

Mohamed Ouessar · Donald Gabriels
Atsushi Tsunekawa · Steven Evett
Editors

Water and Land Security in Drylands

Response to Climate Change

Water and Land Security in Drylands

Mohamed Ouessar · Donald Gabriels
Atsushi Tsunekawa · Steven Evett
Editors

Water and Land Security in Drylands

Response to Climate Change

 Springer

Editors

Mohamed Ouessar
Institut des Régions Arides
Medenine
Tunisia

Atsushi Tsunekawa
Arid Land Research Center
Tottori University
Tottori
Japan

Donald Gabriels
Faculty of Bioscience Engineering
Ghent University
Ghent
Belgium

Steven Evett
USDA-ARS
Bushland, TX
USA

ISBN 978-3-319-54020-7

ISBN 978-3-319-54021-4 (eBook)

DOI 10.1007/978-3-319-54021-4

Library of Congress Control Number: 2017932625

© Springer International Publishing AG 2017

This work is subject to copyright. All rights are reserved by the Publisher, whether the whole or part of the material is concerned, specifically the rights of translation, reprinting, reuse of illustrations, recitation, broadcasting, reproduction on microfilms or in any other physical way, and transmission or information storage and retrieval, electronic adaptation, computer software, or by similar or dissimilar methodology now known or hereafter developed.

The use of general descriptive names, registered names, trademarks, service marks, etc. in this publication does not imply, even in the absence of a specific statement, that such names are exempt from the relevant protective laws and regulations and therefore free for general use.

The publisher, the authors and the editors are safe to assume that the advice and information in this book are believed to be true and accurate at the date of publication. Neither the publisher nor the authors or the editors give a warranty, express or implied, with respect to the material contained herein or for any errors or omissions that may have been made. The publisher remains neutral with regard to jurisdictional claims in published maps and institutional affiliations.

Printed on acid-free paper

This Springer imprint is published by Springer Nature
The registered company is Springer International Publishing AG
The registered company address is: Gewerbestrasse 11, 6330 Cham, Switzerland

Short Biography of Dr. Houcine Taâmallah



Born in Sidi Bouzid (central Tunisia) in 1960, Dr. Houcine Taâmallah completed his undergraduate and M.Sc. studies at the National Agronomic Institute of Tunisia (Institut National Agronomique de Tunisie) (INAT) in 1984 and 1987, respectively. He received a Ph.D. in Agricultural Sciences (Soil and water management) from the Faculty of Applied Bio-engineering Sciences of the University of Ghent (Belgium) in 2007.

After working for a private company (1987–1988), he joined the Arid Zone Research Institute (Institut des Régions Arides) (IRA) (Médenine, Tunisia) in 1988 as a researcher.

Since his appointment at IRA, he contributed actively, as coordinator or team member, to the realization of numerous joint research projects funded by national and international agencies (WB, ABOS, EU, CSFD, UNU, UNESCO, etc.). His research programs focused mainly on land degradation, soil physics and fertility, climate change impacts and adaptation, combating desertification, and drylands management.

He contributed also to training and capacity building through supervision of trainees and students of all levels from national and international centers and organizations and universities, part time teaching at the universities on drylands and natural resources management related issues, and organization of specialized local and international training sessions.

He was solicited to provide expertise for studies and/or projects conducted by numerous national (Ministries of Agriculture, Environment, Planning) and international organizations (FAO, GTZ, OSS, UNU, etc.) in addition to assisting local development agencies (agriculture, environment, development).

He published several scientific papers in national and international journals in addition to his contribution to the edition of books and book chapters.

He moved in 2012 to work as a university professor in soil sciences at the National School of Rural Engineers (ESIER) in Medjez El Bab.

He passed away on May 16, 2013.

Foreword

Drylands are increasingly considered as regions of major concern for the international community because they are subject to natural resource degradation and depletion, particularly in terms of soil and water. Climate change would exacerbate pressure on those resources. The inhabitants of dryland regions are forced to make various adaptations. Therefore, the research community has to play a key role in assisting local societies and development agencies by bringing science to play in guiding field actions.

It is in this spirit that the international conference on '*Integrated Land and Water Resources Management in the Dry Areas Under Climate Change*' (ILDAC2015) was organized in Djerba Island, Tunisia, during May 11–14, 2015. It was organized in memory of *Dr. Houcine Taamallah*, senior researcher in soil sciences and combating desertification, who worked for IRA from 1988 to 2012. It brought around 200 participants of 18 nationalities from Africa, Europe, the USA, and the Middle East. The objectives were as follows:

- Updates on climate change and projections
- Present recent developments in land and water resources management in the drylands
- Provide a forum for debate and exchange among all stakeholders working for drylands development
- Learn from local experiences in combating land degradation and desertification

In order to share the outcomes, this proceedings book contains a selection of 27 papers out of the 50 oral presentations and 190 posters presented in this conference.

We wish to thank all the conference partners that assisted in the organization of this conference. Special thanks are due to donor agencies, ICARDA, the EU, and the Government of Tunisia, who generously contributed in ensuring the

participation of the key people involved in research for development of drylands. A special mention must go to the editors and contributing authors as well as Springer for agreeing to publish these proceedings.

August 2016

Prof. Houcine Khatteli
Director General
Institut des Régions Arides (IRA)
Medenine, Tunisia

Em. Prof. Dr. ir. Donald Gabriels
UNESCO Chair for Eremology
Ghent University
Ghent, Belgium

ILDAC2015 Proceedings Ouessar et al. (editors)

List of Reviewers

Dr. Lamine Babasy (OSS, Tunisia)
Dr. Hédia Chakroun (ENIT, Tunisia)
Dr. Gabriel DEL BARRIO (CSIC-EEZA, Spain)
Dr. Boubakr Dhehibi (ICARDA, Jordan)
Dr. Gunay Erpul (Univ Ankara, Turkey)
Dr. Steven Evett (ARS-USDA, USA)
Prof. Donald GABRIELS (Univ. Ghent, Belgium)
Prof. Giorgio GHIGLIERI (Univ. Cagliari, Italy)
Dr. Caroline King (IIED, UK)
Dr. Mohamed MOUSSA (IRA, Tunisia)
Dr. Kamel Nagaz (IRA, Tunisia)
Dr. Zuhair NASR (INRGREF, Tunis, Tunisia)
Dr. Mohamed Ouessar (IRA, Tunisia)
Prof. Mongi Sghaier (IRA, Tunisia)
Prof. Albert SOLE (CSIC, Spain)
Prof. Atsushi TSUKENAWA (Tottori Univ., Japan)
Dr. Mounira ZAMMOURI (FST, Tunisia)

About the Book

Integrated Land and Water Resources Management in the Dry Areas under Climate Change

Proceedings of the international conference on 'integrated land and water resources management in the dry areas under climate change' (ILDAC2015) Djerba Island, Tunisia, May 11–14, 2015.

Over 40% of the world is drylands, where about 2.3 billion people live in nearly 100 countries. By surface area, it accounts for up to 44% of all the world's cultivated systems. Climate change is a serious reality to cope with. Land degradation, already present in dryland areas, is likely to worsen with high population growth rates and accompanying mismanagement of rangelands and cropped areas.

This book consists of chapters drawn from proceedings addressing these issues. The main themes include climate change impacts, water resources mobilization and management, land degradation remediation, spatial tools, and integrated socio-economic approaches. It brings various rich experiences from all over the world, ranging from traditional know-how to up-to-date high technologies, to bear on the problems of land and water resources management in the drylands.

Contents

1	A Study of Water Stress on Olive Growing Under the Effect of Climate Change in South East of Tunisia	1
	A. Hachani, Mohamed Ouessar and A. Zerrim	
2	Climate Change Impacts in the Maghreb Region: Status and Prospects of the Water Resources	17
	L. Oualkacha, L. Stour, A. Agoumi and A. Kettab	
3	Effect of High Temperature Stress on Wheat and Barley Production in Northern Tunisia	27
	Asma Lasram, Mohamed Moncef Masmoudi and Netij Ben Mechlia	
4	Study of Managed Aquifer Recharge and Climate Change, Using a Numerical Model: The Figuig Aquifer (Eastern High Atlas, Morocco)	35
	Abdelhakim Jilali and Abderrahmane El Harradji	
5	Calibration of AquaCrop Salinity Stress Parameters for Barley Under Different Irrigation Regimes in a Dry Environment	43
	F. El Mokh, Vila-Garcia, K. Nagaz, Mohamed Moncef Masmoudi, N. Ben Mechlia and E. Fereres	
6	Groundwater Recharge of the Kairouan Plain Aquifer: Evidence of Preferential Flow Paths Through the El Haouareb Limestones?	57
	Amal Sebai, Sylvain Massuel, Jamila Tarhouni and Hamza Jerbi	
7	Evapotranspiration of Wheat in a Hilly Topography: Results from Measurements Using a Set of Eddy Covariance Stations	67
	N. Boudhina, Mohamed Moncef Masmoudi, N. Ben Mechlia, R. Zitouna, I. Mekki, L. Prévot and F. Jacob	

8	Performance of Saxton and Rawls Pedotransfer Functions for Estimating Soil Water Properties in the Cap Bon Region-Northern Tunisia	77
	I. Alaya, Mohamed Moncef Masmoudi, Ph. Lagacherie, G. Coulouma, F. Jacob and N. Ben Mechlia	
9	Assessing the Groundwater Pollution Problem by Nitrate and Faecal Bacteria: Case of Djerba Unconfined Aquifer (Southeast Tunisia)	87
	Faiza Souid, Belgacem Agoubi and Adel Kharroubi	
10	Monitoring Soil Moisture Content of <i>Jessour</i> in the Watershed of Wadi Jir (Matmata, Southeast Tunisia)	97
	Fethi Abdelli, Mohamed Ouessar, Salah M’Hemdi, Messaoud Guied and Houcine Khatteli	
11	Direct and Residual Effect of Sewage Sludge in a Sudangrass-Barley Cropping System	111
	Rajia Kchaou, Mohamed Naceur Khelil, Saloua Rejeb, Belgacem Henchi and Jean Pierre Destain	
12	<i>Aflaj</i>’ Water Management in Oman: The Case of <i>Falaj Al-Khatmeen</i> in Birkat Al-Mouz, Wilayat Nizwa	119
	Fairouz Megdiche-Kharrat, Mohamed Moussa and Hichem Rejeb	
13	Response of Vegetable Crops to Irrigation Regimes Using Saline Waters	129
	K. Nagaz, F. El Mokh, Mohamed Moncef Masmoudi, N. Ben Mechlia, O. Belkheiri and G. Ghiglieri	
14	Fog Collection and Participatory Approach for Water Management and Local Development: Practical Reflections from Case Studies in the Atacama Drylands	141
	Martino Correggiari, Giulio Castelli, Elena Bresci and Fabio Salbitano	
15	Salt and Water Dynamic of Potato Crop Under Irrigation with Low Quality Waters	159
	Mguidiche Belhaj Amel, Gazouani Hiba, M’hamdi Douh Boutheina and Boujelben Abdehamid	
16	Development of Methodology for Existing Rainwater Harvesting Assessment in (semi-)Arid Regions	171
	Ammar Adham, Michel Riksen, Mohamed Ouessar, Rasha Abed and Coen Ritsema	

17 Impact of Anthropogenic Activities on Erosive Behavior of Nebhana Watershed Tunisia 185
 Taoufik Hermassi, Hacib El Ammami and Walid Ben Khelifa

18 Short-Term Effects of Olive Mill Wastewater Spreading on Chemical Properties of Soils in Arid Lands, Study Case from Southern Tunisia. 197
 Donia Jendoubi, Houcine Taamallah, Khadija Bouajila, Ahlem Gara, Mohamed Moussa and Mustapha Sanaa

19 Spatio-Temporal Evolution of the Fragmentation Classes of the Mikea Dry Deciduous Forest (Southwestern Madagascar) 209
 Hibraim Rijaso Ravonjimalala, Jan Bogaert, Dominique Hervé, Samuel Razanaka, Jaona Ranaivo, Herizo Randriambanona and Solofo Rakotondraompiana

20 The Impact of Atmospheric Pollution on the Chemical Composition of Soil Around Gabes Cement Plant Southeastern Tunisia 221
 Ines Terwayet Bayouli, Housseem Terwayet Bayouli, Mohamed Tarhouni and Mohamed Nefatti

21 Contribution of Hyperspectral Images (Hyperion) and Spectroscopy for Mapping Soil’s Surface and Materials (Case of the Watershed of Oued Beni Zalten, the New Matmata, Tunisia) 235
 Imen Ben Haj Yahia and Aziza Ghram Messedi

22 Use of Remote Sensing and GIS for Land Degradation Assessment of Qarun Lake Coastal Area, El-Fayoum, Egypt 251
 M.M. Kotb, R.R. Ali and M.A. El Semaary

23 Classification Methods for Detecting and Evaluating Changes in Desertification-Related Features in Arid and Semi-arid Environments 269
 Gabriela Mihaela Afrasinei, Maria Teresa Melis, Cristina Buttau, Claudio Arras, Amar Zerim, Messaoud Guied, Mohamed Ouessar, Bouajila Essifi, Mongi Ben Zaied, Amor Jlali, Hanen Jarray and Giorgio Ghiglieri

24 Evaluation and Validation of SRTMGL1 and ASTER GDEM2 for Two Maghreb Regions (Biskra, Algeria and Medenine, Tunisia). 291
 Claudio Arras, Maria Teresa Melis, Gabriela-Mihaela Afrasinei, Cristina Buttau, Alberto Carletti and Giorgio Ghiglieri

25 An Integrated Cost–Benefit and Livelihood Approach for Assessing the Impact of Water Harvesting Techniques (WHTs) on Livelihoods: A Case Study in the Oum Zessar Watershed, South-East Tunisia 303
Mohamed Arbi Abdeladhim, Mongi Sghaier, Luuk Fleskens and Mohamed Ouessar

26 Assessing the Impacts of Climate Change on Sustainable Development at the Regional Level: A Case Study in Medenine, South-East Tunisia 317
Mohamed Arbi Abdeladhim, Mongi Sghaier, Luuk Fleskens, Lindsay Shutes and Abdallah Akari

27 How Investment in RD&E Offset the Negative Impact of Climate Change on the Tunisian Agricultural Productivity Sector 333
Boubaker Dhehibi, Aymen Frija and Aden Aw-Hassan

Conclusions and Recommendations 347

Introduction

Over 40% of the world is drylands, where about 2.3 billion people live in nearly 100 countries. It accounts for up to 44% of all the world's cultivated systems. Many people living in drylands depend directly upon a highly variable natural resource base for their livelihoods, and about half of all dryland inhabitants—one billion people—are poor and marginalized. This accounts for close to half of the world's poor.

Earth's average temperature has risen by 0.8 °C over the past century, but it is expected that during the twenty-first century the global surface temperature is likely to rise a further 0.3–1.7 °C for the lowest emissions scenario using stringent mitigation and 2.6–4.8 °C for the highest, making climate change a reality to cope with. Small changes in the average temperature of the planet can translate to large and potentially dangerous shifts in climate and weather. Rising global temperatures have been accompanied by changes in weather and climate. Many places have seen changes in rainfall, resulting in more floods, droughts, or intense rain, as well as more frequent and severe heat waves. The planet's oceans and glaciers have also experienced some big changes—oceans are warming and becoming more acidic, ice caps are melting, and sea levels are rising. Moreover, the effects will be severely felt in the dry areas where the temperature is already high and the rainfall is low. As these and other changes become more pronounced in the coming decades, they will likely present challenges to our society and our environment particularly in the drylands.

Land degradation has many facets: soil erosion, vegetation removal, salinization, compaction, pollution, etc. Land degradation costs an estimated US\$40 billion annually worldwide, without taking into account hidden costs of increased fertilizer use, loss of biodiversity, and loss of unique landscapes. The consequences of land degradation are reduced land productivity, socioeconomic problems, including uncertainty in food security, migration, limited development, damage to ecosystems and, in the drylands, desertification. Degraded land is costly to reclaim and, if severely degraded, may no longer provide a range of ecosystem functions and services with a loss of the goods and many other potential environmental, social, economic, and nonmaterial benefits that are critical for society and development.

Water scarcity is the major vulnerability in the world's driest region, the Near East and North Africa (NENA), where per capita water availability is predicted to halve by 2050 even without the effects of climate change. Scientists predict that dry areas in NENA will become drier and droughts will become more frequent; rainfall patterns will become more volatile and unreliable; sea levels will rise and soil salinity will increase in coastal areas; and the occurrence of extreme events, such as frosts and flash floods, will increase. Drought can have devastating consequences for the livelihoods of the poor. It also threatens the fragile ecosystems of the dry areas. Due to climate change, this threat is expected to increase in coming decades.

Geospatial technologies are becoming an integral part of solving the food security equation through integrated research and development, aid to better intervention and delivery programs, and improved policy and outreach. Recent advances in geo-informatics and remote sensing technology have opened new avenues for integrated agro-ecosystems research and applications: land use planning, land degradation monitoring, water resources management, natural resources inventory, integrated spatial decision-making tools, etc.

The people living in the drylands are heavily dependent upon ecosystem services directly or indirectly, for their livelihoods. Communities already have a long record of adaptation to climate variability. However, the impacts of climatic and other man-made stresses have been growing continuously at a rate that often exceeds human and ecosystem tolerance levels. Consequently, many traditional adaptive knowledge and livelihood strategies practiced in drylands for centuries no longer suffice or are inefficient efforts to reduce the vulnerability of drylands populations. Therefore, those populations must reinforce their risk management and coping capacities by augmenting existing adaptation mechanisms and supplementing them with new options that are tailored to unique local contexts.

Chapter 1

A Study of Water Stress on Olive Growing Under the Effect of Climate Change in South East of Tunisia

A. Hachani, Mohamed Ouessar and A. Zerrim

Abstract Climate change (CC) is a main issue of interest at the international as well as the national levels. It is important at this stage to do research to analyze impacts and adaptation strategies. The objective of this study was to evaluate the water stress of olive groves within the context of CC in the South East of Tunisia (watershed of Oum Zessar, Medenine) using hydrological modeling (HidroMORE model). Data on rainfall and temperature were collected from available stations, while those for future scenarios (Horizons 2030 and 2090) were obtained using the Coupled Model Intercomparison Project Phase 5 CMIP5 (GFDL HIRAM C360). In comparison with the reference period (1996–2005) and projecting increases in temperature of 1 and 5 °C, as well as rainfall decreases of 5.4 and 20%, reference evapotranspiration (ET_o) was simulated to increase by 3–9% and evapotranspiration under non-standard conditions (ETC_{adj}) was reduced by 13% and 30%, respectively, for the 2030 and 2090 horizons. Thus, it is expected that the land suitable for olive cultivation will experience shrinkage and this cropping system would become increasingly problematic.

Keywords Olive groves · Climate change · HidroMORE · Water stress

Introduction

Climate change (CC) is a severe problem that the whole world is facing. It is now widely accepted that CC is already happening and further change is inevitable; over the last century (between 1906 and 2005), the average global temperature rose by about 0.74 °C. This has occurred in two phases, from the 1910s to 1940s and more strongly from the 1970s to the present (IPCC 2007). Many studies into the detection and attribution of climate change have found that most of the increase in average

A. Hachani (✉) · M. Ouessar · A. Zerrim
Laboratory of Eremology and Combating Desertification, Institut des Régions
Arides (IRA), 4119 Médenine, Tunisia
e-mail: amalhachani86@gmail.com

global surface temperature over the last 50 years is attributable to human activities (IPCC 2001). It is estimated that, for the twentieth century, the total global mean sea level has risen 12–22 cm, and this rise has been caused by the melting of snow cover and mountain glaciers (both of which have declined on average in both hemispheres) (IPCC 2007). The IPCC also notes that observations over the past century show that changes are occurring in the amount, intensity, frequency, and types of precipitation globally (IPCC 2007). So, it is clear that CC presents a major challenge, a reality for all countries and for Tunisia in several sectors such as agriculture and especially for the olive tree sector, which occupies a strategic place in the Tunisian economy. It is in this framework that this work has been conducted to evaluate the water stress of olive tree within the context of climate change. The aims of this work are to analyze the situation related to climate variability and CC and future projections, then explore different climate scenarios and their effects on water stress of olive plantations in the South East of Tunisia (watershed of Oum Zessar, Médenine) and finally suggest ways and policies of adaptation.

Presentation of the Study Site: Location

The watershed of wadi Oum Zessar was chosen as the site for this study. Based on previous research undertaken in the region (Talbi 1993; Derouiche 1997; De Graaff and Ouessar 2002) this watershed can be considered, from the ecological, hydrological, as well as socio-economical point of view, as representative of arid south-eastern Tunisia. In addition, it has a long history with regard to water harvesting dating from the pre-Roman era (Carton 1888) until today (De Graaff and Ouessar 2002). The study site belongs to the region of south eastern Tunisia (province *government* of Médenine). It is situated northwest of the city of Médenine. It covers administratively the counties (*délégations*) of Béni Khédache, Médenine Nord, and Sidi Makhoulouf (Fig. 1.1). It stretches from the mountains of Matmata (Béni Khédache) in the south-west, crosses the Jeffara plain (via Koutine) and the saline depression (*Sebkha*) of Oum Zessar before ending in the Mediterranean (Gulf of Gabes).

Materials and Methods

Our study was carried out in three main stages: the first was the preparation of climate data for the reference period and the future projection (2030 and 2090) periods. The second stage was devoted to data processing of sequential Landsat images to determine NDVI data cubes. NDVI images were calculated from Landsat 5 and 7 TM images downloaded from USGS. The images were geometrically and atmospherically corrected. For joining all the images as bands in a unique image we have to create the images cube sized to the total area. Some modifications were carried out for the soil and land use maps which would be considered as inputs for

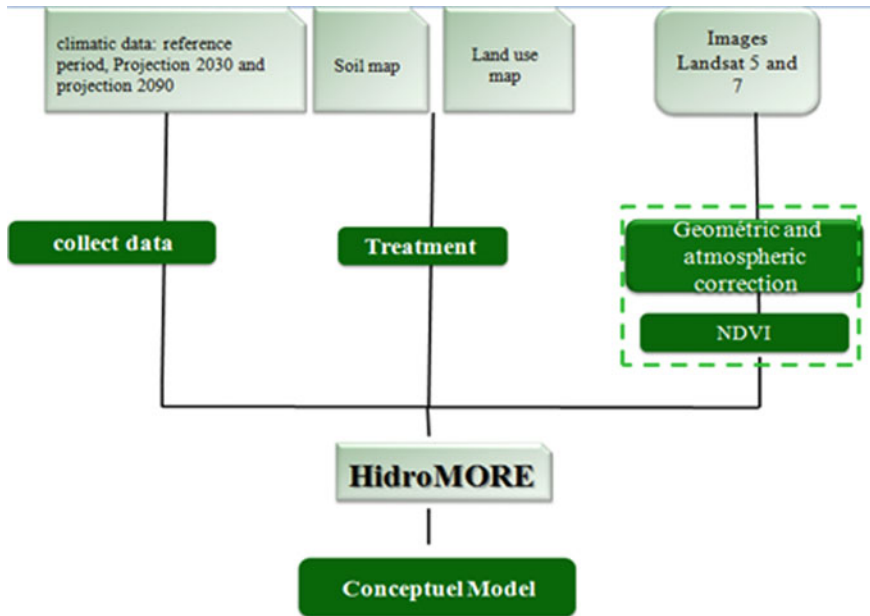


Fig. 1.2 Methodology flowchart

the Coupled model intercomparison project 5 (Taylor et al. 2012) CMIP5 archive. For our study we used the HiRAM-C360 for which the grid has 360×360 points. A user can access CMIP5 model output through the PCMDI data portal (<http://pcmdi3.llnl.gov/esgcat/home.htm>) or through any of the other Earth System Grid (ESG) federated gateways. The ESG data portal web pages make it possible to search for the specific output of interest to a user. A user may search using any combination of model, variable, experiment, frequency (e.g., monthly, daily, 3 hourly), and modeling realm (e.g., atmosphere, ocean, sea ice).

The HidroMORE Model

HidroMORE is considered an operational model allowing the calculation of the superficial water budget with a limited number of input data; they can be estimated from remote sensing or measured by agrometeorological stations, reducing the necessity of adjustments or calibrations. Another relevant aspect of HidroMORE is its capacity to detect the water stress of vegetation, which can be obtained by the soil water balance. HidroMORE implements the FAO-56 dual crop coefficient and water stress, pixel by pixel, in broad areas and it is assisted by satellite images to determine cover parameters, leading to estimates of the basal crop coefficient (K_{cb}) and cover factor (f_c). The crop coefficient is multiplied by the reference

evapotranspiration (ET_o) to estimate the crop water use (ET_c). For that, HidroMORE performs a soil water balance in each pixel of the study zone, determining ET_c by the FAO-56 methodology. The greatest strength of the model is the calculation of ET using the FAO 56 dual crop coefficient, which is applied pixel by pixel in the study area and is based on the derivation of the basal crop coefficient from multispectral images using a relationship between NDVI and K_{cb} (González-Piqueras 2006, Bausch and Neale 1987). The basal crop coefficient was determined in Médenine for mountain and plain olive (Ouessar 2007; Fleskens et al. 2005) during the initial period, the mid-season and during the off-season. When the sap flow measurements are not available, the basal crop coefficient will be established from the minimum value of crop coefficient (Teixeira et al. 2008).

Description of the Input Variables Required By HidroMORE

To implement the model, raster maps of soil properties, land use, NDVI images and meteorological variables such as precipitation and temperature are needed. Once the model is run, raster maps of precipitation, ET_o , ET_c , $ET_{Cad,j}$ defined as the crop evapotranspiration under non-standard conditions which is the evapotranspiration from crops grown under management and environmental conditions that differ from the standard conditions and calculated using a water stress coefficient K_s , percolation (Direct recharge), irrigation, and runoff are obtained. The model also brings the possibility of obtaining detailed information for specific pixels. The input data are introduced into HidroMORE as raster images, but some information, like meteorological information, is only available for the station in maps or images format (Fig. 1.3).

The Conceptual Model

The main objective of a conceptual model was to automate the output data of HidroMORE data. For HidroMORE, the simulation can be run without any NDVI image. These images are not essential but the results of the simulation will be more accurate using them. In case of not using the NDVI, the input data of K_{cb} , crop height and green cover fraction F_{cv} are obtained from the tables. If a NDVI image is available, the user can select the relationship between the NDVI and the input data, using tables or images. So in this framework the calibration was carried out using as input K_{cb} extracted from NDVI and after that from table related to classes of land use map defined by the user. The calibration was performed for the some outputs parameters percolation and $ET_{Cad,j}$ for the years 1986, 1987, 2000, 2001, 2009, 2010 using the image and table simulations.

Another conceptual model was carried out in order to analyze the parameters of the water balance for the reference period (1996–2005) and two future periods (2026–2035) and (2086–2095).

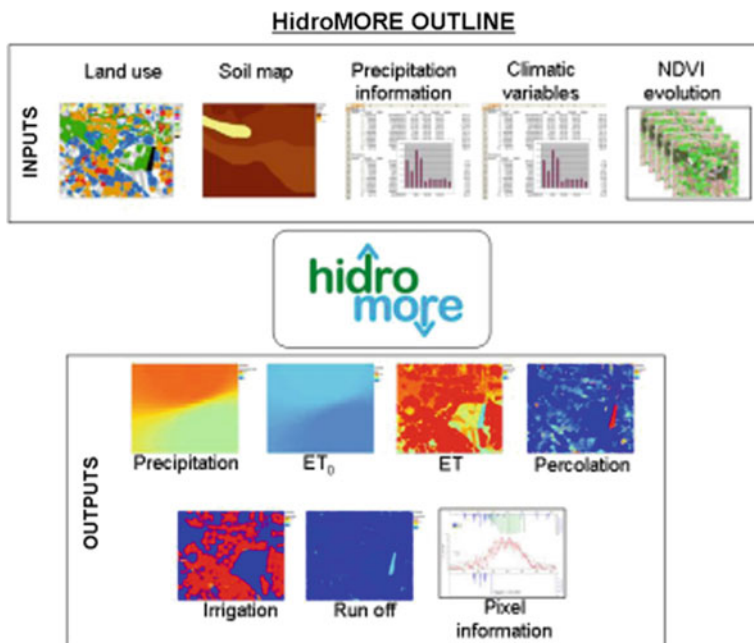


Fig. 1.3 Schematic diagram of inputs and outputs of HidroMORE

Results and Discussion

Calibration

HidroMORE allows two approximations to assess the state of the cover. One is to deduce the K_{cb} and the f_c from $NDVI$ images, and the second is to assess them by tables of K_{cb} and f_c linked to the classes of the land use map defined by the user. The results of these two approximations for Oum Zessar are presented in Fig. 1.4 considering the initial conditions of the soil–vegetation–atmosphere system during the simulation. As observed, these two approximations present similar results in percolation, ET for the studied period 1986, 1987, 2000, 2001, 2009, 2010. However, there are some differences that are not systematic. Table 1.1 shows annual averages of these variables for the studied period. The correlation coefficient was calculated. It was in the order of 0.99 and 0.83 for ETCadj 2009 and percolation 2009, respectively.

HidroMore was applied for the reference period (1996–2005) and future scenarios with the same set of parameters, the same soil map, the same land use map, but with new climate data to see what would be the evolution of the water balance parameters in the watershed Oum Zessar. Thus, since only temperature and precipitation changed between hydrological modeling scenarios, the reference and

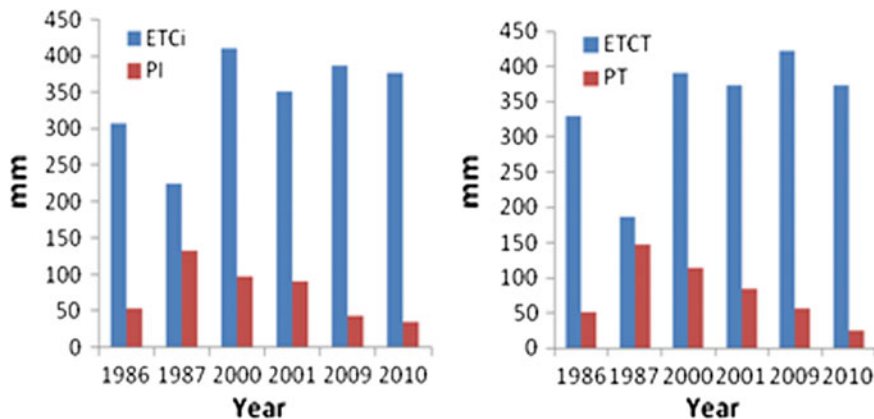


Fig. 1.4 Evapotranspiration ETCi and percolation PI estimated by HidroMORE using the NDVI image (in the *left*) and evapotranspiration ETCT and percolation PT estimated by HidroMORE using the table form for Kcb in HidroMORE (in the *right*)

Table 1.1 Annual averages and correlation in percolation and ET, between two approximations images and tables in 1986, 1987, 2000, 2001, 2009, 2010

Year	R ² : (ETC adj)	R ² : (Percolation)
1986	0.99	0.99
1987	0.94	0.98
2000	0.93	0.82
2001	0.93	0.79
2009	0.99	0.93
2010	0.86	0.83

future scenarios (2030 and 2090 horizons), we can extract the impact of rising temperatures and fluctuating rainfall on the water regime and hence the stress. The value of *ETCadj* tends to be highly variable in space as a result of the availability of water in the soil and the huge fluctuation of precipitation and ETo. The high *ETCadj* zones are in concordance with zones with high amounts of water received from precipitation and from additional collected runoff water since olive trees are generally planted behind water-harvesting structures (*Jessour* and *tabias*). In fact southeast Tunisia provides a typical example of the intensive management of scarce water resources in southern Mediterranean drylands. In this region, communities traditionally constructed earthen dikes with small spillways across the wadis to harvest the surface runoff from the surrounding degraded mountain slopes in the upstream areas. The soil that built up behind the dike formed a terrace that is used for cropping. These ancient water-harvesting systems are referred to as *jessour*. Water harvesting gradually also expanded to the foothills of the mountains. Earthen dikes were made in the gently sloping plains to harvest the runoff from the adjacent mountain slopes. These so-called *tabias* are often built in sequence, with spillways to distribute the water evenly among them. The additional collected runoff water was introduced in HidroMORE model as an irrigation. Precipitation is an important

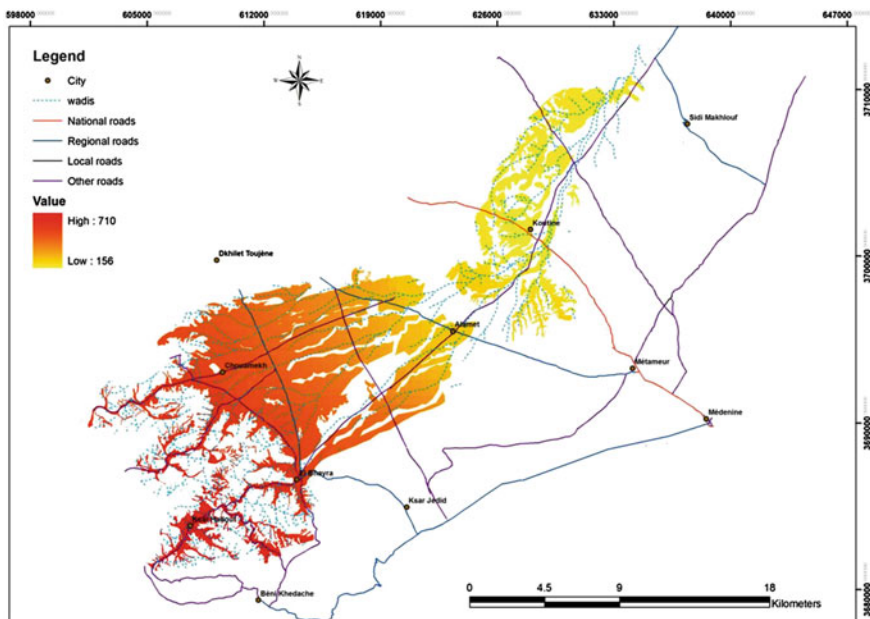


Fig. 1.5 Adjusted evapotranspiration map for the baseline period

variable in the water balance, which affects other variables such as ETC_{adj} for the olive groves especially in rainfed condition. The results of HidroMORE for three scenarios in our study area present how the annual amount of water received from precipitation and additional collected runoff varies as shown in Figs. 1.5, 1.6, 1.7, 1.8, 1.9, and 1.10. For the baseline period, the average of the amount of water received and ETC_{adj} are about 434 mm and 433 mm, respectively. At the 2030 horizon, the total water received was about 379 mm. This amount on water entering into the production system was simulated to go back to the atmosphere as ETC_{adj} which was of the order of 378 mm. At the 2090 horizon, the average of the amount of water received was about 299 mm and ETC_{adj} was 298 mm. It is clear that practically the entire amount of water received will occur as ETC_{adj} . As compared to the estimates obtained from previous studies (Fersi 1985; Derouiche 1997), the evapotranspiration agrees by more than 88% with that obtained from the studies of Fersi (1985) and Derouiche (1997). For the baseline and future scenarios, it is necessary to mention that the fluctuation in ETC_{adj} values is explained by the variability of precipitation and additional collected runoff in watershed. In the simulation, when amount of water received is less than optimum for plant growth, the plant closes its stomata and reduces transpiration, so as the stress increases consequently ETC_{adj} declines

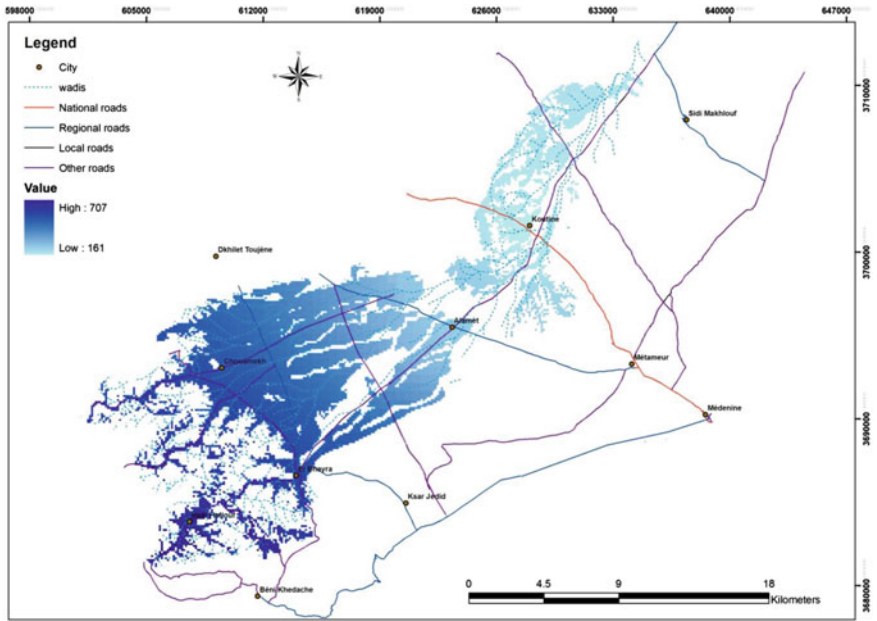


Fig. 1.6 Amount of water received map for the baseline period

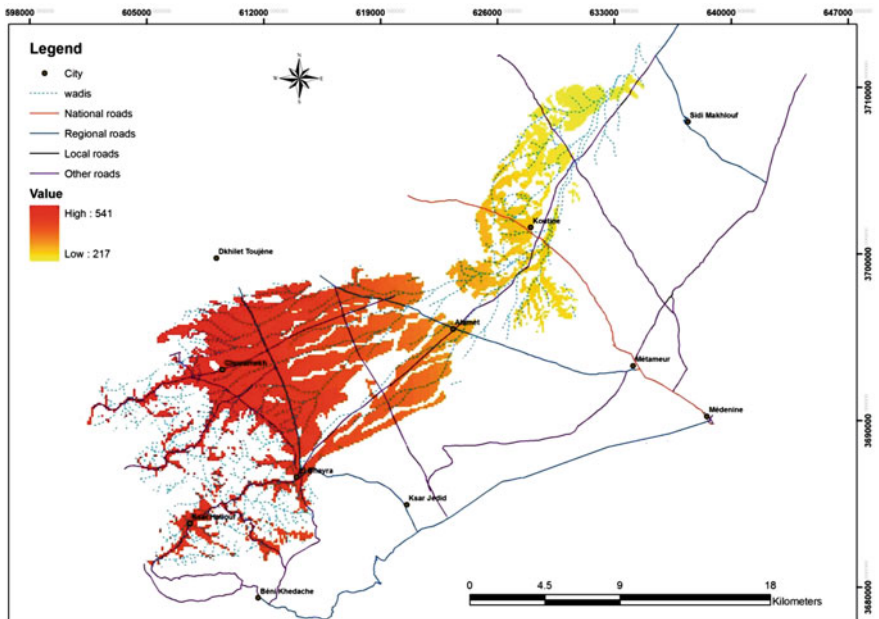


Fig. 1.7 Adjusted evapotranspiration map for 2030 horizon

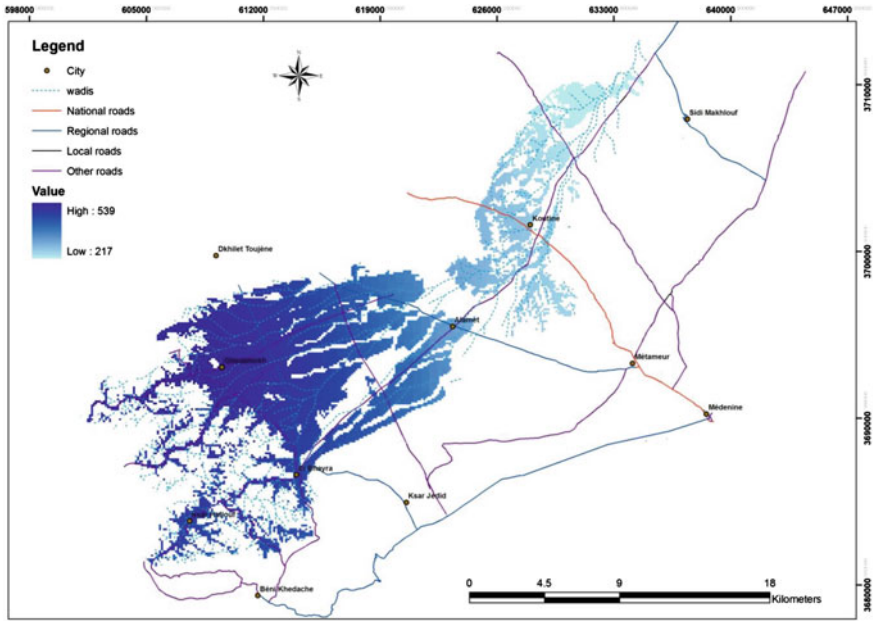


Fig. 1.8 Amount of water received map for 2030 horizon

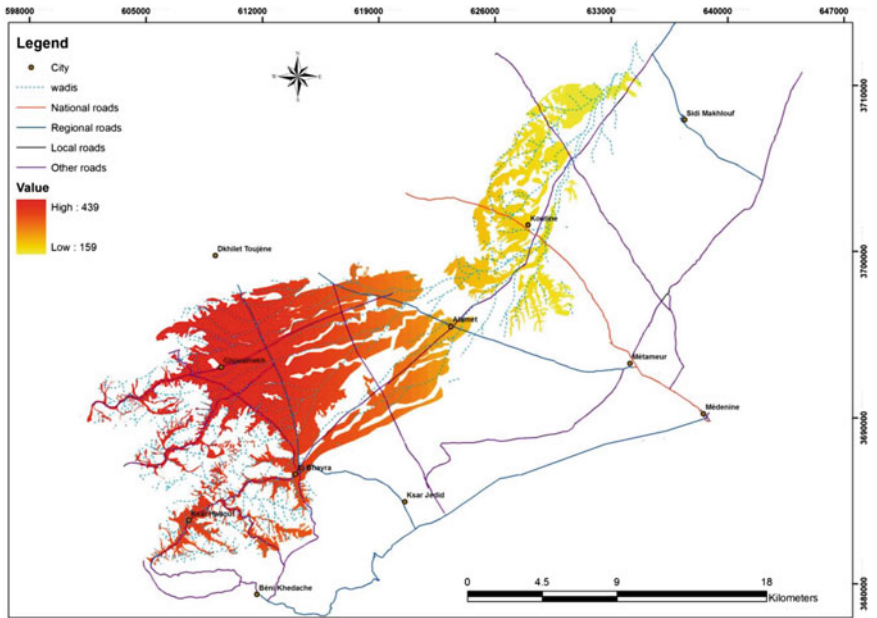


Fig. 1.9 Adjusted evapotranspiration map for 2090 horizon

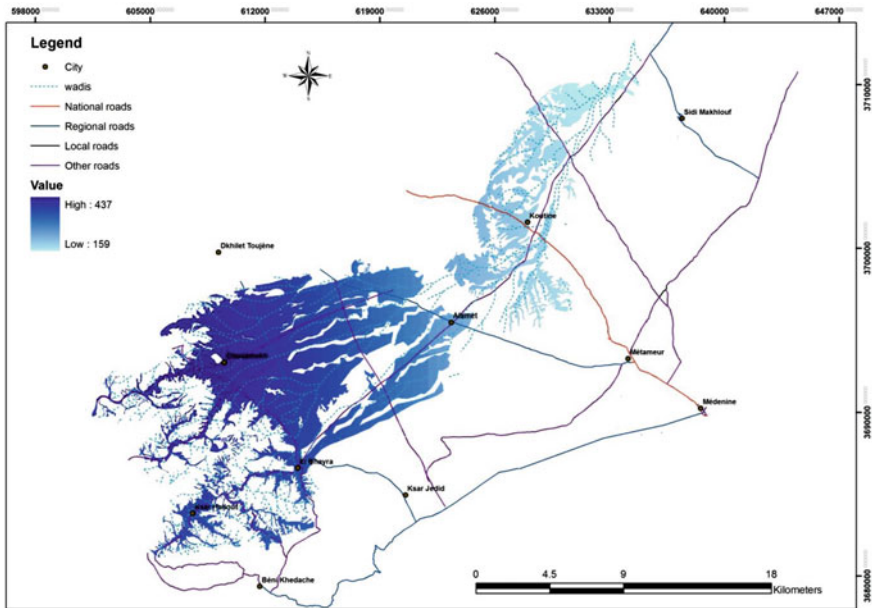


Fig. 1.10 Amount of water received map for 2090

Table 1.2 Classes of suitability for olive trees in the governorate of Medenine (Sghaier et al. 2010)

Class	ETCadj/ETC
Highly suitable	<80
Suitable	60–80
Moderately suitable	60–40
Slightly suitable	40–20
Not suitable	<20

Ratio of ETCadj to ETC

A relationship between *ETCadj* and evapotranspiration under standard conditions (ETC) was calculated to determine the most appropriate and suitable areas for olive growing. The classification of the suitability was done for the entire region of Medenine through the project CI-GRASP as presented in Table 1.2.

Our study site includes the following classes: Slightly suitable/moderately suitable/suitable. These classes agree with the finding of Sghaier et al. (2010) who studied vulnerability of the olive production sector to climate change in the governorate of Medenine. The suitability for olive growing in the study area is presented in Table 1.3 and Figs. 1.11, 1.12 and 1.13 for the baseline period and future scenarios.

Table 1.3 Areas of class of suitability for olive trees in the watershed of Oum Zessar

Horizon	Slightly suitable (%)	Moderately suitable (%)	Suitable (%)
Baseline period	28	46	26
Horizon 2030	19	68	13
Horizon 2090	24	76	0

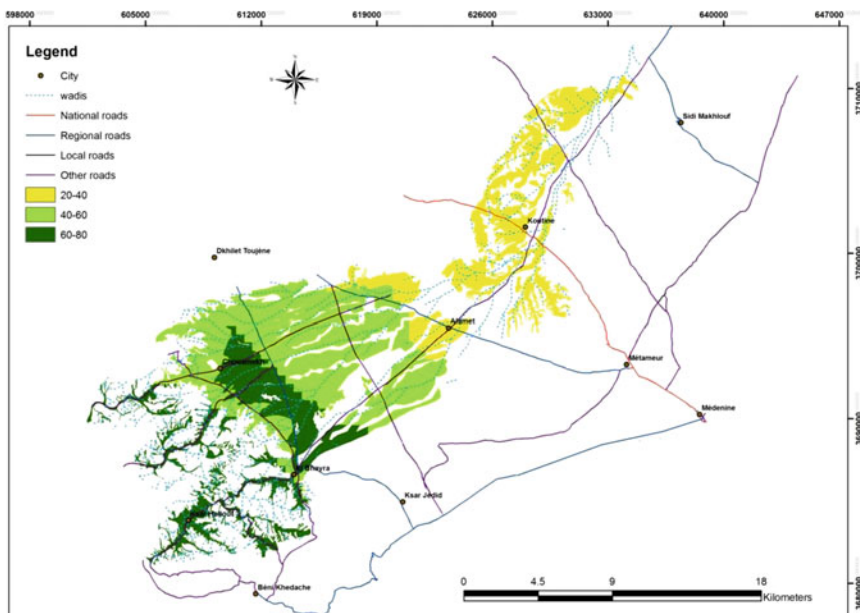


Fig. 1.11 Map of ETC adj/ETC ratio for the baseline period

The area classified as being slightly suitable for olive was about 28%, 19%, and 24% of the area occupied by olive trees for the reference period, 2030 horizon and 2090 horizon, respectively. The area classified as moderately suitable was about 46% for the reference period, and increased to 68% and 76% for 2030 horizon and 2090 horizon, respectively. The area classified as suitable was about 26% of the area occupied by olive trees for the baseline period, and declined to 13% for the 2030 horizon and to zero for the 2090 horizon. It is expected that the land suitable for olive cultivation will experience shrinkage and this cropping system would become increasingly problematic.

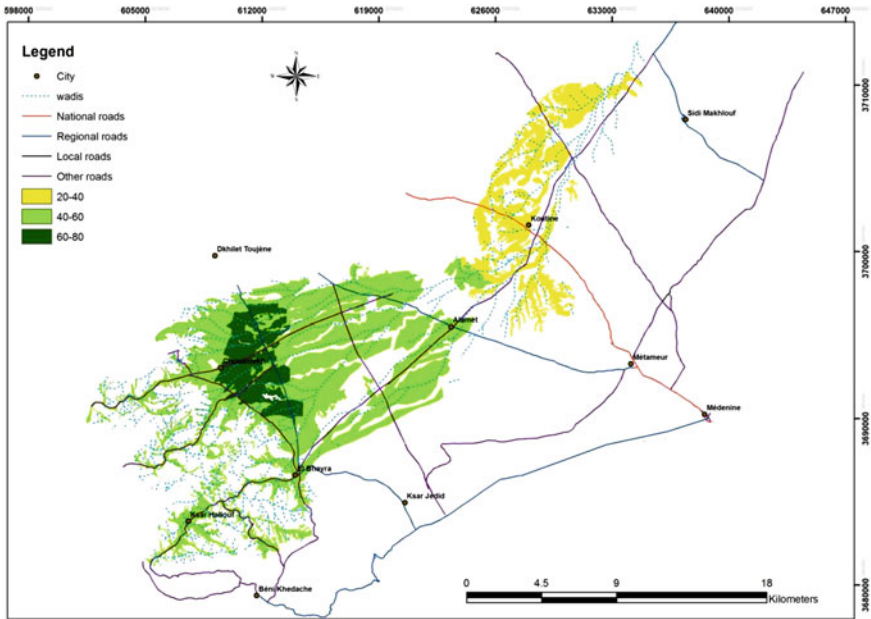


Fig. 1.12 Map of ETC adj/ETC ratio for 2030 horizon

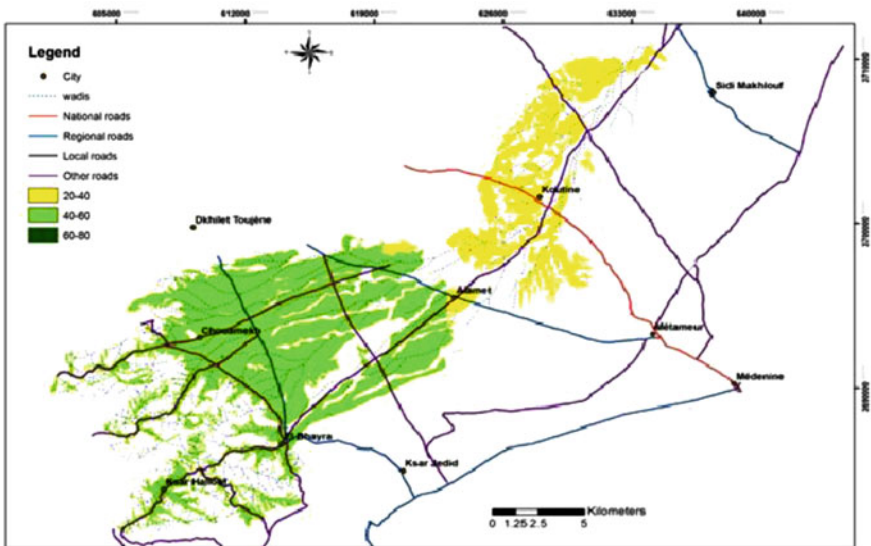


Fig. 1.13 Map of ETC adj/ETC ratio for 2090 horizon

Adaptive Strategy

Adaptation to climate change and variability necessitates the adjustment of a system to moderate the impacts of climate change, to take advantage of new opportunities, and to cope with the consequences (IPCC 2001). Adaptation involves the action that people take in response to, or in anticipation of, projected or actual changes in climate to reduce adverse impacts or take advantage of the opportunities posed by climate change. Since the olive oil sector is highly vulnerable to climatic changes, some measures have to be taken and recommended in order to conserve and improve the welfare of the farmers in the study site. The main potential adaptations are the following:

Early Warning System

Early warning systems for climate change impacts are necessary in order to allow society as a whole to properly and usefully assimilate the masses of new information and knowledge. In fact, a drought early warning system is designed to identify climate and water supply trends and thus to detect the emergence or probability of occurrence and the likely severity of drought. This information can reduce impacts if delivered to decision makers in a timely and appropriate format and if mitigation measures and preparedness plans are in place. Understanding the underlying causes of vulnerability is also an essential component of drought management because the ultimate goal is to reduce risk for a particular location and for a specific group of people or economic sector.

Adapted Crop System Management

If farmers prefer to continue depending on the olive oil sector despite its high vulnerability to climatic stressors, some management tools should be created in order to guarantee a sustainable production of the sector. Among these tools are Select the most drought tolerant olive trees; Control and improve the agricultural practices mainly with regard to respecting the rules of pruning, as well as the manner and the frequency of ploughing.

Change Water and Soil Conservation WSC Techniques and Supplemental Irrigation

To face water scarcity in relation to the expected significant decrease in precipitation, some techniques of soil and water conservation and water harvesting have to be established in the areas receiving more water from runoff. If available, supplemental irrigation will be beneficial both in quantity and quality of the olive oil crop.

Subsidizing Suitable Systems

For many years, planting olive oil trees was subsidized by the agricultural service. These subsidies have encouraged farmers to expand their olive crop area even into marginal and unproductive lands. Moreover, it has encouraged them to plant the unsuitable collective rangelands, which has induced, in some cases, social conflicts between farmers and communities. The subsidy rules should be reviewed and reoriented. Only plantations in appropriate natural conditions should be subsidized.

Conclusion

An evaluation of water stress of the olive tree within the context of CC in the South East of Tunisia (watershed of Oum Zessar, Medenine) was carried out using hydrological modeling (HidroMORE model) coupled with climate change scenarios. The climatic data were collected using the CMIP5 *Coupled Modeling Intercomparison Project* and we chose GFDL HiRAM C 360 as a model since it represented eight stations for our study region. Compared with the reference period, projected temperature increased by 1 and 5 °C, and projected precipitation decreased by 5.4% and 20% for the 2030 and 2090 horizons, respectively. Again compared with the reference period, simulated ETo increased by 3% and 9%, and simulated ETCadj decreased by 13% and 30%, respectively, for the same 2030 and 2090 horizons. Thus, it is expected that the land suitable for olive cultivation will experience shrinkage and this cropping system would become increasingly problematic. In fact, the suitable area is about 26% for the baseline period and declined by 13% for the 2030 horizon and to zero for the 2090 horizon. In any work of hydrological modeling (such as HidroMORE), there is uncertainty at all levels. Thus, improvements could be made through refining further the input parameters of the model, and using multiple satellite images to obtain a good NDVI cube.

Acknowledgements While conducting this study, the main author was partially financially supported by the Institut des Régions Arides (IRA) through the following programs: Eremology and Combating Desertification Laboratory supported by the Tunisian Ministry of Higher Education and Scientific Research, and the EU-funded projects WADIS-MAR (n° ENPI/2011/280-008) and WAHARA (FP7/2007–2013, n° 265570).

References

- Ben Zaied M (2009) Etude d'impact des aménagements CES par application des modèles hydrologiques (Cas du bassin versant d'oued Oum Zessar). Mémoire de Master, ENIT
- Bausch WC, Neale CMU (1987) Crop coefficients derived from reflected canopy radiation: a concept. *Trans ASAE* 30(3):703–709

- Carton D (1888) Essai sur les travaux hydrauliques des Romains dans le Sud de la Régence de Tunis. *Bulletin Archéologique du Comité des Travaux Historiques et Scientifiques*, 438–465. Cas du bassin versant Oum Zessar. M.Sc. thesis, INAT, Tunis
- De Graaff J, Ouessar M (eds) (2002) Water harvesting in Mediterranean zones: an impact assessment and economic evaluation. TRMP paper n° 40, Wageningen University
- Derouiche R (1997) Contribution à l'étude par modèle numérique de l'impact des aménagements de CES sur la recharge de la nappe de Zeuss-Koutine. Graduation dissertation, INAT, Tunis, 68 pp
- Fersi M (1985) Etude hydrologique d'oued Oum Zessar à Koutine. Ministère de l'Agriculture, Tunis
- Fleskens L, Stroosnijder L, Ouessar M, De Graaff J (2005) Evaluation of the onsite impact of water harvesting in Southern Tunisia. *J Arid Environ* 62:613–630
- González-Piqueras J (2006) Crop Evapotranspiration by means of remote sensing determination of the crop coefficient. Regional scale application: 08–29 Mancha Oriental aquifer. Ph.D., Facultat de Física, Universitat de València
- IPCC (Intergovernmental Panel on Climate Change) (2001) Climate change 2001: impacts, adaptation, and vulnerability. Contribution of working group II to the third assessment report of the IPCC. Cambridge University Press
- IPCC (Intergovernmental Panel on Climate Change) (2007) Climate change 2007: impacts, adaptation and vulnerability. Contribution of working group II to the fourth assessment report of the IPCC. Cambridge University Press, Cambridge, UK, 976 pp
- Ouessar M (2007) Hydrological impacts of rainwater harvesting in wadi Oum Zessar watershed (southern Tunisia). Ph.D. thesis, Faculty of Bio-Engineering Sciences, Ghent University, Belgium, 154 pp
- Sghaier M, Ouessar M, Ouled Belgacem A, Taamallah H, Khatteli H (2010) Vulnerability of olive production sector to climate change in the governorate of Médenine (Tunisia). Final report, Projet Ci:Grasp, IRA/PIK/GTZ, 35p+annexes
- Talbi M (1993) Contribution à l'étude de la désertification par télédétection dans la plaine de la Jeffara du Sud-Est tunisien. M.Sc. thesis, Université de Tunis, 305 pp
- Taylor KE, Stouffer RJ, Meehl GA (2012) An overview of CMIP5 and the experiment design. *Bull Am Meteorol Soc* 93(4):485–498. doi:[10.1175/BAMS-D-11-00094.1](https://doi.org/10.1175/BAMS-D-11-00094.1)
- Teixeira A, Hde C, Bastiaanssen WGM, Moura MSB, Soares JM, Ahmad MD, Bos MG (2008) Energy and water balance measurements for water productivity analysis in irrigated mango trees, Northeast Brazil. *Agric For Meteorol* 148:1524–1537

Chapter 2

Climate Change Impacts in the Maghreb Region: Status and Prospects of the Water Resources

L. Oualkacha, L. Stour, A. Agoumi and A. Kettab

Abstract The fifth report of the Intergovernmental Panel on Climate Change reiterates that the Maghreb region is severely threatened by climate change and seems to be one of the most vulnerable regions in the world regarding its water resources responses to the changing climate conditions. The effects of climate change could significantly increase the relevance of water development policies, given that economic growth of the majority of Maghreb countries is closely related to water resources and contributes strongly to the socioeconomic balance and gross domestic product. In the Maghreb region, the need to mainstream climate change into development plans is already recognized and highlighted; the new constitutions have already adopted the sustainable development concept, which opens opportunities for improvement and protection of natural resources. Over the last decades, countries have tried to overcome water stress and scarcity by improving water policy and strategy, infrastructure development, economy of water use, wastewater, and desalinization, among others. However, the great challenge within the Maghreb region is mainstreaming climate change issues into development planning in the contextual framework of the water–energy–food security nexus, whose components are strongly interdependent. The aim of this paper is to analyze the impact of climate change on the water sector in the Maghreb region (Algeria, Morocco, and Tunisia) by means of a SWOT analysis (SWOT standing for Strengths,

L. Oualkacha (✉) · L. Stour
Laboratory of Process and Environment Engineering,
Faculty of Sciences and Technologies of Mohammedia,
Hassan II University of Casablanca, B.P. 146, Mohammedia, Morocco
e-mail: lailaoualkacha@gmail.com

A. Agoumi
Department of Hydraulic, Environment and Climate,
Hassania School of Public Works, Km 7 Route d'El Jadida, B.P. 8108,
Casablanca, Morocco

A. Kettab
Research Polytechnic National School, Alger, Algeria

Weaknesses, Opportunities, and Threats) and to make recommendations on how to improve climate change mainstreaming into water development plans within the region.

Keywords Climate Change · Water resources · Adaptation · Orientations · Maghreb

Introduction

In the Maghreb region, water resources are characterized by irregular distribution in space and time. Climate data indicated that during the twentieth century a temperature increase of 1 °C occurred (Stour and Agoumi 2007), with a pronounced warming trend during the last 40 years and a net increase in the frequency of droughts and floods (Moujahid et al. 2014).

Based on the results of the fifth report of the Intergovernmental Panel on climate change, the Maghreb region is threatened by climate change and seems to be one of the most vulnerable regions in the world regarding water resource responses to climate change. The effects of climate change could influence the viability and relevance of water development policies, given that economic growth and development of the majority of Maghreb countries are closely related to water resources that contribute strongly to the socioeconomic balance and gross domestic product.

Models available for the Maghreb region project that droughts will be more frequent, more intense and longer lasting (Elrafy 2009). Model simulations also announce a drop of 4–27% in annual rainfall with more frequent torrential rain (UNEP 2008); this will increase the competition for water within the Region, carrying the risk of conflicts and can represent strong push-factors for migration.

The World Bank and United Nations experts in 1995, estimates water availability at about 605 m³ per capita per year in Algeria, 758 m³ per capita per year in Morocco and 418 m³ per capita per year in Tunisia (Abdessamad 2005). Therefore, the Maghreb countries (Algeria, Morocco, and Tunisia) have per capita water availability of less than 1000 m³, the threshold for the water-poverty level.

Hydraulic infrastructure development was a priority for the Maghreb governments to cope with droughts and floods in the last decades, hence, today available water resources are already mobilized at a rate exceeding 75% in Morocco (in 2007) and 80% in Tunisia (in 2000) (Desjardins 2010). Agricultural water consumption absorbs more than 80% of the total water demands in Morocco (88%) and Tunisia (90%), and about 59% in Algeria (Abdessamad 2005).

Droughts in rural areas associated with water scarcity enhance push-factors for migration into cities where today more than 60% of the total population are living (Agoumi 2003); this will increase the trend of urbanization and aggravate the socioeconomic conditions.

The Maghreb countries have undertaken numerous efforts to respond to water scarcity and improve groundwater management by adopting water economy use

strategies and plans (Green Plan in Morocco). In Tunisia, wastewater reuse for irrigation was already initiated in 1960 in the Plain of the Soukra, and 800 million cubic meters of water sewage are currently treated and reused for irrigation in Algeria (Lachkar 2015). Many countries in the region have adopted sea water desalination to secure water supply in the coastal cities (Algeria's production of sea water desalination is about 825 m³/day in 2015 (Taibi 2012).

The objective of this paper is to analyze the impact of climate change on the water sector in the Maghreb countries. Analysis is focused on the countries that have already adopted a water adaptation strategy and plan to combat climate change impacts namely: Algeria, Morocco, and Tunisia. The SWOT method is used to undertake this analysis and make recommendations on how to improve climate change mainstreaming into water development plans within the region.

Methodology

The SWOT analysis is focused on the current state of the water resources in the region with a view of climate change impacts; it is used to identify internal strengths and weaknesses, as well as external opportunities and threats within the region with regard to strategic tools and measures for mainstreaming climate change adaptation. The analysis also identifies progress made in institutional, regulatory, technical, and governance aspects. This will permit to make recommendations for promoting and improving business adaptation within the region.

SWOT analysis is based on the following components:

- Collection of official strategic documents (National Strategy and Plan for mainstreaming adaptation, National Communications to the United Nations Framework Convention on Climate Change, etc.),
- Identification of SWOT aspects with a view to institutional, regulatory, technical, and governance issues related to water management.
- Consultation with a group of national and regional experts to validate the results of SWOT analyses.

Climate Change Impacts on Water Resources in the Maghreb Region

Climate change is likely to result in less rainfall, increasing temperature and frequency of droughts and floods. These effects increase water stress through reduced water availability quality groundwater management.

Projections developed for the Maghreb region (national communications of Algeria, Morocco, and Tunisia) depict trends of a decrease in rainfall and a gradual

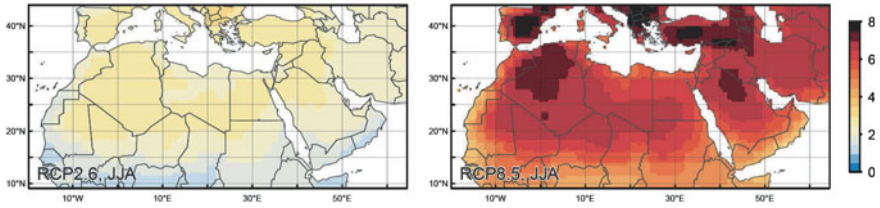


Fig. 2.1 Evolution of the average temperature (°C) of June–July and August during the period 2071–2099 relative to the 1951–1980 period, results of the models RCP2.6 (2 °C world, *left*) and RC8.5 (4 °C world, *right*) (World Bank Group 2014)

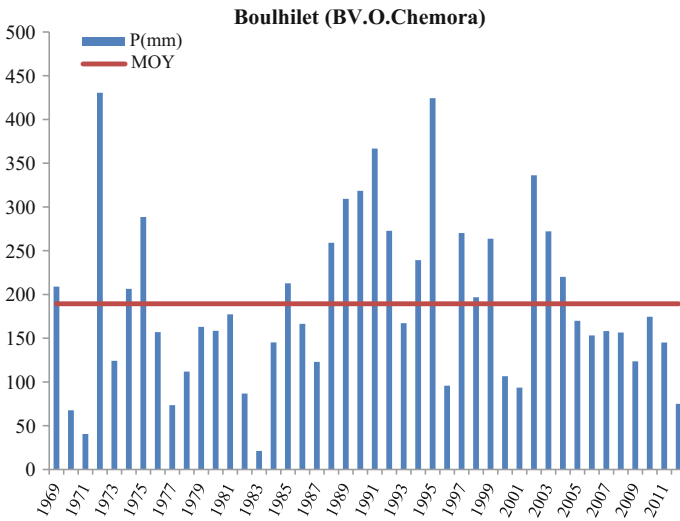


Fig. 2.2 Evolution of annual rainfall of Boulhilet station (Chemora basin) in Algeria (Tatar 2014)

increase in the monthly average temperature in the Maghreb area. The results in Fig. 2.1 of the models RCP2.6 (2 °C world, left) and RC8.5 (4 °C world, right) show the evolution of average Temperature (°C) for June–July and August during the period 2071–2099 relative to the 1951–1980 period. These results show that average temperature will increase by 2–8 °C during 2071–2099 within the region (World Bank Group 2014).

In Algeria, the study of rainfall recorded in hundreds of weather stations (period 1951–1980 and 1961–1990), shows a succession of episodes of excessive and deficient rainfall compared to normal documenting great variability (Hassini et al. 2011). The analysis of rainfall data in Fig. 2.2 demonstrates annual variability and irregular rainfall with excessive and deficit episodes recorded in the Boulhilet station, Chemora basin (Tatar 2014).

In Morocco, the analyses carried out under the “National Water Strategy” show that most basins will experience more water stress by 2030 and water flow at dams

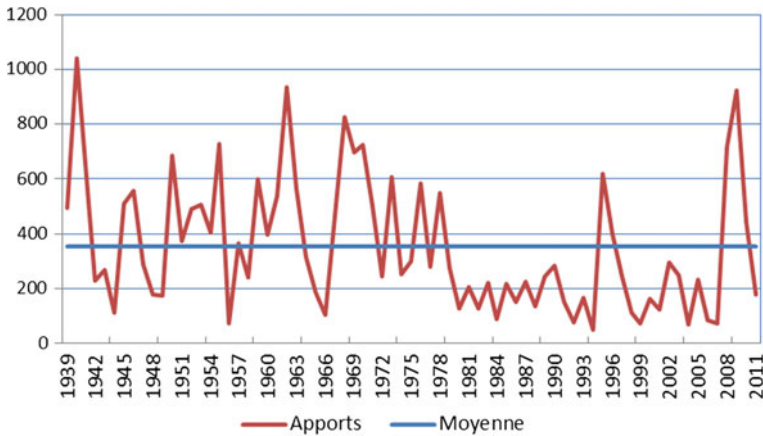


Fig. 2.3 Evolution of water flow at El Kansera dam during 1939–2011 (Secrétariat d’Etat chargé de l’Eau au MAROC 2009)

will continue to decrease (SEE 2009). Figure 2.3 shows a decrease of the water flow at El Kansera dam, especially during 1980–2011 (SEE 2009).

Tunisia also faces the effects of accelerated sea level rise; in fact, Tunisia is among the top 10 impacted countries in terms of population affected and GDP losses due to the accelerated sea level rise (Dasgupta et al. 2007). Hence, Tunisia will have to absorb and compensate for multiple climate change effects. Changes will be noticed in the productivity of fisheries and fishing areas. The most exposed sites are: the Bizerta lagoon, GaraetIchkeul, the Ghar el Melh lagoon, the Kalaat el Andaloussekhas, the wetlands and lagoons in the Gulf of Gabès, the archipelagos and islands of Kuriat, Kneiss, Kerkennah, and Jerba and the entire sandy beach.

Water Strategies and Plans in the Maghreb Countries

During the last decades, the water sector was prioritized in the National strategies and plans; however, the great challenge within the Maghreb region is mainstreaming climate issues into development plans, especially in water policy and the water–energy–food security alliances. The Maghreb countries have tried to carry out transitions to adaptive management; focusing on some specific aspects as highlighted in Table 2.1.

Table 2.1 Measures for water adaptive management

Aspects	Measures for water adaptive management
Governance	Water management decentralization (River Basin Agency)
Legal and institutional	Creation of planning and coordination structures at national and territorial levels
	Adoption of water laws
	Institutional reforms
	Tariff reforms
Infrastructure	Infrastructure for conventional and unconventional water resource development and management (dams, wastewater reuse, water desalination, rainwater management)
Integrated Water Resources Management (IWRM)	IWRM included in development plans at national and territorial levels
	Flood and drought plan management (Morocco)
	Strategic plan for groundwater management
Information management	Transboundary water cooperation (North-Western Sahara Aquifer System shared between Algeria and Tunisia)
	Economy of water use (Morocco's Green Plan)
	Climate data, observations and forecasting networks
Financing	Early warning systems
	Public-Private Partnership (Partnership model for water desalination in Algeria)

SWOT Analysis

The SWOT analysis results are given in Table 2.2.

Table 2.2 SWOT analysis of climate change adaptation in the Maghreb region: Focus on the water resources

Factors that contribute to achieving adaptation goals	Factors that inhibit climate change mainstreaming in water development policies
Strengthens	Weakness
Adoption of the sustainable development concept through the new constitutions in Algeria, Morocco, and Tunisia	Difficulties to operationalize the National Strategies and Plans for Water to adapt to climate change
Development of the water national strategies and plans to adapt to climate change (National Plan against Global Warming adopted on 2009 in Morocco; National Strategy on climate change adopted on 2012 in Tunisia)	Lack of institutional coordination
Targeted research programs	Lack of engagement and involvement of stakeholders and partners
Integrating Water Resources Management process	Lack of mainstreaming climate change into water legislation and regulations
	Lack of structured Monitoring and Evaluation systems
	Weak local and territorial institutions and structures

(continued)

Table 2.2 (continued)

Factors that contribute to achieving adaptation goals	Factors that inhibit climate change mainstreaming in water development policies
Structures for consultation and coordination (Water and Climate Council in Morocco; National Water Council in Tunisia) Decentralization of institutional, regulatory and administrative water management (River Basin Agency in Algeria and Morocco) Hydrological and climatological data and information (National Meteorology Direction in Morocco and National Institute of Meteorology in Tunisia)	Difficulties in implementing regulatory and institutional reforms; especially for water tariffs and taxes Gaps in financing mechanisms and instruments Low human resource capacity building and trained staff Difficulties in integrating drought and flood plans into territorial development plans Short-term planning (2020 or 2030) in contrast to the climate change long-term impacts (2050, 2090)
Opportunities	Threats
International Cooperation and Climate Funds Ratification of the United Nation Framework of Climate Change Convention and the Kyoto Protocol by Algeria, Morocco, and Tunisia Global and rapidly increased exchange of climate change knowledge and information Lessons learned from the Integrating Water Resources Management process at national, regional and international levels	Conflicts for water use at transboundary level (Madjerda shared basin and the shared Aquifer) Diversion of political attention and will toward other immediate concerns and business influenced by international and regional factors

Recommendations

Guidance and recommendations to consider in response to climate change, climate risk, and their impacts on water resources in the Maghreb region are summarized as follows:

- Mainstreaming climate change into water development plans with a view of integrating the “green economy” process and the Post 2015 sustainable development water agenda;
- Develop a long-term vision and operational strategy and planning to mainstream climate change into national and regional water development agenda, ensuring the readjustment of climate change adaptation measures, approaches, and no regret investments that allow to adjust gradually and gain a better understanding of the new climate change realities based on the new and improved data from climate projections;
- Create or strengthen expertise and discussion on uncertainty management (communication and consultation on the risks and uncertainties and promote training of water managers in these new approaches);

- Create or strengthen the climate change center of researches with a view to improve institutional coordination, climate observations (qualitatively and quantitatively), climate projections; research on modeling, sharing experiences, and dissemination of information and data both at the national and local levels;
- Promoting lessons learned from the past experiences of integrating water resources management into development planning and initiate adequate large-scale programs of awareness, communication, training, and education with a focus to climate change;
- Consider, the benefit of international support and opportunities through international negotiations and climate funds;
- Integrate the costs of climate change adaptation into financial mechanisms within the national and territorial plans and promote the public–private partnership;
- Integrate flood and drought plans into development planning processes at national and territorial levels;
- Continue to mobilize unconventional water, ensure efficient water use and institutionalize water quality and groundwater management;
- Create a Maghreb platform to share information, lessons and experiences, and monitoring of water vulnerability with a view to create and institutionalize a climate change water champion within the region;
- Set up a Monitoring and Evaluation system for tracking progress in mainstreaming climate change in water development plans.

Conclusion

The entity of water resources in the Maghreb region requires sustainable management, especially in a future context marked by climate change. National Water Strategies and Plans will contribute to improve this sustainability. However, the implementation of the strategies and plans requires a number of governance and institutional reforms, economic and financial mechanisms, monitoring and evaluation tools, and communication and capacity-building measures.

Sustainable development and climate change mainstreaming require a continuous readjustment of strategies and measures that consider regional and local climate conditions. The success of this readjustment depends on a better coordination and a good understanding of the water–energy–food security nexus in the context of climate change.

The developed strategies are focused on the short and middle terms (2020–2030); however, climate change mainstreaming should consider short, middle but also long-term planning and interventions including necessary investments for adaptation.

References

- Abdessamad (2005) L'eau matière stratégique et enjeu de sécurité au 21^{ème} siècle
- Agoumi (2003) Vulnerability of North African countries to climatic changes, adaptation and implementation strategies for climate change. IISD/Climate Change Knowledge Network
- Dasgupta et al (2007) The impact of sea level rise on developing countries: a comparative analysis. World Bank Policy Research Paper 4136. World Bank, Feb 2007
- Desjardins (2010) Impacts des changements climatiques sur l'agriculture au Maroc et en Tunisie et priorités d'adaptation. Notes d'analyse du CIHEAM N° 56, Mars 2010
- Elrafy (2009) Impact of climate change: vulnerability and adaptation of coastal areas. Report of the Arab forum for Environment and Development
- Hassini et al (2011) Trends of precipitation and drought on the Algerian Litoral: impact on the water reserves. *Int J Water Resour & Arid Environ* 1(4):271–275
- Lachkar (2015) Face au changement climatique, le Maghreb relève le défi de l'eau. <http://www.geopolis.francetvinfo.fr/face-au-changement-climatique>
- Moujahid et al (2014) Drainage urbain et changements climatiques: Limites de la modélisation. Article en cours de publication dans la revue internationale de l'eau. *La Houille Blanche SEE* (Secrétariat d'Etat chargé de l'Eau au MAROC) (2009) Stratégie Nationale de l'Eau
- Stour and Agoumi (2007) Sécheresse climatique au Maroc durant les dernières décennies. *Revue Hydroécologie Appliquée*, tome 16:215–232
- Taibi (2012) Vulnérabilité et adaptation aux changements climatiques en Algérie. Ministère des Ressources en Eau, Algérie
- Tatar (2014) Variabilité climatique et ressources en eau en milieu semi-aride: Cas des bassins versants des Oueds Chemora, Reboa et Gueiss -Hauts plateaux constantinois- Algérie
- UNEP (2008) United Nations Environment Programmes. Climate change and energy in the Mediterranean. Sophia Antipolis, July 2008
- World Bank Group (2014) Turn down the heat confronting the new climate normal, pp 113–159

Chapter 3

Effect of High Temperature Stress on Wheat and Barley Production in Northern Tunisia

Asma Lasram, Mohamed Moncef Masmoudi and Netij Ben Mechlia

Abstract Increasing temperatures due to global warming have raised concerns about food security in the southern Mediterranean region. This work attempts to study the limitation to cereal production in Tunisia. Data from six governorates were used to develop relationships between cereal yields and the sum (STx) of maximum temperatures over the threshold of 15 °C. The data envelopment analysis method was used to identify the attainable regional production among seasons having a total rainfall over 350 mm. Results showed that yields of bread wheat, durum wheat and barley decreased, respectively, by 0.4, 0.26, and 0.32 t ha⁻¹ for each 100 °C-day increase in STx, over the 1973–2013 period. An increasing trend in STx was observed for the major synoptic stations of the studied areas over the last 40 years but with different speeds. Future projections to 2050 showed a 15% rise for STx with a low radiative forcing scenario resulting in cereal yield gaps up to 0.26 t ha⁻¹.

Keywords Climate change · Heat stress · Cereal · Yield

Introduction

Increasing extreme temperature events have raised concerns regarding the risk to cereal production arising from heat stress, especially in Mediterranean areas that are expected to be among the potential “hot-spots” in climate change projections (IPCC 2013). Giorgi (2002) found that the period 1900–1998 was marked by a temperature rise of 0.75 °C and that the contributions of the last decades were more

A. Lasram (✉)
ISA, Chott Mariem BP 47, 4042 Sousse, Tunisia
e-mail: asmalasram@planet.tn

M.M. Masmoudi · N.B. Mechlia
INAT, 43 Avenue Charles Nicolle, 1082 Tunis, Tunisia

significant. He reported also that this warming was slightly higher during the winter and summer. An additional increase by 4 °C was predicted for the year 2100 based on the B2 scenario of carbon emissions (Hertig and Jacobeit 2008). The overall result of climate change on crop production is drawn with uncertainty due to the opposite effects of increased temperature and increased CO₂ concentration. However, several studies agreed on final substantial yield restrictions because they supposed dominant effects of heat stress (Asseng et al. 2015).

Terminal stress, the most recurrent and studied heat stress effect in Mediterranean areas, penalizes grain weight by stopping prematurely the filling process (Talukder et al. 2014). Heat stress also reduces grain set by causing sterility of the flowers during anthesis (Saini and Aspinall 1982) or by abortion the fertilized ovaries thereafter (Calderini et al. 2006). Pre-heading heat stress can also reduce the grain number, which is more decisive for yield (Slafer et al. 2014), and the grain weight, particularly during the booting stage by reducing the size of the flower carpels (Ugarte et al. 2007). Wardlaw and Wrigley (1994) reported that yield decreased linearly when the rise of daily temperature was gradual. Conversely, a drastic heat shock effect is more detrimental and cannot be relieved by a subsequent refresh (Stone et al. 1995). Wardlaw and Wrigley (1994) found that the grain weight decreased around 2–7% °C⁻¹ when the average temperature increased from 15 to 28 °C. Stone and Nicolas (1994) reported a 29% drop in grain weight after 3 days of exposure (from the 10th day after anthesis) to a daytime temperature of 40 °C. This yield gap increased up to 50% when the heat shock period extended (Tewolde et al. 2006). The threshold above which temperature becomes stressful depends on both phenophases and genotypes. Porter and Gawith (1999) listed in their review temperature values between 9 and 25 °C.

Various indicators of extreme events have been proposed and listed by WMO (2009). However, Zhang et al. (2014) found that the Growth Degree Day (with a base temperature adapted to heat stress processes) improved the assessment of the spatiotemporal heat stress variability. Based on mean temperature, this thermal sum attenuates the differences between stations having the same means but diverse temperature amplitudes, as is usually the case comparing coastal and inland regions. This sum merges also the differential effect of diurnal and nocturnal temperatures on crop yields which presented a marked asymmetry of their increase trends in mediteranean area (Lobell and Ortiz-Monasterio 2007).

The objective of this work was to estimate diurnal high temperature effects on yields of the major cereal crops grown in northern Tunisia: durum wheat, bread wheat, and Barley, and to determine the yield trends in a global warming context. We proposed to use the sums of degree days above a certain threshold calculated from only the maximum temperatures instead of mean temperature to assess better both the specific intensity and duration of extreme temperature diurnal events in continental and costal stations.

Methodology

Data Used

The climate data used in this work represent continuous daily maximum temperatures at the synoptic stations for the northern Tunisian cereal areas presented in Table 3.1. Used data are available from the website of the U.S. National Oceanic and Atmospheric Administration (<http://www.noaa.gov>). Missing data for the selected periods represent 3% of all the data, they were replaced by the average of the next and precedent days. Regional durum and bread wheat and barley yields and their corresponding monthly precipitations for the same stations were collected from the annual reports of the Tunisian Ministry of Agriculture from 2000 to 2013.

To limit the effect of the precipitation distribution variation, the data envelopment analysis method, well explained by Cooper et al. (2000), was used for selecting attainable regional yields from those related to “wet” seasons (rainfall from October to May > 350 mm). They corresponded to the highest efficiency coefficients, compared to the heat stress index defined in the next paragraph. STATA 11.0 software was used for analyses.

For future projected climate changes, maximum temperatures were downscaled for the six stations using the MarkSim® DSSAT weather file generator basing on global climate model BCC-CSM1-1 for the two scenarios RCP 2.6 and RCP 8.5. The BCC-CSM1-1 model showed the least relative error performance related to the global seasonal-cycle climatology 1980–2005 as affirmed by Flato et al. (2013). The RCP 2.6 assumes that global annual greenhouse gas emissions peak between 2010 and 2020 with emissions declining substantially thereafter, while in RCP 8.5, emissions continue to rise throughout the twenty-first century.

Table 3.1 Synoptic stations, climatic data periods, and the numbers (N) of selected years related to attainable yields analysis

Gouvernorate	Station	Coordinates	Altitude (m)	Period	N
Nabeul	Kelibia	36.85 °N; 11.08 °E	29	1973–2013	6
Bizerte	Bizerte Carouba	37.25 °N; 9.80 °E	5	1973–2013	6
Jendouba	Jendouba	36.48 °N; 8.80 °E	143	1973–2013	9
Tunis	Tunis Carthage	36.23 °N; 10.23 °E	3	1973–2013	8
Beja	Beja	36.73 °N; 9.18 °E	159	2003– 06-10-13	7
Zaghouan	Zaghouan Mograne	36.60 °N; 10.08 °E	156	2004– 06-12-13	4

Thermal Unit Sums

For cereal crops sown in standard dates (November), tillering generally takes place during January–February while the March–April period is marked by the reproductive processes corresponding to jointing, heading, flowering, and early grain formation stages. The emergence period during December and the grain maturation period during May were not considered in our analysis. Accumulated thermal units (ST_x) were calculated then over the periods from January 1 to April 30 using the daily maximum temperatures (T_x) and the fixed threshold of 15 °C (Eq. 1):

$$ST_{x15} = \left\{ \begin{array}{ll} \sum_{01/01}^{30/04} (T_x - 15) & \text{if } T_x > 15 \text{ }^\circ\text{C} \\ 0 \text{ }^\circ\text{C} & \text{if not} \end{array} \right\} \quad (1)$$

The cardinal temperature of 15 °C was proposed by many authors for spring wheat as the optimal temperature for which the rates of many physiological processes such as photosynthesis (Todd 1982) and growth (Porter and Gawith 1999) were at the maximum observed and beyond which they declined and so did the grain yield as reported by Wardlaw and Wrigley (1994).

Results and Discussion

Attainable Regional Yields

In semiarid areas the effects of heat stress on cereal yields are not easy to quantify because of the overriding water stress limitations. Consequently, the pattern in cereal land use is most commonly based on local mean precipitations amounts and economic considerations rather than the thermal regime. For wet cropping cycles, when water is supposed to be not a limiting factor, attainable yield represents the potential regional yield restricted by heat stress (assuming no nutrient limitations on yield). The data showed that attainable yields of bread wheat were greater than yields of durum wheat, which were higher than those of barley (Fig. 3.1). The production gradient was caused by constitutive differences between the species as the bread wheat presents better fruiting efficiency than durum wheat whereas potential grain weights are higher for durum wheat (Marti and Slafer 2014). The disparities between yields can also be related to the gap between the technical efficiency of the cropping patterns, especially for barley, which is generally marginalized, compared to Triticum. In high-yielding conditions, Tunisian farmers are more motivated to grow durum wheat because of its larger selling price compared to bread wheat. In low-yielding conditions they choose barley because of the common assumption that this latter performs better than wheat under stressful

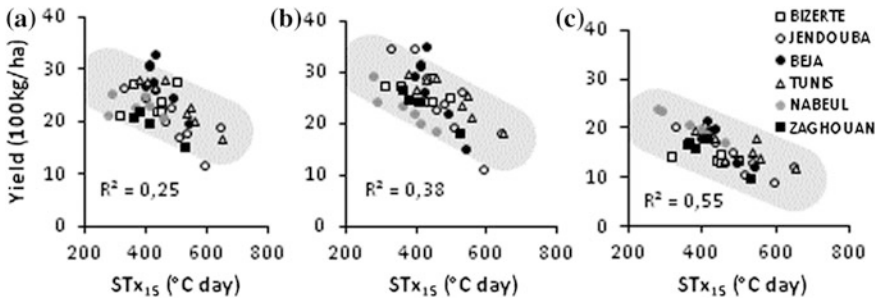


Fig. 3.1 Attainable cereal yields versus cumulative daily maximum temperatures exceeding 15 °C (STx_{15}) during the 2000/2013 period. Data are for durum wheat (a), bread wheat (b) and barley (c), obtained under relatively wet conditions (precipitation during October–May > 350 mm) in six governorates of northern Tunisia

conditions, although this assumption did not find support in scientific work where the two species were compared side-by-side (Savin et al. 2015).

The attainable regional cereal yields during 2000–2013 related to the wet campaigns showed a substantial decreasing tendency with the increase of STx_{15} (Fig. 3.1). The yields decreased around 4.0, 2.6, and 3.2 kg ha⁻¹ °C⁻¹ day⁻¹ for bread wheat, durum wheat, and barley, respectively. Bread wheat seemed to be more sensitive to heat stress compared to durum wheat and barley. As bread wheat presented constitutively better fruiting efficiency, its thermal heat sensitivity is also conforming to the affirmation of larger response of grain number than of average grain mass to changes in environmental conditions (Slafer et al. 2014). Better terminal heat tolerance (during grain filling) of durum wheat compared to bread wheat was pointed out by many authors (Dias et al. 2011; Monneveux et al. 2012). Barley was also found to be less sensitive to heat stress comparing to bread wheat during the pre-anthesis period (Ugarte et al. 2007).

Global Warming Trends

Our study focuses on four stations and a critical period that begins in 1973 and continues until 2013, which is sufficiently long (41 years) to obtain reasonable estimates of the intensities and frequencies of heat events. The increases in mean maximum temperatures related to the January–April period over these years were significantly different from zero ($p < 0.01$) and were about 0.48, 0.43, 0.34, and 0.28 °C/10 years for Kelibia, Tunis, Bizerte, and Jendouba, respectively. These tendencies were adequate to explain the trend rates of STx (Fig. 3.2).

Heat rise was generally faster in the coastal stations compared to Jendouba especially for Kelibia station, which presented the highest coefficient of determination ($r^2 = 0.50$). The relatively small coefficients of determination for the linear

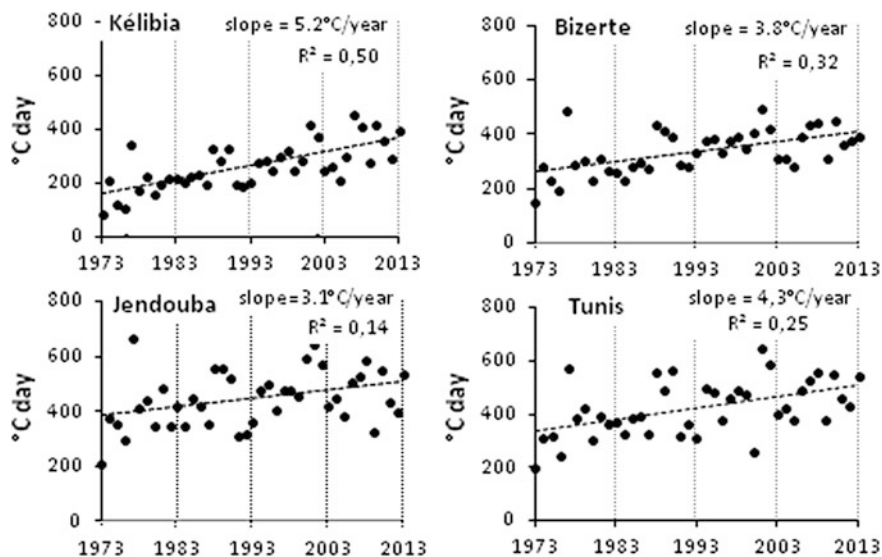


Fig. 3.2 STx₁₅ trends over 1973–2013 period for Kelibia, Bizerte, Tunis, and Jendouba stations

trends reflect the volatile temperature increase rates. Indeed, the seasonal-cycle period 1973/2002 presented slower rise trends and less STx variabilities compared to the last three decades 1983/2013. Only Kelibia station presented a steady rise over all the decades. The actual potential heat stress levels of the different cereal regions in Tunisia STx₁₅ were assessed over the 2000–2013 period and compared to the future projected sums in 2050 using downscaled maximum temperatures generated by the MarkSim® DSSAT weather file generator based on the global climate model BCC-CSM1-1 for the two scenarios RCP2.6 and RCP8.5 (Table 3.2). For the RPC 8.5 scenario only Jendouba and Bizerte stations showed projected values that reflected increases with approximately the same trends measured over 1973–2013. For Kelibia and Tunis stations the projected values were over and underestimated, respectively. Projected yields in north Tunisia could decrease around 0.21, 0.26, and 0.26 t ha⁻¹ for durum wheat, barley and bread wheat, respectively, if we adopted the smaller radiative forcing scenario. These gaps could be doubled for the larger forcing radiative projected climate.

Table 3.2 Actual and future projected values of STx₁₅ (°C day) in cereal tunisian areas (Actual values are averaged over 2000/2013 period)

Station	2000/13	2050 (RPC 2.6)	2050 (RPC 8.5)
Kelibia	336	554	622
Bizerte	384	437	508
Tunis	477	458	538
Zaghuan	404	508	583
Jendouba	493	534	618
Béja	450	450	529

Conclusion

Cumulative heat units based on maximum temperatures could be used as a heat stress index for cereal production. Spatiotemporal variations of this index may explain to a large extent attainable yield of durum wheat, bread wheat, and barley. Analysis of climate records showed an increasing risk of exposure to heat stress that could result in cereal yield gaps up to 0.5 t ha⁻¹ by 2050. Selected new varieties more adapted to heat stress could reduce the gaps caused by the global warming.

Acknowledgments This work was supported by funding from Aclimas (EuropeAid/131046/C/ACT/Multi) and the Middle East and North Africa Water Livelihoods Initiative (US-AID).

References

- Asseng S, Zhu Y, Wang E, Zhang W (2015) Chapter 20—crop modeling for climate change impact and adaptation. *Crop physiology* (2nd edn), pp 505–546
- Calderini DF, Reynolds MP, Slafer GA (2006) Source–sink effects on grain weight of bread wheat, durum wheat and triticale at different locations. *Aust J Agric Res* 57:227–233
- Cooper WW, Seiford LM, Tone K (2000) *Data envelopment analysis: a comprehensive text with models. References and DEA-Solver Software*, Kluwer Academic Publishers, Boston, Applications
- Dias A, Semedo J, Ramalho JC, Lidon FC (2011) Bread and durum wheat under heat stress: a comparative study on the photosynthetic performance. *J Agron Crop Sci* 197:50–56
- Flato G, Marotzke J, Abiodun B, Braconnot P, Chou SC, Collins W, Cox P, Driouech F, Emori S, Eyring V, Forest C, Gleckler P, Guilyardi E, Jakob C, Kattsov V, Reason C, Rummukainen M (2013) Evaluation of climate models. In: Stocker TF, Qin D, Plattner G-K, Tignor M, Allen SK, Boschung J, Nauels A, Xia Y, Bex V, Midgley PM (eds.) *Climate change 2013: The physical science basis. contribution of working group I to the fifth assessment report of the intergovernmental panel on climate change*. Cambridge University Press, Cambridge, United Kingdom and New York, NY, USA
- Giorgi F (2002) Variability and trends of sub-continental scale surface climate in the twentieth century, Part I: observations. *Clim Dyn* 18:675–691
- Hertig E, Jacobeit J (2008) Downscaling future climate change: temperature scenarios for the mediterranean area. *Global Planet Change* 63:127–131
- IPCC (Intergovernmental Panel on Climate Change) (2013) *Climate change 2013*. In: *The physical science basis. Working group I contribution to the fifth assessment report of the intergovernmental panel on climate change*. Cambridge University Press, New York
- Lobell DB, Ortiz-Monasterio JI (2007) Impacts of day versus night temperatures on spring wheat yields: a comparison of empirical and CERES model predictions in three locations. *Agron J* 99:469–477
- Marti J, Slafer AG (2014) Bread and durum wheat yields under a wide range. *Field Crops Res* 156:258–271
- Monneveux P, Jing R, Misra SC (2012) Phenotyping for drought adaptation in wheat using physiological traits. *Front Physiol* 3:429
- Porter JR, Gawith M (1999) Temperatures and the growth and development of wheat: a review. *Eur J Agron* 10:23–36
- Saini HS, Aspinall D (1982) Abnormal sporogenesis in wheat (*Triticum aestivum* L.) induced by short periods of high temperature. *Ann Bot* 49:835–846

- Savin R, Slafer G, Cossani C, Abeledo LG, Sadras V (2015) Chapter 7—cereal yield in mediterranean-type environments: challenging the paradigms on terminal drought, the adaptability of barley and wheat and the role of nitrogen fertilization. *Crop Physiology*, pp. 141–158
- Slafer GA, Savin R, Sadras VO (2014) Coarse and fine regulation of wheat yield components in response to genotype and environment. *Field Crops Res* 157:71–83
- Stone P, Nicolas M (1994) Wheat cultivars vary widely in their responses of grain yield and quality to short periods of post-anthesis heat stress. *Aust J Plant Physiol* 21:887–900
- Stone P, Savin R, Wardlaw I, Nicolas M (1995) The influence of recovery temperature on the effects of a brief heat shock on wheat. I. Grain Growth. *Aust J Plant Physiol* 22:945–954
- Talukder A, McDonald GK, Gurjeet GS (2014) Effect of short-term heat stress prior to flowering and early grain set on the grain yield of wheat. *Field Crops Res* 160:54–63
- Tewelde H, Fernandez CJ, Erickson CA (2006) Wheat cultivars adapted to postheading high temperature stress. *J Agron Crop Sci* 192:111–120
- Todd GW (1982) Photosynthesis and respiration of vegetative and reproductive parts of wheat and barley plants in response to increasing temperature. *Proc Okla Acad Sci* 62:57–62
- Ugarte C, Calderini DF, Slafer GA (2007) Grain weight and grain number responsiveness to pre-anthesis temperature in wheat, barley and triticale. *Field Crops Res* 100:240–248
- Wardlaw IF, Wrigley CW (1994) Heat tolerance in temperate cereals: an overview. *Aust J Plant Physiol* 21:695–703
- WMO (World Meteorological Organization) (2009) Guidelines on analysis of extremes in a changing climate in support of informed decisions for adaptation climate data and monitoring. WCDMP-No. 72
- Zhang Z, Wang P, Chen Y, Song X, Wei X, Shi P (2014) Global warming over 1960–2009 did increase heat stress and reduce cold stress in the major rice-planting areas across China. *Eur J Agron* 59:49–56

Chapter 4

Study of Managed Aquifer Recharge and Climate Change, Using a Numerical Model: The Figuig Aquifer (Eastern High Atlas, Morocco)

Abdelhakim Jilali and Abderrahmane El Harradji

Abstract The impact of climate change on groundwater resources can be significant in arid regions. This is due to the increase in temperature and the decrease in precipitations in such areas. This work studies the effect of Managed Aquifer Recharge (MAR) on the groundwater in the Figuig aquifer (392 km²), which is located in the Eastern High Atlas of Morocco. A numerical model was implemented to evaluate the effect of climate change and MAR up to 2099. Two areas with a surface of 1 and 32 km², respectively, are favored for the construction of dams to serve the purpose of MAR. The extreme A1FI scenario derived from the Intergovernmental Panel on Climate Change (IPCC) was chosen for the simulation of the recharge. The simulation results show that the scenarios are feasible, and that MAR can contribute to an efficient recovery of the groundwater in the Figuig aquifer.

Keywords Managed aquifer recharge · Climate change · Numerical model · Figuig aquifer

Introduction

Due to a constantly increasing demand for water by the population and agriculture, the pressure on groundwater resources has been constantly increasing. As a matter of fact, the intense exploitation of groundwater is qualified as the principal cause of a decrease in piezometric levels and the overall degradation of water quality. As a result, a number of large aquifers in Morocco are now facing a critical depletion. To

A. Jilali (✉)

Laboratory of Mineral Deposits, Hydrogeology and Environment, Faculty of Sciences,
University Mohammed I, Bd. Mohammed VI, B.P: 524, 60000 Oujda, Morocco
e-mail: yamaapa@hotmail.com

A.E. Harradji

Department of Geography—FLSH, University Mohammed I, Oujda, Morocco

remediate this, various departments of the Hydraulic Basin Agency are actively seeking solutions for that situation. The construction of dams to strengthen the irrigation as well as Managed Aquifer Recharge (MAR) are used to increase the piezometric levels and to ameliorate groundwater quality. Several authors have indicated that MAR, consisting of the introduction of rainfall (natural recharge), achieved by dam construction or through the introduction of treated wastewater by surface or well injection can produce excellent results (Masciopinto 2006; Allow 2012; Janardhana Raju et al. 2013; Boisson et al. 2014; Hao et al. 2014; Ouelhazi et al. 2014; Maliva et al. 2015; Parimalarenganayaki and Elango 2015). On the other hand, the system of local khettaras, already in place, is a ground canalization aimed at catching water during rainfall events, with the objective to recharge the aquifer and to use this water for drinking and irrigation. This technique is especially important for people from arid and semi-arid regions characterized by erratic rainfall and long periods of drought (such as the Figuig Oasis in Morocco).

The climatic conditions of the investigated region are arid, with an annual average rainfall of 120 mm (calculated over a period of 76 years, i.e., between 1935 and 2011). The distribution of rainfall from year to year is, however, very variable, and the precipitation differs greatly between the same months in successive years. The average temperature spans the 3–45 °C range, in sporadic cases attaining even 48 °C. Furthermore, the evaporation of rainwater is very high and the precipitation runoffs can reach 80% (Jilali 2014a, b; Jilali and Zarhloule 2015). The Figuig Basin hosts several wadis (periodical streams), such as Tissarfine, Zouzfana, Bouchalikane, and Lakbir. These wadis are dry for most of the time, but strong, occasional storms can take place on the massive watershed and trigger violent floods.

Groundwater modeling is used to understand hydrogeological processes. The simulation of various scenarios, based on a number of assumptions, can be beneficial for the management of piezometric levels and flow budgets. And so, studies of the impact of MAR on the groundwater quality generally show its beneficial effects (Ayuso-Gabella et al. 2011; Bekele et al. 2011; Marie et al. 2014).

The aim of this work is to numerically model the effect of coeval climate change and MAR on the piezometric levels of the Figuig region.

Geographical and Geological Setting

The study area (Figuig aquifer) is located on the eastern side of the Moroccan High Atlas, right beside the Algerian border. It has an overall surface area of 327.46 km² and consists of a plain limited by several mountains (Jebels) including Jebel Grouz, Maïz, Zrigat, Mélias, Sidi Youssef, and a few others (Fig. 4.1).

Recent geological and geophysical surveys carried out in the Figuig area (Younes 2010; Ziani 2010; Amar et al. 2012; Jilali 2014a; Jilali et al. 2015a, b; Jilali and Zarhloule 2015) show that the geology of this region consists of the following strata: (1) Triassic formations of red to green-colored clays and basaltic tuffs,

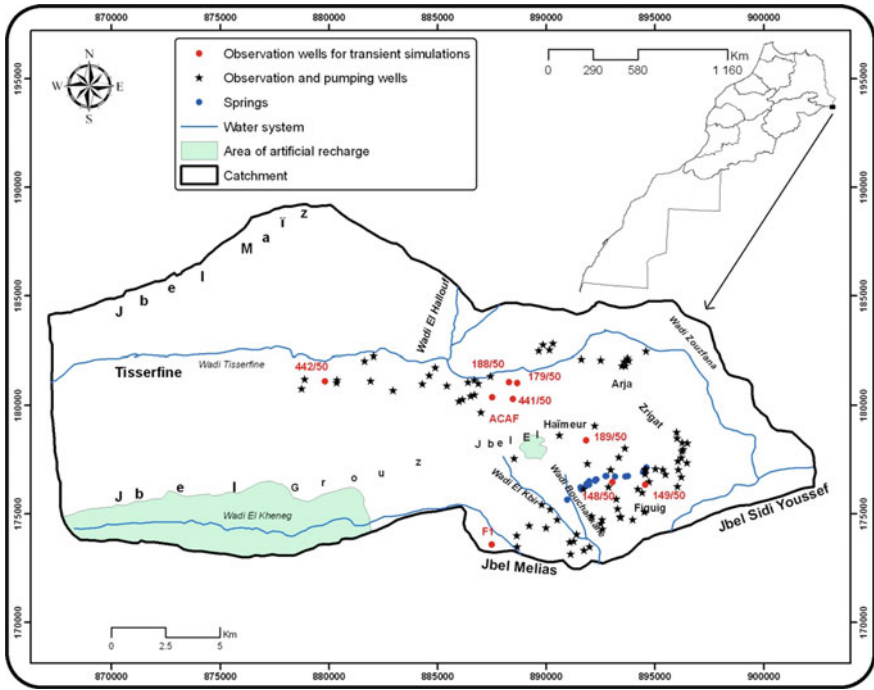


Fig. 4.1 Study area

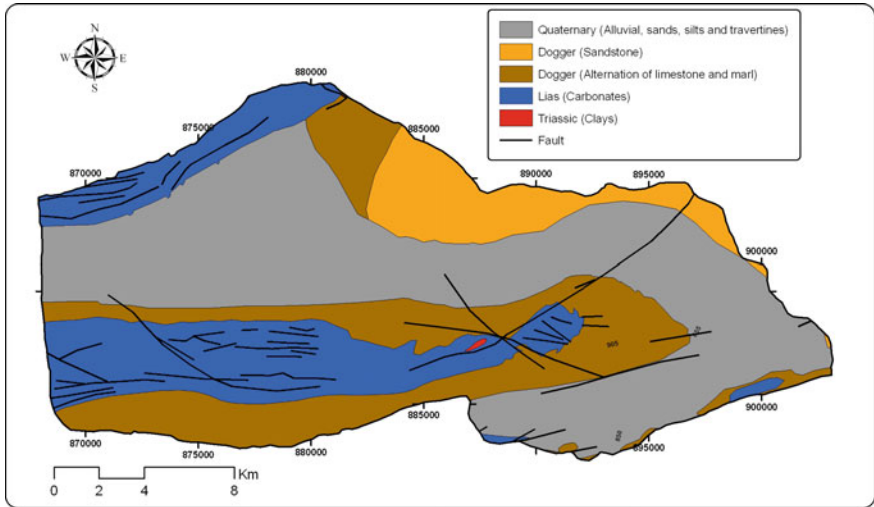


Fig. 4.2 Geology of the study area (Dresnay 1963)

localized in the center of the region (2) Hettengian (Jurassic) formations of black limestones and Sinemurian formations of red to gray dolostones; (3) Thick formations of Pliensbachian (Carixian and Domerian) limestones; (4) Toarcian formations of alternating marls and limestones; (5) Aalenian limestone formations; (6) Bajocian formations of limestones and marls, overlain by a sequence of limestones; and (7) Quaternary formation of alluviums, sand and travertines (Jilali 2014a; Jilali et al. 2015b; Jilali and Zarhloule 2015): see Fig. 4.2. These geological formations are commonly highly fractured, and therefore play a key role in the circulation of groundwater (Jilali 2014a, b; Jilali and Zarhloule 2015).

Methodology

The development of a conceptual model for the Figuiq aquifer was presented in (Jilali 2014a, b), which was based on a steady-state simulation. In this paper, the same parameter structure was used for the transient calibration of the model, but specific yields and storage coefficients in the same zone of hydraulic conductivity were added. Furthermore, a time series of precipitations and pumping wells was introduced in the model for the period between 1984 and 2013. The calibration of the model in transient state is achieved adjusting the specific yields and storage coefficients. The time series of water level of nine boreholes (179/50, 188/50, 189/50, 148/50, 149/50, F1, ACAF, 442/50, and 441/50) was used in the calibration of the model. In addition, piezometric maps of 1995, 2004, and 2010 were used for a verification purpose (Jilali et al. 2015a).

To study the impact of MAR and climate change on the Figuiq aquifer, two ideal areas for MAR (i.e., suitable for the construction of small dams) were selected based on favorable hydrological and hydrogeological conditions. Finally, the extreme scenario A1F1, derived from the Intergovernmental Panel on Climate Change (IPCC 2007) was chosen for the simulation of recharge decreasing by 38% to year 2099 in all of the study area (Jilali 2014a, b), with MAR assumed to having started in 2014 with a constant recharge of 40 mm/year for both study areas.

Results and Discussions

The calibration of the model in transient state was obtained with a root mean square error of 16 m and a mean error of -8 m. The good agreement between the observed and simulated heads for five boreholes (149/50, 179/50, 188/50, 441/50, and ACAF) is shown in Fig. 4.3. In contrast, borehole F1, located in the border area, shows that the calculated hydraulic head is less than the one observed, which is most likely due to the effect of boundary conditions. For the rest of boreholes (442/50, 189/50, and 148/50), the difference between calculated and observed heads is due to the pumping of water from wells in the vicinity (Fig. 4.1). The irrigation in

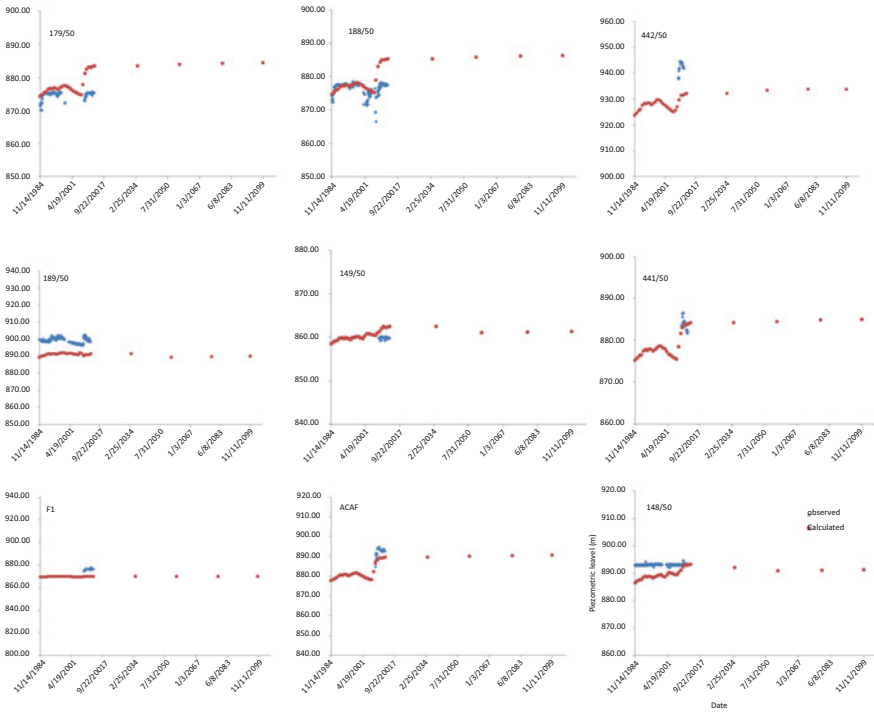


Fig. 4.3 Observed and calculated hydraulic head time series as result of model calibration between 1984 to 2013 and the scenario A1F1 including the MAR from 2014 to 2099

this region is performed once and twice per 15 days for the period from September to April and May to July, respectively.

The study of the paleoclimate in the Figuig oasis between 1950 and 2012, using borehole data shows an overall temperature increase of 1–1.5 °C (Ouzzaouit et al. 2014). In this region, the linear correlation of the mean surface air temperature variation shows an increase of 0.9 °C between 1981 and 2012, and a decrease of annual rainfall by 19 mm for the period of 1965–2012 (Jilali 2014a). After the report of future climate change and adaptation in the oasis regions of Morocco (MEMEE 2011) the scenario A1B of ARPEG-Climate model predicts a rainfall decrease by 10–30% and a mean annual temperature increase by 1.4–1.8 °C for the years 2021–2050, as compared with the years 1971–2000. For this reason, we chose the extreme scenario of climate change A1F1, derived from IPCC (IPCC 2007). The decrease of recharge in the Figuig aquifer region predicted by this model is 38%.

In semi-arid and arid regions, the future climate change projections by different models show an increase in temperature and a decrease in precipitation, therefore a decrease in the recharge of aquifer. To remediate this situation, MAR was proposed in two areas: (1) a small area of 1 km² in Jbel El Haïmeur; (2) a larger area of 32 km² in Wadi El Kheneg. The hydrologic conditions of these two places are

favorable, with practically no sedimentary supply owing to the solid nature of carbonate rocks (big lateral extent), and the construction of a dam in Wadi El Kheneg could also limit the floods in the Oasis of Figuig. The highly fractured limestone (karst) and dolostone sedimentary sequences are, therefore, very suitable for MAR, as the recharge of the aquifer can be facilitated by the numerous fractures. The average hydraulic conductivity derived from pumping tests ranges between 1.1×10^{-4} and 2.15×10^{-4} m/s and constitutes an adequate permeability for MAR (Jilali 2014a; Jilali and Zarhloule 2015). A recharge of 40 mm/year was chosen for the two areas, starting in 2014.

The results of the simulation show an increase in piezometric levels for all of the boreholes. This increase will start in 2034 for boreholes ACAF, 442/50, 441/50, 179/50, and 188/50, and will consist of 1.0, 1.7, 0.8, 1.0, and 1.0 m, respectively (Fig. 4.3). For the remaining boreholes, the increase in piezometric levels will begin in 2056, and will not exceed a maximum of 0.4 m (189/50). The limited improvement for the latter boreholes is due to the effect of pumping wells. The evolution of the flow budget is shown in Fig. 4.4, and the effect of climate change will stop in 2034 with the improvement of water resources due to the MAR. The MAR project is also able to provide the desired additional water supply being sought. This way, the excess water stored in the two areas can be used for irrigation, as in the south the water salinity is high (Jilali 2014a; Jilali et al. 2015a). Clearly, the impact of MAR on groundwater quality will have beneficial effects, nevertheless hydrogeochemical analyses will be required before and after the MAR to ensure a safe water quality. At the present moment, several analyses made in the

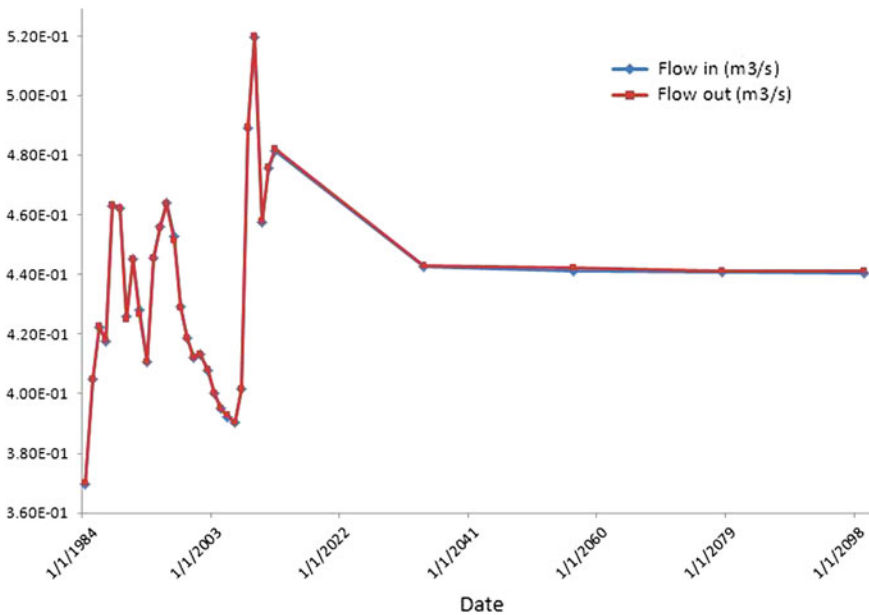


Fig. 4.4 Evolution of flow budget

study area show quite variable results of water quality (Jilali et al. 2015a, b). In light of the foregoing, the region of Figuig has the chance to become an excellent touristic and ecologic region of Morocco, enhanced by the presence of two dams (MAR areas).

Conclusions

In the arid region of Figuig, groundwaters play a key role for the supply of water to the population and the irrigation of palm groves. We are currently observing a huge deterioration of both the quantity and quality of these groundwaters, caused by climate change and the increasing demand for water. In order to alleviate these issues, we propose MAR (Managed Aquifer Recharge) as a suitable solution to these grave issues.

A numerical model was used to evaluate the applicability and the effect of climate change and MAR in the Figuig aquifer. The extreme A1B1 scenario of climate change was selected and it clearly shows that two areas (basins) are very suitable for MAR, based on favorable hydrological and hydrogeological conditions. Nine boreholes should be designed to monitor the piezometric levels in the study area.

The simulation results show that, if MAR is applied, the groundwater levels will rise after 2034 to achieve a maximum of 1.7 m in 2099. The same observation is made with regard to the improvement of the flow budget. In other words, groundwater resources can increase as result of MAR even assuming an extreme scenario of climate change. This MAR simulation is the first in the region, and it can be extended to further regions upstream of the Figuig basin.

References

- Allow K (2012) The use of injection wells and a subsurface barrier in the prevention of seawater intrusion: a modelling approach. *A J Geosci* 5(5):1151–1161
- Amar M, Manar A, Boualoul M (2012) Apport de la cartographie aéromagnétique à l'identification structurale du système aquifère des sources de l'oasis de Figuig (Maroc). *Bull Instit Sci, Rabat, section Sciences de la Terre* 34:29–40
- Ayuso-Gabella N, Page D, Masciopinto C, Aharoni A, Salgot M, Wintgens T (2011) Quantifying the effect of managed aquifer recharge on the microbiological human health risks of irrigating crops with recycled water. *Agric Water Manage* 99(1):93–102
- Bekele E, Toze S, Patterson B, Higginson S (2011) Managed aquifer recharge of treated wastewater: water quality changes resulting from infiltration through the vadose zone. *Water Res* 45(17):5764–5772
- Boisson A, Baisset M, Alazard M, Perrin J, Villesseche D, Dewandel B, Kloppmann W, Chandra S, Picot-Colbeaux G, Sarah S, Ahmed S, Maréchal JC (2014) Comparison of surface and groundwater balance approaches in the evaluation of managed aquifer recharge structures: case of a percolation tank in a crystalline aquifer in India. *J Hydrol* 519, Part B: 1620–1633

- Dresnay RD (1963) Carte géologique du Haut Atlas oriental au 1/200 000, feuille de Bouarfa, Ich, Talzaza et Figuig, Notes et Mémoires du Service Géologique du Maroc, Rabat
- Hao Q, Shao J, Cui Y, Xie Z (2014) Applicability of artificial recharge of groundwater in the Yongding River alluvial fan in Beijing through numerical simulation. *J Earth Sci* 25(3):575–586
- IPCC (2007) *Climate change 2007: impacts, adaptation and vulnerability*. Contribution of working group II to the fourth assessment report of the intergovernmental panel on climate change. Cambridge University Press, Cambridge, UK, p 976
- Janardhana Raju N, Reddy TVK, Muniratnam P, Gossel W, Wycisk P (2013) Managed aquifer recharge (MAR) by the construction of subsurface dams in the semi-arid regions: a case study of the Kalangi river basin, Andhra Pradesh. *J Geol Soc India* 82(6):657–665
- Jilali A (2014a) Contribution à la compréhension du fonctionnement hydrodynamique de la nappe souterraine de l'oasis de Figuig (Haut Atlas Oriental). Université Mohammed Premier, Oujda, p 161
- Jilali A (2014b) Impact of climate change on the Figuig aquifer using a numerical model: Oasis of Eastern Morocco. *J Biol Earth Sci* 4(1):E16–E24
- Jilali A, Zarhloule Y (2015) Structural control of the hydrogeology in Figuig Oasis in the eastern High Atlas of Morocco. *P Geologist Assoc* 126(2):232–243
- Jilali A, Abbas M, Amar M, Zarhloule Y (2015a) Groundwater contamination by wastewater in Figuig Oasis (eastern High Atlas, Morocco). *Nat Environ Pollut Technol* 14(2):275–282
- Jilali A, Amar M, Zarhloule Y, Amar N, Kerchaoui S, Baba E (2015b) Apport de la géophysique à la compréhension des structures géologiques de l'oasis de Figuig (Haut Atlas Oriental, Maroc). *J Mater Environ Sci* 6(1):236–245
- Maliva R, Herrmann R, Coulibaly K, Guo W (2015) Advanced aquifer characterization for optimization of managed aquifer recharge. *Environ Earth Sci* 73(12):7759–7767
- Marie P, Géraldine P-C, Dominique T, Alexandre B, Marina A, Jérôme P, Benoît D, Jean-Christophe M, Shakeel A, Wolfram K (2014) Water quality evolution during managed aquifer recharge (MAR) in Indian crystalline basement aquifers: reactive transport modeling in the critical zone. *Pr Earth Planet Sci* 10:82–87
- Masciopinto C (2006) Simulation of coastal groundwater remediation: the case of Nardò fractured aquifer in Southern Italy. *Environ Model Softw* 21(1):85–97
- MEMEE (2011) Adaptation au changement climatique pour des oasis résilientes “Evaluation du changement climatique futur au niveau des zones oasiennes marocaines”, Maroc, pp 57
- Ouelhazi H, Lachaal F, Charef A, Challouf B, Chaieb H, Horriche F (2014) Hydrogeological investigation of groundwater artificial recharge by treated wastewater in semi-arid regions: Korba aquifer (Cap-Bon Tunisia). *A J Geosci* 7(10):4407–4421
- Ouzzaouit LA, Bakraoui A, Benalioulhaj N, Carneiro J, Correia A, Jilali A, Rimmi A, Zarhloule Y (2014) Recent warming trends inferred from borehole temperature data in Figuig area (Eastern Morocco). *J Afr Earth Sci* 96:1–7
- Parimalarenganayaki S, Elango L (2015) Assessment of effect of recharge from a check dam as a method of Managed Aquifer Recharge by hydrogeological investigations. *Environ Earth Sci* 73(9):5349–5361
- Younes H (2010) Le Lias- Aalénien inférieur de Jbel Maiz (Haut Atlas Oriental): Stratigraphie, évolution paléogéographique et synthèse bibliographique sur les minéralisations associées. Mémoire Thesis, Université Mohammed Premier, Oujda, pp 159
- Ziani N (2010) Le Lias-Aalénien inférieur du Jbel El Haïmeur (Haut Atlas Oriental): stratigraphie, évolution sédimentaire et minéralisations associées. Université Mohammed Premier, Oujda, p 160

Chapter 5

Calibration of AquaCrop Salinity Stress Parameters for Barley Under Different Irrigation Regimes in a Dry Environment

F. El Mokh, Vila-Garcia, K. Nagaz, Mohamed Moncef Masmoudi, N. Ben Mechlia and E. Fereres

Abstract In the arid environment of southern Tunisia, FAO's AquaCrop model version 4.0 has been calibrated to evaluate the effect of irrigation strategies with saline water on barley yield. Data sets during barley cropping seasons 2012 and 2013 in Médenine, southern Tunisia, were used to calibrate and evaluate this model. Barley canopy cover, grain yield, biomass production, and soil salinity and water content were simulated under three irrigation regimes. The RMSE, Willmott index of agreement (d), and r^2 analysis showed good agreement between the simulated and observed data, especially for the biomass production and grain yield. The difference between observed and simulated grain yield under full irrigation was only 1% for the first and second seasons. The difference for biomass was around 2%. The trend of canopy cover was well simulated with slight over estimation in the beginning of the season for both seasons. Salinity stress parameters were adjusted to simulate the combined effect of drought and salinity stress where the electrical conductivity of water (EC_w) was used as the indicator threshold of salinity instead of the saturated soil-paste extract (EC_e) in this case. The model tended to overes-

F. El Mokh (✉) · K. Nagaz
Institut des Régions Arides, 4119 Médenine, Tunisia
e-mail: elmokh.fa@gmail.com

K. Nagaz
e-mail: Nagaz.Kameleddines@ira.rmr.tn

Vila-Garcia · E. Fereres
University of Cordoba and Institute for Sustainable Agriculture (IAS-CSIC),
Cordoba, Spain
e-mail: g82gavim@uco.es

E. Fereres
e-mail: ag1fecae@uco.es

M.M. Masmoudi · N. Ben Mechlia
INAT, 43 avenue Charles Nicolle, 2083 Tunis, Tunisia

estimate the soil water content and the E_c but with reasonable statistical indices for total root zone soil water content (RMSE: 8.6–11 mm, d: 0.78–0.98) and for E_c (RMSE: 1.35–0.94 dS/m, d: 0.63–0.88).

Keywords Salinity · Deficit irrigation · Barley · AquaCrop · Calibration · Testing · Arid environment

Introduction

In many water-scarce countries, irrigation is the dominant user of water. Tunisia is one of these countries where irrigation uses 83% of the total water potential of the country. The situation becomes more severe especially in the arid part of the country as the result of successive years of drought. In this region, the most available water resources have low quality. Thus, there is increasing pressure to use saline waters to intensify agriculture in private farms situated around shallow wells having salinity more than 5 dS/m. Barley (*Hordeum vulgare*) is one of the cereal crops most grown by farmers in the region due to its importance for human consumption and for animal feed. Moreover, barley is considered tolerant to water and salt stress (Maas and Hoffman 1977). Despite its importance, the productivity remains poor with a national average yield of 1.21 t/ha (World Bank 2014). Previous experiments conducted on barley in southern Tunisia by Nagaz et al. (2003) and El Mokh et al. (2014) demonstrated the potential of irrigation management practices in reducing the effect of salinity on both yield and soil salinization.

Given this situation, management strategies that may help to save water and increase water use efficiency need to be applied in agriculture to ensure sustainable and efficient use of low-quality water. Simulation models able to quantify the effects of water on yield can be a helpful tool for evaluating different irrigation management options and therefore developing the agricultural sector. Many crop simulation models are currently available and can be used for estimating crop productivity under deficit irrigation and at farm level to improve the efficiency of water use in agriculture. Examples of tested models for simulating crop growth under water-limited conditions include DSSAT and CropWat, but neither model considers salinity. A model that does consider salinity is version 4.0 of the AquaCrop model that has been developed by FAO (Steduto et al. 2009; Raes et al. 2009). It is simple to manipulate and is relatively accurate, robust and requires relatively limited data inputs. Several studies have been conducted in arid environments using the AquaCrop model to optimize yield and biomass either through deficit or optimal irrigation, e.g., Farahani et al. (2009) and Garcia-Vila et al. (2009) for cotton under full and deficit irrigation regimes in Syria and Spain, Salemi et al. (2011) for winter wheat under deficit irrigation in the arid regions of Iran, and Araya et al. (2010) for barley in the semi-arid regions of Ethiopia. However, the revised version (4.0) of AquaCrop that includes salinity component has not been

tested for barley under an arid environment. Thus, the objective of this study was to calibrate and test the AquaCrop (4.0) model for barley irrigated with saline water and under different irrigation regimes to estimate barley yield.

Materials and Methods

Experimental Conditions and Treatments

Barley crop (cv. Ardhaoui) was sowed in row spaced 0.5 m with a plant density about 70 kg/ha during two contrasting seasons (2011–2012 and 2012–2013) at the Arid Regions Institute of Medenine, Tunisia. The soil was sandy having a field capacity and permanent wilting point of 0.198 and 0.098 m³ m⁻³, respectively, for 0.8 m barley rooting depth.

The crop was planted in 27 and 29 November, respectively, for the first and the second seasons in a randomized complete block pattern. Plants were drip irrigated using saline water having an EC_w about 7.6 dS/m. Drip lines were placed along each row with 4 l/h emitters placed 0.4 m. Irrigation was scheduled to replenish the water depleted in the root zone through the ET to field capacity (FI) and the crop ET was estimated based on water balance method developed on Excel. Details of the estimation of ET_c were given by El Mokh et al. (2014). A deficit irrigation of 50% of full irrigation was applied during the barley growing period (DI-50) and during less sensitive periods of crop growth such as elongation-tillering and maturity stages (DI-Dev + Mat) and at the same time as FI.

Before planting, soil applications were 8.3 t.ha⁻¹ of organic manure, 300 kg.ha⁻¹ of P using diammonium phosphate, and 200 kg.ha⁻¹ of K using potassium sulfate. The nitrogen fertilizer was applied as fertigation during vegetative growth stages with a total rate of 300 kg.ha⁻¹ using ammonium nitrate.

The canopy cover (CC), soil water content, and salinity were measured periodically during both growing season in triply replicated plots for each irrigation strategy. Final biomass and grain yield were measured at harvest.

AquaCrop Model Description

The complete theoretical background and concept of AquaCrop is explained in Raes et al. (2009). The latest version of the AquaCrop model (version 4.0, June 2012) used in this study integrates the salt balance component, which uses the calculation procedure presented in BUDGET (Raes et al. 2001, 2006; Raes 2002; De Nys et al. 2005) to simulate salt movement and retention in the soil profile.

As indicated in the FAO Irrigation and Drainage Paper 29, the average seasonal ECe in the root zone determines the reduction in crop yield and relative biomass reduction, which is determined in AquaCrop model by Eq. (5.1):

$$B_{rel} = 100(1 - K_{s_{salt}}), \quad (5.1)$$

where B_{rel} represents the relative biomass that can be produced with the salinity stress and $K_{s_{salt}}$ is the salinity stress coefficient determined by the average electrical conductivity of the saturated soil-paste extract (ECe).

The salinity stress effects on canopy cover development and plant transpiration are included in the model through four parameters: (i) $K_{s_{sto, salt}}$ that represents the induced stomatal closure, which affects crop transpiration, Tr ; (ii) $K_{s_{exp, f}}$ that represents the effect on canopy development; (iii) $K_{s_{CCx}}$ that represents the reduction in maximum canopy cover; and (iv) $f_{CD_{decline}}$ that represents the triggering of canopy decline.

Input Data

Maximum and minimum temperatures were obtained from historical average data (15 years). The average daily long-term value of ETo during barley growing period was used and it is about 530 mm. Rainfall was measured in the field with a rain gauge and the seasonal amounts of rainfall were 138 and 0 mm, respectively, for the first and the second seasons. The irrigation amounts supplied were 314, 157, and 273 mm in the first season and 425, 213, and 383 mm in the second season, respectively, for FI, DI-50, and DI-Dev + Mat treatments.

Model Calibration and Testing

Canopy cover (CC) parameters were calibrated using measured data of 2011, whereas the testing was done using the data set measured in 2012. The CC represents one key of AquaCrop performance since it separates the ET into crop transpiration and soil evaporation. Thus, the parameterization focused first on the CC curve. The initial canopy cover (CCo) was estimated from plant density at emergence. The maximum CC observed in no water and salinity stress conditions was taken as CC_x . The canopy expansion and decline rates (CGC and CDC) were determined based on a trial-and-error procedure comparing model output to phenological observations of the 2011 barley crop. During the trial-and-error process, the water stress effects on leaf growth, stomatal conductance, and early senescence were parameterized and only the thresholds of the curve were adjusted. Since the irrigation water was saline, barley was subjected to salinity stress under full irrigation and both salinity and water stress under the DI-50 and DI-Dev + Mat

treatments. The calibration of salinity stress was based on Eq. 5.1 where the ECe thresholds were determined for barley crop as indicated in the FAO Irrigation and Drainage Paper 29. At the lower threshold of soil salinity (ECen), $K_{s_{salt}}$ becomes smaller than 1 and the stress starts to affect biomass production. At the upper threshold for soil salinity (ECex) $K_{s_{salt}}$ becomes zero and the soil salinity stress becomes so severe that biomass production ceases (Raes et al. 2012).

Based on FAO paper 24 the lower and the upper ECe threshold for barley were used (8 and 28 dS/m). While during the calibration process, we have not noted the salinity effects with the changes of irrigation strategies. Therefore, the ECe values represent the effect of salinity under soil water content at saturation and not under the real soil water content. In our conditions, the soil water content was below the field capacity for most of the cases. Thus, the ECe threshold may not be the suitable indicator of salt stress. To reduce the mismatch between simulated and measured values, the water salinity thresholds of barley (Ayers and Westcot 1976) ranging between 5 and 19 dS/m were tested instead of ECe. Therefore, the use of these limited values of ECw resulted in better matching during the calibration process.

During the calibration, it was found that the best fit for the normalized water productivity (WP*) for the data of the 2011 season was 13 g m^{-2} , a value suggested by Araya et al. (2010) and Sghair et al. (2014), even though the recommended values in AquaCrop for C_3 crops such as barley range between 15 and 20 g m^{-2} (Steduto et al. 2009). Table 5.1 gives all the parameter values that were modified here from those recommended by Steduto et al. (2012) as a result of the calibration (Table 5.1).

To evaluate the goodness of fit between observed grain yield (Y), final biomass production (B), CC, soil water content (SWC) and soil salinity and simulated outputs, the root mean squared error (RMSE) as indicated in Eq. (5.2) and the Willmott index of agreement (d) shown in Eq. (5.3) were used to compare simulated and measured values:

$$RMSE = \left[\left(\frac{\sum_{i=1}^n P_i - O_i}{n} \right)^2 \right]^{1/2}, \quad (5.2)$$

where S_i and O_i are the simulated and observed values, respectively, and n is the number of observations. Values of RMSE close to zero indicate the best fit of the model. The statistical index of model performance, Willmott's index d , was calculated based on Eq. (5.3):

$$d = 1 - \frac{\sum_{i=1}^n (P_i - O_i)^2}{\sum_{i=1}^n (|P_i - \bar{O}| + |O_i - \bar{O}|)^2}, \quad (5.3)$$

where d describes the covariability of P_i and O_i about the mean of O , and d values closer to 1 indicate more complete agreement.

Table 5.1 Parameter values modified from those recommended by AquaCrop (presented in parenthesis)

	Values	Range (FAO)	Interpretations
Canopy cover per seedling at 90% emergence (CCo)	1.5 cm ²	1.5 cm ²	
Canopy growth coefficient (CGC) (%/day)	7.8	9–12	
Maximum canopy cover (%)	85	50–99	
Canopy decline coefficient (CDC) at senescence (%/day)	5.7	–	
Water productivity (g/m ²)	13	15	(Araya et al. 2010 and Sghair et al. 2014)
Leaf growth threshold p-upper	0.25	0.20	
Leaf growth threshold p-lower	0.65	0.65	
Leaf growth stress coefficient curve shape	3.5	3.0	
Stomatal conductance threshold p-upper	0.65	0.60	
Stomata stress coefficient curve shape	3.0	3.0	
Senescence stress coefficient p-upper	0.75	0.55	
Senescence stress coefficient curve shape	3.5	3.0	
Reference harvest index	38%	30–50%	
Coefficient inhibition of leaf growth on HI	4.0	4.0	Positive impact on HI by inhibition of leaf growth at anthesis
Coefficient, inhibition of stomata on HI	5.0	5.0	Negative impact on HI by inhibition of stomata at anthesis
E _{Ce} threshold p-lower (dS/m)	5*	8	The lower limit of water salinity for barley (Ayers and Westcot 1976)
E _{Ce} threshold p-lower (dS/m)	19*	28	The upper limit of water salinity for barley (Ayers and Westcot 1976)
Soil salinity stress effects			The calibrated relationship between relative biomass and salinity stress
K _{SCCx}	13%		Stress reducing the maximum canopy cover
K _{Sexp,f}	9%		Stress slowing down canopy development
F _{CD} Decline	0.33		Triggering canopy decline
K _{Ssto,salt}	23%		Resulting in stomatal closure

The coefficient of determination r^2 is defined as the squared ratio between covariance and the multiplied standard deviations of observed and predicted values. It ranges from 0 to 1, with values close to 1 indicating good correlation.

Results and Discussion

Soil Water Content

Trends in soil water content in the three treatments and two years of study are simulated in Fig. 5.1. The soil water at full irrigation fluctuated in the wet range or increased with time in the second year while in the other two deficit irrigation it tended to decline with time. The observed values are also indicated in Fig. 5.1 showing good agreement with the simulated values. The relatively large values of d (0.98 and 0.97) obtained in the calibration and testing seasons, respectively, and the relatively small values of RMSE (11.1 and 8.6 mm in the two season, respectively) compared to those obtained (24.5–37 mm) by Iqbal et al. (2014) underscore the good matches between simulated and measured soil water content (Table 5.2).

Soil Salinity

During the model calibration, the initial EC_e and EC_w values were used based on field measurements. In addition, the upper and lower EC_e thresholds for barley

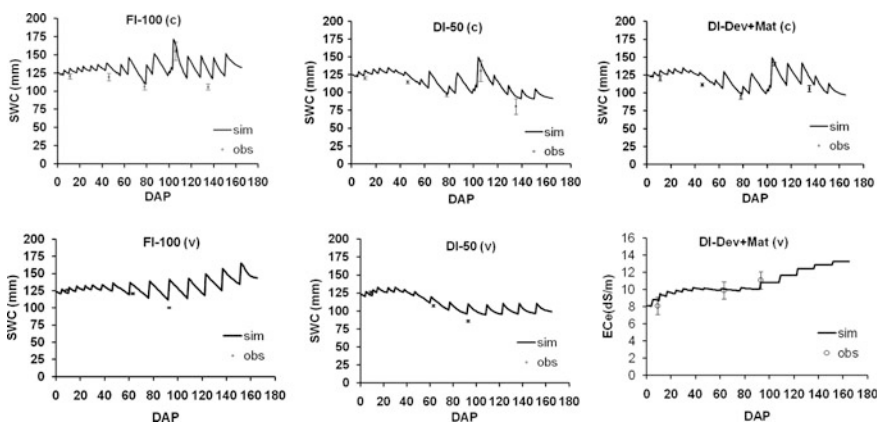


Fig. 5.1 Simulated soil water content (mm) under different irrigation regimes compared with measured values for calibration (c) and testing (v)

Table 5.2 Statistical indicators for model performance for both seasons

Variable	n	RMSE	d	r ²
<i>Calibration</i>				
Yield (kg/ha)	3	0.32	0.78	0.88
Biomass (kg/ha)	3	0.28	0.96	0.96
CC(%)	9	8.09	0.37	0.52
SWC (%)	18	11.1	0.98	0.91
EC (dS/m)	18	1.5	0.58	0.57
<i>Testing</i>				
Yield (kg/ha)	3	0.24	0.93	0.93
Biomass (kg/ha)	3	0.25	0.98	0.97
CC (%)	6	2.7	0.97	0.92
SWC (%)	9	8.6	0.97	0.47
EC (dS/m)	9	0.94	0.88	0.73

were defined based on FAO 29 (Ayers and Westcot 1976). A trial-and-error procedure was used to minimize the mismatch between simulated and measured E_{Ce} values in 2010. Since K_{s,salt} was the main factor that affected the biomass, the threshold was calibrated based on biomass reduction compared to observed values. As mentioned previously, the EC_w was used instead of E_{Ce} as the salinity indicator. In our experiments, the barley crop was subjected to both water and salinity stresses and even for full irrigation the soil water content was generally below field capacity. In this case, the salt concentration in the effective root zone is greater than the E_{Ce}, and is more similar to EC of the soil water content. Therefore, the use of the water EC threshold for barley resulted in acceptable agreement between simulated and measured salt balance in the 0.8 m root zone. Vanuytrecht et al. (2014) highlighted the limitation of using E_{Ce} threshold in water stress condition and suggested the use of EC_w as an indicator of salinity stress in water deficit conditions.

Figure 5.2 shows the evolution of simulated salt accumulation in the root zone compared to measured data sets. The soil salinity was expressed in term of electrical conductivity of a saturated paste extract. The model tended to overestimate the E_{Ce} for all treatments. In fact, the mismatch between estimated and observed E_{Ce} could be explained by leaching due to rains that reduced salt accumulations in the root zone. However, the rain leaching in the model seems to be occurred only after a heavy rain of about 50 mm, whereas, in the real field conditions, even after rainfall events of 20 mm we noted a decrease in the soil salinity and that was reported by El Mokh et al. (2015). Vanuytrecht et al. (2014) mentioned that many efforts were made to improve AquaCrop estimation of soil water balance where more input of soil characteristics will be used to improve the simulation of root deepening and the amount of rain lost by surface runoff. In the second season, and with the absence of rain, results showed good agreement between simulated and measured E_{Ce} for the FI-100 and DI-Dev + Mat treatments, while the model considerably underestimated the E_{Ce} under the DI-50 treatment. The underestimation can be attributed to high

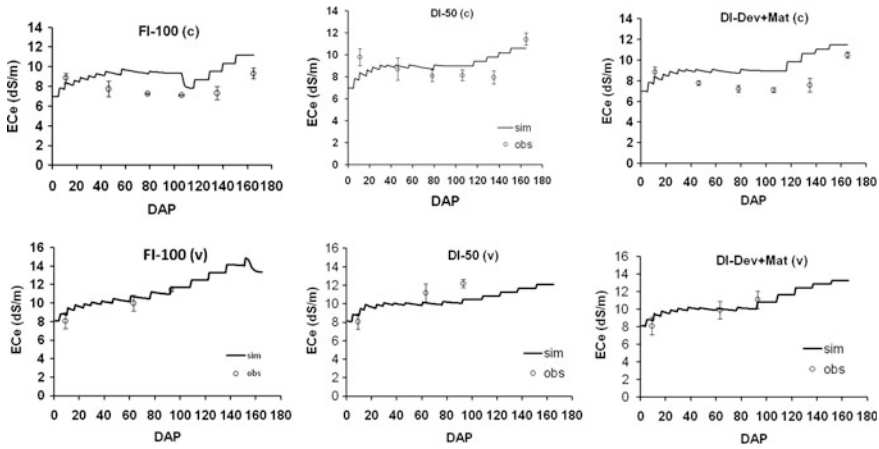


Fig. 5.2 Simulated ECe under different irrigation regimes compared with measured values for calibration (c) and testing (v)

evaporative demand during this period which was not detected by the model since, as mentioned previously, average historical climatic data were used in this study.

The relatively small value of RMSE (1.5 dS/m) and the values of d (0.58) and r^2 (0.57) in the first season indicated what we consider to be reasonable model simulations. In the second season, the ECe values were simulated with a reasonable accuracy as indicated by the RMSE (0.94 dS/m), d (0.88) and r^2 (0.73). Based on these results, the model could be used to simulate salt accumulation in soil, particularly with more improvement of soil components of the model.

Canopy Cover (CC)

During the process of calibration, model parameters were adjusted to minimize the mismatch between simulated and observed CC. For all irrigation regimes, data at three key growth stages were used to perform the calibration: during the development stage, at maximum canopy cover, and during senescence. The model tended to overestimate the CC in the first part of the season at approximately 76 days after planting for the different irrigation treatments (Fig. 5.3). This delay of canopy development in the early season may be due to the winter period affecting canopy expansion in that period (Xiangxiang et al. 2013) in addition of the relatively high salinity about 8 dS/m observed during the initial crop growth that could affect the crop transpiration through the stomatal closure. The simulated CC reached the CC_x for most treatments.

The measured CC declined slightly faster compared to simulated CC especially for the DI-50 treatment over the first season. This early decline can be explained by the starting time of canopy decline that can be considered to be later than the

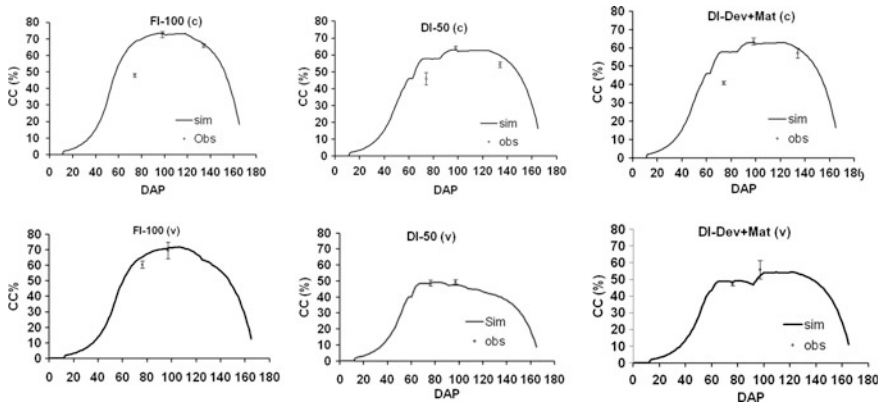


Fig. 5.3 Simulated percent canopy cover (CC) under different irrigation regimes compared with measured values for calibration (c) and testing (v)

starting time of leaf senescence as mentioned by Andarzian et al. (2011); senescence starts generally in the oldest leaf, reducing transpiration and inducing canopy decline.

The relatively small values of d (0.37) and r^2 (0.52) in the calibration season could be due to the mismatch of CC in the first part of the growing period. A reasonable RMSE value (8.09%) was obtained. Nonetheless, good agreement between simulated and measured CC was revealed for the validation season with a relatively large coefficient of determination ($r^2 = 0.92$), d value (0.97) and RMSE (2.7%) (Table 5.2). These statistical parameters confirmed that AquaCrop-simulated CC in a reasonable manner under different irrigation regimes for both seasons.

Final Biomass and Grain Yield

The error percentage of simulated biomass versus measured data was 1.8% in testing seasons. This relatively small value indicated the model performance in simulation of the biomass. The differences between simulated and measured grain yield were relatively high with 8.6%, but remain lower than 10% (Fig. 5.4). In addition, the low RMSE values and the relatively high index of agreement (d) for grain yield (RMSE: 0.24–0.32 t/ha and d : 0.78–0.93) and biomass (RMSE: 0.28–0.25 t/ha and d : 0.96–0.98) (Table 5.2) confirm the performance of the model in simulating biomass and grain yield.

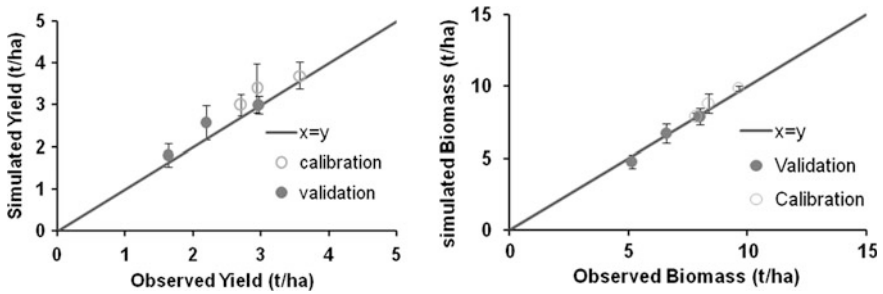


Fig. 5.4 Comparison of simulated and measured biomass production and grain yield for calibration and testing seasons

Conclusion

The scarcity of water resources is already impeding agriculture production and food security. In this situation, the adoption of irrigation management strategies to use poorer quality waters and increase water use efficiency is becoming a necessity. Computer models that simulate crop yield under such condition could be important tools in planning irrigation management. To this end, the parameterization of the AquaCrop model to estimate the effect of water and salinity stresses on barley yield under different irrigation regimes was studied.

Results showed what we consider to be good agreement between observed and simulated data particularly for final biomass and grain yield with RMSE ranging from 0.32 to 0.24 t/ha, Willmott's d values ranging from 0.78 to 0.98, and r^2 values ranging from 0.88 to 0.97. The evolution of canopy cover was well simulated especially for the second season (RMSE: 2.7%, d : 0.97 and r^2 : 0.92), while a slight overestimation of canopy cover in the early season was observed for the calibration season, resulting in moderately poorer values of statistical indices (RMSE: 11.15%, d : 0.37 and r^2 : 0.52). The model tended to overestimate soil water content and ECe, but with reasonable statistical indices for SWC (RMSE: 8.6–11 mm compared to the 50 mm of total available water in the 0.8-m profile, d : 0.78–0.98), and for ECe (RMSE: 1.35–0.94 dS/m, d : 0.58–0.88). These results confirm that AquaCrop was able to simulate with acceptable accuracy barley yield under conditions of saline and limited irrigation water. This study provides first estimate values needed to simulate barley production under these conditions. The calibrated parameters should be tested under different climates, soils, cultivars, irrigations, and field management.

Further investigations should focus on the study of crop production under salt and water deficit conditions to improve models simulation since many countries are facing the problem of soil salinization and water scarcity.

References

- Andarzian B, Bannayanb M, Steduto P, Mazraeha H, Barati ME, Barati MA, Rahnamaa A (2011) Validation and testing of the AquaCrop model under full and deficit irrigated wheat production in Iran. *Agric Water Manag* 100(1):1–8
- Araya A, Solomon H, Kiros MH, Afewerk K, Taddese D (2010) Test of AquaCrop model in simulating biomass and yield of water deficient and irrigated barley (*Hordeumvulgare*). *Agric Water Manag* 97:1838–1846
- Ayers RS, Westcot DW (1976) Water quality for agriculture. Irrigation and Drainage Paper No 29 FAO Rome Italy
- De Nys E, Raes D, Le Gal P, Cordeiro G, Speelman S, Vandersypen K (2005) Predicting soil salinity under various strategies in irrigation systems. *J Irrig Drain Eng* 131(4):351–357
- El Mokh F, Nagaz K (2014) Impact of irrigation with saline water on yield, soil salinization and water productivity of barley in arid regions of Tunisia. *Revue des Regions Arides* 35(3):1217–1225
- El Mokh F, Nagaz K, Masmoudi M, Ben Mechlia N (2015) Yield and water productivity of drip-irrigated potato under different nitrogen levels and irrigation regime with saline water in arid Tunisia. *Am J Plant Sci* 6:501–510
- Farahani HJ, Izzi G, Oweis TY (2009) Parameterization and evaluation of the AquaCrop model for full and deficit irrigated cotton. *Agron J* 101:469–476
- Garcia-Vila M, Fereres E, Mateos L, Orgaz F, Steduto P (2009) Deficit irrigation optimization of cotton with AquaCrop. *Agron J* 101:477–487
- Iqbal MA, Shen Y, Stricevic R, Pei H, Sun H, Amiri E, Rio S (2014) Evaluation of FAO Aquacrop model for winter wheat on the North China plain under deficit from field experiment to regional yield simulation. *Agric Water Manag* 135:61–72
- Maas EV, Hoffman GJ (1977) Crop salt tolerance-current assessment. *J Irrig. Drain Div ASCE* 103:105–134
- Nagaz K, Ben Mechlia N (2003) Etude de la consommation en eau et de la production de l'orge sous irrigation à l'eau salée. *Revue des Régions Arides* 14(1):17–29
- Raes D (2002) BUDGET, a soil water and salt balance model: reference manual. K U Leuven Belgium 80 pp
- Raes D, Geerts S, Kipkorir E, Wellens J, Sahli A (2006) Simulation of yield decline as a result of water stress with a robust soil water balance model. *Agric Water Manag* 81(3):335–357
- Raes D, Steduto P, Hsiao TC, Fereres E (2012) Calculation procedures. AquaCrop version 4.0. FAO Land and Water Development Division, Rome
- Raes D, Steduto P, Hsiao TC, Fereres E (2009) AquaCrop-The FAO crop model to simulate yield response to water. II. Main algorithms and software description. *Agron J* 101:438–447
- Raes D, Van Goidsenhoven B, Goris K, Samain B, De Pauw E, El Baba M, Tubail K, Ismael J, De Nys E (2001) BUDGET, a management tool for assessing salt accumulation in the root zone under irrigation. In 4th Inter regional conference on environment-water, ICID 27–30 August, Fortaleza, Brazil: 244–252
- Salemi HMA, Lee TS, Mousavi SF, Ganji A, Yusoff MK (2011) Application of AquaCrop model in deficit irrigation management of Winter wheat in arid region. *Afr J Agric Res* 610:2204–2215
- Sghair N, Masmoudi M, Ben Mechlia N (2014) Paramétrage du modèle Aquacrop pour la simulation du blé dur. *Revue des Régions Arides* 35(3):1351–1360
- Steduto P, Hsiao TC, Raes D, Fereres E (2009) AquaCrop-The FAO crop model to simulate yield response to water. I. Concepts. *Agron J* 101:426–437
- Vanuytrecht E, Raes D, Steduto P, Hsiao TC, Fereres E, Heng LK, Vila Garcia M, Moreno (2014) Aquacrop: FAO'S crop water productivity and yield response model. *Environ Model Softw*. 1–10. doi:10.1016/j.envsoft.2014.08.005

Wang Xiangxiang W, Qianju W, Jun F, Qiuping F (2013) Evaluation of the AquaCrop model for simulating the impact of water deficits and different irrigation regimes on the biomass and yield of winter wheat grown on China's Loess Plateau. *Agric Water Manag* 129:95–104

World bank (2014) <http://www.worldbank.org/html/cgiar/25years/mand.html>

Chapter 6

Groundwater Recharge of the Kairouan Plain Aquifer: Evidence of Preferential Flow Paths Through the El Haouareb Limestones?

Amal Sebai, Sylvain Massuel, Jamila Tarhouni and Hamza Jerbi

Abstract Groundwater is a key component for the development of semi-arid areas where surface water resources are scarce. Water managers need knowledge about water reserves to cope with their multiple constraints. In the Merguellil basin (Central Tunisia), the Kairouan plain aquifer supplies water for a rapidly growing irrigated agriculture economy but recharge processes are still poorly known. The present paper investigates groundwater transfers from upstream aquifers to the Kairouan plain through the hydraulic threshold of El Haouareb. A conceptual geological 3D model based on lithology analyses was built. Two steady state groundwater models were run using Feflow code in high and low flow conditions. Results suggest that the limestone aquifer that ensures hydraulic connectivity between the upstream and downstream aquifers behaves like a dual-porosity medium with highly significant preferential groundwater flow paths and cannot be simulated as an equivalent porous media.

Keywords Groundwater modeling · Geological modeling · Tunisia · Semi-arid

A. Sebai (✉) · J. Tarhouni · H. Jerbi
Laboratoire des Sciences Technologiques de l'Eau, INAT, Tunis, Tunisia
e-mail: sebai.amal@yahoo.fr

J. Tarhouni
e-mail: elmaainat@yahoo.fr

H. Jerbi
e-mail: hamza.jerbi@ird.fr

S. Massuel
UMR G-EAU (IRSTEA, CIHEAM-IAMM, CIRAD, ENGREF, IRD, SupAgro),
BP434, 1004 Tunis, Tunisia
e-mail: sylvain.massuel@ird.fr

Introduction

The wadi Merguellil basin in central Tunisia has the typical natural resource management issues faced by many developing countries in semi-arid environments. Rainfall is scarce and erratic and evaporation is high in the Kairouan plain. The economic growth of the region relies entirely on the exploitation of groundwater for both irrigated agriculture and the supply of drinking water, and has already caused a serious drop in the water table (e.g., Leduc et al. 2007). The large Plio-Quaternary alluvial aquifer represents a key resource with the highest potential for further agricultural development of the plain. For more than 40 years, the basin has been shaped by regional planning strategies including the creation of numerous water and soil conservation works, hillslope lakes, and big and small dams. In 1989, the El Haouareb dam (95 hm³) was erected at the outlet of the Merguellil catchment (1,200 km²), just before the entrance to the plain. It cuts off the direct natural recharge from the streambed. However, the reservoir is underlain by fissured Cretaceous limestones where infiltration is favored. The limestones connect the Ain El Beidha upstream aquifer to the Kairouan plain aquifer, thereby forming a regional hydraulic threshold. Many studies have been conducted on the Merguellil basin mainly focused on hydrology and sediment transportation (Bouzaiane and Lafforgue 1986; Ayadi et al. 2010), hydrogeology of certain specific aquifers (Besbes 1967; Hamza 1976; Chaieb 1988; Nazoumou and Besbes 2000; Nazoumou 2002), and the study of the functioning and the management of the El Haouareb dam (Kingumbi 1999). More recently, (Alazard 2013) demonstrated that the hydrodynamics of the limestone aquifer is closely linked to the water level in the reservoir. The groundwater from Ain El Beidha meets the infiltrated water from the dam lake and end up flowing into the alluvial aquifer. This area of the basin is therefore a key component of the recharge of the Kairouan plain aquifer. However, the transfer processes within the hydraulic threshold of El Haouareb limestones are not yet well understood. The objective of this study was to test some simple hypotheses regarding groundwater flows through the hydraulic threshold based on the synthesis of current knowledge using hydrodynamic modeling. After gathering and analyzing the available data, a conceptual groundwater flow model was built and compared with hydrodynamic simulations.

Study Area

The wadi Merguellil is one of the three main intermittent rivers that reach the Kairouan plain (3,000 km², Fig. 6.1). The hydrological basin overlays three major interconnected aquifers: Ain El Beidha, Bou Hafna, and Haffouz. Hamza (1983) differentiated three aquifer layers in the synclinal of Ain El Beidha consisting of Mio-Plio-Quaternary deposits.

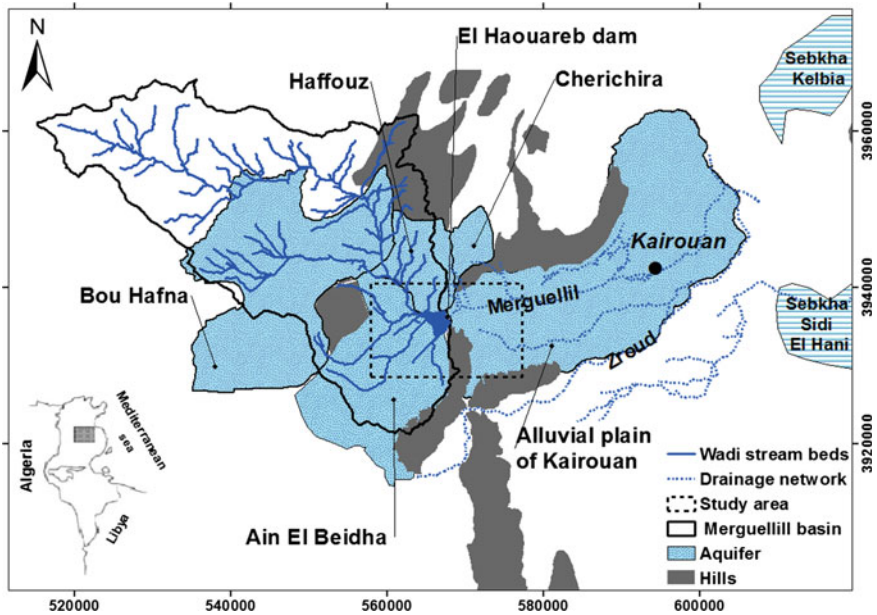


Fig. 6.1 Map of the study area

The hydraulic connection with the Kairouan plain aquifer is ensured through a tectonic pass formed by Cretaceous limestones (Castany 1948). The alluvial Kairouan plain is formed by a collapsed central basin filled by continental deposits of Plio-Quaternary age. Sedimentation is lenticular and formed of alternating layers of coarse sand and marl that are more than 500 m thick (Besbes and de Marsily 1975). The El Haouareb dam has changed the natural recharge processes of the phreatic aquifer of the Kairouan plain. Despite evaporation losses (25% of annual flow), infiltration accounts for the most important term in the water balance of the lake (Kingumbi et al. 2004). It joins the Ain El Beidha groundwater flow and recharges the alluvial aquifer of the Kairouan plain through the hydraulic threshold of El Haouareb. Groundwater coming from Ain El Beidha aquifer now reappears downstream as emergences (Alazard et al. 2011). During long periods of drought when the dam reservoir is empty for months, water is always present in the stilling basin of the dam spillway.

Methodology

A groundwater model was applied to the domain of interest (233 km², Fig. 6.2). To test the hydrodynamic behavior of the limestones, two steady state simulations were performed. The first was inverse modeling of the piezometric levels. The model was

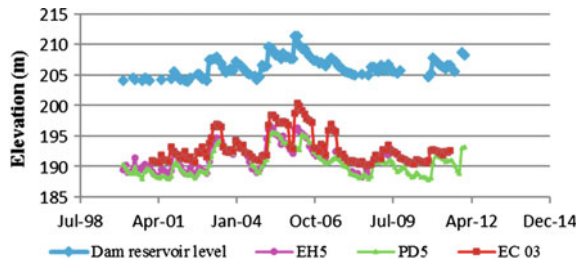


Fig. 6.2 Water levels in the reservoir dam and in three wells in the El Haouareb aquifer: one of spillway piezometers (EC 03), piezometer EH5 and the fifth well located at the foot of the dam (PD5)

then used to calibrate the hydrodynamic parameters of the different geological units based on the adjustment of the water levels in six observation wells. The steady state was fixed at the highest recorded water level of the lake (in 2006) to ensure a maximum impact on the piezometric levels in aquifers. Validation was performed by running the calibrated model to simulate a steady state after the longest drought of the lake (in 2001). The origins of the discrepancies between observed and calculated groundwater levels are discussed.

Data

Numerous data, with variable distribution over time and space, were used for the study. Geological data were collected from logs of deep pumping wells, piezometers, petroleum boreholes, and seismic profiles. Piezometric and water data were provided by the national observation network, the dam monitoring team, and direct field measurements. Geotechnical data from the field report of the construction of the dam were also used.

Geological Pattern

The lithologs were correlated according to the geological maps and to the interpreted seismic profiles. Cross sections were produced to enable the construction of a geological conceptual model. Finally, stratigraphic surfaces were interpolated using kriging for the creation of horizons. The resulting geological model contains five geological units: Mio-Pliocene sands, Oligocene sandstones, Eocene sands, Cretaceous limestones, and Plio-Quaternary clayey sands (Fig. 6.3).

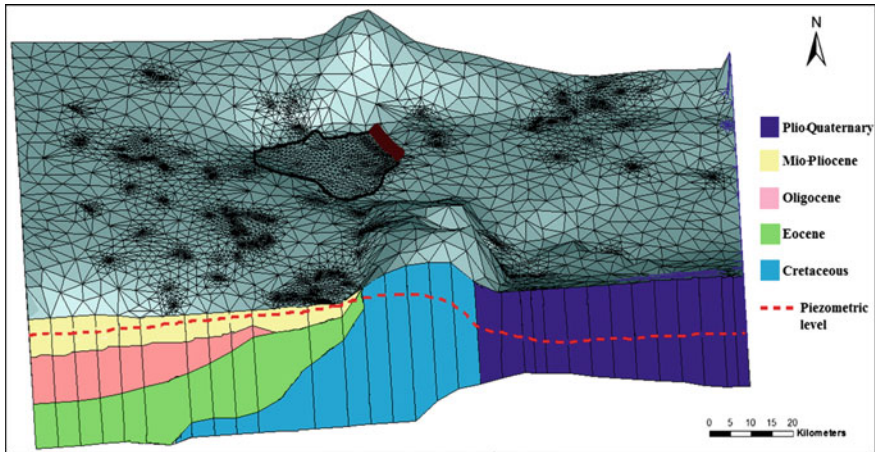


Fig. 6.3 3D conceptual geological model of the study area, 3D geometry of the model domain

Model Setup

Many methods can be used to simulate groundwater flows including the finite difference method, element or integral limits, or the finite element method. In this study, the unconfined groundwater flows were simulated in fully saturated conditions using the FEFLOW code, a three-dimensional finite element numerical model (Fig. 6.3). For numerical purposes, the mesh was refined underneath the lake and around the pumping wells. The final modeling domain comprised 54,505 linear triangular elements and 3,342 nodes.

Fixed hydraulic heads were set on the western and eastern sides of the domain matching the water level contour lines. The water level of the lake was set to the high levels of February 2006 (211,47 m) as a fixed head. The northern and southern boundaries were set as no flow boundaries, following current lines (Fig. 6.4).

Fixed pumping rates were set for public and private wells based on field measurements of mean discharge. The range of hydrodynamic parameters used for calibration was defined from pumping tests and values in the literature (Musy and Soutter 1991). Calibration was performed manually by finely tuning permeability values for matching simulated and observed piezometric levels.

Results and Discussion

The model was able to correctly represent the hydraulic threshold but the best steady state calibration did not satisfactorily fit the six observed groundwater levels (RMSE = 16.5 m) (see Fig. 6.5). Corresponding calibrated permeabilities are listed in Table 6.1.

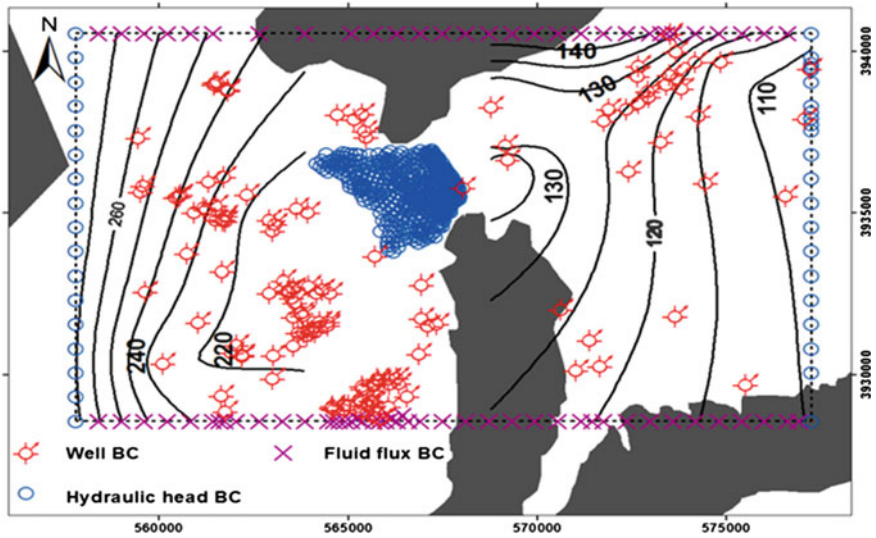


Fig. 6.4 Model features and boundaries, BC: Boundary Condition and the contour lines correspond to the piezometric level in meters

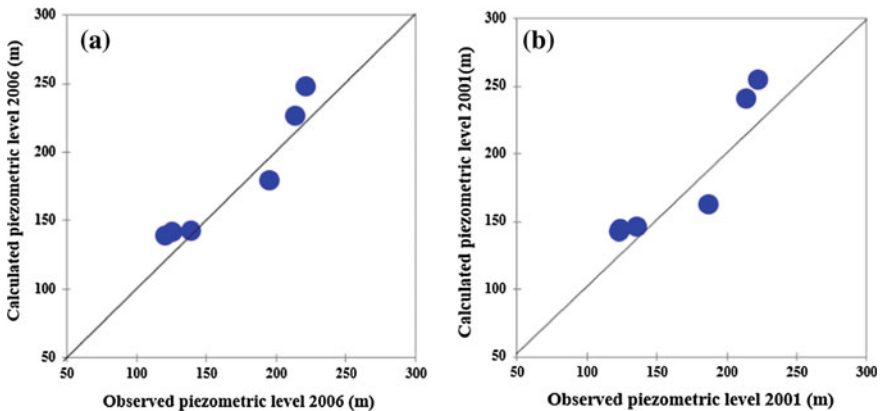


Fig. 6.5 Observed versus calculated piezometric level used, a for calibration (2006), and b for validation (2001)

Analyses of piezometric time series indicated that the influence of the dam could mainly be found in the limestone aquifer. The dynamics of the water levels in this aquifer was strongly correlated with the level of water in the lake. The elevation of the water level in the lake during the high water period (February 2006) was followed by higher groundwater levels in the carbonate aquifer piezometers (spillage piezometers and EH5 piezometer) (see Fig. 6.2).

Table 6.1 Calibrated hydraulic conductivities of geological formations

Aquifers	Lithology	Hydraulic conductivity (m/s) (values from the literature)	Hydraulic conductivity (m/s) (calibrated values)
Mio-Pliocene	Sands, clayey sand	$[1 \times 10^{-5}; 1 \times 10^{-3}]$	0.9×10^{-4}
Oligocene	Sandstone	$[1 \times 10^{-7}; 1 \times 10^{-3}]$	1.0×10^{-3}
Eocene	Marls, nummulite limestone layers	$[1 \times 10^{-8}; 1 \times 10^{-1}]$	7.0×10^{-3}
Cretaceous	Limestone	$[1 \times 10^{-6}; 1 \times 10^{-2}]$	0.1×10^{-4}
Plio-Quaternary	Sand, silt, stiff clays, sandstone	$[1 \times 10^{-5}; 1 \times 10^{-2}]$	1.0×10^{-2}

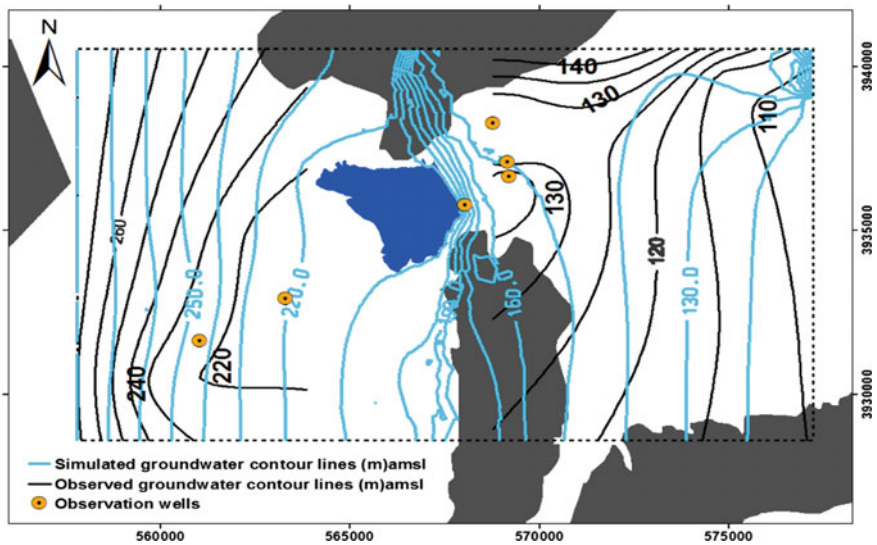


Fig. 6.6 Observed versus simulated groundwater contour lines

Figure 6.6 shows the contour lines of the simulated and observed water levels in the three aquifers. The model was unable to reproduce the piezometric dome (east of the dam) probably due to the absence of preferential flow paths between Ain El Beidha and the Kairouan plain aquifer. This means that the limestone aquifer effectively behaves like a dual-porosity medium with highly significant preferential groundwater flow paths and cannot be simulated as a homogenous porous medium. Evidence of these processes has already been recorded with a significant contrast in groundwater temperature profiles near the dam (Alazard 2013).

Not surprisingly, the steady-state simulation for validation (simulation based on the empty lake in 2001) was unable to reproduce the observed groundwater levels (RMSE = 22.6 m). The calculated hydraulic head was higher than the head observed in 2001 in all piezometers. This was another clue suggesting that the absence of preferential flow paths influences model calibration.

Conclusion

Hydrodynamic model implementation provided interesting results. The hydraulic threshold was correctly reproduced despite the lack of observation points normally required to make a clear and accurate assessment. This proves the correct representation of the stratigraphic layers. However, the best steady-state calibration was unable to correctly reproduce the observed groundwater levels even with an extreme range of permeability values. Moreover, comparison of the contour lines showed that it was impossible to simulate a piezometric dome located near the dam. It is clear that the hydraulic conductivity of the limestone does not explain either the infiltration of water from the dam reservoir or the transfer of Ain El Beidha groundwater through the Cretaceous limestones. The most probable explanation is that the limestone aquifer behaves like a dual-porosity medium with highly significant preferential groundwater flow paths and consequently cannot be simulated as an equivalent porous medium. The next step in our study will be to simulate rapid flows through the Cretaceous limestone aquifer. The continuous approach used in the present study is not feasible, and the El Haouareb zone will be modeled by a network of discrete fractures where each fracture is individualized and assigned a new hydraulic conductivity value.

Acknowledgements The authors would like to thank the Direction Générale des Barrages et des Grands Travaux Hydrauliques for their constant cooperation and the support of the AMETHYST project funded by the French Agence Nationale de la Recherche.

References

- Alazard M (2013) Etude des relations surface—souterrain du système aquifère d'El Haouareb (Tunisie Centrale) sous contraintes climatiques et anthropiques. Thèse de doctorat, Université Montpellier 2
- Alazard M, Leduc C, Virrion R, Guidon S, Ben Salem A, Travi Y (2011) Estimating groundwater fluxes by hydrodynamic and geochemical approaches in a heterogeneous Mediterranean system (central Tunisia). In *Conceptual and modelling studies of integrated groundwater, surface water, and ecological systems*, vol 345. IAHS Publications, Australia, pp 253–258
- Ayadi I, Abida H, Djebbar Y, Raouf Mahjoub M (2010) Sediment yield variability in central Tunisia: a quantitative analysis of its controlling factors. *Hydrol Sci J* 55(3):446–458. doi:[10.1080/02626661003741526](https://doi.org/10.1080/02626661003741526)

- Besbes M (1967) Exploitation du synclinal Oligocène de Bou Hafna-Tunisie. In *Mémoire de l'Ass. Int. Hydrogéologues, Istanbul*, pp 542–544
- Besbes M, de Marsily G (1975) L'analyse d'un grand réservoir aquifère en vue de sa modélisation, 95–107
- Bouzaiane S, Lafforgue A (1986) Monographie hydrologique des oueds Zeroud et Merguellil. DGRE-ORSTOM
- Castany G (1948) Les fosses d'effondrement de Tunisie, Géologie et Hydrologie, Premier fascicule: Plaine de Grombalia et cuvettes de la Tunisie Orientale, vol 3. IMPRIMERIE S.A.P. I., Tunis
- Chaieb H (1988) Contribution à la réactualisation des modèles hydrogéologiques de la plaine de Kairouan. Mémoire de DEA, Université de Tunis, Tunis
- Hamza M (1976) Contribution à l'étude hydrogéologique du synclinal d'Ain Beidha (Tunisie). Thèse de doctorat, Université de Paris VI
- Hamza M (1983) Carte des ressources en eau souterraine de la Tunisie à l'échelle: 1/200.000: Feuille de Kairouan No 11 (trans: BIRH). Ministère de l'Agriculture, Tunis
- Kingumbi A (1999) Bilan et modélisation de la retenue du barrage d'El Haouareb. Mémoire de DEA, ENIT, Tunis
- Kingumbi A, Besbes M, Bourges J, Garetta P (2004) Evaluation des transferts entre barrage et aquifères par la méthode de bilan d'une retenue en zone semi-aride. Cas d'El Haouareb en Tunisie centrale. *Revue des Sciences de l'Eau* 17(2):213–225
- Leduc C, Ben Ammar S, Favreau G, Beji R, Virrion R, Lacombe G, Tarhouni J, Aouadi C, Chelli BZ, Jebnoun N, Oï M, Michelot JL, Zouari K (2007) Impacts of hydrological changes in the Mediterranean zone: environmental modifications and rural development in the Merguellil catchment, central Tunisia. *Hydrol Sci J des Sci Hydrol* 52(6):1162–1178
- Musy A, Soutter M (1991) Physique du sol. Gérer l'environnement, vol 6. Presses polytechniques et universitaires romandes, Lausanne
- Nazoumou Y (2002) Impact des barrages sur la recharge des nappes en zone aride: Etude par modélisation numérique sur le cas de Kairouan (Tunisie centrale). Thèse de doctorat, Université de Tunis El Manar
- Nazoumou Y, Besbes M (2000) Simulation de la recharge artificielle de nappe en oued par un modèle à réservoirs. *Revue des Sci de l'eau* 13(4):379–404

Chapter 7

Evapotranspiration of Wheat in a Hilly Topography: Results from Measurements Using a Set of Eddy Covariance Stations

N. Boudhina, Mohamed Moncef Masmoudi, N. Ben Mechlia,
R. Zitouna, I. Mekki, L. Prévot and F. Jacob

Abstract Several methods allow the determination of evapotranspiration (ET), either by direct measurement or by estimation from weather data. The most used estimation method is the FAO56 (FAO-PM), based on the concept of reference evapotranspiration (ET_o) and crop coefficient (K_c). The eddy covariance technique (EC) developed for measurement of convective fluxes between land surface and the atmosphere is commonly used to estimate ET. However, these methods were established under standard conditions in flat terrain, and their use in hilly areas is questionable. In this work, the variability of ET_o and ET measured by EC and energy balance (EB) in a hilly area of northern Tunisia is studied for different relief configurations. The experiment was conducted using a meteorological (M), and three EC-EB measurement stations in three wheat fields. Two stations were installed on opposite slopes of a ridge with apposing aspects and moderate slopes (A, B), and one station was installed in a flat site (C). Results of monitoring during the mid-season of wheat growth showed similar ET_o levels in all sites for hourly and daily time steps with relative RMSE in the range 0.03–0.08 compared to M. Average ET values in sloping fields (A, B) were, respectively, 15% and 10% lower than in (C). However, hourly values of ET/ET_o obtained from EC measurements were smaller than FAO-K_c, contrarily to those based on the EB method.

N. Boudhina (✉) · M.M. Masmoudi (✉) · N. Ben Mechlia
Institut National Agronomique de Tunisie (INAT), Tunis, Tunisia
e-mail: nissafboudhina@gmail.com

M.M. Masmoudi
e-mail: masmoudi.med@inat.agrinet.tn

R. Zitouna · I. Mekki
Institut National de Recherche en Génie Rural Eaux et Forêts (INRGREF),
Tunis, Tunisia

L. Prévot
Institut National de Recherche Agronomique (INRA), Montpellier, France

F. Jacob
Institut de Recherche pour le Développement (IRD), Montpellier, France

Keywords Evapotranspiration · Wheat · Eddy covariance · Energy balance · Hilly · Slope

List of Acronyms and Abbreviations

EB	Energy Balance
EC	Eddy covariance
ET	Evapotranspiration
ET_EC	Evapotranspiration estimated by Eddy covariance technique
ET_EB	Evapotranspiration estimated by Energy Balance equation
ET _o	Reference evapotranspiration
FAO-56	Food and Agriculture organization, paper 56
FAO-Kc	Kc recommended by FAO-56 bulletin, Table 12
FAO-PM	FAO Penman–Monteith equation
G	Soil heat flux
H	Sensible heat flux
ITC	The integral turbulence characteristics test
Kc	Crop coefficient
LAI	Leaf Area Index
LE	Latent heat flux
Min	Minute
R _n	Net radiation
ST	The steady-state test

Introduction

Methods used for determination of ET are based on weather and crop observations or simulation models. Among these methods there is: (i) the FAO-56 formulation (Allen et al. 1998) which uses the concept of reference evapotranspiration multiplied by a crop coefficient (K_c), (ii) the methods based on the soil water balance and, (iii) the methods based on combinations of the energy balance (EB) and sensible and latent heat flux measurements, such as the eddy covariance technique (EC). In the EC method, vertical wind speed and air temperature/humidity are measured with high frequency and used directly to estimate the convective fluxes of latent (LE) and sensible (H) heat between land surfaces and the atmosphere (Van Dijk et al. 2004). EC systems are often used for testing and calibrating remote sensing-based energy balance models, although several authors reported their systematic underestimation of ET and energy closure problem (Twine et al. 2000; Evett et al. 2012a, b).

Nevertheless, in spite of experimental and instrumental progresses, datasets of EC measurements often experience large portions of missing data. The average data loss in EC systems attributed to maintenance operations, sensitivity of the sensors to

rainfall, and to the method itself which requires spatial and temporal stability of flows, is typically over 35% during a year (Falge et al. 2001). Quality assessment criteria were developed in order to reject inconsistent measurements. The stationarity over 30-min time interval and the spatial homogeneity of turbulence tests are usually applied and result in smaller datasets (Foken and Wishura 1996; Hammerle et al. 2007; Rebmann et al. 2005).

Moreover, most methods for ET estimation are developed and validated in standard conditions and typically for flat areas. Little attention has been given for the hilly catchments, despite the fact that hilly topography is prevailing in large agricultural areas (Hammerle et al. 2007; Feigenwinter et al. 2008; Rana et al. 2007). Hilly topography has an effect on water and energy fluxes in terms of: (i) net and global radiations which are more important on slopes facing south (Raupach and Finnigen 1997; Holst et al. 2005), (ii) soil moisture, which is dependent on the slope, vegetation and the distance from the valley (Tromp van Meerveld and McDonnell 2006; Hugo et al. 2013), (iii) wind, which has a speed and vertical profile dependant on the slope and aspect (Raupach and Finnigen 1997). The representativeness of weather or flux data used for ETo and ET estimation is therefore highly dependent on the location of the measurement station. The aim of this work is to assess ET variability in a hilly area of the south Mediterranean and the sensitivity of ETo and ET of a wheat crop to slope.

Materials and Methods

Experimental Site

The experiment was carried out in a small rain-fed agricultural catchment in the Cap Bon region, northeast Tunisia (Fig. 7.1). Simultaneous measurements of energy

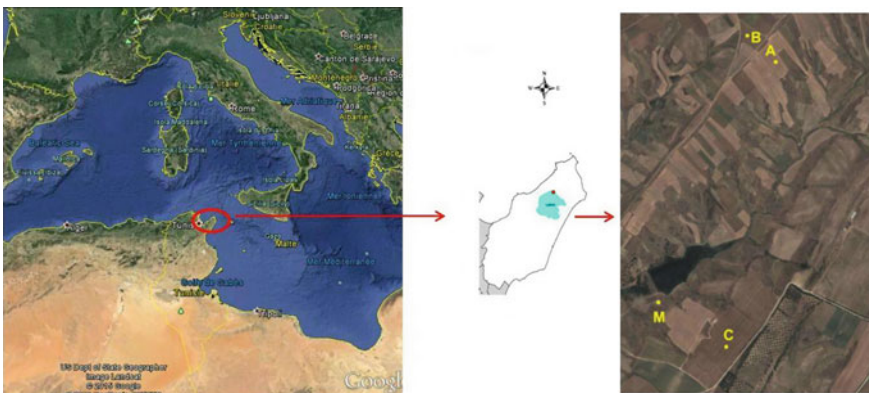


Fig. 7.1 Location of the experimental site and position of the flux (A, B, C) and standard weather (M) stations, Cap Bon, Tunisia

Table 7.1 Location of experimental fields and measurement stations

Field label	Coordinates	Crop	Slope (°)	Aspect (°)	Altitude (m)
A	N36°52'50.2" E10°52'33.1"	Wheat	5.3	152	153
B	N36°52'54.8" E10°52'27.8"	Wheat	6.0	300	155
C	N36°52'12.6" E10°52'40.5"	Wheat	Flat field	–	130
M	N36°52'13.0" E10°52'09.0"	Standard meteorological station			108

fluxes and climatic factors required by the FAO-PM equation were performed in three cereal fields: two stations (A, B) were installed on opposite sides of a ridge on slopes of 5 and 6° respectively, and a station was installed in a flat area (C).

Data from a meteorological station (M), located approximately 100 m southwest of a reservoir at the outlet of the catchment was used for determining ETo (Table 7.1).

The climate in the area is a sub-humid Mediterranean with annual rainfall (P) and reference evapotranspiration (ETo) of 600 mm and 1300 mm, respectively. Traditional and semi-intensive rain-fed agriculture based on cereals (durum wheat, bread wheat, barley, oat, triticale), and legumes (chickpeas, fava beans) are prevailing in the region with landscape organization and land use determined by relief and soil fertility.

Measurements of energy flux terms, and climatic factors were performed in the three fields (A, B, C) and in the weather station (M) from December 2012 to June 2013. However, only the period Mars 7–31, corresponding to simultaneous data availability in all stations and to mid-season stage of wheat growth is considered in this work.

Fields were sown during the same period (December 1, A&B and December 10 for C) and commonly used fertilization and weed control practices were applied in order to have similar growth.

Data Acquisition

Each flux measurement station was equipped with a CR3000 datalogger (Campbell Scientific, USA) and measurement sensors allowing determination of the energy balance (EB) terms. Sensible (H) and latent (LE) heat fluxes, were determined by ECPACK software (Van Dijk et al. 2004) using 20 Hz data of wind vertical velocity, temperature, and air humidity generated by sonic anemometers (CSAT3, Campbell Scientific, USA) and Krypton hygrometers (KH20, Campbell Scientific, USA). Net radiation (Rn) and soil heat flux (G) were measured in each site by a differential radiometer (NR01, Hukseflux, NL) and three soil heat flux sensors

(HPF01, Hukesflux, NL). The stations were also equipped with thermo-hygrometer sensors (HMP45C, Vaisala, FL) in order to determine humidity and air temperature useful in calculating ETo.

The meteorological station (M) provided measurements of solar irradiance (SP100 pyranometer Skye, UK); air temperature and humidity (HMP45C probe, Vaisala, FL); wind speed (A100R anemometer, Vector Instruments, UK); and wind direction (W200P wind vane, Vector Instruments, UK). All instruments had been calibrated by the manufacturer and were connected to a CR10X datalogger (Campbell Scientific, USA) which calculates and stores average values over 30-minute time intervals.

Data Processing and Quality Assessment

The entire set of instrumental and double rotation corrections available in the ECPACK library were applied (Van Dijk et al. 2004). Moreover, Rn measurements were corrected for slope effects using the procedure proposed by Holst et al. (2005).

Quality assessment was applied to H and LE values as proposed by Foken and Wichura (1996) and revisited by Rebmann et al. (2005), considering temporal stationarity (ST) and integral turbulence characteristics (ITC) and used to reject low quality data.

The Penman–Monteith equation (Allen et al. 1998) was used to determine hourly and daily ETo using data obtained at the three sites and at the weather station. Eddy covariance ET (ET_EC = LE) and energy balance ET (ET_EB = Rn-G-H) were determined with hourly time steps in the three sites.

Results and Discussion

Experimental Conditions and Quality Assessment

The average wind speed value recorded during the experiment (4.1 m/s) is twice the global average (Allen et al. 1998). The rainfall during the period January–March 2013 (232 mm) was well distributed and above average cumulated ETo resulting in good soil moisture conditions.

ET_EC and ET_EB were calculated at hourly time steps. Quality assessment was used to identify invalid data using ST and ITC criteria. Records corresponding to maintenance and missing data due to rainfall or condensation were also discarded.

The rejected ET_EC data by quality assessment tests during the cropping season represented 23%, 27%, and 16%, respectively, for fields A, B, and C. The percentages do not consider missing data due to power failure, maintenance and KH20 sensor stops during rainfall events. A relatively greater percentage of good quality

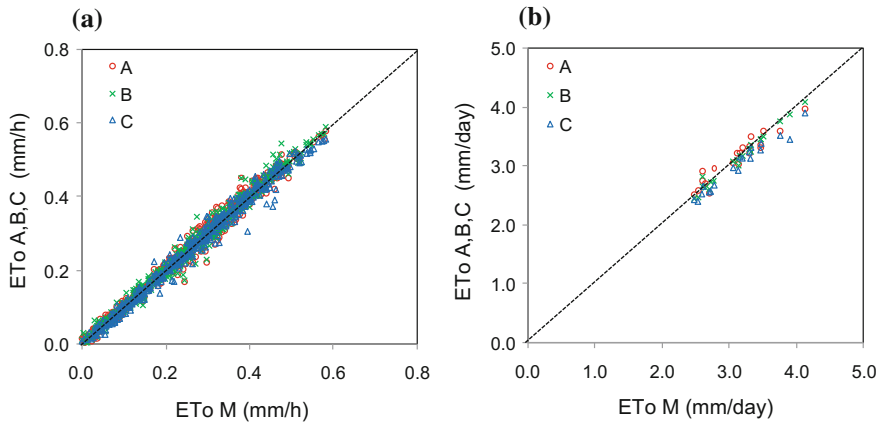


Fig. 7.2 Reference evapotranspiration calculated on hourly **a** and daily **b** time steps using weather data measured in wheat fields A, B, and C as related to ETo derived from standard weather station data M, during the period March 07–31, 2013

data was observed in flat field. Falge et al. (2001) reported an average annual percentage of good quality data of 65%. In contrast, data of sensible heat flux (H) in the three sites had better quality with only 8–9% of the data rejected by quality control tests.

Sensitivity of ETo to Crop Cover and Slope

A comparison between hourly ETo calculated using weather data measured at the meteorological station and in the wheat fields is given in Fig. 7.2. LAI values of 1.4, 2.2, and 1.3 observed, respectively, in sites A, B, and C seem to have relatively small impact on ETo estimations.

Average values of daily ETo calculated from data recorded in M, A, B, and C sites during the period March 07–31 were, respectively, 3.12, 3.08, 3.15, and 2.92 mm/day. High correlation was observed between ETo calculated using meteorological station data and those measured in the wheat fields, with R^2 more than 0.98 for daily and hourly values (Fig. 7.2). The regression lines between ETo of wheat fields (A, B, C) and meteorological station (M) had slopes in the range of 0.98–1.00. Relative root mean square deviations between ETo of site M and those of A, B, C were, respectively, 0.06, 0.07, and 0.06 for daytime hourly data and 0.05, 0.03 and 0.08 for daily data. This suggests that ETo determined using data of a standard weather station, and those measured on cultivated fields with LAI around 2 and with low slopes (5–6°) are comparable.

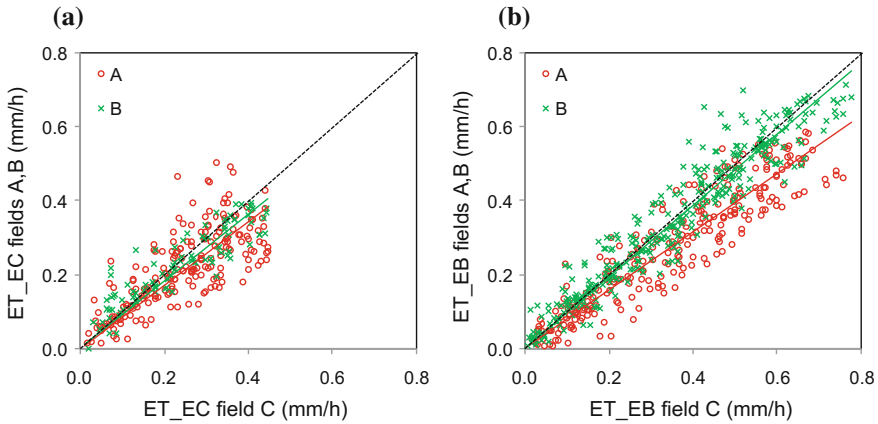


Fig. 7.3 Values of hourly ET observed on sloping fields (*A* and *B*) as function of those observed in flat condition (*C*) during the period March 07–31, 2013, using eddy correlation (a) and energy balance (b) methods

Impact of Slope on ET of Wheat

A comparison of hourly ET values measured by the eddy covariance and energy balance over the mid-season stage (March 07–31) between sloping fields (*A*, *B*) and flat field (*C*) is given in Fig. 7.3. Average value of ET in the flat field during the considered period was 4–22% higher than in the sloping sites. Values obtained with EC method in sloping fields *A* and *B* were, respectively, 15% and 10% lower than in *C*. However, better correlation between flat and sloping fields is observed with EB method.

Coefficients of determination for comparison of ET values observed at hilly sites (*A* and *B*) with those observed in (*C*) were, respectively, 0.89 and 0.93 for EB method, whereas for EC they were 0.54 and 0.74.

Maximum observed hourly ET during the period March 07–31, corresponding to mid-season stage, was around 0.55 mm/h for EC and 0.79 mm/h for EB.

Hourly and Daily Crop Coefficient of Wheat in Sloping Area

Hourly Values of ET/ET_o Ratio

Hourly ET estimations by EC and EB at the three sites (*A*, *B*, *C*) during mid-season stage are represented in Fig. 7.4 versus ET_o measurements in the respective site. The ratio ET/ET_o, which represents the crop coefficient *K_c* for well watered conditions, is the slope of the linear regression line between ET and ET_o.

The regression line slopes of Fig. 7.4a corresponding to ET determined by eddy covariance were 0.82, 0.86, and 0.96, respectively, for *A*, *B*, and *C* sites, well below

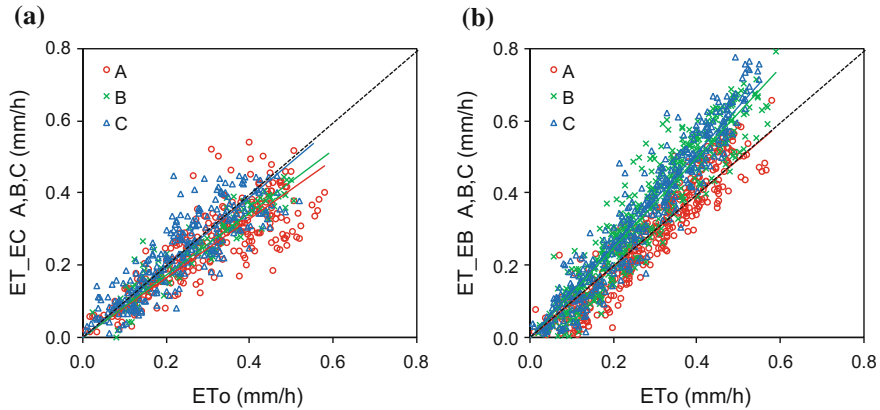


Fig. 7.4 Hourly ET values of wheat estimated by EC (a) and EB (b) methods in sloping (A and B) and flat (C) fields as related to ETo estimations using the FAO-PM equation in the corresponding site, during the mid-season stage of wheat (March 07–31, 2013)

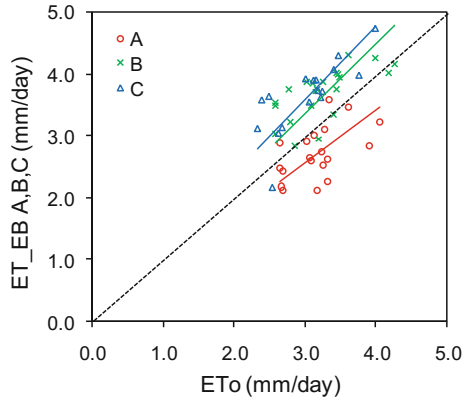
values suggested by FAO (1.15) for mid-season stage. In contrast, ET determined by energy balance is closer to FAO levels with an ET/ETo ratio of 0.98, 1.24, and 1.27, respectively, for A, B, and C sites (Fig. 7.4b). This difference can be explained by a systematic underestimation of ET by the EC method and the closure problem in the surface energy balance, reported in the literature to be in the range of 10–30% (Twine et al. 2000). The relatively smaller crop coefficient in A would be the consequence of less exposure to dominant wind resulting in a lower mean daytime wind speed (4.18 m/s) compared to B (5.09 m/s) and C (4.53 m/s) and less vegetative vigor in term of height (45 cm for A vs. 57 cm for B) and LAI (1.4 for A vs. 2.2 for B).

Daily Values of ET/ETo as Compared to FAO-Kc

Daily ET values could not be determined for EC method because the high proportion of missing and rejected data by quality assessment. However, the lower percentage of rejected data for sensible heat (8–9%) allowed determination of ET using the energy balance equation. Considering that rejection rate is smaller during daytime and that global radiation and ETo during the period 8 h–19 h were found to represent, respectively, 99% and 93% of daily totals, daily ET was taken as the total of hourly values between 8 h and 19 h.

Figure 7.5 shows daily values of ET_EB in the three wheat fields as compared with ETo measured at each site during mid-season stage of wheat.

Fig. 7.5 Daily ET values of wheat estimated by energy balance equation (ET_{EB}) in sloping (A, B) and flat (C) fields versus E_{To} determined at each site during the period March 07–31, 2013



The slopes of the linear regression lines are, respectively, 0.85, 1.15, and 1.20 for A, B, and C sites. These are similar to hourly values; however, the observed slope for site A (0.85) seems to be too low compared to typical FAO-Kc values.

Conclusion and Perspectives

This work concerned assessment of evapotranspiration of cultivated fields in a hilly Mediterranean region. The slope and aspect effects on estimation of reference and actual evapotranspiration of a wheat crop were approached through field experiments involving three eddy covariance stations and a standard weather station. Results show that for slopes of 5–6° and LAI values around 2; relief and crop cover had only small effects on reference evapotranspiration estimates, suggesting the possibility of measuring E_{To} outside the standard conditions. Hourly K_c estimates determined as the ratio between ET_{EC} and PM-E_{To} were below values given by FAO, nevertheless better consistency was observed when ET was estimated by energy balance; this may be explained by the fact reported by several authors suggesting that the EC method overestimates the available energy and underestimates the convective energy. Also, despite the high volume of data recorded using the EC method, the percentage of LE data rejected by quality control tests was considerably greater than the percentage of H data rejected, particularly in sloping fields. Gap filling would have to be systematically used in order to generate daily values needed for operational use in agriculture.

Acknowledgements The financial support of ANR and AIRD for a Phd grant to the first author is acknowledged. Authors want to thank the editorial board and Dr Steven R. Evett for reviewing the paper and for his pertinent comments.

References

- Allen RG, Pereira LS, Raes D, Smith M (1998) Crop evapotranspiration—guidelines for computing crop water requirements—FAO irrigation and drainage paper 56. Food and Agriculture Organization of the United Nations, pp 465
- Evelt SR, Schwartz, RC, Howell TA, Baumhardt RL, Copeland KS (2012a) Can weighing lysimeter ET represent surrounding field ET well enough to test flux station measurements of daily and sub-daily ET? *Adv Water Resour* 50:(79–90)
- Evelt SR, Kustas, WP, Gowda, PH, Anderson, MC, Prueger, JH, Howell, TA (2012b) Overview of the bushland evapotranspiration and agricultural remote sensing EXperiment: 2008 (BEAREX08): A field experiment evaluating methods for quantifying ET at multiple scales. *Adv Water Resour* 50:(5–19)
- Falge E, Baldocchi D, Olson, RJ, Anthoni P, Aubinet M, Bernhofer C, Burba G, Ceulemans R, Clement R, Dolman H, Granier A, Gross P, Gruñwald T, Hollinger D, Jensen N-O, Katul G, Keronen P, Kowalski A, Ta Lai C, Law BE, Meyers T, Moncrieff J, Moors E, Munger JW, Pilegaard K, Rannik U, Rebmann C, Suyker A, Tenhunen J, Tu K, Verma S, Vesala T, Wilson K, Wofsy S (2001) Gap filling strategies for defensible annual sums of net ecosystem exchange. *J Agric Meteorol* 107:(43–69)
- Feigenwinter C, Bernhofer C, Eichelmann U (2008) Comparison of horizontal and vertical advective CO₂ fluxes at three forest sites. *Agric Meteorol* 148:12–24
- Foken T, Wishura B (1996) Tools for quality assessment of surface-based flux measurements. *J Agric Meteorol* 78:83–105
- Hammerle A et al (2007) Eddy covariance measurements of carbon dioxide, latent and sensible energy fluxes above a meadow on a mountain slope. *Bound-Layer Meteorol* 122:397–416
- Holst T, Rost J, Mayer H (2005) Net radiation balance for two forested slopes on opposite sides of a valley. *Int J Biometeorol* 49:275–284
- Hugo AG, Enrique R, Colin Cikoski C, Bruce J, Rafael L, Erkan I (2013) On the observed ecohydrologic dynamics of a semiarid basin with aspect-delimited ecosystems. *Water Resour Res* 49:1–22
- Rana G, Ferrara RM, Martinelli N, Personnic P, Cellier P (2007) Estimating energy fluxes from sloping crops using standard agrometeorological measurements and topography. *Agric Meteorol* 146:116–133
- Raupach MR, Finnigan JJ (1997) The influence of topography on meteorological variables and surface-atmosphere interactions. *J Hydrol* 190:182–213
- Rebmann C, Göckede M, Foken T, Aubinet M, Aurela M, Berbigier P, Bernhofer C, Buchmann N, Carrara A, Cescatti A, Ceulemans R, Clement R, Elbers JA, Granier A, Grünwald T, Guyon D, Havránková K, Heinesch B, Knohl A, Laurila T, Longdoz B, Marcolla B, Markkanen T, Miglietta F, Moncrieff J, Montagnani L, Moors E, Nardino M, Ourcival JM, Rambal S, Rannik U, Rotenberg E, Sedlak P, Unterhuber G, Vesala T, Yakir D (2005) Quality analysis applied on eddy covariance measurements at complex forest sites using footprint modelling. *Theor Appl Climatol* 80(2–4):121–141
- Tromp-van-Meerveld HJ, McDonnell JJ (2006) On the interrelations between topography, soil depth, soilmoisture, transpiration rates and species distribution at the hillslope scale. *Adv Water Resour* 29:293–310
- Twine TE, Kutas WP, Norman JM, Cook DR, Houser PR, Prueger JH, Starks PJ, Wesley ML (2000) Correcting eddy-covariance flux underestimates over a grassland. *Agric Meteorol* 103:279–300
- Van-Dijk A, Moene AF, DeBruin HAR (2004) The principles of surface flux physics; theory, practice and description of the ECPACK library. In: Meteorology and Air Quality Group. Netherlands

Chapter 8

Performance of Saxton and Rawls Pedotransfer Functions for Estimating Soil Water Properties in the Cap Bon Region-Northern Tunisia

I. Alaya, Mohamed Moncef Masmoudi, Ph. Lagacherie, G. Coulouma,
F. Jacob and N. Ben Mechlia

Abstract Appropriate land use and management requires a good knowledge about the main hydraulic properties of the soil, in particular soil moisture at field capacity (FC), permanent wilting point (PWP), and water holding capacity (HC). In the absence of direct measurements, these characteristics could be estimated from data on texture and organic matter content, using pedotransfer functions (PTFs). In this study, FC, PWP, and HC of predominant soil types in Cap Bon (Vertisols, Cambisols, and Calcisols), are estimated using Saxton and Rawls (Soil Sci Soc Am J 70:1569–1578, 2006) PTFs and complete sets of soil analysis data. Results show that when all soil samples (61) are taken together, obtained estimations were well correlated with measured values for FC ($R^2 = 0.72$) and PWP ($R^2 = 0.72$). Similar correlations were observed for Cambisols and Calcisols taken separately ($R^2 = 0.65$ – 0.70 .); but there was an overestimation of FC and PWP for Vertisols (percentage of clay > 50%). However, relatively weak relationships were observed between estimated and measured values for HC in all cases ($R^2 = 0.15$). PTFs seem appropriate to be used in combination with remote sensing methods for generation of soil FC and PWP maps needed in irrigation and agriculture efficient management.

Keywords Hydraulic properties · Pedotransfer functions · Soil · Cap Bon · Tunisia

I. Alaya (✉) · M.M. Masmoudi (✉) · N. Ben Mechlia
Institut National Agronomique de Tunisie, 1082 Tunis, Tunisia
e-mail: alayai@yahoo.fr

M.M. Masmoudi
e-mail: masmoudi.med@inat.agrinet.tn

Ph. Lagacherie · G. Coulouma
Institut National de la Recherche Agronomique, UMR LISAH, Montpellier, France

F. Jacob
Institut de Recherche pour le Développement, UMR LISAH, Montpellier, France

Introduction

The genetic study of soils leads naturally to assess their physical and chemical characteristics and fertility potential for improving their use. On a global scale, FAO has created a World Reference Base for Soil Resources (WRB) representing 32 reference soil groups (IUSS Working Group WRB 2006). WRB is a tool for better correlation between national soil classifications to compare similar soils in different parts of the world.

In Tunisia, soil resources present a great diversity with three predominant groups: alkaline soils developed on calcareous materials distributed in all regions, acid soils located in the extreme northwest of the country and the gypsic and saline soils located mainly in the center and the south (Mtimet 1999).

More than 37% of cultivated lands are used for cereals production and half of that area (1.5 million) is located in the north and dominated by iso-humic soils, brown calcareous soils, Vertisols and slightly developed soils (CPCS Classification 1967). Because of a long dry season and irregularity in rainfall, rainfed cereal crops are frequently subject to water deficit, particularly for soils with limited water holding capacity (Ben Hassine et al. 2003).

The holding capacity of soils represents the maximum water stored in the soil and accessible to plants. It is defined as the difference between soil moisture at field capacity (FC) and at permanent wilting point (PWP). FC is the water content of the soil after the excess water was drained and the downward flow has decreased. PWP is the lowest water content at which a plant can access water from soil. The matric potential corresponding to FC and PWP is commonly estimated at -33 kPa and -1500 kPa, respectively (Musy and Sautter 1991).

FC and PWP values are determined by direct measurements in laboratory: The principle is to drain saturated soil samples by the corresponding suction pressure. For each applied pressure, water retained after equilibrium, is determined by the gravimetric method. These measurement methods are time-consuming and expensive, especially when the number of samples is large (Schaap and Leij 1998; Schaap et al. 2001). Furthermore their values depend on the state of the samples used (disturbed or not). Therefore, models for estimation of these properties from other more available data such as texture were developed (Hall et al. 1977; Gupta and Larson 1979; Rawls et al. 1982; Vereecken et al. 1989; Rawls et al. 1991; Bastet et al. 1999; Pachepsky et al. 2006).

These models called pedotransfer functions (PTFs) (Bouma 1989) are a simple way to have good estimates of hydraulic properties instead of using more complex direct measurements (Rawls and Brakensiek 1982; McBratney et al. 2002), although their efficiency for different soil types remains questionable. Furthermore PTFs developed in one region or from one database had limited accuracy in other conditions (Williams et al. 1992; Tietje and Tapkenhinrichs 1993; Kern 1995; Wösten et al. 2001).

Among PTFs cited in the literature Gijsman et al. (2002) compared the performance of eight methods for estimating water retention parameters against

field-measured data from across the USA and concluded that the texture-based method by Saxton et al. (1986) was the most precise. These latter PTFs have been successfully applied in several studies related to agricultural hydrology and water management, together with models like SPAW (Saxton and Wiley 2006), BUDGET (Raes 2002, Raes et al. 2006) and AquaCrop (Steduto et al. 2009).

The original Saxton et al. (1986) soil water tension equations were revisited by Saxton and Rawls (2006) who developed also relationships for conductivity and introduced adjustments for organic matter, density, gravel, and salinity. The Saxton and Rawls (2006) PTFs were calibrated using the USDA soil database of about 1722 samples of the (A) horizon and are used in many applications.

Soil properties maps are generally based on an extensive soil sampling and analysis and on the use of Krigging technique for spatial extrapolation. Recent development of remote sensing methods for generation of soil texture maps could be used for producing precise soil hydraulic properties maps needed in precision agriculture and for efficient irrigation management (Gomez et al. 2012; Lagacherie et al. 2013). However, this task requires the use of robust PTFs and appropriate methods to extrapolate properties obtained in soil surface to deep layers.

In this work, the use of texture and Saxton and Rawls PTFs for estimation of hydraulic properties will be tested for three soil classes prevailing in the Cap Bon region and results will be analyzed and compared to measured properties.

Materials and Methods

Studied Soils

The samples used in this study were taken in the Cap Bon region, northeast Tunisia, from 17 soil profiles distributed on three types of soil (Vertisols, Cambisols and Calcisols).

For each soil horizon of these soil pits (61 horizons), particles size, bulk density, soil moisture at permanent wilting point (PWP) and field capacity (FC) were determined at the soil analysis laboratory of Arras-France.

Saxton and Rawls Pedotransfer Functions

Data on texture and organic matter content were used to estimate soil hydraulic properties by the equations of Saxton and Rawls. Estimates have considered all of the soil horizons and concerned the water contents at field capacity (FC) and at permanent wilting point (PWP).

Saxton and Rawls PTFs are expressed as nonlinear polynoms using sand (S) and clay (C) percentages and organic matter content (OM).

PWP is defined as the volumetric soil moisture at 1500 kPa (θ_{1500})

$$PWP(mm/m) = 1000 \times \theta_{1500} \quad (1)$$

Where

$$\theta_{1500} = \theta_{1500t} + 0.14 \times \theta_{1500t} - 0.02 \quad (2)$$

$$\begin{aligned} \theta_{1500t} = & -0.024 \times S + 0.487 \times C + 0.006 \times OM \\ & + 0.005 \times S \times OM - 0.013 \times C \times OM + 0.068 \times S \times C + 0.031 \end{aligned} \quad (3)$$

FC is defined as the volumetric soil moisture at 33 kPa (θ_{33})

$$FC(mm/m) = 1000 \times \theta_{33} \quad (4)$$

Where

$$\theta_{33} = \theta_{33t} + 1.283 \times \theta_{33t}^2 - 0.374 \times \theta_{33t} - 0.015 \quad (5)$$

$$\begin{aligned} \theta_{33t} = & -0.251 \times S + 0.195 \times C + 0.011 \times OM \\ & + 0.006 \times S \times OM - 0.027 \times C \times OM + 0.452 \times S \times C + 0.299 \end{aligned} \quad (6)$$

FC and PWP estimates are compared to measured values in order to assess the performance of these equations in estimating soil water content parameters.

Results

In a first assessment, the equations of Saxton and Rawls were applied to the entire set of data (61 samples). Results show relatively good estimations of FC and PWP in comparison with measured values, with similar coefficients of determination for both parameters ($R^2 = 0.72$). FC and PWP values obtained by PTFs were used to estimate available water holding capacity (HC) of the considered soil samples. Estimated HC varied between 7.3 and 15.4% vol., showing a relatively narrow range compared to the measured values (2.3–19.9% vol.), with a poor linear relationship between estimated and measured values ($R^2 = 0.15$).

In a second step, data of the different profiles were arranged under the corresponding three soil classes according to the World reference base for soil resources (IUSS Working Group WRB 2006): cambisols, calcisols and vertisol and results were analyzed separately for each soil type.

Performance of PTFs for Cambisols

The Cambisols (corresponding to Inceptisols according the USDA classification) are soils with a horizon at the beginning of differentiation. They are in a transitional phase of development, from a young to a mature soil. Their parent material is mainly from colluvial, alluvial, or aeolian deposits. These soils are characterized by slight to moderate alteration of parent material and the absence of appreciable amounts of illuviated clay, organic matter, and iron compounds. Most Cambisols have medium texture with high porosity, good water retention capacity and good internal drainage (Driessen et al. 2001). The Cambisols were reported in five surveyed sites (18 horizons). FC and PWP of these soils are increasing clearly with clay content.

The hydraulic properties estimated for Cambisols by the model of Saxton and Rawls have a good correlation with measured values (R^2 in the range 0.6–0.7) (Fig. 8.1a). However weak relationship is observed between estimated and measured values of holding capacity (Fig. 8.1b).

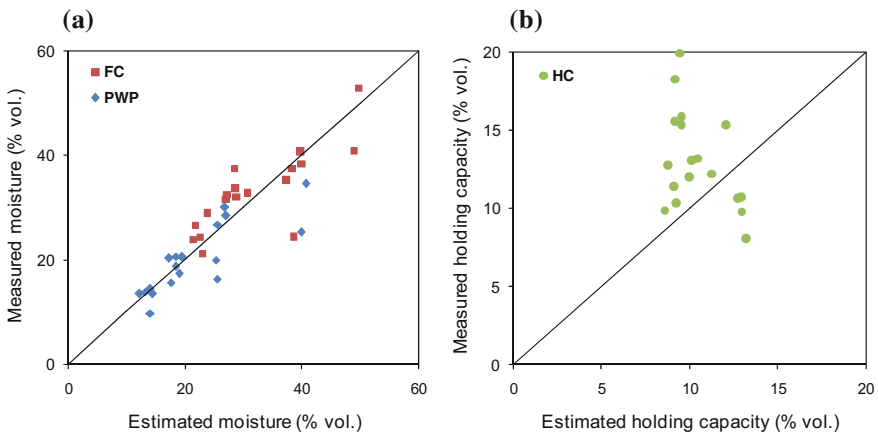


Fig. 8.1 Measured versus estimated values of soil hydraulic properties by Saxton and Rawls PTFs for Cambisols class: **a** field capacity (FC) and permanent wilting point (PWP); **b** holding capacity (HC)

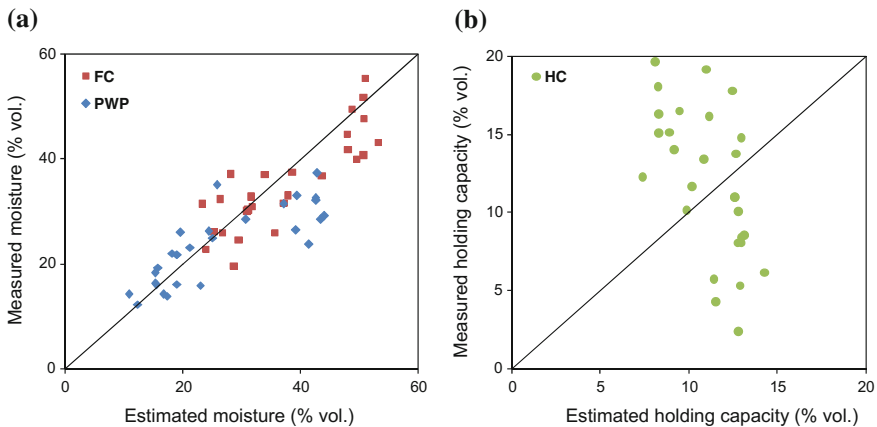


Fig. 8.2 Measured versus estimated values of soil hydraulic properties by Saxton and Rawls PTFs for Calcisols class: **a** field capacity (FC) and permanent wilting point (PWP); **b** holding capacity (HC)

Performance of PTFs for Calcisols

Calcisols are characterized by substantial secondary accumulation of lime. Most Calcisols have a medium or fine texture and good water retention properties. They are widespread in arid and semiarid areas (Driessen et al. 2001).

They were found in 28 horizons in eight profiles among the 17 considered ones. FC and PWP estimated by the Saxton and Rawls model for the Calcisols are also well correlated with measured values with $R^2 = 0.71$ and 0.66 and RMSE of 5 and 7%, respectively (Fig. 8.2).

Holding capacity was poorly estimated by the Saxton and Rawls PTFs with a significantly smaller range of estimated values compared to measured values.

Performance of PTFs for Vertisols

Vertisols are churning heavy clay soils with a high proportion of swelling 2:1 lattice clays that forms deep cracks in drier seasons or years. They derive either from rock weathering products or fine sediments, which have the characteristics of smectite clay. These soils are found mainly in tropical, semiarid to (sub) humid and Mediterranean climates, the essential feature is the alternation of distinct wet and dry seasons. Heavy soil texture and domination of clay minerals lead to a narrow soil moisture range between water stress and water excess (Driessen et al. 2001).

Vertisols were found in four sites with a total number of samples of 15. They are characterized by high percentage of clay (>50%) and did not show a clear relationship between FC or PWP and clay percentage. The use of Saxton and Rawls

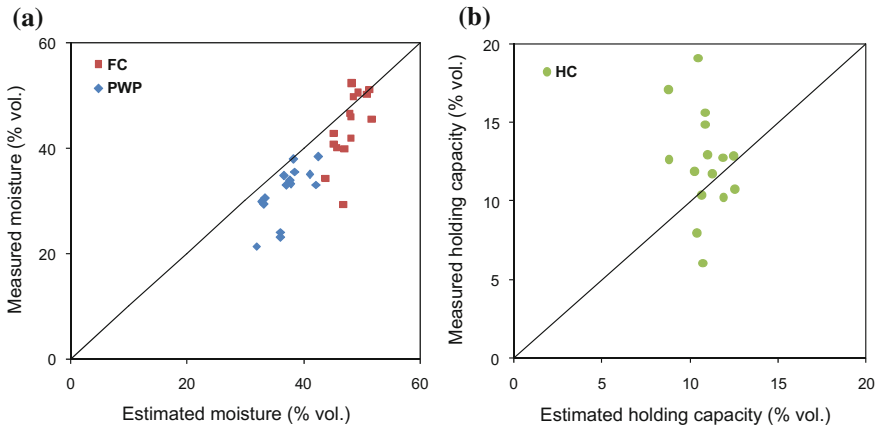


Fig. 8.3 Measured versus estimated values of soil hydraulic properties by Saxton and Rawls PTFs for Vertisols class: **a** field capacity (FC) and permanent wilting point (PWP); **b** holding capacity (HC)

Table 8.1 Coefficient of determination (R^2) and root mean square error (RMSE) between measured and estimated values of volumetric soil moisture at field capacity (FC), permanent wilting point (PWP) and holding capacity (HC) for the three soil types

	Soil type	FC	PWP	HC
R^2	Cambisol	0.64	0.69	0.15
	Calcisol	0.71	0.66	0.09
	Vertisol	0.46	0.46	0.19
RMSE (% vol.)	Cambisol	5.33	4.84	2.14
	Calcisol	5.54	7.20	2.54
	Vertisol	6.42	6.57	3.86

equations to estimate FC and PWP of these soils resulted in overestimated values compared to measured ones (Fig. 8.3a). HC is also poorly estimated by the PTFs and a smaller range was observed for estimated HC as compared to measured values (Fig. 8.3b).

Statistical Evaluation

Statistical evaluation was performed through correlation coefficient and root mean square errors (RMSE) given in Table (8.1). The coefficients of determination and RMSE show that PTFs give larger deviations for Vertisols than for the other two soil types. These deviations are primarily related to the heavy texture of these soils.

Conclusion

In this work, Saxton and Rawls PTFs were tested for estimating hydraulic properties of three types of soil of the Cap Bon region (Vertisols, Cambisols, and Calcisols) using percentage of sand, clay, and organic matter of 61 samples from 17 soil profiles.

PTFs produced relatively good estimates of field capacity and permanent wilting point ($R^2 = 0.72$) when considering all profiles and horizons (61 samples). However, holding capacity was poorly estimated with an R^2 of 0.15 between measured and estimated values.

When considering separately soil classes, results show that estimated values of FC and PWP were well correlated with measured values for Cambisols and Calcisols ($R^2 = 0.65\text{--}0.70$) whereas for Vertisols (clay rate > 50%), PTFs seems to overestimate both parameters. HC remained difficult to assess for the three soil types.

With recent progress in estimating texture and organic matter of soils from remote sensing images, PTFs are likely to become a common method for developing soil hydraulic properties maps (FC and PWP) needed for efficient irrigation and precision agriculture practices.

Acknowledgments The financial support of the ANR projects Digisol-Hymed and Almira is acknowledged.

References

- Bastet G (1999) Estimation des propriétés de rétention en eau des sols à l'aide de fonctions de pédotransfert: développement de nouvelles approches. Univ. d'Orléans
- Ben Hassine H, Ben Salem M, Bonin G, Braudeau E, Zidi C (2003) Réserve utile des sols du Nord-Ouest tunisien évolution sous culture. *Étude et Gestion des Sols* 10:19–33
- Bouma J (1989) Using soil survey data for quantitative land evaluation. *Adv Soil Sci* 9:177–213
- Driessen P, Deckers J, Spaargaren O, Nachtergaele F (2001) Lecture notes on the major soils of the world. FAO, Rome
- Gijsman AJ, Jagtap SS, Jones JW (2002) Wading through a swamp of complete confusion: how to choose a method for estimating soil water retention parameters for crop models. *Eur J Agron* 18:75–105
- Gomez C, Lagacherie P, Bacha S (2012) Using Vis-NIR hyperspectral data to map topsoil properties over bare soils in the Cap Bon region, Tunisia. In: Minasny B, Malone BP, McBratney AB (eds) *Digital soil assessments and beyond*. Springer, pp 387–392
- Gupta SC, Larson WE (1979) Estimating soil water retention characteristics from particle size distribution, organic matter percent and bulk density. *Water Resour Res* 15:1633–1635
- Hall DG, Reeve MJ, Thomasson AJ, Wright VF (1977) Water retention, porosity and density of field soils. Technical Monograph. No 9. Soil Survey of England & Wales, Harpenden
- IUSS Working Group WRB (2006) World reference base for soil resources 2006. World Soil Resources Reports No. 103. FAO, Rome
- Kern JS (1995) Evaluation of soil water retention models based on basic soil physical properties. *Soil Sci Soc Am J* 59:1134–1141

- Lagacherie P, Sneepe AR, Gomez C, Bacha S, Coulouma G, Hamrouni MH, Mekki I (2013) Combining Vis-NIR hyperspectral imagery and legacy measured soil profiles to map subsurface soil properties in a Mediterranean area (Cap-Bon, Tunisia). *Geoderma* 209:168–176
- McBratney AB, Minasny B, Cattle SR, Vervoort RW (2002) From pedotransfer functions to soil inference systems. *Geoderma* 109:41–73
- Mtimet A (1999) Atlas des sols tunisiens. Ministère de l'Agriculture, Tunis
- Musy A, Sautter M (1991) *Physique du sol*. Presses polytechniques universitaires romandes, Lausanne
- Pachepsky YA, Rawls WJ, Lin HS (2006) Hydropedology and pedotransfer functions. *Geoderma* 131:308–316
- Raes D (2002) BUDGET, a soil water and salt balance model: reference manual. Faculty of Agricultural and Applied Biological Sciences, Institute for Land and Water Management, Katholieke Universiteit Leuven, Leuven, Belgium
- Raes D, Geerts S, Kipkorir E, Wellens J, Sahli A (2006) Simulation of yield decline as a result of water stress with a robust soil water balance model. *Agric Water Manag* 81:335–357
- Rawls WJ, Brakensiek DL (1982) Estimating soil-water retention from soil properties. *J Irrig Drain Div* 108:166–171
- Rawls WJ, Gish TJ, Brakensiek DL (1991) Estimation soil water retention from soil physical properties and characteristics. *Advance in soil science*. Springer-Verlag, New-York Inc., 16:213–234
- Schaap MG, Leij FJ (1998) Using neural networks to predict soil water retention and soil hydraulic conductivity. *Soil Tillage Res* 47:37–42
- Schaap MG, Leij FJ, van Genuchten MT (2001) Rosetta: a computer program for estimating soil hydraulic parameters with hierarchical pedotransfer functions. *J Hydrol* 251:163–176
- Saxton KE, Rawls WJ, Romberger JS, Papendick RI (1986) Estimating generalized soil water characteristics from texture. *Soil Sci Soc Am J* 50:1031–1036
- Saxton KE, Rawls WJ (2006) Soil water characteristic estimates by texture and organic matter for hydrologic solutions. *Soil Sci Soc Am J* 70:1569–1578
- Saxton KE, Willey PH (2006) The SPAW model for agricultural field and pond hydrologic simulation. Chapter 17. In: Singh VP, Frevert D (eds) *Mathematical modeling of watershed hydrology*. CRC Press, pp 401–435
- Steduto P, Hsiao TC, Raes D, Fereres E (2009) In AquaCrop-The FAO crop model to simulate yield response to water: I. Concepts and underlying principles. *Agron J* 101:426–437
- Tietje O, Tapkenhinrichs M (1993) Evaluation of pedotransfer functions. *Soil Sci Soc Am J* 57:1088–1095
- Vereecken H, Maes J, Feyen J, Darius P (1989) Estimating the soil moisture retention characteristics from texture, bulk density and carbon content. *Soil Sci* 148:389–403
- Williams RD, Ahuja LR, Naney JW (1992) Comparison of methods to estimate soil water characteristics from soil texture, bulk density and limited data. *Soil Sci* 153:172–184
- Wösten JHM, Pachepsky YA, Rawls WJ (2001) Pedotransfer functions: bridging the gap between available basic soil data and missing soil hydraulic characteristics. *J Hydrol* 251:123–150

Chapter 9

Assessing the Groundwater Pollution Problem by Nitrate and Faecal Bacteria: Case of Djerba Unconfined Aquifer (Southeast Tunisia)

Faiza Souid, Belgacem Agoubi and Adel Kharroubi

Abstract Djerba unconfined sandy aquifer (Southeast of Tunisia) is affected by several contamination phenomenon such as seawater intrusion and anthropogenic activities. This study aims to assess nitrate and faecal pollution in groundwater. More than 70 wells were sampled and analyzed. Geochemical assessment was used to understand the pollution origin and factors controlling this process in Djerba aquifer. Chemical and bacteriological analysis confirms that the sampled wells were seriously affected by both nitrate and faecal pollution problem. Chemical analysis shows that 51% of sampled wells have a nitrate levels more than 50 mg/l. The bacteriological results demonstrated that 95% of wells showed total coliforms densities higher than 10 CFU/100 ml. Thermotolerants coliforms and *Escherichia coli* were detected in all groundwater sampled (96% of wells). These results confirm the impact of anthropogenic activities on groundwater quality. It seems that this contamination is directly related to septic tanks, which are not waterproof; allow the infiltration of the major part of the liquid phase.

Keywords Nitrate · Faecal pollution · Anthropogenic activities · Unconfined aquifer · Djerba · Tunisia

F. Souid (✉) · B. Agoubi · A. Kharroubi

RU: Applied Hydrosiences Research Unit, Higher Institute of Water Sciences and Techniques, University of Gabès, University Campus, 6072 Gabès, Tunisia
e-mail: faizasouid@yahoo.fr

B. Agoubi
e-mail: Belgacem.agoubi@isstegb.rnu.tn

A. Kharroubi
e-mail: adel.kharroubi@voila.fr

Introduction

Anthropogenic activities are the main source of groundwater contamination. Several studies around the world have shown that agricultural activities are the first responsible of elevated nitrate concentrations in groundwater (Sall and Vanclooster 2009; Bonton et al. 2010; Fekkoul et al. 2011). In addition, sewage effluents including septic tanks discharged to unsaturated aquifers, animal excreta, rainfall, and industrial effluents are considered to be important sources for increasing nitrate and faecal contents in the groundwater (Abu Rukah and Alsokhny 2004). Identification of pollution mechanisms needs a combination of several approaches. Nitrate and faecal pollution can be studied using classical geochemical and bacteriological approaches (Aghzar et al. 2002; Howard et al. 2003; Bonton 2010), statistical and geostatistical methods (Sall and Vanclooster 2009; Chica-Olmo et al. 2014) and isotopic techniques (Hosono et al. 2013; Zhang et al. 2014).

Faecal pollution is essentially generated by human and animal waste released in surface or evacuated directly in dug wells used as an uncontrolled discharge for domestic waste; also, septic tanks are a major source of faecal inputs to the unconfined aquifer. In Djerba Island, open dug wells are the principal mean to exploit the quaternary aquifer. In 2005, more than 3,000 wells were inventoried (Kharroubi et al. 2012). This fact, contributes to increase pollution risk of groundwater in Djerba.

This study aims to assess chemical and bacteriological quality of groundwater and highlight nitrate and faecal pollution. Geochemical and bacteriological characterizations in conjunction with cartographic methods were used to understand spatial distribution of pollution tracers and to identify pollution mechanisms governing the island's groundwater quality.

Materials and Methods

Study Area

The study area is a semiarid island located in the southeast of Tunisia and covers 510 km² (Fig. 9.1). The mean annual precipitation is 220 mm. In terms of geomorphology, Djerba is a flat zone with a maximum altitude of 54 m in the south part of the island.

Geological and Hydrogeological Settings

The detailed sedimentological study done by Jedoui (2000) shows the Pleistocene and Holocene sediments outcropping in the south part of the island, with the

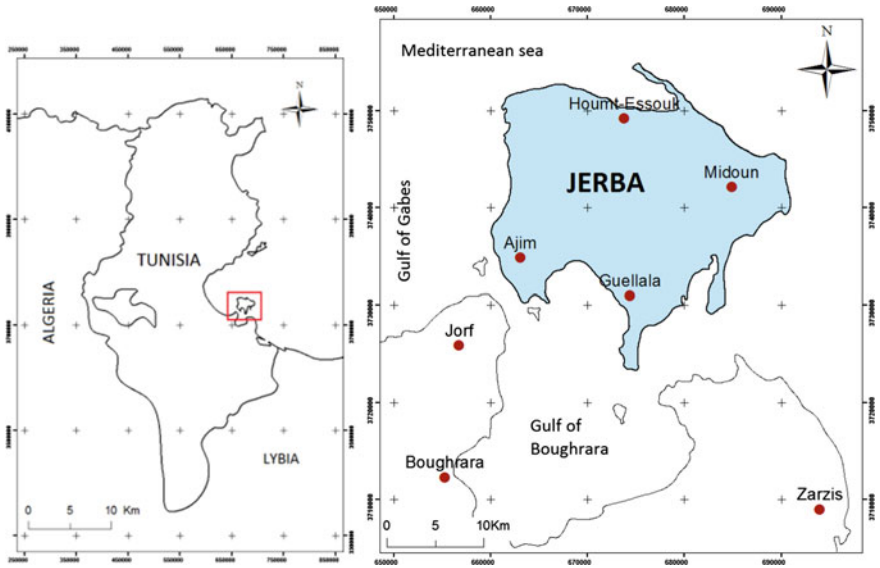


Fig. 9.1 Location map of the study area

occurrence of Holocene oolitic limestone near the north-west and the west coastal parts of the island. Quaternary dunes located principally in the northeast of the island and Holocene bioclastic sands covering the main north coast and another area in the south (Fig. 9.2).

The aquifer is hosted in sandy levels of the Mio-Pliocene intercalated with clay lenses as well as in marine limestone of the Tyrrhenian formation (Jedoui 2000). The aquifer has a variable depth with a maximum of 50 m. This aquifer is recharged via vertical infiltration from precipitation. Kharroubi et al. (2012) studied the geochemistry of unconfined aquifer of Djerba and reported that high mineralization is due to gypsum and carbonate dissolution coupled with the mixed by brackish groundwater and seawater intrusion in many areas.

Water Sampling

Chemical and bacteriological analyses were carried out on groundwater samples collected after wet season (from 25/02/2014 to 14/04/2014) from 79 individual wells. Figure 9.3 shows the location of the selected wells.

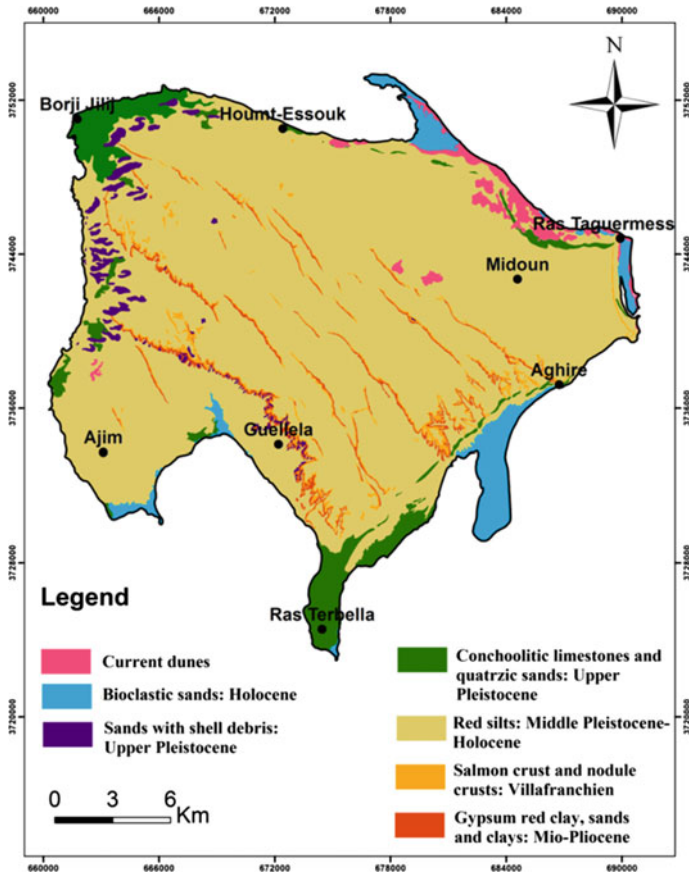


Fig. 9.2 Geological map of Djerba Island (Jedoui 2000)

Physicochemical and Bacteriological Analyses Methods

Parameters analyzed are *pH*, electrical conductivity (*EC*) and salinity using the Consort 933 portable analyzer, NO_3^- is measured using chromatography method.

Total coliforms (TC) and thermotolerants coliforms (ThC) were enumerated by the membrane filtration method (ISO 9308-1 2000). *Escherichia coli* was determined using transplanting TC colonies on tryptophan. Results are obtained after incubation at a temperature of 44 °C and observed after 24 h. Indole production is determined by adding a few drops of Kovac’s reagent.

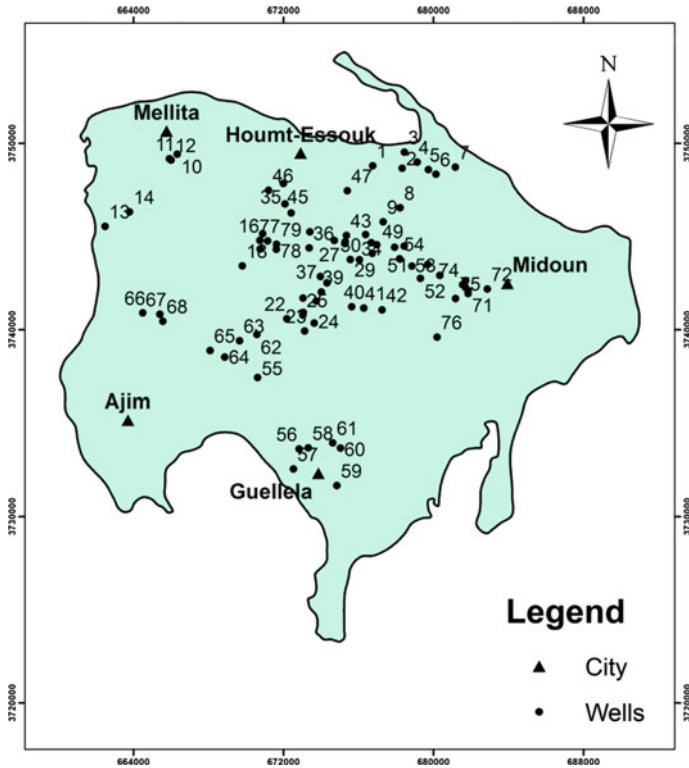


Fig. 9.3 Map showing the geographical locality of the sampled wells

Results and Discussion

Groundwater Quality

Table 9.1 summarizes the results obtained from chemical analysis of water samples for the different tested parameters.

The salinity rates of groundwater ranged between 0.3 and 7 g/l with a mean of 2.41 g/l. Among the physical parameters, pH ranges from 6.82 to 8.04 with an average 7.46, indicating the alkaline nature of sampled waters. EC in the groundwater varied from 0.76 to 12.34 mS/cm, with an average 4.56 mS/cm.

Table 9.1 Chemical analysis results

Parameters	Maximum	Minimum	Mean
pH	8.04	6.82	7.46
EC (mS/cm)	12.34	0.76	4.56
Salinity (g/l)	7	0.3	2.41
NO_3^- (mg/l)	183.35	33.53	67.87

Result of bacteriological analyses showed that 95% of wells presented TC densities higher than 10 CFU/100 ml. ThC and *E. coli* were detected in all groundwater sampled (96% of wells) except three wells whose are deeper than 50 m. In this study, eight sampled wells are used for drinking; analysis results reveal the bacteriological contamination of these wells.

Referring to the WHO (2008) the presence of *E. coli* in drinking water exposes the population to health risk.

Nitrate Pollution

According to the analytical data, 51% of wells presented nitrate concentrations more than 50 mg/l (Table 9.2).

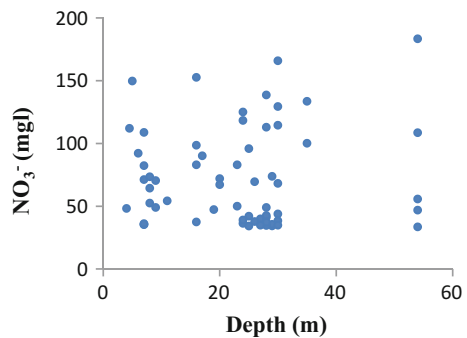
High nitrate concentrations indicate the impact of anthropogenic activities on the groundwater (Ma et al. 2009). In addition, anthropogenic pollution by nitrate is confirmed when nitrate concentration exceeds 5 mg/l (Bonton et al. 2010). Nitrate pollution displayed obvious spatial variations, which may be explained by the absence of sewer system in some suburban zone and by agricultural activities in rural zone. In the island, pollution is generated by municipal and domestic sewages, fertilizers, septic tanks and abandoned wells used as uncontrolled discharge.

NO_3^- versus depth diagram (Fig. 9.4) shows the variation of the concentrations of NO_3^- and the depth of 61 sampled wells. It can be concluded that the nitrate pollution is general and affected deep and shallow wells.

Table 9.2 Ranking of sampled wells according to nitrate levels

Nitrate levels (mg/l)	Number of wells
25–50	39
50–100	25
>100	15

Fig. 9.4 Bivariate plot of NO_3^- versus depth



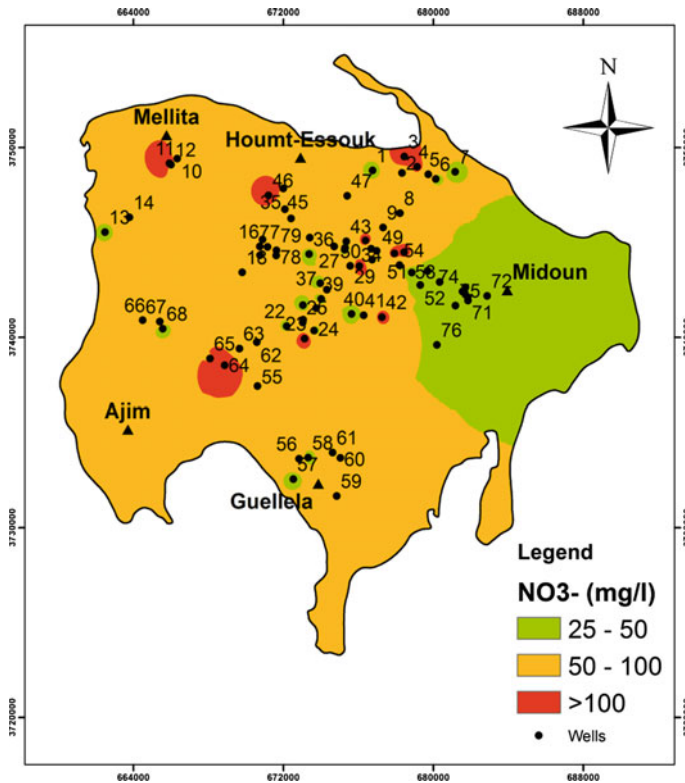


Fig. 9.5 Maps showing the spatial distribution of NO_3^-

The spatial distribution pattern of NO_3^- concentration (Fig. 9.5) presented eminent variability. High NO_3^- concentrations occur in various locality of the island. Extremely high levels of nitrate (exceeds 100 mg/l) was seen in the shallow wells (Northern and Northwestern parts), in wells near septic tanks and agricultural areas (the central and Southwestern parts). They reveal the high inputs of nitrate to the aquifer due to anthropogenic activities and leaching of superficial layers by heavy rain.

This spatial irregularity confirms the existence of punctual sources of pollution (Tandia 1999) such as septic tanks, which are considered like punctual sources of nitrate (Ma et al. 2009). The distance separating the wells from the septic tanks varied between 2 and 40 m, this factor contributes to increase pollution risk. In the island, groundwater is used for domestic purpose and mainly for irrigation. Agricultural irrigation flow is also considered as a source of groundwater pollution (Rouabhia and Djabri 2010) by the contaminated water irrigation return.

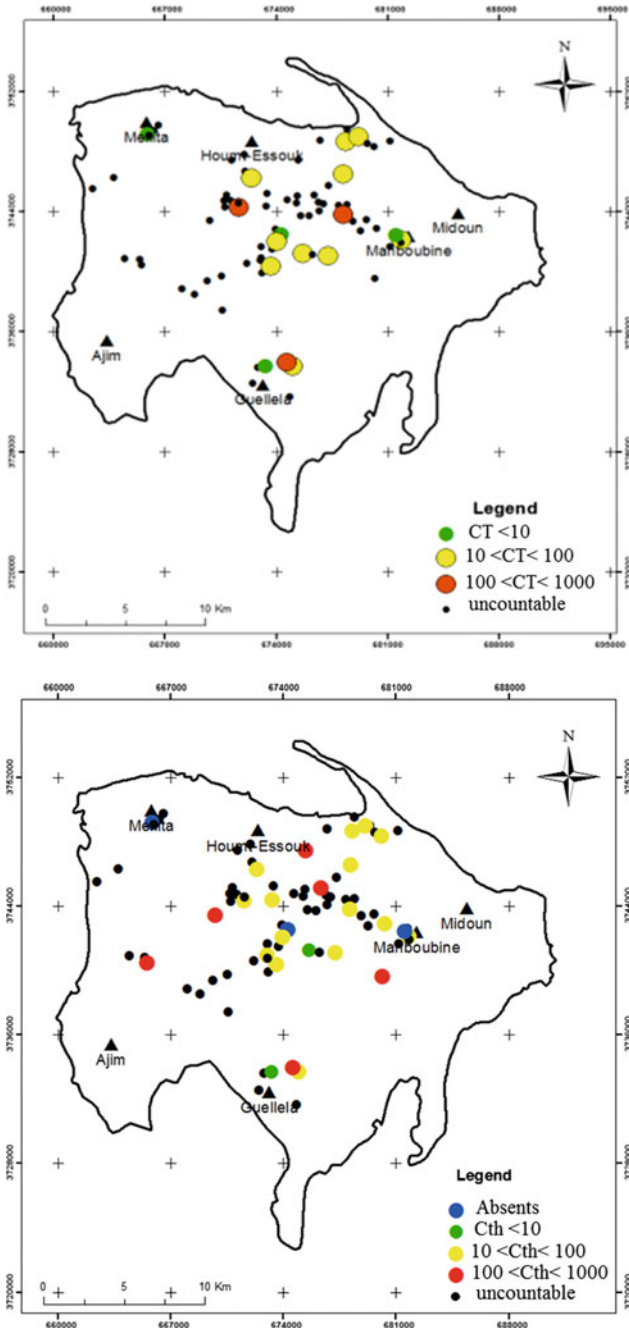


Fig. 9.6 Maps showing spatial distribution of total and thermotolerant coniforms

Faecal Pollution

Referring to Fig. 9.6, spatial distribution of coliforms confirms that the wells are seriously affected by the faecal pollution. The abundance of coliforms, therefore, demonstrates that bacteria are widely distributed in the study area confirming the existence of significant bacteriological pollution in groundwater. In this area, 68% of samples presented high coliforms concentrations (coliforms are uncountable). The presence of *E. coli* in most wells (96%) indicates that these sampling wells were contaminated by means of faecal loads. Faecal pollution is only attributed to the anthropogenic inputs (human and animal faecal sources). *E. coli* is the more precise indicator of faecal pollution (WHO 2008).

Conclusion

This paper gives an overview of the groundwater nitrates and coliforms contamination in Djerba Island. Chemical and bacteriological analyses carried out on groundwater samples of 79 wells show that quaternary aquifer is affected significantly by pollution. Anthropogenic activities (the inadequate sanitation, uncontrolled discharge, septic tanks and agricultural practices) contribute to groundwater quality deterioration through the leaching of superficial layers. Variation of nitrate contamination with the well depth confirms that nitrate contamination is general and affected shallow and deep wells. In contrast, bacteriological pollution decreases with the depth, which may be explained by the purifying effect performed by soil layers.

It is recommended that regional authorities adopted remedial and preventive measures to protect groundwater resources in the island

- Introduction of a proper specification for septic tanks and strict supervision of their construction and their proximity to the wells.
- Public awareness about the danger of the use of abandoned wells like an uncontrolled discharge for domestic waste.
- Installation of adequate sewage system.

References

- Abu Rukah Y, Alsokhny K (2004) Geochemical assessment of groundwater contamination with special emphasis on fluoride concentration, North Jordan. *Chem Erde* 64:171–181
- Aghzar N, Berdai H, Bellouti A, Soudi B (2002) Groundwater nitrate pollution in Talda (Morocco). *Rev Sci Eau* 15(2):459–492

- Bonton A, Rouleau A, Bouchard C, Rodriguez MJ (2010) Assessment of groundwater quality and its variations in the capture zone of a pumping well in an agricultural area. *Agr Water Manage* 97:824–834
- Chica-Olmo M, Luque-Espinar JA, Rodriguez-Galiano V, Pardo-Iguzguiza E, Chica-Rivas L (2014) Categorical indicator kriging for assessing the risk of groundwater nitrate pollution: the case of Vega de Granada aquifer (SE Spain). *Sci Total Environ* 470–471:229–239
- Fekkoul A, Zarhloule Y, Boughriba M, Kabbabi A, Machmachi I, Chafi A (2011) Contamination par les pesticides organochlorés et les nitrates des eaux souterraines de systèmes aquifères de la plaine des Triffa (Maroc Nord Oriental). *ScienceLib Editions Mersenne* 3: N° 110801, ISSN 2111–4706
- Hosono T, Tokunaga T, Kagabu M, Nakata H, Orishikida T, Lin IT, Shimada J (2013) The use of $\delta^{15}\text{N}$ and $\delta^{18}\text{O}$ tracers with an understanding of groundwater flow dynamics for evaluating the origins and attenuation mechanisms of nitrate pollution. *Water Res* 47:2661–2675
- Howard G, Pedley S, Barrett M, Nalubega M, Johal K (2003) Risk factors contributing to microbiological contamination of shallow groundwater in Kampala, Uganda. *Water Res* 37:3421–3429
- International Organization for Standardization “ISO” 9308-1 (2000) Qualité de l’eau-dénombrement des *Escherichia Coli* et des bactéries coliformes-Partie 1: Méthode par filtration sur membrane, Edition 2. Available via ISO. http://www.iso.org/iso/fr/catalogue_detail.htm?csnumber=26404
- Jedoui Y (2000) Sédimentologie et géochimie des Dépôt littoraux quaternaires: reconstitution des variations des climats et du niveau marin dans le Sud Est tunisien. Université de Tunis II, Thèse de doctorat en sciences géologiques
- Kharroubi A, Tlahigue F, Agoubi B, Azri C, Bouri S (2012) Hydrochemical and statistical studies of the groundwater salinization in Mediterranean arid zones: case of the Jerba coastal aquifer in southeast Tunisia. *Environ Earth Sci* 67:2089–2100
- Ma J, Ding Z, Wei G, Zhao H, Huang T (2009) Sources of water pollution and evolution of water quality in the Wuwei basin of Shiyang river, Northwest China. *J Environ Manage* 90:1168–1177
- Rouabhia AEK, Djabri L (2010) L’irrigation et le risqué de la pollution saline. Exemple des eaux souterraines de l’aquifère Miocène de la plaine d’El Ma El Abiod. *Larhyss J* 08:55–67
- Sall M, Vanclooster M (2009) Assessing the well water pollution problem by nitrates in the small scale farming systems of the Niayes region, Senegal. *Agr Water Manage* 96:1360–1368
- Tandia A, Diop ES, Gaye CB (1999) Nitrate groundwater pollution in sub-urban areas: example of groundwater from Yeumbeul, Senegal. *J Afr Earth Sci* 29:809–822
- World Health Organization (2008) Guidelines for drinking-water quality, 3rd edn. WHO, Geneva. http://www.who.int/water_sanitation_health/dwq/fulltext.pdf
- Zhang Y, Li F, Zhang Q, Li J, Liu Q (2014) Tracing nitrate pollution sources and transformation in surface and ground-waters using environmental isotopes. *Sci Total Environ* 490:213–222

Chapter 10

Monitoring Soil Moisture Content of *Jessour* in the Watershed of Wadi Jir (Matmata, Southeast Tunisia)

Fethi Abdelli, Mohamed Ouessar, Salah M'Hemdi, Messaoud Guied and Houcine Khatteli

Abstract Soil moisture is an important indicator to determine the potential production of a crop, especially in recurrent drought threatened countries as Tunisia. It is also important in hydrologic modeling of watersheds. In the context of enhancing the value of *jessour* (plural of *jesr*), and providing scientific knowledge of the evolution of soil water content in this water harvesting technique, TDR measurements were carried out for four consecutive years at three sites in the watershed of wadi Jir (Matmata, southeast Tunisia). The obtained results show that

- The *jesr* ensures water storage in soil, which varies on average between 100 mm and 200 mm. However, in wet periods, this storage *jesr* can exceed 300 mm but can drop as low as 50 mm in dry periods (as recorded in the *jesr* of Téchine).
- Only one effective rainfall annually can ensure adequate water supply for the rest of the hydrological year. During wet periods, olive trees extract water from upper soil horizons whereas they exploit the deeper horizons during summer and drought periods.
- The use of the theoretical potential at permanent wilting point of $pF = 4.2$ seems to be inadequately adapted to olive extraction capabilities and tends to underestimate the amount of water that the adult olive trees can extract.
- Thus, *jessour* can adequately ensure water supply of olive trees while ensuring effective erosion control in the mountains of Matmata and landscape ecology enhancement.

Keywords Water balance · Water harvesting technique · Jessour · TDR · Soil water content

F. Abdelli (✉) · M. Ouessar · M. Guied · H. Khatteli
Laboratoire d'Érémologie et Lutte Contre la Désertification, Institut des Régions Arides (IRA), km 22.5, Route du Djorf, 4100 Médenine, Tunisia
e-mail: abdelli1@yahoo.fr

S. M'Hemdi
Cellule Territoriale de Vulgarisation Agricole de Nouvelle Matmata, Commissariat Régional au Développement Agricole de Gabès (CRDA), Gabès, Tunisia

Introduction

Soil moisture is an important parameter for many applications related to natural resources, such as hydrological modeling (Sheikh et al. 2009; Brocca et al. 2012; Trambly et al. 2012; Mobidelli et al. 2012), forecasting stream flow (Anctil et al. 2004; Komma et al. 2008; Berthet et al. 2009; Huza et al. 2014). Van Steenberghe and Willems (2013), advice to irrigation (Hu and Cheng Si 2014), flood forecasting (Rahman et al. 2015; Massari et al. 2013), knowledge of the vulnerability of plants to climate change (Piedallu 2012; Destouni and Verrot 2014), and the study of soil water balance by remote sensing technique (Gheris 2014; Entekhabi et al. 2010; Chaouch 2008; Shin and Mohanty 2013; Fares et al. 2013). Despite the importance of this parameter, especially the key role which plays in the hydrological and climate modeling, arid regions have received limited attention (Zhang and Ming'an Shao 2014). It is also very limited at the level of the watershed, even of the parcel (Brunet et al. 2003). In this context, we try to bring scientific knowledge for a better understanding evolutionary mechanism of moisture in the soil *jessour*. The *jessour* is an ancient runoff water harvesting technique widely practiced in the arid highlands of the southeastern region of Tunisia, particularly in the mountainous of Matmata (Abdelli et al. 2012). It is based on a retention dam made of earth or stone perpendicular to the runoff, behind which the crops, mainly fruit trees, are cultivated. The dam stops and stores the runoff and supplies in this way water to the crops. About 400,000 ha are covered by *jessour*, particularly in the Matmata mountain chain (El Amami 1984). Though the *jessour* technique was developed for the production of various agricultural commodities, it now also plays three additional roles: (1) aquifer recharge, via runoff water infiltration into the terraces, (2) flood control and therefore the protection of infrastructure and towns built downstream, and (3) wind erosion control, by preventing sediment from reaching the downstream plains, where the wind is very active (Ouessar 2007).

Materials and Methods

Study Area

Three monitoring sites, corresponding to *jessour* of Tijma, Téchine and Adbach (Fig. 10.1), have been characterized and followed almost for four consecutive years (October 2009–January 2014). The measurement frequency is not regular but more frequent after each rainfall event and for longer periods during drought and summer season.

Site selection is conditioned by the presence of *jessour* in the watershed, accessibility to the site, the minimum risk of theft or damage to the equipment, and especially the acceptance of the farmer to install the equipment in his *jesr*.

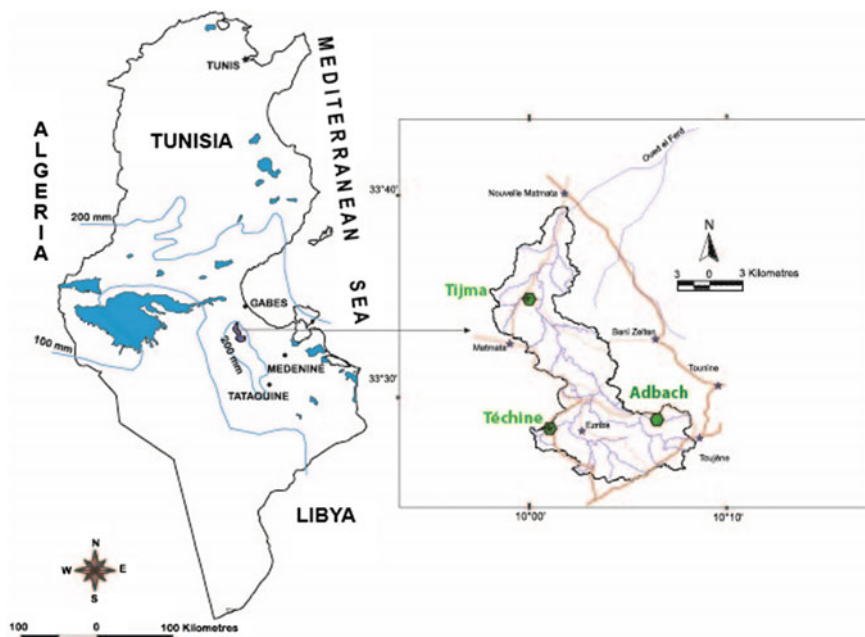


Fig. 10.1 Location map of the study area (the three *jessour*)

Crop practices in three sites are mainly fruit trees (olive, fig, and almond). After the effective rainfall of autumn and/or winter, legumes (e.g., pea, chickpeas, lentil, and faba bean) and barley and wheat are cultivated between fruit trees.

Instrument and Principle of Measurements

Given the importance of water content parameter in soil physics, there is obviously a very large literature on its measurement. Summary presentation of the different methods used and description corresponding experimental protocols and the sources of uncertainty can be found in Sun et al. (2014), Nunzio (2014), Schmutge et al. (1980), Topp (1993), Dos Santos (1997), Robinson et al. (2003), Kirkham (2005), Baran (2005) etc.

For the monitoring of soil moisture in Wadi Jir watershed, the TDR (Time Domain Reflectometry) has been chosen. The TDR is a digital oscilloscope coupled to a pulse generator, connected via a coaxial cable and a connection head to a variable-length transmission line, which is called the probe. The measuring principle is based on the determination of the propagation time of an electromagnetic pulse along an electrode introduced into the soil. The propagation time of pulse depends heavily on soil moisture (Eijkelkamp 2003 and Topp et al. 2003).

Although the TDR was factory calibrated with standard calibration, we used two methods to check it. First one using the calibration set supplied with the equipment (glass beads). After two measurements, one in dry and one in water saturated glass beads, the calibration data was compared with the reference values. The second method was by comparing two techniques simultaneously in the laboratory, those being the TDR and the gravimetric methods. Even with all the errors, the results showed that the TDR is operating properly.

Synthesis of the Soil Profiles Study

To characterize the soil of the studied *jessour*, we conducted surveys of some representative profiles at the rate of one profile in each *jesr* bed. The *jessour* soils are alluvial soils poor in organic matter occupying the talwegs. Texture data show some consistency between 0 and 1.5 m. Thus three sites, Tijma, Téchine, and Adbach can be classified (French classification) as sandy silt to silty sand.

In the *jesr* of Tijma, soils are thick sandy silt soil (over 1.2 m). Samples from the first meter of soil show a small variation in soil particle size with 67–84% sand, 5–13% silt, and 9–18% clay (Fig. 10.2a).

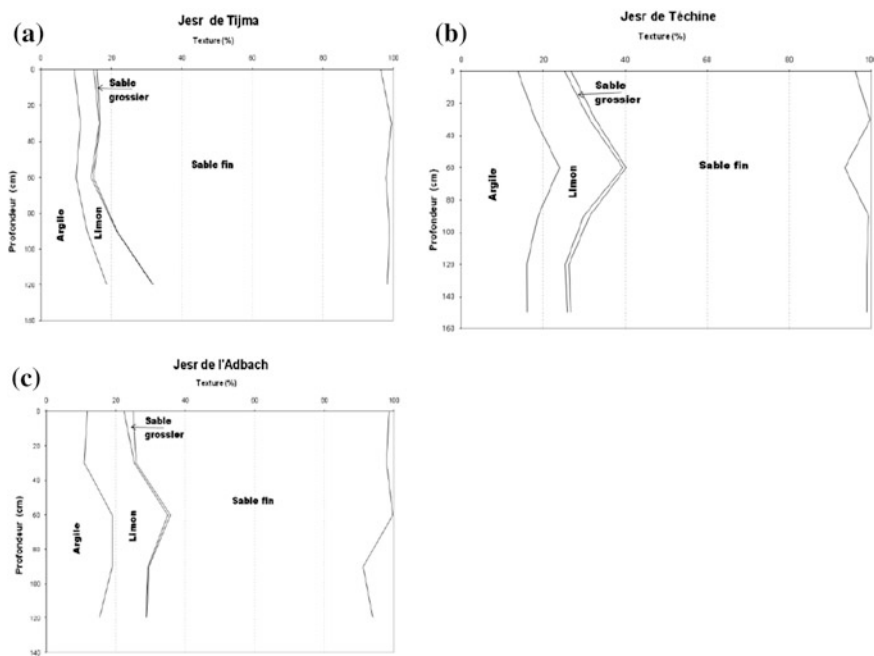


Fig. 10.2 Particle size distribution by soil depth of the three sites **a** Tijma, **b** Téchine and **c** Adbach

The results of particle size analysis of Téchine site are shown in Fig. 10.2b). The terrain is silty-sand with 14–24% clay, 10–16% silt, and 56–74% sand. Note that, contrary to the *jesr* of Tijma where the soil is very sandy at the surface, Téchine trench was dug on very clay and silt plot to 0.5 m deep. Clear limit between the sediment and bedrock is around 1.50 m deep.

The Adbach site is also, as the case of Téchine, silty sand soil with 12–20% clay, 10–17% silt, and 63–77% sand. Figure 10.2c also shows a clay and silt layer between the depth of 0.5 and 0.8 m.

For the three sites, coarse sand rate is less than 1%, except for the case of Adbach where coarse sand rate exceeds the rate of 2% at the soil surface.

Results and Discussion

Temporal Evolution of Water Reserve

The total available water capacity (AWC) is defined as the portion of water available for the vegetation between field capacity and the permanent wilting point water contents (Peiffer 2005).

The two limits of available water capacity (AWC) used in this study correspond to the theoretical threshold set by agronomists to plant crops which by convention corresponds to a $pF = 4.2$, a commonly used value for permanent wilting point (PWP) (Peiffer 2005), and a $pF = 2.5$, a maximum value reached in the field capacity (FC).

Comparison of Average Soil Moisture and at Different Depths with Laboratory Measures at PF2.5 and PF4.2

The volumetric soil moisture content was measured at different depths, in order to take into account, the vertical variability. Unlike surface moisture which is experiencing strong variations (precipitation, rapid evaporation...), moisture of the deep root zone is that really used by vegetation (Gruhier 2010). So the moisture throughout the root zone that has a real impact on exchanges soil-plant-atmosphere (Milly 1992; de Rosnay 1999).

Figure 10.3 shows the soil moisture measurements at eight levels (0–15, 15–30, 30–45, 45–60, 60–75, 75–90, 90–105, and 105–120 cm depth) for a period of 4 years. Note that without effective rainfall during the first two years of measurement (from 29/10/2009 to 01/10/2011), the water content in the surface layers, to a depth of 60 cm, remains below moisture at wilting point (PWP = 10.2%). The deeper horizons, have a moisture evolving between moisture at field capacity (CC = 14.6%) and soil moisture at the wilting point (PWP = 10.2%), with a higher water content in the horizons of depth beyond 1 m. The average of profile soil moisture rate tends toward the value of moisture at the wilting point (PWP = 10.2%) almost for the entire study period except for periods after the effective rainfall events. After the rain of 10/03/2012, there is maximum soil

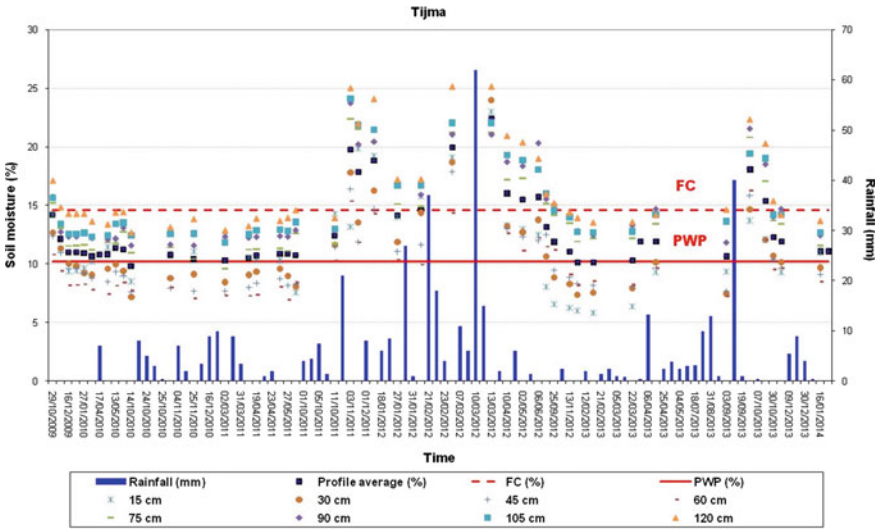


Fig. 10.3 Variation of average soil moisture (% vol.) at different depths in the *jesr* of Tijma

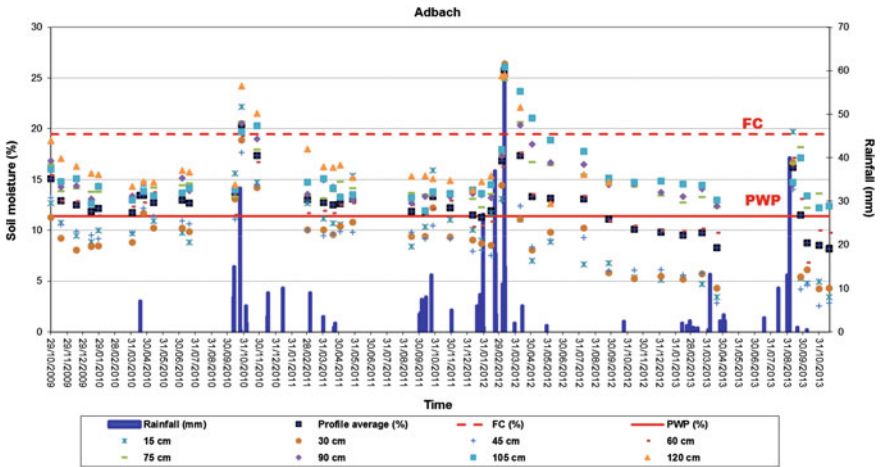


Fig. 10.4 Variation of average soil moisture (% vol.) at different depths in the *jesr* of Adbach

moisture for all horizons with a maximum of average profile of 25.7%. Almost one year later (03/01/2013), the difference in moisture between the surface horizons (depth < 60 cm) and deeper horizons is amply clear. If the superficial horizons remain below the soil moisture at the wilting point (PWP = 10.2%), with a maximum moisture content of 8%, horizons beyond 60 cm depth provide water reserve easily used by the plant (12% < soil moisture < 14%).

Variation of average soil moisture at different depths in the *jesr* of Adbach (Fig. 10.4) shows the same trend as that recorded for the *jesr* of Tijma.

Note that the surface horizons, to a depth of 45 cm, were the driest horizons for the whole profile. The deeper horizons provided water reserves significantly higher than the moisture at permanent wilting point (PWP = 11.4%). Rain recorded in March 10, 2012 produced a maximum of average soil moisture of whole profile of 25.7%. After this rain which maximized the soil moisture for all horizons, there was a dryness in the superficial layers, with lost water that exceeds 50% (soil moisture < 11%), while the deeper horizons remained with soil moisture exceeding moisture at FC. The minimum average soil moisture of the whole profile (9.5%) remained under PWP.

Almost one year later (January 3, 2013), the drying up of superficial layers significantly increase (for soil depths of 15 cm, 30 cm and 45 cm, the recorded soil moisture is 5.2%, 5.5% and 6.2 % respectively). However, the horizons at the depth deeper than 60 cm provide useful water reserve for the plant (13% < soil moisture < 15%).

Variation of moisture in the *jesr* of Téchine (Fig. 10.5) looks different from the evolution recorded in the *jessour* of Tijma and Adbach. The moisture content for all horizons reign below the value of moisture at the permanent wilting point (PWP = 11%) almost for the entire study period except for the periods after the effective rainfall events. Major fluctuations in moisture during precipitation are felt along all the profile, also the drying throughout the profile is in a very fast way. Water reserve in surface soil layers (depth of 30, 45 cm and with less degree the horizon of 15 cm), was consistently greater than the water reserve in the deeper soil layers.

A year without effective rainfall causes a serious drying of the profile. Average moisture rates decrease enormously to go down under permanent wilting point (PWP = 11%). In 22/03/2013, surface layers (depth < 45 cm) have soil moisture ranging between 4 and 6%. The moisture contents of the deeper layers were lower, varying between 3 and 5%.

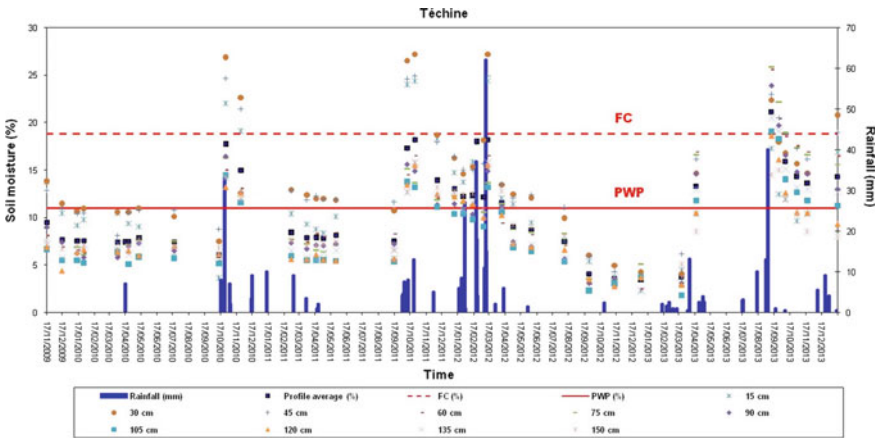


Fig. 10.5 Variation of average soil moisture (% vol.) at different depths in the *jesr* of Téchine

We can conclude that during one hydrological year, water withdrawals differ according to the soil horizons. In wet season, when the soil is well supplied with water, upper horizons provide water to olive trees and potential intercropping. However, during summer period, deep horizons provide water to olive trees to better withstand dry episode.

The permanent wilting point is defined as the water potential from which roots can no longer extract water. However, the soil of *jessour* was able to provide water to adult olive trees up theoretical value of -1.5 MPa ($pF = 4.2$), and this for a long time, especially for the case of *jesr* Téchine. This intense and prolonged dryness caused no mortality of olive trees. This example highlights that the use of theoretical potential at permanent wilting point ($pF = 4.2$) does not represent the real extraction capacity of olives and tends to underestimate the amount of water that can extract adult olive trees. This conclusion is confirmed by Bréda et al. (1995) for sessile oaks in eastern France and Aussenac et al. (1982) for adult individuals of *Quercus* and various *Pinus* in the Mont Ventoux. Even some annual crops (soybeans, alfalfa, corn) can sometimes exploit soil water at a rate lower than that of wilting point (Duchaufour et al. 1979).

Evolution of Soil Water Storage During the Study Period (4 Years)

Soil water (Sw) is calculated using measurements of volumetric soil moisture at each horizon. Quantification of soil water storage is based on the application of the law of continuity. Soil water is the product of the soil layer height by the corresponding volumetric soil moisture.

Thus, soil water stock may be presented by the following two equations (Bréda et al. 2002):

$$Sw(\text{layer}) = \text{Volumetric soil moisture} * \text{Thickness of layer} * \text{Stone in layer} \quad (10.1)$$

$$Sw_{(\text{sol})} = \sum_{i=1}^n Sw(\text{layer}_i) \quad (10.2)$$

$$\text{Stone in layer} = \frac{100 - Sc}{100} \quad (10.3)$$

Sc: stone content (%)

The stone content in *jessour* is considered equal to zero, thus, the load equal to 1.

The depth of soil to be considered is a particularly delicate issue in forest (Bréda et al. 2002). For olive trees in *jessour*, the approximation made consisted of taking

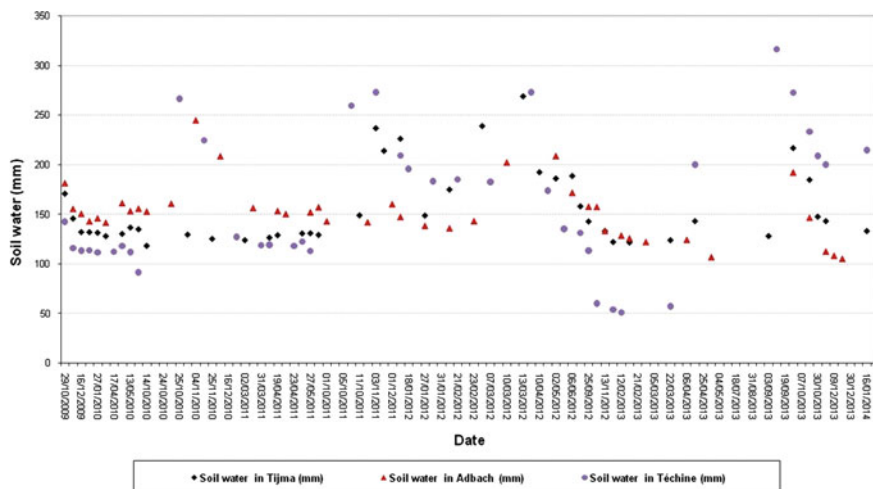


Fig. 10.6 Soil water content (% vol.) evolution during the study period (4 years) in three *jessour*; Téchine, Tijma and Adbach

the depth of sediment in the bed of *jessour* (until bedrock which constitutes a mechanical barrier to the penetration of big roots) as the profile thickness.

Monitoring water content of *jessour* soil (Fig. 10.6) shows that the *jessour* ensures permanent water storage in soil, which varies on average between 100 and 200 mm. On the other hand, it is almost nil outside the *jessour* technique. In wet periods, soil water in the *jessour* may exceed the 300 mm with extreme minimum (50 mm) recorded in the *jessour* of Téchine during drought.

Thus, *jessour*, while ensuring effective erosion control in Matmata mountains, they could restore the broken ecological balance and could enhance the value of water resources in soil.

Soil Water Evolution During One Hydrological Year

Figures 10.7 and 10.8 shows the soil water evolution during a full hydrological year and allow to check two observations

- Soil water changes are rapid when the rains are effective (effective rain is rain that causes an accumulation of run-off water in the bed of *jessour*).
- Only one effective rainfall annually ensures sufficient water supply for the rest of the hydrological year.

In mid-October, after a dry summer, water reserve is very low and in the range of 91 mm in Téchine for a soil depth of 1.50 m and 186 mm in Adbach for soil thickness of 1.20 m (Fig. 10.7.). After the rain of October 24, 2010 (33 mm), the

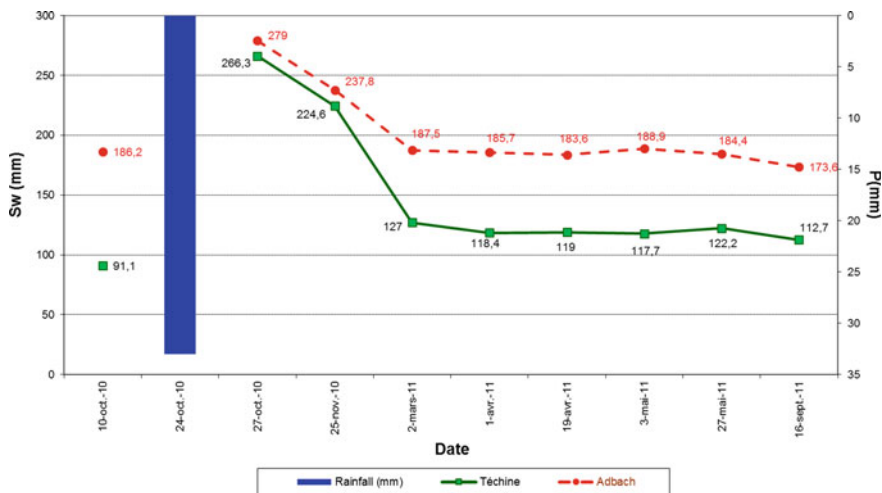


Fig. 10.7 Available soil water (mm) variation in Téchine and Adbach *jessour* (hydrological year 2010–2011)

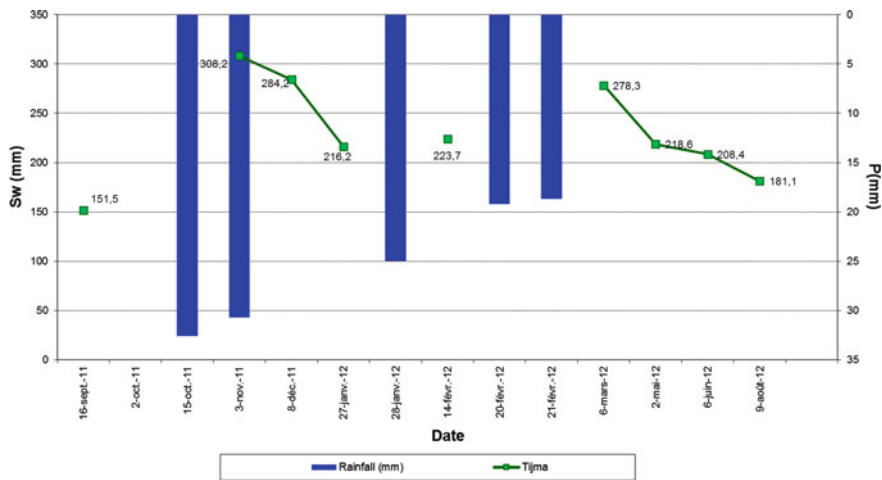


Fig. 10.8 Available soil water (mm) variation in Tijma *jessr* (hydrological year 2011–2012)

largest part of water reserve is restored, reaching the value of 266 mm in Téchine and 279 mm in Adbach in October 27, 2010. Soil water changes, in the *jessr* of Tijma, follows the same appearance as the other two *jessour* (Fig. 10.8).

Since the hydrological year 2010/2011 recorded no effective rainfall in the *jessr* of Tijma, we chose that of 2011/2012 instead of the hydrological year 2010/2011 used in the other two sites.

At the end of the hydrological year, soil water in the soil of three *jessour* is very similar to that established at the beginning of the hydrological year. Therefore, it is a kind of equilibrium position of the water balance established following a single effective rainfall.

We can conclude that the *jesr*, though plays an important role in reducing transport of water and sediment downslope (Schiettecatte et al. 2005), even with a single effective rainfall, can mobilize supplementary water that can significantly improve the water balance. These additional mobilized water quantities are really a good indication of soil retention capacity of the *jessour*, therefore, the effectiveness of *jessour* system.

Conclusions

The volumetric soil moisture monitored by TDR measurement shows a drying tend in surface layer for both *jessour* of Tijma and Adbach, but stability between the surface and deep layers in *jesr* of Téchine.

Only one effective rainfall annually can ensure sufficient water supply for the rest of the hydrological year.

During one hydrological year, water withdrawals differ according to the soil horizons. During wet periods, olive trees extract water from upper soil horizons whereas they exploit the deeper horizons during summer and drought periods.

The soil of *jessour* was able to provide water to adult olive trees up theoretical value of -1.5 MPa ($pF = 4.2$), and this for a long time, especially for the case of *jesr* Téchine. This intense and prolonged dryness caused no mortality of olive trees. This example highlights that the use of theoretical potential at permanent wilting point of $pF = 4.2$ seems to be inadequately adapted to olive extraction capabilities and tends to underestimate the amount of water that can extract the adult olive trees.

The *jesr* ensures water storage in soil, which varies on average between 100 and 200 mm. However, in wet periods, this storage *jesr* can exceed 300 mm but can drop as low as 50 mm in dry periods (as recorded in the *jesr* of Téchine). These additional mobilized water quantities are really a good indication of soil retention capacity of the *jessour*, therefore, the effectiveness of *jessour* system.

Jessour can adequately ensure water supply of olive trees while ensuring effective erosion control in the mountains of Matmata and landscape ecology enhancement.

The study has been able to

- Quantify the soil moisture, thus, the reserve of water in the soil, in order to improve our knowledge exchanges soil-vegetation-atmosphere in the *jessour*; and,
- Illustrate the effectiveness of *jessour* system in terms of enhancing the value of water resources.

Acknowledgements This work was conducted as part of the research program ‘Monitoring of desertification and conservation and valorization of water and soil resources’ of laboratory of Eremologie and Combating Desertification funded by the Institution of Agricultural Research and Higher Education (IRESA) and the Ministry of Higher Education and Scientific Research (MERST) (Tunisia).

References

- Abdelli F, Ouessar M, Khatteli H (2012) Méthodologie d’identification des ouvrages existants et des sites potentiels pour les *jessour*. *Rev Sci Eau* 25(3):237–254
- Ancitil F, Michel C, Perrin C, Andreassian V (2004) A soil moisture index as an auxiliary ANN input for stream flow forecasting. *J Hydrol* 286:155–167
- Aussenac G, Valette JC (1982) Comportement hydrique estival de *Cedrus atlantica* Manetti, *Quercus ilex* L. et *Quercus pubescens* Willd., et de divers pins dans le Mont Ventoux. *Ann Sci Forest* 39(1):41–62
- Baran N (2005) Suivi de la teneur en eau des sols dans les bassins du Gardon d’Anduze et du Touch. BRGM/RP-53654-FR, 38p
- Berthet L, Andréassian V, Perrin C, Javelle P (2009) How crucial is it to account for the Antecedent Moisture Conditions in flood forecasting? Comparison of event-based and continuous approaches on 178 catchments. *Hydrol Earth Syst Sci* 13:819–831
- Bréda N, Granier A, Barataud F, Moyne C (1995) Soil water dynamics in an oak stand. I. Soil moisture, water potentials and water uptake by roots. *Plant Soil* 172:17–27
- Bréda N., Lefèvre Y., Badeau V. 2002. Réservoir en eau des sols forestiers tempérés: spécificité et difficultés d’évaluation. *La Houille Blanche*, n°3, spécial «Forêts et Eau»: 24–32
- Brocca L, Moramarco T, Melone F, Wagner W, Hasenauer S, Hahn S (2012) Assimilation of surface and root-zone ASCAT soil moisture products into rainfall–runoff modelling. *IEEE Trans Geosci Remote Sens* 50(7):2542–2555
- Brunet P., Bouvier C., Perrin J.L., Robain Henri 2003. Suivi annuel des variations de l’humidité du sol à l’aide de sondages Schlumberger. In: *Géophysique des sols et des formations superficielles: Geofcan: actes du 4^{ème} colloque*. Paris (FRA); Paris: University Pierre et Marie Curie; IRD, 2003: 130–136. Colloque Geofcan, 4. Paris (FRA), 2003/09/23-24
- Chaouch N (2008) Détermination de l’humidité du sol dans le bassin versant du Mackenzie à partir des données satellitaires AMSR-E. Ph.D., université du Québec, Canada. pp 176
- De Rosnay P (1999) Représentation de l’interaction sol-végétation-atmosphère dans le modèle de circulation générale du Laboratoire de Météorologie Dynamique. Université Pierre et Marie Curie, Paris VI, Thèse de doctorat, p 176
- Destouni G, Verrot L (2014) Screening long-term variability and change of soil moisture in a changing climate. *J Hydrol* 516:131–139
- Dos Santos P (1997) Développement d’une nouvelle méthode de détermination des profils de teneur en eau dans les sols par inversion d’un signal TDR. Ph.D. thesis, Lab. d’Etude des Transf.en Hydrol. et Environ (LTHE), Univ. Joseph Fourier-Grenoble I, Grenoble, France. 144p
- Duchaufour P, Bonneau M, Souchier B (1979) *Pédologie 2. Constituants et propriétés du sol*. Masson, Paris, p 459p
- Eijkelkamp (2003) TRIME-FM. User manual. pp 24
- El Amami S (1984) Les aménagements hydrauliques traditionnels en Tunisie. Centre de Recherche en Génie Rural (CRGR), Tunis, Tunisia, p 69
- Entekhabi D, Njoku GE, O’Neill EP, Kellogg HK, Crow TW, Edelstein NW, Entin KJ, Goodman DSh, Jackson JT, Johnson J, Kimball J, Piepmeier RJ, Koster DR, Martin N, McDonald CK, Moghaddam M, Moran S, Reichle R, Shi JC, Spencer WM, Thurman WS, Tsang L, Van Zyl J (2010) The soil moisture active passive SMAP mission. *Proc IEEE* 98(5):704–716 (2010)

- Fares A, Temimi M, Morgan K, Kelleners TJ (2013) In-situ and remote soil moisture sensing technologies for vadose zone hydrology. *Vadose Zone J* 12
- Gheris A (2014) Détermination de la variabilité de l'humidité surfacique des sols par les techniques de télédétections. 1er Colloque International Sol, Eau et Environnement (CISEE'2014), Université d'Annaba, Algérie. p 6
- Gruhier C (2010) L'humidité du sol par télédétection micro-ondes en région Sahélienne. Université Pierre et Marie Curie, Paris VI, Thèse de doctorat, p 120
- Hu W, Cheng Si B (2014) Can soil water measurements at a certain depth be used to estimate mean soil water content of a soil profile at a point or at a hillslope scale? *J Hydrol* 516:67–75
- Huza J, Teuling AJ, Braud I, Grazioli J, Melsen LA, Nord G, Raupch TH, Uijlenhoet R (2014) Precipitation, soil moisture and runoff variability in a small river catchment (Ardèche, France) during HyMeX special observation period 1. *J Hydrol* 516:330–342
- Kirkham MB (2005) Principles of soil and plant water relations, chap 13. Elsevier Academic Press, pp 187–202
- Komma J, Blöschl G, Reszler C (2008) Soil moisture updating by Ensemble Kalman Filtering in real-time flood forecasting. *J Hydrol* 357(3–4):228–242
- Massari C, Brocca L, Barbetta S, Papathanasiou C, Mimikou M, Moramarco T (2013) Using globally available soil moisture indicators for flood modelling in Mediterranean catchments. *Hydrol Earth Syst Sci Discuss* 10:10997–11033
- Milly PCD (1992) Potential evaporation and soil moisture in general circulation models. *J Clim* 5:209–226
- Morbideilli R, Corradini C, Saltalippi C, Brocca L (2012) Initial soil water content as input to field-scale infiltration and surface runoff models. *Water Resour Manage* 26:1793–1807
- Nunzio R (2014) Soil moisture at local scale: measurements and simulations. *J Hydrol* 516:6–20
- Ouessar M (2007) Hydrological impacts of rainwater harvesting in wadi oum Zessar watershed (Southern Tunisia). Faculty of Bioscience Engineering, Ghent University, Belgique, Thèse de doctorat, p 154
- Peiffer M (2005) Paramétrisation du bilan hydrique et établissement des flux d'eau et de nutriments dans des séquences de hêtres de plaine. Thèse de Doctorat, Spécialité, Sciences forestières. ENGREF, paris, p 135
- Piedallu Ch (2012) Spatialisation du bilan hydrique des sols pour caractériser la distribution et la croissance des espèces forestières dans un contexte de changement climatique. PhD, Sciences forestières et du bois – AgroParisTech. Nancy – France. p 282
- Rahman MM, Lu M, Kyi KH (2015) Variability of soil moisture memory for wet and dry basins. *J Hydrol* 523:107–118
- Robinson DA, Jones SB, Wraith JM, Or D, Friedman SP (2003) A review of advances in dielectric and electrical conductivity measurement in soils using time domain reflectometry. *Vadose Zone J* 2(4):444–475
- Schietecatte W, Ouassar M, Gabriels D, Tanghe S, Heirman S, Abdelli F (2005) Impact of water harvesting techniques on soil and water conservation: a case study on a micro catchment in southeastern Tunisia. *J Arid Environ* 61:297–313
- Schmugge TJ, Jackson TJ, McKim HL (1980) Survey of methods for soil moisture determination. *Water Resour Res* 16(6):961–979
- Sheikh V, Visser S, Stroosnijder L (2009) A simple model to predict soil moisture: bridging event and continuous hydrological (BEACH) modelling. *Environ Model Softw* 24:542–556
- Shin Y, Mohanty BP (2013) Development of a deterministic downscaling algorithm for remote sensing soil moisture footprint using soil and vegetation classifications. *Water Resour Res* 49. doi:10.1002/wrcr.20495
- Sun Y, Zhou H, Qin Y, Schulze LP, Berg A, Deng H, Cai X, Wang D, Jones SB (2014) Horizontal monitoring of soil water content using a novel automated and mobile electromagnetic access-tube sensor. *J Hydrol* 516:50–55
- Topp GC (1993) Soil water content, chap 51. In: Editeur Carter MR (ed) Soil sampling and methods of analysis. Lewis Publishers, Boca Raton

- Topp GC, Davis JL, Annan AP (2003) The early development of TDR for soil measurements. *Vadose Zone J* 2:492–499
- Tramblay Y, Bouaicha R, Brocca L, Dorigo W, Bouvier C, Camici S, Servat E (2012) Estimation of antecedent wetness conditions for flood modelling in Northern Morocco. *Hydrol Earth Syst Sci* 16:4375–4386
- Van Steenberg N, Willems P (2013) Increasing river flood preparedness by realtime warning based on wetness state conditions. *J Hydrol* 489:227–237
- Zhang H, Shao M (2014) Spatio-temporal variability of surface soil water content and its influencing factors in a desert area, China. *Hydrol Sci J* 60(1):96–110 (2015)

Chapter 11

Direct and Residual Effect of Sewage Sludge in a Sudangrass-Barley Cropping System

Rajia Kchaou, Mohamed Naceur Khelil, Saloua Rejeb,
Belgacem Henchi and Jean Pierre Destain

Abstract In Tunisia, agricultural soils are subjected to progressive degradation. Application of sewage sludge is an important way to recycle nutrient elements and improve soil fertility and physical properties, causing an increase in crop yield. A field experiment was carried out, using ^{15}N isotope techniques, to investigate the effects of labeled sewage sludge (3.7% N, 2.3 atom%) application on sudangrass and its residual effects on barley crops. Sewage sludge was applied at rates equivalent to 113, 226, and 338 kg N ha⁻¹. In addition, one control (no treatment) was also included in the experiment. Sewage sludge application increased the sudangrass yield and total nitrogen uptake as compared to the control treatment. A positive residual effect of sewage sludge application was also observed on yield and N uptake of the subsequent barley crop.

Keywords Sudangrass · Barley · ^{15}N · Sewage sludge

R. Kchaou (✉)

Regional Field Crop Research Center, BP 350, 9000 Beja, Tunisia
e-mail: rajiakm@yahoo.fr

M.N. Khelil · S. Rejeb

National Research Institute of Rural Engineering, Water and Forest,
BP 10, 2080 Ariana, Tunisia
e-mail: khelil_mn@yahoo.fr

B. Henchi

Science Faculty, Biology Department, Tunis Université El-Manar,
2092 Tunis, Tunisia
e-mail: belgacem.hanchi@inrap.mrt.tn

J.P. Destain

The Wallon Agricultural Research Center, 5030 Gembloux, Belgium
e-mail: destain@cra.wallonie.be

© Springer International Publishing AG 2017

M. Ouassar et al. (eds.), *Water and Land Security in Drylands*,
DOI 10.1007/978-3-319-54021-4_11

Introduction

Sewage sludge is a by-product of the treatment of municipal wastewater. Increasing costs of commercial fertilizers, decreasing soil organic matter content with the consequent decrease of soil fertility, and the large amounts of sewage sludge produced worldwide have combined to make cropland application of this residue an attractive disposal option. Many studies have demonstrated the positive effect that land application of sewage sludge has on soils and crop production particularly as a natural source of nitrogen (Akdeniz et al. 2006; Azam et al. 2003; Camilotti et al. 2006; Gutser et al. 2005; Kchaou et al. 2010, 2015; Lasa et al. 2004; Topcuoglu et al. 2003). However, there is little data available on the likely magnitude of the residual value of sewage sludge and its rate of release in subsequent years. This information would be particularly valuable for land that receives sludge regularly where the accumulated residual effects could make a significant contribution in further reducing the requirement for nitrogen fertilizer.

This work aims to investigate the direct and residual effects of using sewage sludge as a nitrogen source on the yield and N uptake in a sudangrass-barley cropping system. For this purpose, ^{15}N isotopic techniques are used to discern the origins of N removed and to quantify the real recovery of ^{15}N labeled sewage sludge by plants.

Materials and Methods

A field trial was conducted at the experimental field of the Rural Water and Forest Research Institute, Tunisia, on a sandy loam soil with 13% clay, 2% C, and 0.055% total N and a pH of 7.7.

An experiment using square microplots (1 m^2) was established utilizing a completely randomized block. The microplots were delimited with galvanized metal barriers that penetrated to a depth of 20 cm and stood 10 cm above the soil surface. Four rates of ^{15}N -labeled sewage sludge (0, 3, 6, and 9 t dry matter (DM) ha^{-1}), providing a total of 113, 226 and 338 kg N ha^{-1} , were applied with four replicates for a final total of 16 plots. The main chemical characteristics of sludge utilized in this study are given in Table 11.1.

To label the sewage sludge, ^{15}N urea (approximately 10% atom excess) diluted with distiller water was mixed with sewage sludge. The mixture was then covered with impermeable paper to minimize the evaporation of water and the loss of N by volatilization and denitrification. Incubation was then conducted under laboratory conditions for 20 days. The sludge nitrogen had a ^{15}N atom excess of 2.3%. Analysis of five different samples gave similar results ($\pm 5\%$ difference between results); which indicates that the labeling was homogeneous.

The ^{15}N -labeled sewage sludge was applied to the soil surface 10 days before sowing.

Table 11.1 Chemical characteristics of sewage sludge utilized in experiments

Characteristics	Units	Sewage sludge
H ₂ O	%	7.8
pH	–	8.08
Total C	%	19.49
Total N	%	3.76
NH ₄ ⁺ -N	%	0.89
Total P	%	1.73
K	%	0.4
Na	%	0.24
Ca	%	8.7
Mg	%	0.58
Cd	mg/kg	0.89
Co	mg/kg	9.28
Cr	mg/kg	97.5
Cu	mg/kg	180.4
Fe ‰	mg/kg	12.5
Mn	mg/kg	155
Ni	mg/kg	28.6
Pb	mg/kg	79.5
Zn	mg/kg	490.2

Heavy metals concentration was below the limits of Tunisian (NT 106.20) legislation about agricultural use of sewage sludge

The microplots were arranged to include four rows of sudangrass (*Sorghum sudanense*) with spacing of 30 cm between rows and 15 cm within rows resulting in seven plants in each row. Sudangrass was irrigated with a watering can. Irrigation water was applied to compensate for evapotranspiration, which was 6–7 mm/day during the experimental period. Approximately 40 mm of water per week were added to each microplot, at a frequency of two irrigations per week.

Two harvests were conducted at the beginning of the flowering stage, after which the yield was measured. Ten central sudangrass plants were used to estimate the fertilizer N recovery. In the first harvest, only the above-ground portions of the plants were collected, while in the final harvest, the whole plants were collected. After that, barley (*Hordeum vulgare*) was sown in the same microplots previously used in four rows (30 cm row spacing). No fertilization was applied as the goal was to determine the residual effect of sewage sludge in barley crops. The barley harvest was taken when plants were at the beginning of the flowering stage. All plant samples were dried at 80 °C, weighed and then grounded. The plant samples were then analyzed for total N and ¹⁵N using a Dumas analyzer coupled with a mass spectrometer (Europa Scientific, UK).

Enrichments are all calculated by $E = A - A_a$ where: A and A_a are the ¹⁵N abundance, respectively, for the plant samples determined by mass spectrometry and for the air, with A_a = 0.3663 atom% ¹⁵N.

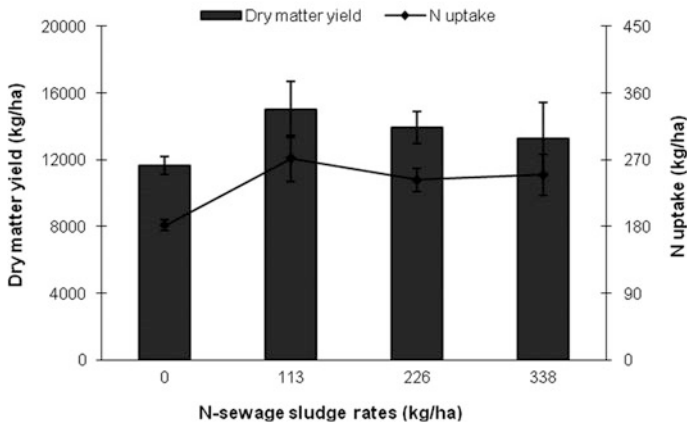


Fig. 11.1 Sudangrass response to sewage sludge application. The vertical bars represent the standards deviation of the averages carried out on four repetitions

The percentage nitrogen derived from fertilizer (NDFP %) and soil (NDFS %) were calculated as follows:

$$\text{NDFP \%} = (E_{\text{pl}}/E_{\text{f}}) * 100,$$

where E_{pl} and E_{f} were the ^{15}N enrichments measured for the plants and the fertilizer, respectively.

$$\text{NDFS \%} = 100 - \text{NDFP\%}$$

The results were assessed using the STAT-ITCF (Ver.V). Analysis of variance was conducted using the Fisher test at the 0.05 level of probability. Differences among means were then evaluated using the Newman and Keuls test. All data shown represent the means \pm the standard deviations of quadruplicate measurements.

Results and Discussion

Dry Matter Production and Nitrogen Uptake by Sudangrass

Sudangrass yield was 11.6 t ha^{-1} in the control (without N) and increased to 15 t ha^{-1} with the lowest rate of sewage sludge. However, there were no significant yield differences among the three sewage sludge treatments. The trends in N uptake were in general similar to those observed for dry matter production (Fig. 11.1). The largest N uptake, 272 kg N ha^{-1} , was attained with 3 t ha^{-1} of sewage sludge.

Sewage sludge application rates above these levels did not lead to additional increases in nitrogen uptake by sudangrass (Fig. 11.1).

In agreement with Powel and Hons (1992), we hypothesized that application of nitrogen as sewage sludge at a rate of 113 kg ha⁻¹ could supply the N requirement of sudangrass; and, indeed, this amount was sufficient to achieve the largest sudangrass yield. Therefore we can conclude that greater amounts of sewage sludge are not recommended since amounts larger than 113 kg ha⁻¹ did not show further increases in dry matter production of sudangrass but did result in significant increases in soil residue nitrate, which could result in N losses (Keskin et al. 2009).

Dry Matter Production and Nitrogen Uptake by Barley

In order to assess the effect of residual N from the previously applied sludge, barley was planted soon after sudangrass harvest with no N added.

Dry matter production represented in Fig. 11.2 showed a significant increase in plots previously amended with sewage sludge in reference to the control treatment with no N applied, but it was unaffected by sewage sludge rates.

The positive residual effect of sewage sludge was reported by other authors and it was generally attributed to the increase of N uptake. Guster et al. (2005) found that nitrogen from sewage sludge often showed little effect on crop growth in the year of application, because of the slow-release characteristics of organically bound N. Furthermore, N immobilization after application can occur, leading to an enrichment of the soil N pool and an increase in the long term of N-use efficiency. Others investigators (Chang et al. 1982; Magdoff and Amadon 1980) explained the residual effect of sewage sludge by the fact that the nitrogen is released continually at slow rate from sewage sludge, resulting in a beneficial extended availability of N after long-term application of sewage sludge.

Fig. 11.2 Residual effect of sewage sludge application on barley above-ground dry matter production. The vertical bars represent the standards deviation of the averages carried out on four repetitions

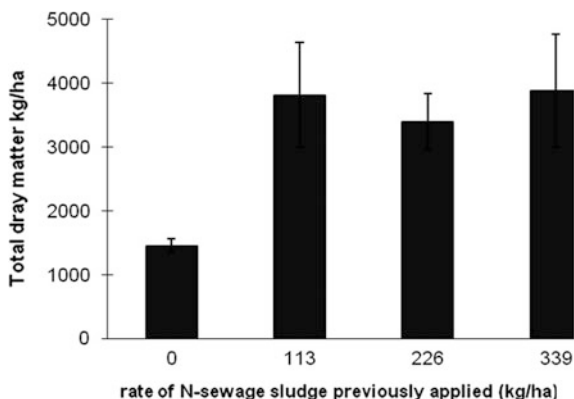
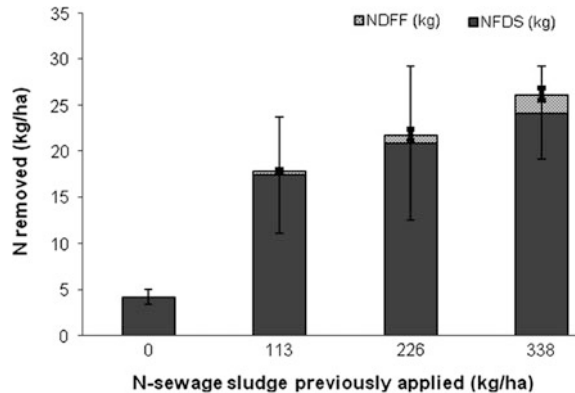


Fig. 11.3 Residual effect of sewage sludge application on nitrogen removed (NDFS and NDFF) by barley above-ground. The *vertical bars* represent the standards deviation of the averages carried out on four repetitions



Nitrogen Derived from Sewage Sludge and from Soil in Barley Crop

Figure 11.3 shows that the total amounts of nitrogen removed by barley in the above-ground biomass increased by 18 kg on average with previous sewage sludge application in comparison with the control. The amounts of ^{15}N sewage sludge removed by barley crops were relatively small in comparison with the amounts of soil N removed (NDFS) (Fig. 11.3).

Fortunately, however, the low efficiency of fertilizer N is compensated by an increase in N availability from soil N expressed by an increase of the amounts of soil N removed in the plots previously amended and in comparison with the control. This increase may be attributed to a priming action or priming effect of the residual added N (Azam 2002). Alternatively, the residual ^{15}N interacts with the native soil N in a way to increase the availability of the later. Stimulation in root proliferation may be suggested as the mechanism responsible for the increase in the uptake of native soil N, through increased microbial activities (Kuzyakov et al. 2000; Zagal 1994). Moreover, enhanced mineralization of native soil N in the fertilized plots can be considered as one of the majors' factors in enhancing barley yields (Azam 1990).

Conclusion

The results obtained in the present study prove the beneficial effects of sewage sludge in sudangrass and barley productions provide an indication of the amounts of N that might be supplied by sewage sludge at the rates applied and confirm that sewage sludge can substitute for commercial fertilizers if applied in the right amounts to soil. Nevertheless, long-term field studies are needed to obtain more accurate assessments of their fertilizing capacity and environmental impact to contribute to the development of sustainable agricultural practices.

References

- Akdeniz H, Yilmaz I, Bozkurt MA, Keskin B (2006) The effect of sewage sludge and nitrogen application on grain sorghum grown (*Sorghum vulgare* L.) in Van Turkey. *Pol J Environ Stud* 15:19–26
- Azam F (1990) Comparative effects of an organic and inorganic nitrogen source applied to flooded soil on rice yield and availability of N. *Plant Soil* 125:255–260
- Azam F (2002) Added nitrogen interaction in the soil-plant system. *Pak J Aronomy* 1:54–59
- Azam F, Lodhi A, Sajjad MH (2003) Response of rice to nitrogenous fertilizer and irradiated sewage sludge. *Pak J Sci Ind Res* 46
- Camilotti F, Andrioli I, Marques MO, Silva AR, Tasso Junior LC, Nobile FO, Nogueira Gde A, Prati F (2006) Productivity and agroindustrial quality of sugarcane cultivated with sewage sludge, vinasse and mineral fertilizers. *Stab-Acucar, Alcool E Subprodutos* 24:32–35
- Chang AC, Page AL, Bingham FT (1982) Heavy metal absorption by winter wheat following termination of cropling sludge application. *J Environ Qual* 11:705–708
- Guster R, Ebertseder T, Weber A, Schraml M, Schmidhalter U (2005) Short-term and residual availability of nitrogen after long-term application of organic fertilizer on arable land. *J Plant Nutr Soil Sci* 168:439–446
- Kchaou R, Khelil MN, Gharbi F, Rejeb S, Henchi B, Hernandez T, Destain JP (2010) Isotopic evaluations of dynamic and plant uptake of n in soil amended with ¹⁵N-labelled sewage sludge. *Pol J Environ Stud* 19(2):363–370
- Kchaou R, Khelil MN, Rejeb S, Henchi B, Destain JP (2015) Sorghum recovery and immobilization of ¹⁵N labeled urea-N as affected by sewage sludge co-application. *J Adv Agr* 363–370
- Keskin B, Yilmaz IH, Bozkurt MA, Akdeniz H (2009) Sewage sludge as nitrogen source for irrigated Silage Sorghum. *J Anim Vet Adv* 8(3):573–578
- Kuzyakov Y, Ehrensberger H, Stahr K (2000) Carbon partitioning and below-ground translocation by *Lolium perenne*. *Soil Biol Biochem* 32:1485–1498
- Lasa B, Quemada M, Frechilla S, Muro J, Lamsfus C, Aparicio-Tejo PM (2004) Effect of digested sewage sludge on the efficiency of N-fertilizer applied to barley. *Nutr Cycl Agroecosyst* 48:241–246
- Magdoff FR, Amadon JF (1980) Nitrogen availability from sewage sludge. *J Environ Qual* 9: 451–455
- Powel JM, Hons FM (1992) Fertilizer nitrogen and stover removal effects on sorghum yields and nutrient uptake and partitioning. *Agr Ecosyst Environ* 39:197–211
- Topcuoglu B, Onal MK, Ari N (2003) Effects of the soil application of municipal sewage sludge on tomato plant. I. Plant nutrient and heavy metal contents. *Ziraat Fakultesi Dergisi Akdeniz Universitesi* 16:87–96
- Zagal E (1994) Influence of light intensity on the distribution of carbon and consequent effects on mineralisation of soil nitrogen in a barley (*Hordeum vulgare* L.) soil system. *Plant Soil* 160:21–31

Chapter 12

***Aflaj*' Water Management in Oman: The Case of *Falaj Al-Khatmeen* in Birkat Al-Mouz, Wilayat Nizwa**

Fairouz Megdiche-Kharrat, Mohamed Moussa and Hichem Rejeb

Abstract *Aflaj* in Oman are sustainable ancient techniques of irrigation based on open channels draining water from wadis, springs or aquifers to communities of users. Omani authorities reported the existence of 4112 *aflaj* of which 3017 are live systems; about 1000 have underground qanats (*dawoodi aflaj*). Agriculture in Oman relies mainly on irrigation by means of *aflaj*. They currently provide 680 million cubic meters yearly and irrigate around 26,500 ha of farmlands. Their water is being managed by an administration headed by a *wakil*. *Falaj Al-Khatmeen* is a *dawoodi falaj* among the five Omani *aflaj* inscribed in the World Heritage List since July 2006. It irrigates the lands of Birkat Al-Mouz in Wilayat Nizwa. This paper provides an overview about *aflaj* in Oman and, through the case study of *falaj Al-Khatmeen*, highlights the main concepts of this traditional knowledge and water management system besides the rights and equity in access to water for stakeholders. Water is shared by *athar* (30 min) according to a very precise irrigation scheduling and rotation (*dawaran*) that can be updated depending on seasons and changes in *falaj* ownership and water flow. The survival of *falaj Al-Khatmeen* relies mainly on the efficiency of its management.

Keywords *Aflaj* · Water management · Irrigation scheduling · Oman

F. Megdiche-Kharrat (✉)
Laboratory "Spaces, Nature and Culture" ENeC UMR 8185, University Paris-Sorbonne
(Paris IV), CNRS-INSHS, Paris, France
e-mail: feirouzmekdish@gmail.com; fairouz.megdiche@paris-sorbonne.fr

F. Megdiche-Kharrat · M. Moussa
Laboratory of Eremology and Combating Desertification, Institute of Arid Regions,
4100 Medenine, Tunisia
e-mail: mohamed.moussa@ira.rnrt.tn

H. Rejeb
Research Unit «Horticulture, Landscape, Environment» UR13AGR06,
ISA-IRESA-University of Sousse BP 47, 4042 Sousse, Tunisia
e-mail: hrejeb62@yahoo.fr

Introduction

In arid and semi-arid zones, rural communities have developed a spectacular procedure of water acquisition. This system is called qanat. It has various names worldwide, such as *falaj* in Oman, *foggara* in Tunisia and Algeria, *kariz* in Afghanistan, and *Mambo* in Japan (Al-Ghafri et al. 2003b).

This study examines one of the famous *dawoodi aflaj* in Oman: *falaj Al-khatmeen* in Birkat Al-Mouz in Wilayat Nizwa (the governorate of Nizwa). This study has as main objectives: to introduce *dawoodi aflaj* as eco-friendly and sustainable groundwater acquisition systems, to explore their management systems through the case study of *falaj Al-khatmeen*, and to determine the actual condition of this *falaj*, besides the issues that may menace its survival and existence.

Description and Mechanism

Beaumont (1971) describes the qanat as “a method for developing and supplying groundwater”, it “consists of a gently sloping tunnel (...) which leads water by gravity flow from beneath the water table at its upper end to a ground surface outlet and irrigation canal at its lower end” (as cited in Megdiche-Kharrat and Moussa 2014).

The cross section of the underground tunnel presents generally an elliptical shape with approximately 1.2 m height and 0.8 m width (Beaumont 1971). Construction of the qanat involves digging a series of wells which are later connected by the underground tunnel (Buhagiar 2007). These vertical shafts facilitate the spoil’s removal and insure ventilation for diggers (Fig. 12.1).

Qanats’ depths and lengths are very variable. For example, the qanat of Zarch is the longest in Iran with a total length of 80 km; the deepest is the qanat of Gonabad that reaches 300 m depth (Yazdi and Khaneiki 2013).

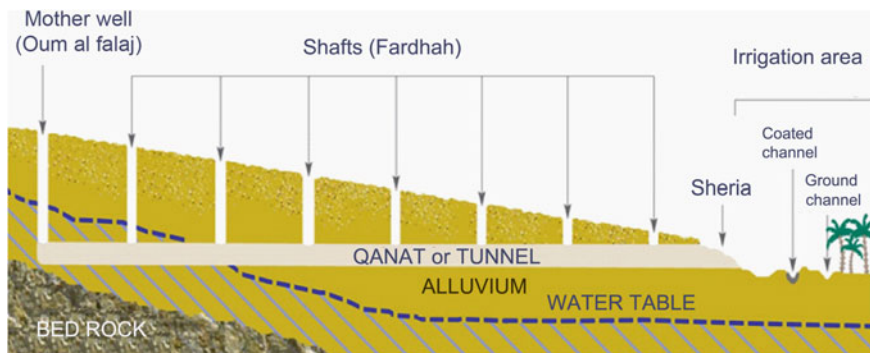


Fig. 12.1 Typical cross section of a qanat. Adapted from Hermosilla and Moussa (2011)

Some qanats are linked to hydraulic structures along their trajectory such as the *Il-Qattara* water gallery in Wied ir-Rum in Malta and its partly rock-cut, partly masonry built water reservoir (Buhagiar 2007).

Origin and History

English (1968) writes: “qanat technology apparently originated in the highlands of western Iran, northern Iraq and eastern Turkey some 2,500 years ago (...) Later Assyrian cities (...) relied on qanats for their drinking water.” This theory was largely debated by Costa (1983) who was trying to turn the attention toward Arabia (specifically Oman) by assimilating the copper mining knowledge and techniques of mid-third millennium BC to those used to convey underground water (Forbes 1964 and Wilkinson 1977 as cited in Megdiche-Kharrat and Moussa 2014). The qanat systems were exported from the Middle East to North Africa and Mediterranean Europe then to the Americas, and to Asia (East and Far East) (Al-Ghafri et al. 2003b).

Aflaj in Oman

In Oman, *aflaj* are commonly defined as tunnels conveying fresh water to houses and agriculture lands. Omani authorities reported the existence of 4112 *aflaj* of which 3017 are live systems (MRMWR 2008). *Aflaj* are the main source for irrigating farmlands. They currently provide 680 million cubic meters yearly for around 26,500 ha of farmlands (Al Amri et al. 2014).

Aflaj are classified into three different types: *ghaili*, *dawoodi*, and *aini* (Al-Marshudi 2007). *Ghaili aflaj* are channeling surface flows from wadis; *aini* ones are connected to springs, and *dawoodi aflaj* drain water from aquifers (Costa 1983). In Oman, there are 1000 known *dawoodi aflaj* (MRMWR 2009) with underground tunnels that count many kilometers in length.

In July 2006, five Omani *aflaj* (including their surrounding environments) were added to the World Heritage List: *falaj Daris* and *falaj Al-Khatmeen* in Willayat Nizwa, *falaj Al-Malki* in Willayat Izki, *falaj Al-Muyassar* in Willayat Al-Rustaq, and *falaj Al-Jeela* in Willayat Sur (MRMWR 2008).

Methods

This study is a part of a research about qanats and *aflaj* as antique ground water acquisition system generators of specific landscapes; and specifically those of Nizwa in Oman. This study went through several steps:

General data collection General data about qanats and *aflaj* was collected mainly from literature review, and from presentations about qanat and architecture at Yazd international conference in the ICQHS-UNESCO center (November 2014, Yazd-Iran).

Site selection *Falaj Al-Khatmeen* is one among the five Omani *aflaj* inscribed in the World Heritage List since July 2006. It has been chosen by researchers for many reasons such as its importance to the local community, its famous water divider, and its important water flow during the whole year (around 2000 l/s).

Specific data collection Specific data about the case study was collected from various resources, mainly, reports published by the Ministry of Regional Municipalities and Water Resources (MRMWR) in Oman, experts papers, and site visits including photographic documentation and UTM coordinates and altitudes record by GPS. All photographs displayed in this paper were taken by the authors in December 2014 and April 2015.

Interviews Interviews were conducted with *aflaj* expert Dr. Abdullah Al-Ghafri (December 2014) and Sheik Khamis Al-Dreishi the *wakil* (manager) of *Falaj Al-Khatmeen* (April 2015).

International workshops The first author participated at the international workshop on Water and the City organized by the ICQHS-UNESCO center and HydroCity in Yazd, Iran (8–17th November 2014); besides the Training Course “Water Integrity for MENA Region-Promoting Integrated Water Resources Management in the Arab Region,” held at the occasion of the third Arab Water Week in Dead Sea, Jordan (14–15th January 2014).

Results

Oman has a topographic diversity that varies from mountains, reaching an altitude of 2000–3000 m (Al-Hajar chain), to coastal plains descending almost to sea level (El-Baz 2002). Most of Omani *aflaj* are located in the northern part of the country which is dominated by mountainous landscape. Rainfall varies from year to year and across the country, ranging from less than 50 mm in central Oman to over 300 mm in the northern mountains (El-Baz 2002). *Falaj Al-Khatmeen* is one of the *dawoodi aflaj* inscribed in the World Heritage List. At the foothill of Al Jabal Al-Akhdhar, it supplies water to Birkat Al-Mouz community.

Location and History of Falaj Al-Khatmeen

Falaj Al-Khatmeen still represents the main source of water for Birkat Al-Mouz area. This village (niyabat Birkat Al-Mouz) is located in the governorate (wilayat) of Nizwa in Al-dhakliya region. This *falaj* is fed by wadi Al-Maiden (MRMWR 2008). Its known previous mother well (*Oum al falaj*) is located at UTM coordinates 40 Q

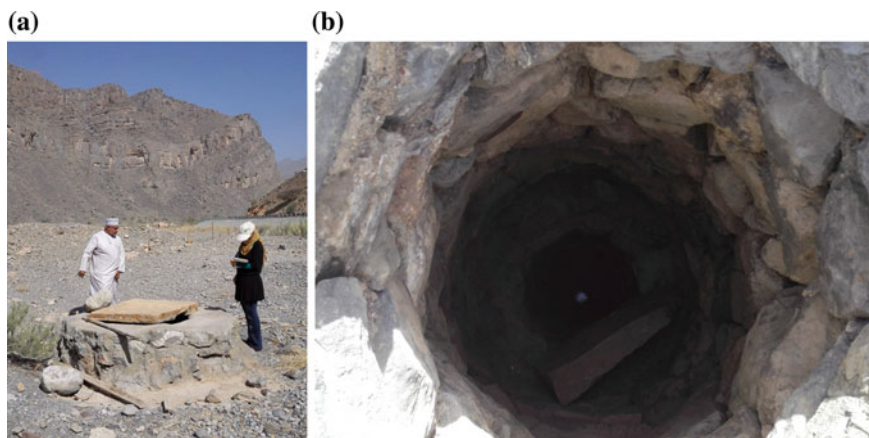


Fig. 12.2 Two of the qanat wells of *falaj AL-Khatmeen*: **a** *Oum al falaj* (mother well) within its surrounding landscape, **b** the fifth well with a halfway closure to protect the qanat

0569292 E, 2536908 N; and at an altitude of 604 m. It was built by the end of 1960s. The newly built one, in the 1990s, is the actual mother well. It is located at UTM coordinates 40 Q 0569207 E, 2536980 N; and at an altitude of 606 m (Fig. 12.2). The *sheria* (first surface emergence of the underground tunnel) is located at UTM coordinates 40 Q 0568340 E, 2535479 N; and at an altitude of 583 m.

Falaj Al-Khatmeen was constructed about 350 years ago under the imamate of the Imam Sultan bin Saif Al-Yorubi who ruled from 1649 to 1679 (MRMWR 2008; see also MRMWR 2009). Its name (*Al-Khatmeen*) comes from the fact that its construction led to a decrease in the water flow of a neighbor *falaj* called *Al-Khatm* in Manah area. Also, *khatama* in Arabic means to stop (MRMWR 2009). While constructing this *falaj*, seven workers died under the recessives of the underground tunnel. The work was interrupted till the Imam promised the workers 2/5th of the *falaj*'s water rights as construction wage (MRMWR 2009).

Physical Data of Falaj Al-Khatmeen

This *falaj* irrigates an area of 1,004,345 m² of which 723,124 m² is agricultural land (Al Amri et al. 2014). Farming products are mainly palm trees (4000 trees regarding 2010 census). About 30 years ago, there were banana, mango, and lemon trees, besides the crop growing of some cereals and vegetables. Livestock are few in some houses. About 20 years ago, there were 10–20 heads from each house/family. The qanat length is 2.450 km. It has 11 shafts in good condition from which four are open and seven are half closed. The flow of the water is 2000 l/s, its electric conductivity is 440 μS/cm, its pH is equal to 7.61, and its temperature is about 30 °C (MRMWR 2009).

Aflaj Management System

Falaj administration structure

Omani *aflaj* management is insured by an administrative body headed by a *wakil*. This administration structure consists of a director (*wakil*), a number of assistants or *arif*, a banker (*qabidh* or *amin al-daftar*), a crier (*dallal*), and expert workers (*bayadir*) (MRMWR 2009). The *wakil* is assigned by the sheik after water shareholders recommendation. He is in charge of the overall *falaj* administration (such as the budget and solving conflicts). The *arif* is responsible about the timing irrigation of shareholders' farms; the *qabidh* controls the *falaj* income coming from the *falaj* benefit shares and allocated lands (Al-Ghafri et al. 2003a).

For *falaj Al-Khatmeen*, there used to be two directors in continuous conflict. There were a *wakil* for *falaj ettaht* (down *falaj* serving inhabitants lands) and another for *falaj alfawq* (upper *falaj* serving government lands). Since 2004, the two directors are working together as *wakil* and assistant-*wakil*, they also accomplish the tasks of *arif* and *qabidh*. *Falaj Al-Khatmeen* has no crier (*dallal*), because the *falaj* shares' value (*waqf*) is fixed (*marbout*) and yearly rented only.

Falaj ownership and various stakeholders

Omani *aflaj* are owned by the government and communities of farmers regarding two types of water ownerships: public and private ownerships (MRMWR 2009). Smaller *aflaj* are owned by single families but larger ones count hundreds of owners (Al-Ghafri et al. 2003b). The public ownership includes using the water of the *falaj* for domestic purpose and for livestock drinking. The private ownership concerns the water used for irrigation regarding shares distribution. For large Omani *aflaj*, there are four various types of private ownership: (1) Owners of land and water; (2) Owners of land and renting water; (3) Owners of water and renting land; (4) Renting land and water (Al-Ghafri et al. 2003b).

Falaj Al-Khatmeen is owned by the government and a community of farmers that counts about 900 water shareholders. Initially, the ownership was divided into five parts: three parts for the government, and two parts for private farmers. This water division is assured spatially by a water divider constructed in the main *falaj* course at the entrance of the village (Fig. 12.3). About 200 m after the *sheria*, the water divider divides the main channel into three subdivisions (2 + 2 + 1). The first course irrigates private local farms. The two others get together again to irrigate *bait al-mal* (government) lands (MRMWR 2008). Thus, from this divider, two *aflaj* diverge: *falaj ettaht* which represents the 2/5 owned by local farmers, and *falaj alfawq* which represents the remaining 3/5 owned by the government.

Water rights and shares distribution

Laws and water rights of the *falaj* are determined since its construction. They are unchangeable during time, by they can be updated for the benefit of the *falaj* and only in a way that does not affect owners' rights (MRMWR 2009). Water is distributed to farmers regarding the number of shares each one owns. The number

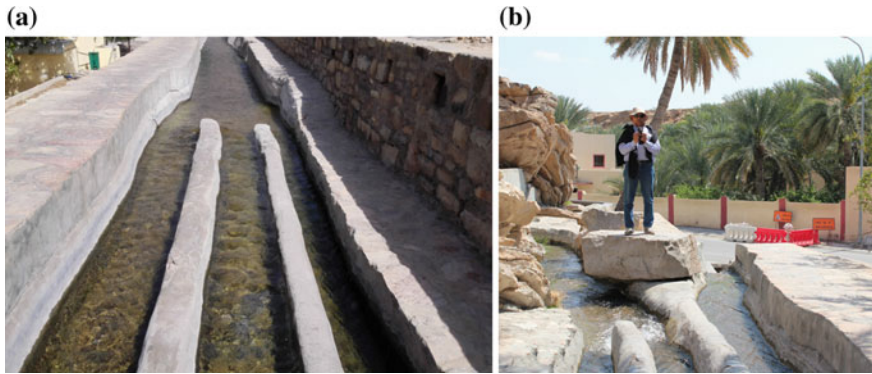


Fig. 12.3 Water divider of *falaj Al-Khatmeen*: **a** Water flowing into the divider, **b** water flowing out of the divider in two distinct *aflaj* (*falaj ettaht* in the right and *falaj alfawq* in the left)

of shares depends on the sizes of the owned lands and/ or the contribution in the construction of the *falaj* itself (Al-Ghafri et al. 2003b). For the majority of *aflaj*, shares are distributed on time basis (one *baddah* is equal to 12 h, and one *athar* is equal to 30 min). In the past, farmers used to estimate *athar* through a complex sundial system in daytime and a stars system in nighttime. Nowadays, they use the modern watch to calculate their shares.

In *falaj Al-Khatmeen*, water is distributed regarding 865 *athar*: 309.5 *athar* for the government (*bait al-mal*), 129 *athar* for the community benefit (*waqf*), 96 *athar* for *falaj* benefit (*waqf al falaj*), and 330.5 *athar* for local farmers (MRMWR 2009). As administration wage, the *wakil* receives yearly the 1/10 of the total amount of the expenses he spent for the maintenance of the *falaj* (MRMWR 2009).

Irrigation Scheduling

Water shares are distributed among shareholders regarding an irrigation rotation (*dawaran*), which means the number of days' interval between two successive irrigations for the same owner. The irrigation rotation depends of the number of shares, shareholders, agricultural land sizes, and water flow. Each day is divided into two timings (*baddah*), in daytime and in nighttime (Al Amri et al. 2014). The *baddah* starting time and length depend of seasons and of used methods (Al-Ghafri et al. 2003a). In traditional method, the night *baddah* is counted from sunset to sunrise and vice versa for the day *baddah*. In *goroobi* and *zawali* methods, the two *baddah* are equal in time (12 h each) and are calculated using the modern watch. In *goroobi* method, the starting time of *baddah* differs from one season to another; the watch is set to 12:00 at sunset every day. However in *zawali* method, the day *baddah* starts at 6:00 am regardless of seasonal change (Al-Ghafri et al. 2003a).

For *falaj Al-Khatmeen*, the irrigation rotation is 9 days, the *wakil* use the *zawali* method to distribute water shares among shareholders. The used irrigation timing units are *athar* (30 min), half *athar* (15 min), and quarter *athar* (7 min 30 s).

Discussion

The Falaj as Sustainable Water Acquisition Technique

Aflaj insure an adapted water use to environmental conditions. The mechanism of *dawoodi aflaj* allows a moderate and sustainable exploitation of the water table. Water is conveyed from aquifer only by gravity and allows its recharge from seasonal rainfall and wadis' runoff. Besides, this system offers sustainable solutions for overcoming drought. The technical solution consists of digging back into the aquifer and searching for lateral sources. As management solutions, farmers adjust water usage by reviewing the areas of cultivated lands and types of crops. Also, the irrigation cycle can be updated to match all farmers needs. *Aflaj* construction and maintenance rely mainly on manpower.

Equity in Access to Falaj Water for Stakeholders

In the past as today, access to *falaj* water for drinking and domestic use is free and available for all community. The administrating body of the *falaj* distributes water-shares equitably regarding ownership of land and water, and resolves conflicts between farmers. However, the traditional system used for shares distribution may lead to inequity in water allocation. But, the newly adopted *zawali* method is accurate and allows precise shares distribution.

Aflaj Management System Assessment Regarding Water Integrity (TAPA Concepts)

Transparency in managing the *falaj* and its water is insured by direct contact between the managing body and multi-stakeholders and an available book of records for sharing information. The *wakil* is assigned by the sheik after water shareholders recommendation. The *wakil* should own important shares, and then he will be directly affected by a bad management of the system. In that case, the stakeholders can dismiss the *wakil* from his functions and choose another one. This insures **accountability**.

Anti-corruption is insured by the **participation** in decision-making regarding the *falaj* and its management at multi-stakeholder levels. Also, the whole system represents a dual common ownership, public, and private. The management of the *falaj* is under the supervision of a control committee of stakeholders.

Problems Facing Falaj Al-Khatmeen

Falaj Al-khatmeen was managed by two directors in continuous conflict that menaced the stability of the administration structure. Since 2004, the two directors are acting as *wakil* and assistant-*wakil* and sharing the management of the *falaj*.

Nowadays, *falaj Al-Khatmeen* faces some other issues, mainly:

- Water table lowering for successive droughts, this led to extending the tunnel by digging back into the aquifer since 1960.
- Digging deep wells and boreholes near the mother well directly affects water level and flow in the *falaj*, actually one legal borehole exists in *falaj*'s source area but it does not affect it too much.
- Wastage of the *falaj*'s fresh water in some activities such as washing cars.
- Usage of some chemical products while cleaning clothes or bathing in the *falaj* despite authorities prohibition.
- Urban expansion menacing farmlands, this was highly noticed during the decade of 1980. Nowadays some laws exist to control housing in that area.
- Because of youth disinterest, expertise in that field is rarely transmitted through generations, *Bayadir* (expert workers) are replaced by expat workers.

Conclusion

Qanats are considered as good examples of human ecosystems (Honari 1989 as cited in Wessels 2005). *Dawoodi aflaj* are environment friendly and sustainable water acquisition systems. They insure free access to freshwater for all community of users, and to a high extent, equity in irrigation water distribution to various stakeholders. In general, *aflaj* management system insures water integrity and covers its TAPA concepts. *Falaj Al-Khatmeen* is a very important Omani *falaj* (listed as World Heritage). It is known for its high water flow and its famous divider. Its current management is very efficient. Thus, the *falaj* still faces many issues such as urban expansion, youth disinterest, and the wastage and pollution of its water.

Acknowledgments It is a pleasant duty for the authors to thank all those who helped in this research, and especially Dr. Abdullah Al-Ghafri and Sheik Khamis Al-Dreishi.

References

- Al Amri S, Al Ghafri A, Abd Rahman N (2014) Water management of Falaj Al Khatmain in Sultanate of Oman. *J Earth Sci Eng* 4(2014):127–133
- Al-Ghafri A, Inoue T, Nagasawa T (2003a) Irrigation scheduling of Aflaj of Oman: methods and its modernization. In: Adeel Z (ed) *Sustainable management of marginal drylands: application of indigenous knowledge for coastal drylands*. In: Proceedings of a Joint UNU-UNESCO-ICARDA international workshop, Alexandria, Egypt, 21–25 September 2002. The United Nations University, Tokyo, Japan, pp 147–166
- Al-Ghafri A, Inoue T, Nagasawa T (2003b) Daudi Aflaj: the Qanat of Oman. In: Proceedings of the third symposium on Xinjiang Uyghor, China, 11 November 2003. Chiba University, Chiba, Japan, pp 29–36
- Al-Marshudi AS (2007) Institutional arrangement and water rights in aflaj system in the Sultanate of Oman. In: Proceedings of the international history seminar on irrigation and drainage, 2–5 May 2007, Tehran, Iran. IRNCID-ICID, Tehran, pp 31–42
- Beaumont P (1971) Qanat systems in Iran. *Bull Int Assoc Sci Hydrol* 16:39–50
- Buhagiar K (2007) Water management strategies and the cave dwelling phenomenon in late medieval Malta. *Med Archeol* 51:103–131
- Costa PM (1983) Notes on traditional hydraulics and agriculture in Oman. *World Archeol* 14 (3):273–295
- El-Baz F (2002) *Wadis of Oman: satellite image atlas*. Office of the Advisor to his Majesty the Sultan for Cultural Affairs, Muscat, Sultanate of Oman
- English PW (1968) The origin and spread of qanats in the old world. *Proc Am Philos Soc* 112 (3):170–181
- Hermosilla J, Moussa M (2011) *Las Galerías de Agua Tunecinas. Las Gobernaciones de Kebili, Tozeur, Gafsa y Gabès*. ESTEPA, Valencia, Spain
- Megdiche-Kharrat F, Moussa M (2014) The qanat as a crucial antique water acquisition system common to arid zones' communities: two case studies, foggaras In Tunisia and Aflaj in Oman. *The International Journal Research Publications*, Singapore (TIJRP)—Research Journal of Social Science and Management—RJSSM, vol 3, no 12. <https://www.theinternationaljournal.org/ojs/index.php?journal=tij&page=article&op=view&path%5B%5D=2864>. Accessed Apr 2014. ISSN: 2251-1571
- Ministry of Regional Municipalities and Water Resources-MRMWR (2008) *Aflaj oman in the world heritage list*. MRMWR, Muscat, Oman
- Ministry of Regional Municipalities and Water Resources-MRMWR (2009) *Experimental project for archiving ownerships and norms and Sunan and data related to aflaj*. MRMWR, Muscat, Oman
- Semsar Yazdi AA, Labbaf Khaneiki M (2013) *Veins of desert: a review on the technique of qanat/falaj/karez*, 2nd edn. IWRMO, Iran
- Wessels JI (2005) Criteria for renovating and using ancient qanats in Syria-case studies. In: Proceedings of the international frontinus symposium, 2–5 October 2003. Frontinus-Gesellschaft, Walferdange, Luxemburg, pp 249–262. ISBN: 3-9806091-2-X

Chapter 13

Response of Vegetable Crops to Irrigation Regimes Using Saline Waters

K. Nagaz, F. El Mokh, Mohamed Moncef Masmoudi, N. Ben Mechlia,
O. Belkheiri and G. Ghiglieri

Abstract Field studies were conducted to examine the response of potato, carrot, fava bean, and pepper to irrigation regimes using saline water in a commercial farm. The irrigation regimes were full (FI100) and deficit (DI70) irrigated with levels of 100 and 70% of crop evapotranspiration (ET_c) when the readily available water, 40% of total available water (TAW), in the FI100 treatment was depleted, and traditional farmer practice (FM). For all experiments, the largest soil salinity values were observed under the farmer treatment compared to the FI100 and DI70 treatments. The highest mean yields of potato (24.4–27.5 t/ha), carrot (28.4–30.3 t/ha), fava bean (19–21.3 t/ha), and pepper (10.9–12.5 t/ha) were recorded for the FI100 treatment. Compared with FI100, significant reductions in potato, carrot, fava bean, and pepper yields were observed under the DI70 treatment, with only a few exceptions, resulting from a reduction in yield components. The farmer's method not only caused significant reductions in yields but also resulted in an increase of water usage of 14–22%, 18–21%, 12.5–19%, and 13.9–15.5% for potato, carrot, fava bean, and pepper, respectively, and increased soil salinity. Water productivity (WP) values reflected the differences in yields and varied between 4.3 (farmer) and 13.7 kg/m³ (DI70) for potato, 4.4 and 11.7 kg/m³ for carrot, 4.8 and 13.7 kg/m³ for fava beans, and 0.8 and 2.6 kg/m³ for pepper across different years and treatments. The FI100 scheduling technique with variable water amounts was more efficient and provided significant advantage in yield, water productivity and net income, compared to the FM treatment in potato, carrot, fava beans, and pepper yields under arid environment. FI100 scheduling technique is suggested for vegetable crops in the arid environment. Under water restriction conditions, adoption of the DI70

K. Nagaz (✉) · F. El Mokh
Institut des Régions Arides, 4119 Médenine, Tunisia
e-mail: Nagaz.Kameleddine@ira.nrmt.tn

F. El Mokh
e-mail: elmokh.fa@gmail.com

M.M. Masmoudi · N. Ben Mechlia
INAT, 43 avenue Charles Nicolle, 2083 Tunis, Tunisia

O. Belkheiri · G. Ghiglieri
Desertification Research Center-NRD, University of Sassari, Sassari, Italy

strategy allows 30% water saving compared with FI100 with relatively small impact on soil salinity and some reductions in yield and net income.

Keywords Salinity · Water management · Irrigation scheduling · Deficit irrigation · Water productivity · Economic evaluation

Introduction

High quality water is a limited natural resource in arid areas of Tunisia. However, large quantities of saline water commonly exist and could be used to intensify agriculture, particularly in the arid part of the country. Local practices give to vegetables an important place in lands irrigated with shallow wells having a salinity more than 3 dS/m. Various species of high economic value crops, such as fava bean, carrot, pepper, and potato are cultivated over contrasting periods to optimize water use. However, local irrigation scheduling practices remain empirical, in terms of timing and irrigation water quantities and lead to water losses during periods with low water needs and water deficits during peaks in plant-water demand. Therefore, good irrigation management is required to improve farmer's practices and achieve tangible productivity improvement.

Many studies have reported substantial increases in crop yields as a result of suitable irrigation management, including studies in saline conditions (Batra 1990; Ayars et al. 1991; Pasternak and De Malach 1995; Minhas 1996; Bustan et al. 2004; Malash et al. 2005; Sermet et al. 2005; Jalota et al. 2006; Ali et al. 2007; Nagaz et al. 2013). It has been demonstrated that optimal irrigation scheduling can be achieved using accurate estimates of crop evapotranspiration (ET_c) mainly without full ground cover which requires that soil evaporation and crop transpiration should be considered separately (Ritchie 1972).

Irrigated farming in arid areas is exposed to the risk of soil salinization due the lack of rain events used for natural leaching. Thus, Irrigation management should consider the impact of irrigation on both the crop yield and the risk of soil degradation.

Vegetable crops are considered sensitive to salinity and water stresses (Maas 1990). Vegetable crops are grown in arid regions of Tunisia during autumn to spring periods, which coincide with the rainy season in small-scale irrigation schemes and irrigated with well waters. Because vegetables are high value crops, the optimal irrigation management strategy is to maximize yield by supplying the irrigation requirement of the crop. However, under local practices, irrigation is applied by farmers according to their experience and supply often exceeds crop requirements.

The impact of irrigation management on yield and water productivity of vegetable crops has not been studied in arid regions of Tunisia. The present work aims to determine irrigation water requirements of vegetables and to assess yield

response to different irrigation regimes using saline waters in an arid region of Tunisia.

Materials and Methods

Field experiment was conducted over 2 years (2012–2014) in farmer field in the South east of Tunisia (33° 27' N, 10° 31' E; altitude 55 m) in Médenine. Average annual precipitation at the site was 151 mm, which means that irrigation is usually required for vegetable crops, particularly during dry years. No rainfall was received throughout the entire growing period of potato, carrot, fava bean, and pepper during the year 2012/2013. During 2013/2014, there was 107 mm of precipitation, most of which fell during November, December and February.

The experiment site soil was sandy with 80.6% sand, 12.6% silt and 6.8% clay. Average water content values for field capacity and permanent wilting point are, respectively, $0.180 \text{ m}^3 \text{ m}^{-3}$ and $0.105 \text{ m}^3 \text{ m}^{-3}$ and organic matter content is less than 0.8%. The total soil available water for an assumed root depth of 1.00 m, was 74 mm.

Fertilizers were supplied during the 2 years according to fertilizer levels used by farmers for vegetable production in the region of Médenine, Tunisia. Before planting of potato, carrot, fava bean, and pepper crops, respectively, 17, 16, 12.5, and 9.5 t/ha of organic manure were applied to the soil. Inorganic nutrient supplies were applied as N in the form of ammonium nitrate, P_2O_5 and K_2O at rates of 300, 300 and 200; 200, 200 and 150; 200, 150 and 150 kg/ha, respectively, for potato, carrot, fava bean, and pepper. The P_2O_5 and K_2O fertilizers were applied as a basal dose before planting. Nitrogen was applied as fertigation in all treatments. For potato, 120 kg/ha of potassium nitrate was applied after the tuber initiation stage.

Potato, carrot, and fava bean were planted every year on September 9, October 14 and 27 in 70 cm rows with plants spaced 40 cm apart, in a randomized complete block design with four replicates and three irrigation treatments. Plants of pepper were transplanted each year into the blocks on May 1. Each plot consisted of eight rows and drip irrigated with a well water having an electrical conductivity (ECi) of 6 dS/m. Each dripper flow rate was 4 l/h.

Three irrigation treatments were applied: two treatments used soil water balance (SWB) and consist in delivering total or a fraction of cumulated ET_c when readily available water in the root zone, which is the amount of water that crops can extract without experiencing any water stress (RAW), was depleted. For SWB method, we adopted replacement of 100% ET_c (FI100), considered as full irrigation, and deficit irrigation treatment supplying 70% ET_c (DI70). A third irrigation treatment consisted of applying the irrigation practices adopted by local farmers where fixed amounts of water are supplied to the crop with fixed intervals.

ET_c was calculated from Penman Monteith method-determined reference crop water use (ET_o) (Allen et al. 1998), using daily climatic data collected from the

meteorological station, located 9 km from the research plot, with a dual crop coefficient (Kc).

A soil water balance model developed in Excel for managing irrigation of annual crops was used to schedule irrigation. The model estimates on daily basis the values of rooting depth and ground canopy cover, calculates all the components of the soil water balance and estimates the next irrigation date considering a depletion limit of 40% of total available water in the root zone (TAW). More details of the model computations are given by Nagaz et al. (2007).

At harvest, yields (t/ha) and yield components were determined for each treatment.

Every year, soil samples were taken before planting and after harvest with a 4 cm auger from three depths for potato and from four depths for carrot, fava bean, and pepper, and then analyzed for electrical conductivity of the saturation extract (ECe).

Water productivity (WP) was calculated based on Eq. (13.1):

$$WP(kg/m^3) = \frac{Y(kg/ha)}{Irrigation\ water(m^3/ha)}, \quad (13.1)$$

where Y is the yield and irrigation water is the amount of irrigation water applied from planting to harvest; 45 and 60 mm irrigation were applied before planting of potato, and carrot, fava bean, and pepper for all treatments in order to start with root zone layer at field capacity.

The net income was calculated for each irrigation treatment by subtracting total production costs from the gross income. The total cost of production includes tillage, seed, fertilizer, irrigation, insecticide, and human labor. Gross return was calculated by multiplying the total amount of yield by its market price.

The least significant difference (LSD) test at 5% level was used to find any significant difference in the above-mentioned criteria, between treatment means.

Results and Discussion

Soil Water Balance

Figure 13.1 presents soil water depletion, estimated by the soil water balance model, for full irrigated (FI100) potato, carrot, fava bean, and pepper for the first year. The water depletion from root zone is considered as the net water requirement. The root zone is replenished to field capacity at each irrigation. Since irrigation was applied only when cumulative water depletion exceeded the readily available water, plants may have suffered a slight stress on the day before irrigation.

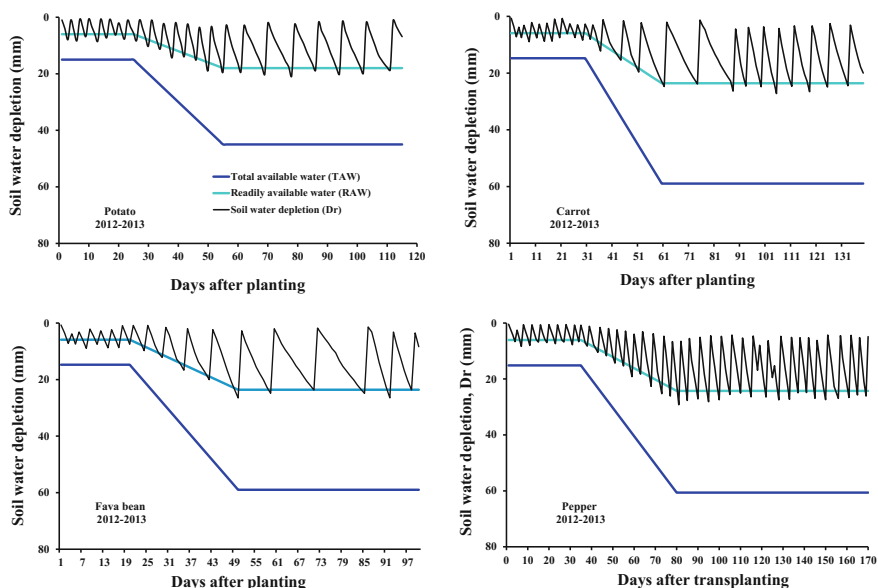


Fig. 13.1 Daily values of water depletion from root zone for the FI100 irrigation treatment during the cropping periods of potato, carrot, fava bean and pepper (2012–2013)

Soil Salinity

The ECe values determined at planting of carrot, fava bean, potato and pepper were, respectively, 3.1, 2.7, and 2.9 dS/m in the first year, and 3.6, 3.2, and 3.3 dS/m in the second year (Fig. 13.2). The results showed that during 2012–2013, an increase in ECe values was recorded under all treatments compared to those at planting. Due to the lack of rainfall during the crop growing periods and the fact that water supply was provided basically through irrigation at rates estimated to equal crop water use, little leaching of the soil was expected. In 2013–2014, the decrease in ECe values at harvest for all treatments was attributed to the leaching of salts by rainfall (107 mm) received during the growing periods of potato, carrot and fava bean, and rains (35 mm) that fell during the maturity stage of pepper. Thus, the relatively higher amounts of rainfall in 2013–2014 seemed to be effective in leaching salts from the root zone.

Figure 13.2 shows a decrease in ECe values for full irrigation treatment (FI100). The DI70 irrigation treatment resulted also in smaller ECe values at harvest. This result may be explained by the fact that even less salt is added in deficit irrigation plots, its concentration in a lower volume of the wetted sphere under the emitters is higher. Apparently, the layout used for soil sampling fails to represent average salts concentration. The highest ECe values were observed for the FM (farmer) irrigation

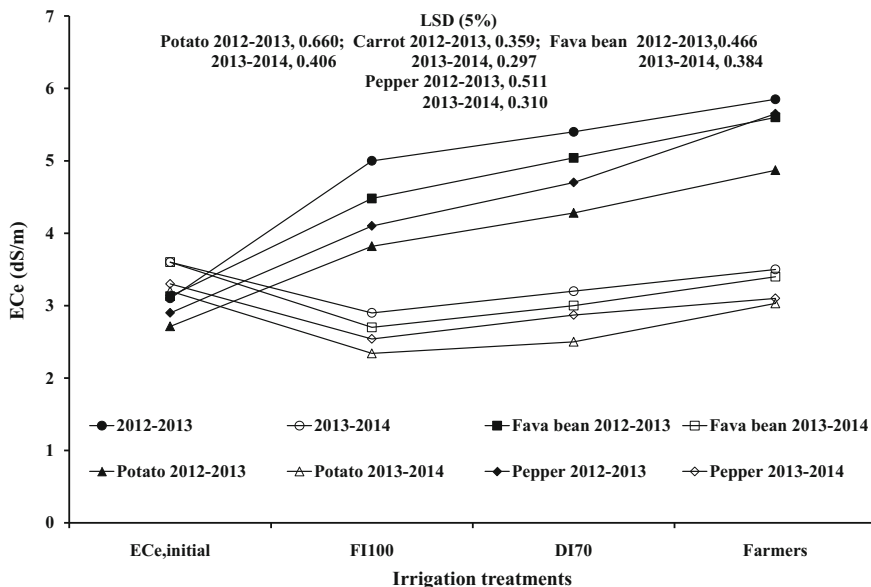


Fig. 13.2 Soil salinity (ECe, dS/m) under different treatments of potato, carrot, fava bean and pepper. The full irrigation treatment (FI100) consisted of giving 100% of ETc, whereas the deficit treatment (DI70) was irrigated with 70% of accumulated ETc

method despite the fact that more water was applied in this treatment. Without adequate scheduling, irrigation with high frequency and small amounts during the first growing period seems to accumulate salts in soil.

Low values of ECe were due to the natural leaching of soluble salts by rainfall that occurred during the second year. Consequently, the impact of using saline water for irrigation on soil salinization appears to be limited for crops with short growing season mainly when the latter coincide with the rainy season and can benefit from the leaching capacity of rainfall events.

Crop Yield

Crop yield under different treatments are presented in Fig. 13.3. Crop yields observed under the FI100 treatment were statistically different from those obtained with the DI70 treatment during the 2 years of the study. The DI70 and FM treatments also show a statistical difference between them. The lowest yields were recorded in FM treatment. The DI70 treatment resulted in 19–24, 11–14, 12–15, and 35–36% more yield than did the farmer’s method, respectively, for potato, carrot, fava bean, and pepper in the first and second years with 30% less irrigation

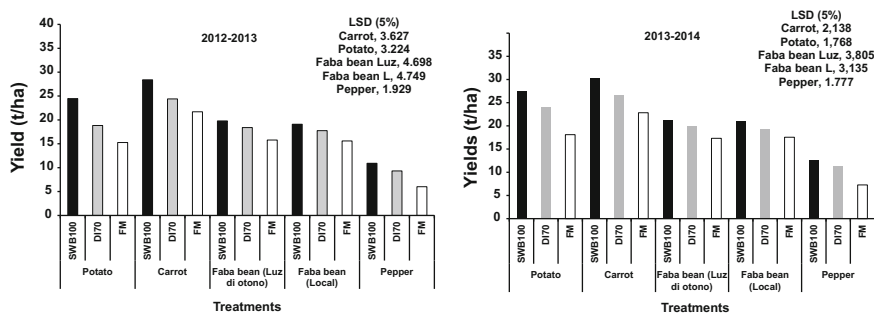


Fig. 13.3 Yields of potato, carrot, fava bean and pepper under different irrigation treatments during 2012/2013 and 2013/2014 field seasons

water than the FI100 treatment while the farmer's method used 12–22% more irrigation water than FI100.

The smaller yields obtained with the farmer's treatment were related with smaller yield components (data not presented) as a result of water deficit during the period between flowering and harvest, the most critical periods of vegetable crops for irrigation. Consequently, the better yields obtained under the FI100 and DI70 treatments were due to better growth and yield components.

Yields were largest in the second year because of the low soil salinity and the higher amount of rainfall (107 mm). During the experimental periods the reduction of water supply by 30% (DI70) seems to have small effect on soil salinization and yield of vegetables in comparison with FI100 method.

The use of the SWB strategy for managing irrigation water resulted in better yields than the method using fixed frequency and amounts practiced by local farmers. The farmer's strategies resulted in greater soil salinity than did the FI100 treatment (Fig. 13.2). The greater E_c values associated with the farmer's method caused important yield reduction of crops. Smaller yields obtained under the farmer's method may be attributed to the fact that the farmer applied water to the crop regardless of the real plant needs. The farmer method is often characterized by periods of over and under-irrigation and this may result in nutrients leaching out of the root zone during early stages of growth and low water availability during periods with high water needs, therefore limiting crop growth and yield.

Previous studies recommended the use of the SWB strategy for conditions similar to those of the present paper (Nagaz 2007). The irrigation scheduling based on crop water needs consisted in applying variable water amounts and intervals adapted to the change of crop water requirement during the growing season. For a small surface farms with an independent water source, as in arid regions of Tunisia where irrigation uses shallow well waters, accurate scheduling is manageable and therefore there is a good chance to optimize water supply to crops.

Water Productivity

Irrigation amounts applied for potato, carrot, fava bean and pepper over the 2-year period are given in Fig. 13.4. Irrigation waters applied before planting are not included in the total.

Results show that fully irrigated potato, carrot, fava bean, and pepper used 249–300, 324–416, 207–285, and 618–631 mm of irrigation water. The water saving achieved from the DI70 treatment was 30% compared to the amount applied to the FI100 treatment. The FM strategy caused significant reductions in yield and resulted in using 12–22% more water and increased soil salinity. With the farmers' irrigation strategy more water was applied (35–98 mm) than that in the FI100 treatment.

Water productivity was calculated as the ratio of marketable yield at harvest to the irrigation amount (Fig. 13.5). The WPs varied by years and by irrigation treatments. Irrigation water productivity values (IWP) varied typically around 0.8–9.2 in 2012–2013 and 1.1–13.7 kg/m³ in 2013–2014.

For all experiments, the WP values obtained with the FI100 treatment were considerably different from those in the DI70 and FM treatments. The WP obtained using the FM method was statistically different from those recorded in the DI70 treatment. The largest IWP were obtained in 2013–2014 with 13.7, 11.7, 13.5, and 2.6 kg/m³ for the DI70 treatment, respectively, for potato, carrot, fava bean and pepper, followed by the FI100 treatment with, respectively, 11.1, 9.3, 10.3, and 2.1 kg/m³. The minimum IWP values of 5.9, 5.8, 7, and 1.1 kg/m³ were obtained for the farmer's treatment during the second experimental year. Values were in the same range in the previous year 2012–2013. The small IWP for the FM during the 2 years was due to reduced yields and greater irrigation water use.

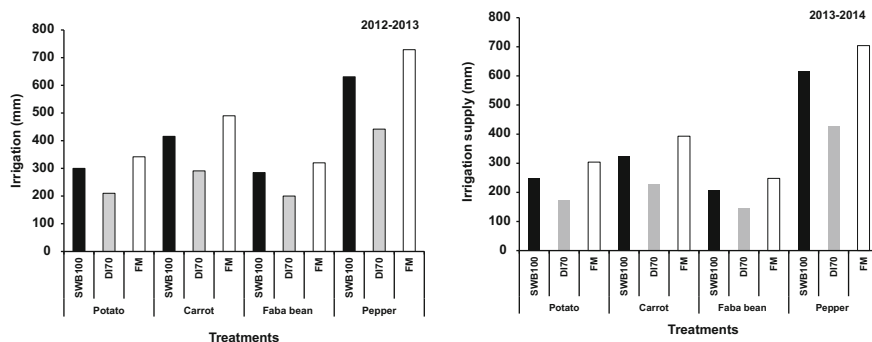


Fig. 13.4 Irrigation amount under different treatments during the period of potato, carrot, fava beans and pepper

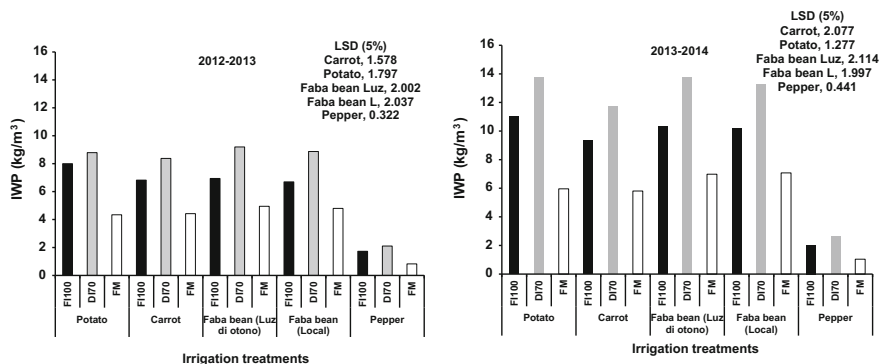


Fig. 13.5 Irrigation water productivity (IWP, kg/m^3) under different irrigation treatments during 2012/2013 and 2013/2014 field seasons

Economic Evaluation

The economic analysis presented in Table 13.1 showed that the greatest net return was observed with the FI100 treatment followed by the DI70 deficit treatment, whereas the farmer's method showed the lowest net return across 2 years. High

Table 13.1 Production costs and net return of vegetable production under different irrigation treatments (US\$/ha)

Treatment	Cost of production	Gross return	Net income
<i>Potato</i>			
FI	3634	9411	5777
DI70	3576	7867	4290
FM	3667	6062	2394
<i>Fava bean</i>			
FI	4292	6510	2217
	4292	6680	2387
DI70	4242	6006	1764
	4242	6227	1984
FM	4337	5366	1028
	4337	5371	1033
<i>Carrot</i>			
FI	2987	7309	4322
DI70	2912	6326	3414
FM	3036	5555	2519
<i>Pepper</i>			
FI	5604	27625	22020
DI70	5485	24312	18827
FM	5665	15676	10010

values of net income under the FI100 treatment were due to better yields as compared with the DI70 and farmer treatments. According to the economic analysis, the net income from the FI100 treatment was found to be reasonable under non-limiting water conditions. Under water scarcity conditions, the DI70 treatment could produce a satisfactory net income.

Conclusions

The effect of irrigation strategies on soil salinity, yield, and water productivity of drip-irrigated potato, carrot, fava bean, and pepper was studied using field experiments conducted in southern Tunisia during 2012–2013 and 2013–2014. The findings were that fully irrigated potato, carrot, fava bean, and pepper used 249–300, 324–416, 207–285, and 618–631 mm of irrigation water and irrigation amount can be reduced by adopting moderate deficit irrigation (DI70). The largest soil salinity values were observed under the farmer's treatment compared to the FI100 treatment. The DI70 treatment resulted in low EC_e values. Yields of potato, carrot, fava bean, and pepper for the DI70 treatment were considerably smaller than those in FI100 treatment. The farmers' method (FM) gave the lowest tuber yields with 12–22% more water. The water productivity was affected by irrigation regime.

Regarding the results of the economic evaluation, it can be concluded that a 30% saving in irrigation water caused a 14.5–25.7% reduction in the net income compared to the fully irrigation (FI100) treatment.

The findings in this study strongly recommend that FI100 could be used for scheduling irrigation of vegetable crops in the arid environment of Tunisia. The DI70 treatment provided inappropriate strategy under water scarcity conditions and allowed 30% water saving compared to the FI100 treatment with relatively small impact on soil salinity and some yield and net income reductions.

Acknowledgments The authors gratefully acknowledge that this work was funded by USAID and managed by ICARDA through the Water and Livelihood Initiative (WLI) and by the European Union, through the WADIS-MAR project (ENPI/2011/280-008).

References

- Allen RG, Pereira LS, Raes D, Smith M (1998) Crop evapotranspiration: Guidelines for computing crop water requirements. Irrigation and Drainage Paper N° 56 FAO Rome Italy
- Ali MH, Hoque MR, Hassan AA, Khair MA (2007) Effects of deficit irrigation on yield, water productivity, and economic returns of wheat. *Agric Water Manage* 92:151–161
- Ayars JE, Hutmacher RB, Steiner JJ, Mantel AB, Vail SS (1991) Irrigation of carrots on a sandy loam soil. *Irrig Sci* 12:193–198
- Batra BR (1990) Effect of different levels of irrigation and fertilization on growth and yield of carrot (*Daucus carota* L.) for root production. *Veg Sci* 17(2):127–139

- Bustan A, Sagi M, De Malach Y, Pasternak D (2004) Effects of saline irrigation water and heat waves on potato production in an arid environment. *Field Crops Res* 90:275–285
- Jalota SK, Sood A, Chahal GBS, Choudhury BU (2006) Crop water productivity of cotton-wheat system as influenced by deficit irrigation, soil texture and precipitation. *Agric Water Manage* 84:137–146
- Maas EV (1990) Crop salt tolerance. In: Tanji KK (Ed) *Agricultural salinity assessment and management*, ASCE manuals and reports on engineering practice no. 71. American Society of Civil Engineers, New York, pp 262–304
- Malash N, Flowers TJ, Ragab R (2005) Effect of irrigation systems and water management practices using saline and non-saline water on tomato production. *Agric Water Manage* 78:25–38
- Minhas PS (1996) Saline water management for irrigation in India. *Agric Water Manage* 30:1–24
- Nagaz K (2007) *Gestion de l'irrigation à l'eau salée en milieu steppique*. Thèse de doctorat en sciences agronomiques INAT Tunisia p 164
- Nagaz K, Masmoudi MM, Ben Mechlia N (2007) Irrigation scheduling calendars development and validation under actual farmers' conditions in arid regions of Tunisia. *Options Méditerranéennes Séries B No. 56(1):249–259*
- Nagaz K, Masmoudi MM, Ben Mechlia N (2013) Field studies on the use of saline water for deficit irrigation in arid Tunisia. In: Hossain Ali M (ed) *Irrigation management, technologies and environmental impact*. Nova Science Publishers Inc., Hauppauge, NY, USA, pp 87–128
- Pasternak D, De Malach Y (1995) Crop irrigation with saline water. In: Pessaraki M (ed) *Handbook of plant and crop stress*. Marcel Dekker Inc., NY, pp 599–622
- Ritchie JT (1972) Model for predicting evaporation from a row crop with incomplete cover. *Water Resour Res* 8:1204–1213
- Sermet O, Caliskan ME, Onder D, Caliskan S (2005) Different irrigation methods and water stress effects on potato yield components. *Agric Water Manage* 73(1):73–86

Chapter 14

Fog Collection and Participatory Approach for Water Management and Local Development: Practical Reflections from Case Studies in the Atacama Drylands

Martino Correggiari, Giulio Castelli, Elena Bresci
and Fabio Salbitano

Abstract The Atacama drylands are characterized by a high level of aridity and water scarcity, abandonment of rural areas by the population and loss of biodiversity, where some areas never get any rainfall. The advection fog is a daily phenomenon and a local resource that can be used by means of a simple low-technology called “Atrapaniebla” (Fog Collector), providing water for human consumption and irrigation. Some case studies offer different scenarios in terms of this technology’s purpose:

- to fulfil the water needs of small isolated communities;
- allows activities like proximity agriculture and reforestation for the rural population;
- to support biodiversity’s preservation and scientific research.

The effectiveness of these projects depends on important factors that are not to be taken for granted, like the communities involvement, the presence in the territory of

M. Correggiari (✉)
Research Unit on Landscape—RUL, Department of Architecture,
University of Ferrara, Ferrara, Italy
e-mail: m.correggiari@gmail.com

G. Castelli · E. Bresci · F. Salbitano
Department of Agricultural, Food and Forestry Systems - GESAAF,
University of Florence, Florence, Italy
e-mail: giulio.castelli@unifi.it

E. Bresci
e-mail: elena.bresci@unifi.it

F. Salbitano
e-mail: fabio.salbitano@unifi.it

F. Salbitano
Atacama Desert Centre (CDA), Pontifical Catholic University of Chile, Santiago, Chile

an active institution and the role of the planned management. This paper analyses different case studies in the Atacama drylands, showing the need of stakeholder involvement and participatory approach. A participatory framework is proposed for project implementation and funding for successful and reliable fog collection and water management.

Keywords Fog water collection · Rural communities · Local management · Participatory planning

Introduction

Arid landscapes cover 41% of the surface of the planet. They include both urban and rural areas and people face problems connected with the growth of the population and with tensions in the environmental context, from the over-exploitation of soil and supplies to the lower availability of resources, water in particular. In the Atacama drylands, the most hyperarid region in the planet, the non-sustainable use of land and water and the impact of climate change are the main causes of the general deterioration of the arid landscapes.

The essential function of water is to maintain life on the drylands because all the human settlements are closely tied to its presence, and therefore water becomes a vitally important economic and eco-social resource. Improved availability of water would facilitate the lives of the local population, supporting rural settlements and reducing the exodus of the population to the cities usage (Marzol and Megia 2008).

As a key component of the water cycle, fog is a crucial factor in driving landscape structure, function and dynamics of coastal, high-altitude, and arid or semi-arid regions. The concept of Fogscape (Salbitano et al. 2010), i.e. fog-dependant landscapes, is definitively applicable to Atacama drylands where the frequency, pattern and intensity of fog events is highly influencing the functioning and dynamics at landscape ecology level (Fig. 14.1). Indeed, the social component of fogscape is very linked to fog water collection that can represent a sustainable drinking water resource for rural communities with low per capita water usage (Domen et al. 2013).

The Chamanchaca (advection sea fog) in the Atacama drylands is a local resource that can be directly used by means of a simple technological device called Atrapaniebla (Fog Collector), which intercepts and captures fog moisture.

The fog collector device has been developed and used for many years in Chile: from the 60s this low-technology has been established in northern Chile, and in the 80s and 90s it started being used for water-collection programmes. It has been successfully tested also in other parts of the world, not only for human consumption but also for forestry and agricultural use (Schemenauer and Cereceda 1991, 1994a, b).

The purpose of the article is to describe past and current fog collection projects in the Atacama drylands and to review the sustainable freshwater use practices. In particular, the main objective is to focus on the methods and management



Fig. 14.1 Advection Fog, Alto Patache, Atacama mountains coast (courtesy of *Cereceda P*, CDA—Centro del Desierto de Atacama)

approaches, underline the strengths and weaknesses of ongoing projects and reflect on the development of design and management innovation and improvement for future applications.

Fog and Fog Water Collection

Fog moisture is a fundamental water source in many coastal ecosystems of the world (Dawson 1998). Fog appears in various shapes and places: advection fog is often generated over the ocean, where humid air passes over cooler water and forms low clouds, which are blown in the coastal areas by winds (Hiatt et al. 2012). Due to morphological factors, the formation of advection fog occurs more often in mountainous coastal areas.

The advection fog in the Atacama's coasts allows the existence of fog oases where ecological communities can periodically activate life cycles and relationships initiating temporary and fragile ecosystems. The patches of fog oases usually cover few hectares, fragmented in a continuous matrix of hyperarid ecosystems. The fog oases temporary patches constitute habitat for endemic or highly adapted plant and animal species.

The relics of forest stands in the semiarid coastal mountain ridge in Chile also attest the role of advection fog in sustaining regional ecosystems. The average annual precipitation in these area does not overtake 150 mm of annual rainfall while fog-derived water can contribute to additional 200 mm per year so enabling the existence of forests in fogscapes. The biodiversity of these ecosystems is definitively higher as compared to drier zones hosting species that developed various forms of adaptation to hyperaridity.

Nevertheless, both fog oases and forest of fogscapes are under risk of degradation, loss and desertification. The ecosystem services associated to fogscapes are fundamental for the future of the region. Support services as biological diversity and habitat complexity; regulating services as climate change mitigation, carbon sequestration, micro- and meso-hydrology; provisional services as water, food and wood will be highly dependent, in the next future, on the conservation and restoration of fog-dependent ecosystems.

Thanks to fog collectors, bare areas once dependent on fog can be reclaimed to ecological restoration and the ecosystem services ensured, with great benefits for the local people.

Sustaining tree plantations by fog water is an action that can initiate easily a secondary succession towards ecosystem recovery. Once the planted trees grow to the size of being able to capture fog by the canopy, they become natural fog collectors and, in absence of anthropogenic disturbances, the succession moves towards more biodiverse and complex habitat while reducing definitively the risk of local erosion and desertification, contributing to groundwater recharge (Domen et al. 2013), and initiating soil evolution (Salbitano et al. 2010).

Fog can be directly used by means of a simple technological device. A plastic net is exposed to the action wind that pushes the fog through the net. Fog droplets are captured and combine to run down the mesh into gutters and tanks for storing and purification. Actually there are some experimentation on size, shape, mesh design and materials, depending on the fog quality and site characteristics.

The standard fog collector (SFC) is a small device used in investigative studies to evaluate the amount of fog water that can be collected in determined sites. The SFC consists in a standard 1 m × 1 m metal frame usually covered in polyethylene Raschel mesh, set at 2 m high (Fig. 14.2).



Fig. 14.2 SFC—Standard Fog Collector, Alto Patache, Atacama (photo: *Martino Correggiari, 2012*)

The large fog collector (LFC) mesh areas typically range from 40 to 48 m². The net is anchored to two poles, forming a natural concave surface in the wind. The SFC and LFC should be oriented perpendicular to the main wind direction for obtaining optimal performances (Schemenauer and Cereceda 1994a, b).

Fog water is collected not only in the Atacama drylands but also in various locations throughout the world (Fig. 14.3). The fog collection is then possible in many mountainous coastal arid areas (Chile, California, Morocco, Peru, South Africa) but it is also present in some islands (Canary Islands, Dominican Republic), and in some particular inland sites with scarcity of water or precipitations (Ethiopia, Guatemala, Yemen, Tanzania). In this context, a natural phenomenon and a simple technological device can concretely influence the dynamics of a certain territory and its population.

Many differences in the fog water collection potentials have been determined for a variety of locations around the world. Collection rates range from 1 to 10 l/m²/day, but they are known to be as 20–30 l/m²/day¹ in some regions (Schemenauer and Cereceda 1994a, b).

The collection rate depends on both environmental factors and fog collector design. The factors that determine the collection rate are the wind speed, the liquid water content of fog, the size distribution of the fog droplets and the design of the mesh material. The collection efficiency is most influenced by the role of the wind, with regard to both speed and direction. Schemenauer and Cereceda (1994a, b) and Marzol and Megia (2008) have shown that the optimal wind speed for collecting a good amount of water is between 3.5 and 9.0 m/s.

Figure 14.4 shows the collection rates for different locations in the world.

The evaluation of sites using SFC for fog collection projects is the first fundamental phase. The evaluation time must be at least a year long, to describe the water potential in the location and the seasonality of the phenomenon. It is necessary to distinguish rainfall from fog collection rate in the provision of water for human use;



Fig. 14.3 Fog collection projects using SFC and LFC around the world

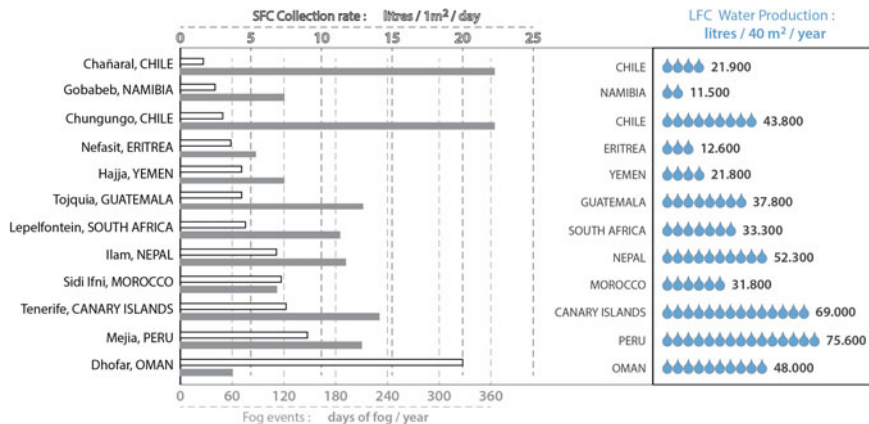


Fig. 14.4 Collection rates and fog water production for selected locations in the world

therefore, the installation of a weather station can be important to give accurate and contemporary data for all meteorological parameters.

The quality of fog water has been proved acceptable for human consumption (Schemenauer and Cereceda 1994a, b). This water is affected by both the surrounding air and the build-up of particles trapped in the mesh: however, most of the fog water harvesting installations around the world meets the WHO standards for metals and ions in drinking water (Abdul-Wahab et al. 2007; Klemm et al. 2012).

In Latin America the fog frequency is very high throughout the year, while in other regions there is less frequency but more collection capacity (Morocco, Canary Islands), still making efficient the use of water fog. In other areas where fog only occurs a few months in the year, such as Oman, Yemen or Eritrea, the storage of fog water for use as drinking water throughout the remainder of the year may be impractical (Schemenauer and Cereceda 1994a, b).

Case Studies

In the drylands, this technology offers an opportunity of sustainable development for small communities, villages or local ecosystems, whose basic needs are highly vulnerable. Moreover, the positive effects could be multiple, as for example the reduction of migration of people away from rural areas, the conservation of traditional activities, the support to local hydrology and ecosystem recovery, etc.

Our interest in research on fog water collection lies in some factors that can determine the success or failure of a fog collection project. For this reason, we have collected different case studies in the Atacama drylands to analyze and compare their development processes. First of all, they show that fog water is a valuable

source of fresh drinking water for human consumption, gardening, and even for reforestation. These case studies reflect the features of other ongoing projects that have various elements in common. One of the main elements is the interaction and collaboration, on different levels, between the local communities and one or more active institutions/organizations, which can be a university research centre, an NGO or a government institution.

Therefore, particular attention should be given to the implementation factors for long-term success in community fog collection projects.

Chungungo—El Tofo—Chile

The fog water project in the village of Chungungo (La Serena, 29°26'52.0"S 71° 17'54.5"W) began in 1987 with the evaluation phase (Fig. 14.5). The work was run by a collaboration between the IDRC, International Development Research Centre of Canada, the investigators of the Pontifical Catholic University of Chile, and the National Forestry Corporation (CONAF).

In 1992, the research group installed 50 fog collectors and the Canadian Embassy provided funds to build a pipeline from the collection site to the village of Chungungo on the coast. The Chungungo Water Committee (CWC) was established as a local organization that included the whole community as partners.

The system grew until there were about 100 fog collectors, 7 km of buried pipeline, a storage tank and a distribution system in the village. An average of 15.000 l of drinking water was provided each day of the year, with peak water production exceeding 100.000 l per day (Cereceda et al. 1997). The Side by side

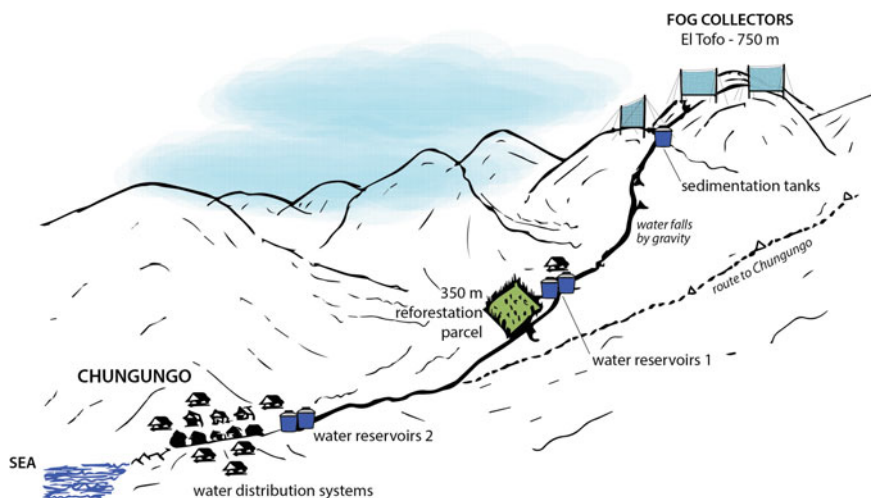


Fig. 14.5 Chungungo fog collection system scheme

with the FCS development, some projects were carried out, like the establishment of forest plots, a fish manufacturing plant and an agricultural orchard.

In the following years the community and the CWC were no longer supported in the management of the project, as a consequence administration problems began because the CWC failed to resolve different issues regarding water distribution, fog collector damages and operational maintenance (Edwards 2005). The maintenance of the fog collectors implied funds that were not available and the pressure of the community, which grew from 300 to over 600 permanent residents, determined the end of the project. In the early 2002, there were about 25 operating fog collectors and in 2003 there were none. Water began once again to be requested at a high cost through the tank trucks, as the community had done before the start of the project.

Chañaral—Falda Verde—Chile

The project began in 2001 to provide water to the coastal location called Falda Verde (Copiapó, 26°17'57.6"S 70°37'24.4"W), 5 km north of the city of Chañaral. The Atacama Fog Collection Group, a group of local fishermen, ran the project and installed 6 large fog collectors of 48 m², after 2 years of studies and measurements, supported by the FogQuest organization and the Pontifical Catholic University of Chile.

Fog collectors initially provided about 600 l of water daily to a greenhouse and an agricultural area in the coast. The greenhouse had tomato plants and the group started an Aloe Vera plantation in the field. A number of organisations provided the necessary funds through donations from the first installation to later additions, like the Rotary Club in Canada, the Australian Embassy and the AngloAmerican Company in Chile. In 2005, four new LFCs as well as some infrastructure to pipe and store the water were installed: this has increased the average daily water production to about 1000 l.

The group members have also built a path that starts from the cultivations and gets the fog collectors on the tops of the first range of mountains, connected with the network of trails of the nearby National Park of "Pan de Azucar", attracting some tourists.

Actually, the Atacama Fog Collection Group manages the maintenance activities and sells the Aloe Vera produced (Fig. 14.6). The project has slowly developed over the years and has found its balance, managed entirely by the Group, producing alternative profits for the community.

Mejia—Lomas de Mejia—Peru

The first experimental campaign in Mejia (Arequipa, 17°03'46.5"S 71°53'19.7"W) was carried out from 1995 to 1999 in the framework of an EU project, with the aims



Fig. 14.6 Aloe Vera plantation in Falda Verde (courtesy of *Cereceda P*, CDA—Centro del Desierto de Atacama)



Fig. 14.7 Fog collectors in the Mejia Lomas (photo: *Elena Bresci*, 1997)

to reintroduce vegetation on the Lomas ecosystem and to investigate the effectiveness of fog collection technology (Fig. 14.7). Five Universities were involved, the San Augustin University of Arequipa from Peru, the Pontifical Catholic University from Chile and others from Europe, Padua, Florence and Toulouse.

In the experimental site of Las Cuchillas, located on the coastal hills close to Mejia (Dept. Arequipa, South Peru) trees of native species (*Caesalpinia spinosa* and *Prosopis pallida*) and exotic species (*Acacia saligna*, *Casuarina equisetifolia*, *Parkinsonia aculeata*) were planted in 1996, in order to check the rehabilitation

potential of the degraded “lomas” ecosystems. The main project’s installations were 20 large fog collectors (with 6000 l average daily water production), three reservoirs, the drip irrigation system, an experimental station and plot.

After the end of the EU project, the tree plantation was monitored over a period of 14 years (2010). Among indigenous species *Caesalpinea spinosa* shows the highest rate of survival. The exotic *Acacia saligna* shows the maximum height, diameter and crown volume increments. The habitat conditions, both in term of diversity/frequency of plant and animal populations, and plant cover have changed substantially over the years. Overall, the tree-covered soil retained much more of both elements than the non-forested areas, thus demonstrating the efficiency of the intervention carried out in terms of combating the greenhouse effect. The various tree species planted, however, showed greatly variable capacity to promote carbon sequestration at soil level.

The water collected by the fog collectors was used not only for plant cultivation, but also for livestock water supply and small-scale farming. But once the goals were achieved, the project slowly ended because of the lack of involvement of the local people in monitoring and maintaining it.

Atiquipa—Lomas de Atiquipa—Peru

This case study is located in Peru, in the southern Lomas, vegetal formations similar to the Fog Oasis in Chile. The residents of the rural community of Atiquipa (Arequipa, 15°47’40.4”S 74°21’47.0”W) are the owners of the Atiquipa’s Lomas, extending across 30.000 hectares of land.

The first phase of evaluation with SFC started in 1995–97, developed by the investigators of the San Augustin University of Arequipa, in collaboration with the Atiquipa villagers. Then, they installed 28 fog collectors divided into two mountain sites, and different ponds thanks to the high water capture (Fig. 14.8).

Water was used essentially in the reforestation of 400 hectares with a plant of great importance to the community’s economy: the “tara” (*Caesalpinea tinctoria*) whose fruits are quoted in the local and international market.

The community involvement has been a key factor to achieve the restoration of a part of this ecosystem; currently the “Environmental Management Plan: 2005–2020” is active. It is overseen by the Atiquipa inhabitants, and the Lomas have received the recognition of “Private Conservation Area”.

These results show that it is possible to capture water enough to recover ecosystems and make subsistence farming through the irrigation of species with little water requirement and resistant to drought.



Fig. 14.8 LFC—Large Fog Collectors in the Atiquipa Lomas (reproduced from *González SM and Torres J 2009*)

Evaluation Criteria

Leaving aside the technical data for individual projects, our attention has shifted to the relationship between the stakeholders involved, and the social and economic aspects. Inside these aspects, which have a wide range definition, we can find the key criteria for the implementation of future fog collection projects.

From the point of view of management processes, past and ongoing projects have shown some limits in the methodological approach. Therefore, priority must be given to the effectiveness of participation processes and management tools, and in any case on the will of all the stakeholders involved.

From the point of view of the community involvement and perspectives, the analysis allowed us to identify some essential factors in the development of a fog collection project, among which the most important are the long-term and active presence of a local organization, the community participation and training and the continuous participatory redesign of the project with all the stakeholders involved.

Methodological Approaches—Participatory Processes

The interest in research on fog water collection does not only lie in the technical aspect because there is enough literature that considers the issues of technical improvement, mesh technology, water sanitation and every aspect to be taken into account in the evaluation of a potential fog collector site. The real interest is in future applications, and what really matters is that water resource will be essential to

improve the quality of life of rural communities (Marzol and Megia 2008) and their surrounding arid landscapes.

The first step is to identify a social need for water. There must be a community with a requirement for more water or cleaner water while conventional means are not able to satisfy their demand (Batisha 2015). In this case, there is a critical point to be solved at the beginning of every type of intervention: the commitment of the community to be an active partner of the project.

Another point of particular importance at the beginning is the identification of a local non-governmental organization (NGO), or other organizations, who work directly in the territory. The organization will have the task to provide training, education and the on-going support for the participation of the community. It is important to have the local population participate in decisions on the water applications, participate in the construction of the system, and, as far as it is practical, take over the maintenance and operation of the system (Batisha 2015).

Therefore, the first phase of the evaluation of fog water potential must be carried on in parallel with the analysis of the community's social, cultural and economic status. The social impact of this type of project and the possibility of a new source of freshwater should be managed by means of a series of community meetings and specific meetings with the women of the village who may be excluded from the village organizational structure. The elders and community councils usually manage community organizational and social structures. Considering these structures, another fundamental factor is the creation of a specific committee for the water management. In this way, the community is empowered and in a legal position to seek out financial and project assistance from different sources. Membership rests on the belief in their founding principles, commitment to the group and collaborative participation (Rosato et al. 2010). The role of the local organization is to ensure the water committee activities and an appropriate and functional water management programme.

In fact, a project that involves the use of new resources and the involvement of the local population must consider a management methodology in the form of an integrated management plan. This implies that the first decision to proceed with the project is made by all the stakeholders involved: the community, the local organization, the sponsors, the institutions. Then the respective skills come into play in a continuous participatory redesign of the project, where technical adjustments and goal corrections must be agreed with community members.

Some projects end when the management passes to community responsibility, because of some common causes: operating costs, poor maintenance, administrative difficulties and lack of involvement. For example, in the Chungungo project only a half of the community members know that the fog collector system was a donation from the institution involved. The village was located 7 km from the LFC and local population had no connection with the fog resource environment resulting in poor knowledge of fog behaviour. All these factors were reflected in a low overall involvement with FCS, resulting in low community participation. This resulted in a low community commitment with the CWC and thus in an inappropriate maintenance of the fog collectors, affecting the efficiency of the FCS.

In the case studies and in other fog collection projects, the population of the communities ranged between 100 and 500 people. High levels of independence were reported in communities with few inhabitants. The belonging to small communities makes the individual person more responsible for the project. Particularly, women need to be involved starting from planning to the implementation stage as they are the primary users and direct beneficiaries of the collected water (Fessehaye et al. 2014).

It is important to understand that the community members are not only the beneficiaries of the project, but in particular they are the main players who will manage the project and the future social impacts. The more the people are encouraged, permitted and willing to invest (within their means of possibility), the more convinced they will be of the project and the higher the likelihood of long-term success. Strong enough long-term commitment to the project is essential to a successful transfer of technology and active, ongoing management by the community. Continuing to support and facilitate this local capacity development has been identified as a crucial objective in the next phases of the project.

To ensure the economic management, during all the development project steps, exit options must be taken into consideration. That may happen very early, before any test measurements are being started, before the decision of construction of large collectors, or after the LFC production phase with limited success (Klemm et al. 2012).

Methodological Approaches—Funding and Costs

In the economic evaluation of fog collection projects, it is preferable to adopt a planned management rather than a process of cause-effect. The latter choice would be the simplest, consisting in the birth of a project idea, fundraising, and the achievement of results: but the focus must be shifted from the result to the method (Fig. 14.9).

An economic study, undertaken to ensure that the projected water costs will be favourable in comparison to other alternatives such as tanker trucks or water pipelines.

The beginning of a project of collecting fog water has to follow the phase of consultation between the stakeholders. Then Initial funds and expertise typically originate from outside.

These funds must be raised from a sponsoring agency with an interest in the territory, from donors who are willing to support the proposed project, or from organizations with a focus on supporting water projects in developing countries.

Typical funding agencies are private and corporate donors, NGOs, UN agencies and the European Union. In many cases, there is a lack of information about potential money sources. For example, in the Atacama region, belonging to Chile and Peru, funds are offered by governmental organizations the local municipalities,

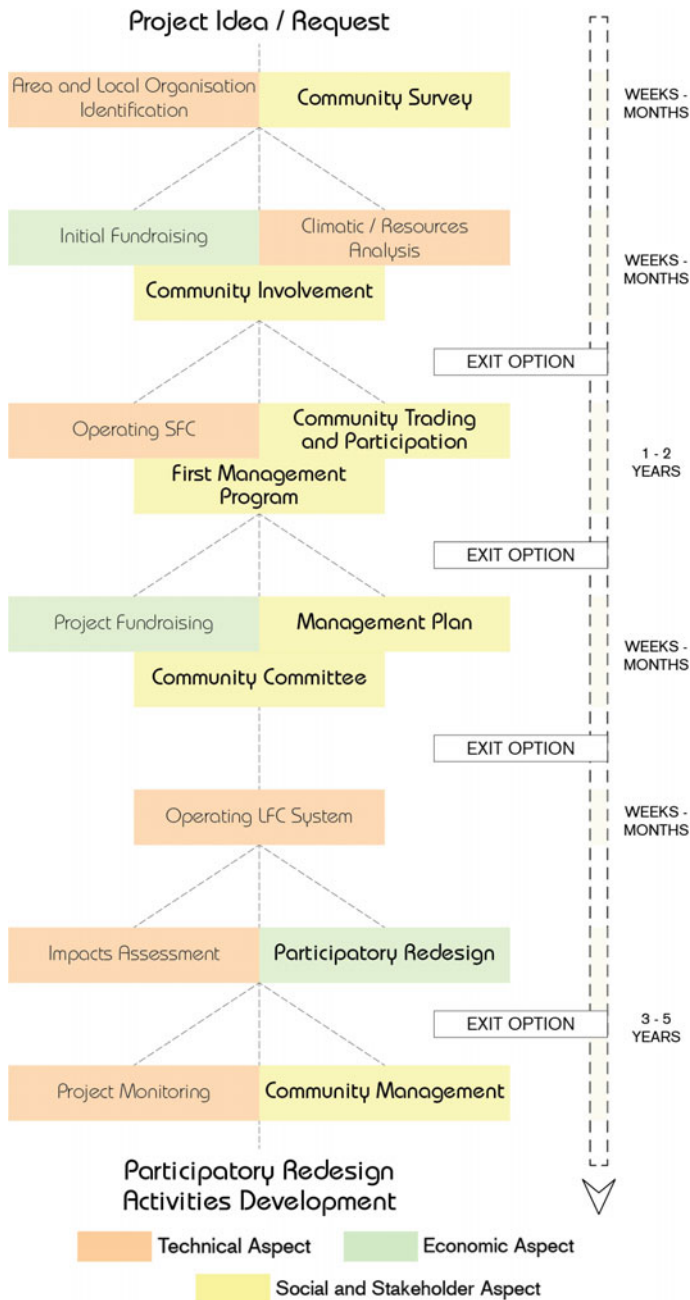


Fig. 14.9 Methodological approaches: hypothesis of a management programme for a fog collection project

private companies and foreign embassies, but local people are not aware of these funds.

The private sector, represented by many industrial companies and mining industries which operate in the Atacama drylands, can be interested in projects of environmental compensation to make up for the pollution they produce and to take advantage of financial opportunities. Environmental compensation is compulsory in Chile, like in many other countries.

One vital source of funds is the community interested in the water project. Not because they have a lot of money to provide, but because their monetary commitment shows their serious involvement in the project. It shows they are not simply looking for a gift but they are rather an active partner in the project.

A complete SFC setup costs around 150 USD, depending on the local market situation. If a field programme with a complete meteorological station is required, then an additional 2.500 USD in instrument and travel costs may be involved plus time for data analysis (Klemm et al. 2012). The estimated start-up cost for an installation of a complete LFC system for a rural village of 150 people on the Atacama coast is of around 75.000 USD, assuming no costs for salaries in external NGOs (Klemm et al. 2012). The cost includes collectors, pipes, storage tanks and, distribution system for an installation with a target goal of 30 l/capita/day, requiring approximately 20 large fog collectors, or around 750 m² of mesh, considering an average collection rate of 6 L/m²/day. A fog collector project in Lima that considers 100 LFC at 350 USD per collector and 500 USD for annual maintenance, shows how an investment of 35.000 USD being paid back after a period of 8 years. Obviously, the funds required depend on the scale of the project and its location.

The integrated management plan of the project should include strategies and funding for ongoing support, unanticipated expenses and repairs and it must require the necessary participation and involvement of the local community in maintaining and managing the installations. The availability of time may be the best possible investment from the community because maintenance requires monitoring, regular tightening of support cables and mesh, immediate repairs to any minor tears, inspections of reservoirs and distribution systems, etc.

Through participatory redesign, it is thus possible to monitor activities and financial aspects, allowing the direct users and potential new investors or sponsors to be informed and given awareness on new project goals and interventions.

As the case studies shown, there are advantages to fog collection projects when they provide benefits and profit for local populations, besides increased water availability (Fig. 14.10). Therefore, local populations could consider their participation as an investment, regarding themselves not only as a marginalised group of neighbours trying to improve their livelihood, but as a group of investors starting their own business (Batisha 2015; Klemm et al. 2012).



Fig. 14.10 Fog collector system and community members in Falda Verde, Chañaral, Atacama (courtesy of *Cereceda P*, CDA—Centro del Desierto de Atacama)

Conclusions

Fog collection, as an alternative source of freshwater, does not represent a global solution for the problem of water availability in drylands, but it allows intervene in a specific way in local situations, usually neglected by the infrastructural innovations that are applied to the most densely inhabited and productive areas of a territory.

A good number of projects show the opportunity to perform various activities: drinking water for human consumption, reforestation and agricultural production. These activities can generate small business and social initiatives and have positive effects on the territory, at an ecological and cultural level. In a holistic landscape framework, these positive effects are reflected on the arid lands' safeguard and local development, thanks to research, educational activities and sustainable tourism. Ecological factors should be considered because fog collectors does not require on-going energy inputs and could be useful for carbon sequestration in connection with reforestation (Batisha 2015).

From the point of view of management processes projects have shown their limits in the methodological approach. The analysis of some different case studies in the Atacama drylands shows that community participation is vital for the elaboration of plans and activities, which improves monetary income and at the same time can provide fund and labour for FCS operation and maintenance. Real sustainability will be reached when the beneficiaries are themselves managers of a fog water collection system. Capacity building, awareness motivation, education and training of the local people are key success factors (Rosato et al. 2010).

The role of a local organization, aiming to implementing all aspects of technology and management, is much more appropriate to offer a long-term role promoting fog collection projects than a foreign-sponsored institution who might withdraw from that territory.

This work reviewed, compared and discussed experiences and theoretical materials, with the purpose of exchanging information and underlining some critical aspects of fog collection project management. Starting from practical experience, we propose an operative framework for stakeholders involvement and a participatory approach based on the redesign concept, with the objective of facilitating future fog project implementation and support the translation of this alternative technology to various local situations in drylands.

References

- Abdul-Wahab SA, Al-Hinai H et al (2007) Fog water harvesting: quality of fog water collected for domestic and agricultural use. *Environ Eng Sci* 24:446–456
- Batisha AF (2015) Feasibility and sustainability of fog harvesting. *Sustainability of water quality and ecology*
- Cereceda P, Schemenauer RS, Velásquez F (1997) Variación temporal de la niebla en El Tofo - Chungungo, Region de Coquimbo, Chile (1987–1995). *Revista de Geografía Norte Grande* 24:103–111
- Dawson TE (1998) Fog in the California redwood forest: ecosystem inputs and use by plants. *Oecologia* 117:476–485
- Domen JK, Stringfellow WT, Camarillo MK, Gulati S (2013) Fog water as an alternative and sustainable water resource. *Clean Technol Environ Policy* 16:235–249
- Edwards M (2005) Community involvement in the fog-water collection system for Chungungo, Chile. Catholic University of Chile, Santiago, Chile
- Fessehaye M, Abdul-Wahab SA et al (2014) Fog-water collection for community use. *Renew Sustain Energy Rev* 29:52–62
- González SM, Torres J (2009) Gestión ambiental de las tierras secas del sur del Perú: cosecha del agua de neblinas en lomas de Atiquipa. Universidad Nacional Agraria La Molina, Perú
- Hiatt C, Fernandez D, Potter C (2012) Measurements of fog water deposition on the California central coast. *Atmos Clim Sci* 2:525–531
- Klemm O, Schemenauer RS, Lummerich A et al (2012) Fog as a fresh-water resource: overview and perspectives. *Ambio* 41:221–234
- Marzol MV, Megia JLS (2008) Fog water harvesting in Ifni, Morocco. An assessment of potential and demand. *Die Erde* 139:97–119
- Rosato M, Rojas F, Schemenauer RS (2010) Not just beneficiaries: fostering participation and local management capacity in the Tojquia fog-collection project, Guatemala. In: 5th international conference on fog, fog collection and dew, Münster, Germany, 2010
- Salbitano F, Calamini G, Certini G et al (2010) Dynamics and evolution of tree populations and soil-vegetation relationships in Fogscapes: observations over a period of 14 years at the experimental sites of Mejía (Peru). In: 5th international conference on fog, fog collection and dew, Münster, Germany, 2010
- Schemenauer RS, Cereceda P (1991) Fog-water collection in arid coastal locations. *Ambio* 20:303–308

- Schemenauer RS, Cereceda P (1994a) A proposed standard fog collector for use in high-elevation regions. *J Appl Meteorol Climatol* 33:1313–1322
- Schemenauer RS, Cereceda P (1994b) Fog collection's role in water planning for developing countries. *Nat Resour Forum* 18:91–100

Chapter 15

Salt and Water Dynamic of Potato Crop Under Irrigation with Low Quality Waters

Mguidiche Belhaj Amel, Gazouani Hiba, M'hamdi Douh Boutheina and Boujelben Abdehamid

Abstract In Tunisia, the scarcity of water for irrigation and the quality of available resources make it necessary to adopt strategies of water management aimed to increase water use efficiency. If from one side, choosing an appropriate irrigation system, like a well-designed subsurface drip system can ensure high values of water distribution uniformity, increasing water use efficiency requires that irrigation scheduling account for actual crop water requirement, depending on soil, plant, climate, and other local conditions. During the growing season (2014) to investigate the effects of low water quality and scheduling on water's dynamic in soil (soil water content moisture distribution, water's stock variation) and water use efficiency (WUE) to produce potato (*Solanum tuberosum* L.). Subsurface drip irrigation was used for two treatments T1 and T2; T2 was irrigated 50% of T1. During the crop season soil water content variation was more important at the end due to root uptake and hard climatic condition, treatment T2 had less water stock and best water use efficiency with 10.83 kg/ha than 5.85 kg/ha for T1.

Keywords Water requirement · Soil water content · Water use efficiency · Root uptake · Subsurface drip irrigation

M.B. Amel (✉) · G. Hiba · M.D. Boutheina · B. Abdehamid
Department of Genius of Horticultural Systems and Environment,
Higher Institute of Agronomy, University of Sousse,
BP 47, 4042 Chott Mariem, Tunisia
e-mail: amelmguidche@yahoo.fr

M.B. Amel
Regional Field Crops Research Center (CRRGC), B. P. 350, 9000 Béja, Tunisia

Introduction

Rainfall patterns are undergoing modifications in numerous parts of the world. Future scenarios predict that in most Mediterranean countries, pro-capita water availability in 2025 will decrease 50% with respect to 1987 (Hamdy et al. 1995), while an established trend of reduction in summer precipitation in the last decades on the Mediterranean basin is already evident. Freshwater demand is steadily increasing worldwide as the demand for industrial and domestic water supplies increase with population. This growing demand for freshwater necessitates that the agricultural sector must move from a scenario of water supply management to water demand management, thus dictating more efficient use of water in the production of food, feed, and fiber. Agricultural scientists should pay greater attention to management of crops for high productivity with a view of limited water supply for irrigation.

Potato (*Solanum tuberosum* L.) is one of the most important crops in the world's various agricultural production volume after wheat, rice, and corn (Fabeiro et al. 2001). Due to its sparse and shallow root system, potato is very sensitive to water stress and tuber yield may be considerably reduced by soil water deficits (Porter et al. 1999). Therefore, irrigation is always needed for production of high-yielding crops (Fabeiro et al. 2001). Due to chronic water shortage good irrigation management is required in order to improve water use efficiency (WUE). Potato is considered relatively susceptible to salinity (Maas and Hoffman 1977) and normally is not suited for stressful conditions. However, its cultivation has been gaining popularity during the last decade in arid areas as a cash crop because temperature and radiation conditions allow for cropping over the spring, fall, and winter seasons (Ben Mechlia et al. 2007). Drip irrigation system is considered one of the most effective to supply water to crop subsurface drip irrigation (SDI), defined by the American Society of Agricultural Engineers (ASAE) (1996), is the application of water below the soil surface through emitters, with discharge rates generally in the same range of the drip irrigation. Well-designed subsurface drip irrigation, providing small quantity of water below the soil surface under high frequency aimed to maintain high water contents and nutrients concentration in the root zone, is considered a powerful system to ensure high distribution uniformity and to enhance irrigation efficiency. At the same time, deficit irrigation (DI) has shown successful results with a large number of crops in various countries. However, for some crops like potato, DI is difficult to manage due to the rapid effect of water stress on tuber yield (Lynch et al. 1995). Irrigation frequency is a key factor for subsurface drip irrigation scheduling; different frequency of watering have an effect on wetting patterns, even under similar irrigation doses, so affecting crop yield. Several Authors have been underlining the positive effect of high irrigation frequency on soil water distribution and on root water uptake. Despite the importance of deficit irrigation applied with subsurface drip irrigation to enhance water use efficiency, a few studies have been carried in the context of Tunisian climate.

Many researchers have reported higher yields and water use efficiency (WUE) of drip irrigation system over the conventional irrigation methods throughout the world in different vegetable crops, such as potato (Unlu et al. 2006; Wang et al. 2006), cucumber (Yuan et al. 2006), capsicum (Sezen et al. 2006), onion (Rajput and Patel 2006), okra (Tiwari et al. 1998), cabbage (Tiwari et al. 2003) and egg-plant (Chartzoulakis and Drosos 1995).

This study was conducted at the Higher Institute of Agronomy of Chott Mariem, Tunisia. It carried to determine water quality and quantity soil on the variation of soil water content, stock variation, salt distribution, and water use efficiency.

Materials and Methods

Experiments were carried out at the higher Institute of Agronomy of Chott-Mériem, Tunisia (Long. 10, 56° E, Lat. 35, 91° N, Altitude 19 m a.s.l.). The climate is semi-arid, characterized by an average annual precipitation of 230 mm and reference evapotranspiration of about 2100 mm year⁻¹.) Climatic data during the growing season of potato crop was presented in Fig. 15.1. Soil is sandy loam (clay = 8%, silt = 31% and sand = 61%) with a bulk density equal to about 1.60 g cm⁻³ for the layer 0–80 cm, and $\theta_{cc} = 0.36$, $\theta_{pfp} = 0.06$, and RU = 240 mm. Potato crop '*Solanumtuberosum* L.' cv. Spunta, was planted on January 15, with 40 cm spacing between plants along the row and 80 cm between rows. Experiments were carried out in 2014 on two plots with the same design and irrigated with water having an EC_w value of 3.32 dS m⁻¹, chemical composition was presented in Table 15.1. Potato is irrigated by a SDI system, with a single pipe per plant row. Each pipe, having a diameter of 16 mm and emitters spaced 40 cm apart, was installed at 20 cm depth. Each emitter flow rate equal was 4 l/h at a nominal pressure of 100 kPa. Standard meteorological data are recorded from a weather station placed about 300 m far from the experimental area. Eight watering were supplied during the growing period of potato for. Time-DOMAIN reflectometry (TDR) was used to determine the volumetric soil water content, a total of three measurement tubes were installed around one emitter; in particular, the access tubes were located near the emitter, as well as at 25 and 50 cm from emitter. Soil water content was measured every 10 cm, in the layer 0–50 cm.

Field experiments aimed to test two different treatments (T1; T2) maintained under the same management, except that for irrigation depth. Irrigation timing T1 was scheduled according the average soil matric potential in the root zone, T2 received about the half of the volume provided in T1, by reducing proportionally irrigation timing.

Soil salinity expressed by electrical conductivity of saturated paste extract (ECe) was determined periodically during the crop season. Soil is sampled to 0.6 m depth at 0.2 m increments along the vertical profile near emitter. Each salinity simple was carried near new emitter since the method was destructive. Considering that the method was destructive, each measurement was carried out in

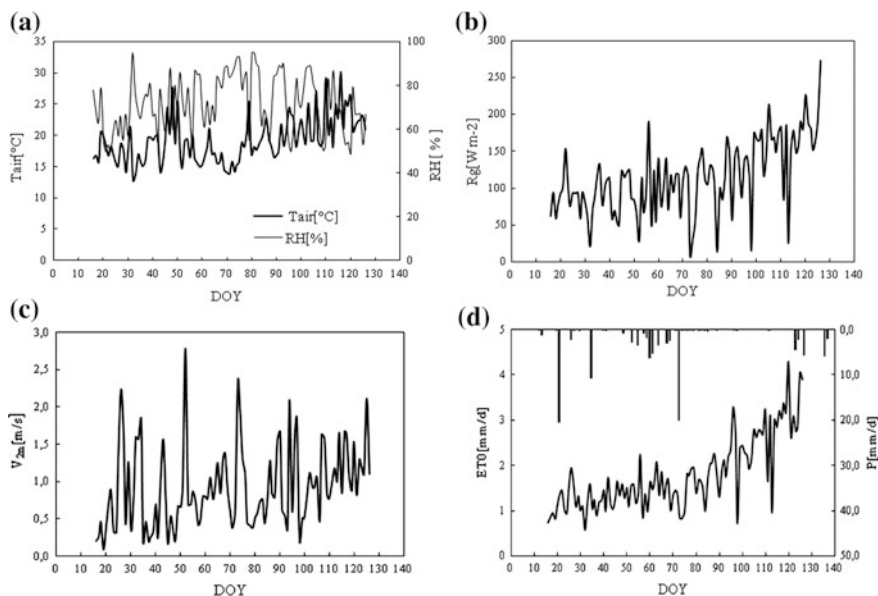


Fig. 15.1 Climatic data variation during the crop season of potato crop

Table 15.1 Chemical composition of irrigation water

Analysed parameter	Unit	Results
K ⁺	g/l	0.18
Na ⁺	g/l	0.46
Cl ⁻	g/l	0.71
Mg ²⁺	g/l	0.012
Ca ²⁺	g/l	0.1

correspondence of a different emitter. At harvest, ten plants within each plot are harvested by hand to determine fresh tuber yield.

Water use efficiency (WUE) is defined as the yield obtained per unit of water consumed, whether from irrigation or total received, therefore including the precipitation. The WUE was calculated as follow: $WUE (kg ha^{-1} mm^{-1}) = Yield (kg ha^{-1}) / (Irrigation + Rain (mm) \text{ from planting to harvest})$.

Results and Discussion

Soil Water Content

Soil water content variation measured during the growing period at different depth under two treatments irrigated with saline water is presented in Fig. 15.2. Irrigation

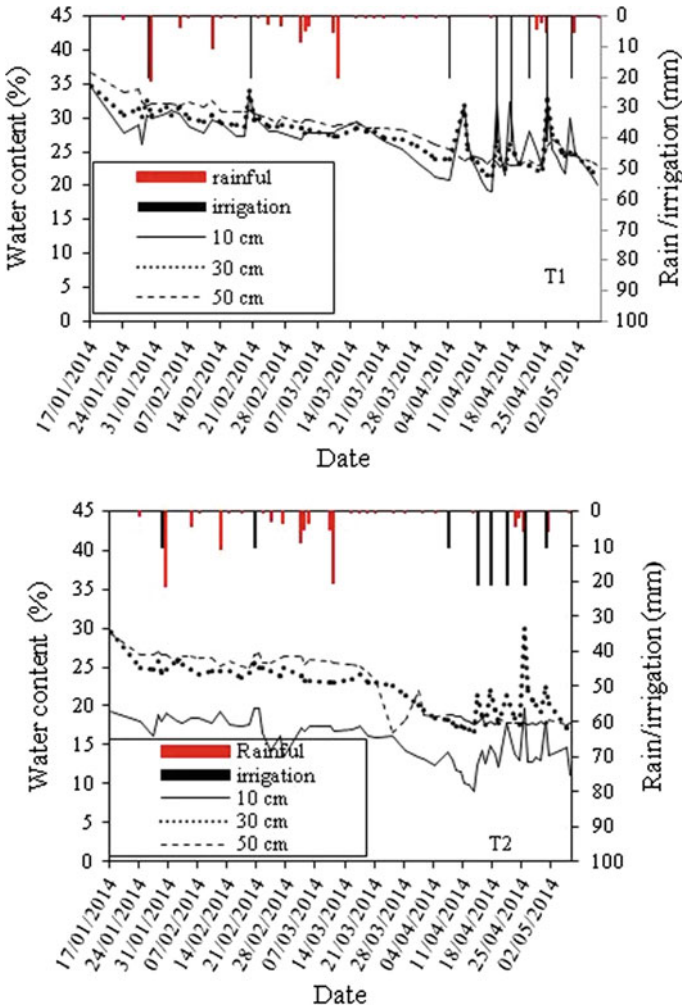


Fig. 15.2 Soil water content variation for both treatments T1 and T2 during the growing season of potato crop

timing T1 was scheduled according the average soil matric potential in the root zone, T2 received about the half of the volume provided in T1, by reducing proportionally irrigation timing

For treatment T1 soil water content varies between 18 and 35%. The low value of soil water content was from January 17 to March 7, from March 7 variation was more important this is due to root uptake in the stage of full development of potato crop. Soil water content increases after irrigation or rain and decreases between two irrigations. Difference in soil water content in different layer could be explained water infiltration and difference of root system development. For T2 soil water

content was between 17 and 30%, at 30 cm depth soil water content are more uniform since this layer supplied by the capillary reassembled layer below at. For both treatment, soil water content at 50 depth is more uniform than 10 and 30 cm. Douh and Boujelben (2012) evaluate the soil moisture distribution under drip irrigation system buried at 5, 20, and 35 cm and demonstrated that more uniform soil moisture content was observed at a depth of 35 cm compared to that in 20 and 35 cm depth and highest moisture values were recorded at deeper soil layer for all treatments. Malash et al. (2008) reported that soil moisture was at a minimum in the root zone (20–40 cm layer), but showed a gradual increase at 40–60. They also reported that soil water content decreased gradually as the distance from the irrigation water source on soil surface increased.

Water Stock Variation

Figure 15.3 illustrates the stock variation under T1 and T2 treatments. The stock change was positive after water supply by irrigation or rainfall events and negative between two successive water supplies due to the root extraction or water loss by drainage. Comparing the stock variation of both treatments T2 has stock variation more important than T1, therefore due the root extraction taking into account that the irrigation rate is 50% T1. In previous work, Douh and Boujelben (2012) mentioned that lowest amplitude variation in soil water stock gave optimum development of the crop root system in more steady soil humidity.

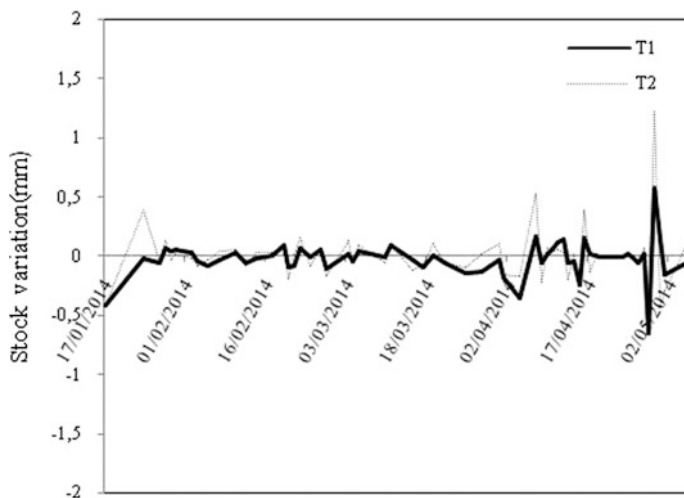


Fig. 15.3 Stock variation for both treatments T1 and T2 during the growing season of potato crop

Salt Distribution

Soil salinization was measured in order to evaluate the effect of two strategies of irrigation T1 and T2 on soil salinity in the first 60 cm layer. Conductivity of the extract of paste has been determined for each soil sample. A weighted average of soil salinity has been performed using the Kriging interpolation.

Figures 15.4 and 15.5 shows salt distribution around emitter buried at 20 cm coordinated (0, -20). After plantation and in the starting of development (January 28) of potato, E_{Ce} value varied between 0.8–4 dS/m and 1.8–3.5 dS/m, respectively, for T1 and T2 treatments. T1 was noted a best uniformity in the distribution curves of equal electrical conductivity, and it is observed that the values of conductivity have the same size.

The pattern of E_{Ce} around the drip line showed values more important than the threshold value (1.7 dS/m) throughout the soil profile, salinity was the least near the drip line with values less than about 1.8 dS/m for T1 and 2.8 for T2, but salinity

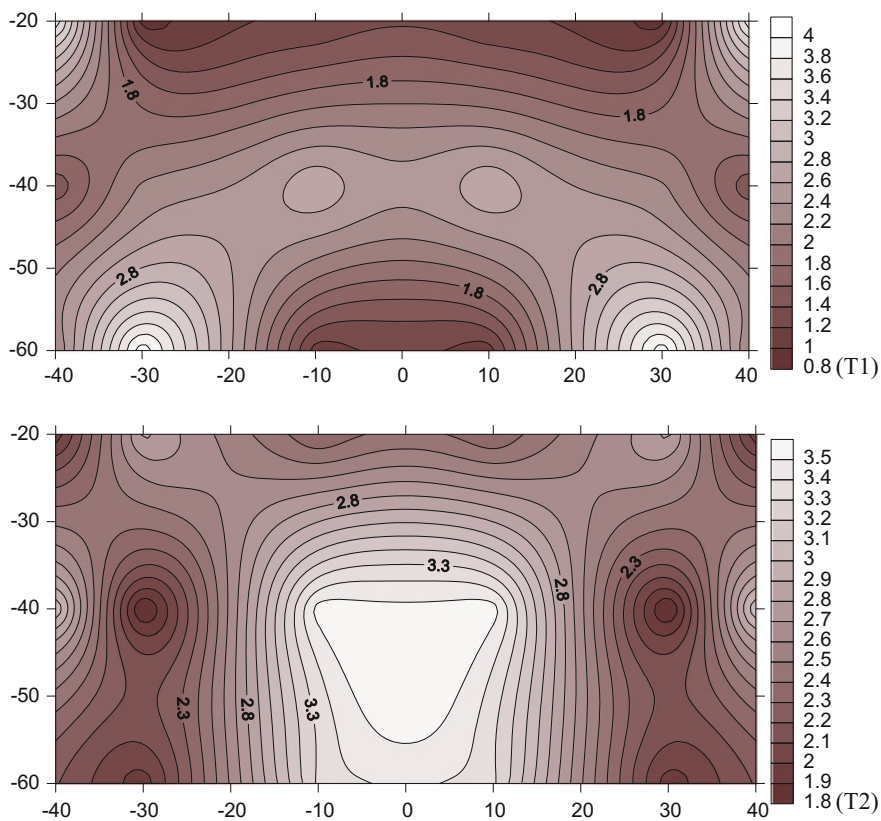


Fig. 15.4 Salt distribution around emitter for T1 and T2 at the beginning of the experiment

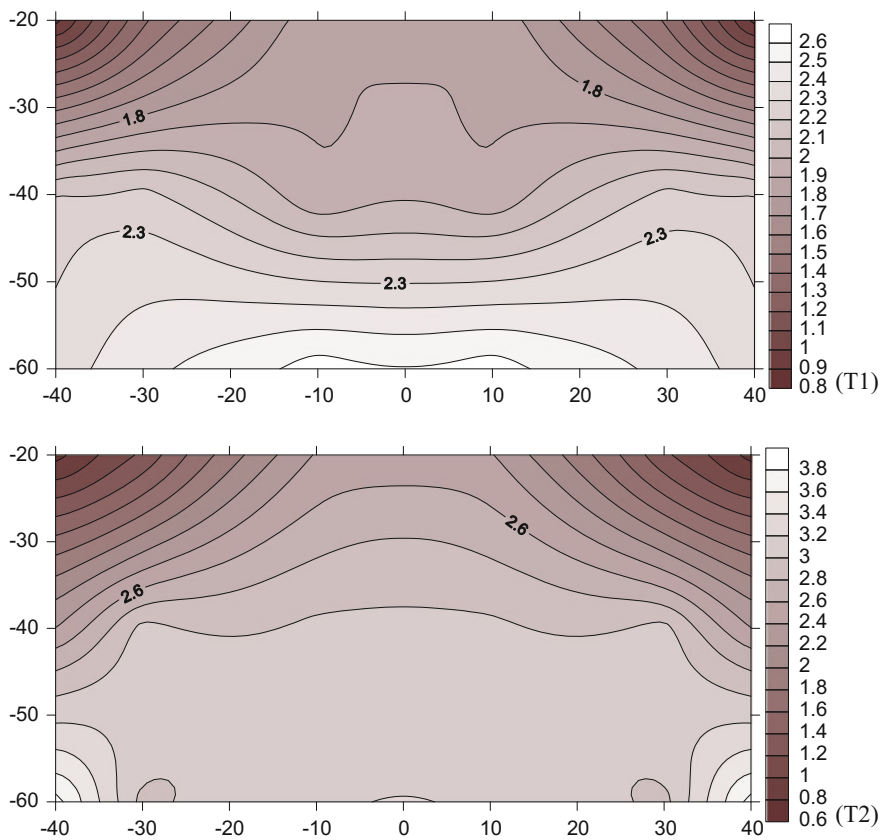
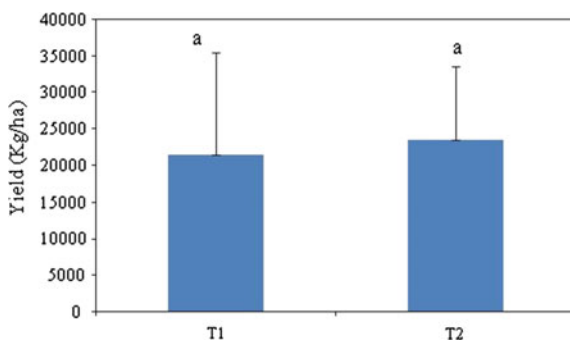


Fig. 15.5 Salts distribution around emitter for T1 and T2 treatments at the end of the experiment

Fig. 15.6 Potato crop yield



increased with horizontal distance from the drip line and with depth. Salinity also increased above the drip line as depth decreased indicating salt accumulation above the drip line.

At Salinity above the drip line increased as depth decreased. The high salinity near the drip line reflected the well water EC. The low levels of salinity near the edge of the pattern probably reflected leaching of salts due to ponding from a severe winter rain. At the end of the development of potato crop there is an increase in salinity in treatments T1 and T2 indeed there is a higher value of electrical conductivity below the drippers at the last layer, which explains the leaching of salts outside the wetting zone using water have an electrical conductivity 3.56 dS/m.

Yield

Yield of potato crop was 21490.75 kg/ha and 13978.37 kg/ha, respectively, for T1 and T2 (Fig. 15.6), T1 have more important yield even if difference was statistically not significant according to a t-test. Deficit irrigation creates water stress that can affect the growth and development of potato plants. At all stages of growth, water stress reduces photosynthetic efficiency, but the drought during the periods of tuber initiation and bulking has the most drastic effect on the yield (MacKerron and Jefferies 1986; Haverkort et al. 1990; Lynch et al. 1995; Yuan et al. 2003). As showed by El Hendawy (2008) that corn yield, yield components, increased with increasing irrigation rates in drip irrigation.

Water Use Efficiency

Water use efficiency (WUE) values (Fig. 15.7) were affected by irrigation treatments. WUE was highest (10.3 kg/m^3) with T2 treatment and was lowest (5.9 kg/m^3) in case of T1 treatment ($P < 0.05$). Lower water use efficiency in T1 treatment can be attributed to reduced yield but also to higher water consumptive use presented in Table 15.2.

Fig. 15.7 Total Water use efficiency (WUE, kg/m^3) for treatments T1 and T2

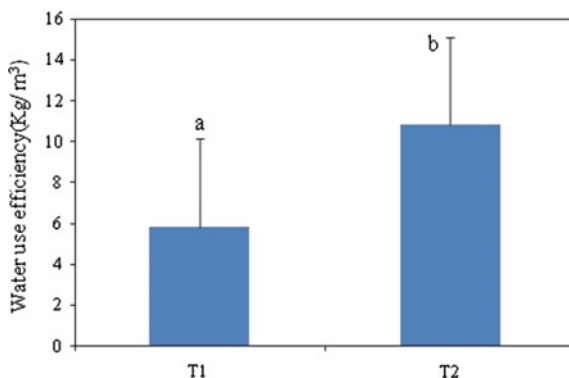


Table 15.2 Irrigation and rain for both treatment T1 and T2

	Irrigation (mm)	Rain (mm)
T1	208.3	108.6
T2	104	108.6

These results are in agreement with those of Yaseen et al. (2014) and Al-Mefleh et al. (2012) who mentioned that increasing irrigation levels did not increase the WUE in melon.

Conclusion

Soil water content and salt distribution was more uniform in treatment T2 in which received 50% of the volume provided in T1. For both the treatment salinity increases within depth and around the drip line. Yield for treatment T1 was more important than T2 but there is no significant difference but water use efficiency for treatment T2 was about 10.83 kg/m³ more important than T1. Water content, salt distribution, and water use efficiency for potato irrigated by water well have 3.32 dS/m was presented in this work. Depending on irrigation scheduling, soil water content, and salt distribution was more uniform in treatment T2. Using well water having an EC_i of 3.32 dS/m was possible to produce potato at about 5.85–10.28 kg m⁻³.

References

- Al-Mefleh NK, Samarah N, Zaitoun S, Al-Ghzawi A (2012) Effect of irrigation levels on fruit characteristics, total fruit yield and water use efficiency of melon under drip irrigation system. *J Food Agric Environ* 2:540–545
- ASAE (American Society of Agricultural Engineering) (1996) I. Soil and water terminology, 43rd edn, S 526. St. Joseph, Mich
- Ben Mechlia N, Nagaz K, Abid-Karray J, Masmoudi MM (2007) Productivity of the potato crop under irrigation with low quality in options Méditerranéennes: Série B. *Etudes et Recherches* 57
- Chartzoulakis K, Drosos N (1995) Water use and yield of greenhouse grown eggplant under drip irrigation. *Agric Water Manag* 28:113–120
- Douh B, Boujelben A (2012) Diagnostic des pratique de l'irrigation localisée souterraine en tunisie effet sur la valorisation du stock en eau du sol, le rendement d'une culture de maïs et l'efficience de l'utilisation de l'eau. *Larhyss J* 10:115–126
- El Hendawy SE, Abd El-Lattief EA, Ahmed MS, Schmidhalter U (2008) Irrigation rate and plant density effects on yield and water use efficiency of drip-irrigated corn. *Agric Water Manag* 95:836–844
- Fabeiro C, de Santa Martin, Olalla F, de Juan JA (2001) Yield and size of deficit irrigated potatoes. *Agric Water Manag* 48:255–266
- Hamdy A, Abu-Zeid M, Lacirignola C (1995) Water crisis in the Mediterranean: agricultural demand management. *Water Int* 4:515–526

- Haverkort AJ, Van de Waart M, Bodlaeader KBA (1990) The effect of early drought stress on numbers of tubers and stolons of potato in controlled and field conditions. *Potato Res* 33:89–96
- Lynch DR, Foroud N, Kozub GC, Farries BC (1995) The effect of moisture stress at three growth stages on the yield, components of yield and processing quality of eight potato varieties. *Am Potato J* 72:375–386
- Maas EV, Hoffman GJ (1977) Crop salt tolerance: current assessment. *J Irrig Drain Div Am Soc Civ Eng* 103:115–134
- MacKerron DKL, Jefferies RA (1986) The influence of early soil moisture stress on tuber numbers in potato. *Potato Res* 29:299–312
- Malash NM, Flowers TJ, Ragab R (2008) Effect of irrigation methods, management and salinity of irrigation water on tomato yield, soil moisture and salinity distribution. *Irrig Sci* 26:313–323
- Porter GA, Opena GB, Bradbury WB, McBurnie JC, Sisson JA (1999) Soil management and supplemental irrigation effects on potato. I. Soil properties, tuber yield, and quality. *Agron J* 91:416–425
- Rajput TBS, Patel N (2006) Water and nitrate movement in drip-irrigated onion under fertigation and irrigation treatments. *Agric Water Manag* 79:293–311
- Sezen SM, Yazar A, Eker S (2006) Effect of drip irrigation regimes on yield and quality of field grown bell pepper. *Agric Water Manag* 81:115–131
- Tiwari KN, Mal PK, Singh RM, Chattopadhyay A (1998) Response of okra (*Abelmoschus esculentus* (L.) Moench.) to drip irrigation under mulch and non-mulch conditions. *Agric Water Manag* 38:91–102
- Tiwari RB, Singh V, Parihar P (2003) Role of front line demonstration in transfer of gram production technology. *Maharashtra J Ext Educ* 22(1):19
- Unlu M, Kanber R, Şenyiğit U, Onaran H, Diker K (2006) Trickle and sprinkler irrigation of potato (*Solanum tuberosum* L.) in the middle Anatolian region in Turkey. *Agric Water Manag* 79:43–71
- Wang W, Anderson BT, Phillips N, Kaufmann RK, Potter C, Myneni RB (2006) Feedbacks of vegetation on summertime climate variability over the North American Grasslands. Part I: Statistical analysis. *Earth Interact* 10
- Yaseen R, Shafi J, Ahmad W, Rana MS, Salim M, Qaisrani SA (2014) Effect of deficit irrigation and mulch on soil physical properties, growth and yield of maize. *Environ Ecol Res* 2:122–137
- Yuan BZ, Nishiyama S, Kang Y (2003) Effects of different irrigation regimes on the growth and yield of drip irrigated potato. *Agric Water Manag* 63:153–167
- Yuan XT, Yang HS, Zhou Y, Mao YZ, Zhang T, Liu Y (2006) The influence of diets containing dried bivalve feces and/or powdered algae on growth and energy distribution in sea cucumber *Apostichopus japonicus* (Selenka) (Echinodermata: Holothuroidea). *Aquaculture* 256:457–467

Chapter 16

Development of Methodology for Existing Rainwater Harvesting Assessment in (semi-)Arid Regions

Ammar Adham, Michel Riksen, Mohamed Ouessar, Rasha Abed and Coen Ritsema

Abstract Arid and semiarid regions face water scarcity and climatic uncertainty. Rainwater harvesting (RWH) has been used for generations to cope with these challenges. Numerous methods have been applied to select suitable sites for RWH. However limited attention has been given to evaluation of RWH structure performance. In this study, a comprehensive methodology to evaluate and optimize the performance of existing RWH techniques in (semi-)arid regions was developed and tested. Engineering, biophysical, and socioeconomic aspects were integrated by using analytical hierarchy process (AHP) supported by geographic information system (GIS). Sixteen RWH locations (subcatchments) in the Oum Zessar watershed in Tunisia were examined. Based on the criteria selected, some 88% of the sites scored between 2 and 3 (low to moderate) on a 1–5 suitability scale; 6% scored higher than 3, and 6% received suitability scores less than 2. Improving RWH design by raising spillway heights by 50% increased overall suitability, with 69% of the sites scoring between 3 and 4 after such optimization. Our highly flexible, widely applicable methodology proved effective, easy to use and low cost. Its further application is recommended to support designers and decision-makers in assessing and optimizing the performance of both existing and new RWH systems.

Keywords RWH · AHP process · Optimization · Subcatchments · Jessour · Tabias

A. Adham (✉) · M. Riksen · R. Abed · C. Ritsema
Soil Physics and Land Management Group, Wageningen University,
P.O. Box 47, 6700 AA Wageningen, The Netherlands
e-mail: engammar2000@gmail.com; engammar2000@yahoo.com

M. Ouessar
Institut des Régions Arides, Route de Djorf km 22.5, 4119 Medenine, Tunisia

A. Adham
University of Anbar, Ramadi, Iraq

Introduction

Water scarcity and climatic uncertainty are the major challenges in arid and semiarid regions. For generations, rainwater harvesting (RWH) has been used to induce, collect, store, and conserve local surface runoff for agriculture (Gupta et al. 1997). Tunisia is a Mediterranean country facing severe water shortages. These are furthermore expected to worsen, due to climate change, growing demand for water for agriculture and urban development, and the expanding tourism industry (Ouassar 2007; Adham et al. 2017). Throughout history, Tunisians have developed and implemented several types of water harvesting techniques; jessour, tabias, terraces, cisterns, recharge wells, gabions check dams, and mescats are the most common (Oweis 2004; Ammar et al. 2016).

Identification of suitable sites plays an important role in ensuring the success and sustainability of RWH systems. Throughout history, numerous methodologies have been applied in different regions to identify a suitable site for RWH (Adham et al. 2016a). The Soil Conservation Service (SCS) with curve number (CN) method has been applied by several researchers to assess how much runoff can be generated from a runoff area such as De Winnaar et al. (2007) in South Africa and Kadam et al. (2012) in India.

Nowadays, GIS and remote sensing (RS) are often used to map the biophysical environment and to identify suitable sites for RWH (Kahinda et al. 2008; Mechlia et al. 2009; Ziadat et al. 2006). Researchers have furthermore integrated GIS and RS with multicriteria analysis (MCA) to assess sites suitability for RWH (Elewa et al. 2012; Jabr and El-Awar 2005; Mbilinyi et al. 2007). These tools and methods, however, have tend to yield inadequate insight into the overall performance of RWH systems, as their scope tends to be rather limited. For example, some assessments have considered only cost-benefit analysis, using few criteria, or lack to consider the relative influence (weight) of different criteria on the performance of an intervention (Fleskens et al. 2005; Ngigi et al. 2005; Ouassar et al. 2008). To understand the performance of RWH and ensure the success of new RWH implementations, evaluation tools are needed that integrate engineering, biophysical, and socioeconomic aspects.

The main objective of this study was to develop and test a methodology to assess and to optimize the performance of existing rainwater harvesting systems in (semi-) arid regions. The Oum Zessar watershed in southeastern Tunisia was selected as a case study, where we applied and tested our evaluation and decision support tool. The methodology presented was designed to be easy to use, to provide accurate results without the need for complex analysis, and to be flexible enough to apply under different site characteristics simply by changing the criteria selected. Analytical hierarchy process (AHP) was used to help meet these requirements.

Materials and Methods

Methodology Overview

AHP is a multicriteria decision-making method that provides a structured technique for organizing and analyzing elements in complex decision processes based on mathematics and expert knowledge (Adamcsek 2008). Thomas Saaty developed AHP in the 1970s. Since then, it has been extensively applied in various disciplines. A main element of AHP is the hierarchical representation of the components of a problem, revealing the relationships between the levels. The highest level is the main goal (objective), with the lower levels made up of criteria and sub-criteria (indicators) feeding into that main goal (Saaty 2008). Our AHP-based RWH assessment tool consists of eight steps (Adham et al. 2016a):

- i. Define the main objective of the intervention.
- ii. Identify main criteria and sub-criteria (indicators).
- iii. Develop a decision hierarchy structure.
- iv. Collect and process data for each indicator.
- v. Classify the values for each indicator in terms of suitability classes.
- vi. Identify the relative importance of each criterion (using a pairwise comparison matrix).
- vii. Assess RWH performance (suitability of site).
- viii. Optimize RWH performance.

The main objective of the RWH systems evaluated here was collection and storage of runoff water during the rainy season to mitigate water scarcity during the drier seasons. Figure 16.1 presents our main criteria and sub-criteria (indicators).

For each of the main criteria we derived indicators, which we then reclassified and assigned suitability values from low to high: 1 (very low suitability), 2 (low suitability), 3 (medium suitability), 4 (high suitability), and 5 (very high suitability) as shown in Table 16.1. These values were determined in consultation with experts and using information from the literature. For our first main criterion, climate, two indicators were derived: rainfall and drainage flow. Areas with high rainfall were considered highly suitable for RWH, as large amounts of water were expected to provide sufficient rainwater for harvesting to meet crop requirements (Al-Adamat 2008; De Winnaar et al. 2007). Drainage flow represents the distance from water courses to a dyke, with less loss expected over shorter distances (Elewa et al. 2012; Mbilinyi et al. 2007).

Second main criterion, structure design, three indicators were derived. Storage capacity is the ratio of the total volume of water inflow to the existing storage capacity. Structure dimension represents the ratio between the design height deemed ideal and the existing height of the RWH dykes or barriers examined. Values close to one were ranked as highly suitable (Jabr and El-Awar 2005). The ratio of catchment size to cropping area (CCR) indicates whether a terrace area was appropriately sized (not too large) to provide sufficient water for crops. Scores were

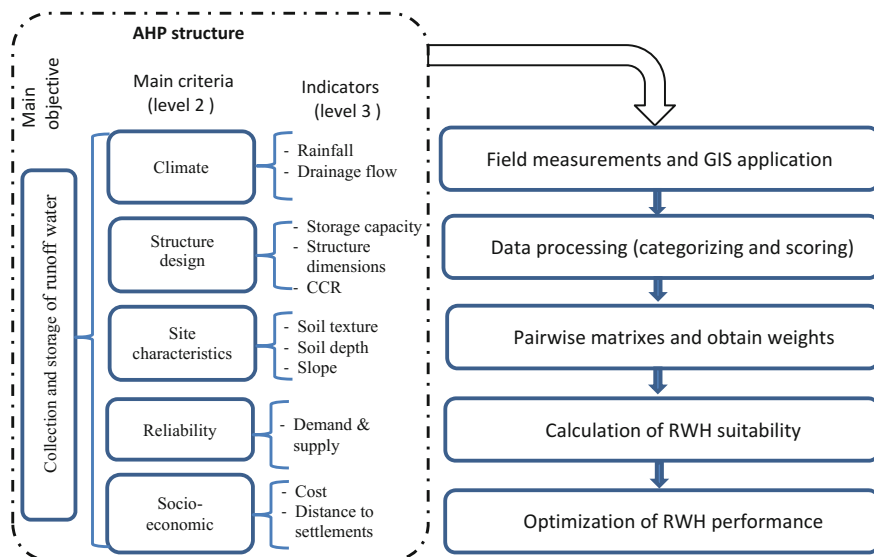


Fig. 16.1 Analytical hierarchy process (AHP) structure and methodology for assessing rainwater harvesting (RWH) site in arid and semi-arid regions. CCR catchment to cropping area ratio. After Adham et al. 2016a

assigned based on the physical features of our case study area and findings from previous studies (e.g., Schiettecatte et al. 2005).

For our third main criterion, site characteristics, three indicators were derived: soil texture, soil depth, and slope. The textural class of soils was determined by the percentage of sand, silt, and clay. Clay soils have the greater water-holding capacity and were therefore considered more suitable for RWH (Mbilinyi et al. 2007; Kahinda et al. 2008). Furthermore, sufficient soil depth was considered necessary to allow excavation to the prescribed optimum depths for RWH. Based on the previous studies, soils with depths of 1.5 m or more received the highest rankings (Kadam et al. 2012; Mekdaschi Studer and Liniger 2013). Slope was measured because one of the most common RWH techniques (jessour) is most effective in areas with a high slope, while another (tabias) is more suited to locations with slight slopes (Mbilinyi et al. 2007).

The fourth criterion, reliability, one indicator was derived: the ratio between the total demand and the total supply of water. Values close to one were considered highly suitable (Jabr and El-Awar 2005; Adham et al. 2016a).

For our final criterion, socioeconomic conditions, two indicators were derived. The cost of each RWH system was calculated based on the World Overview of Conservation Approaches and Technologies (WOCAT) database (Mekdaschi Studer and Liniger 2013) and interviews with local farmers. Lower cost systems received higher scores. For distance to settlements, higher scores were given to systems located nearer settlements since the examined RWH sites targeted local communities (Al-Adamat 2008).

Table 16.1 Analytical hierarchy process (AHP) structure and methodology for assessing rainwater harvesting (RWH) site in arid and semi-arid regions

Criteria (indicator)	Classes	Values	Scores (jessr/tabia)	Scores (tabia) ^a
Rainfall (mm)/year	Very low	<100	1	
	Low	100–175	2	
	Medium	175–250	3	
	High	250–325	4	
	Very high	>325	5	
Drainage flow (m)	Very high	0–50	5	
	High	50–125	4	
	Medium	125–200	3	
	Low	200–300	2	
	Very low	>300	1	
Storage capacity ratio (–)	Over requirement	<0.5	2	
	Sufficient	0.5–1.0	4	
	Optimum requirement	1.0–2.0	5	
	Critical	2.0–4.0	3	
	Very critical requirement	>4.0	1	
Structure dimensions ratio (–)	Over design	<0.5	3	
	Suitable	0.5–0.75	4	
	Optimum	0.75–1.0	5	
	Under design	1.1–1.25	2	
	Critical	>1.25	1	
Catchment to cropping area [CCR ratio (–)]	Medium suitability	<0.5	2	
	Very high suitability	0.5–0.75	4	
	Suitable	0.75–1.25	5	
	Low suitability	1.25–2.0	3	
	Very low suitability	>2.0	1	
Soil texture (clay content %)	Very high suitability	>20	5	
	High suitability	15–20	4	
	Medium suitability	11–15	3	
	Low suitability	8–11	2	
	Very low suitability	<8	1	
Soil depth (m)	Very deep	>1.5	5	
	Deep	0.9–1.5	4	
	Moderately deep	0.5–0.9	3	
	Shallow	0.25–0.5	2	
	Very shallow	<0.25	1	

(continued)

Table 16.1 (continued)

Criteria (indicator)	Classes	Values	Scores (jessr/tabia)	Scores (tabia) ^a
Slope (%)	Flat	<1.5	1	2*
	Undulating	1.5–3	3	5
	Rolling	3–5	4	4
	Hilly	5–10	5	3
	Mountainous	>10	2	1
Reliability ratio (–)	Sufficient	<0.35	2	
	Very Sufficient	0.35–0.75	4	
	Medium Suff.	0.75–1.1	5	
	Large deficit	1.1–1.75	3	
	Very large deficit	>1.75	1	
Distance to settlement (km)	Very high suitability	<0.5	5	
	High suitability	0.5–0.75	4	
	Medium suitability	0.75–1.25	3	
	Low suitability	1.25–1.75	2	
	Very low suitability	>1.75	1	
Cost (\$ per m ³ of water)	Very high cost	>12	1	
	High cost	9–12	2	
	Medium cost	6–9	3	
	Suitable cost	3–6	4	
	Profitable cost	<3	5	

CCR catchment to cropping area ratio after (Adham et al. 2016a)

^aSuitability classes for slopes differ for jessour and tabias

The next step was to weight each criterion by applying a pairwise comparison matrix. Using index values from 1 to 9, two criteria were systematically compared. Values 1, 3, 5, 7, and 9 corresponded, respectively, to a criterion being ‘equally’, ‘moderately,’ ‘strongly,’ ‘very strongly,’ and ‘extremely’ important relative to the other being compared. The values 2, 4, 6, and 8 were intermediate (Saaty 2008; Adham et al. 2016a). A major advantage of AHP is the ability to check expert opinions for consistency in the pairwise comparison process. The consistency of each matrix was verified by calculating consistency ratios (*cr*). The *cr* should be less than or equal to 10%, otherwise, it is judged as insufficiently consistent to generate weights. Insufficient consistency would imply a need to revise and improve the indicators (Ying et al. 2007).

The final step in the assessment methodology was calculation of the overall suitability of each RWH site. The following formula was applied:

$$S = \sum_{i=1}^n W_i X_i, \quad (16.1)$$

where S = suitability,
 W = weight of criteria i ,
 X = score of criteria i ,
 i, n = number of criteria.

Overall suitability, like the indicators, was categorized into five classes from 1 to 5. The classes were thus representative of the general strength of the RWH intervention. It is important to check this with the stakeholders through discussion of the results with them, including the preliminary conclusions and their recommendations.

To optimize the performance of the RWH structures and to improve the water yield. An improvement in structural design was examined by raising spillway heights by 50%.

Case Study: The Oum Zessar Watershed

Description of Study Area

The Oum Zessar watershed in southeastern Tunisia has a surface area of 367 km² (Fig. 16.2). It has average annual rainfall of 150–230 mm, with mean temperatures ranging from 19 to 22 °C (Ouessar 2007; Adham et al. 2016b). For generations, the region's inhabitants have developed and constructed several types of RWH structures to recharge groundwater and satisfy water requirements for agriculture.

Jessour and tabias are the RWH techniques most commonly found in the region, though; spreading of water and groundwater recharge structures in wadi beds are also used. For our case study, a sub-catchment in the middle of the watershed was examined. We tested our RWH assessment tool here on 16 RWH structures (9 tabias and 7 jessour) covering a total area of some 19 ha (see Fig. 16.2).

Data Collection

Data were collected from various sources. Meteorological data, for seven meteorological stations in and around the study watershed, were collected from the Institute des Régions Arides (IRA) in Tunisia. Field measurements were carried out in the sub-catchment from December 2013 through March 2014. ArcGIS10.2 and Google Earth imagery were also applied to extract the needed data. All collected, measured, and calculated data were stored and processed using Excel. Table 16.2

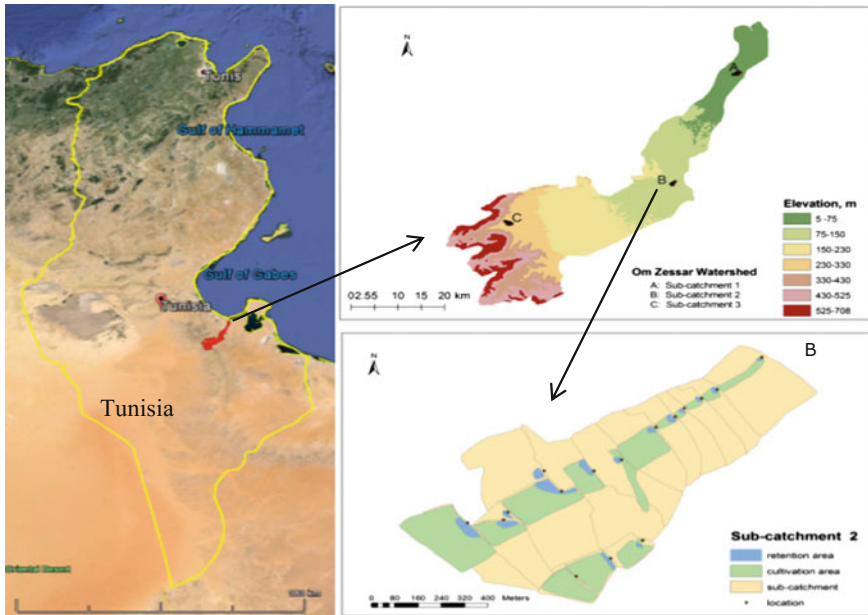


Fig. 16.2 Location of Oum Zessar and the test sub-catchment within it

summarizes the main steps in data collection, measurement, and calculation for each criterion.

Results and Discussion

Results

Table 16.1 lists the values assigned to the various categorizations of indicators based on the expert opinions and the literature. Figure 16.3 (left) presents the weights assigned using the pairwise comparison matrix. The climate criterion was given the greatest weight, and the socioeconomic criterion the least, 31% and 11%, respectively. The values for each criterion (indicator) were calculated, ranked and reclassified based on the five suitability classes, after which Eq. 16.1 was applied to get the final suitability score for each site (Fig. 16.3, right). The consistency of each matrix was determined using the consistency ratio (cr). For the main criteria matrix, cr was 2.8%. Since AHP calls for a cr of 10% or less, the obtained cr values were more than satisfactory.

The highest overall score for RWH site suitability was 3.03 (indicating modest suitability), for site 1. The lowest score was 1.98 (low suitability), for site 11. The socioeconomic criteria (cost, distance) and design criteria (structure dimensions,

Table 16.2 Main steps for data collection, measurement, and calculation for each criterion

Main criteria	Indicators	Step 1	Step 2
Climate	Rainfall	Collected from IRA, provided by seven meteorological stations in the Oum Zessar watershed for 1979–2004	Applying the Inverse Distance Weight (IDW) in ArcGIS 10.0
	Drainage flow	Google Earth images and ArcGIS software	Distance flow (m)
Structure design	Storage capacity	Potential runoff quantity (V_1 in m^3) from a catchment area calculated as $V_1 = C \times P \times A$	Calculation of the total volume of water inflow (V_i), which is $V_i = V_1 + V_2 + V_3$
	Structure dimensions	Field measurements	Calculation of the ratio between existing and ideal dyke height
	Catchment to cropping area ratio (CCR)	Field measurements and minimum impluvium area/terrace area ratio (Ca/C), calculated as $Ca/C = (WR - P)/CP$	Calculation of ratio between design and existing “impluvium area/terrace areas”
Site characteristics	Soil texture	Field measurements and sampling analysis	Measurement of clay content (%) of soils
	Soil depth	Field measurements	Categorization of sites up to 1.4 m
	Slope	Digital elevation model (30 m resolution)	Application of ArcGIS 10.0
Reliability	Demand and supply	Calculation of crop water requirements plus losses	Calculation of the ratio between total demand and total supply of water at each site
Socioeconomic	Cost	Based on the WOCAT database and interviews with the local farmers	Calculation of cost per cubic meter of water collected in each storage area including maintenance and construction of jessour/tabias
	Distance to settlements	Google Earth and ArcGIS	Measurement of distance (km)

C The mean annual runoff coefficient (–) equals 0.18 (Schietecatte et al. 2005); P mean annual precipitation (mm); A catchment area (m^2); V_2 (m^3) overflow volume from upstream dyke(s); V_3 (m^3) volume of rainfall onto the storage area; WR annual crop water requirements; *WOCAT* The World Overview of Conservation Approaches and Technologies

storage capacity, and CCR) had significant negative effects on the overall RWH suitability obtained for most of the sites. The lowest scores were recorded for the socioeconomic criteria. All sites registered low performance in this regard, due to the high cost of implementing and maintaining RWH structures in relation to the small quantities of water harvested. Low performance in this respect may be explained by a lack of adequate procedures for selecting suitable sites in

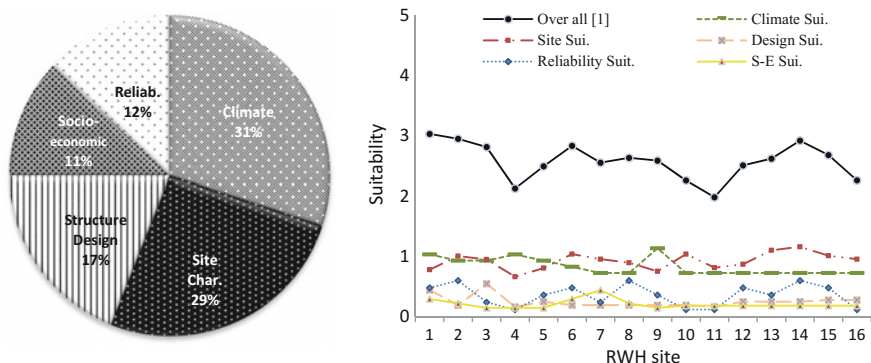


Fig. 16.3 Weights assigned to the main criteria (left), with overall and per criterion suitability of each site in the sub-catchment (right)

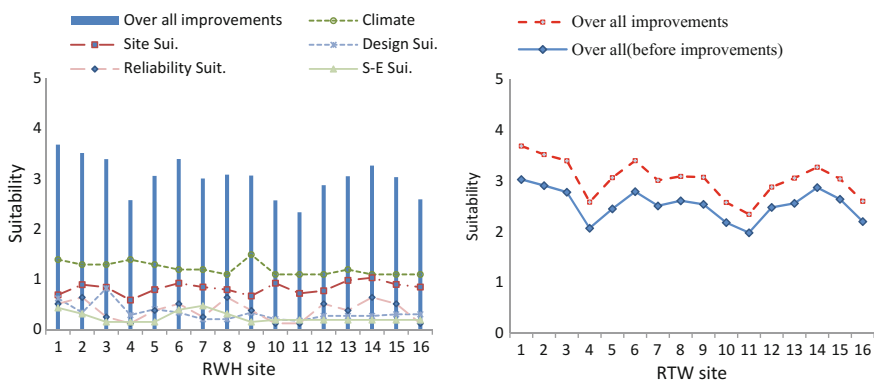


Fig. 16.4 Overall suitability of each site and suitability with respect to each of our five main criteria (climate, structural design, site characteristics, reliability, and socioeconomic conditions) after incorporating improved design (left); overall suitability scores for each site before and after improvements (right)

combination, in our case, with structures being built with insufficient engineering design. These results were confirmed by field observations of RWH structure performance.

To optimize the performance of RWH, an attempt was made to improve the overall suitability scores by raising the spillway heights by 50% which had a generally positive impact. And, due to the relatively small area the rainfall was the same in all subcatchments, therefore we assumed constant rainfall (in climate criteria) in all subcatchments and gave it the same score. These adjustments had a generally positive impact on the overall scores, as improved storage capacity by increasing water storage, reduced the cost of each cubic meter of water storage and changed the overall suitability. After the improvements, 11 of the 16 sites recorded scores greater than 3 (Fig. 16.4).

Discussion

Our methodology for assessing the suitability of sites for RWH structures integrate engineering (technical), biophysical and socioeconomic aspects. Five main criteria and various sub-criteria (indicators) were identified, and an AHP decision hierarchy structure was applied to determine their relative importance. We tested this new methodology in the Oum Zessar watershed in southeastern Tunisia.

Sixteen RWH sites (9 tabias and 7 jessour) were assessed and optimized. The results find that 88% of the sites were of low to modest suitability (scores between 2 and 3), and 6% of the sites were of low suitability (scores less than 2). Only 6% of the sites scored higher than 3, implying mid-level or higher suitability. Our observations and discussions with experts confirmed that these results accurately represent the real performance of the structures at each site. This validation suggests that the methodology might be reliably used elsewhere to assess the performance of other RWH structures.

Due to the relatively small size of the sub-catchment under study, the rainfall indicator received the same score at all sites. While this meant that rainfall had no impact on the relative suitability of the sites obtained in the current study, rainfall would likely be a key indicator in comparisons spanning larger and more diverse regions.

Though the weight for the climate criterion, 31%, was higher than that for the site characteristics criterion, 29%, (see Fig. 16.3, left), the site characteristics criterion received the highest scores at most of the sites (Fig. 16.3, right). These results are in line with the findings of other authors, such as Al-Adamat (2008) and Mbilinyi et al. (2007).

In most cases, low suitability (performance) of RWH structures was attributed to shortcomings in engineering design and maintenance and to the high cost of water harvesting. This was confirmed by the low scores registered on these criteria (see Fig. 16.3, right).

Our methodology, furthermore, provided a clear indication of which criteria might best be addressed to optimize performance and improve RWH system yield. In particular, structural engineering was a factor. Our calculations indicated that improving dyke design by raising spillway heights by 50% would result in considerably better performance. And, the overall suitability increased about 69% of all sites got a score between 3 and 4 as shown in Fig. 16.4.

The methodology presented here was designed to be easy to use, to provide accurate results without the need for complex analysis, and to be flexible enough to apply under various circumstances simply by changing the criteria selected. Thus, the time and money required can be kept within reasonable limits, while still delivering accurate and useful information. Nonetheless, it must be kept in mind that in the use of AHP, expert opinions and the consulted literature highly affect the weights assigned to each criterion. Substantial care must therefore be taken in the weighting procedure.

Conclusion

This study introduced a new RWH evaluation and decision support tool employing AHP supported by GIS. The tool, moreover, was put to the test in the Oum Zessar watershed in southeastern Tunisia. There, the performance of 16 RWH systems was assessed, and alternatives for system optimization were explored. Engineering (technical), biophysical, and socioeconomic criteria were integrated to produce five main criteria, which were further broken down into sub-criteria (indicators), and weighted and assessed drawing on inputs from experts, stakeholders, and the literature. Stakeholders confirmed that the methodology provided accurate results in our case study area. Furthermore, it offered insights into how poor RWH performance might be improved. Raising spillway heights had a generally positive impact on RWH performance, as this adjustment improved storage capacity, leading to increased water availability. This, in turn, reduced the cost per cubic meter of water harvested, optimizing overall RWH structure performance.

The methodology could be implemented more widely to evaluate potential sites for new RWH projects, thus increasing the likelihood of satisfactory long-term performance. Moreover, the tool could be utilized in a variety of circumstances, owing to its flexibility and the ease with which it can be adapted for use with different criteria and indicators of RWH performance. A final advantage is a low time and cost required for such assessments, which makes the methodology a feasible option for local RWH managers and communities.

To confirm the wider applicability and reliability of our method, future studies are highly recommended that test the methodology in different regions and with different kinds of criteria. Moreover, additional socioeconomic criteria (e.g., ownership, family size, etc.) warrant further investigation. Findings of such work could provide greater insight on reliability and enable greater generalization of our methodology for assessment and optimization of RWH system performance.

Acknowledgments This study was conducted in the framework of the cooperation between The Higher Committee For Education Development in Iraq (HCED) and Wageningen University (The Netherlands). Field work was carried out in collaboration with the Institut des Régions Arides (IRA) in Tunisia. Special thanks are due for Ammar Zerrim and Messaoud Guied for the technical and field measurements assistance. Great thanks as well to Demie Moore in the Soil Physics and Land Management Group for the English review and support.

References

- Adamcsek E (2008) The analytic hierarchy process and its generalizations. 43
Adham A, Riksen M, Ouessar M, Ritsema CJ (2016a) A methodology to assess and evaluate rainwater harvesting techniques in (semi-)arid regions. *Water* 8:198

- Adham A, Wesseling JG, Riksen M, Ouessar M, Ritsema CJ (2016b) A water harvesting model for optimizing rainwater harvesting in the wadi Oum Zessar watershed, Tunisia. *Agric Water Manag* 176:191–202
- Adham A, Wesseling JG, Riksen M, Ouessar M, Abed R, Ritsema CJ (2017) Assessing the impact of climate change on rainwater harvesting in the Oum Zessar watershed in southeastern Tunisia (minor revision by *Journal of Hydrology*)
- Al-Adamat R (2008) GIS as a decision support system for siting water harvesting ponds in the Basalt Aquifer/NE Jordan. *J Environ Assess Policy Manag* 10:189–206
- Ammar A, Riksen M, Ouessar M, Ritsema C (2016) Identification of suitable sites for rainwater harvesting structures in arid and semi-arid regions: a review
- De Winnaar G, Jewitt GPW, Horan M (2007) A GIS-based approach for identifying potential runoff harvesting sites in the Thukela River basin, South Africa. *Phys Chem Earth Parts A/B/C* 32:1058–1067
- Elewa HH, Qaddah AA, El-feel AA et al (2012) Determining potential sites for runoff water harvesting using remote sensing and geographic information systems-based modeling in Sinai Department of Water Resources, National Authority for Remote Sensing and Space Sciences (NARSS), *Environmental GIS L. Am J Environ Sci* 8:42–55
- Fleskens L, Stroosnijder L, Ouessar M, De Graaff J (2005) Evaluation of the on-site impact of water harvesting in southern Tunisia. *J Arid Environ* 62:613–630
- Gupta KK, Deelstra J, Sharma KD (1997) Estimation of water harvesting potential for a semiarid area using GIS and remote sensing. In: *Remote sensing and geographic information systems for design and operation of water resources systems. Proceedings of the Rabat symposium S3, IAHS Publ No, vol 242*, pp 53–62
- Jabr WM, El-Awar FA (2005) GIS & analytic hierarchy process for siting water harvesting reservoirs, Beirut, Lebanon. *J Environ Eng* 122:515–523
- Kadam AK, Kale SS, Pande NN et al (2012) Identifying potential rainwater harvesting sites of a semi-arid, Basaltic Region of Western India, using SCS-CN method. *Water Resour Manag* 26:2537–2554. doi:[10.1007/s11269-012-0031-3](https://doi.org/10.1007/s11269-012-0031-3)
- Kahinda JM, Lillie ESB, Taigbenu AE et al (2008) Developing suitability maps for rainwater harvesting in South Africa. *Phys Chem Earth Parts A/B/C* 33:788–799. doi:[10.1016/j.pce.2008.06.047](https://doi.org/10.1016/j.pce.2008.06.047)
- Mbilinyi BP, Tumbo SD, Mahoo HF, Mkiramwinyi FO (2007) GIS-based decision support system for identifying potential sites for rainwater harvesting. *Phys Chem Earth Parts A/B/C* 32:1074–1081
- Ben Mechlia N, Oweis T, Masmoudi M et al (2009) Assessment of supplemental irrigation and water harvesting potential: methodologies and case studies from Tunisia. ICARDA, Aleppo, Syria
- Mekdaschi Studer R, Liniger H (2013) *Water harvesting: guidelines to good practice*
- Ngigi SN, Savenije HHG, Rockström J, Gachene CK (2005) Hydro-economic evaluation of rainwater harvesting and management technologies: farmers' investment options and risks in semi-arid Laikipia district of Kenya. *Phys Chem Earth Parts A/B/C* 30:772–782
- Ouessar M (2007) Hydrological impacts of rainwater harvesting in wadi Oum Zessar watershed (Southern Tunisia). Ghent University
- Ouessar M, Bruggeman A, Mohtar R, et al (2008) Future of drylands—an overview of evaluation and impact assessment tools for water harvesting. In: *The future of drylands*. Springer, pp 255–267
- Oweis TY (2004) Rainwater harvesting for alleviating water scarcity in the Drier environments of West Asia and North Africa. In: *International workshop on water harvesting and sustainable agriculture, Moscow, Russia*, p 182
- Saaty TL (2008) Decision making with the analytic hierarchy process. *Int J Serv Sci* 1:83. doi:[10.1504/IJSSCI.2008.017590](https://doi.org/10.1504/IJSSCI.2008.017590)

- Schiettecatte W, Ouessar M, Gabriels D et al (2005) Impact of water harvesting techniques on soil and water conservation: a case study on a micro catchment in southeastern Tunisia. *J Arid Environ* 61:297–313. doi:[10.1016/j.jaridenv.2004.09.022](https://doi.org/10.1016/j.jaridenv.2004.09.022)
- Ying X, Zeng GM, Chen GQ et al (2007) Combining AHP with GIS in synthetic evaluation of eco-environment quality—a case study of Hunan Province, China. *Ecol Model* 209:97–109. doi:[10.1016/j.ecolmodel.2007.06.007](https://doi.org/10.1016/j.ecolmodel.2007.06.007)
- Ziadat F, Oweis T, Mazahreh S et al (2006) Selection and characterization of badia watershed research sites

Chapter 17

Impact of Anthropogenic Activities on Erosive Behavior of Nebhana Watershed Tunisia

Taoufik Hermassi, Hacib El Ammami and Walid Ben Khelifa

Abstract The aggressiveness of the climate and soil vulnerability associated with low and degraded vegetation on steep slopes make the flows concentration into violent runoff causing usually huge amounts of erosion. Furthermore, ongoing socioeconomic transformations in the rural environment have contributed into the amplification of this phenomenon. Indeed, this erosion is responsible for land fertility decrease, crops falling yields, reduction of farmers' income and silting of dams. These hydraulic structures are built by the national community at great expense. Given the limited financial resources of Tunisia and the high cost of erosion reduction, the establishment of maps for priority intervention becomes a necessity for the planner. The objective of this study is to determine a methodology for assessing the quantitative impact of human actions on erosion behavior in Nebhana watershed, located in central part of Tunisia. This study finds its interest in the fact that the developed erosion map is a decision support tool and a basis for determining the priority intervention areas as part of the Water and Soil Conservation Management Programs. Erosion mapping was carried out using empirical model based on the Revised Universal Soil Loss Equation (RUSLE). In Nebhana watershed, the average soil loss is about 3.5 t/ha/yr from the period 1965 to 2010. Between 2010 and 2015, the increase in soil and water conservation area allowed to reduce the average soil water erosion rate to around 3.2 t/ha/yr, that is a reduction of around 10% of dam silting. This work showed that the use of GIS for the analysis and processing of digital map data has made it easy and fast development of the erosion map that provides synthetic and systematic information on the intensity and spatial distribution of the phenomenon of water erosion.

Keywords Water erosion · Nebhana · Quantification · Soil and water conservation structures · RUSLE model

T. Hermassi (✉) · H. El Ammami · W. Ben Khelifa
National Research Institute for Rural Engineering, Water and Forestry (INRGREF),
Hedi Karray street, El Menzah IV., P.O. Box n°10, 2080 Ariana, Tunisia
e-mail: taoufikhermassi@yahoo.com

Introduction

In Tunisia, the predominance of less resistant surfaces, irregular weather, torrential flows, the low density of vegetation cover, and land overuse are particularly favorable to accelerated water erosion phenomenon that seriously threatens the water and soil resources. If it is possible to reduce water erosion using appropriate techniques but we need first to define the high erosion areas for priority action (Morschel and Fox 2004).

Water erosion in Tunisia is severe and affecting more than about 3 million hectares of agricultural land, and threatens the sustainability of big dams to mobilize surface water. On the other hand, it causes a loss of the richest topsoil organic matter and nutrients which leads to decrease productivity of agricultural land and a deficit to meet the nutritional needs as well as economic and social problems. Furthermore, since the 60s, Tunisia initiated a planning policy to conserve of soil and which was supported in 90s, by the two strategies of soil and water conservation management.

In order to determine the appropriate soil and water conservation techniques, and to fight against erosion to extend the life time of dams and to develop waterway structures, the quantification and the mapping of soil loss, caused by water erosion, becomes an indispensable need.

The objective of this study is to determine the amount of sediment that can be delivered annually by Nebhana watershed, and to map erosion risk areas.

Location and Description of the Study Site

The Nebhana watershed is located in central Tunisia. It represents one of the three major watersheds in the region draining southeast flanks of the Tunisian Dorsale until the Sebket El Kelbia northeast of Kairouan. This area covers four governorates: Sousse, Kairouan, Siliana, and Zaghuan and spreads over an area of approximately 3983 km². In this study, we are interested only in Nebhana dam sub basin with an area of 865 km² (Fig. 17.1).

This basin is bounded on the west side by the limestone plateau of Kesra and the marly limestone massifs of Jebel Serdj (1357 ma.s.l) and Bargou (1266 ma.s.l), on the east side by the marly limestone massifs of Jebel Rihana (600 ma.s.l) Boudabous (816 ma.s.l), Ouchetla (646 ma.s.l) and Bouhajar (462 ma.s.l), on the north side by DjebelTouilla (640 ma.s.l) and El Mnassir (658 ma.s.l) and on the south side by the hills separating it from the wadi Merguellil.

The soil map shows that the Nebhana dam watershed is occupied mainly by Lithosols and Fluviosols (40% of the total area). Rendzina and Cambisols cover 27% of the total area of the study area.

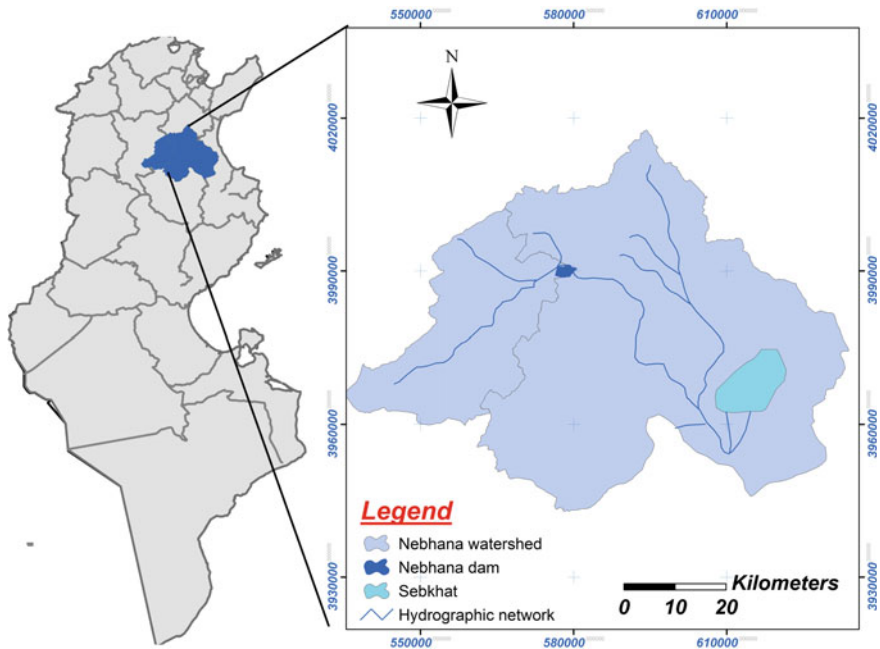


Fig. 17.1 Location of Nebhana watershed

The land use map shows that most of the surface of Nebhana dam watershed is occupied by forests (40% of total area) located throughout the basin and farmlands (30%) consisting mainly of fruit trees and cereals. Rangelands (28%) are found in the central and the northern parts of the watershed.

Between 1965 and 1985, the soil and water conservation techniques were very limited. However, almost 23% of the catchment area has been treated by soil and water conservation structures in the period from 1985 to 2010.

The soil and water conservation structures consist mainly of pastoral plantations, stone cordons or gully corrections, mechanical or manual terraces, and spreading perimeter. The soil and water conservation structures include hill lakes and hillside dams intended for the protection of Nebhana dam against silting up, groundwater recharge, and improving agricultural productivity. Sixteen lakes and two hillside dams have been already constructed in the Nebhana watershed (Fig. 17.2).

For the period 2010 to 2015, we assumed that the watershed was managed according to the planning study (DG ACTA 2011) which stipulates an increase in the water and soil conservation area to 40% of the total area of the watershed (Fig. 17.3).

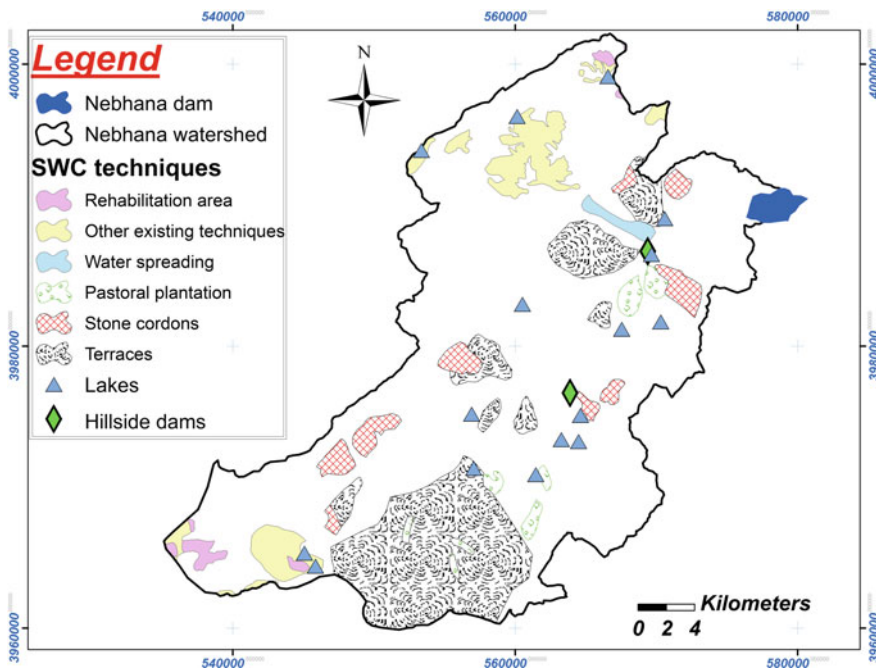


Fig. 17.2 Soil and water conservation structures map of Nebhana watershed (1985–2010)

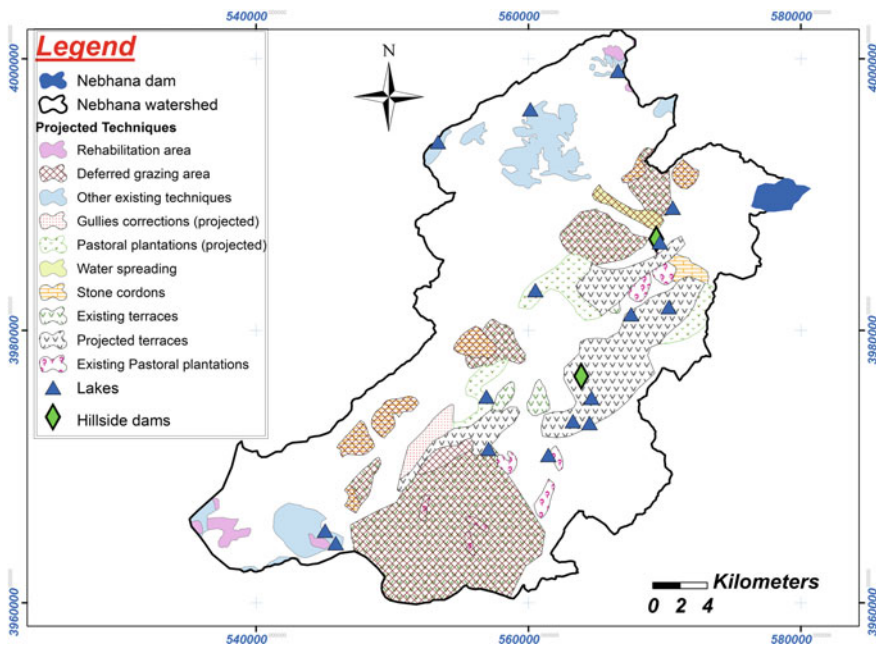


Fig. 17.3 Soil and water conservation structures map of Nebhana watershed (2010–2015) (DG ACTA 2011)

Soil Erosion Model

The researchers developed models which are simplified representations of reality in a physical or analytical form. Thus, the erosion modeling is a tool for understanding and predicting the soil degradation. Indeed, modeling helps for understanding the relationships between the parameters that cause soil loss. Erosion models simulate a mathematical description of processes such as detachment, transport, and deposition of soil particles.

Simplified empirical models, such as the Universal Soil Loss Equation (USLE) (Wischmeier and Smith 1965), present a simple structure, compared to physical models. USLE model is the most used empirical model that assesses long-term averages of sheet and rill erosion. This model is based on plot data (Wischmeier and Smith 1978). The revised version RUSLE (Renard et al. 1997) has been applied to various spatial scales worldwide (Vrieling et al. 2008). RUSLE model is tested at the catchment scale, the country scale, and the continent scale. Currently this type of approach is recognized as simple and robust. The erosion modeling by integrating empirical models in a GIS allows both estimation and spatial distribution of water erosion hazard in watersheds (Hermassi et al. 2014).

The RUSLE equation was used to determine the average annual soil loss A (t/ha/yr) as a function of six erosion factors

$$A = R \times K \times L \times S \times C \times P,$$

where R is rainfall erosivity factor (MJ.mm/ha.h.yr), K (t.ha.h/ha.MJ.mm) is soil erodibility factor, L is slope length (m), S is slope steepness (%) (LS : topographic factor), C is crop management factor (dimensionless), and P a conservation practice factor (dimensionless).

Rainfall erosivity factor (R) is considered the most important factor in erosion response estimation. It is based on the kinetic energy and the maximum intensity in a 30 min period event (Wischmeier and Smith 1958). The method of Arnoldus (1980) based on Fournier index was used. R factor for Nebhana watershed was calculated with reference to nine rain gauge stations, it was estimated from daily rainfall records for the period 1994–2014. The average annual erosivity values ranged from 61 to 95 MJ.mm/ha.h.yr. The average annual erosivity found was 77 MJ.mm/ha.h.yr.

The average annual erosivity map for Nebhana watershed is presented in Fig. 17.4.

Soil erodibility factor (K) represents the vulnerability of soil particle to detachment and transport by rainfall and runoff. The K factor was defined using the soil map (scale: 1/50 000), several experiments conducted in the Tunisian semiarid areas (Cormary and Masson 1964; Dumas 1964; Masson 1971; Collinet et al. 2001; Zante et al. 2003), and the literature (Wischmeier and Smith 1978; Cormary 1963). The erodibility values and their spatial distribution are found in the Fig. 17.5.

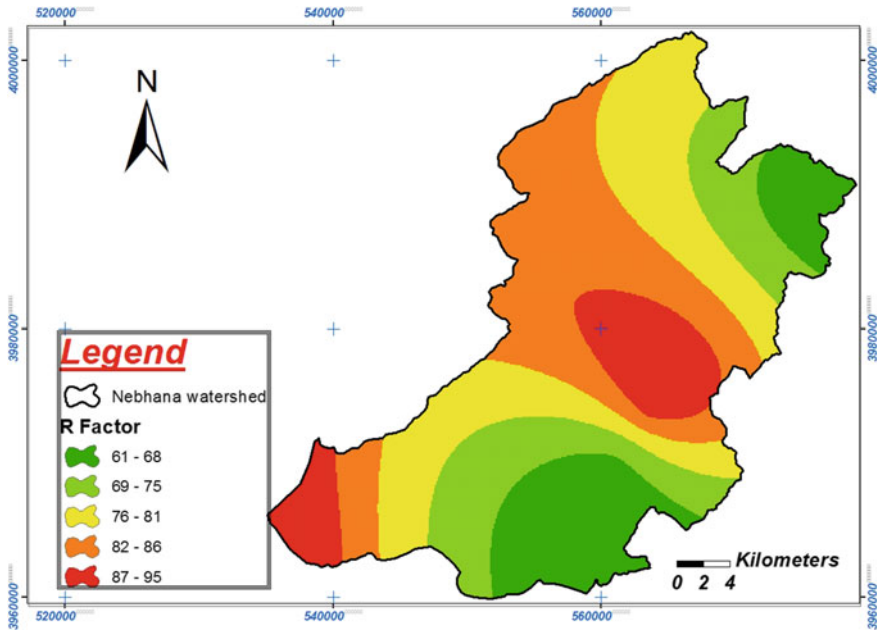


Fig. 17.4 Rainfall erosivity map of Nebhana watershed

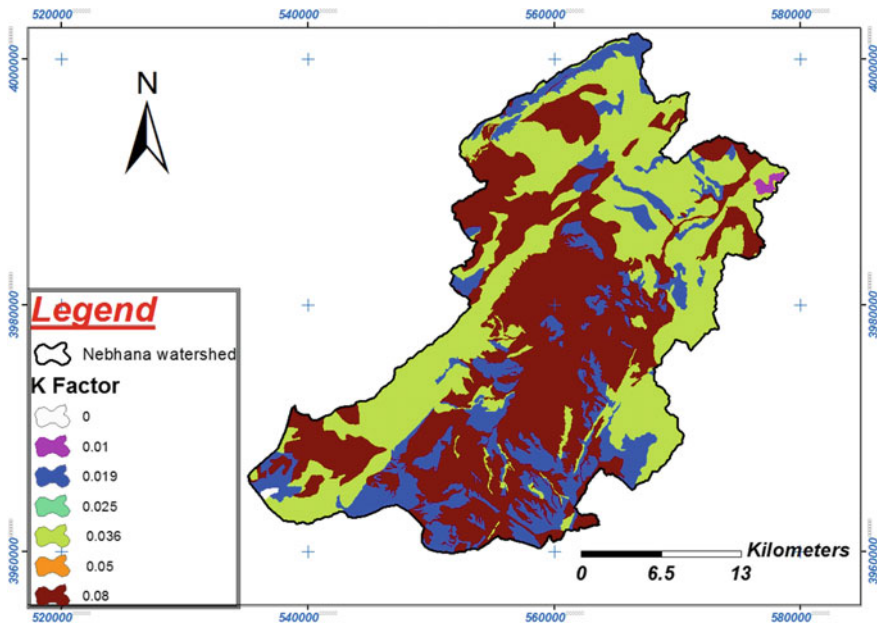


Fig. 17.5 Soil erodibility map of Nebhana watershed

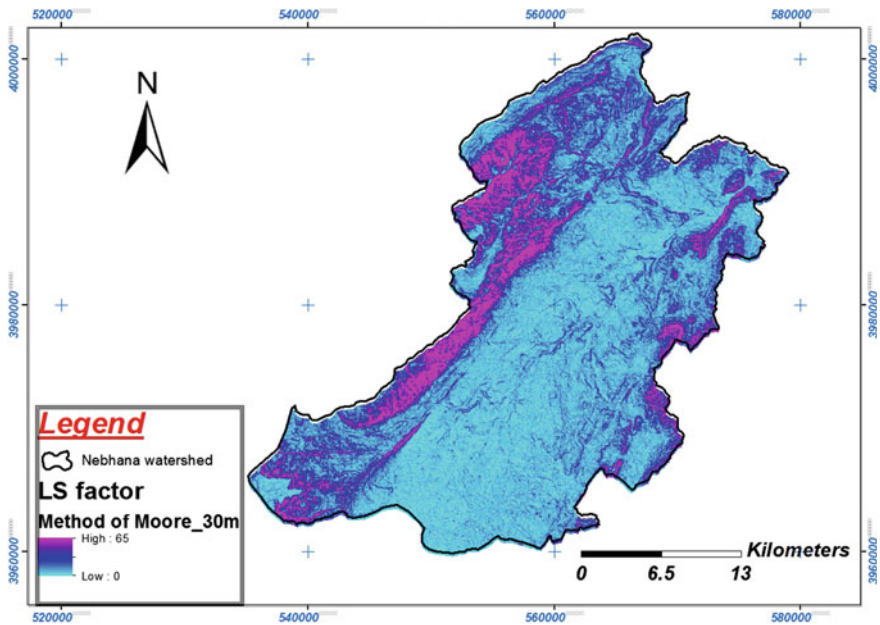


Fig. 17.6 Topographic factor map of Nebhana watershed

Topographic factor (LS) (slope length (m) and steepness (%)): The LS factor was derived based on the Aster (Advanced Spaceborne Thermal Emission and Reflection Radiometer) GDEM (Global Digital Elevation Model) images acquired in 2011 with a resolution of 30 m.

The topographical factor LS was determined using the equation recommended by Moore et al. (1991). Its spatial distribution is shown in the Fig. 17.6.

Crop management (C): is defined as the combined effect between vegetation cover and its management system on erosion (Wischmeier and Smith 1978). Its values were essentially derived from the literature (Masson 1971) and based on satellite images (Landsat 2000 with a resolution of 20 m), the topographic map (scale 1:25 000) (Ministry of Agricultural and Hydraulic Resources, mission 1998; scale: 1:20 000) (Fig. 17.7).

Conservation practice (P) factor: reflects the impact of conservation practices that reduce the amount and velocity of runoff, thus reducing the impacts of erosion. For Nebhana watershed, they were derived from aerial photo interpretation (Ministry of Agricultural and Hydraulic Resources, missions of 1998 and 2010; scale: 1/20 000). Its corresponding values are defined as recommended in the literature (Masson 1971; Wischmeier 1975). The values and the spatial distribution of P-factor are given in the Fig. 17.8.

The preparation of the thematic maps as spatial data base was performed to run the RUSLE model.

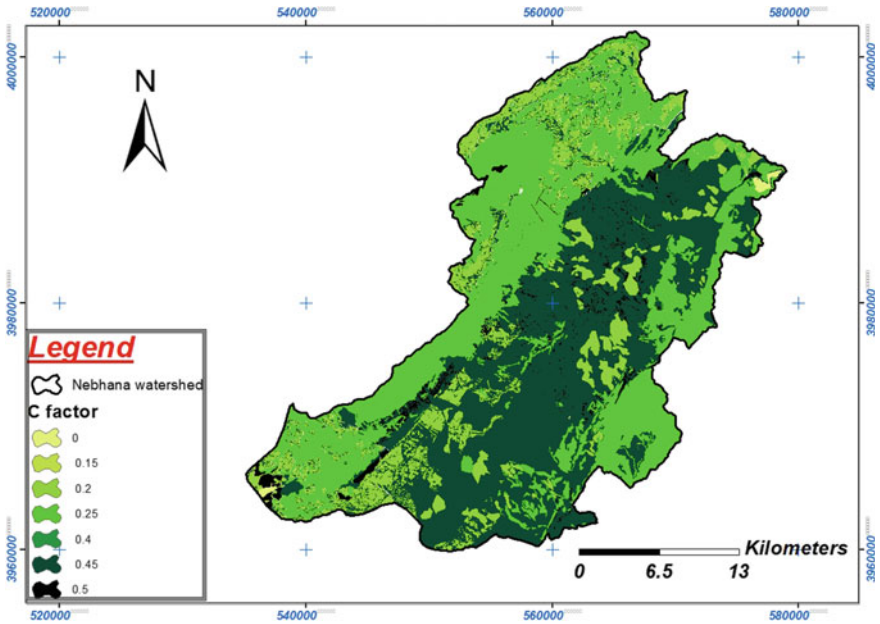


Fig. 17.7 Crop management factor map of Nebhana watershed

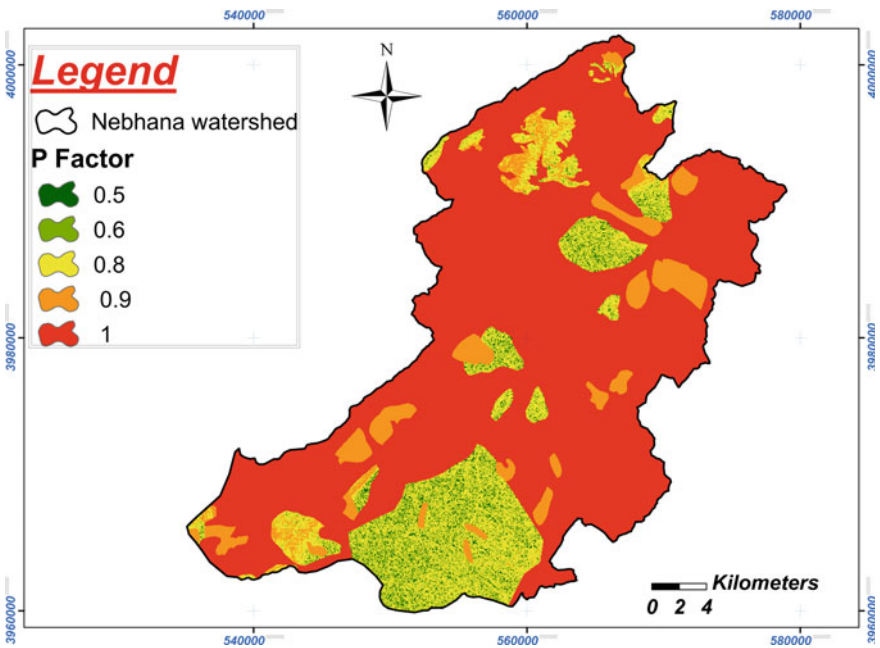


Fig. 17.8 Conservation Practice factor map of Nebhana watershed

All data were spatially organized within a GIS environment (ArcGIS 10.0) with the same resolution and coordinate system. The Nebhana watershed was divided into regular 25×25 m grids. This procedure was followed by the overlay of the five parameter layers (R, K, LS, C, and P).

The average annual soil loss for the watershed was computed from the sum of all grid cells.

Because RUSLE is an empirically based model, it is essential to calibrate the model concerning both the grid size and model factors. Although parameter estimation is relatively easy, and well-explained documentation is available (Renard et al. 1996), the calibration and validation of some parameters is essential because of the large number of formulas used to estimate notably the rainfall erosivity factor and the topographic factor. We performed the model calibration on observed soil loss determined from bathymetric measurements on the dam reservoir.

Indeed, we have used the first period (1965–1985) for calibration, the second period (1985–2010) for the validation, and the third period (2010–2015) for the simulation of the current situation.

Discussion

In order to estimate annual soil loss, the five factors were multiplied according to the relationship in RUSLE model. In total, six layers with annual soil loss were computed. The soil loss was classified into soil erosion risk maps with five different soil erosion risk levels.

As shown in Fig. 17.8, most of the catchment is affected by to moderate soil erosion risk (1–4 t/ha/yr). The upstream is more affected by erosion; it can reach more than 10 t/ha/year due to steep slopes and low vegetation cover. The downstream is less affected and erosion does not usually exceed 2 t/ha/yr; this behavior is explained by the gentle slopes and shallow soil depths. We note that only 20% of the catchment area contributes to the heavy soil erosion.

The spatial distribution of potential soil loss rates predicted by RUSLE is shown in Fig. 17.9.

Different results were obtained for the different methods used to derive LS factor; therefore it must go through a calibration and validation procedure to choose the method that is satisfactory for both periods (1965–1985 and 1985–2010).

For the calibration, the RUSLE model slightly underestimates the specific erosion throughout the catchment. The average loss is about 3.5 t/ha/yr, or a total annual volume of approximately 28 million m^3 of sediments. The validation confirms the results obtained by the calibration for simulating erosion at Nebhana watershed.

Between 2010 and 2015, the increase in soil and water conservation area allowed to reduce the average soil water erosion rate to around 3.2 t/ha/yr (a total volume of 24.5 million m^3 sediments), that is a reduction of around 10% dam silting. If this scenario will be accompanied by measures of prohibiting grazing, pastoral plantations, or biological fixation, this reduction would reach 16%.

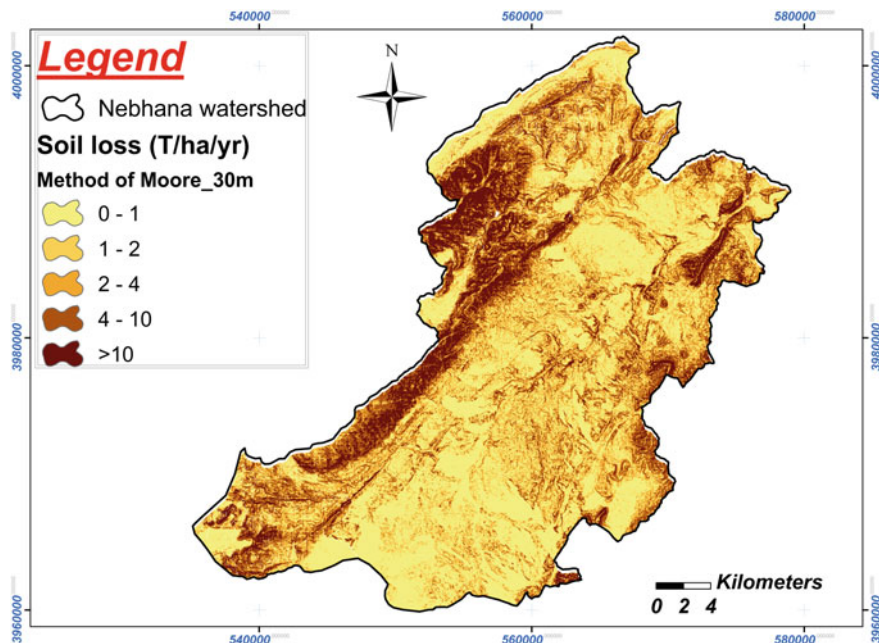


Fig. 17.9 Soil erosion risk map of Nebhana watershed

Conclusion

This study attempts to assess soil erosion patterns from year 1965 to 2015 due to soil and water conservation changes based on estimating annual soil loss by applying RUSLE model in Nebhana catchment, Tunisia.

Soil and water conservation structures are very important in rural areas of the semiarid regions; they are used to collect the water, to protect the soil, and to increase the agricultural production. The RUSLE model is a powerful tool to study the impact of the anthropogenic activities, for land use, anti-erosion techniques design, and management and planning scenarios analysis at watershed scale.

The RUSLE model gives satisfactory estimates of erosion. It is increasingly used in integrated planning studies to determine the most sensitive areas in a watershed and on which emergency interventions are required and/or provide for different management scenarios for hill slopes.

The application of this model to other semiarid Tunisian watersheds allows their validation and their use in development of soil and water conservation programs. In the future, the RUSLE model can be used as a tool for assessing climate change and land use management impacts on soil erosion and losses.

This study also showed that the use of GIS has made easy and fast, the development of the erosion map that provides synthetic and systematic information on the intensity, spatial distribution of the phenomenon of water erosion.

References

- Arnoldus HMJ (1980) Methodology used to determine the maximum potential average soil loss due to sheet and rill erosion in Morocco. *Bull. FAO* 34
- Collinet J, Zante P, Balieu O, Ghesmi M (2001) Cartographie des risques érosifs sur le bassin versant du barrage collinaire de Zanfour (Nord Dorsale tunisienne). CRDA du Kef, IRD, Tunis, 39 p. + annexes
- Cormary Y, Masson J (1964) Application à un projet type de la formule de perte de sols de Wischmeier. Etude de conservation des eaux et du sol au Centre de recherches du génie rural de Tunisie, 5–26 p
- Cormary Y (1963) Projet type CES. Utilisation des photographies aériennes. Intégration des paramètres climatiques, pédologiques et agricoles dans l'élaboration d'un projet de CES sur le bassin versant de l'Oued Hallouf. Dossier CGR. No. 30 Note CES-C5
- DG ACTA (2011) Etude de planification des aménagements CES du gouvernorat de Kairouan. 150 pp
- Dumas J (1964) Relation entre l'érodibilité des sols et leurs caractéristiques analytiques ORSTOM Tunis, série pédologie, 3, 307–333
- Hermassi T, Cherif MA, Habaieb H (2014) Etude du transport solide au niveau du bassin versant de Merguellil, Tunisie Centrale: Cas des bassins versants d'Ettiour et de Rajela". *Int Water J La Houille Blanche* 4:88–96 (2014). doi:[10.1051/lhb/2014043](https://doi.org/10.1051/lhb/2014043)
- Masson JM (1971) L'Érosion des sols par l'eau en climat méditerranéen. Méthodes expérimentales pour l'étude des quantités érodées à l'échelle du champ. Université des Sciences et techniques du Languedoc-Montpellier 2, thèse de doctorat, Montpellier, 213 p. + annexes
- Moore ID, Grayson RB, Ladson AR (1991) Digital terrain modelling: a review of hydrological, geomorphological, and biological applications. *Hydrol Process* 5(1)
- Morschel J, Fox D (2004) Une méthode de cartographie du risque érosif: application aux collines du Terrefort Lauragais. *MappeMonde* n°76 (4-2004)
- Renard KG, Foster GR, Weesies GA, McCool DK (1996) Predicting soil erosion by water. A guide to conservation planning with the revised universal soil loss equation (RUSLE). *Agriculture Handbook* 703. US Govt Print Office, Washington, DC
- Renard KG, Foster GR, Weesies GA, McCool DK, Yoder DC (1997) Predicting soil erosion by water: A guide to conservation planning with the revised universal soil loss equation (RUSLE). *Agriculture Handbook* No. 703, p 384 USDA-ARS
- Vrieling A, De Jong SM, Sterk G, Rodrigues SC (2008) Timing of erosion and satellite data: a multi-resolution approach to soil erosion risk mapping. *Int J Appl Earth Obs Geoinf* 10(3): 267–281
- Wischmeier WH (1975) Estimating the soil loss equations cover and management factor for undisturbed lands. In *Present and Prospective Technology for Predicting Sediment Yields and Sources*, ARS-S-40, Agr Res Scriv, US Department of Agriculture, Washington, DC, pp 118–125
- Wischmeier WH, Smith DD (1965) Predicting rainfall-erosion losses from cropland east of the rocky mountains. *Agricultural Handbook* No. 282. US Department of Agriculture, Washington, DC
- Wischmeier WH, Smith DD (1978) Predicting rainfall erosion losses: a guide to conservation planning. *Agricultural Handbook* No. 537. US Department of Agriculture, Washington, DC, 58
- Wischmeier WH, Smith DD, Uhland RE (1958) Evaluation of factors in the soil loss equation. *Agric Eng* 39(458–462):474
- Zante P, Collinet J, Leclerc G (2003) Cartographie des risques érosifs sur le bassin versant de la retenue collinaire d'Abdessadok (nord dorsale tunisienne), Institut de Recherche pour développement, Tunisie, pp 13–18 + annexes

Chapter 18

Short-Term Effects of Olive Mill Wastewater Spreading on Chemical Properties of Soils in Arid Lands, Study Case from Southern Tunisia

Donia Jendoubi, Houcine Taamallah, Khadija Bouajila, Ahlem Gara, Mohamed Moussa and Mustapha Sanaa

Abstract Olive mill wastewater (OMW) is occurred from the production of olive oil in olive mills. Many olive mills are scattered in most Mediterranean countries which produce it seasonally. This led to an environmental problem in these olive oil-producing countries, due to the elevated level of salinity, polyphenols, and the pollution burden. However, OMW is also characterized by richness in organic and mineral compounds. Consequently, OMW spreading can be an alternative for a low cost soil organic amendment. This work aimed to study the effect of OMW spreading on the chemical properties of soils in arid regions. Amendments with OMW were applied on two different soils in arid regions from Southern Tunisia with a quantity of 300 L per 100 m² (per plot), in a completely randomized experimental setup. The main objective of this work is to identify the short-term effect of OMW on fertility of sandy soil, for the supply of soil on organic carbon, inorganic nitrogen, available phosphorus and exchangeable potassium during 2010 as well as assessment of its effect on pH, salinity of soils in arid regions. Obtained results show that under the conditions of our experiment, applying of this organic effluent has changed significantly the content of exchangeable potassium (197% and 221%, respectively, for Dar Dhaoui (A) and El Fje (B) soil), mineral nitrogen, phosphorus (370% and 445%, respectively for (A) and (B) soil), and organic matter in soil (from 0.92% to 1.51% and from 0.87% to 1.95%, respectively, for (A) and (B) soil). Consequently, OMW is considered as a rich organic material and may constitute a potential potassic amendment for dryland soils poor in this element, which has the tendency to increase the content of major elements and the soil organic matters. OMW application did not cause a significant change in soil pH, due to the low quantity of OMW used in the soil. However, we highlighted the value of OMW as an organic amendment that requires further study on optimizing

D. Jendoubi (✉) · K. Bouajila · A. Gara · M. Sanaa
National Agronomic Institute of Tunisia (INAT), Tunis, Tunisia
e-mail: donia.jendoubi@yahoo.com

H. Taamallah · M. Moussa
Arid Regions Institute (IRA), 4119 Medenine, Tunisia

used doses to avoid the possible risks. According to the obtained results we can confirm that OMW can be very useful as an organic amendment in agriculture.

Keywords Olive mill wastewater · Soil · Fertility · Arid regions · Monitoring

Abbreviations

OMW Olive Mill Wastewater

CEC Cation Exchange Capacity

Introduction

The olive mill wastewater (OMW) is derived from the extraction of oils from olive fruits (*Olea europea* L.) either by the centrifuge method or the pressure method. However, the produced wastewater has a high variable chemical composition, which depends upon the variety, maturity, and the processing method.

Unfortunately, the common and major problem of the producers and millers is the removal of waste. Therefore, this causes a strict problem for the community too, through the potential risk of pollution.

Several studies have tried to assess the effect of the olive mill wastewater spreading on crops and soil properties, such as cited in the review of Demichelli et al. (1996). But unfortunately, the results remain inconsistent and not explicit. For this reason, more attention for this crucial problem is really required, especially considering the Italian case, in which 106 t of OMW have to be removed every year (Kapellakis et al. 2008). By assessing OMW effect on soil fertility, many studies have proved an enhancing effect on chemical properties, such as the organic carbon, potassium, and phosphorus contents (Taâmallah et al. 1997; Tomati and Galli 1992; Leïla et al. 2014).

The coastal areas of Mediterranean countries are mainly characterized by arid climate conditions, low soil fertility, and water shortage (García et al. 1994; Alianello 2001). Therefore, OMW spreading appears as a suitable alternative for land fertilization (Cabrera et al. 1996).

However, even with the prospect of the contamination risk of water and/or soil following OMW spreading, the consideration of the OMW as fertilizer is promoted through its beneficial compositions, such as N, P, K, Mg, and Fe and organic carbon (Bonari et al. 1991; Alianello 2001; Mekki et al. 2006b; Lozano-García et al. 2011).

Throughout the last three decades, many studies were made, aiming to assess the impact of OMW spreading on the bare soil fertility (Paredes et al. 1987; Levi-Minzi et al. 1992; Cabrera et al. 1996) and its effects on the crops performances (Mekki

et al. 2006b; Mechri et al. 2007, 2011; Arienzo et al. 2009; Chartzoulakis et al. 2010; Lozano-Garcia et al. 2011; Moraetis et al. 2011; Nikolaos et al. 2013).

In this study, we evaluated two arid regions of Southern Tunisia characterized by sandy soils. We tested the short-term effect of OMW field applications in order to monitor some reliable and sensitive chemical soil parameters.

Materials and Methods

Experimental Sites

The field sites are located in two typical arid ecosystems of south of Tunisia, in the governorate of Medenine; the first site called El Fje, Northern Medenine (33°20'N and 10°29'E), characterized by 16 m of altitude level. The coldest month is December, during which temperature drops down to -1 °C. August is the warmest month of the year, during which temperatures can reach more than 48 °C. The rainfall is low and erratic. It receives between 150 and 240 mm per year, with an average of 30 rainy days (Paredes et al. 1987). The second site is Dar Dhaoui site, Ben Guerdane (33°17'N and 10°46'E), characterized by a relatively dry Saharan weather. The warmest month is July, during which temperatures can reach more than 46 °C and the coldest month is February, during which temperatures can drop down to 1 °C. Maximum rainfall is recorded during the month of January but in average, it receives low quantities not exceeding 15.8 mm each month.

Soil and OMW Characteristics

In both sites, soils have been classified as isohumic sierozems dating from the Mio-Pliocene and lack horizon differentiation. The major feature of soil heterogeneity is the depth of the gypsous crust under a relatively homogeneous sand-loam horizon. The main physical and chemical characteristics of soil in the region of Dar Dhaoui are summarized in Table 18.1.

The main physical and chemical characteristics of soil of El Fje are summarized in Table 18.2.

The main physical and chemical characteristics of the OMW are presented in Table 18.3.

Table 18.1 The main physical and chemical characteristic of soil of Dar Dhaoui

Depth (cm)	Calcium (%)		Total N %	O.M %	ECe mS/cm	pH	da	Exchangeable bases		Granulometry (%)		
	Total	Active						K+ (ppm)	Na+ (ppm)	ST	C	S
0-20	4.21 ± 1.32	0.66 ± 0.28	0.032 ± 0.005	0.87 ± 0.61	0.77 ± 0.08	8.11 ± 0.03	1.59	48.33 ± 6.29	14.41 ± 0.56	94.6	2.6	0.7
20-40	4.98 ± 1.75	2.5 ± 1	0.045 ± 0.01	0.84 ± 0.51	0.77 ± 0.02	8.17 ± 0.02	1.53	45.83 ± 10.10	13.76 ± 2.6	93.7	2.8	0.8

N: nitrogen; **ECe**: electrical conductivity of the saturated paste extract; **da**: density apparent; **K⁺**: potassium; **Na⁺**: sodium; **OM**: organic matter; **C**: clay (<0.002 mm); **S**: silt (0.002-0.05 mm), **ST**: total sand (0.05-2 mm)

Table 18.2 The main physical and chemical characteristic of soil of El Fje

Depth (cm)	Calcium (%)		Total N %	O.M %	ECe mS/cm	pH	da	Exchangeable bases		Granulometry (%)		
	Total	Active						K+ (ppm)	Na+ (ppm)	ST	C	S
0-20	11.11 ± 1,32	5 ± 0,86	0.03 ± 0,005	0.98 ± 0,43	2.78 ± 0,08	7.84 ± 0,04	1.73	57.5 ± 4,33	9.82 ± 5,1	79.55	4.30	15.22
20-40	8.81 ± 1,32	5.66 ± 0,76	0.03 ± 0,01	0.91 ± 0,2	2.89 ± 0,19	7.77 ± 0,11	1.28	49.15 ± 3,81	16.05 ± 1,13	78.9	4.5	13.7

N: nitrogen; **ECe:** electrical conductivity of the saturated paste extract; **da:** density apparent; **K⁺:** potassium; **Na⁺:** sodium; **OM:** organic matter; **C:** clay (<0.002 mm); **S:** silt (0.002-0.05 mm), **ST:** total sand (0.05-2 mm)

Table 18.3 Selected physical and chemical properties of the olive mill wastewater

Parameter	Value
pH	4.13
% DM	12.5
EC (mS/cm)	15.75
% OM	88.16
% MM	11.84
% Phosphorus	0.19
% TNM	0.07
% K ⁺ (%MS)	2.92
% Na ⁺ (%MS)	0.30
Content of Ca ⁺⁺ and Mg ⁺⁺ (meq/l)	3.5

DM: Dry matter, **OM:** Organic matter, **MM:** Mineral matter, **TNM:** Total nitrogen matter

Experimental Set up

OMW spreading applications were made in January 2010, soil sampling was conducted from both experimental sites with an area of 100 m² each one (10 m width by 10 m in length), with 3 replicates each treatment: unirrigated (T0) and irrigated with a quantity of 300 L of OMW per 100 m² (per plot), equal to 3 m³/hectare. Undisturbed soil samples were taken from 0 to 20 and 20 to 40 cm depth for each treatment, they were randomly collected. Soil sampling was done before OMW spreading and every end of month during the year 2010.

Laboratory Measurements

Soil samples were air dried, milled, and sieved (2 mm). The soil samples were analyzed for pH, electrical conductivity (EC), the exchangeable potassium K⁺ was determined by photometry method, and the phosphorus was determined by spectrophotometer following the method of Olsen (Pauwels et al. 1992).

NO₃⁺ and NH₄⁺ were analyzed by distillation according to the Bremner and Keeney method. Soil organic carbon was determined following the Walkley–Black chromic acid wet oxidation method (Pauwels et al. 1992).

Results and Discussion

In both study sites, the short-term effects of OMW spreading were evaluated on soil chemical parameters compared to a control samples (Table 18.4).

Table 18.4 Soil chemical parameters in two sampling horizons in two study sites after 1 year of olive mill wastewater (OMW) addition, compared to controls

Soil parameters/site	Dar Dhaoui				El Fje			
	Control		OWM		Control		OWM	
	0–20 cm	20–40 cm	0–20 cm	20–40 cm	0–20 cm	20–40 cm	0–20 cm	20–40 cm
OM (%)	0.92		1.51		0.87		1.95	
EC (mS/cm)	0.76		1.2		3.06		2.61	
pH	8.11	8	7.8	7.85	7.8	8.05	7.7	7.85
CEC (ppm)	1.5		4.7		0.9		5.7	
K+ (mg/kg)	38.5	35	197%	112%	39.5	24.16	221%	145%
P2O5 (mg/kg)	9.9	7.72	370%	204%	9.65	9.69	445%	257%
NH4+ (mg/kg)	8.99	8.61	25	18	12.5	10.5	34.3	25
NO3- (mg/kg)	10.85	10.66	143%		11.53	10.98	215%	

Effect of Short-Term OMW Application on Soil Organic Matter

About 65% of OMW is constituted of organic matter. But, the content of organic carbon on the OMW dry mass may range between 4.0 and 17.0% according to the extraction method (Paredes et al. 1987; Poiana et al. 2004). A very significant improvement was observed after 5 and 15 years of OMW soil amendment, of which Mahmoud et al. (2010) proved an OM increase to 22.7 and 36.8 g kg⁻¹, respectively, in the soil top layer.

As a result of short-term spreading with OMW in this study, organic matter content in the soil samples taken from 0 to 20 cm horizon in Dar Dhaoui site increased from 0.92% in control sample to 1.51% after one years of OMW application. Also OMW spreading in El Fje site resulted in an increase in the content of the soil organic matter in the surface layer from 0.87% to 1.95% one year after OMW application. Thus, obtained results show that there is a significant difference between OMW treatment and control. Many soil scientists have proved a concrete improvement and positive effect on soil fertility after OMW amendment (Mekki et al. 2006a, b; Brunetti et al. 2007; Sierra et al. 2007; Mechri et al. 2008). The same tendency was observed also for the organic carbon content in the bulk soil after OMW spreading (e.g., Yaakoubi et al. 2010; Chartzoulakis et al. 2010).

Soil Exchangeable Potassium

The initial content of the soil exchangeable potassium was 38.5 mg/kg in the 0–20 cm horizon and 35 mg/kg in the 20–40 cm horizon. Indeed, after OMW spreading in both sites, values were found improved to 197% in the 0–20 cm horizon

and 112% in the 20–40 cm horizon, higher than the observed ones in the control in Dar Dhaoui site. Concerning the soil of El FJE, results show that these soils are poor in potassium with 39.5 mg/kg at the surface layer and 24.16 mg/kg in the 20–40 cm horizon. After OMW intake, a greater improvement in K exch was observed. It reaches 221% in the 0–20 cm horizon and 145% in the 20–40 cm horizon. According to the previous observations of many authors (Mechri et al. 2007; Di Siero et al. 2008; Chartzoulakis et al. 2010; Kavvadias et al. 2010; Paredes et al. 1999), these significant increases are explained by the fact that the OMW are very rich on K⁺. And it is obvious that the high rates of K⁺ are beneficial for crop productivity (Arienzo et al. 2009) and it must have ecological and economic advantages through the reduction of the use of potassic fertilizers (Di Siero et al. 2008).

Soil Available Phosphorus

Soils of Dar Dhaoui are initially very poor in phosphorus with a P₂O₅ content of 9.9 mg/kg at the surface layer and 7.72 mg/kg in the 20–40 cm. An increase of 370% in the 0–20 cm horizon and 204% in the 20–40 cm horizon were observed after OMW input. As regards of soils of El FJE, results show that these soils are also poor in this element with 9.65 mg/kg at the surface layer and 9.69 mg/kg in the 20–40 cm horizon. An improvement in available phosphorus was observed following OMW application. It reaches 445% in the 0–20 cm horizon and 257% in the 20–40 cm horizon. Several authors (Cabrera et al. 1996; Alianello 2001; Piotrowska et al. 2006; Sierra et al. 2007; Di Siero et al. 2008) obtained similar results. So despite its relatively low content of phosphorus, OMW can contribute to improving the soil on this element mainly in arid soils where organic matter levels are very low.

Arid Tunisian soils are mostly alkaline, calcareous, coarse texture, and cation exchange capacity (CEC) is very low. Soils are saturated at 95% by calcium and are relatively poor to very poor in exchangeable potassium (Taâmallah et al. 1997). Therefore, being rich in potassium, OMW may be a possible potassic amendment for dry land soils, which are naturally poor in this element.

Soil Mineral Nitrogen

As regards ammonia nitrogen N–NH₄⁺, the OMW treatment determined a limited increases in both sites. The analysis carried out before OMW application in the region of Dar Dhaoui show that ammonia nitrogen is very low in these soils. It corresponds to 8.99 mg/kg at the surface layer and 8.61 mg/kg in the 20–40 cm horizon. The ammonia nitrogen released from the mineralization of organic matter that depends on biological conditions (temperature, aeration and humidity). The results showed limited increases in the OMW treated soils; it reached 25 ppm at the

surface layer and 18 ppm in the 20–40 cm horizon. Moreover, N-NH_4^+ was very low in the untreated soil in El Fje site. It corresponds to 12.5 mg/kg at the surface layer and 10.5 mg/kg in the 20–40 cm horizon. However, for OMW treated soils, a significant increase was noticed to highlight an improvement of 215% at the surface layer. This increase could be linked to the soil texture, which is dominated by sand fraction (79% ST). Complementary to the soil of Dar Dhaoui, it is characterized by substantial sandy texture (95% ST). As already proved by many authors (Arienzo et al. 2009; Sierra et al. 2007), a significant increase was detected in short period.

As regards nitrate nitrogen N-NO_3^- , analysis carried out before OMW application in the soil of Dar Dhaoui show very low contents which correspond to 10.85 mg/kg at the surface layer and 10.66 mg/kg in the 20–40 cm horizon. After OMW spreading, an improvement of 143% of N-NO_3^- content was detected at the surface layer compared to the control. In El Fje site, a very low content of N-NO_3^- was shown before OMW spreading which correspond to 11.53 mg/kg at the surface layer and 10.98 mg/kg in the 20–40 cm horizon. OMW application led to a slight increase of 215% compared to the control sample. The very low contents of N-NO_3^- obtained in both soils are due firstly to the soil texture, which was sandy and consequently promote the leaching of nitrates, which are very mobile. Our obtained results confirm those of López-Piñeiro et al. (2006), presenting a significant increase of NO_3^- after OMW amendment, that seems related to the NH_4^+ increases (Stevenson et al. 1999). Also, the mineralized-N forms should be closely correlated to soil chemical and physical properties, observation times and climatic conditions that can have an effect on the biological activity.

Soil Salinity

As shown by Roig et al. (2006), an increase in EC (from 5.5 up to 12.0 dS m^{-1}) might be connected to the extraction system of the olive oil. Commonly, the increase of EC in the soil after OMW spreading was explained by the fact that the OMW are heavily concentrated into salt (Sierra et al. 2001).

As a result of short-term irrigation with OMW, EC was not affected by the OMW treatment at both sites in comparison with control. Despite their high salinity, OMW which the EC is 15.75 mS/cm did not cause an increase in soil electrical conductivity in Dar Dhaoui site. This is due to the low dose of used OMW and did not pose risk of salinization. Indeed, EC varies from 0.76 to 1.2 mS/cm immediately after application, then it comes down to a value of about 0.94 mS/cm at the end of the year in the topsoil. However, the application of OMW induced a slight increase in EC of topsoil layer in El Fje site compared to the control, which reached 3.06 mS/cm immediately after OMW application, then it decrease to 2.61 mS/cm. This is probably due also to the low dose of used OWM. These results confirm those observed by Taamallah et al. (1997), who found that applying a dose of 50 m^3/ha do not cause a large increase in electrical conductivity of the soil and therefore do not affect soil salinity.

Soil pH

As most arid Tunisian soils are characterized by relatively high content of calcium, the surface layer of samples seems to have a basic pH value (8.11) in soil of Dar Dhaoui and 7.8 in soil of El Fje. Although it has been reported that addition of OMW sewage material would cause a decrease in soil pH value (Bouranis et al. 1995), the results obtained in Dar Dhaoui site show that the OMW application causes a slight decrease in the pH in the topsoil (0–20 cm), which reaches 7.95 just after OMW application and then decreases to 7.8 in the end of year. Same trend was observed in El Fje site, which pH decrease from 7.8 to 7.7 just after OMW application and then decreases to 7.85 in the end of year. This is probably due firstly to the low dose of used OMW and secondly to the buffering capacity of dry land soils. Ben Rouina and Taamallah (2000) have regularly monitored the pH of a calcareous soil irrigated with OMW; it appears that the pH remains unchanged over the years. This is due to high buffering capacity of the soil relatively rich in calcium. This result confirms also those of Levi-Minzi et al. (1992), which showed that OMW only modify slightly the soil pH due to the buffering capacity of the soil.

Conclusion

In conclusion, these results confirm that enhancing effects or the positives trends are detected in soil chemical parameters in both sites. As regards exchangeable potassium, available phosphorus, ammonium nitrogen, and nitrate nitrogen contents, a positive effect in the first 40 cm of at both sampling sites was shown. Consequently the detected increases of these mineral items should be counted as a beneficial indicator, that make OMW spreading as a possible amendment for dry land soils poor in these elements.

While treated plots, we perceived a temporal increases that intend to improve the organic matter properties of the soil compared to the untreated ones. This temporal behavior is concrete and obvious in the soil organic matter tendency, which can be considered as a beneficial indication of OMW soil amendment. Approximately, no change was detected regarding pH of OMW treated soils, in spite of its acidity. This is due to buffering Tunisian soil rich in calcium. But, in case of irrigation with large quantities of this effluent could only be conducted in alkaline soils.

And despite the salty characteristic of these wastewaters, a small increase of the electrical conductivity was detected, and then it decreases with time and climate conditions. This is due also to the low dose usage of OMW in our experiment. The beneficial OMW impacts on chemical soil properties prove that effluent can be considered as an alternative of soil fertilization in agriculture, through its richness on organic matter and nutrients.

References

- Alianello F (2001) Effetti della somministrazione di acque reflue di frantoioleari sulle caratteristiche chimiche e biochimiche del suolo. Progetto editoriale PANDA "I sottoprodotto dei frantoioleari" 3:29–40. Ed. L'Informatore Agrario
- Arienzo M, Christen EW, Quayle W, Kumar A (2009) A review of the fate of potassium in the soil-plant system after land application of wastewaters. *J Hazard Mater* 164:415–422
- Ben Rouina B, et Taamallah H (2000) L'utilisation des margines comme fertilisant en agriculture. Collaboration Institut des Régions Arides de Medenine – Institut de l'Olivier de Sfax. Rapport technique
- Bonari E, et Ceccarini L (1991) Spargimento delle acque di vegetazione dei frantoioleari sul terreno agrario. *L'Informatore Agrario* 13:49–57
- Bouranis DL, Vlyssides AG, Drossopoulos JB, Karvouni G (1995) Some characteristics of new organic soil conditioner from the co-composting of olive oil processing waste-water and solid residue. *Commun Soil Sci Plant Anal* 26:2461–2472
- Brunetti G, Senesi N, Plaza C (2007) Effects of amendment with treated and untreated olive oil mill wastewaters on soil properties, soil humic substances and wheat yield. *Geoderma* 138:144–152
- Cabrera F, López R, Martínez-Bordiú A, Dupuy de Lome E, Murillo JM (1996) Land treatment of olive oil mill wastewater. *Int Biodeterior Biodegradation* 215–225
- Chaarria L, Elloumb N, Gargouric K, Bourouinac B, Michichid T, Kallela M (2014) Evolution of several soil properties following amendment with olive mill wastewater. *Desalin Water Treat* 52(10–12). The online platform for Taylor & Francis Group content, pp 2180–2186
- Chartzoulakis K, Psarras G, Moutsopoulou M, Stefanoudaki E (2010) Application of olive mill wastewater to a Cretan olive orchard: effects on soil properties, plant performance and the environment. *Agric Ecosyst Environ* 138:293–298
- Demichelli M, Bontoux L (1996) Studies survey on current activity on the valorization of by-products from olive oil industry, Institute for Prospective Technological, Seville, Italy
- Di Serio MG, Lanza B, Mucciarella MR, Russi F, Iannucci E, Marfisi P, Madeo A (2008) Effects of olive mill wastewater spreading on the physicochemical and microbiological characteristics of soil. *Int Biodeterior Biodegradation* 62:403–407
- García C, Hernandez MT, Costa F, Ceccanti B (1994) Biochemical parameters in soils regenerated by addition of organic wastes. *Waste Manag Res* 12:457–466
- Kapellakis IE, Tsgarakis KP, Crowther JC (2008) Olive oil history, production and by product management. *Environ Sci Biotechnol* 7:1–26
- Kavvadias V, Doula MK, Komnitsas K, Liakopoulou N (2010) Disposal of olive oil mill wastes in evaporation ponds: effects on soil properties. *J Hazard Mater* 182:144–155
- Levi-Minzi R, Saviozzi A, Riffaldi R, Falzo L (1992) Lo smaltimento in campo delle acque di vegetazione. *Effetti sulle proprietà del terreno. Olivae* 40:20–25
- López-Piñero A, Fernández J, Rato Nunes JM, García A (2006) Response of soil and wheat crop to the application of two-phase olive mill waste to Mediterranean agricultural soils. *Soil Sci* 171:728–736
- Lozano-García B, Parras-Alcántara L, Del Toro Carrillo de Albornoz M (2011) Effects of oil mill wastes on surface soil properties, runoff and soil losses in traditional olive groves in southern Spain. *Catena* 85:187–193
- Mahmoud M, Janssen M, Haboub N, Nassour A, Lennartz B (2010) The impact of olive mill wastewater application on flow and transport properties in soils. *Soil Tillage Res* 107:36–41
- Mechri B, Ben Mariem F, Baham M, Ben Elhadj S, Hammami M (2008) Change in soil properties and the soil microbial community following land spreading of olive mill wastewater affects

- olive trees key physiological parameters and the abundance of arbuscularmycorrhizal fungi. *Soil Biol Biochem* 40:152–161
- Mechri B, Attia F, Braham M, Ben Elhadj S, Hammami M (2007) Agronomic application of olive mill wastewaters with phosphate rock in a semi-arid Mediterranean soil modifies the soil properties and decreases the extractable soil phosphorus. *J Environ Manag* 85:1088–1093
- Mechri B, Cheheb H, Boussadia O, Attia F, Ben Mariem F, Braham M, Hammami M (2011) Effects of agronomic application of olive mill waste water in a field of olive trees on carbohydrate profiles, chlorophyll a fluorescence and mineral nutrient content. *Environ Exp Bot* 71:184–191
- Mekki A, Dhouib A, Aloui F, Sayadi S (2006a) Olive wastewater as an ecological fertilizer. *Agron Sustain Dev* 26:61–67
- Mekki A, Dhouib A, Sayadi S (2006b) Changes in microbial and soil properties following amendment with treated and untreated olive mill wastewater. *Microbiol Res* 161:93e101
- Moraetis D, Stamati F E, Nikolaidis N P, Kalogerakis N (2011) Olive mill wastewater irrigation of maize: impacts on soil and groundwater. *Agric Water*
- Nikolaos G, Ioannis V, Alexandros P, Eleftheria S, Nikolaos Cand Adamantia C (2013) Chemical and biological properties of a sandy loam soil amended with olive mill waste, solid or liquid form, in vitro. *Int J Recycl Org Waste Agric*. <http://www.ijrowa.com/content/2/1/13>
- Paredes MJ, Moreno E, Ramos-Cormenzana A, Martinez J (1987) Characteristics of soil after pollution with wastewaters from olive oil extraction plants. *Chemosphere* 16:1555–1564, *Management* 98:1125–1132
- Paredes C, Ceggara J, Roing A, Sanchez-Monedero MA, Bernal MP (1999) Characterization of olive mill waste-water (alpechin) and its sludge for agricultural purposes. *Biores Technol* 67:111–115
- Pauwels JM, Van Ranst E, Verloo M, et Mvondoze A (1992) *Manuel de laboratoire de pédologie*. Ed. AGCD. 265 p
- Piotrowska A, Iamarino G, Rao MA, Gianfreda L (2006) Short-term effects of olive mill wastewater (OMW) on chemical and biochemical properties of a semiarid Mediterranean soil. *Soil Biol Biochem* 38:600–610
- Poiana M, Mincione A, Mincione B, Sicari V (2004) Caratteristiche chimiche e fisiche dei residui delle industrie olearie e agrumarie. In: *Valorizzazione di acque reflue e sottoprodotti dell'industria agrumaria e olearia*, Laruffa, pp 13–21
- Roig A, Cayuela ML, Sánchez-Monedero MA (2006) An overview on olive mill wastes and their valorization methods. *Waste Manag* 26:960–969
- Sierra J, Martí E, Garau MA, Cruañas R (2007) Effects of the agronomic use of olive oil mill wastewater: field experiment. *Sci Total Environ* 378:90–94
- Sierra J, Martí E, Montserrat G, Cruañas R, Garau MA (2001) Characterisation and evolution of a soil affected by olive mill wastewater disposal. *Sci Total Environ* 279:207–214
- Stevenson FJ, Cole MA (1999) *Cycles of soil: carbon, nitrogen, phosphorus, sulfur, micro nutrients*, 2nd edn. Wiley Inc, New York
- Taâmallah H, Ben Rouina B, De Gryse S, Hartmann R, et Kheriddine N (1997) Effets de l'épandage des margines sur certaines propriétés du sol. Etude préliminaire. *Atelier National sur les traitements et la valorisation des sous produits de l'olivier*. Boughrara- Sfax Tunisie
- Tomati U, Galli E (1992) The fertilizing value of wastewaters from the olive processing industry. In: Kubat J (ed), *Humus, its structure and role in agriculture and environment*. Elsevier Science, Amsterdam, pp 117–126
- Yaakoubi A, Chahlaouia A, Rahmanib M, Elyachiouic M, Nejdib I (2010) Effect of olive mill wastewater spreading on the physicochemical characteristics of soil. *Desalin Water Treat* 16:194–200

Chapter 19

Spatio-Temporal Evolution of the Fragmentation Classes of the Mikea Dry Deciduous Forest (Southwestern Madagascar)

Hibraim Rijaso Ravoanjimalala, Jan Bogaert, Dominique Hervé,
Samuel Razanaka, Jaona Ranaivo, Herizo Randriambanona
and Solofo Rakotondraompiana

Abstract In southwestern Madagascar, the Mikea forest is a highly diverse ecosystem of great biodiversity, which mixes dry deciduous forest in the eastern part and xerophytic thicket in the western coastal area. However, dry forests and shrubs are rapidly destroyed due to slash-and-burn cultivation (*hatsaky*) and exploitation of forest resources by riparian communities and external operators. The aim of this paper is to evaluate forest fragmentation in the Mikea national park, by comparing past and recent forest maps. The analysis of forest fragmentation is based on landscape indices. The changes in forest cover have been detected from time-series SPOT satellite images registered over 15 years (1999, 2005, and 2014). Between 1999 and 2014, forest area is reduced by 39.8% which is equivalent to an annual forest loss rate of 4.6%. The forest fragmentation is associated with a significant decrease in forest patch size. The mean patch size decreases from 37,228 to 18,731 ha from 1999 to 2014. The primary direct causes are economic driven due to intense anthropogenic activities such as wood charcoal production, logging, accompanied by frequent wild land fires. The indirect cause is the absence of a sustainable environmental management and conservation strategy.

H.R. Ravoanjimalala (✉) · S. Razanaka · J. Ranaivo · H. Randriambanona
Centre National de Recherches sur l'Environnement (CNRE),
Antananarivo, Madagascar
e-mail: ravoanjimalala@gmail.com

H.R. Ravoanjimalala · S. Rakotondraompiana
Laboratoire de Géophysique de l'Environnement et Télédétection (LGET),
Institut et Observatoire de Géophysique d'Antananarivo (IOGA),
Université d'Antananarivo, Antananarivo, Madagascar

J. Bogaert
Gembloux Agro-Bio Tech, Université de Liège, Gembloux, Belgique

D. Hervé
UMR 220 GREDD (IRD-UPVM), Institut de Recherche pour le Développement,
Montpellier, France

Keywords Forest fragments · Deforestation · Remote sensing · Biodiversity · Mikea forest · Landscape metrics

Introduction

Phillipson et al. (2006) consider Madagascar as a major hotspot of global biodiversity. In the southwestern region of Madagascar, the Mikea forest is a dense dry forest where the forest degradation rate is considered as higher than in any other region in Madagascar (Ravonjimalala et al. 2015). The area of Mikea forest is 184,630 ha in 2011. It is bounded in the North by the Mangoky River and in the South by the Manombo River. A little known human group called Mikea including about 1000–2000 people lives inside this forest. Mikea people still have a traditional way of life (Stiles 1998). Region biodiversity includes among others two (02) endemic birds species, *Uratelornis chimaera* and *Monias benschi* (Rakotonomenjanahary and Hawkins 2000) as well as two (02) mammals species, *Microgale jenkinsae* and *Macrotarsomys* (Goodman and Soarimalala 2005; Lourenço et al. 2004).

The forest cover change and its consequences have been recognized as a threat to the environment (Laurance 1999). It affects forest fragmentation and loss of biodiversity through connectivity decrease (Liu et al. 2014; Martínez et al. 2015). Forest fragmentation is a transformation of the landscape in which a massive intact natural forest is divided into several small forest plots, more or less isolated (Bogaert et al. 2004; Collins et al. 2009; Fahrig 2003). It is one of the leading agents of species extinction at local and global scales (Bregman et al. 2014). Unfortunately, the process of forest fragmentation is not yet sufficiently widely studied, less than deforestation, notably within tropical dry forests (Worku et al. 2014) although this type of forest is known for its vulnerability related to a weak potential for regeneration and restoration (Vieira and Scariot 2006).

The main objectives of this study are to quantify forest fragmentation mechanisms from deforestation.

Material and Method

Study Area

The region under study is situated at about 100 km north of the city of Toliara, (22° 31' 39.47" S; 43° 32' 2.57" E, 120 m a.s.l.) surrounding the village of Analamisampy (Fig. 19.1). The climate is semi-arid with an annual rainfall ranging from 600 to 1000 mm. 90% of the rainfall occurs during the rainy season (November–March) while the rainfall during the dry season (April–October) is below 50 mm (Blanc-Pamard et al. 2005). The average annual temperature is about 24.1 °C.

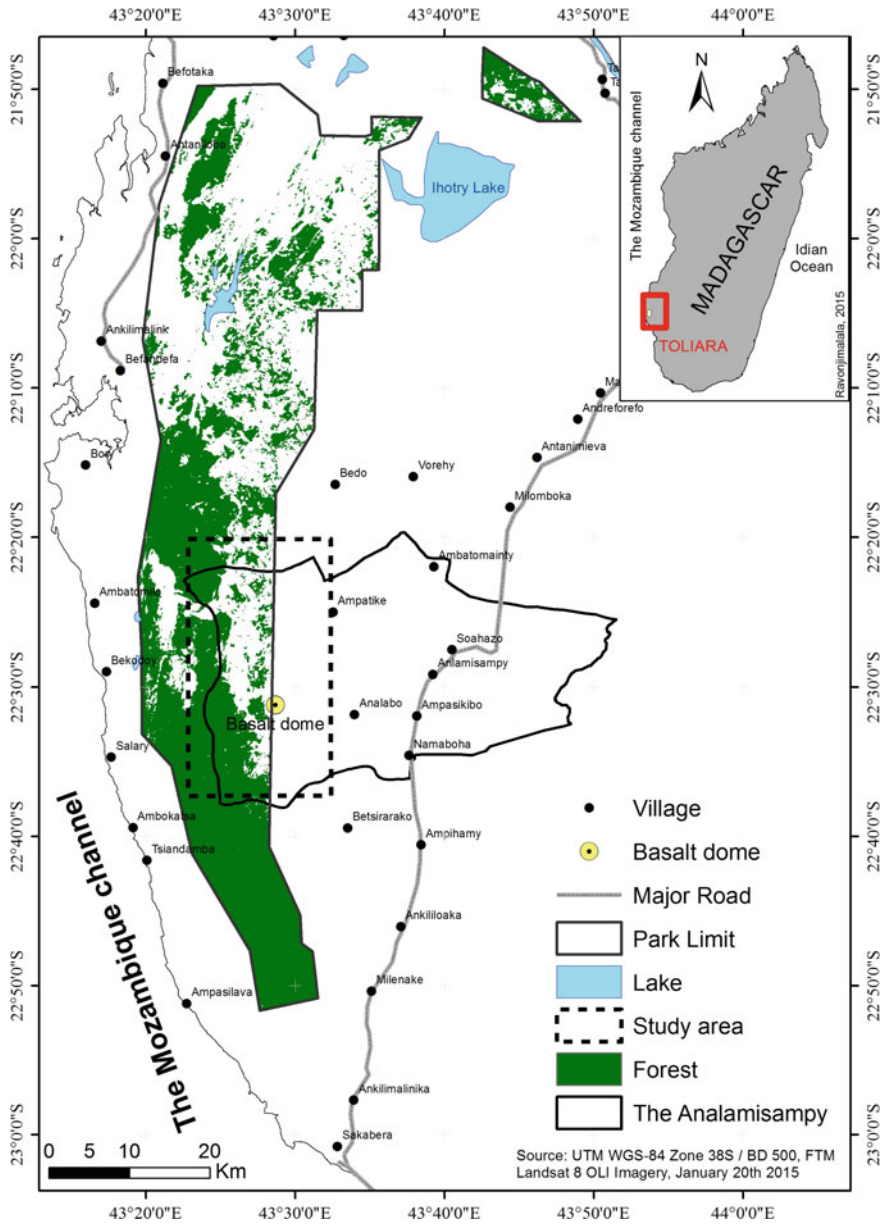


Fig. 19.1 Study area

Table 19.1 Characteristics of the satellite images

Date	Satellite type	Resolution (m)	Resolution (m)	Path/Row
		XS	PAN	
99-04-01	SPOT 4	20	10	162–395
05-05-01	SPOT 4	20	10	162–395
14-11-28	SPOT 5	10	2.5	162–395

Spatial Images

Three (03) SPOT images (KJ 162/395) were employed to map land cover and to identify its evolution through time. Dates of images were 1999, 2005, and 2014. These images have a spatial resolution of 20 m for multispectral channels (XS) and 10 m for the panchromatic channel (PAN). Their characteristics are given in Table 19.1. Atmospheric correction was applied to all images in order to correct the effect of atmosphere on pixel spectral values (Mustak 2013), using the method proposed by Bernstein et al. (2005). An image fusion operation between PAN and XS channels with pan sharpening method (Aiazzi et al. 2007) is applied to the 1999 and 2005 scenes. It enables to obtain synthetic images with 10 m resolution.

Image Classification

We used an object-based classification method which is more adapted to very high resolution images (Blaschke 2010). Object-oriented classification was done in two steps. The first step consisted in the segmentation of the images into meaningful objects, which gathered pixels sharing spectral and textural homogeneity. The implemented segmentation type used contour filters to define the outline between segments (Meinel et al. 2000).

The second phase was the classification of the segments (or objects), using a support vector machine (SVM) algorithm because of its ability to solve complex classification patterns, which are generally the case when working with landscapes (Huang et al. 2013).

Landscape Metrics

The quantitative methods of landscape ecology are based on the application of landscape metrics (Turner and Gardner 1991). These metrics render quantitative information about landscape composition and configuration allowing a more

Table 19.2 Summary table of landscape metrics. All equations are available in McGarigal and Marks (1995)

Index name	Acronym	Analysis level	Landscape structure concept
Class area (ha)	CA	Class	Fragmentation
Number of patches	NP	Landscape/Class	Fragmentation
Patch density (#/100 ha)	PD	Landscape/Class	Fragmentation
Largest patch index	LPI	Landscape/Class	Fragmentation
Mean patch area (ha)	AREA_MN	Landscape/Class	Fragmentation
Mean euclidean nearest neighbour distance (m)	ENN_MN	Class	Connectivity/Isolation
Shannon's diversity index	SHDI	Landscape	Heterogeneity

objective comparison of different patterns in space and time. Consequently, landscape metrics have widely been used in literature to study large natural areas, forest evolution, or urban expansion (Başkent and Kadioğullari 2007). Table 19.2 describes the landscape metrics used in this study. We selected landscape metrics suitable to characterize fragmentation classes.

Results and Discussion

Forest Cover Classification and Change

The forest cover maps in Fig. 19.2 show the evolution of forest cover during 15 years. A basalt dome and the limit of the Mikea National Park, fixed in 2007, are given as benchmarks. The area of forest lost in 15 years is 37,227 ha, which represents 80% of the total forest area. The maps show the different forms of the forest fragments in the study area.

Quantitative Metric Analysis of Dry Deciduous Forest Pattern Change

We calculated landscape metrics using FRAGSTATS software (McGarigal et al. 2012). Comparison of landscape metrics outcomes between years provides valuable information about landscape heterogeneity, fragmentation, and connectivity. This study particularly investigated the forest fragmentation process using a set of classic and accurate landscape metrics. Table 19.3 shows the mean values of the landscape metrics for forest/non-forest land uses.

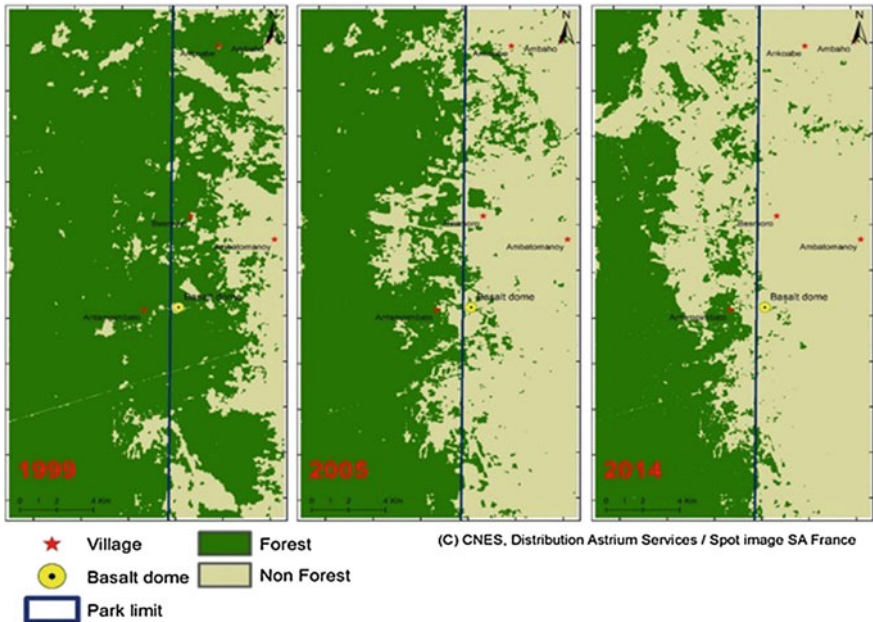


Fig. 19.2 Forest cover in the 3 analyzed years

Table 19.3 Landscape metrics for 1999, 2005, and 2014

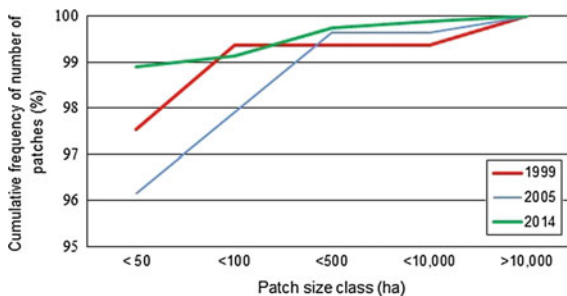
	Type	CA	NP	PD	LPI	AREA_MN	ENN_MN	SHDI
1999	Forest	37,228	304	0.7	78	122	95	0.5
	Non-forest	9,149	436	0.9	10	21	138	
2005	Forest	26,625	421	0.9	53	63	142	0.7
	Non-forest	19,752	277	0.6	39	71	145	
2014	Forest	18,647	438	0.9	30	43	131	0.7
	Non-forest	34,205	144	0.3	58	192	145	

The number of patches (NP) per class gives an idea about the evolution of the fragmentation of a class between periods. Comparisons of NP values for forest between 1999 and 2014 show an increase of the index value from 304 to 438.

The forest class area (CA) gives the overall forest size over the area. The former decreases from 37,228 ha (80%) in 1999 to 18,647 ha (40%) in 2014.

The increased number of small patches in an area is considered as one of the basics of forest fragmentation assessment. While the total number of forest fragments increases from 304 to 421 during the first period (1999–2005), the increase is less important (421–438) during the second period (2005–2014). In 1999, the forest area is found in patches between 10,000 and 40,000 ha; the remaining forest fragments can be observed in isolated patches with an area lower than 100 ha. In

Fig. 19.3 Evolution of cumulative frequency of NP distribution over forest patch size classes in the Mikea dry deciduous forest



2005, the majority of forest plots have a size less than 100 ha, only three fragments have a size between 100 and 500 ha and only one lies between 500 and 2000 ha.

Other forest changes have been found by comparing the distribution of forest patch sizes between the three years (Fig. 19.3). Forest fragment sizes less than 100 ha can be considered as isolated patches. The cumulative frequency of the number of patches indicates a slight similar trend between patch class size intervals in 1999 and 2005. The forest area loss almost affected the entire class area. Weaker values observed for forest class areas less than 100 ha in 2005 may be associated to the disappearance of these small patches by intensive slash and burn during the 1999–2005 period.

The fragmentation process mostly affected the largest forest fragments aside the forest boundary leading to an increase of patch density (PD) and a decrease of LPI and AREA_MN (Table 19.3). An increase of patch density (PD) is also observed in the area. As a result, these metrics indicate that the landscape has become more fragmented between 1999 and 2014. The last landscape level metric calculated shows that there was no important change in SHDI between 1999 and 2014, which indicates that heterogeneity has not affected.

The Fig. 19.2 and the Table 19.3 differentiate two landscape classes, forest vs. non forest. Significant changes of fragmentation index values have been observed for both classes. Non-forest classes expanded and spread all over the region area. The decrease in the ENN_MN of forest patches and the stability of ENN_MN for non forest patches between 2005 and 2014 could suggest an improvement of the structural connectivity between the forest patches.

Causes of Deforestation and Metrics Change from Survey

Comparisons of the classification results over the three different years allowed to detect forest dynamics in the study area. The deforestation rate is quantified using the formula proposed by Puyravaud (2003), generally used to quantify the deforestation trend at a global scale:

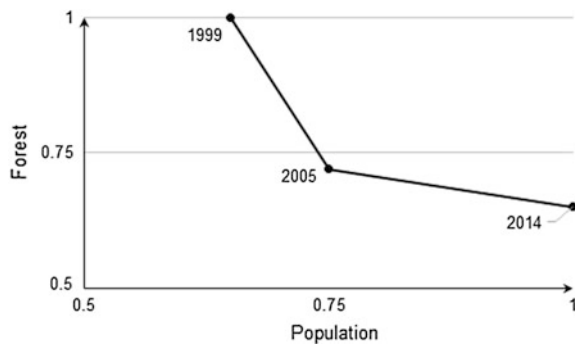
$$t = \frac{100}{t_2 - t_1} \ln \frac{A_2}{A_1}$$

where t represents the deforestation rate, A_1 is the forest landscape state in the initial year t_1 and A_2 is its state for the subsequent year t_2 (Puyravaud 2003). It shows a slight increase which means an obvious decrease of the forest area, about 4.58% per year (Table 19.3).

Landscape metric computation also evidenced the trends of forest fragment loss in the study area. The analysis reveals that the fragment loss affects all the size classes, which means a randomness of forest area re-affectation for agricultural purposes in the study area. The decrease of class areas less than 500 ha between 1999 and 2005 may be associated to the elimination of the isolated forest patches, the increase recorded between 2005 and 2014 could be a consequence of the creation of new small fragments (Fig. 19.3). The large fragments (>500 ha) seem to be stable but in fact they are shrinking and shifting into the lower size classes if they do not disappear entirely, and new large fragments are created (Fig. 19.3). This patch structure evolution reflects human logging strategy. A gradual fragmentation process leads to large fragments at the forest border which are fragmented further in smaller and more isolated forest patches, which are finally converted into non-forest land use.

In addition, biological and ecological characteristics of dry forest emphasize this trend. In fact, such forest types have a relative slow regeneration due to the high increase of population density in the region (Fig. 19.4). Furthermore, slashed and dead fallen trees are also used to provide timber and woody charcoal. These causes related to human activities seem to be the main direct drivers of forest cover changes and transitions in the region.

Fig. 19.4 Comparison of deforestation and population trend



Conclusion

This work mainly links forest cover loss in the dry deciduous forest of Mikea localized in the southwest of Madagascar to the underlying fragmentation process during 15 years. The combination of spatial observation approaches and landscape metrics acquired from FRAGSTATS helped to highlight the spatial dynamics of dry deciduous forest.

Forest cover loss and the forest fragmentation seem to follow the same trajectory: the use of forest as a resource for people to survive (mainly firewood and woody charcoal for domestic use). This could be evidenced through the evolution of forest fragmentation patterns.

The dynamic pattern of the dry forest in the study area follows the general trend of landscape fragmentation by human activities and settlement sprawl. The incorporation of biological and ecological factors in the analysis of the different fragmentation classes could help to understand the impact of this fragmentation phenomenon on biodiversity.

Acknowledgments This research was supported by a RAMI PhD grant from the Agence Universitaire de la Francophonie (AUF), the Gembloux Agro-Bio Tech, Université de Liège (Belgique) and the FPPSM project (French MAE) for field work. Special thanks to the SEAS-OI station and CNES-ISIS for providing satellite data to the “Centre National de Recherches sur l’Environnement” (CNRE) Madagascar and the “Remote Sensing and Environmental Geophysics Laboratory”/Institute & Observatory of Geophysics, Antananarivo (IOGA), University of Antananarivo. Many thanks for the FPPSM project (IRD, CNRE, ESSA-Forest, ENI, CNA, and DBEV) for research managing and logistical-technical supports.

References

- Aiazzi B, Baronti S, Selva M (2007) Improving component substitution pansharpening through multivariate regression of MS + Pan data IEEE. *Trans Geosci Remote Sens* 45:3230–3239. doi:[10.1109/TGRS.2007.901007](https://doi.org/10.1109/TGRS.2007.901007)
- Başkent EZ, Kadioğullari AI (2007) Spatial and temporal dynamics of land use pattern in Turkey: a case study in İnegöl. *Landsc Urban Plan* 81:316–327. doi:[10.1016/j.landurbplan.2007.01.007](https://doi.org/10.1016/j.landurbplan.2007.01.007)
- Bernstein LS, Adler-Golden SM, Sundberg RL, Levine RY, Perkins TC, Berk A, Ratkowski AJ, Felde G, Hoke ML (2005) Validation of the QUick atmospheric correction (QUAC) algorithm for VNIR-SWIR multi-and hyperspectral imagery. In: Shen SS, Lewis PE (eds). pp 668–678. doi:[10.1117/12603359](https://doi.org/10.1117/12603359)
- Blanc-Pamard C, Milleville P, Grouzis M, Lasry F, Razanaka S (2005) Une alliance de disciplines sur une question environnementale: la déforestation en forêt des Mikea (Sud-Ouest de Madagascar). *Natures Sci Sociétés* 13:7–20. doi:[10.1051/nss:2005002](https://doi.org/10.1051/nss:2005002)
- Blaschke T (2010) Object based image analysis for remote sensing ISPRS. *J Photogramm Remote Sens* 65:2–16. doi:[10.1016/j.isprsjprs.2009.06.004](https://doi.org/10.1016/j.isprsjprs.2009.06.004)
- Bogaert J, Ceulemans R, Salvador-Van Eysenrode D (2004) Decision tree algorithm for detection of spatial processes in landscape transformation. *Environ Manag* 33:62–73. doi:[10.1007/s00267-003-0027-0](https://doi.org/10.1007/s00267-003-0027-0)

- Bregman TP, Sekercioglu CH, Tobias JA (2014) Global patterns and predictors of bird species responses to forest fragmentation: implications for ecosystem function and conservation. *Biol Conserv* 169:372–383. doi:10.1016/j.biocon.2013.11.024
- Collins CD, Holt RD, Foster BL (2009) Patch size effects on plant species decline in an experimentally fragmented landscape. *Ecology* 90:2577–2588. doi:10.1890/08-1405.1
- Fahrig L (2003) Effects of habitat fragmentation on biodiversity. *Anu Rev Ecol Evol Syst* 34:487–515. doi:10.1146/132419
- Goodman SM, Soarimalala V (2005) A new species of *Macrotrarsomys* (Rodentia: Muridae: Nesomyinae) from southwestern Madagascar. *Proc Biol Soc Washingt* 118:450–464. doi:10.2988/0006-324X(2005)118[450:ANSOMR]20CO;2
- Huang Y, Yin X, Ye G, Lin J, Huang R, Wang N, Wang L, Sun Y (2013) Spatio-temporal variation of landscape heterogeneity under influence of human activities in Xiamen City of China in recent decade. *Chinese Geogr Sci* 23:227–236. doi:10.1007/s11769-012-0577-2
- Laurance WF (1999) Effects on the tropical deforestation crisis. *Biol Conserv* 91:109–117. doi:10.1016/S0006-3207(99)00088-9
- Liu S, Dong Y, Deng L, Liu Q, Zhao H, Dong S (2014) Forest fragmentation and landscape connectivity change associated with road network extension and city expansion: a case study in the Lancang River Valley. *Ecol Indic* 36:160–168. doi:10.1016/j.ecolind.2013.07.018
- Lourenço WR, Goodman SM, Ramilijaona O (2004) Three New Species of *G Rospus* Simon From Madagascar (S Corpiones B Uthidae)
- Martínez del Castillo E, García-Martin A, Longares Aladren LA, de Luis M (2015) Evaluation of forest cover change using remote sensing techniques and landscape metrics in Moncayo natural park (Spain). *Appl Geogr* 62:247–255. doi:10.1016/j.apgeog.2015.05.002
- McGarial K, Marks BJ (1995) FRAGSTAT: spatial pattern analysis program for quantifying landscape structure United States. Department of Agriculture Pacific Northwest Research Station, 120 pp
- McGarigal K, Cushman SA, Ene E (2012) Spatial pattern analysis program for categorical and continuous maps computer software program produced by the authors at the University of Massachusetts. <http://www.umass.edu/landeco/research/fragstats/fragstats.html>. Accessed 3 Aug 2016
- Meinel G, Neubert M, Sensing R, City L (2000) A comparison of segmentation programs for high resolution remote sensing data. *Spring* 35:1097–1105
- Mustak S (2013) Correction of atmospheric haze in Resourcesat-1 Liss-4 Mx Data for urban analysis: an improved dark object subtraction approach. *ISPRS—Int Arch Photogramm Remote Sens Spat Inf Sci XL-1/W3:283–287*. doi:10.5194/isprsarchives-XL-1-W3-283-2013
- Phillipson PP, Schatz GR, Lowry IIPP, Labat FN (2006) A catalogue of the vascular plants of Madagascar. In: Ghazanfar SA, Beentje HJ (eds) *Taxonomy and ecology of African Plants: their conservation and sustainable use*. Proceedings XVIIth AETFAT congress, Royal Botanic Gardens, Kew
- Puyravaud JP (2003) Standardizing the calculation of the annual rate of deforestation. *For Ecol Manag* 177:593–596. doi:10.1016/S0378-1127(02)00335-3
- Rakotonomenjanahary OM, Hawkins AFA (2000) Le Projet “Zicoma” ou “Zones d’Importance pour la Conservation des Oiseaux a Madagascar”. *Ostrich* 71:168–171. doi:10.1080/0030652520009639901
- Ravonjimalala HR, Razanaka S, Randriambanona H, Hervé D, Rakotondraompiana S (2015) Evolution de la déforestation pour la culture de maïs sur défriche-brûlis dans la forêt de Mikea avant et après sa mise sous statut d’aire protégée. In: Hervé D, Razanaka S; Rakotondraompiana S, Rafamantanantsoa F, Carrière S (eds) *Transitions agraires au sud de Madagascar Résilience et viabilité deux facettes de la conservation*. Actes du séminaire de synthèse du projet FPPSM “Forêts parc et pauvreté au sud de Madagascar”, 10–11/06/2013, Antananarivo, IRD/SCAC-PARRUR Ed. MYE, pp 85–94
- Stiles D (1998) The Mikea Hunter-Gatherers of Southwest Madagascar: ecology and economics African study 19:127–148
- Turner MG, Gardner RH (1991) Quantitative methods in landscape ecology. *Ecol Stud* 82:536

- Vieira DL, Scariot A (2006) Principles of natural regeneration of Tropical Dry Forests for regeneration. *Restor Ecol* 14:11–20. doi:[10.1111/j1526-100X200600100x](https://doi.org/10.1111/j1526-100X200600100x)
- Worku A, Pretzsch J, Kassa H, Auch E (2014) The significance of dry forest income for livelihood resilience: the case of the pastoralists and agro-pastoralists in the drylands of southeastern Ethiopia. *For Policy Econ* 41:51–59. doi:[10.1016/j.forpol.2014.01.001](https://doi.org/10.1016/j.forpol.2014.01.001)

Chapter 20

The Impact of Atmospheric Pollution on the Chemical Composition of Soil Around Gabes Cement Plant Southeastern Tunisia

Ines Terwayet Bayouli, Housseem Terwayet Bayouli,
Mohamed Tarhouni and Mohamed Nefatti

Abstract This study fits into the framework of the evaluation of the impact of atmospheric pollution on the chemical composition of soil that was carried out around Gabes cement plant situated in Southeast of Tunisia commonly characterized by a high pollutant potential due to industrial encroachment. Crossing the inventoried sector, four sites are subject of the study along a pollution gradient potential started from the cement plant. The statistical analysis ANOVA shows a highly significant variation ($p < 0.001$) between sites of soil contents of chemical components measurements (Total limestone CaCO_3 , active limestone CaCO_3 , sodium Na, potassium K) marking a pollutant effect. Electrical conductivity and pH are also influenced from sites located near the plant to further ones along distance from the cement plant.

Keywords Air pollution · Chemical composition · Soil · Cement plant

I. Terwayet Bayouli (✉)

Laboratory of Arid Crop Oasis, Faculty of Sciences of Gabes, Institut des Régions Arides de Médenine, 22.5 km Route Aljorf, 4119 Medenine, Tunisia
e-mail: bayouli_ines@yahoo.fr

H. Terwayet Bayouli · M. Tarhouni · M. Nefatti

Laboratory of Rangeland Ecology, Institut des Régions Arides de Medenine, 22.5 km Route Aljorf, 4119 Medenine, Tunisia
e-mail: Beyoulihousem@yahoo.fr

M. Tarhouni

e-mail: Mohamed.tarhouni@gmail.com

M. Nefatti

e-mail: nefatti.mohamed@ira.nrnt.tn

Introduction

Even though the atmospheric emissions rate limits—imposed on industrial facilities—have become stricter recent years, inadequate measures are still prevalent in the case of emergent countries (Gabrila et al. 2014). Particulate matter and pollutants in general can be transported by winds and dispersed by turbulent movement of air before reaching receptors. One of industries, which can cause particulate matter, is cement production accompanied by emissions of dust and is being thus of a main environmental concern highlighting cement manufacture (Isikli et al. 2006).

Cement industries are important pollution emission sources of both organic and inorganic chemicals, and produce an input of metals and metalloids such as As, Cd, Ca, Co, Cr, Cu, Ni, Pb, and Zn (Isikli et al. 2006; Schuhmacher et al. 2004; Alkhashman and Shawabkeh 2006).

Established in 1977, Gabes cement plant, permanently programmed in the fourth Plan (1973–1977) is part of a sectorial objective related to the supply of the Tunisian market, which has become a major consumer of cement. The choice of its location in Gabes is explained by the availability of raw materials (limestone, marly limestone and clay), also by the existence of a significant infrastructure (port, plants, pipelines and industrial complex) and its central position in the south then it became an important market of cement (25% of the Tunisian needs). Nevertheless, the environmental effects related to the construction and operation of the cement, despite that they were relatively localized; they affect a huge number of significant areas. Indeed, the quarrying of raw materials, the industrial process leading to the production of cement and the transportation of the final product to the customer represent all aspects that are likely to have significant environmental impacts (Haydar 1986).

Several publications have evaluated the soil pollution around a cement plant. All of them focused on heavy metals contamination but the impact of cement plant on the chemical composition of soil is still missed. The main goal of this study is to evaluate the impact of cement pollution on ions balance of soil.

Experimental Design

Site Description

Soil samples were taken from the neighbourhood of the cement plant of Gabès (southeastern of Tunisia). Four sites were chosen for soil study according to distance to the cement plant. Before sampling, we must choose the most homogeneous sites (same slope, nature of soil, same depth, the same pH and same size).

Soil Sampling Method

Soils can be contaminated by atmospheric fallout, runoff water, contributions of exterior materials of natural origin or not or have undergone alterations that have modified the original distribution of the existing pollution. The soil sampling should be specific. Therefore, it is necessary first to define the nature of the needs, which justify the investigation of soil and determine the most appropriate approach. There are several methods and standards for sampling and soil analyzes that can be adapted or simplified for the study of polluted soils (Laperche and Mossman 2004).

In our case, a random sampling was performed while moving away from the cement (same characteristics of sites). We took into consideration the uniformity of ecological and geomorphological conditions in the light of data required on soil at sites around the plant uniform surrounding bio-geological conditions of the soil, status check (lack of agricultural activities), homogeneous size and topology of the site, avoiding the combination of other sources of pollution (roads because discharge). Three samples (between 0 and 20 cm deep) were performed, using an auger, at each site. Soil samples were transported in bags and Stocked in the shade before analysis.

Determination of Ionic Balance

This is to determine the concentrations of various ions (anions and cations) of soluble soils. Anions (chlorides, carbonates, bicarbonates and sulphates) and cations (potassium and sodium) are determined from the extract of the saturated paste of ground soil and prepared for the measurement of the electrical conductivity. Saturated paste is obtained by weighing 250 g soil samples and then added to each sample, a definite volume of distilled water until being dough brilliant, fairly compact and sliding on the spatula (Baize 2000). All ions contents were measured using AFNOR X31-071 (1987) methods.

Analysis of Variance (ANOVA)

The analysis of variance (ANOVA) is a classification criterion applied to all results. It compares the average of the groups formed by the classification criteria or subjected to analysis. This analysis allows us to see if there is significant variability between sites or not regarding the average parameters calculated based on the distance (Tarhouni 2008). The critical threshold beyond which a significant difference between the mean observed is fixed and coded as follows:

NS = non-significant difference $p > 0.05$; * = significant difference $p \leq 0.05$; ** $P \leq 0.01$; *** $P \leq 0.001$. ANOVA were performed using SPSS 11.5 software.

Results and Discussion

The pH measurement results of different soil samples collected near Gabès cement plant are given in Fig. 20.1.

All pH found are alkaline. In the first site the pH was 8.07 and it grows in the second, third and fourth site to reach 8.15, 8.35 and 8.65, respectively. The analysis of variance (ANOVA) shows highly significant differences between sites ($p = 0.0 < 0.001$). This difference is explained, by the pollution gradient. The more we get closer to the plant, the more the pH is lower and this is because of the acidic pollutants rejection.

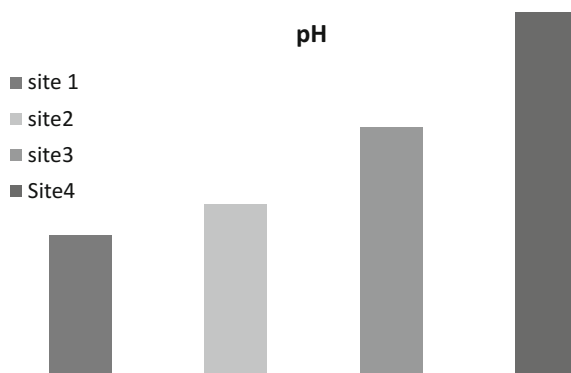
Moreover, the alkalinity of the soil appears in calcareous soils. It can occur naturally in sodic soils due to the accumulation of exchangeable sodium. It has been shown that sodic soils have low structural stability due to their high exchangeable sodium (FAO 2000). Such soils having high OH^- concentrations are associated with high levels of carbonates and bicarbonates. In our case the basicity of the soil may be due to environmental conditions since gypsum is placed on a limestone substrate outcrop. However, any type of pollution induces changes in soil pH level of factories surrounding areas by acidifying or alkalizing them.

We remind that Legros (1996) defined the alkalinity as the sum of ions and cations as follows:

$$\text{Alkalinity} = 2[\text{Ca}^{2+}] + 2[\text{Mg}^{2+}] + [\text{Na}^+] + [\text{K}^+] + [\text{NH}_4^+] - 2[\text{SO}_4^{2-}] - [\text{Cl}] - [\text{NO}_3^-]$$

From this relationship, it can be concluded that the concentrations of cations Ca^{2+} , Mg^{2+} , Na^+ , K^+ and NH_4^+ increase as one moves away from the cement plant.

Fig. 20.1 Changes in soil pH near Gabes cement plant in the spring of 2012 a/b/c denote the groups identified by the SNK test



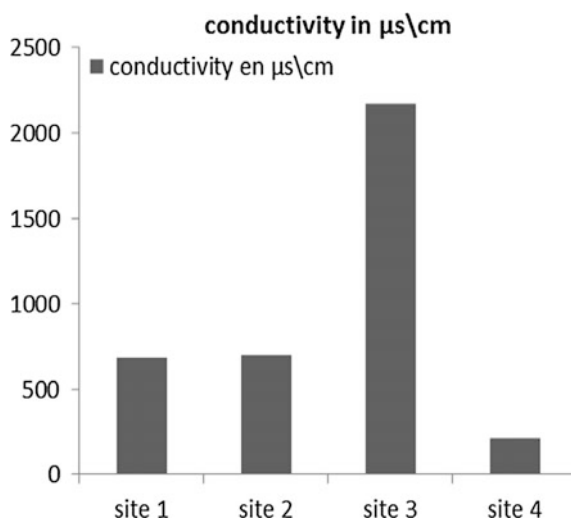
However concentrations SO_4^{2-} , Cl^- and NO_3^- have more severe levels in the first sites and progressively decrease away from the cement plant. Assuming that the plant emits sulphur dioxide and nitrogen oxides and if we refer to cycles of nitrogen and sulphur, which show that at topsoil level the sulphur may take the form of sulphates (SO_4^{2-}), we deduce that the relatively high concentration of anions SO_4^{2-} and NO_3^- at the closest sites to the plant are resulting of pollutants emissions. The dust from cement plants are mostly alkaline and may have advantageous and disadvantageous effects on plants (Gigauri et al. 1992; Iqbal and Shafiq 1995).

The pH is a crucial factor for the mobility of metal ions as it influences the number of negative charges that can be brought into solution (McLaughlin et al. 2000). Generally, with increasing pH, cations are less soluble and anions are more soluble (Blanchard 2000). It also entails the dissolution of organic matter and subsequent formation of more soluble organometallic complexes (Chaignon 2001). Such alkaline conditions (especially sodium), induce various nutritional plants disorders such as chlorosis (caused by the inability of plants to absorb enough iron and manganese). Copper and zinc deficiencies can also appear as well as phosphorus deficiency which is due to the low solubility. If the soil contains a lot of CaCO_3 , potassium is easily leached and a deficiency can be manifested. Nitrogen can also be deficient because of the low content of organic matter (FAO 2000).

Electrical Conductivity Measurement

Electrical conductivity is measured to deduce the salinity of soil samples near Gabès cement plant (Fig. 20.2).

Fig. 20.2 Variation of electrical conductivity near Gabès cement plant in the spring of 2012 a/b denote the groups identified by the SNK test



The electrical conductivity is a measure of the ion concentration. The more a solution is rich in salts, acids or bases the more its conductivity is high (Gavrilovic et al. 1996). Figure 20.2 notes that the highest electrical conductivity is observed in the third site followed by the first and the second site. The lowest value is recorded in the fourth site (about 200 $\mu\text{s}/\text{cm}$). Analysis of variance revealed a significant variability of the conductivity between the sites ($p = 0.009 < 0.01$). These results show that the fourth site is poor in ion and salt while other sites are richer. This enrichment of ionic elements is due to emissions from the cement plant. This is consistent with the hypothesis of Bocard (2006) which suggests that a highly polluted area is characterized by a negative spontaneous potential and a strong electric chargeability. Indeed the closest floors to the cement plant are more polluted (more loaded with ionic elements).

Furthermore the conductivity, mineralization indicator, increases with the ion content and the nature of the dissolved salts. Leaching of soil and dissolution of atmospheric CO_2 can be an important factor of mineralization (Cissé 2012). Any increase in CO_2 levels in the atmosphere can induce, in a well-defined process, mineralization of soil upon which conduction is depending.

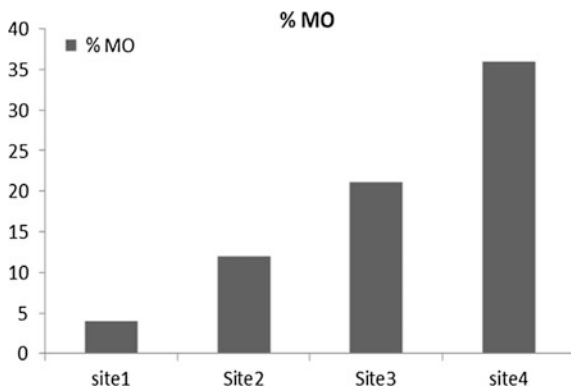
Organic Matter Measurement

The variation of the organic matter content is measured and shown in Fig. 20.3.

We notice from this figure that the organic matter content increases from one site to another. The nearest site to the plant is characterized by the lowest content (0.074%). As long as we move away from the cement, organic matter content substantially increases respectively of 0.22, 0.39–0.68% at the second, third and fourth site. The analysis of variance showed a highly significant variability between sites ($p = 0.00 < 0.001$).

Weather conditions (high temperatures, low humidity) discriminates the accumulation of organic matter improving then the structure and soil aeration that

Fig. 20.3 Variation of organic matter content



promote the development of aerobic bacteria essential for digestion and exchanges in the rhizosphere (Soltner 2003). Particularly in arid regions and at the horizon of 0–20 cm for any type of soil, the threshold of the organic matter content varies from 0.5 to 2.5% (Ben Hassine et al. 2008). We notice that the organic matter contents of the sites near the plant are below the threshold with the exception of the fourth site. The low organic matter content can then be due to climatic conditions close to the plant. In contrast, this content appears to be normal in the farthest site. For this reason, we can say that emissions from the plant are the primarily responsible of the attenuation of the organic matter content.

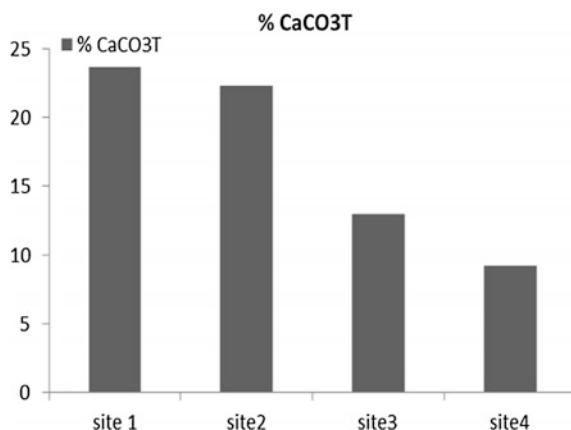
Organic matter typically contributes to the soil chemical fertility. It represents a nutrient reserve (mainly nitrogen, phosphorus and sulphur) (Balesdent 1996). Also, the large organic matter at the surface of soil reduces the impact of raindrops, allowing the water to slowly infiltrate into the ground. The runoff surface and erosion are then reduced (Donahy 1958). We deduce, therefore, that low content (below the threshold) can reduce a significant portion of nutrient reserves of plants. However, the carbon accumulation in the soil can be due to a slowdown in the decomposition of organic matter related to a decrease of pH (Brink and Belay 2006).

Measurement of CaCO₃ Content

The analytical results of total calcium content are shown in Fig. 20.4.

As noticed the total calcium content decreases when we are getting far away from the cement plant and passes from 23.68% (site 1), 12.99% (site 3) to 9.25% (site 4). Analysis of variance shows that these differences are highly significant ($p = 0.00 < 0.001$). The high total calcium content in the first two sites is explained by their close distances towards the cement plant that emits, in great part, a large amount of CaCO₃. This result confirms those of Bacic et al. (1999). Indeed,

Fig. 20.4 Changes of total CaCO₃ content near Gabes cement plant in the spring of 2012 a/b/c denote the groups identified by the SNK test



the carbonated materials can be transported and deposited either in the form of dust or by rain or by precipitation solution mechanism and fall in large quantities at the nearest locations of factories (Moti 1997).

Measurement of Active Limestone Content

The CaCO_3 content of the soils studied is given in Fig. 20.5.

From this figure, we see that there is a gradual decrease in the content of active CaCO_3 with distance from the plant. This decrease is explained by emissions from the cement plant that was deposited in the immediate vicinity of the plant (site 4 shows the lowest CaCO_3). Site 1 shows a content of about 41% of CaCO_3 ; while this content is about 13% (site 2), 7% (site 3) and 2% (site 4). The analysis of variance showed a highly significant variability between sites ($p = 0.00 < 0.01$). A study made in Estonia by Ots et al. (2010) shows that the dust emitted by the cement industry, at a distance of 2.5 km from the sampled area, contains higher concentrations of CaCO_3 than farther areas.

It should be reminded that the active calcium carbonates are calcium carbonate dissolved in the soil. High levels of carbonates in the soil yet raise series of problems due to the induction of nutrients deficiencies referred to the insolubility of P, Fe, Mn, Zn, Cu (Aljumaa 1993).

Measurement of Sulphate Content

To determine the sulphate content of each site, a standard curve is proceeded.

Sulphate concentrations of different sites (Fig. 20.6) are deducted from the equation of the standard curve ($y = 0.2677 + 0.0078x$). From this figure, we see that

Fig. 20.5 Changes in the content of active CaCO_3 near Gabes cement plant in the spring 2012 a/b/c/d denote the groups identified by the SNK test

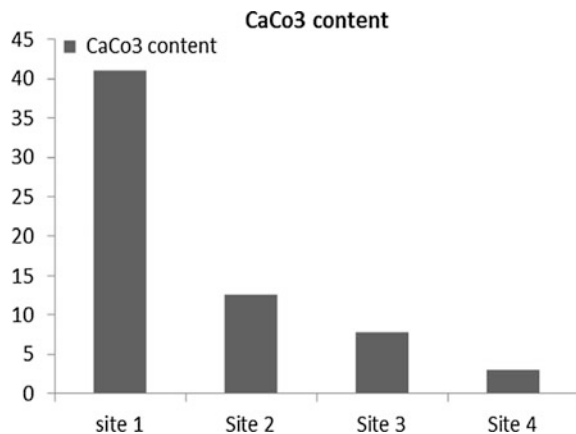
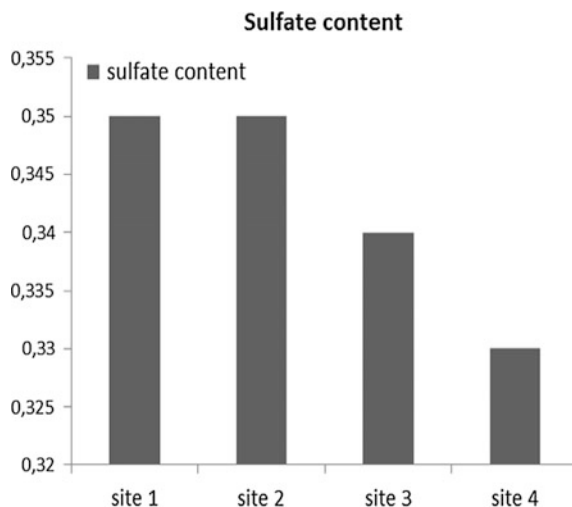


Fig. 20.6 Variation of the sulphate content near Gabes cement plant in the spring of 2012



the sulphate content ranges from 0.33 to 0.35 mEq/L. Two highest levels were registered in the first two sites (0.35 mEq/L). The third and the fourth site show respective contents of 0.34 and 0.33 mEq/L. The ANOVA applied to the measurement results of the sulphate content, provides a non-significant variability between sites ($p = 0.86 > 0.05$).

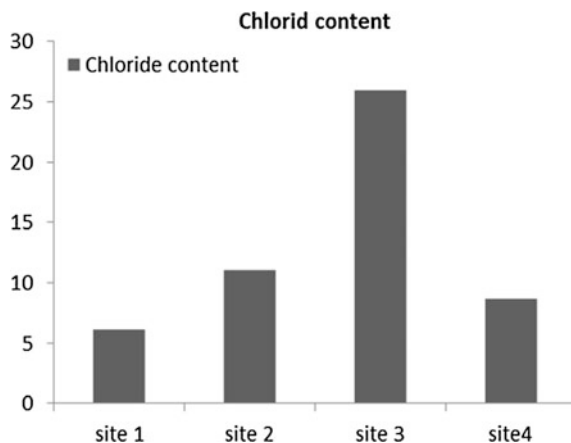
The small decrease in sulphate content from the cement plant, despite the emissions of sulphur dioxide, is probably explained by the inclusion of sulphur in various forms on the biogeochemical cycle. Since emitted in the form of sulphur dioxide, sulphur in the atmosphere falls back to the ground and infiltrate where it takes the form of sulphate (SO_4^{2-}). It is recognized that soil exposed to air pollution, intensively, usually contain high concentrations of sulphates (Wainwright 1984). In turn, Bremner and Banwart (1976) estimate that soils have a large capacity to absorb sulphur gases that are oxidized to sulphates. This absorption is much stronger in wet soils compared to dry soils (Bremner and Banwart 1976; Ghorse and Alexander 1976). Pollution sulphate causes a high content of nutrients and increases the potential of toxic compounds in wet soils (Jeroen et al. 2009).

Measurement of Chloride Content

Chloride content shows a progressive increase of more than 5–25 mEq/L between site 1 and site 3. This content drops in the site 4 and is about 8 mEq/L. statistically these variations are not significant ($p = 0.16 > 0.05$).

Ordinary chloride content in the soil is less than 20 mEq/L. Any increase in content is considered as an index of industrial pollution (Le pimpec et al. 2002). It is generally dependent on the increase of the conductivity. Our results (Fig. 20.7)

Fig. 20.7 Variation of the chloride content near Gabes cement plant in the spring of 2012



show that the levels found of chlorides are less than 20 mEq/L except in the third site (about 26 mEq/L). This can be explained by the location of the site, which lies at the foot of a mountain range. It therefore receives larger amount of runoff and will be enriched in chloride comparing to other sites.

Measurement of Sodium (Na^+) Content

Once the standard curve is plotted, the sodium concentration of the different samples of soil is determined following the equation $y = 0.2857 + 1.0171x$.

From Fig. 20.8 we see that the sodium content increases between sites 1 (22.32), 2 (6.38) and 3 (4.69) to decrease at site 4 (2.65) mEq/L. The analysis of variance gives highly significant results between sites ($p = 0.00 < 0.001$). This gradual increase in sodium levels can be due to soil salinization and alkalisation. Indeed, the increased alkalinity of the soil is referred to an increase of sodium carbonates, bicarbonates and sulphates of sodium (Alperovitch and Dan 1972).

Admitting that particles emitted by the cement plant are formed by an heterogeneity of compounds including those salted (Na^+ , Cl^-). These latter will be transported by wind over long distances before falling into the ground. The size, shape and chemical composition of particles influence strongly their dispersion and residence time in the atmosphere. Very large particles are deposited near sources of emissions. In contrast, the finer particles remain longer in the air and can be transported by the wind over longer distances (Gombert 2005). We can deduce that sodium compounds emitted by the plant are fine particles since there is an increasingly higher content in function of the distance. Geomorphological features of the third site promote its sodium enrichment (this site is at the foot of a hill that

Fig. 20.8 Changes in the sodium content near Gabes cement plant in the spring of 2012 a/b denote the groups identified by the SNK test

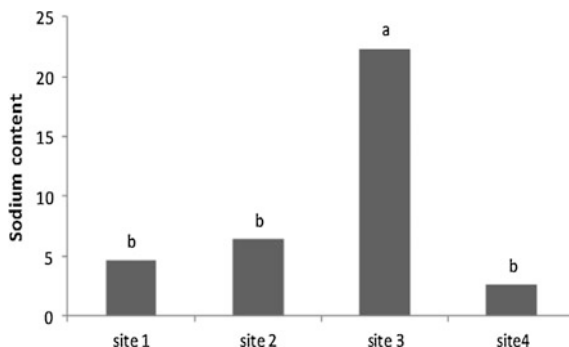
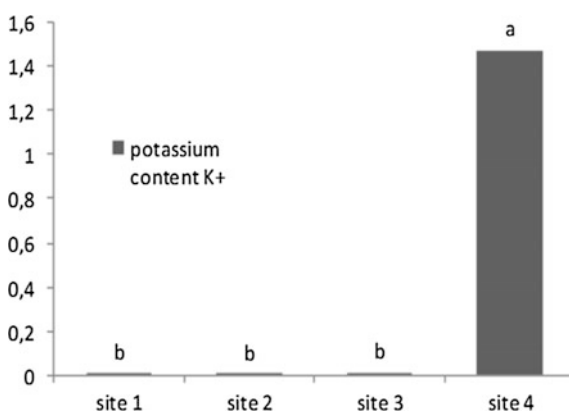


Fig. 20.9 Variation of potassium content near Gabes cement plant in the spring of 2012 a/b denote the groups identified by the SNK test



forms a kind of barrier receiving emissions of the cement plant, the flow and the precipitation drain these pollutants to piedmont of the site).

Measurement of Potassium K^+ Content

From Fig. 20.9 we deduce the potassium concentrations of various soil samples.

Figure 20.9 elucidates that the potassium content is almost zero in the first 3 sites (0.006, 0.004 and 0.013 mEq/L for sites 1, 2 and 3, respectively). It is growing significantly in the fourth site to up 1.4 mEq/L. The variation of the potassium concentration between sites is highly significant ($p = 0.00 < 0.001$). In addition, a gradual increase in the potassium content is marked according distance to the cement plant. This shows that the cement industry plays a crucial role in the variation of the potassium content since there is a high fluctuation between the nearest site (1.5 km) and the most distant (12 km), supposedly the least affected by the effect of air pollutants.

According to Balestrini and Tagliaferri (2001), the percentage of the precipitation behaves as a determinant agent of the leaching regulation of K^+ . This is confirmed by Likens et al. (1994) estimated that the precipitation is the only variable that predicts the potassium concentration in the soil. It should be noted also that the rainfall average recorded in Gabes region, in 2012, exceeded the averages recorded before. The lowest level of nearest sites can be explained by an altered composition and altered minerals brought by rainfall and the contributions of air pollutants emitted from the plant. Indeed, all contributions are alkaline effluents that can dissolve soil organic carbon. At a long term, this can cause potassium accumulation in the soil (Arienzo et al. 2008). Any acid contribution or acid deposition, such as those provided by the plant, may cause a reduction in the potassium content of the soil. In addition, Peuportier (2008) reported that sulfuric dioxide and nitrogen oxides, generated by industries, become sulphates and nitrates (or even sulfuric and nitric acids dusts), which then drop as rainfalls and wash the soil nutrients like potassium. If the soil contains a high concentration of $CaCO_3$, potassium can be easily washed and can cause a state of deficiency (FAO 1997).

Conclusion

Pollutants emitted by the cement plant, brought by air and deposited on the ground have a direct effect on the chemical composition of the soil that is proved by the increasing content of both total $CaCO_3$ and active $CaCO_3$ contents revealing a strongly loaded sites by $CaCO_3$ at close distance also soil is very poor in term of organic matter content at nearly localized sites as noticed with lack of any source of disturbance save the cement plant, that decrease of organic matter content is due to cement plant emissions and consequently it alters soil fertility and plant growth. Similarly a great variation between the buffer site (site 4) and the other sites in sodium and potassium contents especially the latter one corroborates our hypothesis predicting that cement plant emissions have a direct effect on chemical soil components whether increasing or decreasing directly or indirectly thus it can disturb at a long term biogeochemical cycles as well as every beings upon them are depending tending from microorganisms to superior plant species.

Acknowledgements We thank Professor Houcine Khatteli the director of Arid Regions Institute, Medenine Tunisia, for the facilities that he had offered for the realization of this work. Many thanks also go to the CRDA staff of Gabès governorate for their help and the generous field data.

References

- AFNOR X31-071 (1987) « Qualité des sols: méthodes d'analyse ». Edité par l'Afnor, France, 17 pp
- Aljuma K (1993) Le calcaire actif des fluvisols de la plaine alluviale de l'euphrate, vol III, 105 pp
- Alkashman O, Shawabkeh R (2006) Metals distribution in soils around the cement factory in southern Jordan. *Environ Pollut* 140:387–394
- Alperovitch N, Dan J (1972) Sodium affected soil in Jordan Valley. *Geoderma* (Elsevier) (8):37–57
- Arienzo M, Christen EM, Quayle W, Kumar A (2008) A review of the fate of potassium in the soil plant system after land application of waste waters. *J Hazard Mater* 164:415–422
- Bacic T, Lynch AH, Cutler D (1999) Reactions to cement factory dust contamination by *Pinus halepensis* needles. *Environ Exp Bot* 41:155–166
- Baize D (2000) Guide des analyses en pédologie. Edition INRA, Paris, 207 pp
- Balesdent J (1996) Un point sur l'évolution des réserves organiques des sols en France. *Etude et gestion des sols* 3(4):245–260
- Balestrini R, Tagliaferri I (2001) Atmospheric deposition and canopy exchange processes in Alpine forest ecosystems (Northern Italy). *Atmos Environ* (Amsterdam) 35:6421–6433
- Ben Hassine H, Aloui T, Gallali T, Bouzid T, El Amri S, Ben Hassene R (2008) Evaluation quantitative et rôles de la matière organique dans les sols cultivés en zones subhumides et semi arides méditerranéenne en Tunisie. *Agro solution. Ressources* 2(19):5–19
- Blanchard C (2000) Caractérisation de la mobilisation potentielle des polluants inorganiques dans les sols pollués. Ecole Doctorale de Chimie de Lyon, Thèse, 302 pp
- Bocard C (2006) Marées noires et sols pollués par des hydrocarbures. Enjeux environnementaux et traitements des pollutions. Editions Technip, Paris, France, 291 pp
- Bremner JM, Banwart WL (1976) Sorption of sulfur gases by soils. *Soil Biol Biochem* 8(2):79–83
- Brink M, Belay G (2006) Cereales et légumes secs. Edition Prota 2006 Pays bas, 313 pp
- Chaïgnon V (2001) Biodisponibilité du cuivre dans la rhizosphère de différentes plantes cultivées. Cas de sols viticoles contaminés par des fongicides. Thèse: Ecole doctorale, Sciences de l'Environnement : Système Terre, Université d'Aix-Marseille, INRA, 167 pp
- Cissé O (2012) Les décharges d'ordures en Afrique Mbeubess à Dakar au Sénégal. Editions IAGU Karthala, 42 pp
- Donahy R (1958) Nature des sols et croissance végétale. Ed. D'organisation. Paris, 312 pp
- FAO (1997) Manuel pratiques intégrées de gestion et de conservation des sols. Editions de FAO, 79 pp
- FAO (2000) Manuel de pratiques intégrées de gestion et de conservation des sols. Bulletin des terres et des eaux de la FAO. Editions FAO, Nigeria, 208 pp
- Gabrila A, Abi L, Eduardo D, Wannaz, Ana C, Mateo S, Maria L, Pignata (2014) Biomonitoring of airborne particulate matter emitted from a cement plant and a comparison with dispersion modelling results. *Atmos Environ* 82:154–163
- Gavrilovic M, Maginot MJ, Wallach J (1996) Manipulations d'analyse biochimique. Edition doin, France, 459 pp
- Geurts JJM, Sarneel JM, Willers BJC, Roelofs JGM, Verhoeven JTA, Lamers LPM (2009) Interacting effects of sulphate pollution, sulphide toxicity and eutrophication on vegetation development in fens: a mesocosm experiment. *Environ Pollut* (157):2078–2081
- Ghiorse WC, Alexander M (1976) Effect of the microorganisms on the sorption and fate of sulfur dioxide and nitrogen dioxide in soil. *J Environ Qual* 5:220–230
- Gigauri GN, Devdariani TV, Ratman PA, Ramishvili IA, Kvachadze NK, Magalashvili NT, Dzhokhadze GK (1992) Effect of cement dust on the condition of woody plants. *Lesoved* 6:65–73
- Gombert S (2005) Pollution atmosphérique par les métaux : Biosurveillance des retombées. Editions EDP sciences et ADEME éditions, 87 pp

- Haydar A (1986) Industrialisation de gabes et ses conséquences. Etude géographie urbaine et économique. Édité par l'université de Tunis, faculté des lettres et sciences humaines de Tunis. Imprimerie officielle Imprimerie officielle tunisienne, vol XIX, 194 pp
- Iqbal MZ, Shafiq M (1995) Effect of cement dust pollution on the growth of some tree species. *Pak J Sci Ind Res* 38:368–370
- Isikli B, Demir T, Akar T, Berber A, Urer SM, Kalyoncu C, Canbek M (2006) Cadmium exposure from the cement dust emissions. A field study in around residence. *Chemosphere* 63:1546–1552
- Laperche V, Mossmann JR (2004) Protocole d'échantillonnage des sols urbains pollués par du plomb. Editions BRGMP/ RP 52928-FR, 27 pp
- Le pimpec P, Lienard A, Bonnard R, la Font M, Cazin B, Bossard ph. Hubert B, Bray M (2002) Guide pratique de l'agent préleveur charge de la polie de milieux aquatiques. Editions Maurice Merlin. France, 71 pp
- Legros JP (1996) Cartographie des sols - De l'analyse spatiale à la gestion des territoires. Presses polytechniques et Universitaires romandes, Lausanne, 321 pp
- Likens GE, Driscoll CT, Buso DC, Siccama TG, Johnson CE, Ryan DF, Lovett GM, Fahey T, Reiners WA (1994) The biogeochemistry of potassium at Hubbard Brook. *Biogeochemistry* (25):61–125
- McLaughlin MJ, Zarcinas BA, Stevens DP, Cook N (2000) Soil testing for heavy metals. *Commun Soil Sci Plant Anal* 31(11–14):1661–1700
- Moti M (1997) Mémoire (Cartographie par informatique des carbonates de la vallée de l'Artibonite (Haïti)). Faculté des sciences supérieures de l'université Laval, Quebec Canada, 81 pp
- Ots K, Indrikson A, Varnagiryte I, Mandre M, Kiznetsova T, Kloiseiko J, Tlik M, Koresar K, Lukjanova A, Kikamagi K (2010) Changes in the canopies of *Pinus Sylvestris* and *Picea abies* under alkaline dust impacts in the industrial region of Northeast Estonia. *For Ecol Manag Sci Direct* 262:82–87
- Peuportier B (2008) Eco-conception des bâtiments et des quartiers collection sciences de la terre et de l'environnement. Editions MINES Paris tech les presses, 330 pp
- Schuhmacher M, Jose L, Garretta DJ (2004) Pollutants emitted by a cement plant: health risks for the population living in the neighborhood. *Environ Res* 95:198–206
- Soltner D (2003) Les bases de la production végétale. Tome I. Le sol et son amélioration. Collection Sciences et Techniques Agricoles. 23^{ème}. Ed. Paris, 472 pp
- Tarhouni (2008) Indicateurs de biodiversité et dynamique du couvert végétal naturel aux voisinages de trois points d'eau en zone aride tunisienne: Cas de parcours collectifs de Ouara. Université de Tunis Elmanar, 169 pp
- Wainwright M (1984) Sulfur oxidation in soils. *Adv Agron* 37:349–396

Chapter 21

Contribution of Hyperspectral Images (Hyperion) and Spectroscopy for Mapping Soil's Surface and Materials (Case of the Watershed of Oued Beni Zalten, the New Matmata, Tunisia)

Imen Ben Haj Yahia and Aziza Ghram Messedi

Abstract Degradation in arid zone is reflected on the ground by the modification of the soil surface components. Several studies have investigated the mapping of the soil surface and components in drylands. A few studies are the outcome of ground-based observations, while others widely use multispectral remote sensing and calculating indices that are limited to samples of electromagnetic spectrum. This paper proposes an innovative method that is applied to geomorphology and environmental research. It seeks to develop a new methodology for mapping soil surface and components, based on hyperspectral remote sensing with a wide range of electromagnetic spectrum. Our case of study is Beni Zalten watershed, which is situated in the natural region of Matmata (Southeast of Tunisia). The region is characterised by limited natural resources, complex physical conditions and irrational human use. This led to the fragility of the environment and the proliferation of water-erosion problems. Therefore, mapping the soil surface and components of Beni Zalten watershed is highly useful to evaluate soil erosion sensitivity and eventual study on erodibility. The methodological approach of our research is essentially based on a Hyperion satellite image dating from December 2009, spectrophotometry measurements and spectroscopy data. This approach depends on a series of pre-treatments (radiometric and atmospheric corrections and reflectance passage), adding to a series of treatments (spectral similarity method: the spectral angle mapper SAM and a method to extract endmembers from the image: Spectral HourglassWizard). This paper is organised around three main parts: First, we will present the physical and human context. Then, we will describe the data and

I.B.H. Yahia (✉) · A.G. Messedi
Laboratoire de Cartographie Géomorphologique des Milieux, des Environnements
et des Dynamiques (CGMED), FSHST, Université de Tunis,
Boulevard du 9 Avril 1938, Tunis, Tunisia
e-mail: imene.bhy@gmail.com

methodology. Finally, we will present our results and discuss the hyperspectral remote sensing and spectroscopy contribution to the cartography of soil surface and components in an arid zone.

Keywords Hyper spectral remote sensing · Hyperion · Spectroscopy · Soil surface and components · Arid zone

List of Abbreviations

CNCT	Center of cartography and Remote Sensing
VIS	Visible
NIR	Near infrared
MENA	Middle East North Africa
nm	Nanometer
Quac	Quick atmospheric correction
MNF	Minimum noise fraction
PPI	Pixel purity index
SAM	Spectral angle mapper
ICA	Independent component analysis

Introduction

This paper presents the first attempt to map the soil surface using an image with very high spectral resolution of Hyperion sensor. This innovative method is applied to geomorphology and environmental research. We will discuss a new advanced technology, which is hyperspectral remote sensing.

The choice of the Hyperion image is principally found on the fineness of the spectral resolution of the sensor that is well suited to the context and to our study area. Indeed, drylands are the areas of low cloud cover and rare vegetation and soils. That is why optical measurements are particularly useful for the identification of materials and surface condition. Motivated by this technological advancement, our mainly purpose of this study is at the same time methodological and thematic. Thus, the study aimed to focus on methods and techniques suitable for the atmospheric correction and reflectance passage in hyperspectral remote sensing.

In addition, we try to value an existing spectroradiometer and spectrophotometer database. The development of an appropriate method facilitates the detection, the analysis, and spatialization of the main indicator of soil degradation. The study's objective, in this case, is to produce thematic maps of the different types of soil surface and components, based on the radiometric data. Beni Zalten watershed scale (Southeast of Tunisia) will be our study application, where such cartography can be used as a support for land degradation studies.

Presentation of the Study Area: Human and Physical Context

The study area is located in the South East of Tunisia at the New Matmata delegation (Gabes Governorate). The sub-watershed of Beni Zalten belongs to a Mediterranean climate of the arid zone (Fig. 21.1). In fact, this region of Tunisia is generally very little watered, but what characterises the climate is its great irregularity, heavy rains may succeed to long periods of drought (Bonvallot 1992).

The study area covers one hundred square kilometres (104 km²) and includes the total watershed of Beni Zalten, which is part of the natural region of Matmata. The region is distinguished by its high relief, and its river system fashioning deep small valleys.

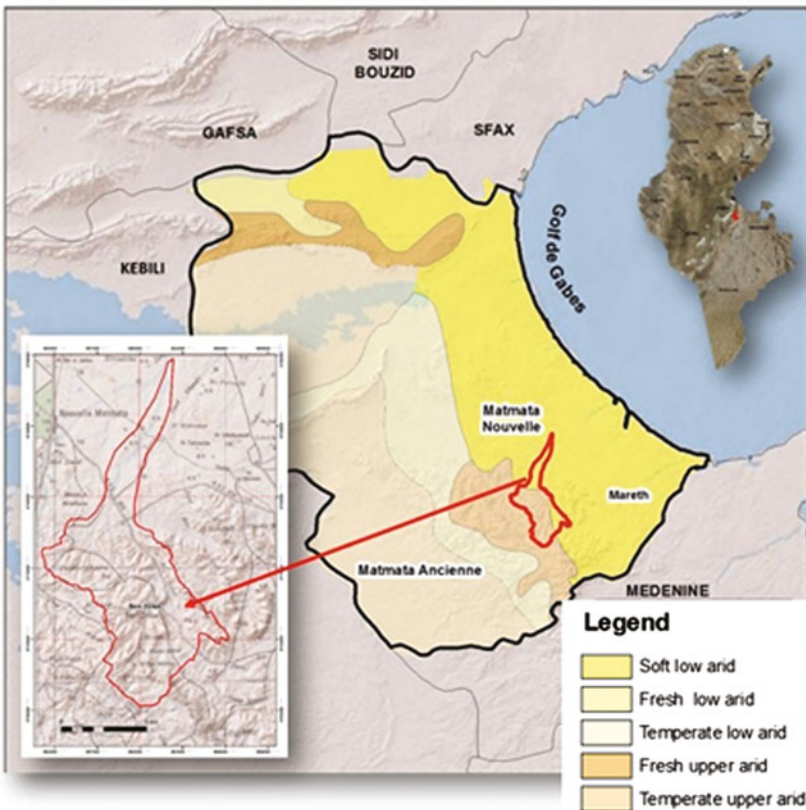


Fig. 21.1 Location of the study area

The average altitude at the sub-watershed of Beni Zalten is moderately high (around 298 m). The area presents a mosaic of morphological landscapes with steep hill slopes (chain of Matmata), short piedmonts (a system of cones and glazes), and more or less narrow and long plains accumulation. In these landscapes, morphological dynamics is characterised by active erosion on piedmonts and long banks of oueds; it interests rarely low sandy plains (Belaid 1967; Bonvallot and Ben Amar 1979) in Mtimet (1983).

The region of Matmata is a natural and human environment, which is rather special in the south of Tunisia. Djebalias, which have developed for millennia (djebel dwellers are originally Berber), characterise this region, and they are deemed by a housing and agricultural activities adapted to this environment: these are troglodyte houses (Photo 21.1). The culture system is based on tree crops in the ravines and talwegs (Photo 21.2) (Mtimet 1983) and behind Jessour.

Recently, there has been a tendency to leave troglodyte houses and farming behind jessour, which will cause the loss of traditional know-how of the arrangement construction, as well as the increase of soil erosion. We can conclude that Beni Zalten watershed is a complicated system. In fact, this hydraulic unit can be considered as a typical case study of the arid zone, since it includes severe physical and human conditions, and limited natural resources. Such conditions led to the fragility of the environment by the proliferation of water-erosion problems. Therefore, mapping soil surface and components in Beni Zalten watershed can be extremely beneficial to estimate the soil degradation indicators.



Photo 21.1 Troglodyte houses



Photo 21.2 Culture system using tabias

Methodology

Data Collection: Image and Measurements

Data collection is a fundamental and crucial phase since certain data are necessary for the radiometric image correction process, several data are used for identification and extraction of image spectre that can be a support for mapping soil's and material surface conditions.

Measurements Performed with the ASD PSII Spectroradiometer

The measurements performed with the spectroradiometer was collected in the period between 19 and 20 September 2006, and 24 and 29 December 2007.¹ The first one measured different types of surface conditions, while the second was used to measure pseudo-invariants. These would be used to complete radiometric calibration of images reflectance by the empirical model. This spectroradiometer measures the luminance of a target in the spectral range VIS-NIR (350–1052 nm).

Measures taken on ground in the region of Beni Zalten by ASD PSII spectroradiometer used to create a radiometric database (Table 21.1).

Measurements Performed with the Spectrophotometer

In the laboratory, samples absorptances harvested from the soil's surface are measured using a spectrophotometer to identify the reflectance of the pure soil

¹Collect by the CNCT.

Table 21.1 Radiometric database. (*Source* project MENA) (Middle East North Africa)

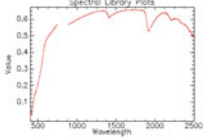
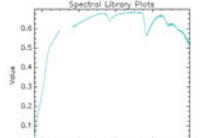
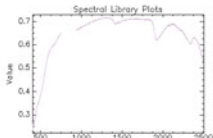
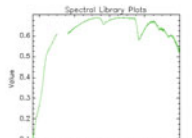
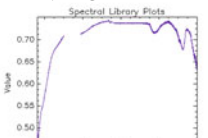
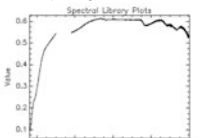
Reference	X	Y	Soil's surface
EBZ1	603,312	3,709,195	Patina
EBZ2	603,312	3,709,195	Nodules ^a
EBZ3	603,312	3,709,195	Debrislitters
EBZ4	603,312	3,709,195	Raw mineral
EBZ5	603,256	3,709,203	Loamy soil with coarse elements
EBZ6	603,100	3,709,450	Limestonecrust
EBZ7	602,666	3,710,418	Loamysoilplowed
EBZ8	602,666	3,710,418	Slakingcrust
EBZ9	597,458	3,723,487	Deep loamy soil with hardpan

^aSmall mineral or rock mass, which is in a rock of different composition

sample nevertheless radiometric value of other components of area such as vegetation, stones, etc. (Table 21.2).

A large number of measurements were provided to us by the CNCT. It was first necessary to calculate their reflectance from the values of absorptance. However, some values were negative. Therefore, we kept only the measures that have positive values.

Table 21.2 Spectral library plots of the ground Sample (*Source* MENA project)

Sample	Spectral Library Plots	Sample	Spectral Library Plots
	<p>MENA 3</p> 		<p>MENA 17</p> 
	<p>MENA 10</p> 		<p>MENA 18</p> 
	<p>MENA 13</p> 		<p>MENA 19</p> 

Hyperion Image

In this study, a hyperspectral image of Hyperion sensor, acquired in 12 December 2009 was provided by the CNCT. The image covers a large part of the total area of the sub-watershed of Beni Zalten. It is spread over the geomorphological landscape (Fig. 21.2).

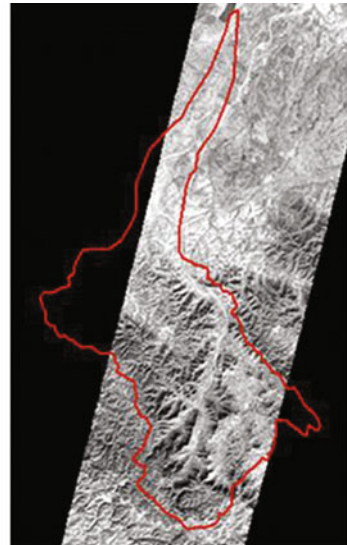
The fineness of the spectral resolution of Hyperion sensor is adapted to the context of our study because of its capacity to identify materials and provide high spectral information. This will replace other more costly and sometimes inaccessible type of data.

The hyperion sensor (hyperspectral imager) is embarked on the Earth Observing1 (EO1) satellite. It was launched since 21 November 2000 as the first hyperspectral instrument. An Hyperion image contains 242 spectral bands ranging from 356 to 2577 nm. The spatial resolution of Hyperion sensor is 30 m. The image processing is performed mainly using the ENVI[®] software.

The Soil's and Materials Surface Mapping Approach

In this work, we looked to develop a method that evaluates and maps the surface soil and components' conditions. We are focusing especially on the contribution for the hyperspectral remote sensing measure (Fig. 21.3). For this article, the global methodological approach takes into consideration the different data pre-treatments and treatments.

Fig. 21.2 The part of the sub-watershed covered by the Hyperion image



 **boundarie of the watershed**

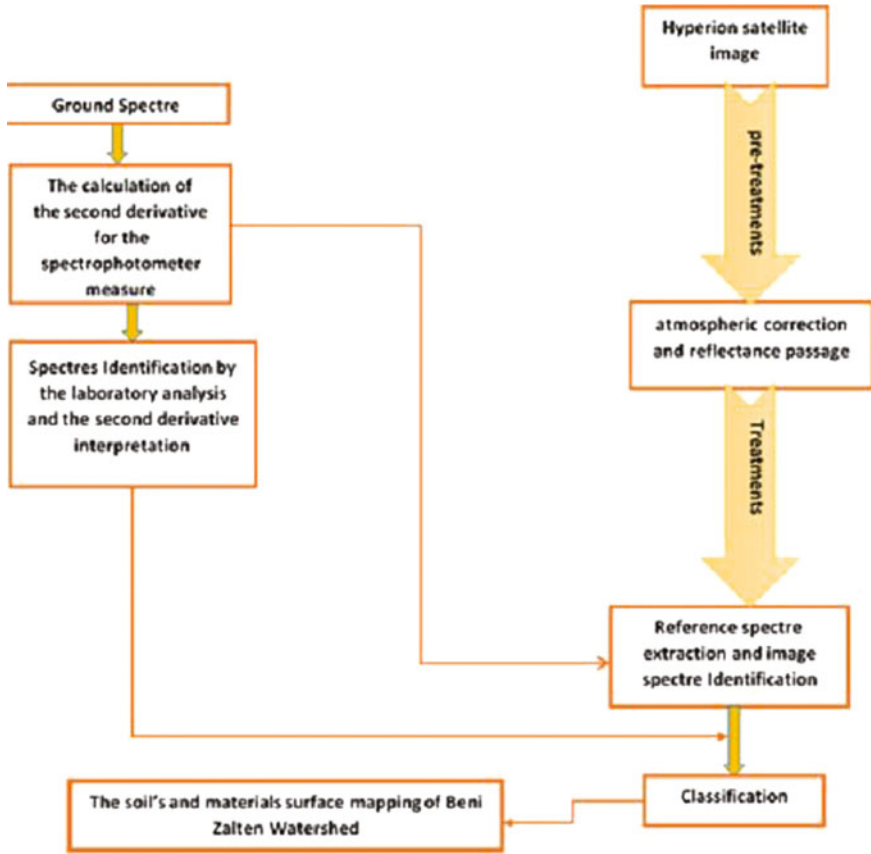


Fig. 21.3 Methodological approach

In fact, we first proceeded with pre-treatments to transform the image into reflectance. Then, in a second step, we extracted and identified the references spectrums using treatments assembly (The calculation of the second derivative). We carried out, in the last step, a number of treatments in order to achieve a classification. This last part is considered as the support of our soil surface and components mapping.

Pre-treatments of the Hyperion Image

Due to various factors such as the effects of interaction with the atmosphere and the geometric effects, the flow of radiation collected by the sensors cannot operate directly. A series of corrections should be made to characterise the target by eliminating noise and minimising errors. The acquisition company may perform some of these corrections. Then, according to its objectives, the user may

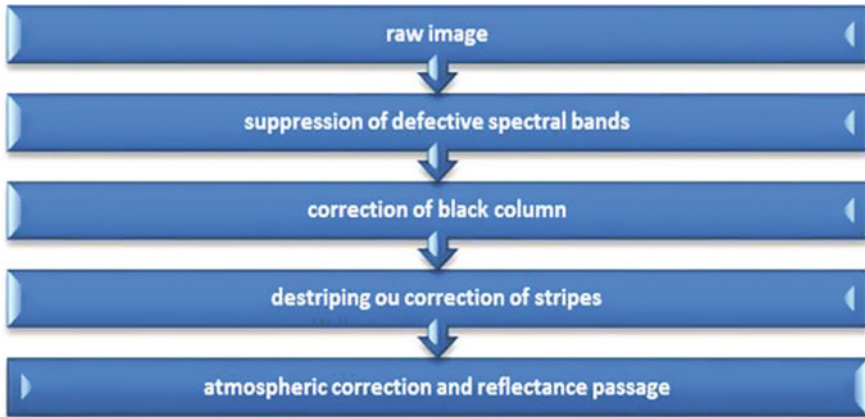


Fig. 21.4 Organizational chart of the image corrections

supplement other corrections. In our case, atmospheric correction and reflectance passage was preceded by a suppression of defective spectral bands, correction of black columns, and correction of stripes (Fig. 21.4).

We used and compared two methods of atmospheric correction and reflectance passage. These are the empirical line based on invariants, and correction from the image data Quick Atmospheric Correction QUAC. The comparison of methods is based on a reflectance Aster image. Our purpose is to search correlation between the corrected images (by QUAC and by empirical line), and the normalized image (ASTER) by the calculation of regression line. After this comparison, we opted for QUAC method, which presents a high correlation degree.

Spectral Data Processing

A sample is a mixture of several materials. To determine the composition of each sample, we have to study its reflectance spectrum. We opted for two methods, which are complementary; the first is based on a delicate interpretation of second derivative spectra. Indeed, the calculation of second derivatives is done in order to exaggerate the absorption rays (Fig. 21.5). We have to determine the characteristic mineral of each absorption ray. We have also deduced that the samples represent a mixture of minerals.

The second method is to use the analyst to determine the spectral composition of each spectrum by comparing it to a spectral library of our choice. This method can be considered as objective since the process is completely automated, but the flood of information it provides can be misleading. The best is to consider the results of the two methods for interpretation.

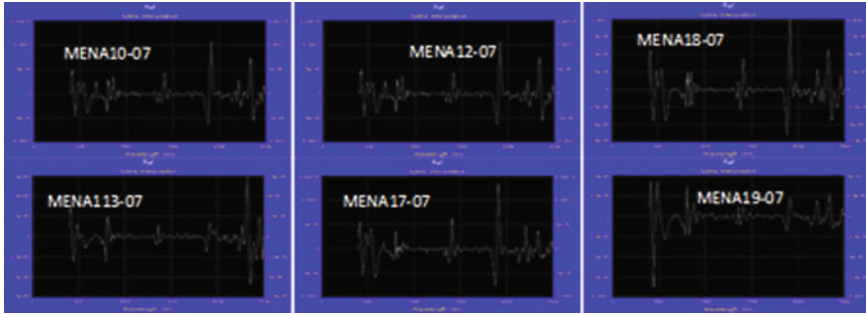


Fig. 21.5 Second derivative of spectral reflectance

The Method of Extracting Endmembers “Spectral HourglassWizard”

To extract endmembers from the image using the method Spectral Hourglass Wizard, we have to go through the following steps: minimum noise fraction (MNF), pixel purity index (PPI), and n-Dimensional visualisation and extraction of endmembers (Fig. 21.6).

The extraction of the prototype signature is based on the calculation of purity index. The latter requires the extraction of MNF components. In our application, we considered the first 30 components as significant. This deduction is founded on the curve of proper value (Fig. 21.7). Spectral HourglassWizard method allowed us to extract 30 sample spectral curves for typical soils prototype (Fig. 21.8).

The prototype spectrum is compared to the spectrum library of Envi® software. The result demonstrates that almost the totality of spectrum corresponds to a mixture of minerals already mentioned in the ground sample.

Fig. 21.6 Diagram of the processing

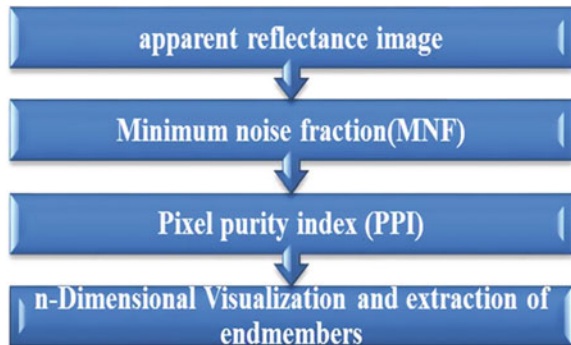


Fig. 21.7 Curve of proper value

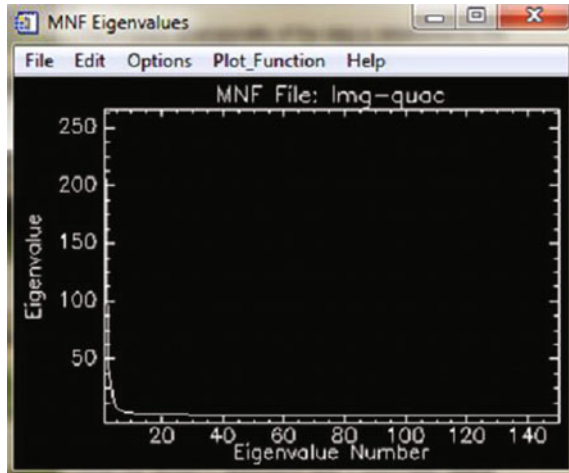
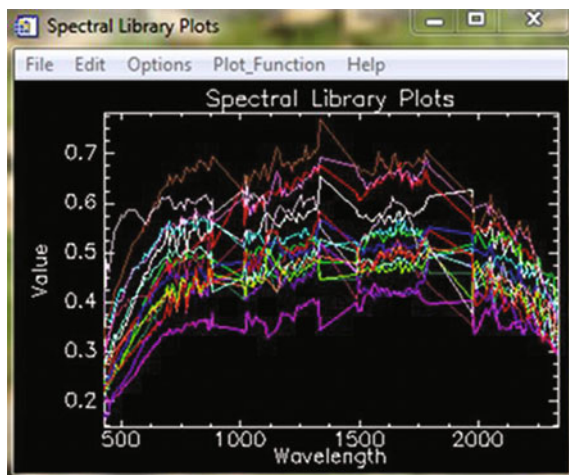


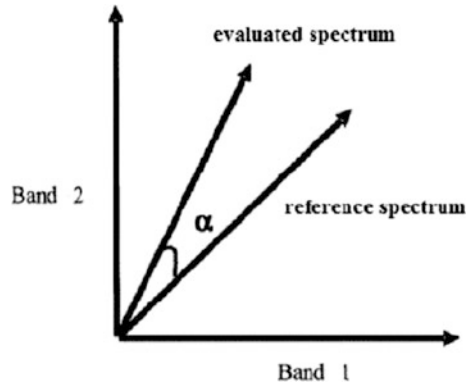
Fig. 21.8 Prototypes signatures of pure spectrum



The Method of the Classification Spectral Angle Mapper (SAM)

It was based on the classification Spectral Angle Mapper (SAM) that has been widely used as a measure of spectral similarity. It calculates the spectral similarity between the reference spectrum (spectrum of the spectral library or field) and the test spectrum (image spectrum) (Fig. 21.9). This method assumes that the data has been reduced to the apparent reflectance, and used only the “direction” of the spectra, not their “length”.

Fig. 21.9 The representation of the angular deviation between the image spectrum of the reference spectrum



Results and Discussion

Map of the Soil Surface in the Sub-Watershed of Beni Zalten

Following our classification, a map of the soil surface was drawn (Fig. 21.10). According to the comparison of the results of this map and topographic data, surface states dominated muddy ploughed are located mainly in the lowlands and the foothills. This coincides largely with the cultures behind jessour in order to benefit from runoff. Contrariwise, the surface soils with dominance of silt with coarse elements extend especially in hilly areas where access is difficult. The slaking crusts silty limestone with nodules is mainly present in the lowlands and on the slopes and terraces of wadis.

Map Abundance of Materials in the Watershed of Beni Zalten

According to SAM classification, which we use to develop the map of abundance of materials in the watershed of Beni Zalten (Fig. 21.11), we note that the present minerals are Alunite, the Jarosite, the goethite, dolomite, calcite, clay, pyrite, hematite, zoisite, quartz, illite. It was also reported the abundance of unclassified pixels that can correspond to other mixtures of materials are not shown by the samples taken.

It is important here to analyse the spatial repartition of the predominant elements, which seems related to the geographic distribution of soils. Thus, minerals and their associations are often due to the characteristics of a specified region. In this study, we used laboratory spectral analysis of the soil's samples collected in the field.² There are seven samples on which spectral and granulometric analysis were

²Collect by the CNCT.

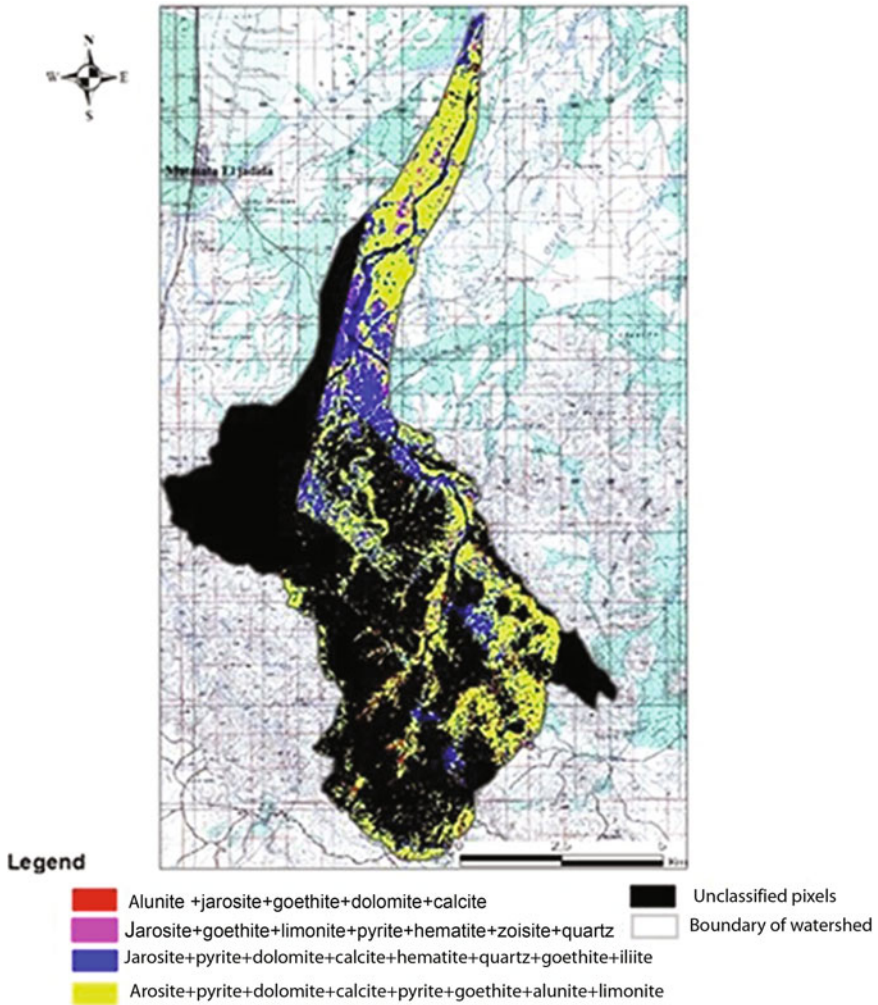
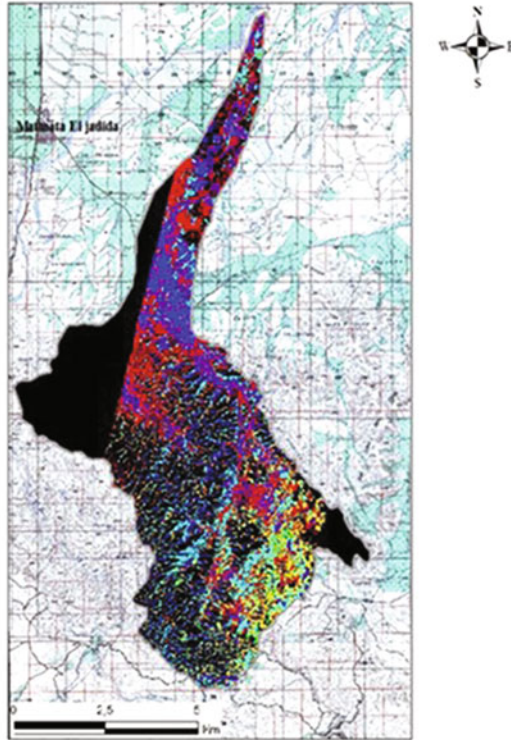


Fig. 21.10 Soil’s surfaces in the watershed of Beni Zalten. (Source Hyperion image and field spectra, Background topographic maps of New Matmata and Zmertène)

effectuated. By performing a simple correlation between the laboratory analysis and our material abundance map, we were able to characterise each mineral association (Table 21.3). We can note that the presence of *jarosite*, which exists in all mineral association, has been recognised as a likely indicator of water at the surface (Brand et al. 2015)



Legende

- Slaking Crust
 - Debris litters
 - Crusting surface with limestone nodules
 - Loamy Soil with coarse elements
- Loamy soil plowed
 - Unclassified pixel
 - Boundary of the watershed

Fig. 21.11 Material abundance map in the sub-watershed of Beni Zalten. (Source Hyperion image and laboratory spectra, Background topographic maps of New Matmata and Zmertène)

Table 21.3 Correlation between mineral association and geographic area

Mineral association	Geographic area
Alunite, Jarosite, goethite, dolomite, calcite	Bad land area and the olive trees in the shallows
Jarosite, pyrite, dolomite, calcite, Hématite, quartz, goethite, illite	Confluence of Oued El gharbaoui and Oued Ben Zao
Jarosite, goethite, limonite, pyrite, hématite, zoisite, quartz	Heterogeneous agricultural area: olive, fodder and cereals (very limited in space)
Jarosite, dolomite, calcite, pyrite, goethite, limon, alunite	Deep loamy soils: extensive cereal: the downstream part of the catchment area and in the valleys Intermountain in the upstream area

Conclusion

We can affirm that hyperspectral remote sensing has a big potential for identifying, qualifying and mapping, soil surface and components. Such potential was provided by the use of the Hyperion image (242 bands from visible to mid-infrared) and field spectrum.

Methodologically speaking, the characterization and mapping of surface conditions allowed giving us an idea about the prevailing soil surface in the sub-watershed of Beni Zalten and the spatial distribution of each represented entity. The use of a series of pre-treatments and treatments was helped us to extract and analyse the reflectance information of the hyperion image.

However, some weaknesses can be identified in our approach. In fact, the adoption of the pixel purity index hypotheses to extract the prototype signature can be unrealistic. Such hypotheses is based on the existence of large area, which characterised with mono-surface state. Nevertheless, the surface covered by our image is 30×30 m and such surface is composed with mixed element. Indeed, we can find other hypotheses like the method of Independent Component Analysis (ICA) of Ben-Tal and Zibulevsky (1997).

While there is confusion at some steps, the results agree mostly with field observations. However, we might have a better result if we had benefited of measures, which cover a greater range of the electromagnetic spectrum.

Although there are difficulties with the methods adopted or at the data used, the identification and mapping of soils surface and materials by hyperspectral remote sensing is considered very useful. Indeed, they can be used, among others, for the study of erodibility, modelling of soil loss, learned about the susceptibility to degradation of soil, and providing decision elements for future development in the sub-watershed of Beni Zalten.

Acknowledgements Our thanks to the National Centre for Cartography and Remote Sensing for providing us spectroradiometric data and the results of laboratory analysis.

References

- Belaid R (1967) Carte de l'érosion de la Tunisie. Direction H.E.R., Service Pédologique, Tunis
- Ben-Tal A, Zibulevsky M (1997) Penalty/Barrier multiplier methods for convex programming problems. *SIAM J* 347–366
- Bonvallot J (1992) Plaidoyer pour les Jessour. In: Le Floc'h E et al. (eds) *L'aridité, une contrainte au développement*, ORSTOM Editions. Paris, France, pp 507–518
- Bonvallot J, Ben Amar M (1979) Comportement des ouvrages de petite hydraulique dans la région de Médenine (Tunisie du Sud) au cours des pluies exceptionnelles de mars 1979. Tunis: DRES; ORSTOM (161), p 33
- Brand HEA, Scarlett NVY, Grey IE (2015) Formation of Jarosite minerals in the presence of seed material. In: 46th Lunar and planetary science conference, p 2
- Mtimet A (1983) Contribution à l'étude pédologique des limons des Matmata (sud tunisien). Thèse de doctorat. Paris VI, p 183. <http://eo1.usgs.gov/sensors/hyperion>

Chapter 22

Use of Remote Sensing and GIS for Land Degradation Assessment of Qarun Lake Coastal Area, El-Fayoum, Egypt

M.M. Kotb, R.R. Ali and M.A. El Semary

Abstract El-Fayoum Oasis is a depression or basin in the western desert that is adjacent to the Nile, Egypt. It locates about 130 km southwest of Cairo. Qarun Lake is the only natural contemporary lake in Middle Egypt. The lake is saline with an elevation about 44 m below sea level. It receives drainage water from El-Fayoum Depression but has no surface outflow. Wadi El-Rayan Lakes have been receiving drainage water since April 1973. El-Fayoum is now an intensively agricultural region supported by abundant freshwater from the Nile River via the Bahr Yusef Canal. The main objective of this study is to use Landsat multitemporal images to detect and monitor the changes of Qarun Lake coastal area. To fulfill this objective, Landsat data (path 177/row 40) are as follows: Landsat MSS 1973, Landsat TM 1988, Landsat ETM + 2003 and Landsat-8 2015, and topographic maps (1992) scale 1:50,000 were used. Geometric correction, Image enhancement, and visual interpretation were carried out on the images and maps. Digital elevation model (DEM) and the vector contour lines of the study area were used. ArcGIS 9.2 software had been applied for mapping environmental changes around Qarun Lake in the investigated area. ENVI 4.2 software was also used to produce the physiographic map of the study area. The obtained results from the digitized topographic map (1942) showed that the surface area of Qarun Lake was about 21 km². From that time, the surface area of the Lake was more or less stable and it was in a balance with land use in El-Fayoum Depression base on the interpretation of the remotely sensed data. In 1973 the surface area of Qarun Lake reached the maximum (240 km²) due to receiving the excessive drainage water from El-Fayoum Depression. The surface area of Qarun Lake decreased to about 230 km² by 1988. Since that time until 2013 the surface area of the lake was almost stable.

M.M. Kotb (✉)

The head of the Soils and Water Department, Faculty of Agriculture,
Beni Suef University, Beni Suef, Egypt
e-mail: kotbmostafa2003@yahoo.com

R.R. Ali · M.A. El Semary

Biological and Agricultural Division, Soils and Water Use Department,
National Research Centre, Dokki, Cairo, Egypt

Keywords Qarun Lake · El-Fayoum Depression · Land degradation assessment · Remote sensing · GIS · Egypt

Introduction

El-Fayoum Oasis locates in the Western Desert of Egypt, about 130 km southwest of Cairo between latitudes $29^{\circ} 02'$ and $29^{\circ} 35'$ N and longitudes $30^{\circ} 23'$ and $31^{\circ} 05'$ E (Fig. 22.1). Emanuele et al. (2010) stated that the Oasis occupies a depressed area, surrounded by hills in the South and by a 300 m escarpment in the North: the elevation ranges from 40–45 m below the sea level.

The total rainfall in El-Fayoum Depression does not exceed 7.2 mm/year. The mean minimum and maximum temperatures are about 14.5°C and 31.0°C , respectively. The annual mean temperature is 22°C . The evaporation rates range from 3.06 to 10.26 mm/day, with an annual mean of about 6.75 mm/day, (CLAC 2004). According to the aridity index classes (Hulme and Marche 1990), the climatic condition of El-Fayoum Depression was classified as arid climate.

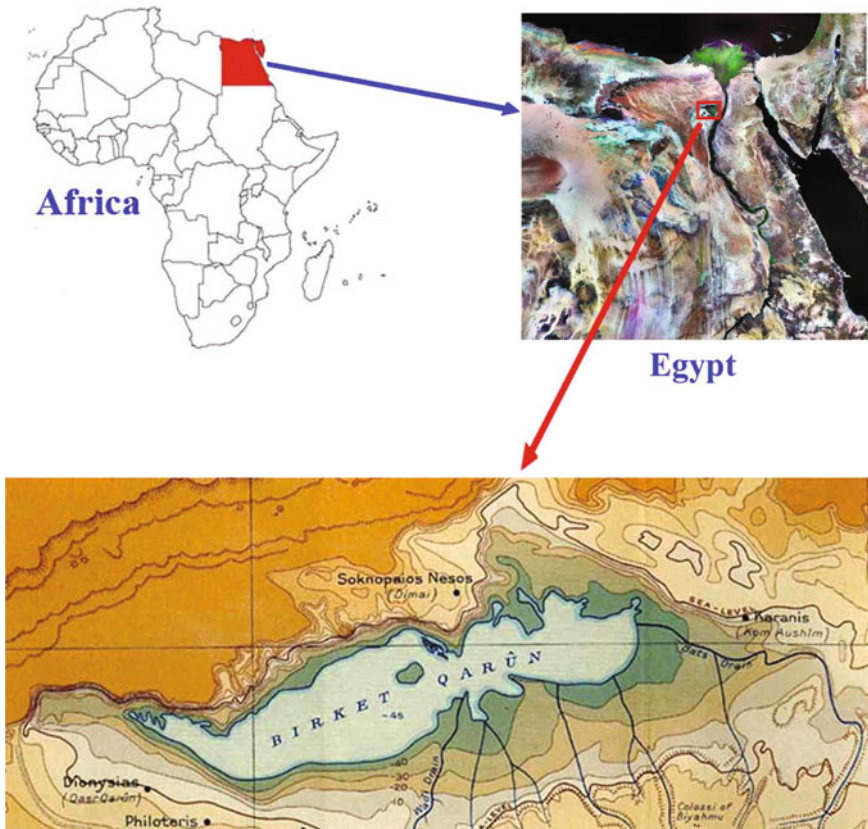


Fig. 22.1 Location of the study area

The relative humidity values vary between 42.6 and 67.4%, the lowest value (42.6%) is recorded in May, while the highest one (67.4%) is recorded in December.

The annual mean of wind speed is 4.46 knots. The Khamaseen wind blows over the area during the period of February–June interval, from the western direction across the Western desert. It is usually warm strong and loaded with sand particles and dust.

The soil temperature regime is Thermic Erian (1982) mentioned that the area is prevailed mainly by Torric moisture regime. He added that the Aquic or Peraquic moisture regimes can be expected in the margins of lakes, river banks, and soils of shallow water table. Moreover, Abdel All (1990) classified the soil moisture regime of El-Fayoum Depression as Torric and Ustic in addition to Aquic in the margin areas subjected to Qarun Lake and the soils of high water table.

Geological Aspect

El-Fayoum Depression has an erosional origin, closely controlled by tectonics and it dates back to no more than the Upper Oligocene or later, Issawi et al. (2001). Said (1962); Tamer (1968); Khalil (1970); Khater (1973); Hanna and Labib (1977); and Shendi (1984) point out that the Fayoum formations recognized into three groups of sediments of distinctly different origins: Nile River sediments, desertic sediments, and lacustrine deposits.

Soil Aspect

Landforms

Abd El-All (1984) and Shendi (1984) identified the main landforms in El-Fayoum Depression as: (a) Nile alluvial (lake terraces, basins, gullies, channels and low parts). (b) Interference zone (lake terraces, basins, gullies, channel high and low parts). (c) Desertic formations (high parts, low parts, plateau, escarpments, slopes, ridges, dry valley, summits, isolated hillocks, rocky table land, sandy areas peneplain, and marches). While, Abo El-Enean (1985) stated that the main landforms in El-Fayoum are; Fans, recent lake terraces, older lake terraces, depression ridges, Fayoum plain, Graham basin old wadies.

Landscape

Ali (2005) and Ali and Abdel Kawy (2013) showed that the soils of El-Fayoum Depression were belonged three landscape units; i.e., alluvial plain (12.22%), fluvio-lacustrine plain (34.20%) and lacustrine plain (53.58%). He stated that the main land forms were terraces, while the overflow and decantation basins represent the rest of the area.

Soil Mineralogy

Various authors; Basta, et al. (1969), Khalil (1970), Labib (1970), Abdel Aal et al. (1976), Hanna and Labib (1977), Kassem and Elwan (1980), Wahab et al. (1988) and Shendi (1990) studied soil mineralogy of El-Fayoum Depression, their observations can be concluded as; the light minerals of sand fraction are mainly composed of quartz in the forms of subangular to subrounded grains, associated with minor amounts of feldspars (microcline, orthoclase and Plagioclase) and micas. The heavy minerals are mainly consisted of iron oxides, amphiboles, pyroxenes and epidotes. The clay fraction of the Nile deposits of El-Fayoum Depression are mainly composed of kaolinite, montmorillonite and illite in the coarse clay (1–2 μ), whereas the fine clay (<0.2 μ), is dominated by montmorillonite group. Smectites (dioctahedral iron rich types) are the dominant clay minerals in the different clay fraction of El-Fayoum sediments except for the coarse clay of the aqueous desertic deposits where kaolinite takes place. Illite, attapulgite, chlorite, quartz, interstratified of illite–montmorillonite, illite–chlorite and montmorillonite–chlorite were also found in both clay fraction.

Soil Classification

Wahab et al. (1988), Harun (2004) and Abd-Elmabod (2014) classified the soils of El-Fayoum Depression according to the soil taxonomy system of the USDA into three orders; Vertisols, Entisols and Aridisols. These soils belong the following subgroups: Vertic Torrifluvents, Typic Haplocalcids, Typic Torrifluvents, Typic Haplogypsis, Typic Haplosalids, Typic Torripsamments.

Land Capability and Productivity

According to ASRT (1991) The El-Fayoum Depression is classified into five grades according to their production capacity. The first and second grades do not exceed 20.2% of the total cultivated area, whereas about 70.2% are accommodating the third and fourth classes.

Hydrology and Drainage

An agricultural drainage system network was established in El-Fayoum Depression as an effort to decrease the accumulation of excess drainage water in Qarun Lake and to protect the nearby agricultural land from inundation (Anon 2003). Qarun Lake receives only the discharge water from the irrigation network; even if some authors such as Hussein et al. (2008) mentioned that it may discharge water speculate a small groundwater flux. Qarun Lake is considered one of the most important ancient natural lakes. It is the remaining part of the ancient Moeris Lake. It comprises 1155 km². It is 5 m depth in east, 13 m in west. You can practice water sports, fishing, and bird watching. The best period for fishing is from July to September (ICFG 2016).

Problems of Pollution

Hussein et al. (2008) concluded that Qarun Lake was suffering from various pollution types due to the industrial and agricultural waste disposal as well as domestic waste, which affect the fish and animal life in the lake with the great dangerous impact on the human health.

Under the same condition in another oasis in Egypt (Siwa Oasis) Kotb et al. (2015) pointed out that some environmental hazardous were occurred due to the improper management of groundwater resources. Additionally, the same authors found an increase in the surface area of the water bodies against arable lands.

Due to receiving more water for irrigation for the new reclaimed areas, El-Fayoum Depression has unique geographical satiation, due to this satiation of the depression, the mismanagement of irrigation water and insufficient drainage system, and environmental problems which lead to an increase in the surface area of Qarun Lake were observed. These led to some environmental problems such as increase of soil salinity and waterlogged areas due to the increase of the groundwater table of the areas adjacent to the Qarun Lake.

The present study aims to monitoring and assessment of changing on the surface area of Qarun Lake and its effect on the adjacent areas, using Landsat multitemporal images.

Materials and Methods

Topographic maps of 1942 at scale 1:100,000 and 1992 at scale 1:50,000 of El-Fayoum were used as a basic data (Fig. 22.2). Four Landsat images (path 177/row 40) acquired in 1973, 1988, 2003, and 2015 (Landsat MSS 1973, Landsat TM 1988, Landsat ETM + 2003, and Landsat-8 2015) were used to detect and monitor water bodies over the Qarun Lake (Fig. 22.3). Table (22.1) illustrates the specifications of the used satellite data.

Geometric Correction

In this study, geometric correction was carried out using a total of 48 ground control points from topographic maps to geocode the image of 1992. Then, this image was used to register all the other images. The RMSE between different images was less than 0.4 pixel which is acceptable. ENVI 4.7 software was used for this function.

Image Enhancement and Visual Interpretation

The goal of image enhancement is to improve the visual interpretability of an image by increasing the apparent distinction between the features. The process of visually interpreting digitally enhanced imagery attempts to optimize the complementary abilities of the human mind and the computer (Lillesand and Kiefer 1994). Contrast stretching was applied on all images and the False Color Composites (FCC) were



Fig. 22.2 A topographic map (1942) of El-Fayoum Depression at scale 1:100,000

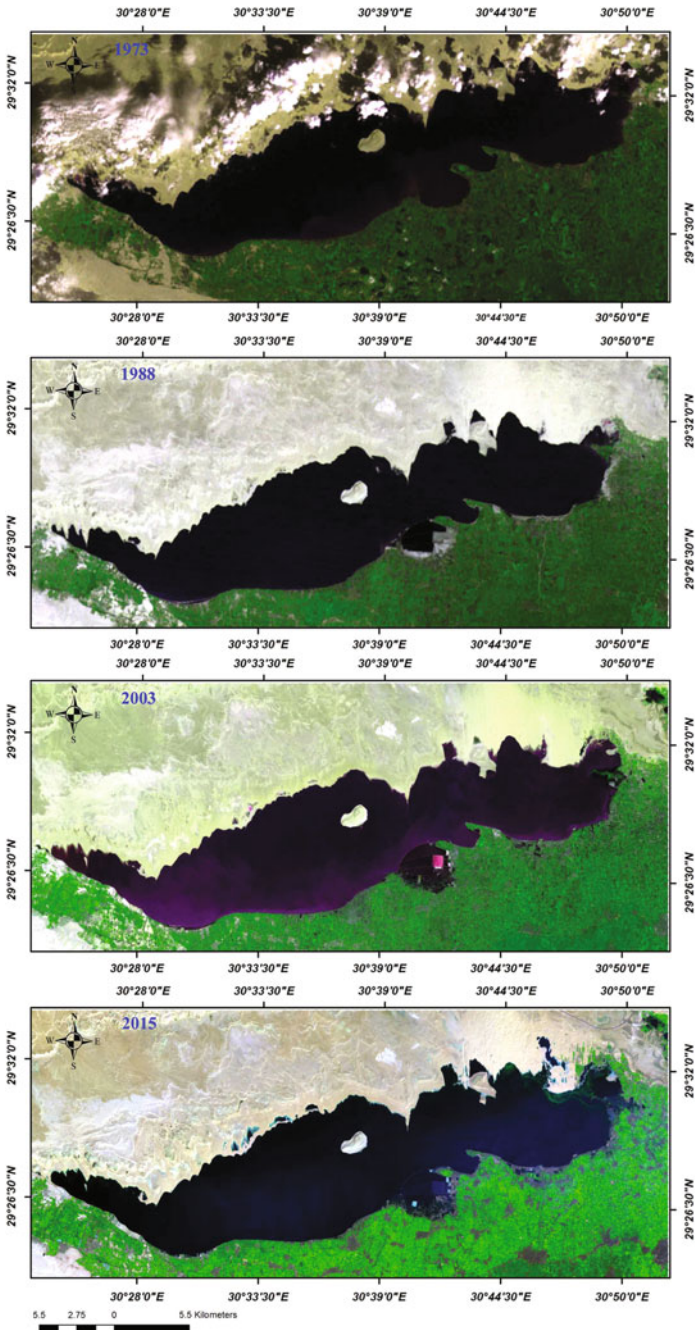


Fig. 22.3 Multitemporal satellite images of Qarun Lake from 1973 to 2015

Table 22.1 Specification of Landsat MSS, TM, ETM+ and Landsat-8

Band	Spatial resolution (m)				Spectral resolution (μm)			
	Landsat MSS	Landsat TM	Landsat ETM+	Landsat-8	Landsat MSS	Landsat TM	Landsat ETM+	Landsat-8
1	60	30	30	30	0.52–0.60	0.45–0.52	0.45–0.52	0.43–0.45
2	60	30	30	30	0.63–0.69	0.52–0.60	0.53–0.61	0.450–0.51
3	60	30	30	30	0.76–0.90	0.63–0.69	0.63–0.69	0.53–0.59
4	60	30	30	30	2.08–2.35	0.76–0.90	0.78–0.90	0.64–0.67
5	–	30	30	30	–	1.55–1.75	1.55–1.75	0.85–0.88
6	–	120	60	30	–	10.4–12.5	10.4–12.5	1.57–1.65
7	–	30	30	30	–	2.08–2.35	2.09–2.35	2.11–2.29
8	–	–	30	15	–	–	0.52–0.90	0.50–0.68
9	–	–	–	30	–	–	–	1.36–1.38
10	–	–	–	100	–	–	–	10.6–11.19
11	–	–	–	100	–	–	–	11.5–12.51

Where: Visible and near infrared (NIR) Bands are 1 to 4; Middle IR bands are 5 and 7
Thermal IR band is 6 and Panchromatic band is 8

produced. These FCC are visually interpreted using on-screen digitizing in order to delineate land cover classes that could be easily interpreted such as urban and water.

Regardless of the technique used, the success of change detection from imagery will depend on both the nature of the change involved and the success of the image preprocessing and classification procedures (Milne 1988). In the case of the chosen study area, field observation and measurements have showed that the change in land cover between the four dates was both marked and abrupt. Images were calibrated to radiance using the inputs of image type, acquisition date and time. The images were stretched (normalized) using linear 2%, smoothly filtered, and their histograms were matched. Consequently, the atmospheric correction is carried out using ENVI 4.7 software. The images were classified using supervised classification method and maximum likelihood algorithm, and then the post-classification change detection technique was applied. This technique requires the comparison of independently produced classified images. It is the most effective technique, because of the used images are atmospherically corrected, separately classified, and stretched to avoid the differences that related to atmosphere and sensors type between dates.

Landform Mapping, Soil Survey, and Soil Analysis

Digital elevation model (DEM) of the study area has been generated from the elevation points (recorded during the field survey by GPS), and the vector contour lines; digitized from the topographic map of the year 1992 (scale 1:50,000); ArcGIS 9.2 software was used for this function.

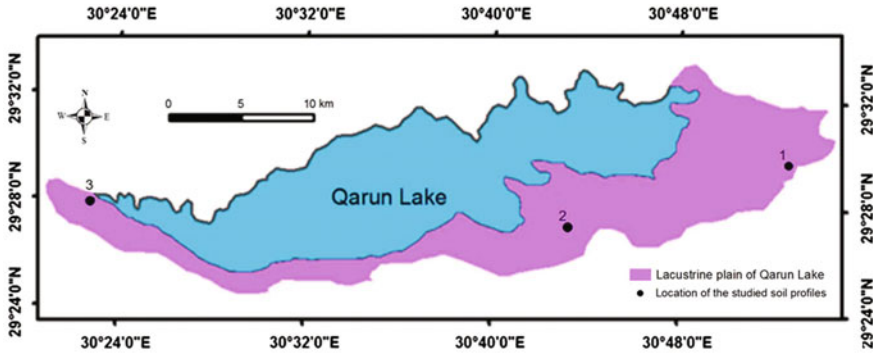


Fig. 22.4 Location of the studied soil profiles

Landsat-8 image of the year (2015) and digital elevation model (DEM) was used in ENVI 4.2 software to produce the physiographic map of the study area, following the methodology described by Dobos et al. (2002). First, the surface elevation, slope, and landform configuration were extracted from DEM, then the land use/land cover and soil pattern were extracted from Landsat-8 image by using ENVI 4.7 software. Consequently, the data extracted from satellite images generate a preliminary geomorphologic map. Accordingly, field survey is carried out throughout the investigated area in order to gain an appreciation on soil patterns, landforms, and the landscape characteristics. Then the obtained data from land survey and laboratory analyses were linked with their relevant landform units using ArcGIS 9.2 software.

Morphological description of three soil profiles representing the different physiographic units (Fig. 22.4) were carried out according to the field book for describing and sampling soils (FAO, 2006).

Representative of seven disturbed soil samples have been collected from the studied soil profiles according to the morphological variations and were used for laboratory analyses. The laboratory analyses were carried out using the soil survey laboratory methods manual (USDA 2004).

The soils were classified to the subgreat group level on the basis of the key to soil taxonomy (USDA 2010).

Results and Discussion

Digital Elevation Model (DEM)

Digital Elevation Model (DEM) has been obtained from the elevation points and topographic map of the year 1992 (Fig. 22.5). Qarun Lake appears as a depression compared to upland surrounding areas, where the highest closed areas is about 50 m above sea level and suddenly decrease to about 45 m below sea level.

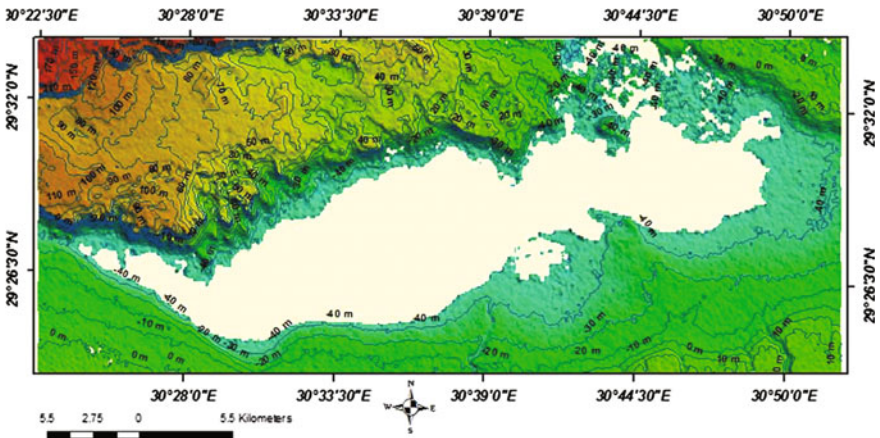


Fig. 22.5 The Digital Elevation Model (DEM) of Qarun Lake

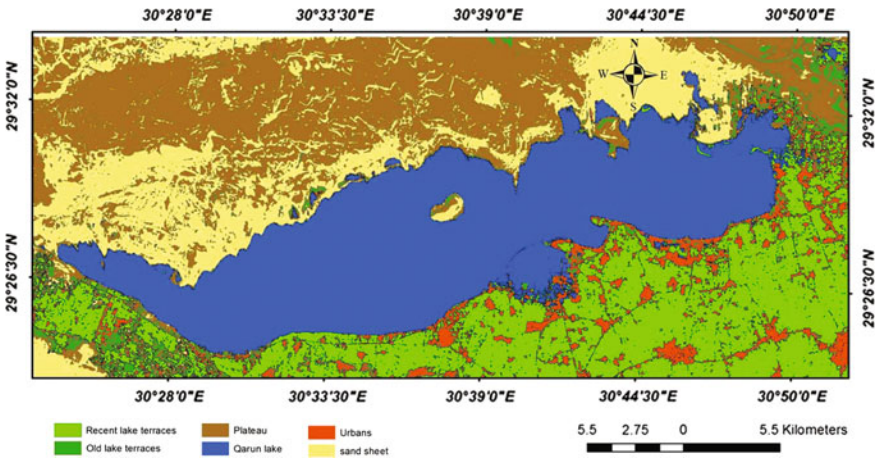


Fig. 22.6 Landforms of areas adjacent to Qarun Lake

Landforms and Soils

Based on the field survey data, Landsat ETM + (2015) images and digital elevation model (DEM), the landforms in the study area were defined according to Dobos et al. (2002), as shown in Figs. 22.6, 22.7 and Table 22.2.

The lacustrine plain is the main landscape in the southern part of Qarun Lake; it includes lacustrine terraces of various elevations. It covers an area of about 194 km² (i.e., 19,420 hectare), including soils of relatively high terraces (7413 hectare), soils of the moderately high terraces (4436 hectare), and soils of the relatively low terraces (7571 hectare). These are represented by soil profiles 1, 2 and 3,

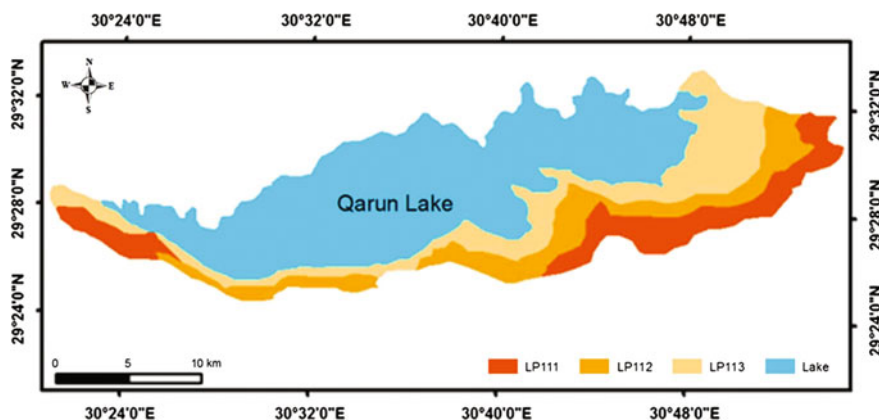


Fig. 22.7 Landforms and soils of south Qarun Lake

Table 22.2 Legend of landforms and soils map of south Qarun Lake

Landscape	Lithology/Origin	Relief/Molding	Land form	Area (km ²)	Taxonomic unit	Map unit
Lacustrine terraces						
Lacustrine	Lacustrine	Flat to	Relatively high	74.13	Typic Haplosalids	LP111
Plain	deposits	almost flat	Moderately high	44.36	Vertic Torrifuvents	LP112
			Relatively low	75.71	Typic Haplosalids	LP113

respectively and are classified to the subgreat group level as Typic Haplosalids (representing 100% of the lacustrine plain). The correlation between physiography and soils indicates that the mapping unit in this landscape is consociation at this survey level. The soil depth, salinity, ESP, and CaCO₃ of this landscape ranges from (50 to 90 cm), (11.35 to 36.22 dS/m), (9.14 to 17.26%) and (5.60 to 28.91%), respectively (Tables 22.3, 22.4).

A comparison between the changes of surface areas of Qarun Lake was assessed. This estimation was done from 1942 based on the calculations of a digitized topographic map (1942) at scale 1:100,000; satellite image interpretations from 1973 to 2015, as indicated on different satellite image (Landsat, MSS 1973 and TM 1988, Landsat ETM + 2003 and Landsat-8, 2015), Figs. 22.8 and 22.9.

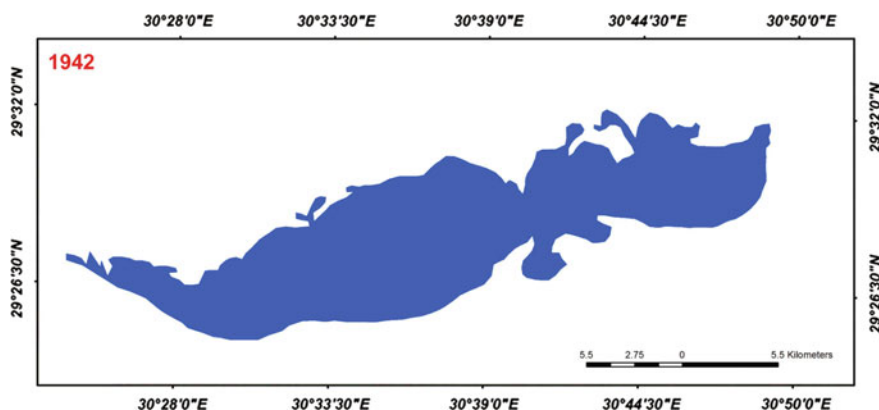
The obtained results showed the surface area of the lake was about 22 km². From that time the surface area of Qarun Lake was more or less stable and it was in a balance with land use in El-Fayoum Depression. But by the end of 1960s, after the High Dam has been established, the Nile water be controlled; a big amount of fresh water became available for agriculture. The Egyptian Government at that time

Table 22.3 Some chemical and physical analysis of the studied soil

Mapping unit	Profile no.	Depth cm	pH 1:2.5	EC dS/m	CEC meq/100 g soil	ESP %	O.M %	CaCO ₃ %
LP111	1	0–25	8.20	11.35	35.22	13.44	1.81	22.61
		25–60	8.10	31.54	37.55	9.14	1.04	21.58
		60–90	7.95	16.33	46.39	9.63	0.41	28.91
LP111	2	0–35	8.31	16.52	34.50	9.55	1.80	5.60
		35–65	8.42	36.22	39.75	14.73	0.55	9.84
LP111	3	0–25	8.25	12.50	35.40	17.26	1.55	21.66
		25–50	8.34	32.44	39.18	12.40	0.64	14.80

Table 22.4 Some chemical and physical analysis of the studied soil

Mapping unit	Profile no.	Particle size distribution %				
		C. sand	F. sand	Silt	Clay	Texture
LP111	1	5.60	41.3	18.3	34.8	SCL
		3.70	20.4	26.5	49.4	C
		12.6	36.7	16.2	34.5	SCL
LP111	2	3.9	22.5	26.4	47.2	C
		2.8	20.6	15.2	61.4	C
LP111	3	6.9	22.3	24.6	46.2	C
		3.2	21.6	31.6	43.6	C

**Fig. 22.8** Multitemporal satellite images and mapping of water bodies of Qarun Lake study area from 1973 to 2015

planned to increase the agricultural land in all the country. El-Fayoum Depression was one of those extension areas.

A sudden increase of the surface area of Qarun Lake was happened due to the increase of using water for irrigation in El-Fayoum Depression just after the High

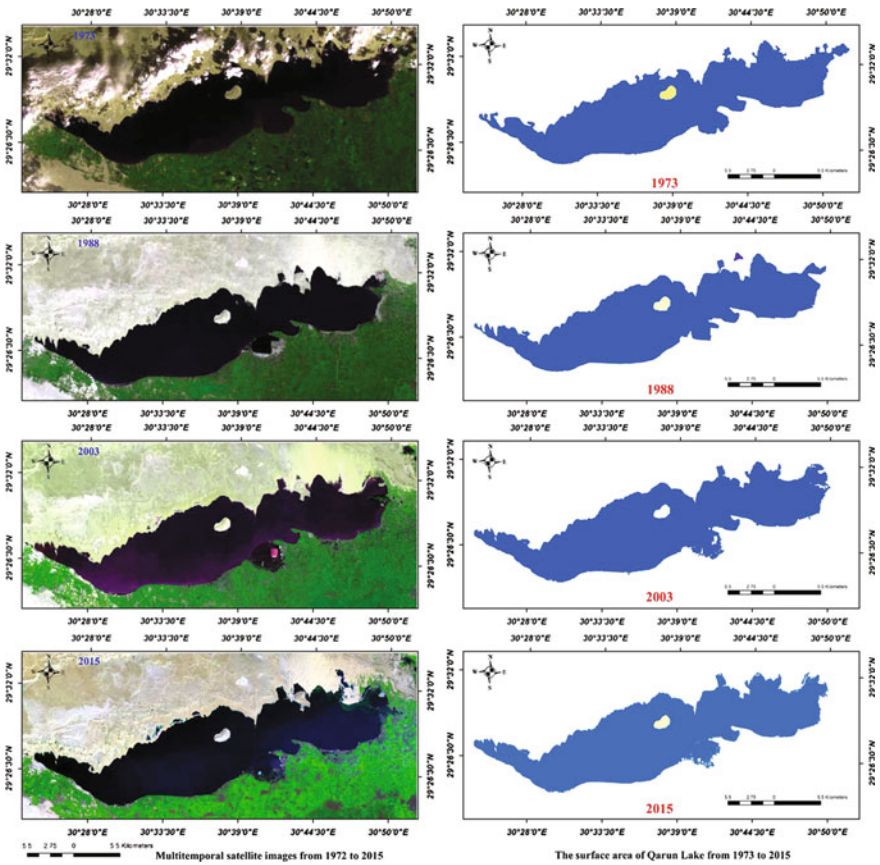


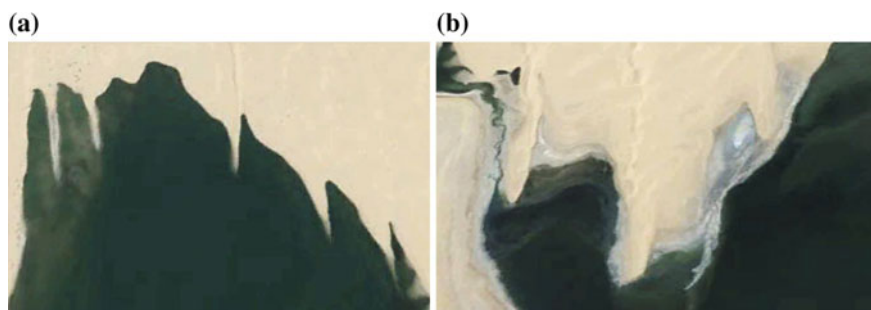
Fig. 22.9 Multitemporal satellite images and mapping of water bodies of Qarun Lake study area from 1973 to 2015

Dam had been constructed at Aswan south of Egypt. This was one of the negative effects of the mismanagement after the establishment of the High Dam in Aswan, Egypt. In 1973 the surface area of Qarun Lake reached its maximum area (240 km²) due to receiving all excessive drainage water of El-Fayoum Depression.

The government of Egypt at that time decided to convey a part of the excessive drainage water of El-Fayoum Depression to a new depression southwest El-Fayoum, which is called (El-Rayan Depression) that started to receive some drainage water in 1973. Accordingly, the surface area of Qarun Lake decreased to about 230 km² by the year 1988 and from that time until 2015 its surface area was almost stable (Table 22.5). These changes in the environmental conditions due to the human impact through mismanagement of water resources of the study area are shown in Fig. 22.9.

Table 22.5 Area of different lakes from 1984 to 2013 in Qarun Lake, (km²)

Year	Total area km ²	Island km ²	Surface area of Qarun Lake km ²
1973	241.91	2.28	239.63
1988	231.76	2.39	229.37
2003	248.76	2.38	246.38
2015	247.59	2.20	245.39

**Fig. 22.10** The effect of sand dune on Qarun Lake A & B are some parts affected by sand dune encroachment

During the period from 1988 to 2003, the increase of human activities in different sectors in particular the agricultural proposes in the both horizontal and vertical extension caused changes in the hydrological conditions in the study area. In spite of El-Rayan Depression started receiving some drainage water by the year 1973 the surface area of Qarun Lake increased from 230 km² in the year 1988 to 246 km² in the year 2003. Within the period from 2003 to 2015 the surface area of Qarun Lake was almost stable as the assigned value for 2015 is 245 km². This could be explained by somehow happened in the water budget of El-Fayoum area and/or by increase of the amount of drainage water be conveyed to El-Rayan Depression.

The Effect of Sand Dune on Qarun Lake

As the topographic saturation of El-Fayoum Depression there are some sand dunes and accumulation of sand areas move from north and northwest direction facing Qarun Lake (Fig. 22.10). The effect of these types of accumulation sands encroach water on the lake and pushing the water of the lake to south direction. So, with same amount of water volume, the coming sand from north push the water body southward to cover low areas mainly the agricultural lands and these have somehow a role to degrade the arable lands by rising ground water table salinization and waterlogged areas.

The Negative Impact of Qarun Lake

The effect of Qarun Lake on the surrounding areas is recognized especially in south and southeast parts during the last 50 years. This is due to two factors; the first one is the receiving drainage water. The second factor is the effect of sand movement, somehow by pushing the water southward direction due to the accumulation of sands from the north and/or northwest direction. This causing some environmental problems such as increasing ground water table, salinization and waterlogged areas. This has negative socioeconomical effects on the life of the native people. Most of those people depending mainly on the agricultural sector. With increasing land degradation rates of the areas adjacent to Qarun Lake and lowering of agricultural productivity, the poverty increases which rise more social problems. In the same trend, according to Abd-Elmabod et al. (2010 and 2012) the adjacent soil type to Quarn Lake (Typic Haplosalids) it was more degraded than the other soil types of El-Fayoum Depression as a result of high salinity due to the negative effect groundwater level.

By the same way, Kotb et al. (2015) applied the remote sensing and GIS techniques for monitoring of the water bodies and their effect on the land resources in Siwa Oasis, Egypt. They found a huge fluctuation on the surface areas of the water bodies of the main lakes in Siwa. This effect led to increase on the ground water table, salinization, and waterlogged areas. They mentioned that in some very severely affected areas, the people had left their villages and transferred to other places.

References

- Abd El-All TS (1984). Pedological and physical studies on some soils of the expansion areas in Fayoum Governorate, Egypt. M.Sc. Thesis, Fac. of Agric., Cairo Univ., Egypt
- Abdel Aal Shi, El-Demerdash S, Khalil MN, Naga MA (1976) Mineralogy of the clay fraction of the Fayoum soils, ARE. Desert Inst. Bull. 26(2): 255–262
- Abdel El-All TS (1990) Cyclic formation of soils on different geomorphic factures of Fayoum area, Egypt. Ph.D. Thesis, Fac. of Agric., El Fayoum Univ., Egypt
- Abd-Elmabod SK (2014). Evaluation of soil degradation and land capability in mediterranean areas under climate and management change scenarios. Andalusia Region, Spain and El-Fayoum Province, Egypt. Ph.D. Thesis, University of Seville
- Abd-Elmabod SK, Ali RR, Anaya-Romero M, De la Rosa D (2010) Evaluating soil contamination risks using MicroLEIS DSS in El-Fayoum Province, Egypt. In: 2nd International conference on chemical, biological and environmental engineering (ICBEE). Cairo, Egypt, pp 1–5
- Abd-Elmabod SK, Ali RR, Anaya-Romero M, Jordán A, Muñoz-Rojas M, Abdelmaged TAL, Zavala LM, De la Rosa D (2012) Evaluating soil degradation under different scenarios of agricultural land management in Mediterranean region. Nat Sci 10:103–116
- Abo El-Enean SM (1985) Pedogenesis of El-Fayoum Area, Ph.D. Thesis, Fac. of Agric., Al-Azhar Univ., Cairo, Egypt

- Ali RR (2005) Geomatics based soil mapping and degradation risk assessment of the cultivated land in El-Fayoum Depression, Egypt. *Egypt J Soil Sci* 45(3):349–360
- Ali RR, Abdel Kawy WAM (2013) Land degradation risk assessment of El Fayoum depression. *Egypt Arabian J Geosci* 6(8):2767–2776
- Anon (2003) Food production in freshwater ecosystems. I: Wadi El-Raiyan Lakes (Egypt). Final Report to MERC/AID
- ASRT (1991) Changes occurred in the fertility of Egyptian soils, 2nd report, Academy of Scientific Research and Technology (ASRT) 1991. Egypt, Cairo
- Bitelli G, Curzi PV, Mandanici E (2009) Morphological and lithological aspects in the north-eastern Libyan desert by remote sensing. *Proc SPIE* 7478:74781W
- CLAC (2004) Central Laboratory for Agricultural Climate (CLAC)
- Dobos E, Bliss N, Worstell B, Montanarella L, Johannsenm C, Micheli E (2002) The use of DEM and satellite data for regional scale soil databases. In: *The 17th WCSS, 14–21 August 2002, Thailand*
- Emanuele M, Gabriele B, Pietro VC (2010) Hyper and multispectral image analysis in North-Eastern Libyan Desert. In: *Proceeding ‘Hyperspectral 2010 Workshop’*. Frascati, Italy, 17–19 March 2010 (ESA SP-683, May 2010)
- Erian WF (1982) An approach to apply the American Soil Taxonomy on some soils of Egypt. M.Sc. Thesis, Fac. of Agric., Cairo Univ., Egypt
- Hanna FS, Labib F (1977) The soils of the Fayoum Depression. *Egypt J Soil Sci* 17(1):33–43
- Harun ORM (2004) Soil evaluation systems as a guide to identify an economical feasibility study for agricultural purposes in El Fayoum Governorate. Fayoum, Cairo University, Egypt. Ph.D. Faculty of Agric
- Hulme M, March R (1990) Global mean monthly humidity surfaces for 1930–59, 1960–89 and projected for 2020, UNEP/GEMS/GRID. Climatic Res. Unit, Univ. of East Anglia, Norwich, England
- Hussein H, Amer R; Gaballah A; Refaat Y, Abdel-Wahab A (2008) Pollution monitoring for Lake Qarun. *Adv Environ Biol* 2:70–80. *EurekaMag.com*, Life earth and health sciences. <http://eurekamag.com/research/032/855/032855380.php>
- ICFG, Information Center, Fayoum Governorate. http://www.sis.gov.eg/En/Templates/Articles/tmpArticles.aspx?CatID=2648#.VuAVc_krKM8. Accessed 8 Mar 2016
- Issawi B, Osman RAK, Meibed AZ (2001) The Fayoum depression-Qarun lake: a geological study. In: *Proceeding the second international conference on the geology of Africa*. Assiut University, pp 307–322
- Kassem YS, Elwan AA (1980) Origin and uniformity of the soils adjacent to Qarun Lake, Fayoum Governorate. *Egypt J Soil Sci* 20(1):57–63
- Khalil JB (1970) Petrological studies on some sediments from Fayoum area and the Nile valley, Egypt. M.Sc. Thesis, Fac. of Sci., Cairo University, Cairo, Egypt
- Khater EA (1973) Pedological studies on Fayoum, Governorate, Egypt. M.Sc. Thesis, Fac. of Agric., Cairo University, Egypt
- Kotb MM, Ali RR, El-Semary MAM (2015) Using remote sensing and GIS techniques for monitoring of the water bodies and their effect on the land resources in Siwa Oasis, Egypt. *Glob J Curr Res* 3(2):53–60
- Labib F (1970) Contribution to the mineralogical characterization of the most important soil parent materials in the United Arab Republic. Ph.D. Thesis, Fac. of Agric., Ain Shams Univ., Egypt
- Lillesand TM, Kiefer RW (1994) *Remote sensing and image interpretation*, 4th edn. Wiley, New York
- Milne AK (1988) Change detection analysis using landsat imagery a review of methodology. In: *Proceedings of IGARSS 88 symposiums, 13–16 Sept 1988*. Edinburgh, Scotland, pp 541–544
- Said R (1962) *The geology of Egypt*. El-Sevier Publishing Company, Amsterdam, pp 99–106
- Shendi MM (1984) Pedological studies on soils adjacent to Qarun Lake, Fayoum Governorate, Egypt. M.S. Thesis, Fac. of Agric., Cairo University, Egypt

- Shendi MM (1990). Some mineralogical aspects of soil sediments with special reference to both lithology and environmental conditions of formation in Fayoum area, Egypt. Ph.D. Thesis, Fac. of Agric. at El-Fayoum, Cairo University, Egypt
- Tamer NA (1968) Subsurface geology of the Fayoum regions. M.Sc. Thesis, Fac. of Sci., Alexandria University, Egypt
- Wahab MA, Ghazy A, Hanna FS (1988) Clay mineralogical studies on the soils of Fayoum Depression. Egypt J Soil Sci 28(1):23-34

Chapter 23

Classification Methods for Detecting and Evaluating Changes in Desertification-Related Features in Arid and Semi-arid Environments

Gabriela Mihaela Afrasinei, Maria Teresa Melis, Cristina Buttau, Claudio Arras, Amar Zerrim, Messaoud Guied, Mohamed Ouessar, Bouajila Essifi, Mongi Ben Zaied, Amor Jlali, Hanen Jarray and Giorgio Ghiglieri

Abstract Land cover, land use, soil salinisation and sand encroachment, which are desertification-indicating features, were integrated into a diachronic assessment, obtaining quantitative and qualitative information on the ecological state of the land, particularly degradation tendencies. In arid and semi-arid study areas of Algeria and Tunisia, sustainable development requires the understanding of these dynamics as it withstands the monitoring of desertification processes. Two different classification methods of salt and sand features have been set up, using historical and present Landsat imagery. Mapping of features of interest was achieved using both visual interpretation and automated classification approaches. The automated one implies a decision tree (DT) classifier and an unsupervised classification applied to the principal components (PC) extracted from Knepper ratios composite. Integrating results

A revised version of this chapter has been accepted for publication in Euro-Mediterranean Journal for Environmental Integration—Springer.

G.M. Afrasinei (✉) · M.T. Melis · C. Buttau · C. Arras · G. Ghiglieri
Laboratory of TeleGIS, Department of Chemical and Geological Sciences,
University of Cagliari, Via Trentino, 51-09127 Cagliari, Italy
e-mail: gabrielafrasinei@gmail.com

C. Arras
e-mail: nrd@uniss.it

G. Ghiglieri
e-mail: ghiglieri@unica.it; nrd@uniss.it

C. Arras · G. Ghiglieri
Desertification Research Center–NRD, University of Sassari, Viale Italia, 39-07100 Sassari,
Italy

A. Zerrim · M. Guied · M. Ouessar · B. Essifi · M.B. Zaied · A. Jlali · H. Jarray
Institutes des Région Arides - IRA, Route du Djorf Km 22.5, Medenine, Tunisia
e-mail: Ouessar.Mohamed@ira.rnrt.tn

with ancillary spatial data, we could identify driving forces and estimate the metrics of desertification processes. In the Biskra area (Algeria), it emerged that the expansion of irrigated farmland in the past three decades has been contributing to an ongoing secondary salinisation of soils, with an increase of over 75%. In the Oum Zessar area (Tunisia), there has been a substantial change in several landscape components in the last decades, related to increased anthropic pressure and settlement, agricultural policies and national development strategies. One of the concerning aspects is the expansion of sand encroached areas over the last three decades of around 27%. This work is partly supported and developed within the WADIS-MAR Demonstration Project, funded by the EU Commission through the SWIM Programme (www.wadismar.eu).

Keywords Arid and semi-arid areas · Desertification · Salinisation · Sand encroachment · Land cover/use mapping · Change detection · Decision tree classification · Knepper ratios · Principal component analysis · Landsat series

Background

Salinity built-up is a concerning and increasing problem that has rendered impracticable extensive agricultural land, whereas soil salinisation is present to different extents in more than 50% of the irrigated drylands (Elnaggar and Noller 2010; Fares and Philip 2008; Masoud and Koike 2006). The two arid and semi-arid sites of the Maghreb region that are discussed in this chapter are affected by two major land degradation processes: soil salinisation and sand encroachment. Natural and anthropologic factors have a strong impact on the ecological state and quality of soils, especially in such drylands where agricultural and animal husbandry practices are intensive, being the main branches of the local economy. Desertification phenomena and land degradation processes threaten the sustainability and reliability of economic growth, hence monitoring is an indispensable requirement for reviewing and improving resource management.

The present work proposes a versatile workflow for the qualitative and quantitative estimation of spatio-temporal variations of desertification phenomena in roughly accessible drylands. It comprises auxiliary, ground truth data and remote sensing methods. The current research was undertaken in the framework of the WADIS-MAR Demonstration Project, funded through the Sustainable Water Integrated Management (SWIM) Programme, by the European Commission (www.wadismar.eu). It aims at the endorsement of an integrated, sustainable management of agriculture and water harvesting in the Biskra region of Algeria and the Dahar-Jeffara area (Oum Zessar study area) of central-eastern Tunisia (Ghiglieri et al. 2014).

Considering the main forms of land degradation that are specific to drylands, soil salinity and especially secondary salinisation represent the main threat to sustainable agriculture in the Biskra region. The economy of the Biskra area is

agricultural-based, and it represents one of the most important date palm producer and exporter at national and also international scale. In order to cope with increasing production demand and population needs, agricultural activities intensified, over-soliciting already fragile soils. Moreover, the climatic setting predisposes the concentration of salts in ephemeral surficial and slow-flowing underground waters that eventually are brought to surface through seepage due to excessive evapotranspiration, thus favouring salt crust formation (Fares and Philip 2008). In the Oum Zessar study site in Tunisia, on the other hand, sand encroachment represents the main threat for the agro-pastoral activities, which represent the base of the regional economy (Ouerchefani et al. 2013; Ouessar 2007). However, even if salinisation is present to a much lesser extent, the issue of salinisation must not be overlooked.

Remote sensing and the employment of geospatial tools have been confirmed as valid instruments and methods for diachronic analyses through the assessment of desertification indicators in order to support decision-makers (Abbas et al. 2013; Allbed and Kumar 2013; Vogiatzakis and Melis 2015; Zewdie 2015; Vacca et al. 2014; Melis et al. 2013b; Fichera 2012). The employment of change detection analysis offers the possibility to quantitatively and qualitatively estimate change rates and, therefore, argue driving factors (Afrasinei 2016).

Common and acknowledged digital image classification methods, such as supervised, unsupervised or spectral mixture, have been widely applied for the delineation of salt features, but no agreed-upon and replicable technique has been acknowledged to be optimal. The state-of-the-art reports problems regarding misclassification and spectral mix-up with other land cover types, especially impermeable features, bare land and areas that have a high content of carbonate minerals (Elnaggar and Noller 2010; Fares and Philip 2008; Khan et al. 2001).

In the Oum Zessar study area, in Tunisia, the main desertification issues are of anthropic origin, as pressure increased in recent years due to changes in socio-economic policies (Afrasinei et al. 2015a; Ouessar 2007, 2010; Sghaier et al. 2010; Schiettecatte et al. 2005).

Sand encroachment is one of the most serious environmental problems in South Tunisia, and previous research shows that several unwary human activities have contributed to the intensification of this process, namely overgrazing, change in land use, from pasture to agriculture and other disturbances coming from inappropriate agricultural practices (Ouerchefani et al. 2013). The studies conducted in the arid and semi-arid Tunisia that approach the sand encroachment and salinisation issues (Lorenz et al. 2013; Ouerchefani 2012; Essifi et al. 2009; Dalel Ouerchefani 2008) are limited to either local test sites or regional scale, and results on driving forces and trends need more insight. The contributing factors are reported as being mainly of anthropogenic nature and not of natural, windborne one, with the Grand Oriental Erg is the source area. In this sense, studies argue that the aeolian sand transport in Southern Tunisia is influenced by the predominant active winds ($u > 3 \text{ m}^{-1}$), coming from the east, south-east and north. This implies a movement towards Sahara and not the opposite (Khatelli and Gabriels 1998, 2000), but the results need further validation.

Considering (1) vast spatial and temporal coverage required for monitoring, (2) limited or no access to ground verification, and (3) the need to correctly delineate features of interest (land cover types, salty and sandy areas), we propose a customised methodological workflow involving remote sensing techniques and mapping land cover and land use (LCLU) through both visual interpretation and automated image classification methods.

Salt and sandy features can be delineated and characterised spectrally based on the high content of main minerals when mapping using multi- or hyperspectral satellite imagery. Band ratios are simple but highly efficient band operations that have been used also by the geological remote sensing community to identify hydrothermally altered minerals, hydrated sulphates and carbonates and other types of land features as described by Langford (2015) (Mia and Fujimitsu 2012). Specific red-green-blue (RGB) composites have been defined through the combination of various ratios, such as the Knepper ratios (Langford 2015). Up-to-date literature shows that Knepper ratios have been used only in geological remote sensing until now (Afrasinei et al. 2017; Langford 2015; Afrasinei et al. 2015a, b). In this study, we propose its employment for salt and sand features extraction (Afrasinei et al. 2015a, b).

The two automated classifications that are developed in this work comprise either supervised multi-stage decision tree classifier (DT) (Matthew 2012; Srimani and Prasad 2012; Elnaggar and Noller 2010), or unsupervised Iterative Self-Organizing Data classification applied to principal components (PC) of Knepper ratios.

For what the Tunisian study area is concerned, the classification methods, either visual or automatic, are supported by a thorough, systematic ground truth (GT) campaign. In the case of the Biskra site, a large and complex set of auxiliary data were employed in the different stages of the analysis, as field survey was difficult to acquire due to the current political and social context.

The scope of this study was not only to map the land cover and soil conditions for a certain point in time but also to construct a customised and replicable methodology in order to repeat this investigation in different moments in time in similar environmentally sensitive areas and minimise previously reported issues of misclassification (Li 2014; Nutini et al. 2013; Ceccarelli 2013).

Study Sites

Wadi Biskra Study Area, Algeria

This study site, of approx. 5000 km², is located in the Biskra Wilayat, in the north-eastern sector of the Northern Sahara. Representing a vast piedmont area, it is delimited by the Aures mountainous domain in the North and by the Sahara plain in the South (Fig. 23.1a). The area is also known as the *Zibans* (meaning *oasis* in

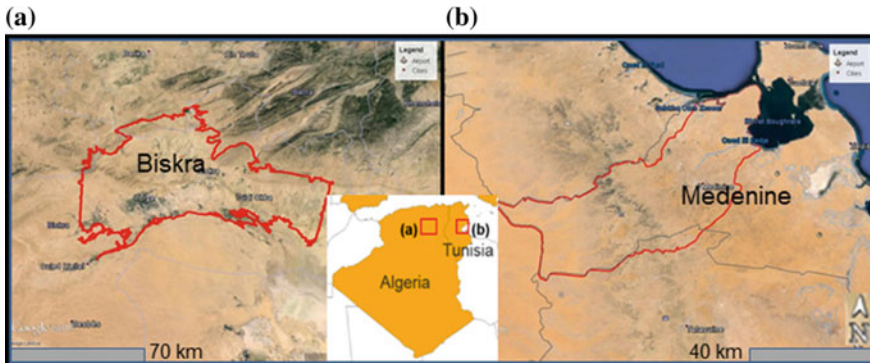


Fig. 23.1 Study areas: Biskra, Algeria (a) and Oum Zessar, Tunisia (b)

berbere language), being possible to distinguish two agricultural sub-zones: (1) the *Occidental Zab* or the *Zibans palmeraie* (meaning palm groves), based on date palm plantations and (2) the *Oriental Zab* based on open field and industrial cultures. These latter cultures do not require a shallow aquifer (unlike phoeniculture), and this favoured their expansion in the past 30 years, but, instead, they require deep pumping of groundwater that has a higher salinity than the shallow acquirers of the Occidental Zab (Bougherara and Lacaze 2009).

In the Occidental Zab, the highly productive and superficial aquifers (average salinity of 2–4 g/l) provide the conditions for a high production of high-quality dates (Ghiglieri et al. 2014). The irrigated area of around 70,000 ha has been reported to require the drawing of more than 600 million m³ per year (NRD 2011).

Various studies have focused on obtaining qualitative and quantitative parameters of these aquifers, some of which have employed up-to-date approaches of three-dimensional (3D) modelling, bringing to the attention of end users their limited and fragile features (Arras et al. 2016; Arras et al. 2015; Pelo et al. 2015; Arras et al. 2014a, b; Buttau et al. 2013; Buttau and Funedda 2008; Buttau et al. 2007).

From the geological point of view, the Biskra area is located in the eastern part of the Saharan Atlas (Aures), between the folded Atlas domain in the northern part of the area and the Saharan desert and flat domain in the South. Its main lithological characteristics are given by the presence of Quaternary and Mio-Pliocene sands and clays, Mid-Eocene gypsum clays and evaporitic deposits, Lower Eocene limestone, gypsum clays and halite, Turonian dolomitic limestone and dolomites and Cenomanian clay, marlstone and gypsum (Buttau et al. 2013; Algerienne 1980).

The climatic regime of this area is hot and dry, with an average annual temperature of about 22 °C, with a total annual rainfall average of approx. 150 mm. However, the average rainfall within a year is less than 20 mm. The minimum rainfall is almost null in the months of July and August, and the maximum occurs in March and November.

Oum Zessar Study Area, Tunisia

The area of about 3000 km² mainly overlaps the Médenine Governorate and stretches from the Great Oriental Erg in the West and crosses the Dahar Plateau and Jeffara plain, reaching the Mediterranean Sea to the East (Fig. 23.1b).

It is denominated generically 'Oum Zessar' because it comprises the whole Oum Zessar watershed (of about 35 000 ha), and it bares its name due to its importance for optimal characteristics for water supply in the surrounding area. The land use types are: extended rangelands, extended olive groves (mainly in the Jeffara plain), local scale arboriculture, episodic cereals and small-farming irrigated agriculture. Crop sites, mainly arboriculture, are mainly found within torrential bodies behind water harvesting structures: *jessour* and *tabias*. (Ouessar 2011) which are favoured by the geomorphological context of the area, such as a high presence of alluvial landforms and paleo-valleys (Marini et al. 2008; Waele and Melis 2008).

The geological setting is given by (1) Mesozoic deposits outcropping mainly in the Dahar domain, underlining the importance of the Cretaceous carbonate deposits with gypsum intercalations for the current study and the (2) Mio-Pliocene continental deposits and (3) Quaternary alluvial and aeolian deposits found mainly in the Jeffara plain (Arras et al. 2015).

The shallow aquifers of the Mio-Plio-Quaternary deposits and the Turonian dolomitic limestone are exploited for the domestic use, with a salinity that ranges from 0, 6 to 5 g/l. The water table ranges from 30 to 2–3 metres near the coastal plain. The area receives between 150 and 240 mm of total annual rainfall and is defined by mild to cold winters and warm to very hot summers (up to 48 °C), with almost null rainfall from June to August.

Methodology and Data Analysis

The methodological approach was tailored considering several criteria based on the objectives of this work and the issues aimed to solve. It was approached from both the theoretical and empirical perspective, explained as follows. The theoretical one refers to the existing environmental problem of salinity and sand encroachment, and the approach that the state-of-the-art literature advises to be adopted when attempting to define current state, driving forces and the trends of these phenomena. The empirical perspective refers to the chosen schema of methods, considering the availability of ancillary data, coping with the difficulty or impossibility to acquire ground data and misclassification issues. This latter one refers to the spectral confusion that is very common among desert features, as they are very reflective.

The mapping methods scheme refers to the employment of two different classification approaches: mapping through on-screen visual interpretation and digital image automatic classification. The first phase of this research consisted of the comprehensive knowledge of the areas and the generation of the LCLU maps used

as support and base map for the following analysis phases. Since base cartographic data were limited or outdated in these areas (dating from the 60s, in the case of Biskra area) as well as not of full spatial coverage, this first phase was necessary in order to update pre-existing maps or even create new ones, being indispensable for the holistic knowledge and acquaintance with the study area.

Secondly, two different automated classifiers were assessed, designed and applied: (1) a decision tree classifier (DT) and (2) a customised unsupervised classification method. These methods were chosen in accordance with reported limitations of variously experimented classification methods in similar case study contexts by the scientific community (Elnaggar and Noller 2010; Pal and Mather 2003). The DT contains five new indices (Afrasinei et al. 2017; Afrasinei et al. 2015b) tailored for this particular type of study, that were constructed manually through thorough spectral analysis, band transformation techniques, image statistics and expert knowledge (Rao et al. 2006; Elnaggar and Noller 2010; Matthew 2012; Srimani and Prasad 2012). The IsoDATA classification was applied to the PC extracted from the Knepper ratios (Langford 2015), as described in Section ‘[Principal Component Analysis of the Knepper Composite](#)’. Given the political and social context in Algeria, the ground survey was not possible to undertake personally, therefore it was acquired in collaboration with the Algerian WADIS-MAR partners. Being difficult to acquire it in the proper amount required by such studies, multi-source ancillary data were employed throughout the study phases.

Thirdly, the IsoDATA-Knepper-PC resulting maps are compared with the DTA results and with the visually interpreted LCLU maps and assessed for error assessment through the application of the confusion matrix. Change detection is applied in both cases, and the results are discussed through correlation to social and economic ancillary data. The ESRI ArcGIS (version 10.2) software was employed for geoprocessing and spatial data analysis and ENVI ITT VIS Exelis version 5.2 for digital image management (pre-treatment, processing and post-classification). A schematic flowchart is illustrated in Fig. 23.2.

Dataset

A comprehensive database of various data types (containing either spatial data or non-spatial) was put together within the WADIS-MAR project, having homogeneous geometries and projections. For easiness of interrogation, manipulation, overlay and geoprocessing, hard copy information was digitalised and stored within a database in a GIS environment, comprising agricultural calendars, pedological surveys and well reports, as well as topographical, geological maps and aerial photographs. These consisted the support data used for the first phase of analysis and LCLU mapping through visual interpretation.

Most of the data were made available by the WADIS-MAR local partners such as the National Agency of Hydraulic Resources of Algeria (ANRH), the Technical Institute of Development of the Sahara Agronomy (ITDAS), Arid regions Institute

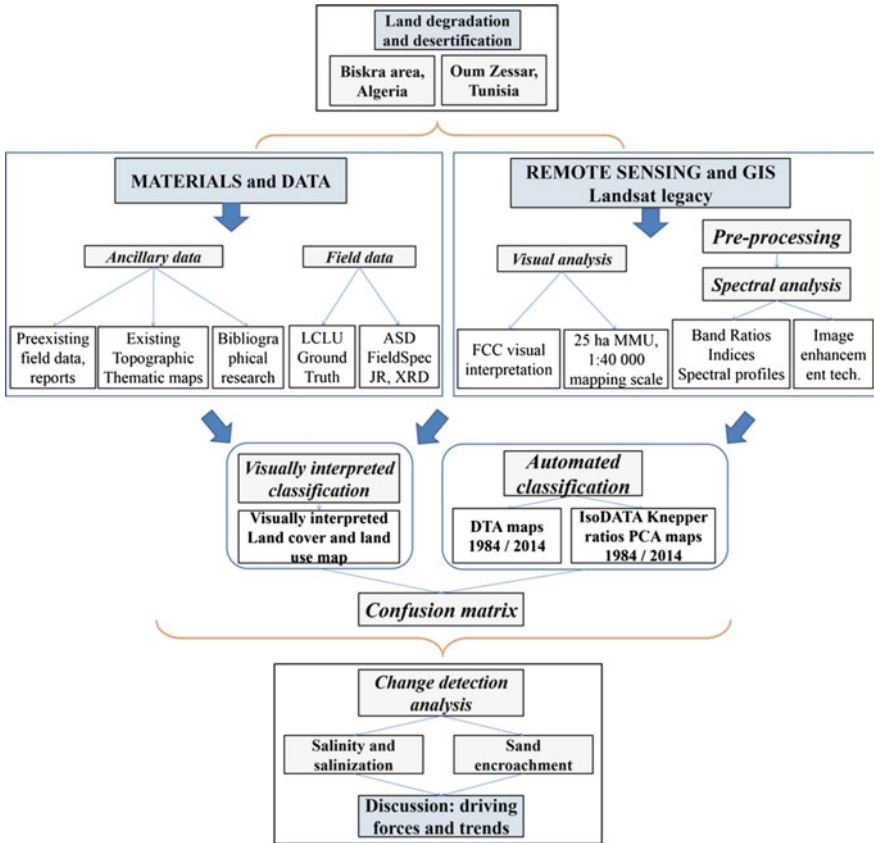


Fig. 23.2 Methodological flowchart

(IRA) and *Observatoire du Sahara et du Sahel* (OSS). Google Earth and its community-based ground truth data were also used as ancillary information.

In addition to this, field data was acquired in the Oum Zessar area from April to June 2014, according to a stepwise methodology. These observations served as ground truth data for the adjustment of the previously interpreted LCLU maps and as field data on salt-affected areas and sand encroachment areas.

The results consist in a ready-to-use geodatabase of 400 observation points with attached geotagged photographs and attributes obtained partly from land cover sheets and attributes recorded onsite in ArcPAD GIS software on Mobile Mapper GPS. A part of these points was also used as training data for further supervised classification and, the other part, for validation.

The Landsat satellite imagery (courtesy of USGS, <http://earthexplorer.usgs.gov>) was downloaded and selected discarding exceptional humid years and considering only the scenes with less than 10% cloud coverage. Climate data was taken into consideration when choosing the imagery acquired during the dry season or at the

Table 23.1 Landsat scenes used for Biskra area and climate data. Climatic data legend: T—average temperature (°C); TM—maximum temperature (°C); Tm—minimum temperature (°C); SLP—atmospheric pressure at sea level (hPa); H—average relative humidity (%); PP—total rainfall and/or snowmelt (mm); VV—average visibility (km); V—mean wind speed (km/h); VM—maximum sustained wind speed (km/h) (Tutiempo Network)

Landsat	WRS path	WRS row	Year	Date	T	TM	Tm	SLP	H	PP	VV	V	VM
LT5	194	36	1984	2 Sept	29.6	36.2	23.4	1017.2	29	0	13.7	10.2	25.9
LC8	194	36	2015	7 Aug	35.8	43	29	1010.2	28	0	11.6	9.6	22.2

end of it, as it has been reported to be the most suitable period of the year for remote sensing salinity mapping (Elnaggar and Noller 2010). Scenes starting from 1984 to 2015 were employed in the analysis of the two study areas (Tables 23.1 and 23.2). It must be mentioned that in the case of Oum Zessar area, two scenes were needed for the full coverage of the study area, so the closest dates as possible were chosen for the mosaic construction of each year.

Visual Interpretation

Visual interpretation is still one of the most widely used methods for identifying and classifying spatial features in a digital image. In this study, the visual interpretation and construction of the LCLU maps served as support for the following phases of the study. Their quality and validity (Elnaggar and Noller 2010) are confirmed through to the use of acknowledged methodology (ETC/LC and Agency 1999; Feranec and Otahel 2000; Büttner et al. 2000; Jaffrain and EEA 2011), a large set of ancillary data, a mapping scale of 1:40,000 and a minimum mapping unit of 25 hectares (MMU). This phase was also supported by ground truth data in the Tunisian study area (Elnaggar and Noller 2010).

Integrating also a geomorphological study (Marini et al. 2008), we managed to delineate and define classes using objective criteria of a set of seven variables (precision of contours, colour/hue, size, texture, structure, spatial distribution and location (ETC/LC and Agency 1999) and keys of interpretation. This procedure allowed us to define and describe the identified classes in detail and define a customised LCLU nomenclature to the local context with a detail up to the fourth level of (according to CORINE (ETC/LC and Agency 1999), CORINE outside Europe (ESA and FAO) and AFRICOVER 2000). In the Biskra area, the interpretation of the June 2011 Landsat scene resulted in 37 feature classes, employing the data described in the previous sections, given the difficulty to undertake ground verification. For the Oum Zessar area, the 36 classes were delineated based on the visual interpretation of Landsat 8 images of 17 May 2013, path 190, row 37 and 24 May 2013, path 191, row 37, combined with ancillary data and the ground truth data described in the previous *Dataset* section.

Table 23.2 Landsat scenes used for Oum Zessar area and climate data. Climatic data legend: T—average temperature (°C); TM—maximum temperature (°C); Tm—minimum temperature (°C); SLP—atmospheric pressure at sea level (hPa); H—average relative humidity (%); PP—total rainfall and/or snowmelt (mm); VV—average visibility (km); V—mean wind speed (km/h); VM—maximum sustained wind speed (km/h) (Tutiempo Network)

Landsat	WRS path	WRS row	Year	Date	T	TM	Tm	SLP	H	PP	VV	V	VM
LT5	190	037	1984	18 Jun	28.3	34.5	17.7	1017.3	37	0	8	15.6	25.9
LT5	191	037	1984	25 Jun	29	34.4	21.3	1015.1	49	0	8	19.3	25.9
LC8	190	037	2014	21 Jun	28.6	32.8	21.6	1013	68	0	23	11.9	18.3
LC8	191	037	2014	28 Jun	30.6	36	20.8	1017.7	47	0	24.9	9.6	14.8

Image Processing and Classification Methods

For both areas, level LIT products were radiometrically calibrated to obtain top of atmosphere reflectance and atmospherically corrected by applying Dark Object Subtraction, thus obtaining surface reflectance. The information contained in the metadata of each scene was used to understand the level of product pre-processing undergone by the provider. Since these products were LIT level, meaning that their provider pre-processing employed ground control points and relief models, geometric correction was not performed (Hamid Reza and Majid Shadman 2012). The relevance of applying topographic correction was determined through an assessment of its effects when applied in arid regions such as our study areas, where land features are very reflective, and the thresholds for their separation are very sensitive. Thus this type of correction was not performed since the state-of-the-art literature reported that topographic correction in desert areas is prone to over-correct values in plain areas and lose valuable information (Vanonckelen et al. 2013).

Decision Tree Classifier Design

A complex spectral analysis was undergone in order to determine optimal data for each decision node. Several vegetation, water and mineral indices were reviewed and applied, choosing the relevant ones reported as successful saline (Allbed and Kumar 2013; Mulder et al. 2011; Hamid Reza and Majid Shadman 2012; Khan et al. 2005; Elnaggar and Noller 2010) and sandy areas delineation (Ouerchefani et al. 2013; Essifi et al. 2009), respectively, in similar environmental and biogeographical areas. The outcomes of these tests showed discrepancies regarding correct delineation of features and accuracy of class assignment. Therefore, in order to construct the decision tree, the best band ratios or indices constructed through compound band mathematical operations were determined for the discrimination of features of interest, with the highest possible accuracy. The choice of optimal band ratios and spectral indices was done through a complex spectral analysis for all scenes of both areas. This involved 2D scatter plots, vertical and horizontal spectral profiles

assessment, band transformation techniques with emphasis on image spectral enhancement, among the other types (spatial and radiometric). Image statistics were used to calculate each node's threshold.

In order to delineate each feature of interest, regions of interest (ROIs) were created either from 2D scatter plots or through direct delineation on images and consequently, statistics were extracted from each band. The bands that were highly uncorrelated (had the highest covariance), were used for band operations as they provided less redundant data and the maximum information content. This retrieval of information is obtained from the combination of bands that have higher covariance among them, and the higher the standard deviation is, the more information content is derived from composite bands (Afrasinei et al. 2015b).

Out of a total of eleven indices, five new ones proposed by (Afrasinei et al. 2015b), were employed in the DTA for Biskra area (Table 23.3), which were constructed through relatively complex mathematical band operations.

Two new indices are proposed within this study and they were employed in the DT used for Oum Zessar area, as presented in Table 23.4. All the indices were constructed differently for each area, depending on the spectral and biophysical-geographic particularities of each area, but also on the basis of the features of interest to be extracted: in Biskra area, salt-affected areas had priority, followed by the main land cover types, whereas in Oum Zessar area, the sandy ones, followed by the saline ones and eventually land cover.

Principal Component Analysis of the Knepper Composite

The principal components were extracted from Knepper composites (Langford 2015). This gave us the input for understanding to what degree Knepper PC can

Table 23.3 Decision tree classification nodes and thresholds—Biskra study site, Algeria (decision nodes)

Decision nodes	Node expressions	Band operations
NDVI (Allbed and Kumar 2013)	b1 GE 0.240	$(\text{NIR}-\text{R})/(\text{NIR} + \text{R})$
NDWI (SEOS 2014)	b2 GE 0.010	$(\text{NIR}-\text{SWIR1})/(\text{NIR} + \text{SWIR1})$
NDWI USGS (McFeeters 1996; Khan et al. 2005)	b3 GE -0.390	$(\text{R}-\text{NIR})/(\text{R} + \text{NIR})$
WR [derived from (van der Meer et al. 2012)]	b4 GE 1.01	R/NIR
SMI*	b5 GE 0.740	$\text{sqrt}(((\text{B}^2) + (\text{G}^2) + (\text{R}^2))/\text{SWIR2})$
MI*	b6 GE 0.0280	$(\text{B}*\text{G}*\text{R})/\text{NIR}$
IRI_SWIR1*	b7 GE 0.880	$\text{sqrt}(((\text{NIR}^2) + (\text{SWIR2}^2))/\text{SWIR1})$
IRI_NIR*	b8 GE 1.70	$\text{sqrt}(((\text{SWIR1}^2) + (\text{SWIR2}^2))/(\text{NIR}^2))$
S2 (Allbed and Kumar 2013)	b9 LE -0.320	$(\text{B}-\text{R})/(\text{B} + \text{R})$
HIS*	b10 GE 1.740	$(\text{B} + \text{G}+\text{R})/\text{SWIR2}$
1/5 (Melis et al. 2013a)	b11 GE 0.220	B/SWIR1

*Indices proposed by (Afrasinei et al. 2017)

Table 23.4 Decision tree classification nodes and thresholds, Oum Zessar area, Tunisia (decision nodes)

Decision nodes	Node expressions	Band operations
NDVI	b1 GT 0.1450	$(\text{NIR}-\text{R})/(\text{NIR} + \text{R})$
Ratio 5/2	b3 GT 4.20	(NIR/B)
Diff 5-2	b5 GT 0.370	$(\text{NIR}-\text{B})$
Ratio 6/3	b7 GT 3.10	$(\text{SWIR1}-\text{G})$
Diff NDVI-NDWI	b8 GT 0.260	$((\text{NIR}-\text{R})/(\text{NIR} + \text{R})) - ((\text{NIR}-\text{SWIR1})/(\text{NIR} + \text{SWIR1}))$
MMI*	b4 GT 0.60	$(\sqrt{\text{R}*\text{R}} + (\text{SWIR1}*\text{SWIR1}))$
Modif SI*	b6 GT 0.450	$(\sqrt{\text{B}*B} + (\text{NIR}*\text{NIR}))$
NDWI	b2 GT -0.050	$(\text{NIR}-\text{SWIR1})/(\text{NIR} + \text{SWIR1})$

*Indices proposed in this study

spectrally distinguish the features of interest, namely the mineral components and vegetation types. Moreover, this phase aimed to assess its prospective as a simple user-independent approach of fast classification, an auxiliary to decision tree classifier, since this latter one is highly dependent on how thresholds are calculated and requires much computational labour for the determination of rules. The obtained images were classified using IsoDATA unsupervised classifier for both areas.

Results and Discussions

DT Classifier

The normalised vegetation index, two water indices, existing and new salinity indices, as well as simple band ratios were employed in the DT classifier, and the final map was obtained. The choice of the indices or band operations that were derived through the previous spectral analysis has proven to give optimal results (Melis et al. 2013a). Considering mean values and standard deviation, the threshold values of the decision nodes were derived from each index image statistics. The DT classifier was applied to the 1984 and 2015 images in the case of Biskra area and to the 1984 and 2014 images for the Oum Zessar area. The example of Biskra area is presented in Figs. 23.3 and 23.4, where classes are defined according to (Afrasinei et al. 2017; Afrasinei et al. 2015b) and the Oum Zessar one, in Figs. 23.5 and 23.6.

The DT components and class description were tailored for each study site considering their particular biophysical characteristics, bearing in mind especially their specific lithology and the main types of vegetation cover that can be spectrally distinguished among themselves, respectively.

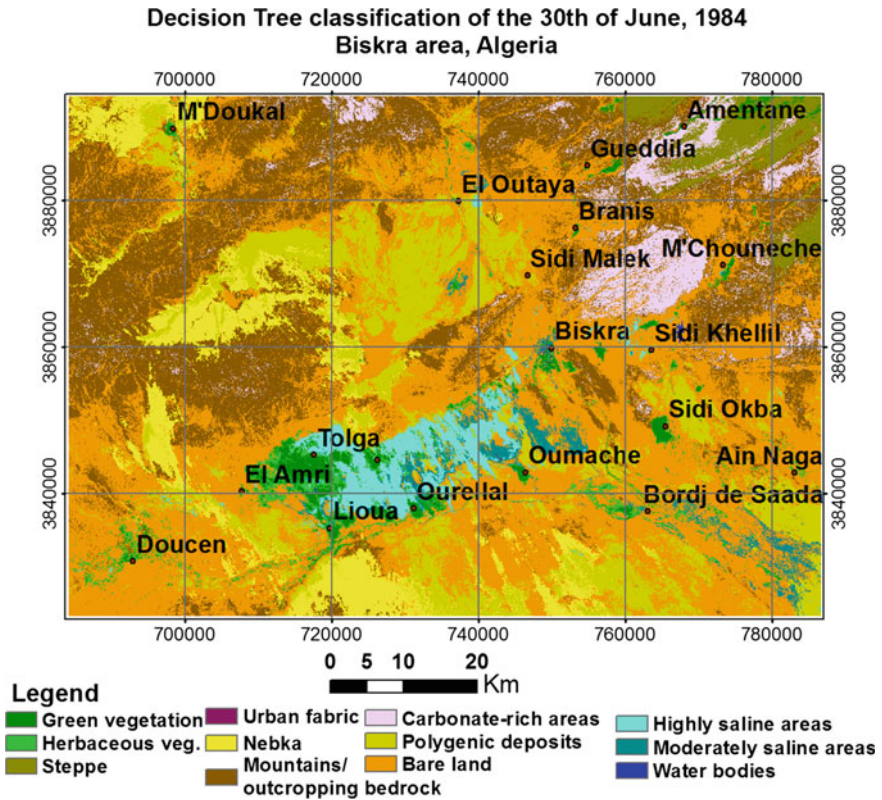


Fig. 23.3 Customised decision tree classification applied to the 1984 Landsat scene, Biskra area, Algeria

IsoDATA Classifier of Knepper-ratios composite Principal Components

The principal components analysis indicated that the information regarding the abundant salt minerals were found within the third component in both years' images in the case of Biskra area. The highest amount of irredundant data of the three input images (namely the Knepper ratios) was related to sand minerals, emphasised by the first principal component. The second component emphasised clay minerals, usually overlying alluvial fans areas where sandy, loamy or clayey soils are usually present.

Consequently, the resulting PC bands were further classified using unsupervised classification, IsoDATA in ENVI 5.2. ITT VIS Exelis Boulder, CO, applied with 100 iterations and a 2% threshold to obtain a clear delineation of saline areas and sandy areas. The seven major classes were not delineated correctly using IsoDATA classification since it presented misclassification issues in both areas and it gave an overall accuracy inferior to 60%. Therefore, only the 'saline soil' and 'moderately

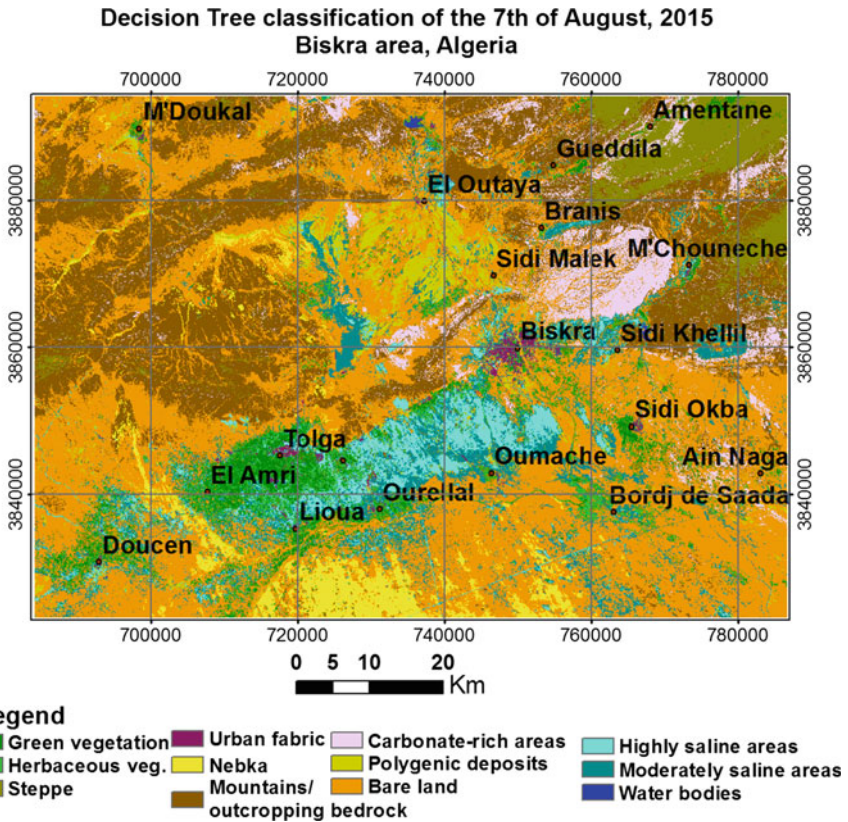


Fig. 23.4 Customised decision tree classification applied to the 2015 Landsat scene, Biskra area, Algeria

saline areas’ classes were employed for the confusion matrix analysis for change detection. In the Oum Zessar area, the third principal component contained the sandy areas information, and good results were also obtained on the spectral distinction between the aeolian sand West of Dahar and the inner-plain one. IsoDATA was applied on the three resulting components, but with several issues of misclassification.

Discussion

The observations that were made on the Biskra satellite images during the pre-classification phase related to the analysis of the features of interest from the spectral point of view revealed that the main elements that influence the reflectance of salty soils are the content and mineralogical typology of salts. In addition, the

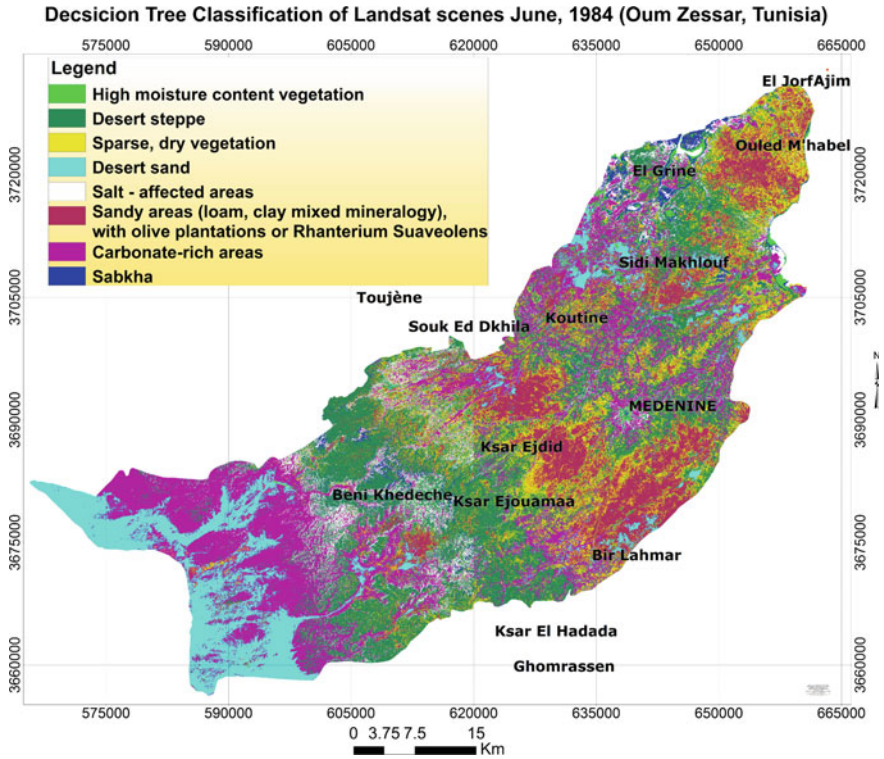


Fig. 23.5 Customised decision tree classification of the 1984 Landsat mosaic image, Oum Zessar area, Tunisia

physical properties are also important, such as moisture content, surface roughness, impurities or colour.

The spectral signature is influenced by the mineralogy of the chloride, carbonate or sulphate salts, hence elementary anion groups (carbonate, sulphate, hydroxyl and hydroxide) that trigger the behaviour of tones, either exciting them or favouring combinations, which are related to the internal vibration modes translated into the presence/absence of absorption features (Metternicht and Zinck 2008). Given this premise, we can explain why we encountered difficulties in correctly identifying the saline features, even though it must be mentioned that the *highly saline areas* class have presented the highest degree of misclassification because of spectral similarity to areas that have a strong carbonate component and implicitly outcropping limestone. Various tests were conducted on the images applying salinity indices indicated by the literature (Masoud 2014; Allbed and Kumar 2013; Khan et al. 2005), but no substantial outcomes were achieved. This is argued by the fact clayey soils, silty soils, impervious surfaces, bare rock and land, as well as carbonate-rich areas presented high similarity to saline areas so as to be classified altogether in one unique class.

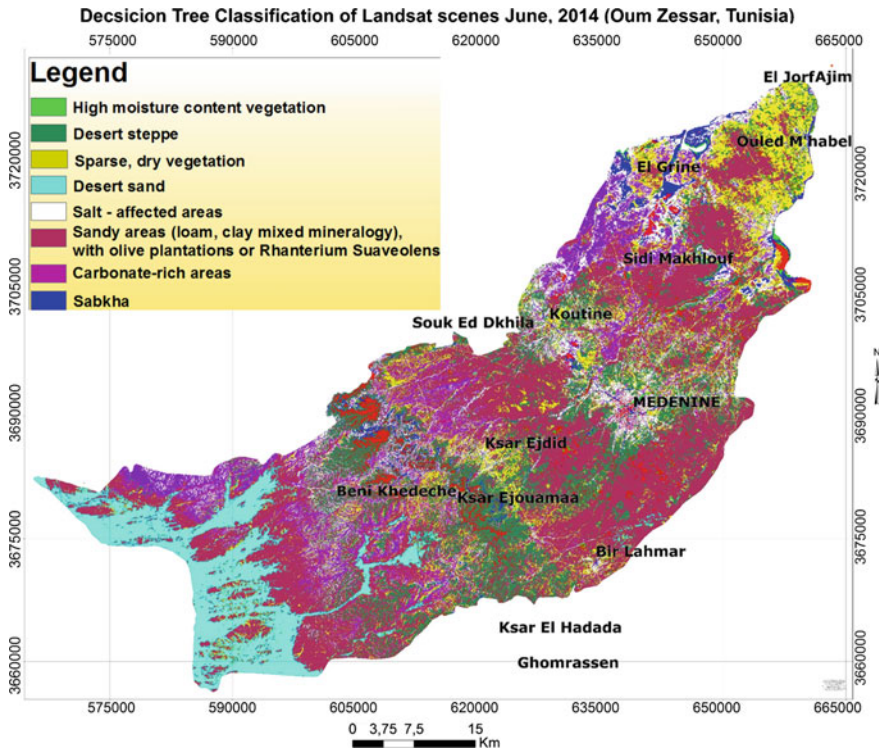


Fig. 23.6 Customised decision tree classification of the 2014 Landsat mosaic image, Oum Zessar area, Tunisia

We managed to minimise these issues, and both classifiers showed agreeable results and an overall accuracy of over 80%.

However, it must be mentioned, as an overall observation, that from both spectral analysis and classification phases, we can determine that common drylands features that are highly reflective may present high levels of similarity to those of areas with high salt concentration. Such typical drylands features are braided stream beds, eroded surfaces with skeletal soils and non-saline silt-rich structural crusts, as previously stated in literature (Metternicht and Zinck 2008).

Change detection statistics of the 1984 and 2015 years showed an increase of approx. 76% of the surface of salt-affected areas, including ‘moderately saline areas’ class, mainly in the disfavour of steppe vegetation (18%), orthents (2%), green vegetation (around 16%) and other small percentages of other classes.

In the Oum Zessar area, the *aeolian sand* class presented an increase of 10, 13% and the desert one, of 10, 44%, between 1984 and 2014. However, the PCA of the Knepper composites, between the same years has shown an increase of 21% of the *aeolian sand* class and 19% of the *desert sand* class, as resulted from the change detection statistics. The *desert sand* class had presented problems of spectral

confusion with another feature (possibly saline areas in the western extremity of the image), as shown from comparison to IsoDATA of Knepper PCA and ground truth data. Thus, the index employed to extract it needs further revision. The class was identified but it was overestimated. Thus, we reached our goal of separating the *desert sand* class from the inner plain aeolian sand, but we cannot fully appreciate the change between the two dates, as it needs further revision. It is also important to specify that the sparse vegetation on sand encroached areas, mainly *psammophyte* species have decreased by 40% which can be argued by the fact that in the past decades the rainfed agriculture and especially olive plantations overlay mostly to the sandy areas of the plain.

The most important aspect obtained from this analysis was the net separation between inner plain aeolian sandy areas and the desert ones along paleo-valleys that converge towards the Great Oriental Erg. Both classification methods have shown good separability between the two classes, for both years in discussion.

Conclusions

Based on a vast bibliography, this work combines and proposes a specifically tailored workflow for thematic mapping, indices construction, classification built-up and change detection analysis. The customised decision tree classifier was proven to be more flexible and adequate for the extraction of highly and moderately saline areas, and major land cover types, as it allows multi-source information and higher user control, yielding an overall accuracy of more than 85%.

The results showed that the secondary salinisation of soils is an ongoing process in the Biskra area of Algeria. The main driving factors are related to human activities, namely the intensification of agriculture, through the enlargement of date palm plantation and market gardening fields in the Occidental Zab, and the expansion of open field and large-scale industrial agriculture practices in the Oriental Zab. In the last three decades, the salinized areas have increased by 76%.

In the Oum Zessar study area, in Tunisia, the analyses show a substantial change in several components of the environment since the 80s, related to increased anthropic pressure, settlement and agricultural policies and national development strategies. One of the concerning aspects that emerged from this study is that the Jeffara plain, is more affected by sand encroachment over the last decade, namely by around 27%, also adding changes in several other classes of land cover.

Acknowledgements We wish to acknowledge the Desertification Research Centre team of the University of Sassari, the WADIS-MAR project and its team, and the TeleGIS Laboratory team of the University of Cagliari (Italy) for the scientific and financial support and the possibility of conducting the current research. This study was also developed within the PhD course in Environmental and Land Engineering Sciences, financed by the Italian Ministry of Instruction, University and Research (MIUR, *Ministero dell'Istruzione, dell'Università e della Ricerca, Italia*). We also acknowledge the contribution given by the fellow researchers and professors of the Chemical and Geological Department of the University of Cagliari, in particular Prof. Franco Frau,

Prof. Andrea Vacca and Dr. Marco Pistis. We also wish to thank the Tunisian and Algerian WADIS-MAR partners and the Spatial Analysis Laboratory of Wollongong University NSW, Australia for the undertaken research training programme for the provided data and support.

References

- Abbas A, Khan S, Hussain N, Hanjra MA, Akbar S (2013) Characterizing soil salinity in irrigated agriculture using a remote sensing approach. *Phys Chem Earth* 55–57:43–52. doi:[10.1016/j.pce.2010.12.004](https://doi.org/10.1016/j.pce.2010.12.004)
- Afrasinei GM (2016) Study of land degradation and desertification dynamics in North Africa areas using remote sensing techniques. doi: [10.13140/RG.2.1.2412.6327](https://doi.org/10.13140/RG.2.1.2412.6327)
- Afrasinei GM, Melis MT, Buttau C, Bradd JM, Arras C, Ghiglieri G (2017) Assessment of remote sensing based classification methods for change detection of salt-affected areas (Biskra area, Algeria). *J Appl Rem Sens* 11:16025. doi: [10.1117/1.JRS.11.016025](https://doi.org/10.1117/1.JRS.11.016025)
- Afrasinei G-M, Melis MT, Frau F, Demurtas V, Buttau C, Arras C, Ghiglieri G (2015a) Spectral characterization methodology of saline and sand encroachment areas using proximal sensing e remote sensing in Tunisia. In: *Proceedings of the XIX Conferenza Nazionale ASITA*, 29 settembre–1 ottobre 2015, Lecco, Italy
- Afrasinei GM, Melis MT, Buttau C, Bradd JM, Arras C, Ghiglieri G (2015b) Diachronic analysis of salt-affected areas using remote sensing techniques: the case study of Biskra area, Algeria. In: *In Proceedings of SPIE 9644, earth resources and environmental remote sensing/GIS applications VI*, 96441D-41D-15, p 96441D. doi:[10.1117/12.2194998](https://doi.org/10.1117/12.2194998)
- Algerienne MdIH (1980) Notice explicative de la carte hydrogeologique de Biskra au 1/200.000. *Ministere de l'hydraulique*. Algerienne MdH, Alger, Algeria
- Allbed A, Kumar L (2013) Soil Salinity mapping and monitoring in arid and semi-arid regions using remote sensing technology: a review. *Adv Remote Sens* 02(04):373–385. doi:[10.4236/ars.2013.24040](https://doi.org/10.4236/ars.2013.24040)
- Arras C, Buttau C, Carletti A, Funedda A, Ghiglieri G (2014a) Geological 3D model for the design of artificial recharge facilities into the Oued Biskra inféro-flux aquifer (NE Algeria). *Rendiconti Online Societa Geologica Italiana*
- Arras C, Buttau C, Carletti A, Funedda A, Ghiglieri G (2014b) Geological modelling for hydrogeological purposes in Oum Zessar area (SE Tunisia). *Rendiconti Online Societa Geologica Italiana*
- Arras C, Longo V, Testone V, Carletti A, Buttau C, Da Pelo S, Ouessar M, Ghiglieri G (2015) Electrical resistivity tomography for the identification of the alluvium-triassic boundary in Medenine region (SE Tunisia). *Rendiconti Online Societa Geologica Italiana* 35:10–12. doi:[10.3301/ROL.2015.51](https://doi.org/10.3301/ROL.2015.51)
- Arras C, BabaSy M, Buttau C, Da Pelo S, Carletti A, Afrasinei GM, Ghiglieri G (2016) Preliminary results of a 3-D groundwater flow model in an arid region of NE Algeria using PMWin: the Inféro-flux phreatic aquifer (Biskra). *Rend Online Soc Geol It* 41:18–21. doi: [10.3301/ROL.2016.82](https://doi.org/10.3301/ROL.2016.82)
- Bougherara A, Lacaze B (2009) Etude preliminaire des images Landsat et Alsat pour le suivi des mutations agraires des Ziban (extrême nord-est du Sahara algérien) de 1973 à 2007. *Journées d'Animation Scientifique (JAS09) de l'AUF Alger Journées d'Animation Scientifique (JAS09) de l'AUF Alger Journées d'Animation Scientifique (JAS09) de l'AUF Alger*
- Buttau C, Funedda A (2008) 3D Model of hinterland verging folds In the variscan foreland of SW Sardinia. *FIST (Federazione Italiana Scienze della Terra)*, Rimini
- Buttau C, Funedda A, Carletti A, Virdis S, Ghiglieri G (2013) Studio geologico strutturale per indagini idrogeologiche dell'area compresa tra le regioni di Batna e Biskra (NE Algeria). *Rend Online Soc Geol It* 29:13–16

- Buttau C, Funedda A, Pasci S, Oggiano G, Carmignani L, Sale V (2007) Structural analysis by 3D modelling of the transcurent area of Lanaitto Valley (NE Sardinia). Federazione Italiana Scienze della Terra), Rimini
- Büttner G, Maucha G, Bíró M, Kosztra B, O.Petrik (2000) National CORINE land cover mapping at scale 1:50.000 in Hungary. FÖMI Remote Sensing Centre, Budapest, Hungary
- Ceccarelli T (2013) Land cover data from Landsat single-date imagery: an approach integrating pixel-based and object-based classifiers. *Eur J Remote Sens* 699–717. doi:[10.5721/EuJRS20134641](https://doi.org/10.5721/EuJRS20134641)
- Dalel Ouerchefani HTeAB (2008) Apport de la classification spectrale des compositions colorées des indices pour la cartographie des sols salins dans un milieu aride du Sud tunisien. *Journal Canadien de Télédétection* 34(5):438–446
- Elnaggar AA, Noller JS (2010) Application of remote-sensing data and decision-tree analysis to mapping salt-affected soils over large areas. *Remote Sens* 2(1):151–165. doi:[10.3390/rs2010151](https://doi.org/10.3390/rs2010151)
- Essifi B, Ouessar M, Rabia MC (2009) Mapping long-term variability of vegetation greenness and sand dunes around watering points in the rangelands of Dahar and El Ouara (Tataouine-Tunisia) during the period 1975–2000 using remote sensing. *J Arid Land Stud* 19(1):319–322
- ETC/LC, Agency EE (1999) CORINE Land cover. Technical guide. ETC/LC, European Environment Agency
- Fares MH, Philip CG (2008) Characterization of salt-crust build-up and soil salinization in the united arab emirates by means of field and remote sensing techniques. In: Remote sensing of soil salinization. CRC Press. doi:[10.1201/9781420065039.ch8](https://doi.org/10.1201/9781420065039.ch8)
- Feranec J, Otahel J (2000) The 4th level CORINE land cover nomenclature for the phare countries. Slovak Academy of Sciences, Bratislava, Slovak Republic, EEA Phare Topic Link on Land Cover Institute of Geography
- Fichera CR (2012) Land cover classification and change-detection analysis using multi-temporal remote sensed imagery and landscape metrics. *Eur J Remote Sens* 1–18. doi:[10.5721/EuJRS20124501](https://doi.org/10.5721/EuJRS20124501)
- Ghiglieri G, Sy MOB, Yahyaoui H, Ouessar M, Ouldamura A, Gil AS, Arras C, Barbieri M, Belkheiri O, Zaied MB, Buttau C, Carletti A, Pelo SD, Dodo A, Antonio, Funedda, Iocola I, Meftah E, Mokh F, Nagaz K, Melis MT, Pittalis D, Said M, Sghaier M, Torrentó C, Virdis S, Abderezak, Zahrouna, Enne G (2014) Design of artificial aquifer recharge systems in dry regions of Maghreb (North Africa). In: Tuscia UdSd (eds) Dipartimento di Scienze Ecologiche e Biologiche, FlowPath2014—National meeting on hydrogeology, Viterbo. Dipartimento di Scienze Ecologiche e Biologiche, Università degli Studi della Tuscia
- Hamid Reza M, Majid Shadman R (2012) Decision tree land use/land cover change detection of Khoram Abad city using landsat imagery and ancillary SRTM data. *Scholars Research Library (Annals of Biological Research)* 4045–4053
- Jaffrain G, EEA (2011) CORINE land cover outside of Europe. Nomenclature adaptation to other bio-geographical regions. Universidad de Malaga, ETCSIA, Spain
- Khan NM, Rastoskuev VV, Sato Y, Shiozawa S (2005) Assessment of hydrosaline land degradation by using a simple approach of remote sensing indicators. *Agric Water Manag* 77 (1–3):96–109. doi:[10.1016/j.agwat.2004.09.038](https://doi.org/10.1016/j.agwat.2004.09.038)
- Khan NM, Rastoskuev VV, V.Shalina E, Sato Y (2001) Mapping salt-affected soils using remote sensing indicators—a simple approach with the use of GIS IDRISI. Paper presented at the 22nd Asian conference on remote sensing, Singapore
- Khatelli H, Gabriels D (1998) A study on the dynamics of sand dunes in Tunisia: mobile barkhans move in the direction of the Sahara. *Arid Soil Res Rehabil* 12(1):47–54. doi:[10.1080/15324989809381496](https://doi.org/10.1080/15324989809381496)
- Khatelli H, Gabriels D (2000) Effect of wind direction on aeolian sand transport in Southern Tunisia. *Int Agrophys* 14:291–296

- Langford RL (2015) Temporal merging of remote sensing data to enhance spectral regolith, lithological and alteration patterns for regional mineral exploration. *Ore Geol Rev* 68:14–29. doi:[10.1016/j.oregeorev.2015.01.005](https://doi.org/10.1016/j.oregeorev.2015.01.005)
- Li M (2014) A review of remote sensing image classification techniques: the role of spatio-contextual information. *Eur J Remote Sens* 389–411. doi:[10.5721/EuJRS20144723](https://doi.org/10.5721/EuJRS20144723)
- Lorenz RD, Gasmi N, Radebaugh J, Barnes JW, Ori GG (2013) Dunes on planet tatoonine: observation of barchan migration at the star wars film set in Tunisia. *Geomorphology* 201:264–271. doi:[10.1016/j.geomorph.2013.06.026](https://doi.org/10.1016/j.geomorph.2013.06.026)
- Marini A, Melis MT, Pitzalis A, Talbi M, Gasmi N (2008) La carta della unità geomorfologiche della regione di Medenine (Tunisia meridionale). *Mem Descr Carta Geol d'It LXXVIII* pp 153–168
- Masoud AA (2014) Predicting salt abundance in slightly saline soils from Landsat ETM + imagery using spectral mixture analysis and soil spectrometry. *Geoderma* 217–218:45–56. doi:[10.1016/j.geoderma.2013.10.027](https://doi.org/10.1016/j.geoderma.2013.10.027)
- Masoud AA, Koike K (2006) Arid land salinization detected by remotely-sensed landcover changes: a case study in the Siwa region. *NW Egypt J Arid Environ* 66(1):151–167. doi:[10.1016/j.jaridenv.2005.10.011](https://doi.org/10.1016/j.jaridenv.2005.10.011)
- Matthew CH (2012) Classification trees and mixed pixel training data. In: *Remote sensing of land use and land cover. Remote sensing applications series*. CRC Press, pp 127–136. doi:[10.1201/b11964-12](https://doi.org/10.1201/b11964-12)
- McFeeters SK (1996) The use of Normalized Difference Water Index (NDWI) in the delineation of open water features. *Int J Rem Sens* 17:1425–1432.
- Melis MT, Afrasinei G, Belkheir O, Carletti A, Iocola I, Pittalis D, Viridis S, Ghiglieri G (2013a) Caratterizzazione spettrale delle aree interessate da salinizzazione nel bacino del Oued Biskra in Algeria a supporto delle politiche di gestione dell'acqua nell'ambito del progetto WADIS-MAR. Proceeding of the Atti 17a Conferenza Nazionale ASITA, 5–7 november 2013, Riva del Garda, Italy
- Melis MT, Dessi F, Locci F, Bonasoni P, Vuillermoz E (2013b) Share geonetwork: a web-service platform for environmental data sharing, pp 87951 V-8, <http://dx.doi.org/10.1117/12.2027602>
- Metternicht G, Zinck JA (2008) Spectral behavior of salt types. In: *Remote sensing of soil salinization*. CRC Press. doi:[10.1201/9781420065039.ch2](https://doi.org/10.1201/9781420065039.ch2)
- Mia B, Fujimitsu Y (2012) Mapping hydrothermal altered mineral deposits using landsat 7 ETM + image in and around Kuju volcano, Kyushu. *Jpn J Earth Syst Sci* 121(4):1049–1057. doi:[10.1007/s12040-012-0211-9](https://doi.org/10.1007/s12040-012-0211-9)
- Mulder VL, de Bruin S, Schaeppman ME, Mayr TR (2011) The use of remote sensing in soil and terrain mapping—a review. *Geoderma* 162(1–2):1–19. doi:[10.1016/j.geoderma.2010.12.018](https://doi.org/10.1016/j.geoderma.2010.12.018)
- NRD (2011) WADIS-MAR Water harvesting and Agricultural techniques in dry lands: an integrated and sustainable model in MAghreb regions. Concept Note, http://www.wadismar.eu/images/wadis-mar_Concept_note.pdf, Accessed 20 July 2016
- Nutini F, Boschetti M, Brivio PA, Bocchi S, Antoninetti M (2013) Land-use and land-cover change detection in a semi-arid area of Niger using multi-temporal analysis of Landsat images. *Int J Remote Sens* 34(13):4769–4790. doi:[10.1080/01431161.2013.781702](https://doi.org/10.1080/01431161.2013.781702)
- Ouerchefani D (2012) Caratterizzazione Et Suivi Des Etats De Surfaces Éolisés En Tunisie Pré-Saharienne: Approches Stationnelle Et Spatiale. Université de Tunis El Manar, Faculté des Sciences de Tunis, Laboratoire de Ressources Minérales et Environnement
- Ouerchefani D, Dhaou H, Delaitre E, Callot Y, Abdeljaoued S (2013) Geographic information system (GIS) and remote sensing for multi-temporal analysis of sand encroachment at Oglet Merteba (South Tunisia). *Afr J Environ Sci Technol* 7(10):938–943. doi:[10.5897/AJEST2012.1414](https://doi.org/10.5897/AJEST2012.1414)
- Ouessar M (2007) Hydrological impacts of rainwater harvesting in wadi Oum Zessar watershed (Southern Tunisia). Ghent University Ghent Belgium
- Ouessar M (2010) Water Harvesting and CC adaptation in the dry areas of Tunisia. Water Scarcity, Drought, and Population Mobility, Damascus, Syria, Regional Consultation Meeting Climate Change Impacts in the Arab Region

- Ouessar M (2011) Physical and socio-economic characteristics of the watershed of Wadi Oum Zessar, Tunisia
- Pal M, Mather PM (2003) An assessment of the effectiveness of decision tree methods for land cover classification. *Remote Sens Environ* 86(4):554–565. doi:[10.1016/S0034-4257\(03\)00132-9](https://doi.org/10.1016/S0034-4257(03)00132-9)
- Pelo SD, Ghiglieri G, Buttau C, Cuzzocrea C, Carletti A, Biddau R, Fenza P, Arras C, Funedda A, Cidu R (2015) 3D hydrogeological modelling supported by geochemical mapping as an innovative approach for management of aquifers applied to the Nurra district. *Rendiconti Online Societa Geologica Italiana, Sardinia, Italy*
- Rao P, Chen S, Sun K (2006) Improved classification of soil salinity by decision tree on remotely sensed images, pp 60273K-60273K-60278
- Schietecatte W, Ouessar M, Gabriels D, Tanghe S, Heirman S, Abdelli F (2005) Impact of water harvesting techniques on soil and water conservation: a case study on a micro catchment in southeastern Tunisia. *J Arid Environ* 61(2):297–313. doi:[10.1016/j.jaridenv.2004.09.022](https://doi.org/10.1016/j.jaridenv.2004.09.022)
- SEOS (2014) Remote Sensing and GIS in Agriculture Vegetation Indices (NDVI, NDWI). <http://www.seos-project.eu/modules/agriculture/agriculturec01-s03.html>. Accessed 22 Mar 2017
- Sghaier M, Ouessar M, Belgacem AO, Taamallah H, Khatteli H (2010) Vulnerability of olive production sector to climate change in the governorate of Médenine (Tunisia). Final report. CI, GRASP project
- Srimani PK, Prasad SN (2012) Decision tree classification model for land use and land cover mapping—a case study. *Int J Curr Res*
- Tutiempo Network SL en.tutiempo.net, www.tutiempo.net/en/. Accessed 20 July 2016
- Vacca A, Loddo S, Melis MT, Funedda A, Puddu R, Verona M, Fanni S, Fantola F, Madrau S, Marrone VA, Serra G, Tore C, Manca D, Pasci S, Puddu MR, Schirru P (2014) A GIS based method for soil mapping in Sardinia, Italy: A geomatic approach. *J Environ Manag* 138:87–96. doi:[10.1016/j.jenvman.2013.11.018](https://doi.org/10.1016/j.jenvman.2013.11.018)
- Van der Meer FD, van der Werff HMA, van Ruitenbeek FJA, Hecker CA, Bakker WH, Noomen MF, van der Meijde M, Carranza EJM, Smeth JB de, Woldai T (2012) Multi- and hyperspectral geologic remote sensing: A review. *Int J Appl Earth Obs Geoinform* 14:112–128. doi: <http://dx.doi.org/10.1016/j.jag.2011.08.00>
- Vanonckelen S, Lhermitte S, Van Rompaey A (2013) The effect of atmospheric and topographic correction methods on land cover classification accuracy. *Int J Appl Earth Obs Geoinf* 24:9–21. doi:[10.1016/j.jag.2013.02.003](https://doi.org/10.1016/j.jag.2013.02.003)
- Vogiatzakis IN, Melis MT (2015) Changing perceptions in Mediterranean Geography: the role of geospatial tools. In: Theano S, Terkenli ADA (eds) *Connections, mobilities, urban prospects and environmental threats. The Mediterranean in transition*. Cambridge Scholars Publishing, Lady Stephenson Library, Newcastle upon Tyne, NE6 2PA, UK
- Waele J, Melis MT (2008) Geomorphology and geomorphological heritage of the Ifrane-Azrou region (Middle Atlas, Morocco). *Environ Geol* 58(3):587–599. doi:[10.1007/s00254-008-1533-4](https://doi.org/10.1007/s00254-008-1533-4)
- Zewdie W (2015) Remote sensing based multi-temporal land cover classification and change detection in northwestern Ethiopia. *Eur J Remote Sens* 121–139. doi:[10.5721/EuJRS20154808](https://doi.org/10.5721/EuJRS20154808)

Chapter 24

Evaluation and Validation of SRTMGL1 and ASTER GDEM2 for Two Maghreb Regions (Biskra, Algeria and Medenine, Tunisia)

Claudio Arras, Maria Teresa Melis, Gabriela-Mihaela Afrasinei, Cristina Buttau, Alberto Carletti and Giorgio Ghiglieri

Abstract In this paper, we present the comparison and validation of the Shuttle Radar Topography Mission Version 3.0 Global 1 Arc-Second (SRTMGL1) Digital Elevation Model (DEM) and the Advanced Spaceborne Thermal Emission and Reflection Radiometer Global Digital Elevation Model Version 2 (ASTER GDEM2) applied to two areas of Maghreb region (Biskra, Algeria and Medenine, Tunisia). These are the two target areas assessed in the frame of WADIS-MAR project (<http://www.wadismar.eu>), which is one of the five demonstration projects implemented within the Regional Programme SWIM (<http://www.swim-sm.eu>) and funded by the European Commission. Newly released SRTMGL1 is available for free download since October 2014 over the African continent through United States Geological Survey (USGS) web data tools. Given the previously reported issues regarding optical sources DEMs, SRTMGL1 can provide significant advantages in elevation modelling and geoscience applications, but studies regarding its quality assessment and validation are in their early infancy. We employed the two data sets in a visual and quantitative comparison and subsequently, their validation was conducted using ground control points (GCPs) collected within the target areas. Results show that SRTMGL1 presents an overall major accuracy and higher sensitivity to small-scale features and slight variations in landforms.

C. Arras (✉) · M.T. Melis · G.-M. Afrasinei · C. Buttau · A. Carletti · G. Ghiglieri
Department of Chemical and Geological Sciences, University of Cagliari,
Via Trentino 51, 09127 Cagliari, Italy
e-mail: cla.arras1@studenti.unica.it

A. Carletti
e-mail: nrd@uniss.it

G. Ghiglieri
e-mail: ghiglieri@unica.it

C. Arras · A. Carletti · G. Ghiglieri
Desertification Research Centre-NRD, University of Sassari, Viale Italia 39,
07100 Sassari, Italy

Keywords SRTMGL1 · ASTER GDEM2 · DEM · Validation · Maghreb region

Introduction

“Digital Elevation Model (DEM) is a computational representation of the continuous variation of relief over space from which topographic parameters can be digitally generated” (Jing et al. 2014). Several methods can be used to generate DEMs including airborne and satellite-borne stereoscopic photogrammetry, RADAR/SAR interferometry, Light Detection and Ranging (LIDAR) and other traditional approaches (e.g. GPS, levelled benchmarks) (Athmania and Achour 2014). In past decades, global DEMs have become invaluable sources of information in geosciences (Varga and Bašić 2015) especially in regions where, due to particular political or environmental issues, direct field surveys are difficult or even impossible.

The release of spaceborne ASTER and SRTM elevation datasets has provided significant advances in elevation modelling. These DEMs data are global, so they are available for the most part of populated world areas and are free of charge (download from <http://www.earthexplorer.usgs.gov>) at a spatial resolution of 1 arc-second for both sets (NASA SRTM Version 3.0 Global 1 arc-second dataset SRTMGL1 data released over Africa on October 2014, https://lpdaac.usgs.gov/about/nasa_shuttle_radar_topography_mission_srtm_version_30_global_1_arc_second_data_released_over). However, studies on the accuracy assessment of DEM data sets at local and regional scales are fundamental to understand their potential limitations related to particular purposes and applications (Jing et al. 2014).

In the present work, after a brief description of the study areas and the DEMs characteristics, we present the methodology and results for their visual and quantitative comparison and then their validation using GCPs collected in the target areas. This article contributes to the DEM accuracy literature because SRTMGL1, in particular, has begun its worldwide release in phases starting with September 2014 and studies regarding its quality assessment and validation are in their early infancy.

Study Areas

Arid and semi-arid regions of Maghreb suffer under dry climatic conditions and ongoing desertification processes. In particular, sand encroachment and soil salinization increasing phenomena (Afrasinei et al. 2015) affect the Medenine (Southern Tunisia) and Biskra (North-Eastern Algeria) regions, respectively. For this reason, these target areas have been selected within the frame of WADIS-MAR project (<http://www.wadismar.eu>) to realise an integrated water harvesting and managed aquifer recharge system. WADIS-MAR is one of the five demonstration projects implemented within the Regional Programme SWIM (<http://www.swim-sm.eu>), funded by the European Commission. In both areas, different elevation ranges and

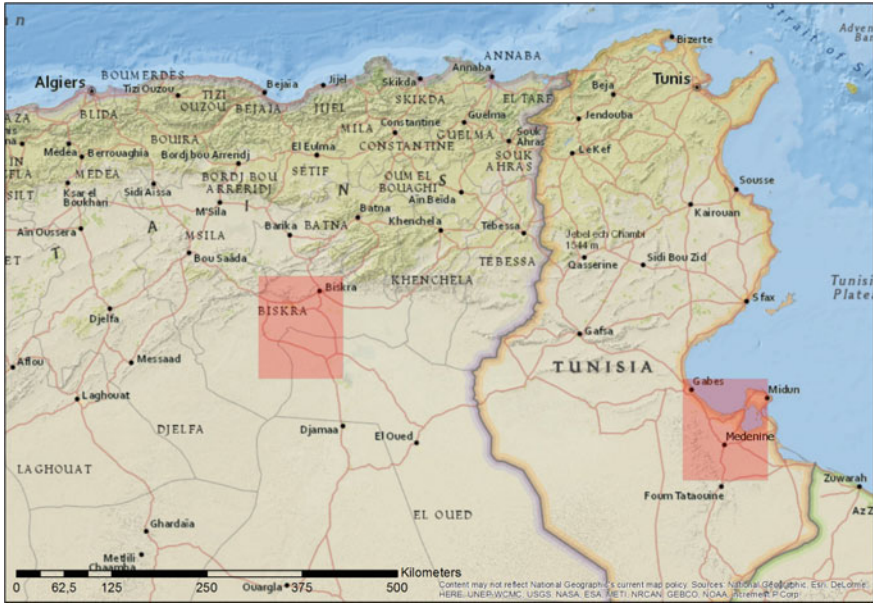


Fig. 24.1 Location of the study areas and DEM tiles extension

several morphological features are identified, ranging from mountains and hills to plains and depressions.

The Medenine area is characterised by the presence of a wide flat area, the Jeffara Plain. It is bordered by the Dahar Plateau to the Southwest, where the maximum elevation reaches about 700 m, and by the Mediterranean Sea to the Northeast where, close to the coastal line, elevations reach negative values corresponding to the *sabkhas* (Marini et al. 2008). The DEM tiles extend over 33°00'N to 34°00'N and 10°00'E to 11°00'E (geographic projection), covering an area of about 7.700 km² (excluding the sea area) (Fig. 24.1).

The Biskra area can be divided into two major domains: the Atlas Mountains to the North and the Sahara platform to the South. Elevations range from about 1100 m in the Atlas domain to about -70 m in the southeastern zone, where the Chott Melrhir depression is set. The DEM tiles extend over 34°00'N to 35°00'N and 5°00'E to 6°00'E (geographic projection), covering an area of about 10.200 km² (Fig. 24.1).

Digital Elevation Models

Two open source DEMs with same resolution and coverage were used for the present study purposes: (1) the Shuttle Radar Topography Mission Version 3.0 Global 1 Arc-Second (SRTMGL1) and (2) the Advanced Spaceborne Thermal

Table 24.1 Height statistics across the Medenine and Biskra regions extracted from SRTMGL1 and ASTER GDEM2 data sets

Study area	Model	Min (m)	Max (m)	Mean (m)	Std dev. (m)
Medenine	SRTMGL1	-37	700	107.11	145.7
	ASTER GDEM2	0	715	108.03	146.06
Biskra	SRTMGL1	-50	1070	154.40	116.55
	ASTER GDEM2	-77	1096	150.76	118.77

Emission and Reflection Radiometer Global Digital Elevation Model Version 2 (ASTER GDEM2).

The SRTMGL1 data set is the result of cooperative work between the National Imagery and Mapping Agency (NIMA) and the NASA (National Aeronautics and Space Administration) of United States (US). Elevations data were collected during an 11-day mission in February 2000, and measurements were undergone using the X-band and C-band Interferometric Synthetic Aperture Radar (InSAR) sensor (5.6 and 5.3 cm wavelengths, respectively). SRTM C-band data are available over Africa at $1^\circ \times 1^\circ$ tiles and 1 arc-second resolution (about 30 m) since 8 October 2014. Africa is the first continent to be released after the US and its territories as the global 1 arc-second data. The absolute vertical accuracy of the elevation data is 16 m (at 90% confidence) (Sulzer and Gspurning 2009).

ASTER GDEM was built up by the METI (Ministry of Economy, Trade and Industry) of Japan together with the NASA. It is provided at 1 arc-second resolution and is accessible for free since the 29 June 2009 (ASTER GDEM validation team (a)). The absolute vertical accuracy of the elevation data is 20 m (at 95% confidence) (Athmania and Achour 2014). A new data set, ASTER GDEM2, was released in (2011) with 260.000 overlapping images added to the original one. The aim was to enhance the spatial resolution and the water body coverage accuracy and to reduce the occurrence of data artefacts (ASTER GDEM validation team (b)).

Table 24.1 shows the SRTMGL1 and the ASTER GDEM2 statistics for both study areas.

Ground Control Points

DEMs accuracy assessment needs at least 20 measured elevation data with high precision in each major land cover category to obtain consistent results, as suggested by the American Society of Photogrammetry and Remote Sensing (ASPRS). For the study purposes, GCPs were collected in different ways depending on the study areas. For the Medenine region, 28 GCPs (Fig. 24.2a) were collected using an altimeter device during a survey campaign carried out in June 2014, while for the Biskra region were used 107 GCPs (Fig. 24.2b) derived from survey reports provided by the *Ministère des Ressources en Eau* (MdH 1980).

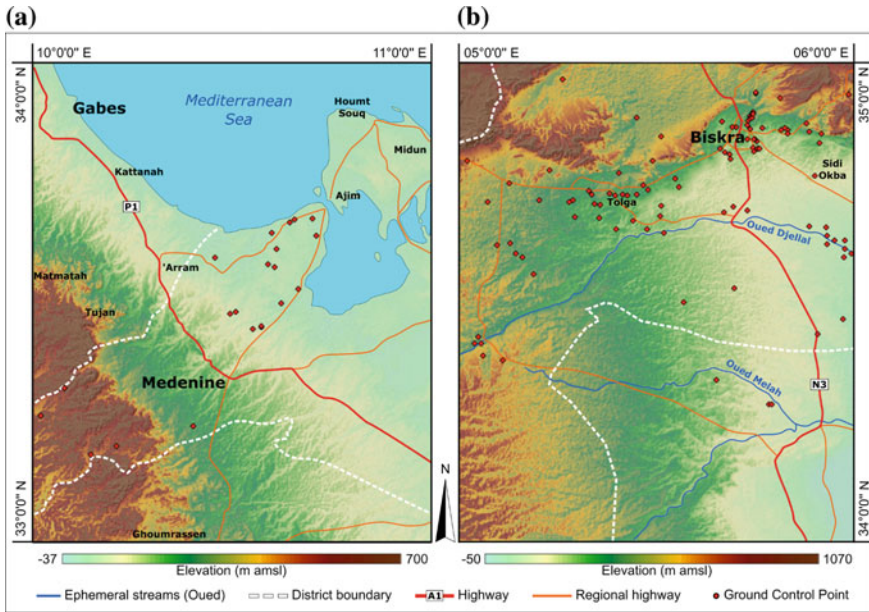


Fig. 24.2 Location of the GCPs plotted on the a Medenine and b Biskra hill-shaded SRTMGL1 data sets

Methodology

Objective of this study was to verify the vertical displacement between SRTMGL1 and ASTER GDEM2 through comparison methods and to assess their accuracy with respect to GCPs available within the study areas.

After downloading the SRTMGL1 and ASTER GDEM2 tiles for both the study areas, a pre-processing phase was required. Previous investigations have shown that DEMs are subjected to systematic horizontal shifts (Denker 2004; ASTER GDEM validation team 2009). Correct georeferencing and co-registration are necessary in order to ensure that corresponding pixels on images pair represent the same geographic location and the possibility of differences caused by shifts of unchanged object boundaries is excluded (Aleksandrowicz et al. 2014). The Universal Transverse Mercator (UTM) is selected as the projected reference system, where Zone 32 and Zone 31 correspond to the Tunisian and the Algerian DEM tiles, respectively. Subsequently, the two sets of images were verified for correct overlay and results showed that no horizontal shift existed between the two DEM tiles.

The processing phase includes a visual and quantitative comparison between DEMs and then their validation through GCPs. Visual comparison, which is based on the production of relative difference map and shaded relief map (Jing et al. 2014), aims to locate areas of significant vertical displacement between the two data sets and to identify large-scale systematic effect (Hilton et al. 2003) and artefacts

such as stripe effects. The quantitative comparison is based on geostatistical and statistical measures (Athmania and Achour 2014). The mutual correspondence (difference) between the models allowed the evaluation of possible significant systematic errors or outliers between the DEMs (Varga and Bašić 2015). For the pixel-to-pixel comparison, the “raster calculator tool” from ESRI ArcGIS was used and the difference between SRTMGL1 and ASTER GDEM2 was carried out. However, model validation using GCPs is the method that delivers consistent accuracy evaluation, on the condition that elevation data are independently set and of sufficient precision (Hirt et al. 2010). The DEMs elevation values were extracted corresponding to the GCPs locations and then, the subtracted values between the DEMs extracted values and the GCPs values were obtained using the ArcGIS “field calculator tool”.

Results

Figure 24.3 and Table 24.2 show the plot differences between SRTMGL1 and ASTER GDEM2 for (a) the Medenine and (b) Biskra region, respectively. Both the resulting images are characterised by a slight stripe effect oriented NNE-SSW. Hirt et al. (2010) ascribed this effect to the ASTER model. Further visual analysis on the images and statistics have shown that in the Biskra area, where both DEMs

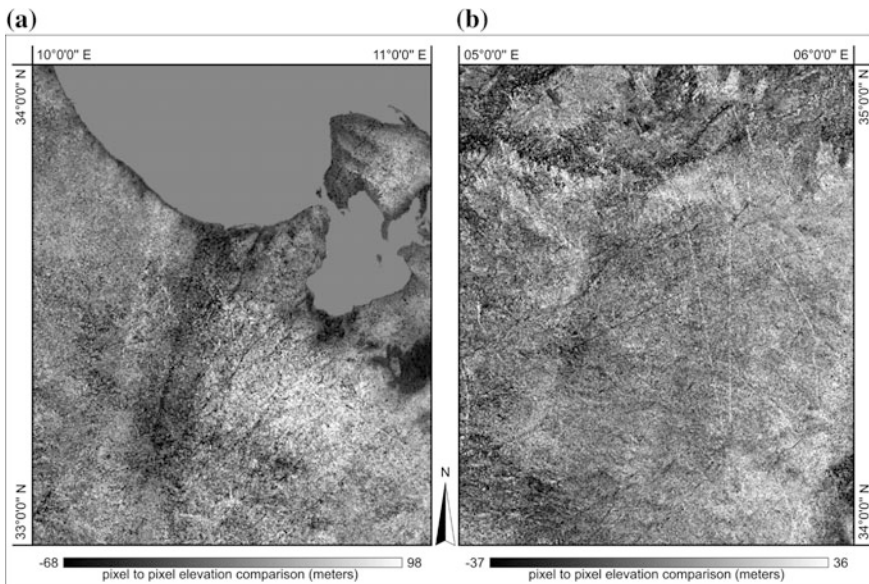


Fig. 24.3 Model-to-model (SRTMGL1–ASTER GDEM2) comparison results for the **a** Medenine and **b** Biskra regions

Table 24.2 Model-to-model comparison statistics for both the study areas

Study area	Max negative shift (m)	Max positive shift (m)	Mean (m)	Std dev. (m)
Medenine	-73	106	-0.9	6.17
Biskra	-108	116	3.64	6.67

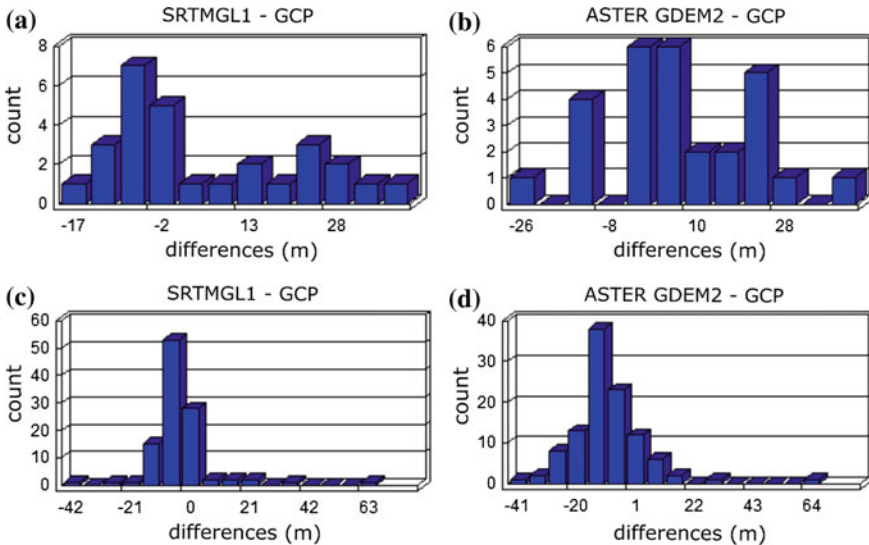


Fig. 24.4 Displacement distribution of the SRTMGL1 and ASTER GDEM2 data sets relative to the GCPs for the **a, b** Medenine and **c, d** Biskra regions

presented negative values over the *chott*, ASTER GDEM2 values were sparse and sporadic, unlike SRTMGL1 values that were uniform and all the negative values best fitted the depression area. In the Medenine area, both data sets showed zero values over the sea domain while only the SRTMGL1 managed to identify negative values corresponding to the *sabkhas*. This demonstrates a higher sensitivity of the radar sensing towards flat depression areas either endorheic or coastal.

Results of model validation through GCPs for both the study areas are illustrated in Fig. 24.4, Table 24.3 and Table 24.4, for Medenine and Biskra area, respectively. Mean Error (ME) was used as global accuracy measure. The accuracy assessment in the Medenine area shows that SRTMGL1 has a lower mean vertical bias (6.75 m) compared to the ASTER GDEM2 (8.07 m). In the case of the Biskra tile, SRTMGL1 was underestimated by about 1 m, while the ASTER GDEM2 model presents a negative shift of about 6 m. However, it must be mentioned that in Medenine area, SRTMGL1 presents a slightly major standard deviation with respect to ASTER GDEM2 while in the Biskra area the situation is the opposite. For a better understanding of displacement factors, a brief analysis of the influence of morphology has been undergone. We have taken into consideration the two

Table 24.3 Statistics of the model to GCP for both SRTMGL1 and ASTER GDEM2, respectively (Medenine area)

Study area	Comparison	Morphology	Max ⁻ (m)	Max ⁺ (m)	Mean (m)	Std dev. (m)
Medenine	SRTMGL1–GCP	Total coverage	-17	42	6.75	16.01
		Plain/coastal domain	-17	35	3.47	14.09
		Mountain domain	-5	42	21.8	15.74
	ASTER GDEM2–GCP	Total coverage	-26	44	8.07	15.20
		Plain/coastal domain	-26	26	5	13.66
		Mountain domain	7	44	22.2	13.92

Table 24.4 Statistics of the model to GCP for both SRTMGL1 and ASTER GDEM2, respectively (Biskra area)

Study area	Comparison	Morphology	Max ⁻ (m)	Max ⁺ (m)	Mean (m)	Std dev. (m)
Biskra	SRTMGL1–GCP	Total coverage	-42	69	-1.25	11.32
		Plain domain	-18	41	-0.91	9.77
		Mountain domain	-42	69	-1.83	12.76
	ASTER GDEM2–GCP	Total coverage	-41	67	-6.38	13.02
		Plain domain	-30	32	-7.29	11.60
		Mountain domain	-41	67	-5.63	14.35

major morphologies in both areas, namely mountain and plain domains. Table 24.3 presents the statistics summary for Medenine area, where SRTMGL1 model-to-GCP difference shows the maximum negative displacement located in the plain area, whereas the max positive one, in the mountain domain. In Table 24.4, correspondent to Biskra area, SRTMGL1 presents both max negative and positive shifts in the mountain domain.

Given the fact that the ASTER GDEM2 shows the same shift pattern, one of the immediate explanations can be the fact that in the Medenine area there were only 5 of 28 GCPs in the mountain domain, too scarce to provide valid statistics. Another explanation could be that SRTMGL1 and ASTER GDEM2 data sets are more erroneous in high elevation zones, as reported by Mukherjee et al. (2013). In the Biskra area, GCPs were distributed relatively even in the two landforms and the

results are slightly different than the ones in the Medenine area. The aforementioned standard deviation results may be influenced by the small amount of GCPs used in the Medenine area and their concentration in the plain coastal sector, but it may be also given by the presence of outliers that SRTMGL1 presents because of its high sensitivity to lowland features, while in the ASTER GDEM2 data these are completely absent. However, for model-to-GCP comparison, both models present the minimum shift values (close to 0) in the plain coastal sector in Medenine area but in the Biskra area, these are found in the mountain domain (not presented in the statistic table), that would confirm a problem related to the different characteristics of the sets of GCPs used in the two areas.

Conclusions

Digital Elevation Model represents one of the most valuable data set for geomatics and geoscientific purposes ranging from environmental to anthropogenic applications (Toutin 2008) and examples of attributes which can be extracted from them include (Gomasasca 2004):

- topographic and geomorphic data as slope and aspect for geological analysis on slope stability;
- hydrological data as hydrographic network and watershed which become input data for hydrological modelling on superficial runoff and flood simulations.

DEMs are also useful for the detection and estimation of landslides or lava flows volumes based on variations of elevations between two DEMs taken before and after the events. Undoubtedly, the quality of the obtained attributes depends on the accuracy of the DEMs data.

In this study, both the spaceborne ASTER GDEM2 and SRTMGL1 (newly released over Africa since October 2014) data set were employed in a visual and quantitative statistical comparison between each other, after which their accuracy was assessed using GCPs. Either visual or statistical comparison detected discrepancies between the two DEMs related to artificial error patterns ASTER GDEM2 data (stripes and cloud anomalies), being constructed from optical stereo imagery. The results of the model accuracy assessment through GCPs allow us to understand the behaviour of each DEM in different environments: coastal (flat areas) and inner-land (mountain areas). The results show the possible presence of outliers that do not have the same distribution pattern in the two study areas. This provides information on the advantages and drawbacks of SRTMGL1 which may present higher outliers in the mountain domain but a higher precision in lower landforms, on the one hand. On the other hand, we can infer that ASTER GDEM2 is affected by cloud cover and is often altered by the presence of artefacts. It shows lower precision or inability to identify certain features hence, smaller outliers are given by the standard deviation analysis.

The aforementioned arguments confirm that DEMs developed from optical sources such as ASTER GDEM2 and aerial photography may be negatively impacted by certain factors. In contrast, SRTMGL1 data penetrates clouds and are more sensitive to small-scale features, but both of them are sensitive to the top of impervious or high vegetation features even if SRTMGL1 to a lesser extent. This could also be explained by the fact that SRTMGL1 has void-filled data.

To cope with these issues and to understand the reason of the outliers' occurrence, a future step would be to identify them and to assess to which extent it is important to validate the results before and after their removal.

Acknowledgements We wish to acknowledge the TeleGIS Laboratory team, University of Cagliari (Italy) and the WADIS-MAR team for the possibility of conducting the current research. We also wish to thank the Tunisian and Algerian WADIS-MAR partners, IRA, ITDAS and ANRH for the provided data and information.

References

- Afrasinei GM, Melis MT, Buttau C, Bradd JM, Arras C, Ghiglieri G (2015) Diachronic analysis of salt-affected areas using remote sensing techniques: the case study of Biskra area, Algeria. In: Proceedings of SPIE 9644, earth resources and environmental remote sensing/GIS applications VI, 96441D, 20 Oct 2015. doi:[10.1117/12.2194998](https://doi.org/10.1117/12.2194998)
- Aleksandrowicz S, Turlej K, Lewiński S, Bochenek Z (2014) Change detection algorithm for the production of land cover change maps over the European Union countries. *Remote Sens* 6(7):5976–5994
- ASTER GDEM Validation Team (a) ASTER Global DEM validation-summary report (2009). <https://ersdac.or.jp>
- ASTER GDEM Validation Team (b) ASTER Global Digital Elevation Model Version 2—summary of validation results 2011. <https://www.lpdac.usgs.gov/>. Accessed 9 Jan 2013
- Athmania D, Achour H (2014) External validation of the ASTER GDEM2, GMTED2010 and CGIAR-CSI-SRTM v4. 1 free access digital elevation models (DEMs) in Tunisia and Algeria. *Remote Sens* 6(5):4600–4620
- Denker H (2004) Evaluation of SRTM3 and GTOPO30 terrain Data in Germany. In: Jekeli C et al (ed) GGSM 2004 IAG international symposium Porto, Portugal. Springer, Heidelberg, pp 218–223
- Gomarasca MA (2004) Elementi di geomatica. Associazione Italiana di Telerilevamento, 618
- Hilton RD, Featherstone WE, Berry PAM, Johnston CPD, Kirby JF (2003) Comparison of digital elevation models over Australia and external validation using ERS-1 satellite radar altimetry. *Aust J Earth Sci* 50(2):157–168. doi:[10.1046/j.1440-0952.2003.00982.x](https://doi.org/10.1046/j.1440-0952.2003.00982.x)
- Hirt C, Filmer MS, Featherstone WE (2010) Comparison and validation of the recent freely available ASTER-GDEM ver1, SRTM ver4. 1 and GEODATA DEM-9S ver3 digital elevation models over Australia. *Aust J Earth Sci* 57(3):337–347
- Jing C, Shortridge A, Lin S, Wu J (2014) Comparison and validation of SRTM and ASTER GDEM for a subtropical landscape in Southeastern China. *Int J Digit Earth* 7(12):969–992, doi:[10.1080/17538947.2013.807307](https://doi.org/10.1080/17538947.2013.807307)
- Marini A, Melis MT, Pitzalis A, Talbi M, Gasmi N (2008) The geomorphic units map of the Medenine Region (southern Tunisia). La carta della unità geomorfologiche della regione di Medenine (Tunisia meridionale). *Mem. Descr. Carta Geol. d'It.* LXXIII, pp 153–168

- MdH – Ministère de l'Hydraulique (1980) Carte hydrogéologique de Biskra au 1/200.000, notice explicative. Direction des études de milieu et de la recherche hydraulique – Service Hydrogéologie
- Mukherjee S, Joshi PK, Mukherjee S, Ghosh A, Garg RD, Mukhopadhyay A (2013) Evaluation of vertical accuracy of open source digital elevation model (DEM). *Int J Appl Earth Obs Geoinf* 21:205–217. doi:[10.1016/j.jag.2012.09.004](https://doi.org/10.1016/j.jag.2012.09.004)
- Sulzer W, Gspurning J (2009) High mountain geodata as a crucial criterion of research: case studies from Khumbu Himal (Nepal) and Mount Aconcagua (Argentina). *Int J Remote Sens* 30(7):1719–1736
- Toutin T (2008) ASTER DEMs for geomatic and geoscientific applications: a review. *Int J Remote Sens* 29(7):1855–1875. doi:[10.1080/01431160701408477](https://doi.org/10.1080/01431160701408477)
- Varga M, Bašić T (2015) Accuracy validation and comparison of global digital elevation models over Croatia. *Int J Remote Sens* 36(1):170–189

Chapter 25

An Integrated Cost–Benefit and Livelihood Approach for Assessing the Impact of Water Harvesting Techniques (WHTs) on Livelihoods: A Case Study in the Oum Zessar Watershed, South-East Tunisia

Mohamed Arbi Abdeladhim, Mongi Sghaier, Luuk Fleskens and Mohamed Ouessar

Abstract Despite broad interest in use of water harvesting techniques (WHTs) to reduce pressure on natural resources in arid zones, few ex post assessments are available on how WHTs impact livelihood sustainability. This paper assesses the impact of WHTs on the livelihood conditions of inhabitants in the Oum Zessar watershed in south-east Tunisia. We used an integrated impact assessment (IIA) framework incorporating extended cost–benefit analysis (ECBA) and the sustainable livelihoods approach (SLA). The former internalizes environmental impacts while the latter enables assessment of the contributions of WHTs to rural livelihoods in the watershed. We began by using ECBA to estimate the profitability of investments in WHTs. We then scaled up our impact perspective from the local level to the watershed level using SLA based on survey data from beneficiary households upstream, midstream and downstream. Our goal was to better understand and evaluate changes in livelihoods and associated environmental effects. We focused on the links between cost–benefit of WHTs and sustainable livelihoods, looking in particular at the capitals that connect the two. Our ECBA results suggest that WHT techniques did benefit the local population at both the private and the social level (IRR > 20%; NPV > 2000 TD/ha). Sensitivity analysis confirmed this result. SLA findings point to a central role of social capital in promoting sustainable livelihoods, followed by physical capital enhanced by WHTs construction,

M.A. Abdeladhim (✉) · M. Sghaier · M. Ouessar
Institu des Régions Arides (IRA), Medenine, Tunisia
e-mail: mohamed.abdeladhim@wur.nl

M.A. Abdeladhim · L. Fleskens
Soil Physics and Land Management (SLM), Wageningen University,
Wageningen, The Netherlands

especially in the upstream and downstream segments of the watershed. Recommendations were derived from these outcomes for more integrated watershed management policy.

Keywords Water harvesting techniques · Sustainable livelihoods approach (SLA) · Extended cost–benefit analysis (ECBA) · Externalities · Oum Zessar watershed · Tunisia

Introduction

Population growth, climate change and changes in consumer behaviour associated with globalization have exerted substantial pressure on Tunisia's natural resources (Abaab 1986; Abaab and Guillaume 2004; MARH and GIZ 2012; MEDD 2006). This is particularly true in the Oum Zessar watershed in the arid south-east of the country. There, these drivers have combined to effect environmental changes, oftentimes associated with natural resources degradation. Green and blue water scarcity is especially rife, and climatic factors have undermined crop yields, with knock-on effects on local socio-economic conditions (Gamoun et al. 2015).

To stimulate development at the national and regional levels, the government has enacted various programmes related to natural resources management and agricultural modernization. Examples are the soil and water conservation strategies of 1991–2000 and 2001–2010 and the current national strategy for climate change adaptation (MARH and GIZ 2012). These policies have aimed to reduce the pressures exerted on natural resources, especially land and water, and enhance the capacities of local populations to adapt to climate change and to improve local socio-economic conditions.

Successful implementation of sustainable development strategies, such as those related to soil and water conservation and natural resources management, nonetheless continues to be hampered by weak evidence of their impact on livelihood conditions. For example, most previous studies in south-east Tunisia have focused on on-site biophysical (Ouassar et al. 2009) and socio-economic costs and benefits (Fleskens et al. 2002, 2005; Schiettecatte et al. 2005; Sghaier et al. 2002), without relating these to economic profitability or effects on the livelihood conditions of local inhabitants. Fleskens et al. (2005) measured WHTs' effects on olive yields in an upstream area of the Oum Zessar watershed and calculated the on-site costs and benefits of WHT implementation. Ouassar et al. (2009) modelled the effects of WHTs on the catchment water balance using a soil and water assessment tool (SWAT). The SWAT was calibrated and validated using data from 38 runoff events. In south-east Tunisia, Sghaier et al. (2002) applied an interdisciplinary approach based on the Forces-MOD model, conceived by the World Bank and the Food and Agriculture Organization of the United Nations (FAO), and an extended cost–benefit analysis (ECBA) to evaluate the costs and benefits of WHTs in the Oum Zessar watershed.

Despite the above studies, the off-site effects, adjacent and downstream of WHTs, remain poorly understood and quantified. Indeed, moving from the exclusive study of on-site impacts, to include off-site effects, requires an understanding of the complex biophysical interactions within a watershed, as biophysical and socio-economic downstream effects must also be predicted.

In the current study, we incorporated on-site and off-site impacts by integrating two methods: ECBA and the sustainable livelihood approach (SLA). Our objective was to assess the economic profitability of WHTs and to analyse the impacts of WHTs on livelihood conditions in the Oum Zessar watershed. Cost–benefit analysis (CBA) has often been applied to support decision-making, as it provides information on the direct impacts of land management practices, though without taking into account wider effects on livelihood conditions. SLA is a tool for helping us understand the factors that influence people’s capacity to achieve sustainable development in particular circumstances. It differs from conventional evaluation methodologies in that it focuses on well-being rather than the financial outcomes of an intervention. Wellbeing encompasses not only income, but also physical, natural, social and human assets (Côté and Healy 2001).

Our approach compared the outcomes of analyses using SLA and conventional ECBA. Use of SLA to examine livelihoods may reveal how a natural resources management intervention melds with livelihood strategies, and how projects might enhance or constrain people’s livelihoods. Thus, the integrated approach presented here sought a scaled up understanding of land management impacts based on WHTs, from the farm level to the watershed level.

Background

The Oum Zessar Watershed

We carried out our study in the Oum Zessar watershed, Governorate of Medenine, south-east Tunisia (Fig. 25.1). Rural inhabitants of the Oum Zessar watershed face harsh environmental conditions. Indeed, aridity, water scarcity, lack of livelihood options and population growth pose serious challenges. The watershed, however, is important due to its strategic location and contribution to the regional economy. Furthermore, it provides key environmental services, as it harbours pastoral resources, is a source of honey and aromatic and medicinal plants and offers productive hunting grounds. Furthermore, the watershed plays a role in carbon sequestration, climate regulation and soil and water conservation. Finally, it has a cultural role as an ecotourism destination and seat of intellectual and spiritual inspiration (Ouled Belgacem et al. 2011). Watershed inhabitants have demonstrated themselves to be highly resilient despite their harsh surroundings.

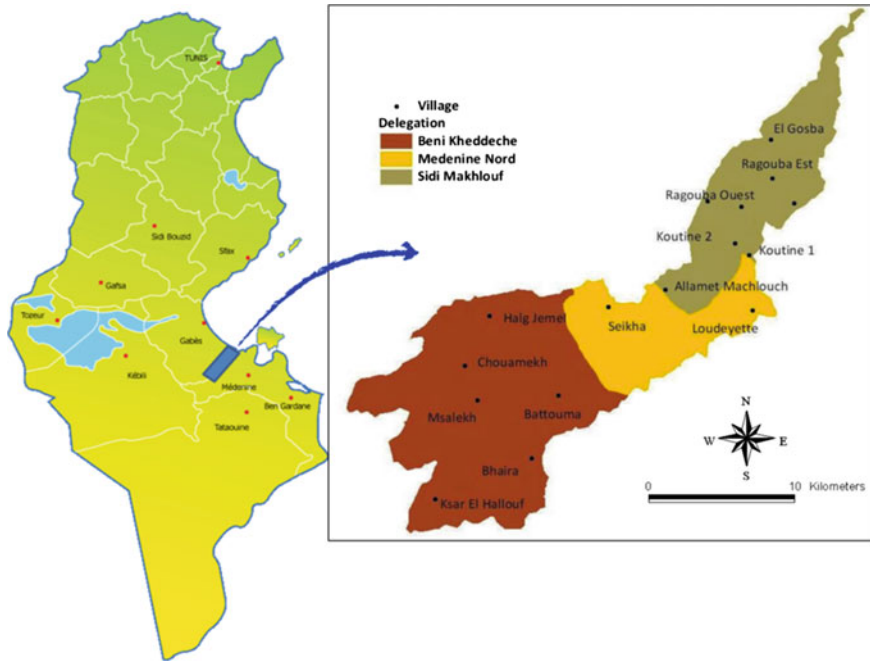


Fig. 25.1 Location of the Oum Zessar watershed in the Province of Medenine

Administratively, the Oum Zessar watershed stretches over the territory of ten villages, under three districts, namely, Beni Khedache (three upstream villages), Medenine North (three midstream villages) and Sidi Makhlouf (four downstream villages).

Three major hydro-geophysical zones characterize the watershed:

- an upstream, mountainous zone corresponding to the administrative territory of the Beni Khedache district;
- a midstream zone starting from the Bhayra Chouamakh region at the foot of the mountainous zone and corresponding to part of the administrative territory of the Beni Khedache and Medenine North districts;
- a downstream zone from Koutine to the sea (Gulf of Gabes), corresponding to the administrative territory of the Sidi Makhlouf district.

The site under study experienced rapid land use change and transformation of the agrarian system in its recent history. These changes in turn have affected both livelihood conditions and the natural environment. Primary concerns are the negative impacts of land use changes on soil fertility, diminishing incomes from production and increasing competition for water (Pinstup-Andersen and Pandya-Lorch 1998; Sghaier et al. 2012a). Rainfall distribution is irregular in the study area. Annual precipitation is very low, 160 mm on average. Successive dry

Table 25.1 Population of the Oum Zessar watershed by district

District	Population 2004	Population number 2014
Beni Khedache	6978	6320
Medenine North	11736	13371
Sidi Makhlouf	5783	6149
Total	24497	25839

Source (INS 2014)

years, irregular rainfall and extreme climate events are factors driving land degradation in the area. As a result, there is little water available for plant growth, low biomass production and grain yield, and in consequence, little vegetative protection of soils (Ouassar et al. 2009).

Total population of Beni Khedache, Medenine North and Sidi Makhlouf nonetheless grew from 100,400 inhabitants in 2004 to 108,900 inhabitants in 2014 (INS 2014). Medenine Nord, with a population density of 101–200 persons per sq km, is the most densely populated district, followed by Sidi Makhlouf, with 51–100 people per sq km. Beni Khedache, with a density of just 11–25 persons per sq km, is the most sparsely populated district. This is explained by the massive rural exodus from Beni Khedache due to natural resources degradation and lack of job opportunities. Some 24% of the three districts' total population resides in the Oum Zessar watershed (Table 25.1).

Agriculture in the Oum Zessar watershed is characterized by the coexistence of irrigated and rainfed production (cereals, fruits, etc.) with pastoralism (rangeland). However, land uses have changed with the privatization of the traditional collective lands and evolution towards a more intensive agro-pastoral system (Sghaier et al. 2012b).

Methods

The current study applied an integrated impact assessment (IIA) framework consisting of an extended cost–benefit analysis (ECBA) and the sustainable livelihoods approach (SLA). The ECBA was used to internalize environmental impacts. Conventional CBA is a decision support tool for assessing the social and economic costs and benefits associated with an existing or proposed project, programme, or policy over a given period. CBA compares the present value of a stream of benefits (positive effects) with the present value of all investments and recurrent costs (negatives) (Akroush et al. 2014; Ranasinghe 1994, 1997). ECBA extends CBA by including the social and environmental impacts of a proposed project, programme or policy, thus incorporating indirect effects as well. Typical ECBA consists of multiple stages: (i) problem definition (i.e. what are the project objectives, what are the alternatives, whose welfare is considered and over what time period),

(ii) identification of the project's physical impacts (i.e. environmental impact analysis), (iii) valuation of impacts, (iv) discounting of cost and benefit flows, (v) selection of the project to be implemented based on the net present value test and (vi) sensitivity analysis (i.e. determination of the robustness of the outcomes to small changes in parameter values) (Kuosmanen and Kortelainen 2007).

Our ECBA took into account external economic and environmental phenomena, and considered tangible as well as intangible effects of soil and water conservation programme interventions involving WHTs and undertaken since 1980s in the Oum Zessar watershed. We considered only jessour,¹ as this was the most widely used WHT in the area. Two evaluation criteria were considered: the net present value (NPV) and the internal rate of return (IRR). Each provided a single figure representing the impact of a project on economic welfare. However, each provided slightly different information. The NPV was used to estimate the total welfare gained over the service life of a project, while the IRR was used to quantify the rate of benefit realized. Both measures are widely applied in CBA (Wholey et al. 2010).

Our data for the ECBA were derived from a statistical database maintained by the regional directorate for agricultural development (CRDA 2013) and from a socio-economic and technical survey conducted during 2012–2013 in the Oum Zessar watershed among beneficiaries of the soil and water conservation programme. Fifteen beneficiary households were selected for interviews from three representative sub-catchments (Chaabat el Anez, Beni Khedache, upstream in the watershed; Eloudayet, Medenine Nord, midstream in the watershed; and Oued Moussa, Sid Makhlouf, downstream in the watershed). Sub-catchments and beneficiary households were chosen during a 1-day workshop attended by scientists and policymakers.

The survey posed questions on the type of intervention (new implementation or rehabilitation of a WHT), investment costs, maintenance costs and crop yields at the household and farm levels. Prices were gathered from rural markets and interviews with farmers. We used averages of data collected from those interviewed. All prices were expressed in Tunisian dinars (TDs; 1 US dollar = 2.027 TDs). Costs and returns were estimated for each component, both upon its implementation and, hypothetically, effects if the intervention had not been implemented, over a 30 year period. Results were reported per hectare. The rather long, 30 year, time horizon was considered appropriate because the benefits accruing from investments in WHTs in general, and particular those associated with tree production, appear only after a long period (Fleskens et al. 2005). A range of discount rates (8, 10 and 12%) were applied in the sensitivity analysis.

Supplementing our ECBA results, we applied SLA, which is an analytical tool for assessing the impact of a programme or intervention on people's ability to achieve sustainable development in their particular circumstances. SLA is based on

¹'Jessour' is the plural of a *jesr* which is a typical macro-catchment WHT encountered in the mountains of Matmata, south-east Tunisia. A *jesr* is made up of a small dyke to retain runoff and sediments, alongside a terrace (cropping area) and the impluvium (catchment area) (Ouessar et al. 2009).

five capital assets with which livelihoods are considered to be built: social, human, physical, financial and natural. Enhancing these capital assets is viewed as an avenue to improved wellbeing (Baumann 2002). We applied SLA to explore interdependencies between the assets and activities on which the inhabitants of our study area depended for their livelihoods (Dearden et al. 2002; Karl et al. 2002; Norton and Foster 2001). The analysis considered WHTs to be physical capital. We thus assessed the impact of this physical capital on the wellbeing of Oum Zessar watershed inhabitants.

To evaluate the five types of livelihood capital in the upstream, midstream and downstream segments of the watershed, we made use of data from a socio-economic survey (139 households interviewed) conducted in 2012–2013. The survey population was all inhabitants of the Oum Zessar watershed which had benefited directly or indirectly from a public or private water harvesting unit. Our sampling procedure consisted of two steps. The first step was a triple stratification of the watershed into biophysical zones, administrative zones and farm types. The second step was systematic sampling by randomly drawing a number of farms proportional to the total population in each class from a list of farmers provided by the regional commissariat of agricultural development. Finally, 59 households from Beni Khedache (upstream), 33 households from Medenine Nord (midstream) and 47 households from Sidi Makhlouf (downstream) were selected. Interviewers approached the households and asked them questions regarding the effects of WHT technologies on human, social, natural, financial and physical assets. The beneficiaries were also asked questions regarding the livelihood assets with WHT implementation and, hypothetically, if WHTs had not been implemented. Our set of indicators was adapted from the land degradation assessment in drylands (LADA) tool (Nachtergaele et al. 2010) (Table 25.2).

Table 25.2 Indicators surveyed in SLA, by types of livelihood capital

Natural capital	Financial capital	Physical capital	Human capital	Social capital
Number of livestock	Agriculture income	Number of WHTs (jessour)	Education level	Membership of local associations (NGOs)
Farm size	Livestock income	Ownership of ploughing equipment	Household size	Distance to nearest hospital
Land quality	Off-farm income		Age of household head	Certificate of land ownership
Water quality			Annual household expenditure	Access to drinking water network
Number of olive trees				

Using the survey outcomes, a scoring session was held with scientists and experts from the Institute of Arid Regions. Ten experts participated, representing a variety of disciplines. The scoring exercise consisted of five steps. In step 1, a list of the main indicators representing WHT-related livelihood assets was developed. In step 2, indicator values were calculated from the survey data. In step 3, each participant gave each indicator a score from 0 to 100, regarding the current state of livelihood assets. In step 4, an average score was calculated for the whole watershed and for each watershed segment (i.e. upstream, midstream and downstream). Finally, in step 5, a pentagon diagram was elaborated depicting an average household profile in each segment of the catchment and overall.

Results and Discussion

Economic Profitability of WHTs

The investment costs of jessour implementation encompass dyke and spillway construction and maintenance. Digging planting holes for olive trees are another cost aspect, as is the purchase of tree saplings and outlays for watering, manure and labour (Fleskens et al. 2005). Locally sourced inputs (sand, stone and cement) were also considered construction costs (Table 25.3). Maintenance costs include allowances for dyke repairs and spillway height adjustments and supplemental irrigation for maintaining the productive capital (olive trees) during dry years, as the terraced areas are used mainly for growing olive trees. In years with sufficient autumn precipitation, the impluvium provides moisture for cereal cultivation and for grazing as well.

To quantify future maintenance costs and yields of jessour, six hypotheses were applied:

H1: The cultivated area represents 30% of the total area, with the rest being impluvium and tracks.

H2: The number of olive trees remains constant into the future.

H3: The farmer provides supplemental irrigation to preserve olive trees during drought periods, implying that maintenance costs must include the cost of such additional irrigation.

H4: Annual maintenance costs equal 5% of the total investment cost.

H5: Maintenance costs every fifth year equal 20% of the total investment cost; this corresponds to outlays required to prevent spillway destruction in a heavy rainfall event.

H6: Crop production (barley, watermelon, etc.) was taken into account once every 4 years, given that the probability of three successive dry years is small.

As shown in Tables 25.4 and 25.5, we ran the CBA at three levels: financial, economic and extended. The financial analysis used market prices and dealt with private interests. The economic analysis used shadow prices and dealt with societal

Table 25.3 Jessour investment costs, comprising outlays for development and maintenance

	Input type (per jessour)	Specification	Units	Value (TD)	
Construction costs	Labour	Dyke construction	Labour days	100	
		Spillway construction	Labour days	50	
		Planting holes	Labour days	40	
Total				190	
	Local intermediate consumption	Sand	Kilogramme	156	
		Cement	Sack	110	
		Stone	Vehicle	160	
		Plants	Number	25	
		Mechanical works			120
		Total (TD)			
Maintenance costs					
	Supplemental irrigation			40	
	Annual maintenance costs (5% of total implementation cost)			36	
	Maintenance cost every 5 years (20% of total implementation cost)			144	
Total				220	
Total investment				980	

Table 25.4 Internal rate of return (IRR) and sensitivity analysis for investments in water harvesting techniques (WHTs) at the farm level

	IRR (%)		
	Observed	Costs (+10%)	Benefits (-20%)
Financial CBA (%)	24	27	21
Economic CBA (%)	27	22	23
Extended CBA (%)	23	21	20

Table 25.5 Net present value (NPV) of investments in water harvesting techniques (WHTs)

	NPV (TD)				
	12%	10%	8%	Costs (+10%)	Benefits (-20%)
Financial CBA	2,491	3,615	5,231	2,340	1,691
Economic CBA	3,023	4,283	6,092	2,884	2,140
Extended CBA	2,073	3,027	4,402	1,910	1,333

interests. Finally, the extended CBA incorporated environmental externalities. Findings were reported on a per hectare basis.

The financial analysis found an IRR of 24% and a positive NPV of 3,615 TD/ha, using a 10% discount rate. These results represent the effectiveness of WHTs at the household level, despite the heavy investments required, the delayed benefits of tree crops and the adverse environmental conditions and climatic fluctuations.

Moving up from the financial analysis to the economic analysis, the market prices of costs and benefits were adjusted to reflect their social value. Market distortions were also reduced (subsidies, transfer payments, taxes, etc.). These adjustments were performed using conversion factors adapted to the Tunisian context (Belli et al. 2001).

Taking into account the social context, the WHT interventions became more valuable, with a NPV of 4,283 TD/ha (discount rate of 10%) and an IRR of 27%. This was a clear improvement compared to the financial analysis (Tables 25.2 and 25.3). When market distortions were reduced, WHTs became more profitable, suggesting that the soil and water conservation strategy as a whole would become more effective too.

Finally, an extended CBA was applied. Only one type of off-site impact was considered, i.e. flooding as a negative consequence of WHT infrastructure. Incorporation of this consideration slightly reduced the IRR and NPV, respectively, from 27% and 3,615 TD/ha to 23% and 3,027 TD/ha. The ECBA shows that, despite environmental externalities in the form of increased flood damage, WHTs did benefit the local population at both the household and societal levels.

Sensitivity analysis yielded somewhat varied outcomes with different discount rates. But this did not affect the general trend, even when the off-site effects were incorporated into the analysis (see Tables 25.3 and 25.4). Results also remained robustly positive using the higher discount rate of 12% (NPV of 2,073 TD/ha) and incorporating reduced benefit (i.e. in the case of ECBA considering greater flooding damage due to failure of jessour) (NPV of 1,333 TD/ha and IRR of 20%). The profitability of WHTs thus seemed quite satisfactory, despite the considerable investment required and rather low agricultural yields after implementation. However, it is difficult to identify and internalize all external positive and negative effects (e.g. groundwater recharge and salinity reduction, sedimentation and erosion prevention, etc.), due to lack of data on the economic valuation of ecosystem goods and services provided by WHTs and reflecting the value of natural capital.

Impacts on Livelihood Conditions

We went on to explore how the soil and water conservation programme, in particular WHT implementation, impacted livelihood conditions. Pentagon diagrams (Fig. 25.2) show that the livelihood assets in the watershed as a whole and in the three segments (upstream, midstream and downstream) were expected to change during the coming 15 years, according to the interviewees. Indeed, the natural

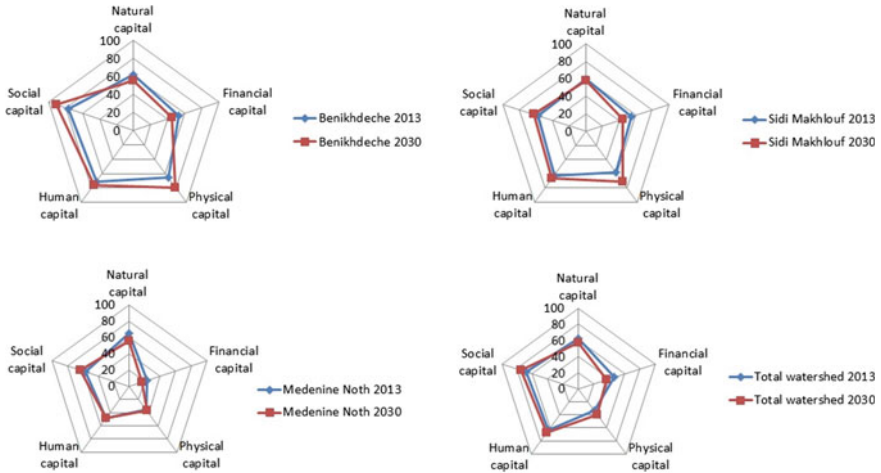


Fig. 25.2 Pentagon diagrams depicting the five types of livelihood capital for an average household profile in each catchment area and overall

capital was expected to decline, while human, social, physical and financial capitals were expected to rise.

At the whole watershed level, average scores for the future were higher than those for the present regarding social, human and physical assets (Fig. 25.2). On a 0–100 scale, social, human and physical, respectively, will increase from 68, 63 and 62 to 75, 67 and 69. Conversely, a decrease of natural assets was expected due to anthropogenic pressures.

In the three catchment segments (upstream, midstream and downstream), in the current situation, social capital was found to be predominant, with respective scores of 77, 56 and 58, followed by physical capital, which was most available upstream (in the Beni Khedache district, with a score of 65) and downstream (in the Sidi Makhlouf district, with a score of 71) (Fig. 25.2).

Thus, stakeholders’ expectations suggest increasing human capital in the watershed, because of enhanced education and improvements in living conditions. New WHTs were expected to help stem the rural exodus as well, due to their effect in enhancing local living conditions. Increased pressure on governments was anticipated to lead to provision of a wider range of rural social services. Expectations of financial capital were lower, due to relatively low agricultural and livestock incomes. This went hand in hand with the expectation that natural capital would slowly diminish.

To summarize, Fig. 25.3 presents the trends of the five types of capital in the study area over time. Households were optimistic concerning four types of capital (human, social and physical), as these were expected to increase. Natural capital was expected to decline over time, due to increased pressure on natural resources, particularly water, soil and vegetation. WHT implementation was expected to

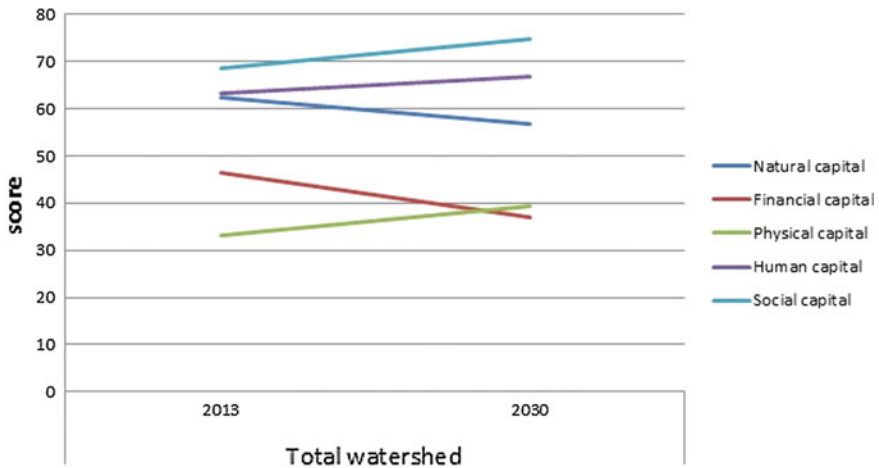


Fig. 25.3 Trends in the five types of livelihood capital over time

modestly diminish natural resources degradation, but it was not expected to be able to maintain the current situation, given the harsh environmental realities in the watershed.

Conclusion

This paper presented an IIA framework incorporating ECBA and SLA and used the method to assess the impact of WHT implementation on livelihood conditions in the Oum Zessar watershed in Tunisia. Coupling the two methods proved useful in this case. It enabled us to first quantify the impact of WHTs implementation and second to scale up our impact assessment from the farm level to the regional level and to explore effects on different types of capital considered to influence the wellbeing of the local population. The very multifunctionality of WHTs dictates an urgent need to adopt such IIA methods, to effectively support land management strategies. Indeed, the scientific community increasingly views IIA methods as a way to expand the information base for policy and address the complex issues posed by sustainable livelihood development.

The Oum Zessar watershed faces a multitude of environmental problems and challenges that far exceed the resources available to reverse current trends. What is required is a fully integrated development plan that takes into account all the necessary technical, agricultural, socio-economic, political and institutional aspects of natural resources management. The integrated impact assessment framework applied here could be a useful tool for livelihood strategy assessments. The findings presented in this paper suggest that WHTs did improve rural livelihoods in a very arid dry region of south-east Tunisia.

References

- Abaab A (1986) Mutations socio-économiques de la Jeffara orientale (Sud tunisien): Revue de l'Occident musulman et de la Méditerranée 41(1):327–333
- Abaab A, Guillaume H (2004) Entre local et global: pluralité d'acteurs, complexité d'intervention dans la gestion des ressources et le développement rural. IRD Ed Collect Latitudes 23:261–290
- Akroush S, Shideed K, Bruggeman A (2014) Economic analysis and environmental impacts of water harvesting techniques in the low rainfall areas of Jordan. *Int J Agr Resour Gov Ecol* 10(1):34–49
- Baumann P (2002) Improving access to natural resources for the rural poor. A critical analysis of central concepts and emerging trends from a sustainable livelihoods perspective. LSP working paper (FAO)
- Belli P, Anderson JR, Barnum HN, Dixon JA, Tan J-P (2001) Economic analysis of investment operations, analytical tools and practical applications. WBI, World Bank, Washington, DC
- Côté S, Healy T (2001) The well-being of nations: The role of human and social capital: Organisation for Economic Co-operation and Development, Paris
- CRDA (2013) Rapport annuel du Commissariat Régional au Développement Agricole
- Dearden P, Roland R, Allison G, Allen C (2002) Sustainable livelihood approaches: from the framework to the field: sustainable livelihood guidance sheets. Department for International Development, University of Bradford, UK
- Fleskens L, Stroosnijder L, Fetoui M (2002) Economic evaluation of on-site impact of water harvesting in southern Tunisia. In: de GJ, Ouessar M (eds) *Water harvesting in Mediterranean zones: an impact assessment and economic evaluation*. Tropical resource management papers 40. Wageningen University, pp 89–100
- Fleskens L, Stroosnijder L, Ouessar M, De Graaff J (2005) Evaluation of the on-site impact of water harvesting in southern Tunisia. *J Arid Environ* 62(4):613–630
- Gamoun M, Patton B, Hanchi B (2015) Assessment of vegetation response to grazing management in arid rangelands of southern Tunisia. *Int J Biodivers Sci Ecosyst Serv Manage* 1–8
- INS (2014) N. I. o. S.. <http://www.ins.nat.tn/>
- Karl M, Potters J, Colatei D, Dohrn S (2002) Participatory policy reform from a sustainable livelihoods perspective review of concepts and practical experiences. Livelihood Support Programme
- Kuosmanen T, Kortelainen M (2007) Valuing environmental factors in cost–benefit analysis using data envelopment analysis. *Ecol Econ* 62(1):56–65
- MARH, and GIZ (2012) Stratégie Nationale sur le Changement Climatique Rapport de la stratégie, 165 p. http://www.environnement.gov.tn/fileadmin/medias/pdfs/dgeqv/chang_climatique_3.pdf
- MEDD (2006) Programme d'action régional de lutte contre la désertification du Gouvernorat de Médenine: Publication du Ministère de l'Environnement et du Développement Durable (MEDD)
- Nachtergaele F, Biancalani R, Bunning S, George H (2010) Land degradation assessment: the LADA approach. In: Proceedings 19th world congress of soil science, Brisbane, Australia
- Norton A, Foster M (2001) The potential of using sustainable livelihoods approaches in poverty reduction strategy papers. Overseas Development Institute London
- Ouessar M, Bruggeman A, Abdell F, Mohtar R, Gabriels D, Cornelis W (2009) Modelling water-harvesting systems in the arid south of Tunisia using SWAT. *Hydrol Earth Syst Sci* 13:2003–2021
- Ouled Belgacem A, Sghaier M, Ouessar M (2011) Vulnérabilité de l'écosystème pastoral face au changement climatique dans le Gouvernorat de Médenine. MEAT/GIZ, Tunis. <http://www.environnement.gov.tn/>
- Pinstrup-Andersen P, Pandya-Lorch R (1998) Food security and sustainable use of natural resources: a 2020 vision. *Ecol Econ* 26(1):1–10
- Ranasinghe M (1994) Extended benefit-cost analysis: quantifying some environmental impacts in a hydropower project. *Proj Appraisal* 9(4):243–251

- Ranasinghe M (1997) Bounds on the value of waterfalls: a case study from a hydropower project. *Proj Appraisal* 12(3):185–192
- Schiettecatte W, Ouessar M, Gabriels D, Tanghe S, Heirman S, Abdelli F (2005) Impact of water harvesting techniques on soil and water conservation: a case study on a micro catchment in southeastern Tunisia. *J Arid Environ* 61:297–313
- Sghaier M, Arbi AM, Tonneau J-P, Ounalli N, Jeder H, Bonin M, McNeil D, Nesheim I, Brouwer F (2012a) Land degradation in the arid Jeffara region, Tunisia: land use policies for sustainable development: exploring integrated assessment approaches. Edward Elgar, p 89
- Sghaier M, Arbi AM, Tonneau JP, Ounalli N, Jeder H, Bonin M (2012b) Land degradation in the arid Jeffara Region, Tunisia. In: McNeil D, Nesheim I, Brouwer F (eds) Land use policies for sustainable development: exploring integrated assessment approaches. Edward Elgar, p 89
- Sghaier M, Mahdhi N, De Graaff J, Ouessar M (2002) Economic assessment of soil and water conservation works: case of the oued Oum Zessar watershed in south-eastern Tunisia. In: De Graaff J, Ouessar M (eds) Water harvesting in Mediterranean zones: an impact assessment and economic evaluation. Wageningen University, The Netherland, pp 101–113
- Wholey JS, Hatry HP, Newcomer KE (2010) Handbook of practical program evaluation. Wiley

Chapter 26

Assessing the Impacts of Climate Change on Sustainable Development at the Regional Level: A Case Study in Medenine, South-East Tunisia

Mohamed Arbi Abdeladhim, Mongi Sghaier, Luuk Fleskens,
Lindsay Shutes and Abdallah Akari

Abstract This paper applies multiple analytical and empirical methods to evaluate the sustainability impacts of climate change and prospective adaptation measures based on water harvesting techniques (WHTs) at the regional level. We developed a sustainability composite index (SCI) for an arid zone in Tunisia, specifically the south-eastern Province of Medenine. To quantify the SCI, a static computable general equilibrium model (CGE) was adapted to the region. To provide a database for the CGE model, we built a regional social accounting matrix (RSAM). A bottom-up approach was applied to build a regional supply and use matrix for the agricultural sector incorporating natural resources (land and water) as intermediate inputs. Our regional SAM included ten production factors, 18 production sectors producing 22 goods and services, two household types (urban and rural), one representative enterprise, two public sectors (central and regional administration), taxes accounts, two capital accounts (savings/investment and changes in stocks), the rest of the world and the rest of the country. We used the RSAM to calculate the regional GDP. Two simulations were run, focused on the 2030 time horizon from the baseline year of 2006: (i) declining natural capital due to the effects of climate change and (ii) implementation of a regional climate change adaptation strategy based on water harvesting technologies (WHTs). Scenario identification drew on

M.A. Abdeladhim (✉) · L. Fleskens
Soil Physics and Land Management (SLM), Wageningen University,
Wageningen, The Netherlands
e-mail: mohamed.abdeladhim@wur.nl

M.A. Abdeladhim · M. Sghaier
The Institute of Arid Regions of Medenine (IRA), Medenine, Tunisia

L. Shutes
Agricultural Economics Research Institute (LEI), The Hague, The Netherlands

A. Akari
University of Economic Sciences and Management of Tunis, Tunis, Tunisia

previous research and was performed in close collaboration with regional stakeholders. Based on the outputs of the CGE model, the impacts of the two scenarios on the main regional economic indicators were analysed. Using multi-criteria analysis (MCA), we calculated an aggregated SCI for regional development. Results suggest that implementation of the regional climate change adaptation strategy would have positive impacts, but would be insufficient to maintain the SCI at its current level.

Keywords Climate change · Sustainable development · Regional CGE model · Composite indicator

Introduction

Sustainable development in the Province of Medenine, south-east Tunisia, is threatened by a mismatch between human needs (employment, income, energy, grazing and so on) and natural resources availability (mainly agricultural land and blue and green water) (Sghaier et al. 2012). Indeed, pressure exerted on natural resources to meet human needs has induced natural resources degradation and led to significantly diminished economic sector productivity and competitiveness. Since 1980s, the government has implemented various land use policies at the regional level to address natural resources degradation. However, despite such early interventions, productivity has remained low, and local livelihoods have remained at risky and deficient.

Research by the Ministry of Agriculture and Hydraulic Resources (MARH) in collaboration with Germany's GIZ (MARH and GIZ 2012), using the HDCM3¹ climate model, predicts worsening water stress and land degradation in the region due to climate change. In fact, Medenine is extremely vulnerable, and its capacity to adapt to the impacts of climate change could reasonably be questioned. MARH and GIZ (2012) have recommended a suite of adaptation measures, including (i) using recharge wells to raise groundwater resources, (ii) mobilizing runoff water with traditional and innovative water harvesting technologies (WHTs) and (iii) rehabilitating rangelands using modern management methods such as the rest technique and planting of exotic herbaceous species and shrubs.

For their effective implementation, however, an ex ante assessment tool and set of measurement indicators are needed to better understand the threat posed by climate change and the potential impacts of the different adaptation measures.

Interactions between socio-economic development and environmental degradation are exceedingly complex. In the face of this complexity, integrated assessment

¹Hadley Centre Coupled Model, version 3.

modelling (IAM) has been proposed to provide a better information base for sustainable development strategies (Abaza et al. 2004). IAM provides structured knowledge about human–environment interactions to support decision-making and design of sustainable development interventions (Schöber et al. 2010). Parker et al. (2002) defined IAM as a methodology for combining several qualitative approaches and quantitative models representing different systems and scales into a solid framework for integrated assessment.

Given data constraints, identification of appropriate sets of indicators to measure sustainability at the regional level is often an onerous task. Choosing appropriate sustainability indicators requires knowledge of what is important to the viability of the particular systems involved, and how these combine to contribute to sustainable development. The number of representative indicators must be kept as small as possible, but be as large as required (Bosello et al. 2011). Since the Brundtland Report of 1987 and the Rio Summit of 1992, academics have sought to overcome the limitations of gross domestic product (GDP) as a measure of sustainable development. Progress has been made in three main directions: (i) composite indicators (monetary or non-monetary aggregated indicators), (ii) indicator sets (dashboards or sets of indicators representing economic, social, and environmental dimensions) and (iii) satellite accounting systems.

Composite indicators integrate large amounts of information into easily understood formats, facilitating communications with decision-makers. However, Freudenberg (2003) argued that methodological difficulties are rife in construction of composite indicators, the result being that they can mislead and be easily manipulated.

Böhringer and Löschel (2006) investigated the use of computable general equilibrium (CGE) modelling to measure the impacts of interference on policy-relevant indicators of sustainability (economic, social, environmental and institutional). They found CGE modelling to be a powerful tool for measurement of sustainability. However, they concluded that (i) an integrated assessment framework was needed to link standard CGE models to theme-specific complementary models having an environmental and social focus and (ii) participatory processes were needed in which stakeholders and other interested parties could communicate a range of values, perceptions and judgments to policymakers.

The current paper explores the idea of combining CGE modelling with analytical tools such as multi-criteria analysis (MCA), to evaluate the sustainability impacts of, and vulnerability and adaptation to, climate change at the regional level. To this end, a sustainability composite index (SCI) was developed. A regional-level social accounting matrix (SAM) was constructed to provide a database for the CGE model. Our discussion is based on the methodological framework of the 2007–2011 LUPIS project (Land Use Policies and Sustainable Development in Developing Countries; see <http://www3.lei.wur.nl/lupis/>; project no. GOCE-036955).

Case Study and Methodology

Case Study

The Province of Medenine, south-east Tunisia, spans 0.92 million ha. It is an arid zone with extreme climatic conditions. Annual rainfall is less than 200 mm, distributed over approximately 30 days. Pressure on water and land resources is rising, due to population growth, urbanization, land use intensification and climate change (Nesheim et al. 2014). Demand for water for agriculture competes with demands from industry, tourism and households (Hamzaoui-Azaza et al. 2011; Romagny et al. 2004). Competition for water will surely increase in the future, as climate change simulations project reduced precipitation and rising temperatures (Sghaier et al. 2011). This presents a considerable challenge to local livelihoods and natural resources management (Omrani and Burger 2012).

Methodological Framework

In line with the methodological framework of the LUPIS project, our ex ante, integrated impact assessment of climate change and adaptation strategies at the regional level distinguished three phases: pre-modelling, modelling and post-modelling (Reidsma et al. 2011) (Fig. 26.1).

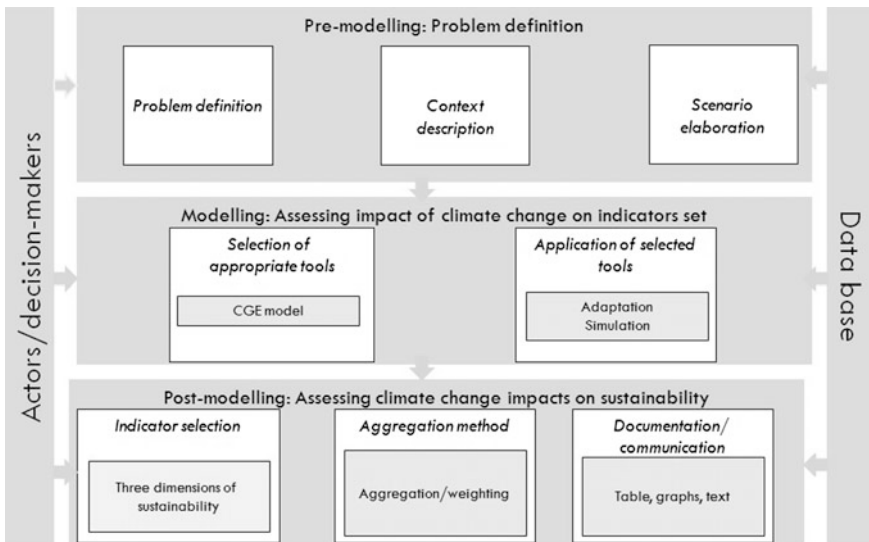


Fig. 26.1 Methodological framework for assessing the impact of climate change on sustainability in arid zone. Adapted from Reidsma et al. (2011)

Pre-modelling phase. The pre-modelling phase consisted of the problem definition, the case study description and scenario elaboration (identification of policy options). This phase was carried out in close collaboration with local and regional stakeholders. Land degradation and climate change in Medenine, and the negative implications of these processes for the socio-economic situation, were identified as the central issue (Bezlepina et al. 2011). From a typology of land use policies developed for the region under study, and in consultation with scientists and regional and local stakeholders, actions from the national climate change adaptation strategy were selected as ‘policy options’ for assessment in the modelling phase. The case study was defined mainly in narrative terms in the pre-modelling phase. Only later, in the modelling phase, was this narrative translated into models and knowledge rules (Nesheim et al. 2014).

Modelling phase. The modelling phase consisted of tool selection and application. The main criteria for tool selection were appropriateness of the model for the case study and availability of the needed data. A CGE model was chosen, as this responded best to stakeholders’ and policymakers’ need for an ex ante, regional, economy-wide assessment of the impacts of climate change and potential effects of adaptation strategies.

CGE models are a standard empirical tool, widely used for assessing the impacts of exogenous shocks and policy changes transmitted through various markets (Wing 2004). Various studies have used CGE modelling to assess the socio-economic impacts of natural resources degradation and climate change at the global level (Berritella et al. 2006; Bosello et al. 2011; Sassi et al. 2009), the national level (Briand 2004; Decaluwe et al. 1999; Holden et al. 2005; Horridge 1999; Robinson and Gehlhar 1995) and the regional level (Berck et al. 1991; Mushtaq et al. 2014; Ochuodho et al. 2012; Seung et al. 1998; Smajgl et al. 2009). Major ex post studies have provided sets of indicators representing economic, social and environmental dimensions of sustainability (Böhringer and Löschel 2006).

The current work linked a CGE model to a complementary MCA to derive a composite indicator simplifying the complexity of sustainability into an easier-to-interpret measure to support decision-making.

Our regional CGE model depicted the specific conditions of the study region. We considered the region to be a ‘price-taker’; that is, its export supply and import demand had no impact on prices outside the region. In the model framework, according to the national input–output table, we included 18 production sectors and 22 commodities. Four groups of production factors were taken into account: land, water, labour and capital. The behavioural relationships in the CGE model were represented by a mix of nonlinear and linear relationships. In accordance with microeconomic theory, households were assumed to maximize their utility subject to their income constraint. A Stone–Geary utility function was used, introducing a subsistence level of consumption to a Cobb–Douglas utility function. Producers were assumed to maximize their profit, subject to initial capital availability. The production function used was a combination of a constant elasticity of substitution (CES) function and a Leontief function, as shown in Fig. 26.2 (Abdeladhim et al. 2011; Chant 2008).

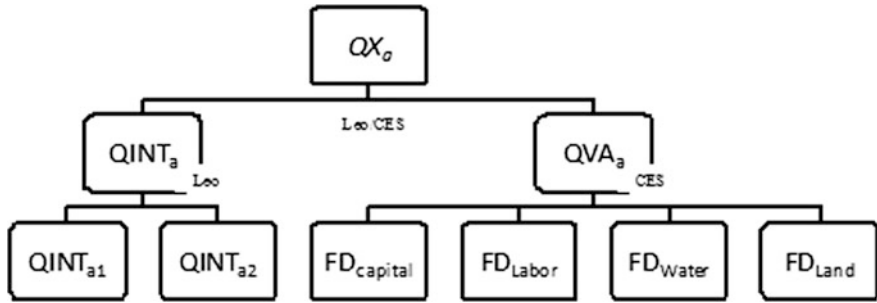


Fig. 26.2 Production function structure. Leo indicates Leontief technologies, CES indicates a constant elasticity of substitution function, QX is the output of an activity, QINT is the aggregate intermediate input, QINTD1 and QINTD2 are representative intermediate inputs and QVA is the aggregate quantity of value added. FD is factor demand and is shown for capital, labour (unskilled urban labourers, skilled urban labourers, unskilled rural labourers and farmers), land (agricultural land, non-agricultural land, grazing land) and water (surface water, groundwater)

The realistic economic data needed to numerically solve the CGE model were entered into an accounting table known as a social accounting matrix (SAM). In a SAM each economic account has both a row and a column. The expenditures for each account are recorded as column entries while the incomes for each account are recorded as row entries. Thus, a SAM is a form of double entry bookkeeping in matrix form, in which entries in each cell identify the magnitude, source (expenditure) and destination (income) account of a transaction.

The form of the SAM determines what agents can be included within the model, and the transactions recorded in the SAM identify the transactions that took place in the base year. In developing a SAM, a top-down or bottom-up approach may be applied. For our Medenine SAM, we used a hybrid procedure. If data were available at the regional level, we integrated it directly into the matrix. If insufficient data were available, we used the top-down technique, regionalizing national data. The RAS method was used to estimate, update and balance the SAM. RAS is an iterative procedure of biproportional adjustment of rows and columns developed independently by various researchers, such as Kruithoff and Sheleikhovski in the 1930s (Ahmed and Preckel 2007).

In accordance with the aims of our study, the economic situation of the study area and data availability, we developed a typical structure for a regional SAM with a base year of 2006. Choice of that base year was determined by two main criteria: (i) data availability and (ii) climate and socio-economic conditions (these factors in the base year should be comparable to a normal year). The SAM incorporated accounts for production (activities), commodities, factors of production, various actors (institutions), the rest of Tunisia and the rest of world.

The activities accounts were disaggregated into the categories agriculture, industry and tourism. Agriculture received special attention and was further disaggregated into livestock, fishing, irrigated agriculture and rainfed agriculture. The agricultural commodities account was disaggregated into 11 agricultural

commodities. The categories for both the commodities and the activities were selected based on the characteristics of the study area and information gathered from the agricultural census compiled by the Ministry of Agriculture (MARH 2006). Thus, the agricultural activities accounts were representative of agriculture in the region. Local farms produced a combination of commodities and could therefore be viewed as multiproduct firms.

The actor (institutional) accounts represented households, enterprises and the national and provincial government. Due to data constraints, we aggregated the rest of the world and the rest of Tunisia. Because we sought as large a structure as possible for the regional SAM, we included a large set of regionally relevant commodities and activities, especially for the agricultural sector.

Household consumption figures were derived from a consumption survey produced by the Institute of Statistics (INS) every 10 years (2005). The survey divides the national territory into six regions: north-east, north-west, central-east, central-west, south-west and south-east. The Province of Medenine is part of the south-east region. The survey distinguishes rural and urban consumption only at the national level. We assumed that rural and urban national consumption patterns were the same throughout the province. Given that we had 22 commodities, all of the commodities included in the survey could be incorporated into the set of commodities in the Medenine SAM. In doing so, some assumptions had to be made, for example, that total cereals consumption demand was met by dry cereals. To calculate the rural and urban household consumption in Medenine, we used an adjustment procedure to convert the south-east regional rural and urban consumption pattern into a provincial consumption pattern.

We considered four groups of production factors: water, land, labour and capital. To capture the characteristics of the region, these were further disaggregated into ten factors (Table 26.1). The remuneration of factors used by agricultural activities was estimated from data provided by regional statistics (i.e. a 2006 survey of the livestock and animal production system in the province by the Regional Statistics Office of Medenine and regional-level farm structure surveys concerning agricultural production, including the factors of production used). Labour incomes were

Table 26.1 Production factors

Aggregated factor	Factors	Definition
Water	fGWATR	Groundwater
	fSWATER	Surface water
Land	fGRAZLAND	Grazing land
	fALAND	Arable land
	fNALAND	Non-agricultural land
Labour	fFARMER	Farm labourers
	fRUNSK	Rural unskilled labourers
	fURBANSK	Urban skilled labourers
	fURBANUNSK	Urban unskilled labourers
Capital	fCAPT	Capital

categorized as farm, unskilled urban, skilled urban and unskilled rural. Assumptions were made here as well, for example, that skilled rural labourers did not engage in agricultural activities. Remuneration of factors of production by non-agricultural activities was given by the regionalized input–output table.

Groundwater and surface water resources were allocated to the irrigated activities and evaluated according to the water prices paid by local farmers to the water management authority. Rainfall water was allocated to rainfed agriculture and breeding activities according to the drylands and grazing land area, evaluated according to opportunity cost. Dry and irrigated agricultural land and grazing land were evaluated according to their rental values, whereas the costs of non-agricultural land were estimated in line with commercial values, according the land use (industry, tourism, etc.). Capital remuneration was calculated as a residual and therefore equalled value added less the remuneration of all other factors.

Post-modelling phase. The post-modelling phase entailed calculation of the composite sustainability index using SMART method: the Simple Multi-Attribute Rating Technique (Edward 1977). SMART is considered the simplest variant of MCA analysis. The typical composite indicator x_j takes the following form:

$$x = \sum_{i=1}^m w_i a_i / \sum_{i=1}^m w_i \quad i = 1, \dots, m, \tag{1}$$

where X is the composite index, a_i is the normalized indicators, and w_i is the weight of a_i , $\sum_{i=1}^m w_i = 1$.

All indicators used were CGE model outputs. Each indicator represented a dimension of sustainable development. The weights given to each indicator or dimension signified the importance of that indicator or dimension in our sustainability composite index (SCI). For purposes of simplification, we attributed equal weights to all indicators (Fig. 26.3).

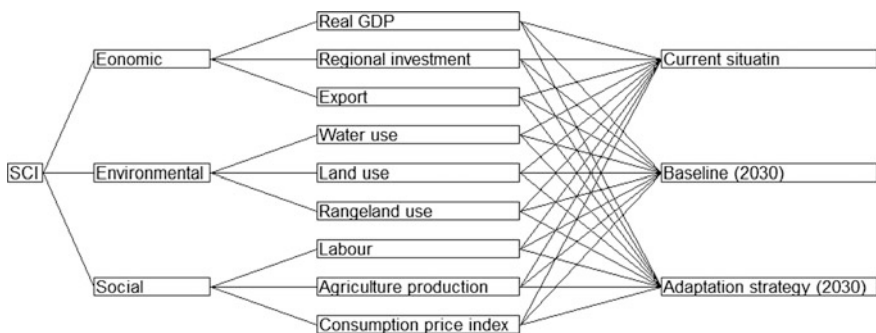


Fig. 26.3 Indicator framework for sustainability impact assessment. The sustainability composite index (SCI) chain drew on three sustainable development dimensions and associated indicators. Adapted from Reidsma et al. (2011)

Figure 26.3 presents the results of a brainstorming session in which relationships were sought between dimensions and indicators in consultation with regional decision-makers and scientists during a 1-day workshop in the framework of the LUPIS project. The dimensions of sustainable development were linked to the main goal of the MCA: deriving the SCI. In line with the brainstorming outcomes, we included three alternatives in our hierarchical tree: the base year, business as usual (policy scenario 1, denoted S1), and the adaptation strategy (policy scenario 2, denoted S2). The indicator values were derived from the modelling phase for the current situation, the business-as-usual scenario and the adaptation strategy. The indicators were the lowest level of criteria in the proposed MCA tree. Inclusion of all values (preferences, indicator values) in the MCA would yield separate matrices for each hierarchical level. The Criterium DecisionPlus software was used to calculate the regional SCI via SMART.

Scenario Definition

Business-as-usual (S1 in Fig. 26.4). We developed the business-as-usual scenario based on MARH and GIZ (2007), which used HDCM3 to quantify effects. Specifically, a low climate change picture was taken, globally the emissions and temperature changes described in the A2 storyline of the Special Report on Emissions Scenarios by the Intergovernmental Panel on Climate Change (IPCC). The severity of climate change impacts on production factors (land and water), agriculture and livestock productivity were quantified as follows:

- groundwater reduced by 28%,
- surface water reduced by 5%,
- rainfed arboriculture areas reduced by 80%,
- rangelands reduced by 80%,
- crop areas reduced by 20%.

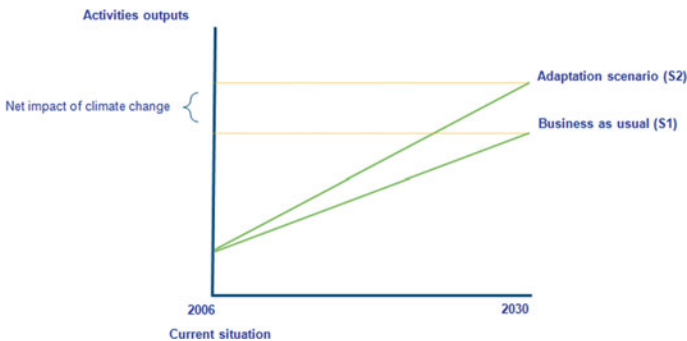


Fig. 26.4 Scenario definition

Adaptation scenario (S2 in Fig. 26.4). As noted, MARH and GIZ (2012) recommended an extensive suite of adaptation measures. We quantified the impacts of these measures on production factors (land and water) based on consultations with experts from the regional commissariat of agricultural development in Medenine. We considered three of these measures in our CGE model: (i) using recharge wells to raise groundwater resources by 20%, (ii) mobilizing up to 15% of runoff water using traditional and innovative WHTs and (iii) rehabilitating 40% of rangelands using modern management methods such as the rest technique and planting exotic herbaceous species and shrubs.

Results

Impacts on Sustainable Development Indicators

The CGE model is static, so the base year is simply the initial structure of the economy as reflected in the regional SAM. The two counter-factual scenarios: business as usual (S1) and the adaptation scenario (S2) were introduced via, respectively, an exogenous decrease and increase in natural resources supply. The results of the two scenarios were explored by comparing their impacts relative to the base year.

A priori, a reduction in the supply of natural resources due to climate change, as projected by MARH and GIZ (2012), would likely lead to reduced production in agriculture and tourism, as groundwater and land are production factors in the technology structures of these activities. Subsequently, production in agriculture and tourism would indirectly influence intermediate consumption in all economic activities and the final consumption of institutions, as well as overall output (GDP) of the region. In contrast, increasing natural resources, via implementation of the adaptation actions proposed within the national strategy, was expected to enhance productivity. But in either case the underlying question was the same: would the adaptation strategy be sufficient to maintain the SCI at its current level?

Figure 26.5 presents the simulated impacts of the projected climate changes (S1) and adaptation strategy (S2) on regional welfare, GDP, domestic production, private consumption, total factor use, investment, imports and exports (in percentage deviation from the base year).

Comparing the economic indicators under S1 and S2 with those for the current situation (base year), we found all economic indicators diminished from those in the base year. Regional GDP was predicted to decline by 2.5% by 2030 as a result of climate change. Implementation of adaptive measures in the region resulted in GDP gains in S2, but GDP was still expected to shrink slightly, by 0.41% relative to the current situation (base year). Domestic production, private consumption, total factor use, investment, imports and exports were found to decline, respectively, by 1.70%, 1.15%, 0.29%, 5.39%, 0.74% and 0.73% in S1. The mitigating impact of the

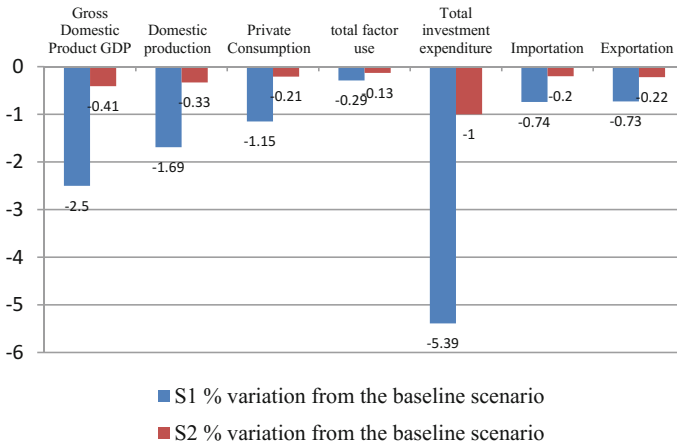


Fig. 26.5 Climate change (S1) and adaptation strategy (S2) impacts on economic indicators

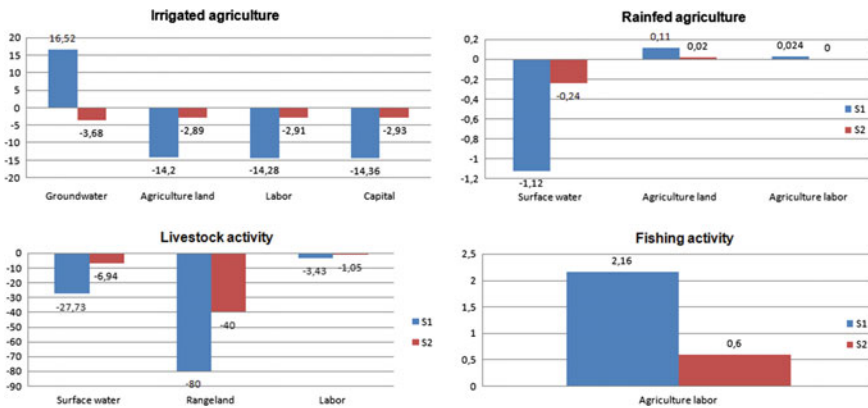
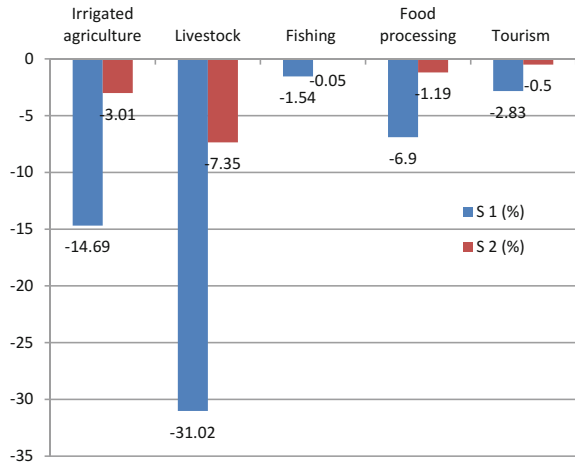


Fig. 26.6 Factor use by activity (percentage change from base year)

adaptive measures implemented in S2 directly affected the economic indicators in the Medenine region. Indeed, they declined much less, compared to the current situation, when adaptive measures were in place.

Reallocation of production factors across sectors also offset the direct impact of climate change, contributing to the magnitude of the value-added contraction of production sectors (Fig. 26.6). Compared to the base year, factor demand by agricultural activities (irrigated agriculture, rainfed agriculture, livestock and fishing) in S1 and S2 was somewhat modified. Use of groundwater by irrigated agriculture increased by 17% in S1, to offset the decrease in surface water. Meanwhile, groundwater use dropped by 4% in S2. Because output was reduced in irrigated agriculture, labour was released from the sector (a decline of 14% and 3%, respectively, in S1 and S2). This released labour was employed either by other

Fig. 26.7 Impacts of climate change and the adaptation strategy on the value added of activities



agricultural activities (rainfed agriculture and fishing) or in activities outside the agricultural sector. In fact, labour demand in fishing, which was less affected by climate change, increased by 2.16% and 0.6%, respectively, in S1 and S2. Livestock saw the greatest decline in production factor demand, due to the dramatic reduction of rainwater, which is a key production factor in this sector.

The aggregated value added was influenced by the diminishment of natural resources. For example, irrigated agriculture’s value added dropped by 15% in S1 and by 3% in S2, relative to the base year. As expected, livestock value added fell as well (by 31% and 7%, respectively, in S1 and S2). Due to the agricultural productivity losses, value added in the food processing sector, which is a user of agricultural products, dropped by 7% in S1 and by 1% in S2. The tourism sector, which is a user of groundwater, experienced a decline in value added by 3% and 0.5% for the two scenarios, respectively. The impact of diminished natural resources on the other industrial and services activities was not significant, because there was no strong link between these sectors and water availability (Fig. 26.7).

Impacts on the Sustainability Index

SCI. Figure 26.8 depicts the overall sustainability index (SCI) for each scenario. Based on the chosen weighting system and the calculated values derived from the CGE model, the current situation was found to have the highest SCI score (0.67) and was thus much more profitable than the two other scenarios. The adaptation strategy scenario scored higher than the business-as-usual (climate change) scenario (0.58 vs. 0.49). Based on a classic production function analysis, in which the total output (GDP) is the aggregation of value added and intermediate consumption, the decline of natural capital stocks caused by climate change would affect economic performance and subsequently the SCI.

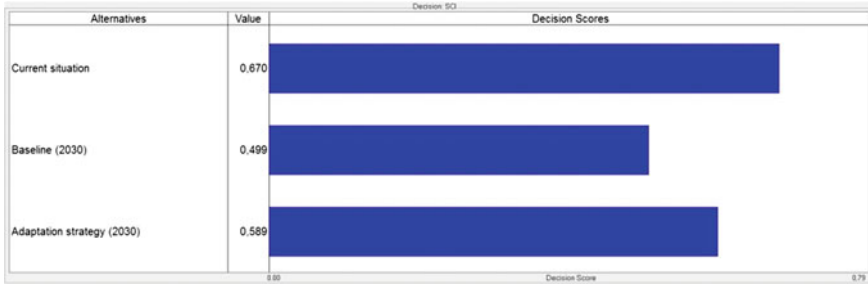


Fig. 26.8 Sustainability index for the base year, the climate change (S1) and the adaptation (S2) scenarios

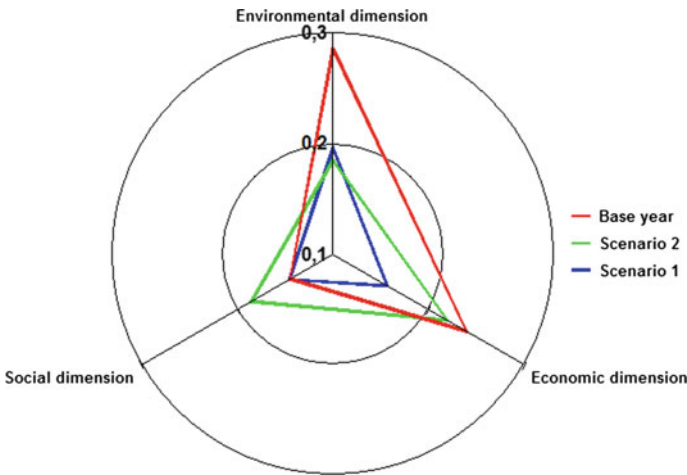


Fig. 26.9 Contribution of each sustainable development dimension to the sustainability composite index (SCI) for the base year, S1, and S2

As shown in Fig. 26.9, environmental sustainability is highest in the current situation, and reduced in S1 and S2. Social sustainability, ranked second in the current situation, but gained prominence in S2. The importance of economic sustainability was stable for the base year, S1, and S2.

Sensitivity Analysis

The sensitivity analysis tested the stability of our results using alternative values for the relative weight of sustainability dimensions. Sensitivity analyses were performed for all dimensions. If small deviations from the original weight of alternative do not change the preferred choice, that result is considered robust. If small

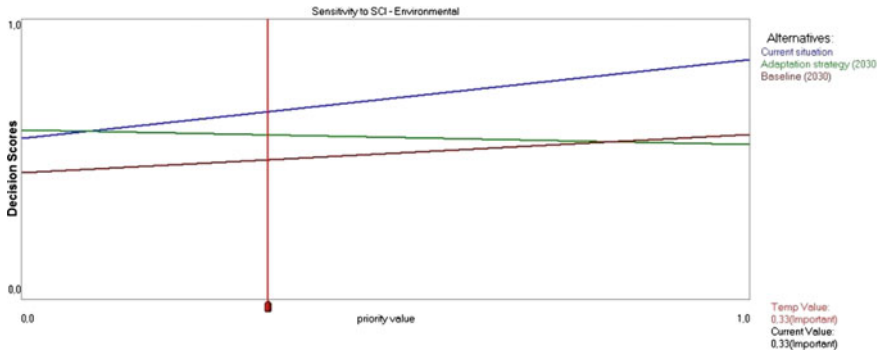


Fig. 26.10 Sensitivity analysis for the environmental dimension of sustainable development

changes do lead to large changes in the preferred alternatives then the different alternatives require re-evaluation.

Figure 26.10 presents the main alternative scores for the environmental dimension of sustainable development. As seen, with the current value set at 0.33 (thus weighting all sustainability dimensions equally), the base year emerged as the best option. Reducing the relative weight of this dimension to 0.09, and attributing equal weight to keeping the values of the other dimensions (such that the total is 1), changed the decision outcome, as the adaptation scenario then becomes the best option. Increasing the value to 0.82 (again redistributing the remaining 0.18 equally over the other dimensions) also changed the outcome, as in this example, the business-as-usual scenario would then emerge as preferable to the adaptation strategy scenario. Therefore, doubling the weight of the environmental dimension altered the preferred alternative.

Conclusion and Discussion

This paper investigated the use of integrated impact assessment based on a quantitative method (CGE model) and qualitative and participatory analysis (MCA). Our objective was to evaluate the impact of climate change and potential adaptation measures based on WHTs on sustainability at the regional level. The social relevance of the pre-modelling, modelling and post-modelling phases was enhanced by interactions between scientists and stakeholders, as dialogues were held during workshops and meetings. These interactive and participatory events mobilized many actors and represented a huge opportunity to develop a collaborative approach with decision-makers, including members of the regional development administration and local institutions. Decision support tools were thus implemented with a greater understanding of the potential regional-level effects of climate change and adaptation strategies and of sustainable development programmes and outcomes.

To calculate the economy-wide impact of climate change, two simulations were run: (i) business as usual and (ii) a regional climate change adaptation strategy. Results showed a positive impact of the adaptation strategy on the SCI, but it was still insufficient to maintain the SCI at its current level.

Indeed, the *ex ante*, integrated policy impact assessment produced a diverse picture across the various sectors. Our analyses may thus provide a valuable tool for regional stakeholders and policymakers assessing potential policies and deciding on potential adaptation measures. Nonetheless, our results should be interpreted with caution, given the limitations of the current work. Climate change, for instance, is a dynamic phenomenon, yet our model is static and thus ignores the time factor. Furthermore, the stock of labour and capital were assumed to be equally available at the regional level under the different scenarios. This excludes the possibility of capital mobility between regions. In addition, perfect substitutability was assumed between factors of production, natural resources (water and land), physical capital and labour (CES production function).

References

- Abaza H, Bisset R, Sadler B (2004) Environmental impact assessment and strategic environmental assessment: towards an integrated approach. UNEP/Earthprint
- Abdeladhim MA, Sghaier M, Fleskens L, Akari A (2011) Assessing climate change impacts on sustainable development at the regional level: a case study of the province of Medenine south-east of Tunisia
- Ahmed SA, Preckel PV (2007) A comparison of RAS and entropy methods in updating IO tables. In: 2007 Annual meeting, American Agricultural Economics Association, pp 1–20
- Berck P, Robinson S, Goldman G (1991) The use of computable general equilibrium models to assess water policies. *The economics and management of water and drainage in agriculture*. Springer
- Berritella M, Bigano A, Roson R, Tol RS (2006) A general equilibrium analysis of climate change impacts on tourism. *Tour Manage* 27:913–924
- Bezlepkina I, Brouwer F, Nesheim I, Verburg R, Silvis H, Chen L, Chant L, Imbernon J, Bonin M, Bonnal V (2011) D1. 3: final report. LUPIS. Land use policies and sustainable development in developing countries. Specific targeted project integrating and strengthening the European research area. LEI, part of Wageningen UR
- Böhringer C, Löschel A (2006) Computable general equilibrium models for sustainability impact assessment: status quo and prospects. *Ecol Econ* 60:49–64
- Bosello F, Campagnolo L, Eboli F, Parrado R, Portale E (2011) Extending energy portfolio with clean technologies in the ICES model. In: 14th annual conference on global economic analysis, Venice. Citeseer, pp 16–18
- Briand A (2004) Comparative water pricing analysis: duality formal-informal in a CGE model for Senegal. In: Conference input-output and general equilibrium: data, modeling and policy analysis. Brussels, pp 2–4
- Chant L (2008) The macroeconomic impact of HIV/AIDS in South Africa. University of Sussex
- Decaluwe B, Patry A, Savard L (1999) When water is no longer heaven sent: comparative pricing analysis in a AGE model. *Cahiers de travail*, p 99
- Edwards W (1977) How to use multi-attribute utility measurement for social decision making. *IEEE Trans Syst Man Cybern* 7:326–340

- Freudenberg M (2003) Composite indicators of country performance: a critical assessment. OECD science, technology and industry working papers, no 2003/16. OECD Publishing, Paris
- Hamzaoui-Azaza F, Ketata M, Bouhlila R, Gueddari M, Riberio L (2011) Hydrogeochemical characteristics and assessment of drinking water quality in Zeuss-Koutine aquifer, southeastern Tunisia. *Environ Monit Assess* 174:283–298
- Holden S, Lofgren H, Shiferaw B (2005) Economic reforms and soil degradation in the Ethiopian highlands: a micro CGE model with transaction costs. In: International conference on policy modeling (EcoMod2005)
- Horrige JM (1999) A general equilibrium model of Australia's Premier City. Victoria University, Centre of Policy Studies/IMPACT Centre
- MARH (2006) Enquête sur les Structures des Exploitations Agricoles 2004–2005. <http://www.onagri.nat.tn/uploads/divers/enquetes-structures/index.htm>
- MARH & GIZ (2012) Stratégie Nationale sur le Changement Climatique Rapport de la stratégie, 165 p. http://www.environment.gov.tn/fileadmin/medias/pdfs/dgeqv/chang_climatique_3.pdf
- Mushtaq S, Cockfield G, White N, Jakeman G (2014) Modelling interactions between farm-level structural adjustment and a regional economy: a case of the Australian rice industry. *Agr Syst* 123:34–42
- Nesheim I, Reidsma P, Bezlepkina I, Verburg R, Abdeladhim MA, Bursztyn M, Chen L, Cisse Y, Feng S, Gicheru P (2014) Causal chains, policy trade offs and sustainability: analysing land (mis) use in seven countries in the South. *Land Use Policy* 37:60–70
- Ochuodho T, Lantz V, Lloyd-Smith P, Benitez P (2012) Regional economic impacts of climate change and adaptation in Canadian forests: a CGE modeling analysis. *Forest Policy Econ* 25:100–112
- Omrani N, Burger D (2012) Water management issues in Southern Tunisia under a climate change context. Climate change and the sustainable use of water resources. Springer
- Parker P, Letcher R, Jakeman A, Beck M, Harris G, Argent RM, Hare M, Pahl-Wostl C, Voinov A, Janssen M (2002) Progress in integrated assessment and modelling. *Environ Model Softw* 17:209–217
- Reidsma P, König H, Feng S, Bezlepkina I, Nesheim I, Bonin M, Sghaier M, Purushothaman S, Sieber S, van Ittersum MK (2011) Methods and tools for integrated assessment of land use policies on sustainable development in developing countries. *Land Use Policy* 28:604–617
- Robinson S, Gehlhar CG (1995) Land, water, and agriculture in Egypt: the economywide impact of policy reform
- Romagny B, Guillaume H, Ben Oueddou H, Palluault S (2004) Ressources en eau, usages et concurrences dans la Jeffara tunisienne.: série Usages, appropriation, gestion des écosystèmes, Documents de recherche du LPED 1, UMR 151 IRD, Université de Provence
- Sassi O, Crassous R, Hourcade J-C, Gitz V, Waisman H, Guivarch C (2009) IMACLIM-R: a modelling framework to simulate sustainable development pathways. *Int J Global Environ Issues* 10:5–24
- Schöber B, Helming K, Wiggering H (2010) Assessing land use change impacts—a comparison of the SENSOR land use function approach with other frameworks. *J Land Use Sci* 5:159–178
- Seung CK, Harris TR, Macdiarmid TR, Shaw WD (1998) Economic impacts of water reallocation: A CGE analysis for Walker river basin of Nevada and California. *J Reg Anal Policy* 28:13–34
- Sghaier M, Abdeladhim MA, Tonneau J, Ounalli N, Djeder H, Bonin M (2011) Land degradation in the arid Jeffara Region, Tunisia. In: McNeill D, Nesheim I, Brouwer F (eds) Land use policies for sustainable development: exploring integrated assessment methods. Edward Elgar, Cheltenham
- Sghaier M, Arbi AM, Tonneau JP, Ounalli N, Djeder H, Bonin M (2012) Land degradation in the arid Jeffara Region, Tunisia. In: McNeill D, Nesheim I, Brouwer F (eds) Land use policies for sustainable development: exploring integrated assessment approaches. Edward Elgar
- Smajgl A, Morris S, Heckbert S (2009) Water policy impact assessment—combining modelling techniques in the Great Barrier Reef region. *Water Policy* 11:191–202
- Wing IS (2004) Computable general equilibrium models and their use in economy-wide policy analysis. Technical note, Joint program on the science and policy of global change, MIT

Chapter 27

How Investment in RD&E Offset the Negative Impact of Climate Change on the Tunisian Agricultural Productivity Sector

Boubaker Dhehibi, Aymen Frija and Aden Aw-Hassan

Abstract The aim of this paper is to examine the impact of research, development extension (RD&E) and climate change (measured in terms of change in rainfall) on the productivity growth of agriculture in Tunisia during the period 1970–2011, using output-based Törnqvist index combined with econometric regression. Results show that RD&E and climate change are significantly affecting the long-run productivity growth of the Tunisian agriculture. Climate change lessens the productivity of agriculture in the long run whilst RD&E boosts its productivity. Empirical findings suggest that an increase in agricultural RD&E investment is critical to improving long-run productivity growth in the face of adverse climate change.

Keywords Agricultural productivity · Climate change, RD&E, Tunisia

Introduction

The Growth of agricultural Total Factor Productivity (TFP) is increasingly crucial for food security and farmers' livelihoods in Tunisia (Dhehibi et al. 2014a). The role of TFP growth in accelerating and sustaining the pace of agricultural growth has gained great interest and is well recognized in the specialized literature (Fuglie 2010). However, long-term productivity growth in agriculture faces several challenges such as climate change, availability of suitable land, labor and infrastructure. Growth in agricultural production mainly relies on sustained productivity growth. Moreover, most climate change impact assessments on the food and agricultural sector have been focusing on the implications for production, with less consideration of other components such as productivity growth. Regarding agricultural

B. Dhehibi (✉) · A. Frija · A. Aw-Hassan
Sustainable Intensification and Resilient Production Systems Program (SIRPSP)—Social, Economics and Policy Research Team (SEPRT), International Center for Agricultural Research in the Dry Areas (ICARDA), P.O. Box 950764, Amman 11195, Jordan
e-mail: b.dhehibi@cgiar.org

productivity, another important determinant factor is the stock of knowledge considered as a lead driver of productivity growth (Hall and Grant 2006). Given methodological limitations for the quantification of the stock of knowledge, investment in RD&E is generally used as a proxy (Griliches 1979). Strategic policy making and appropriate funding for sustained productivity growth in agriculture is therefore crucial to investigate.

To fill this gap, the objective of this research is to contribute to understanding the importance of investments in research, development, extension (RD&E) and climate change on the Tunisian agriculture productivity. Firstly, we focus on the period 1970–2012, which was characterized by several policy dynamics in terms of RD&E investments. In fact, since the late 1980s the agricultural sector has been driven by the Agricultural Sector Adjustment Program (ASAP)¹ which considered a gradual discontinuation of input subsidies advocating for increased involvement of the private sector, and emphasizing the cultivation of export crops. Secondly, the contribution of RD&E and overall rainfall patterns in the country (North, Center and South rainfall values have been considered) to the (year-to-year and longer term) productivity growth have been analyzed. Finally, we try to explore the connection between productivity dynamics and RD&E and climate change during the selected time period.

This paper is organized as follows. Section “[The Agricultural Sector in Tunisia: An Overview](#)” provides general overview of the Tunisian’s agriculture sector. Section “[Overview of Literature](#)” review on the recent productivity literature. Section “[Data Sources and Analytical Framework](#)” fulfils two objectives: First, it describes the different sources of data. Second, it provides the analytical framework of the current study. In Section “[Analysis and Empirical Results](#)”, empirical results are presented and discussed while highlighting the main findings from this research. The final section concludes.

The Agricultural Sector in Tunisia: An Overview

Agriculture assumes significant social and economic importance in the Tunisian economy. The main contribution of the agricultural sector is not only in terms of GDP, around 8% in 2011, but as a source of employment engaging approximately 810,000 people in 2012 (FAOSTAT 2013) or 19.5% of the working population (Dhehibi et al. 2014b). However, Tunisia is characterized by low rainfall and limited renewable water resources. It is influenced by the arid and semi-arid climate that covers more than 3/4 of its area. Major crops, in terms of cultivated area, are tree crops (especially olives and dates) followed by cereals. While tree crops are strategic for exports (Tunisia is the fourth world exporter of olive oil), cereal crops are very important for domestic human and livestock domestic consumption.

¹Funded by the International Monetary Fund and the World Bank and implemented by the Tunisian government.

Rain fed cropped areas (except rain fed trees areas) and productions are highly dependent to the climate variability. As an example of this fluctuation, total cereal production in 2002 was around 0.51 Million tons while in 1996 and 2003 it was around 2.9 Million tons. The same figure is observed for all other cereal crops where the yields of durum wheat (between 0.5 and 2 tons/ha), soft wheat (between 0.5 and 2.5 tons/ha), and barley (between 0.4 and 1.5 tons/ha) are highly variable from 1 year to another. Not only yields are variable, the cereal cropped areas are also depending stochastically on the climate conditions. For the expected “bad” years, farmers usually avoid planting cereals which make both yields and areas decreasing. As a consequence, cereal importations are done almost each year to cover the gap between domestic production and consumption. The stabilization of agricultural yields and the decrease of the sector dependency to climate variations are necessary for food security and agricultural trade balance in Tunisia. Many solutions have been proposed including the improvement of farmers’ skills, financing, mechanization, intensification, and the extension of the irrigated areas. The latter strategy can be considered as the most important in Tunisia during the last four decades. In fact, during that period, massive efforts have been made to develop surface and groundwater infrastructure and to promote the irrigation sector. Currently, 75% of total fresh water consumed in Tunisia is being used for irrigation (MARH 2013). Currently, irrigated area is covering around 450,000 ha (MARH 2013), which is around 8% of the total agricultural area. This percentage is low but is reflecting a (almost) maximum surface that can be irrigated given the available water resources and water use efficiency levels. However, irrigated areas in Tunisia are producing 35% of the agricultural output value, 20% of total agricultural exports and 27% of agricultural employment (Atiri 2007). Around 48% of these irrigated areas are irrigated from groundwater sources, including both superficial and deep aquifers. Overall water resources in the country are estimated to be only around 4700 million m³ (Atiri 2007) including 650 million m³ of non-renewable resources (13.8% of the total water resources). Surface water is estimated to 2700 million m³.

Despite these considerable and continuous efforts to promote irrigation and stabilization of yields, shortage and imports of many food commodities in Tunisia are still persistent. In terms of trade balance, the agriculture and agro-food trading recovery rate in Tunisia was in average 87% over the period 2000–2009. This rate is also highly fluctuating with a minimum value of 48% (in 2002) and a maximum value of 121% (in 2006) (Bachta 2011). According to the same source, during that period (2000–2009) positive and successive trading recovery rates were only recorded for three successive years. In addition to the dependence to climate, some main structural problems of the Tunisian agriculture are also being pointed as main source of low agricultural productivity. The small farm size at national level is one of these problems. In fact, the average farm size in Tunisia in 2005 was about 10.2 ha (MARH 2013). Total farm number is 516,000 farms, managing an area of 5.3 million ha. According to the same source, in 2005, 54% of these farms have a size lower than 5 ha and 75% of farms have a size lower than 10 ha indicating a main constraint for the modernization of the agricultural sector.

Overview of Literature

Productivity growth is a crucial element in increasing per capita income and living standards of a country (Islam and Salim 2009). In the meantime and in addition to the importance of investments in agricultural RD&E, another imperative factor that affects agricultural productivity is the impacts of climate change and variability (Antle 2008). Climate in recent decades has been of particular interest due to observed global warming and greenhouse effects (Nelson et al. 2009). In the below section we are going to present a synthetic overview on the RD&E expenditure and agriculture productivity from one side and the nexus between climate change and agricultural productivity from another side.

RD&E Expenditure and Agriculture Productivity

In the specialized literature, several studies analyzed the link between RD&E expenditures and agriculture productivity. Solow's (1957) decomposition of economic growth is widely used to examine the contribution of different factors to the productivity residual. He found expenditure on RD&E as the factor gaining most attention. Griliches (1979) argues that the stock of a firm's technical knowledge is itself considered as a production factor. Thus, RD&E activities could be added to the existing knowledge stock of the firm which is not only affecting its productivity but also has spillover effects on the productivity of other firms because of the "partially public good nature" of knowledge. Recent studies have also found a significant contribution of RD&E expenditure to the agricultural productivity. Thirtle and Bottomley's (1989) study on UK agricultural sector found a significant contribution of agricultural RD&E expenditure to total factor productivity (TFP). They used five different TFP indices and found that, for all indices, a 1% increase in R&D expenditure increased TFP by between 0.25 and 0.44%.

By examining the effects of RD&E expenditure on TFP in agriculture in 47 African countries, Lusigi and Thirtle (1997) used the multilateral *Malmquist* indices of TFP for agriculture over the period of 1961–1991. Agricultural output included food and non-food items. Whereas, inputs included livestock, labor, land, fertilizers, machinery, land quality, and agricultural research expenditures. Their findings indicate that the average rate of TFP growth was 1.27%. When the *Malmquist* TFP index is decomposed into technical progress (which is result of investment in RD&E) and efficiency technical progress is shown to have grown at an annual average rate of 0.9% and efficiency growth was 1.15% per year. Fitting deterministic and stochastic frontier models showed that the effect of agricultural RD&E on TFP was highly significant. In their study of the role of RD&E in the agricultural productivity In New-Zeland (for the period 1926–2001), Hall and Grant (2006) used the "capital theoretic" approach and found that estimates of the stocks of both domestic and foreign knowledge were highly correlated with productivity growth.

Particularly, spillover effects from foreign investment were highly relevant. They concluded that foreign R&D investments are important for New-Zealand, but domestic research will be still needed to adapt spillovers from these foreign investments and stock of knowledge. Very recently, Islam and Salim (2009) examine the short-run and long-run impact of RD&E and climate change (measured in terms of change in rainfall) on the productivity growth of agriculture in Western Australia. Results show that R&D and climate change both affect the long-run productivity growth of Western Australian agriculture. Climate change lessens the productivity of agriculture in the long run whilst R&D boosts its productivity.

Climate Change and Agriculture Productivity

The concern of climate change mainly stems from the significant change in global climate in recent decades and which is predicted to continue throughout the 21st century. In an early study of this issue in US agriculture, Adams et al. (1990) assess the effect of temperature and precipitation variation on the yields of irrigated and rain fed winter wheat, maize and soybeans over the period 1951–1980. Their simulation results show that low precipitation and high temperature adversely affect crop yields; although results can vary across regions. Sensitivity of agriculture to climate variability also depends on the overall level of economic development (Mendelsohn et al. 2001). The negative effect of climate variability tends to be lower in the developed countries due to the availability of advanced technologies. In such situations capital can be a good substitute of climate risks and uncertainty. Mendelsohn et al. (2001) validated this hypothesis by testing climate responses function for three countries with different levels of economic development (USA, Brazil, and India). In the same line, Torvanger et al. (2004) analyzed the effect of climate change on the agricultural productivity in Norway. Particularly, the historical effect of temperature and precipitation on yields of four crops (wheat, barley, oats, and potatoes) was tested over the period 1958–2001. Their results showed that the effect on yields is missed. In 18% of cases, increasing temperatures have had a positive impact on yields, while in 20% of cases, increased precipitations were causing a decrease of the yields. In a very recent paper Gornall et al. (2010) reviews recent literature concerning a wide range of processes through which climate change could potentially impact global-scale agricultural productivity, and presents projections of changes in relevant meteorological, hydrological and plant physiological quantities from a climate model ensemble to illustrate key areas of uncertainty. National studies in Tunisia already report an increasing trend of temperature and a higher variability of rainfall in Tunisia during the 20th century (MARH 2011). According to the same report, this trend is expected to continue, with a possible scenario of increasing average temperatures with a minimum of +0.8 °C, and a decrease of rainfall with about –8% by 2020. This is expected to have deep implications on the agricultural sector in Tunisia, including increasing water scarcity, soil erosion, and decreasing yields.

Climate studies on Tunisia have shown that the country is very exposed to climate change and that its economy, population and ecosystems are therefore very vulnerable. According to the United Nations framework convention on climate change (2015), Tunisia proposes reducing its greenhouse gas emissions across all sectors (energy; industrial processes; agriculture, forestry and other land use; waste) in order to lower its carbon intensity by 41% in 2030, relative to the base year 2010. Mitigation efforts will particularly centre on the energy sector, which alone accounts for 75% of the emissions reductions contributing to this decrease in carbon intensity. As part of the energy transition policy advocated by the State, it is estimated that the energy sector will reduce its carbon intensity in 2030 by 46% compared with 2010. Tunisia, which has already made significant strides towards mitigation in its baseline, is looking to reduce its carbon intensity unconditionally and through its own efforts by 13% compared to 2010, i.e. by around 1/3 of its INDC. To achieve the rest of its objective, i.e. an additional drop in carbon intensity of 28% in 2030 compared to 2010, Tunisia is relying on the support of the international community for funding, capacity building and technology transfer. The reduction in emissions compared to the baseline scenario would be in the order of 26 million tCO₂ eq in 2030, and 207 million tCO₂ eq for the period 2015–2030. Implementation of the Tunisian contribution towards mitigation requires substantial funds to be mobilized—an estimated 18 billion US dollars—to cover investment needs and finance capacity building programmes. The national effort required to achieve Tunisia's unconditional contribution is estimated at nearly 10% of the total mitigation investment needs. The national effort exclusively concerns the energy sector, which accounts for the most significant part of the investment needs. In terms of adaptation, Tunisia remains very vulnerable to the global warming anticipated in the region and the corresponding implications of major increases in temperature, reduced precipitation and rising sea levels. The socio-economic and environmental impact will particularly affect water resources, agriculture, natural and artificial ecosystems, the coastline, health and tourism. The additional costs of the necessary adaptation measures for these sectors and fields will come to some 2 billion dollars and should be borne completely by the international community as part of the global fight against climate change. Altogether, the total additional financing required for mitigation and adaptation would be around 20 billion US dollars to fund investment requirements and capacity building.

Data Sources and Analytical Framework

Data Sources and Descriptive Statistics

FAO's data was the main source used for this study. Time series (1961–2012) of agricultural (including livestock and crop) productions, land areas, labor, machinery and fertilizers use were the main outputs and inputs used to construct the Torqnovist

index for the case of Tunisia. To complete the missing data, other national sources of aggregated statistical information were used when considered as more accurate or up to date. Government investments in agricultural RD&E were collected from the annual statistical records of the Ministry of Agriculture, Hydraulic Resources and Fisheries of the Tunisian Government (MARH). Moreover, key determinants of TFP were mostly collected from national sources and other international databases.

Table 27.1 Descriptive statistics of the input, output and TFP determinants variables

Input/output variables	Minimum	Maximum	Mean	S.D
Seeds (tons)	95417	188153	139075	19084
Seeds current value (million TND)	1.400	233.714	41.539	47.776
Pesticide use value (million TND)	0.566	265.505	55.508	72.678
Pesticides quantity (ha of cereals treated)	67142	530000	280794	135653
Fertilizers consumption (1000 tons)	48.446	288.100	177.607	76.898
Fertilizers consumption value (million TND)	4.156	541.080	121.902	138.406
Total animal feed (tonnes)	96836	2274053	842596	658353
Animal feed value (million TND)	1.988	1043.678	211.260	256.058
Number of tractors	10654	46878	28211	8619
Value of tractors (current value million TND)	0.107	7.074	2.187	1.930
Labor (1000 workers)	466.453	593.300	495.432	34.577
Labor (current value million TND)	56.970	1855.852	660.937	537.923
Capital stock (quantity)	291.231	942.372	624.189	207.191
Capital stock (current value Million TND)	32.546	489.975	180.674	152.821
Natural resources (ha of agricultural land)	8492000	10072000	9179750	484474
Natural resources value (residual)	-44.270	1756.456	473.876	555.724
Total agricultural output	68.699	5376.150	1747.883	1675.120
TFP determinant variables	Minimum	Maximum	Mean	S.D
Annual stock of RD&E expenditure in the Tunisian Agricultural sector (TND)	1498	19490	7573.21	5445.62
Annual mean rainfall in the North of Tunisia (mm)	10.39	64.09	44.07	11.42
Annual mean rainfall in the Center of Tunisia (mm)	14.79	48.04	27.39	8.33
Annual mean rainfall in the South of Tunisia (mm)	5.10	27.80	12.94	5.43
Human capital-health status as measured by life expectancy (years)	48.34	75.24	64.23	8.96
Annual rural GDP (current TND/capita/year)	25.68	1808.96	496.30	486.26
Agricultural employment share (%)	11.93	25.52	16.89	3.93
Trade openness: (import + export)/total production	10.16	41.49	21.32	8.08
Road density (km of roads by km ² of agricultural area) (expressed in 1000 km)	0.76	5.24	2.36	1.08

Source Author's elaboration from dataset (2014)

Table 27.2 Causality Results of the TFP, RD&E and climate (rainfall) in the Tunisian agricultural sector (1970–2011)

Parameters	Dependent variable LnTFPG _t		
	Estimated coefficients	t-ratios	p-value
Constant	0.915	2.43**	0.021
LnRDE _t (annual stock of RD&E expenditure in the Tunisian agricultural sector)	0.05	1.44***	0.141
LnRFTN _t (annual mean rainfall in the North of Tunisia)	0.21	1.63***	0.113
LnRFTC _t (annual mean rainfall in the Center of Tunisia)	-0.109	-0.835	0.410
LnRFTS _t (annual mean rainfall in the South of Tunisia)	0.054	0.347	0.731
LBTD _t (balanced territorial development indicators)	0.037	0.309	0.759
LRR _t (resources reallocation: share of agricultural employment)	0.057	0.213	0.833
LTO _t (trade openness)	-0.169	-1.471***	0.151
LINF _t (infrastructure)	0.090	1.79***	0.100
T	43		
R ²	0.37		
F-statistic	0.784 (p < 0.63)		
Durbin-Watson	2.85		

Source Author's calculation

*Significant at 1%; **Significant at 5%; ***Significant at 10%

The climatic data for Tunisia was obtained from the Tunisian National Meteorological Institute (INM), and average annual data for the Northern, Central and Southern regions of Tunisia were used. The rationale of this regional division within the country is due to the differences in bio-climatic stages and type of agricultural activities (rainfed, irrigated, tree crops, oases, etc.) among regions. The analysis covers the period 1970–2011. Summary statistics of variables used in the empirical specification are presented in Tables 27.1 and 27.2.

Analytical Framework

Both frontier and non-frontier approaches can be used to measure the TFP growth. These two specifications can also be estimated using both parametric and non-parametric methods (Mahadevan 2004). In this paper, the Törnqvist–Theil index was used to estimate TFP for agriculture sector in Tunisia. This index was used to construct both the aggregate output and input indexes. According to this approach, growth in total factor productivity (TFP) is considered as equivalent to

growth in technical change. Further explanations of the conceptual framework and basic measurement issues of productivity using Törnqvist Index can be found in Diewert (1978, 1980), Christensen (1975), Capalbo and Antle (1988) and Coelli et al. (2005).

The Törnqvist output, input and TFP index in logarithm form can be expressed as follows:

Output index:

$$\text{Ln}\left(\frac{Q_t}{Q_{t-1}}\right) = 1/2 \sum_j (R_{j,t} + R_{j,t-1}) \text{Ln}\left(\frac{Q_{j,t}}{Q_{j,t-1}}\right) \quad (27.1)$$

Input index:

$$\text{Ln}\left(\frac{X_t}{X_{t-1}}\right) = 1/2 \sum_i (S_{i,t} + S_{i,t-1}) \text{Ln}\left(\frac{X_{i,t}}{X_{i,t-1}}\right) \quad (27.2)$$

TFP index:

$$\text{Ln}\left(\frac{\text{TFP}_t}{\text{TFP}_{t-1}}\right) = \text{Ln}\left(\frac{Q_t}{Q_{t-1}}\right) - \text{Ln}\left(\frac{X_t}{X_{t-1}}\right) \quad (27.3)$$

where $R_{j,t}$ is calculated as the output (j) share in total revenue for the time (t); $Q_{j,t}$ is the quantity of output (j) for the time (t); $S_{i,t}$ is calculated as the input (i) share in total input cost; $X_{i,t}$ is the input (i) for the time (t).

The TFP Törnqvist–Theil index measures TFP changes by calculating the weighted differences in the growth rates of outputs and inputs. The growth rates are in log ratio form, and the weights are revenue and cost shares for outputs and inputs, respectively. The TFP index as defined in the last equation can be used as an approximation of technological progress, assuming that producers behave competitively, production technology is input–output separable, and there is no technical inefficiency (Antle and Capalbo 1988). This research further assumes that TFP is derived through RD&E expenditure investment, climate change (proxied by the quantity of rainfall) and other determinants such as balanced territorial development, resources reallocation, trade openness and infrastructure. Thus:

$$\text{TFP}_t = A_t \text{RDE}_t^\alpha \text{RFTN}_t^\beta \text{RFTC}_t^\gamma \text{RFTS}_t^\delta \text{OTFPD}_t^\vartheta \quad (27.4)$$

where RDE denotes the stock of RD&E expenditure in the Tunisian agricultural sector, and RFTN, RFTC and RFTS is rainfall in the North, Center and South of Tunisia, respectively and OTFPD are other drivers (determinants) of the TFP growth in Tunisia. α , β , γ , δ and ϑ are their respectively weights. The constant A is the technical progress component not triggered by the conventional factors. We estimate Eq. (4) as the TFP specification to find the importance of RD&E and

climate change (RFTN, RFTC and RFTS) to agricultural production in Tunisia. In a logarithm form, we used the below empirical model (expected signs in parentheses):

$$\begin{aligned} \text{LnTFPG}_t = & C + \alpha \text{LnRDE}_t + \beta \text{LnRFTN}_t + \gamma \text{LnRFTC}_t + \delta \text{LnRFTS}_t + \vartheta_1 \text{LnHC}_t \\ & + \vartheta_2 \text{LnBTD}_t + \vartheta_3 \text{LnRR}_t + \vartheta_4 \text{LnTO}_t + \vartheta_5 \text{LnINF}_t + \varepsilon_t \end{aligned} \quad (27.5)$$

where TFPG is the Total Factor Productivity Growth in the Tunisian agricultural sector; RDE (+) = Annual stock of RD&E expenditure in the Tunisian Agricultural sector (TND); RFTN (+) = Denotes the Annual mean rainfall in the North of Tunisia (in mm); RFTC (+) = Denotes the Annual mean rainfall in the Center of Tunisia (in mm); RFTS (+) = Denotes the Annual mean rainfall in the South of Tunisia (in mm); HC (+) = Human Capital: Health status as measured by life expectancy (Years); BTD (+) = “Balanced Territorial Development” indicators (which is measured by the annual rural GDP/capita expressed in current TND/Capita/Year); RR (+) = “Resources Reallocation”: (Measured as the share of annual agricultural employment compared to the total annual employment and expressed in %); TO (+) = Trade Openness = (agricultural Import + agricultural export)/(total agricultural production). This indicator is also expressed in percentage and, INF (+) = Infrastructure: Road density (km/km² agricultural land).

Equation 5 will be specified under a log-linear form, which will allow to consider the estimated coefficients of the function as elasticities. Equation 5 also has low “residual variance” compared to other functional forms (Jud and Hyman 1974). It also provides better adjustment of the data, in terms of parameter signs and statistical significance, than the linear form. The OLS (Ordinary Linear Squared) method, can produce spurious regression performances when if applied to non-stationary data series. It allows to obtain higher R², lower Durbin-Watson (DW) statistics, and better t-values for the estimated parameters. Regressions of TFP score have been typically conducted by specifying the set of explicative variables under the logarithmic form, which is also similar to the first order differentiation of variables in time series analysis. Using logarithmic forms to express the explicative variables may ensure a stationary data series, which in turn can allow for reliable use of the OLS method (Hendry 1995).

Analysis and Empirical Results

TFP Growth Rate Determination

The annual average growth rates in the total output index, total input index and total factor productivity index (TFPI) between 1966 and 2011 are shown in Fig. 27.1. The results estimated for individual years appeared to vary widely because of

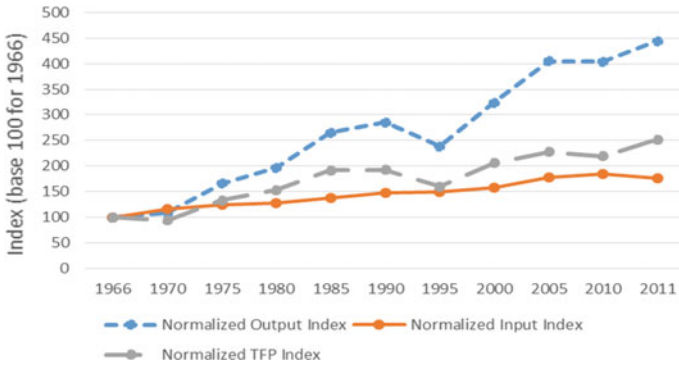


Fig. 27.1 Törnqvist output, inputs, and total factors productivity indexes, for the Tunisian agricultural sector (1966–2011) (own elaboration)

fluctuations in the prices of inputs and outputs. The TFP index shows an important fluctuation over the analysis period. This fluctuating trend is mainly due to the fluctuation of the Output index, which is explained by the variability of rainfed agriculture in Tunisia due to highly variable climate conditions.

RD&E Expenditure, Climate Change and TFP Determinants Nexus

Before exploring the econometrics findings of the Eq. 5, the first step was the assessment of the partial correlation aspects among output, TFP, RD&E and climate change indicators. The quantitative results show that both RD&E and RFT (North, Center and South) are highly correlated with output and TFP growth, meaning that correlation coefficients is not valid to draw significant conclusions about the causality between these variables. The estimation of the relationships (Eq. 5) is presented in Table 27.2. The estimation is performed by normalizing all the variables. All the elasticities were estimated by maximum likelihood (ML). Except the RFTC and TO, the rest of variables have the expected signs. However, not all the coefficients are statistically significant. The variable for RD&E is statistically significant at a 1% level. However, the variables RFT's are significant at a 1% level for the RFTN while that of RFTC and RFTS are not statistically insignificant. Thus, according to the estimates of the model 5 it can be inferred that RD&E and RFTN have significant impact on the TFPG. However, the magnitude of the coefficient and significance level of rainfall in the north (RFTN) is higher than those of RD&E, implying RFTN is strongly influencing TFPG. The results presented in Table 27.2 indicates that a 1% increase in RD&E expenditure. This indicates that RFTCN would increase TFPG by 0.05 and 0.21%, respectively. However, this positive

relationship is consistent with empirical studies that find a direct correlation between investments on agricultural RD&E and TFP (Fuglie 1999; Ruttan 2002; Dhehibi et al. 2014a; Chebil et al. 2014). Given the direct impact of RD&E on output is partially considered in TFP, this positive and significant coefficient might capture spillover impacts from the private sector investment or other government sectors' R&D and possibly additional return (through technical and allocative efficiency) derived from RD&E (Islam and Salim 2009).

Results of the regression had shown the importance of others factors that could have significant impact on the Tunisian TFPG. Empirical findings indicate the negative impact of trade openness (TO) and the positive impact of infrastructure. Whereas, the balanced Territorial development coefficient (BTD) and resource reallocation (RR), measured as agricultural employment share (in % from the national employment) are not statistically significant. As expected, the estimation results indicate that infrastructure has positive impact on the Tunisian TFP. The correspondent coefficient is positive and significant but with small magnitude. Table 27.2 demonstrates that the rise of 1% in investments in roads resulted in an average increase of 0.09% in TFP, at 10% of significance. This result can be explained by the current difficulties found in the production transportation in Tunisia, mainly in the new agricultural irrigated areas.

Regarding the terms of trade (TO) coefficient, the results demonstrate that the increase of 1% in the TO lowered the TFP by 0.17% on average, at 10% of significance. The negative impact of this coefficient may be due to the deterioration of the terms of trade that Tunisia has experienced during the period of analysis. This means depreciation in the terms of trade which compels the economy to decrease its final demand as the cost of imported goods increase, a development that does not favor TFP growth. Indeed, our results are in accordance with Schiff and Valdés (1992) findings. These authors have indicated that trade policies that lowered agriculture's terms of trade have been a major cause of the slow growth in developing countries which is the opposite of the intended effect from industry-led growth strategies.

Concluding Remarks and Policy Implications

This study examines the impact of RD&E spending and climate change, proxied by rainfall, on agricultural productivity growth in Tunisian agriculture by using time series analysis. Empirical results show that RD&E expenditure and rainfall are important for the growth of agricultural productivity. These results are online with the existing recent studies in Tunisia and elsewhere (Dhehibi et al. 2014a, b; Chebil et al. 2014). Chebil et al. (2014) found that RD&E expenditures in the cereal sector of Tunisia have a positive and significant impact on the TFP of this sector. In addition, they find out that the Drought index is significantly and negatively affecting the TFP of this crop. For our case, comparing the elasticities of RD&E expenditures (which is around 0.05) and the rainfall variables (RFTN, RFTC, and RFTS), (which

are 0.21, -0.109 , and 0.054 , respectively) shows that climate variability has a heavier negative effect on the TFP, compared to the low positive effect of RD&E expenditures. By keeping the same RD&E strategy, there is much evidence that the TFP of the agricultural sector in Tunisia will be negatively affected by climate variability which is expected to further increase with climate change.

All these results suggest two recommendations with straightforward implications: (a) Optimal rainfall use is necessary; mainly in the north part of the country where rain is relatively abundant and yields of different rain fed crops have a large potential to further increase, once technical packages and farmers' skills can be enhanced, (b) The increase and prioritization of RD&E expenditures in the agricultural sector are also necessary to redress the expected deteriorating climate conditions. These investments have the potential to boost the long term perspectives/opportunities for a sustainable productivity growth.

Acknowledgements This work was undertaken as part of the project "Agricultural Productivity with an Emphasis on Water Constraints in the Middle East and North Africa", funded by the Economic Research Service (ERS)—United States Department of Agriculture (USDA), as grant (No. 58-6000-2-0108). Authors fully acknowledge the support provided by the ERS. The opinions expressed here belong to the authors, and do not necessarily reflect those of the ERS".

References

- Adams Richard M et al (1990) Global climate change and US agriculture. *Nature* 345(6272):219–224
- Atiri A (2007) Evolution institutionnelle et réglementaire de la gestion de l'eau en Tunisie, Vers une participation accrue des usagers de l'eau. L'avenir de l'agriculture irriguée en Méditerranée. Nouveaux arrangements institutionnels pour une gestion de la demande en eau. Actes du séminaire Wademed, Cahors, France, 6–7 Novembre 2006. CIRAD, Montpellier, France
- Antle J, Capalbo S (1988) An Introduction to recent developments in production theory and productivity measurement. In: Capalbo S, Antle J (eds) *Agricultural productivity measurement and explanation. Resources for the future*. Washington DC, pp 17–95
- Antle John M (2008) Climate change and agriculture: Economic impacts. *Choices* 23(1):9–11
- Bachta MS (2011) L' Agriculture tunisienne : Performances et Menaces de non Durabilité, pp 1–31
- Capalbo SM, Antle JM (eds) (1988) *Agricultural productivity measurement and explanation, Resources for the future*. Washington DC
- Coelli TJ, Prasada Rao DS, O'Donnell CJ, Battese GE (2005) *An introduction to productivity and efficiency analysis*, 2nd edn. Springer, USA
- Christensen LR (1975) Concepts and measurement of agricultural productivity. *Am J Agric Econ* 57(5):910–915
- Chebil A, Frija A, Alyani R (2014) Measurement of total factor productivity and its determinants: case of wheat sector in Tunisia. ERF In: 21st annual conference—democracy and economic development, Gammarth, Tunisia, March 20–22, 2015, 14 p
- Dhehibi B, Telleria R, Aw-Hassan A (2014a) Total factor productivity in Tunisian agriculture: measurement and determinants. *New Médit* 13(1):4–14
- Dhehibi B, Frija A, Telleria R, Aw-Hassan A (2014b) The effect of trade liberalization on the sustainability of agricultural sectors in Egypt and Tunisia: a new framework based on TFP

- growth structure. In: International conference: building sustainable agriculture for food security in the Euro-Mediterranean area: challenges and policy options, 20–21 November, 2014, Rabat, Morocco, 22 p
- Diewert WE (1978) Superlative index numbers and consistency in aggregation. *Econometrica* 46:883–900
- Diewert WE (1980) Capital and theory of productivity measurement. *Am Econ Rev* 70(2):260–67
- FAOSTAT (2013) FAO of the UN. <http://faostat.fao.org/site/535/default.aspx#ancor>. Accessed 30 Aug 2013
- Fuglie KO (1999) Investing in agricultural productivity in Indonesia. *Forum Penelitian Agro Ekonom* 17(2):1–16
- Fuglie KO (2010) Total factor productivity in the global agricultural economy: evidence from FAO data. The shifting patterns of agricultural production and productivity worldwide. The Midwest Agribusiness Trade Research and Information Center, Iowa State University, Ames, Iowa. Chapter 4, pp 63–95. (http://www.card.iastate.edu/books/shifting_patterns/pdfs/chapter4.pdf)
- Griliches Z (1979) Issues in assessing the contribution of research and development to productivity growth. *Bell J Econ* 10(1):92–116
- Gornall J, Betts R, Burke E, Clark R, Camp J, Willett K, Wiltshire A (2010) Implications of climate change for agricultural productivity in the early twenty first century. *Philos Trans R Soc Lond B Biol Sci* 365(1554):2973–2989
- Hall J, Grant MS (2006) The role of R&D in productivity growth: the case of agriculture in New Zealand: 1927 to 2001. New Zealand treasury working paper no 06/01
- Hendry DF (1995) *Dynamic econometrics*. Oxford University Press, Oxford
- Islam N, Salim RA (2009) Can R&D investment offset the negative impact of climate change on agricultural productivity? Working paper. Department of Agriculture and Food, Government of Western Australia, November 2009, 26 p
- Jud D, Hyman J (1974) International demand for Latin American tourism. *Growth Change* 5(1):25–31
- Lusigi A, Thirtle C (1997) Total factor productivity and the effects of R&D in African agriculture. *J Int Dev* 9(4):529–538
- Mahadevan R (2004) *The economics of productivity in Asia and Australia*. Edward Elgar Publishing Limited, UK
- Ministère de L'Agriculture et des Ressources Hydrauliques (MARH) (2011) *Elaboration de la Stratégie Nationale sur le Changement Climatique de la Tunisie*. ALCOR-TEC report, Menzeh, Tunisia
- MARH (2013) *Rapports d'activités 1998–2012*
- Mendelsohn R, Dinar A, Sanghi A (2001) The effect of development on the climate sensitivity of agriculture. *Environ Dev Econ* 6:85–101
- Nelson GC, Rosegrant MW, Koo J, Robertson R, Sulser T, Zhu T, Ringler C, Msangi S, Palazzo A, Batka M, Magalhaes M, Valmonte-Santos R, Ewing M, Lee D (2009) *Climate change: impact on agriculture and costs of adaptation*. Food policy report, International Food Policy Research Institute, Washington, DC
- Ruttan VW (2002) Productivity growth in world agriculture: sources and constraints. *J Econ Perspect* 16(4):161–184
- Solow RM (1957) Technical change and the aggregate production function. *Rev Econ Stat* 39:312–320
- Schiff M, Valdés A (1992) *The plundering of agriculture in developing countries*. The World Bank, Washington DC
- Thirtle C, Bottomley P (1989) The rate of return to public sector agricultural R&D in the UK, 1965–80. *Appl Econ* 21(8):1063–1086
- Torvanger A, Twena M, Romstad B (2004) *Climate change impacts on agricultural productivity in Norway*. Centre for International Climate and Environmental Research (ICERO) Working paper no 2004:10. Blindern, Norway

Conclusions and Recommendations

Climate change is a reality that must be faced and the region of North Africa and the Mediterranean Basin in general will be one of the most affected (hot spot). Compared with other regions, North Africa contributes only marginally to the pollution responsible for global warming and therefore the research efforts should focus more on adaptation aspects as mitigation. Particular attention should be given to rangeland, representing the majority of the surface but also hosting the main source of livestock farm income. More research is required for pastoral water problems including watering of livestock, provision of drinking water to the shepherds, and the distribution of watering points in grazing routes.

Natural but more importantly anthropogenic factors are responsible for land degradation in dry environments. Remedial means can be preventative or curative. Preventive measures combine several options such as natural resources management, awareness raising, and legislation to better manage the fragile ecosystems in arid environments. Remedial measures include among others, dune fixation, soil and water conservation, and rangeland rehabilitation. On the other hand, there is a need to promote exchanges of experiences between countries with similar problems in the field of management of arid ecosystems and encourage participatory approaches with end users.

Water resources in the drylands are already very scarce. Huge efforts have been already devoted to mobilization (dams, soil and water conservation, water harvesting, groundwater recharge, etc.), which resulted in very high percentages exceeding some cases 90% of the runoff/flood water. Therefore, future efforts need to be oriented to management of the demand: water-saving techniques, crop selection, strategic planning, farmer organization, water pricing, amongst others. Nevertheless, the exploitation of non-conventional water resources (treated wastewater, drainage water, saline aquifers) and renewable energies (solar, wind, geothermal) are still limited and there are a lot of unused potentials.

As drylands extend over large areas, the remote sensing and spatial technologies are found to be very effective tools particularly in surveying and monitoring of accelerated landscape changes and recurrent droughts. The increased availability of

free earth observation data would encourage their wider use and the development of spatial decision-making platforms. However, some indices (NDVI, etc.) and methods may require careful attention when applied in specific environments.

When dealing with natural resources management, the sectoral approach is inconsistent with the holistic and integrated participatory approach. The contradiction lies in the fact that development agents are required to implement participatory development projects while the governing administration continues to be built on a sectoral basis. Policymakers are urged to address seriously this institutional aspect. The technical approach to research and development has also shown its limits. Indeed, in the absence of an institutional, legal, and appropriate policy, the chances of adoption of technologies and innovations are very small, which explains the low degree of dissemination of research results. On the other hand, the production systems in arid environments are changing very rapidly, which requires more attention in order to produce scenarios that can help decision-makers.